JULIUS-MAXIMILIANS-UNIVERSITÄT
WÜRZBURG

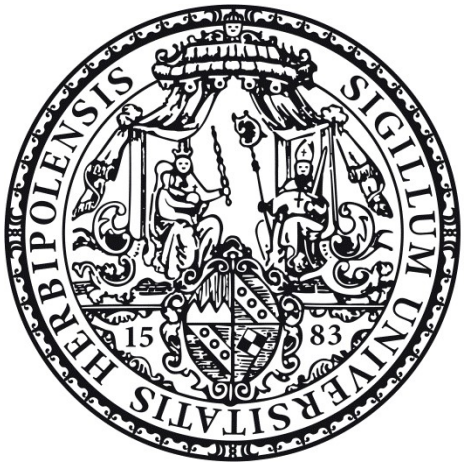

NHC-ligated Nickel(0)-Complexes: Bond Activation, Redox Behavior and Catalysis

Dissertation zur Erlangung des naturwissenschaftlichen Doktorgrades
der Julius-Maximilians-Universität Würzburg

vorgelegt von

Lukas Tendera

aus Bad Rodach

Würzburg 2022

Eingereicht am: _____

an der Fakultät für Chemie und Pharmazie der Julius-Maximilians-Universität Würzburg.

Gutachter der schriftlichen Arbeit:

1. Gutachter: Prof. Dr. Udo Radius
2. Gutachter: Prof. Dr. Holger Braunschweig

Prüfer des öffentlichen Promotionskolloquiums:

1. Prüfer: Prof. Dr. Udo Radius
2. Prüfer: Prof. Dr. Holger Braunschweig
3. Prüfer: _____

Datum des öffentlichen Promotionskolloquiums: _____

Doktorurkunde ausgehändigt am: _____

Die in der vorliegenden Arbeit beschriebenen Experimente wurden im Zeitraum von November 2018 bis September 2022 am Institut für Anorganische Chemie der Julius-Maximilians-Universität Würzburg unter der Leitung von Prof. Dr. Udo Radius durchgeführt.

Für meine Familie

Table of Contents

Chapter I

NHC Nickel Chemistry - an Overview

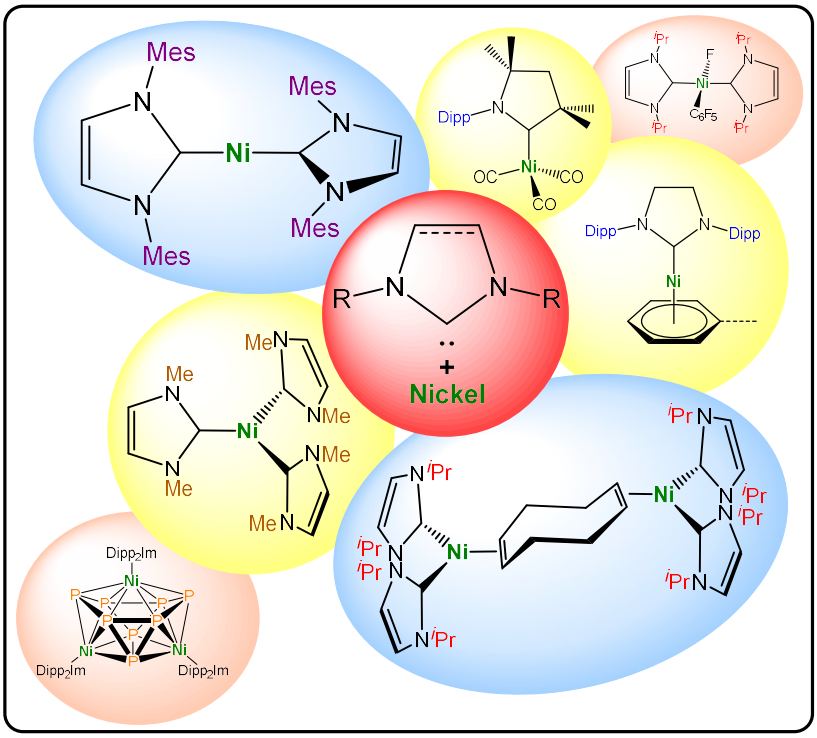

1 NHC Nickel Chemistry – an Overview

1.1 Introduction

The isolation of the first “bottleable” *N*-heterocyclic carbene (NHC), Ad_2Im (= 1,3-diadamantylimidazolin-2-ylidene) by Arduengo *et al.* in 1991[1] triggered one of the most remarkable developments in modern chemistry, rendering NHCs[2] and related molecules[3] ubiquitous and indispensable in many research areas such as main group[4] and transition metal[5] chemistry, homogeneous catalysis,[6] organocatalysis,[7] and medicinal chemistry.[8] The extraordinary stability and robustness of NHCs has allowed for the synthesis of a wide variety of such molecules, as their electronic and steric parameters can be tailored by both, nitrogen and backbone-carbon functionalization. Thus, fine-tuning of NHCs constitutes an efficient method of influencing their interaction with main group elements or transition metals and leads consequently to different reactivities of either the NHC or the resulting complexes. Intensive investigations were carried out in this direction leading to the isolation of numerous NHCs, typically bearing neutral moieties on their backbone or nitrogen atoms.

Already at the beginning of the 1960s Wanzlick was interested in the isolation of stable NHCs but he only obtained the corresponding dimers (tetraaminoethylenes), which led to the proposal of the well-known Wanzlick equilibrium.[9] Nevertheless, Wanzlick[10] and Öfele[11] independently reported the synthesis of the first NHC stabilized transition metal complexes of mercury(II) and chromium(III) by *in situ* deprotonation of imidazolium salt precursors, about 20 years before the actual isolation of a stable NHC. Later on, Lappert *et al.* expanded the studies on NHC stabilized transition metal complexes starting from the known tetraaminoethylenes and suitable metal precursors like $[Pt_2(PEt_3)_2(\mu\text{-}Cl)_2(Cl)_2]$, for example (see Figure I.1).[12]

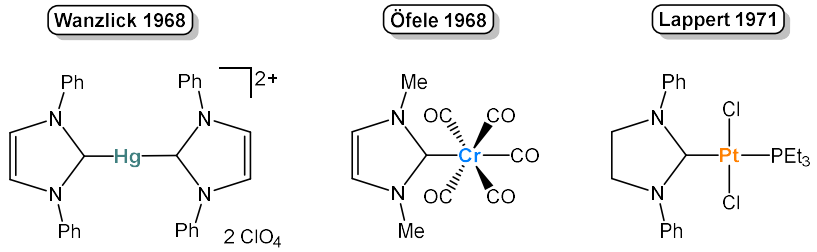

Figure I.1 Early NHC-stabilized transition metal complexes.[10-12]

With the discovery of the first isolable *N*-heterocyclic carbene Ad_2Im by Arduengo and co-workers, the chemistry of NHCs finally experienced an enormous boost. This milestone created the basis for countless extraordinary chemical novelties and can be referred to as the starting point of the success story of NHCs. Shortly after the isolation of Ad_2Im Arduengo *et al.* also reported the synthesis of four other stable NHCs, namely Me_2Im^{Me} (1,3,4,5-tetramethylimidazolin-2-ylidene), Tol_2Im (1,3-ditolylimidazolin-2-ylidene), *p*-Cl-Ph_2Im (1,3-di-(*p*-chlorophenyl)-2-ylidene) and Mes_2Im **A** (1,3-dimesitylimidazolin-2-ylidene).[13] The reaction of Mes_2Im **A** with copper(I) and silver(I) triflates led to the isolation of the cationic two-coordinate complexes $[Cu^I(Mes_2Im)_2][OTf]$ and $[Ag^I(Mes_2Im)_2][OTf]$, respectively.[14] One year later, it was again Arduengo *et al.*, who reported the first bis-NHC stabilized, low-coordinate 14-electron nickel(0) complex $[Ni(Mes_2Im)_2]$ **1** and the platinum analogue $[Pt(Mes_2Im)_2]$ obtained from the reaction of **A** with $[M(\eta^4\text{-COD})_2]$ (M = Ni, Pt; COD = 1,5-cyclooctadiene).[15] These compounds were the first NHC transition metal complexes synthesized from a free carbene and a suitable metal precursor. In recent years, NHC-nickel complexes have displayed some very interesting reactivity and applicability in different transition metal-catalyzed processes, which strongly depend on the electronic and steric nature of the NHCs employed. This overview presents the chemistry of NHC-stabilized nickel complexes, their synthesis, characterization, reactivity, and application in catalysis. Due to the large amount of work in catalysis using systems generated *in situ* from imidazolium salts and nickel precursors the introduction is restricted to the current knowledge for isolated, well-defined $[Ni(NHC)_2]$ complexes, as such systems are employed throughout the thesis.

1.2 Synthesis and General Properties of NHCs

Since 1991 many different NHCs have been successfully synthesized and used in various chemical applications. For all NHCs the carbenic centre is contained by *N*-heterocyclic rings of varying sizes (mainly five- and six-membered) with at least one nitrogen atom present to stabilize the carbene. In particular, the well-known imidazolin-ylidenes, imidazolidin-ylidenes, benzimidazolin-ylidenes and tetrahydropyrimidin-ylidenes, which all have a carbene center with two adjacent nitrogen atoms, are nowadays heavily applied. Additionally, NHCs containing only one nitrogen atom and an additional carbon atom next to the carbene center, i.e. the cyclic (alkyl)(amino)carbenes (cAACs), which were first reported by Lavallo and Bertrand *et al*.[16] are nowadays frequently used. These cAACs exhibit strongly increased *π*-accepting properties relative to conventional NHCs, like the imidazolin-ylidenes, and thus have found special use in the stabilization of subvalent main group compounds or main group radicals.[3e, 4d, 4i, 17] Furthermore, heterocycles containing additional heteroatoms such as oxygen (oxazolin-ylidenes)[18], sulfur (thiazolin-ylidenes)[19] or nitrogen (triazolin-ylidenes)[20] have also been reported in the literature. Another class are the mesoionic (MIC) or “abnormal” NHCs (*a*NHC),[21] in which the carbene center is located at the 4-position of an imidazole ring. The general structures of the different classes of NHCs and the structures of the selected carbenes Mes_2Im **A** (= 1,3-dimesitylimidazolin-2-ylidene), Mes_2Im^{H2} **B** (= 1,3-dimesitylimidazolidin-2-ylidene), $Dipp_2Im$ **C** (= 1,3-(2,6-di-*iso*-propylphenyl)imidazolin-2-ylidene), $Dipp_2Im^{H2}$ **D** (= 1,3-(2,6-di-*iso*-propylphenyl)imidazolidin-2-ylidene), $cAAC^{Me}$ **E** (1-(2,6-di-*iso*-propylphenyl)-3,3,5,5-tetramethylpyrrolidin-2-yliden), $^{i}Pr_2Im$ **F** (1,3-di-*iso*-propylimidazolin-2-ylidene), and $^{i}Pr_2Im^{Me}$ **G** (1,3-di-*iso*-propyl-4,5-dimethylimidazolin-2-ylidene), which are often used in $[Ni(NHC)_2]$ chemistry, are shown in Figure I.2.

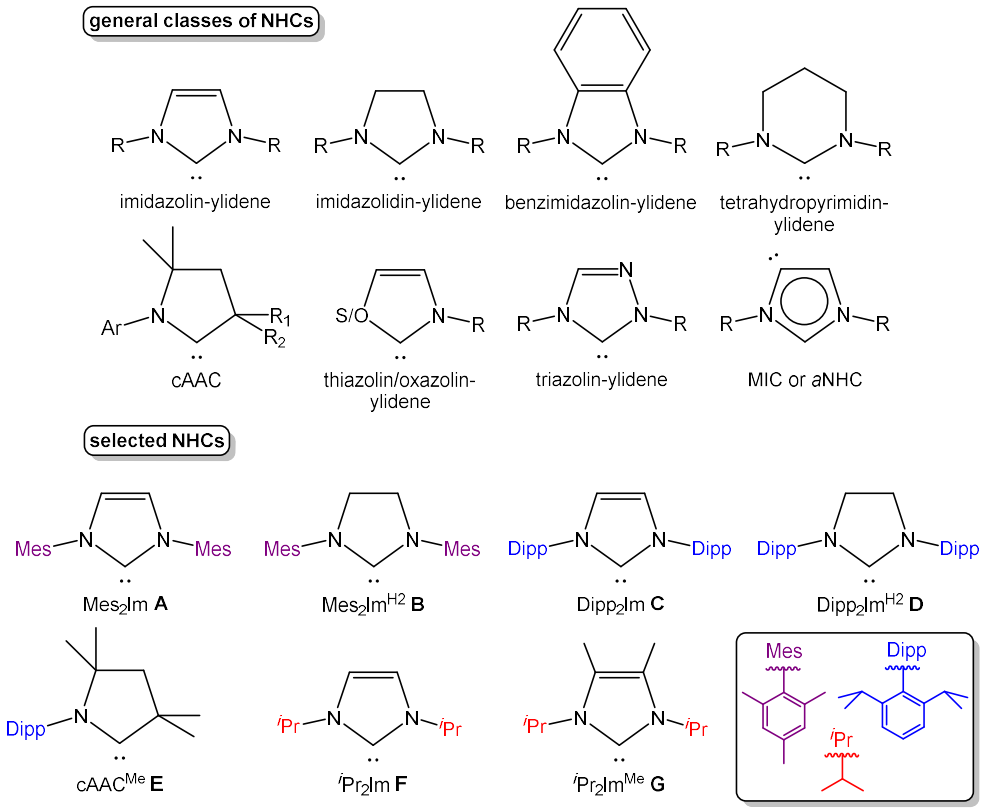

Figure I.2 Important general classes of NHCs and selected NHCs **A-G**.[2]

As mentioned above, the first isolated carbene was Ad_2Im, which was obtained as a colorless crystalline solid by a simple deprotonation of the corresponding imidazolium-chloride salt using NaH and a catalytic amount of DMSO in THF (Scheme I.1a).[1] This synthetic route remains the most used preparation method for many of the known NHCs. However, the isolation of the free carbene is often not necessary for a wide range of applications. Especially in many organocatalytic reactions, where the carbene is generated *in situ* from the imidazolium salt in combination with a suitable base. Besides the simple deprotonation, alternative synthetic strategies have been reported (see Scheme I.1b). The isolation of free NHCs can be achieved, for example, by desulfurization of thioureas with potassium[22] or by heating a zwitterionic azolium-carboxylate under extrusion of CO_2.[23] Further possibilities are the reductive dehalogenation of chloro-substituted azolium-salts[24] or the vacuum pyrolysis with small molecule elimination, e.g. MeOH, from a suitable precursor.[20, 25]

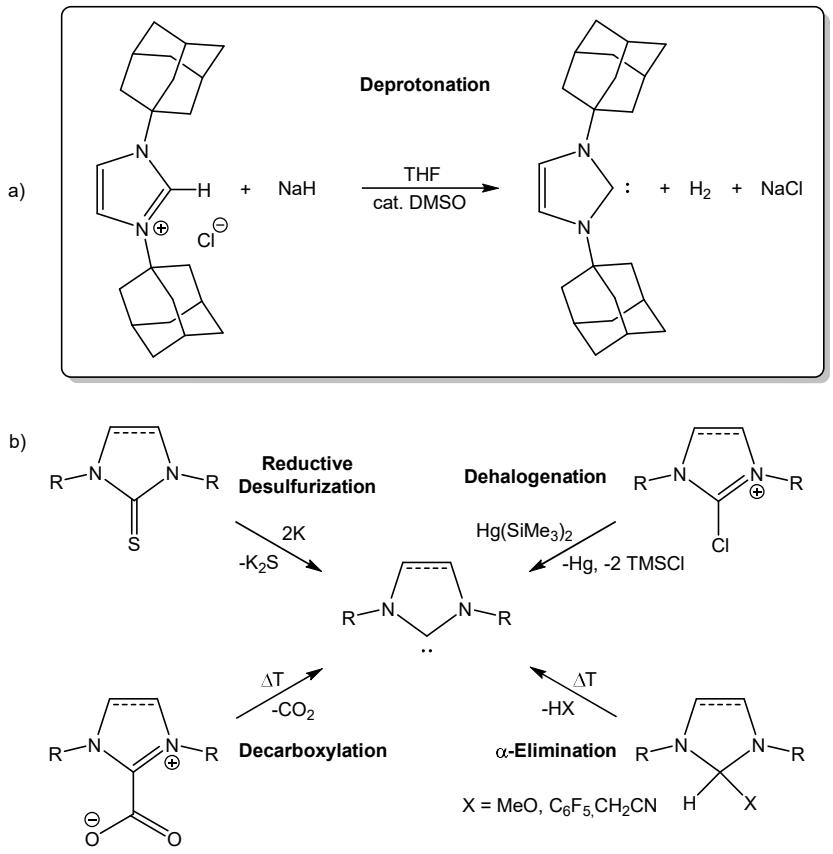

Scheme I.1 a) Arduengo's first synthesis of Ad_2Im *via* the most commonly employed deprotonation method.[1] b) Alternative synthetic routes to free NHCs.[20, 22-25]

The selected carbenes **A-G** are all conveniently synthesized by using the deprotonation method and can be isolated as crystalline or amorphous solids, except for $^{i}Pr_2Im$, which is a liquid at room temperature. Purification is achieved either by simple precipitation and filtration from a non-polar solvent like hexane[26] or by sublimation/condensation[27] of the crude product. The procedures for the synthesis of the azolium-salt precursors of **A-G** as well as the reagents for the deprotonation are shown in Scheme I.2.

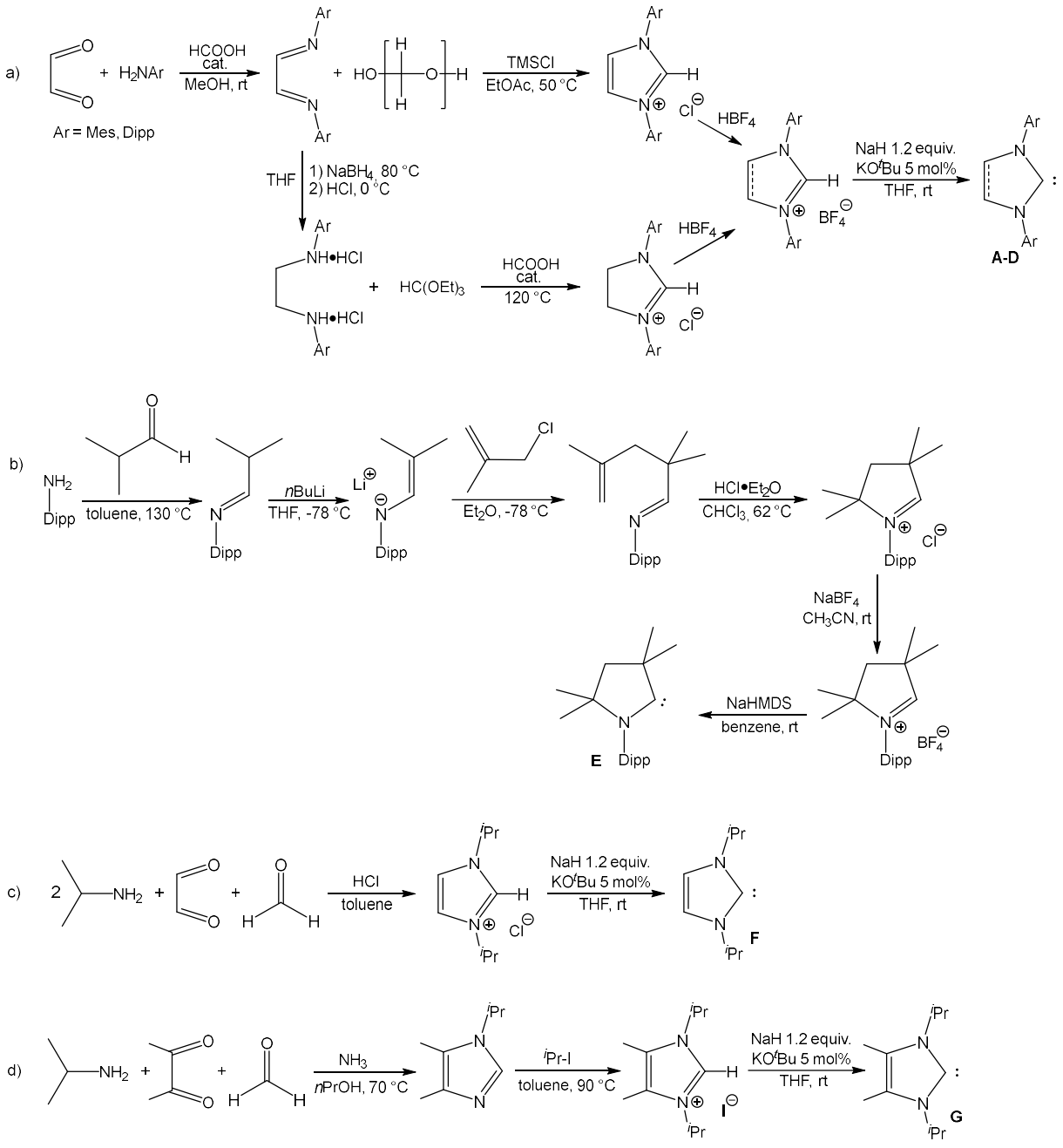

Scheme I.2 Synthesis of the *N*-aryl substituted imidazolin-ylidenes Mes_2Im **A**, Mes_2Im^{H2} **B**, $Dipp_2Im$ **C** and $Dipp_2Im^{H2}$ **D** (a), of $cAAC^{Me}$ **E** (b) and of the *N*-alkyl substituted imidazolin-ylidenes $^{i}Pr_2Im$ **F** (c) and $^{i}Pr_2Im^{Me}$ **G** (d).[16, 26-27]

1.3 Electronic and Steric Properties of NHCs

The range of possible applications of *N*-heterocyclic carbenes are a result of their unique electronic and structural properties (compare Figures I.3, I.4 and I.5).[2e, 28] A quantitative MO analysis (Figure I.3) reveals that the frontier orbitals of Me_2Im (= 1,3-dimethylimidazolin-2-ylidene)[29] may be considered as those of a 6 π-electron aromatic system, superimposed on the carbene σ-type orbital $12a_1$ at -5.74 eV, which is the HOMO of the molecule. The orbitals $2b_1$, $2a_2$, $3b_1$, $3a_2$ and $4b_1$, similar to those of the well-known cyclopentadienyl anion, are the occupied orbitals of the π-system and have no nodal plane (orbital $2b_1$ in C_{2v} symmetry, at -10.26 eV) or one nodal plane ($2a_2$, -7.41 eV and $3b_1$, -6.25 eV), whereas the unoccupied π-orbitals ($3a_2$, +0.57 eV and $4b_1$, +1.08 eV) have two nodal planes. These pairs of orbitals are not degenerate due to the heteroatomic substitution of the aromatic ring and thus in C_{2v} symmetry. The $4b_1$ orbital (LUMO+1, +1.08 eV) is mainly centered at the carbene carbon atom and is mostly composed of the carbene p_x-orbital (62 %), while for the $3b_1$ orbital the p_x contribution is lower (22 %, based on gross Mulliken contributions of AOs to the MOs). The HOMO of Me_2Im is the $12a_1$ orbital at -5.74 eV, usually referred to as the carbene σ-orbital, which contains carbene carbon p_z (49 %) and s (33 %) character. This level of theory predicts to an energy gap of 6.82 eV between $12a_1$ and $4b_1$.[29a] [1]

[1] The preceding text section of Chapter 1.3 and Figure I.3 were mainly adapted from a previous publication of our group (ref. 29a).

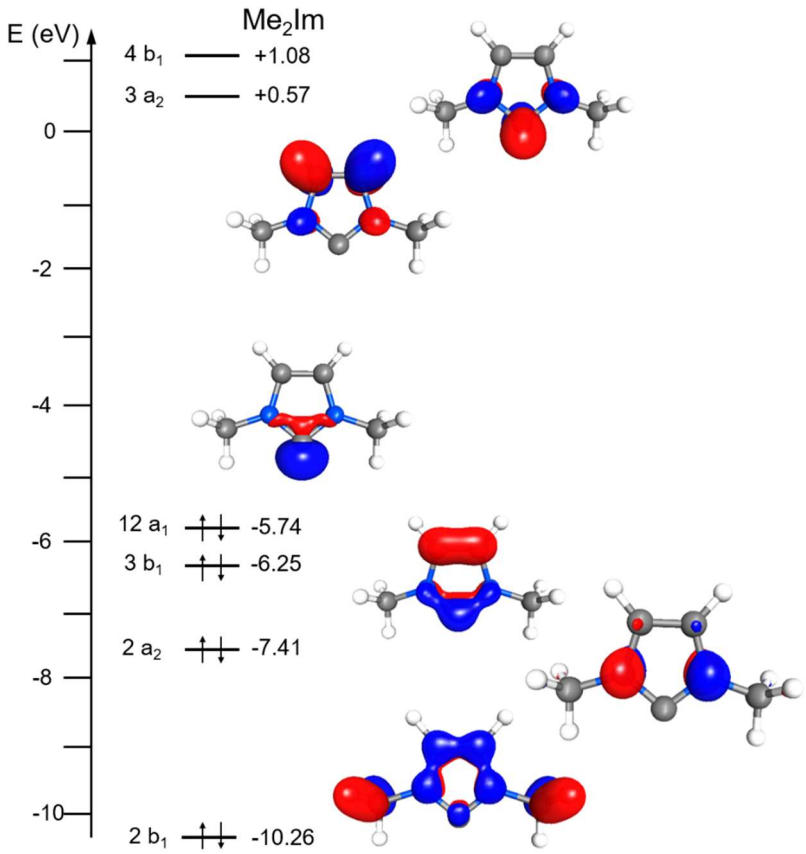

Figure I.3 Main electronic features of Me_2Im (= 1,3-dimethylimidazolin-2-ylidene). Energies were calculated at the DFT/B3LYP/def2-TZVPP level of theory.[29]

This concept can also easily be explained by simple inductive and mesomeric effects (Figure I.4). [2b] Stabilization of the unoccupied p-orbital at the carbene occurs *via* a +M-effect through overlap of this orbital with the nitrogen p(π)-orbitals, which in turn leads to an energetic rise of the combination located at the carbene carbon atom (π-conjugation). On the other hand, the higher electronegativities of the nitrogen atoms located within the ring lead to an inductive withdrawing of σ-electron density (-I-effect) from the σ-sp^2-orbital and therefore to an increase of the s-contribution in the sp^2-orbital, lowering the HOMO-energy (σ-polarization). Both effects result in an electronic stabilization of the singlet ground state due to the increased gap between the carbene s- and p-orbital.[30] Additionally, the *N*-substituents protect the carbene center sterically and prevent dimerization, the latter is known as the Wanzlick-equilibrium of NHCs.[2f, 9] Due to these stabilizing effects NHCs stand out as very good σ-donating ligands surpassing phosphines. The π-accepting abilities of NHCs differ and depend on (i) the general structure of the heterocycle and (ii) the electronic situation of the transition metal complex it is bound to.[29]

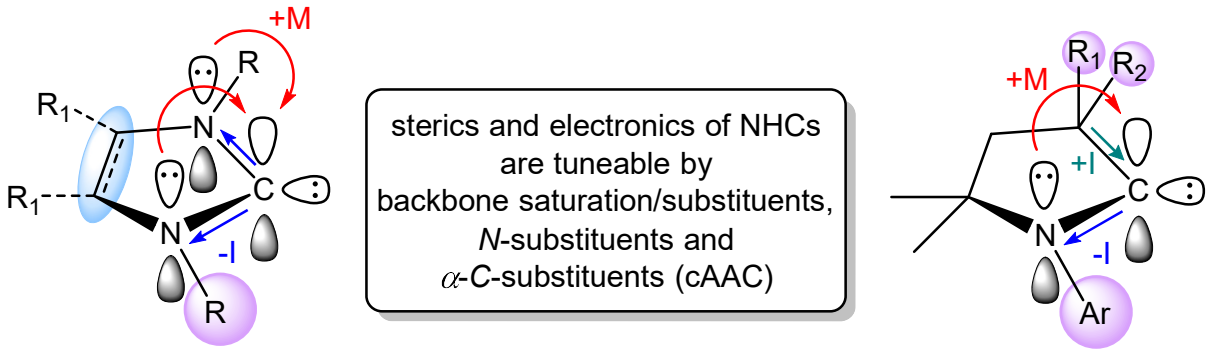

Figure I.4 Electronic and steric effects of NHCs and cAACs.

While classic five-ring imidazolin-ylidenes are relatively weak *π*-acceptors, the cAACs for example, reveal even better *σ*-donor properties and a very good *π*-accepting character. Results from DFT calculations (B3LYP/def2-TZVPP-level, see Figure I.5) on the commonly used carbenes Me_2Im and **A-G** revealed that the *σ*-type HOMO of $cAAC^{Me}$ **E** (-5.20 eV) is slightly higher in energy compared to the HOMOs of the imidazoline- or imidazolidine-type NHCs which lie within 0.5 eV in the range between -5.94 eV and -5.43 eV. Furthermore, cAAC ligands have a lower energy carbene *π**-orbital (-0.36 eV for $cAAC^{Me}$ **E** compared to +0.49 eV - +1.25 eV for the NHCs), which leads to a smaller singlet–triplet energy gap and thus to an increased electrophilicity at the carbenic carbon atom. Backbone saturation or substitution also affect the donor/acceptor properties, while having a relatively low, but still noticeable impact on the sterics.[31] The obtained energy values for the frontier orbitals of the unsaturated NHCs Mes_2Im **A** and $Dipp_2Im$ **C** and their saturated analogues Mes_2Im^{H2} **B** and $Dipp_2Im^{H2}$ **D** reveal slightly better donor and acceptor capabilities for the saturated NHCs. In contrast to that, a comparison of the orbitals of $^{i}Pr_2Im$ **F** and $^{i}Pr_2Im^{Me}$ **G** shows that backbone methylation significantly increases both, the energy of the *σ*-type HOMO (-5.43 eV for **G** compared to -5.63 eV for **F**) and the energy of the *π**-orbital (+1.25 eV for **G** compared to +1.15 eV for **F**) and thus leads to better *σ*-donor and weaker *π*-acceptor properties of the backbone-methylated carbene $^{i}Pr_2Im^{Me}$ **G**. In summary, the stereo-electronic properties, stability and reactivity of NHCs depend on the ring size,[32] the substituents at nitrogen[33] and on backbone substitution,[31, 34] which can be easily fine-tuned.

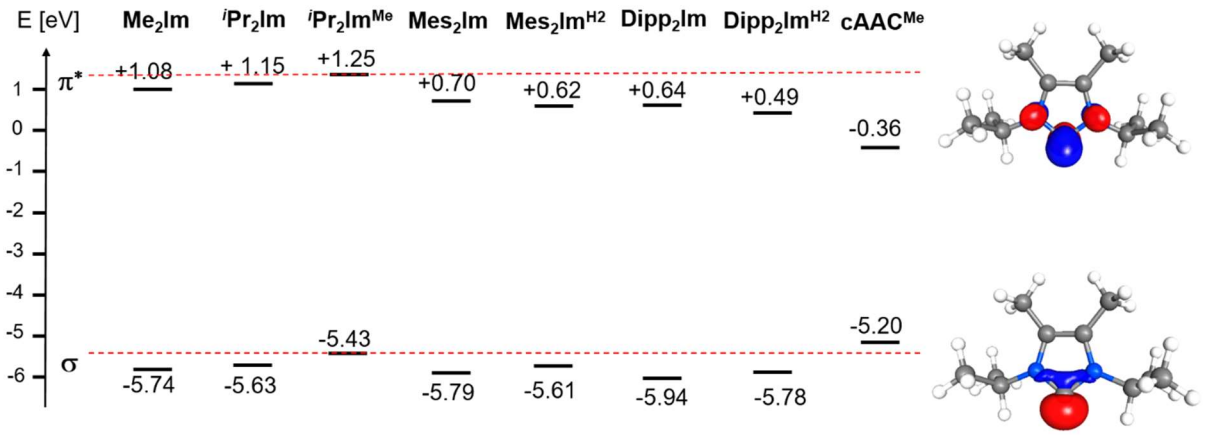

Figure I.5 The calculated energies of the carbene s- and p-orbitals of commonly used NHC ligands Me_2Im and **A-G** (DFT/B3LYP/def2-TZVPP level of theory).

Since the number and applications of experimentally accessible NHCs has increased rapidly in the last thirty years, different methods have been developed to rationalize the steric and electronic properties of different NHCs.[35] Therefore various parameters have been evaluated by experimental or computational strategies to facilitate the choice of the correct NHC for any purpose. The most commonly used methods for quantifying the donor/acceptor abilities of NHCs are the Tolman electronic parameter (TEP),[36] which refers to the *σ*-donor strength, and the ^{31}P NMR (δ_P) or ^{77}Se NMR (δ_{Se}) shifts of phosphorus or selenium NHC-adducts, which evaluate the *π*-accepting character of the carbene.[37] To compare the steric impact of NHCs, calculation of the "percent buried volume" ($\%V_{bur}$) and steric maps have emerged as useful tools.[38] These methods will be briefly discussed in the following section. Nonetheless, it is worth mentioning that many other quantification methods have been established such as the determination of pK_a-values of azolium-salts,[39] electrochemical measurement of the Lever electronic parameter (LEP),[40] evaluation of nucleophilicity and *Lewis* basicity,[41] additional computational methods to determine the computed ligand electronic parameter (CEP),[42] the metal-ligand electronic parameter (MLEP),[43] the molecular electronic potential (MESP),[44] and the carbene relative energy of formation (CREF).[45]

The TEP-value describes the net donor ability of electron donating ligands like phosphines or NHCs to a metal center and can be obtained from the analysis of the C–O-stretches of different transition metal carbonyl complexes.[35a, 36] Traditionally the TEP of a ligand (L) was obtained by measuring an IR-spectrum of complexes of the type [(L)Ni(CO)$_3$] and quoting the frequency of the A_1 stretching mode of the C≡O bonds as the TEP. This concept is based on the fact that a more electron donating ligand leads to a higher electron density at the metal center and thus increased backdonation to the π^*-antibonding orbital of the carbonyl ligands of the complex, resulting in lower stretching frequencies. Therefore, a stronger donor ligand is accompanied with a smaller TEP value, a weaker donor is associated with a higher TEP value. In the 1970s Tolman first evaluated the TEP of a series of phosphine ligands from complexes of the type [(R$_3$P)Ni(CO)$_3$], which were prepared starting from [Ni(CO)$_4$] and the phosphine.[36] Due to the toxicity and volatility of [Ni(CO)$_4$][46] and this synthetic approach often not forming the desired complexes, [(NHC)Ni(CO)$_3$], for NHCs,[47] nowadays the TEP is often determined from the easily available and less hazardous complexes [IrCl(CO)$_2$(NHC)] or [RhCl(CO)$_2$(NHC)]. The TEP-values of both systems can be linked to each other and to the [(NHC)Ni(CO)$_3$] system by a linear regression. In 2013, Nelson and Nolan reviewed the electronic properties of about 300 NHCs including a standardization of their TEP values derived either from the Ni-, Ir- or Rh-carbonyls.[35a] As it was missing until then, our own group added the experimentally derived data for the widely used cAAC^{Me} ligand in 2016 by preparing the corresponding [(cAAC^{Me})Ni(CO)$_3$] complex.[48] Although the TEP is a useful tool to estimate the relative donor strength of a NHC, it always has to be interpreted with care since it is an indirect method related to π-interactions between the metal and the carbonyl ligand. Those interactions are also affected by the sterics of the NHC, the influence of other ligands, and the different bonding situations between the metal and the NHC, which cannot be of pure σ-donating character in all cases. However, some general trends were observed when comparing the TEPs of different NHCs and phosphines: (i) NHCs are stronger σ-donors than phosphines, (ii) the donor strength of the NHC increases with its ring size (iii) a higher number of nitrogen atoms in five membered NHCs leads to weaker donor abilities, (iv) *N*-alkyl substituents lead to lower TEP values compared to *N*-aryl substituents, (v) backbone substitution with electron withdrawing or electron donating substituents can affect the TEP and (vi) NHCs with an unsaturated backbone reveal a lower TEP than their saturated analogues, whereby the latter has to be treated

with care since imidazolidin-ylidenes are also more *π*-accepting than imidazolin-ylidenes and therefore compete with the carbonyl ligands. Figure I.6 provides the TEP values of the NHCs **A-G** and some other selected examples.[35a]

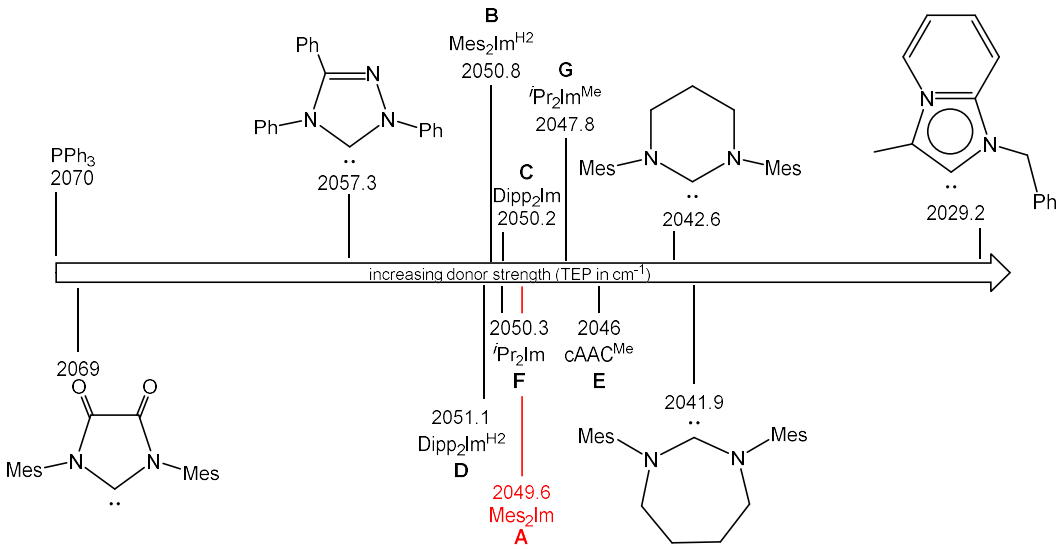

Figure I.6 Tolman electronic parameter (TEP in cm^{-1}) of selected NHCs including the NHCs **A-G**.[35a]

To rationalize the *π*-accepting ability of NHCs, Bertrand *et al.*[37b] and Ganter *et al.*[37c, 37d] independently developed NMR-spectroscopic methods based on NHC-phosphinidene and NHC-selenium adducts, respectively. Both adducts can be described by two resonance forms (see Figure I.7), which either describe a charge-separated single bond between the carbenic carbon atom and the heteroatom, leaving a positive charge at carbon, or a formal double bond between the carbene carbon atom and the phosphorus or selenium atom with a significant amount of *π*-backdonation. Accordingly, a higher degree of *π*-acceptance of the carbene leads to a more downfield-shifted signal of the ^{31}P NMR (δ_P) or ^{77}Se NMR (δ_{Se}) resonance in these NHC phosphinidenes or NHC selenes. As expected, the adducts of cAACs reveal by far the most downfield-shifted δ_P and δ_{Se} values of all NHCs, in line with their very good *π*-accepting ability.[48-49] A comparison of the NHCs with the same *N*-substituents reveals that the saturated carbenes are usually much better *π*-acceptors than their unsaturated analogues. For the phosphinidene and selenium adducts of the NHCs **A-G** the previously reported δ_P and δ_{Se} values follow these trends as expected,[37, 48-49] with cAAC^{Me} **E** being the best and $^{i}Pr_2Im^{Me}$ **G** being the worst *π*-acceptor respectively

(see Figure I.7). It is worth noting that these values must be interpreted with care as they are strongly dependent on the solvent, concentration, temperature, and pH values. Furthermore, the backdonation of phosphorus or selenium to the NHC is also influenced by the donor-capability of the NHC itself, due to the nature of synergic bonding.[35d] Just recently, Bertrand *et al.* showed that non-classical selenium-hydrogen bonding interactions, for example, can additionally cause a significant deviation from the expected ^{77}Se NMR (δ_{Se}) shifts of the NHC-selenium adducts.[50]

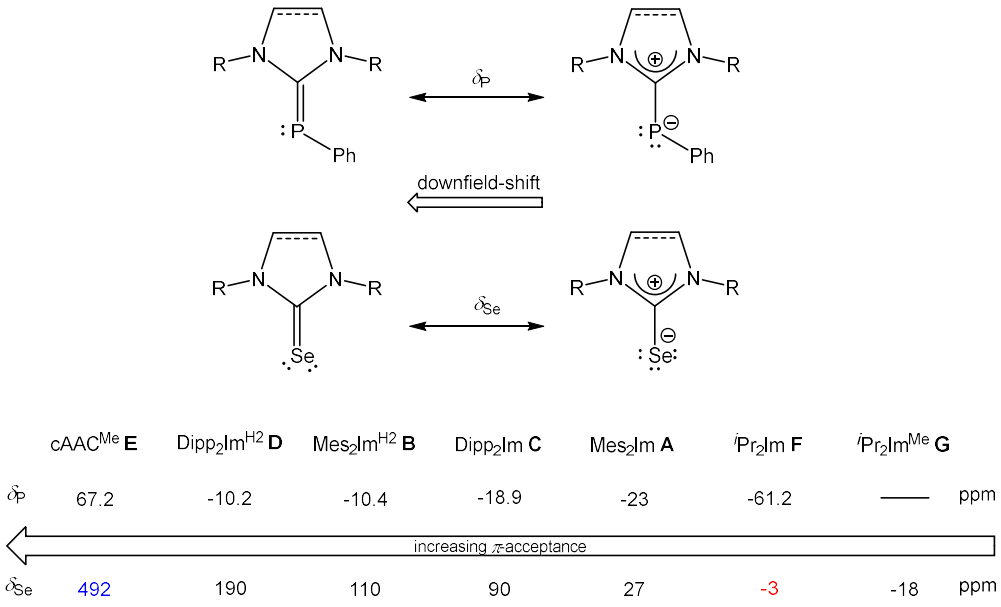

Figure I.7 Resonance structures of phosphinidene and selenium NHC-adducts and ^{31}P NMR (δ_P) or ^{77}Se NMR (δ_{Se}) shifts of the adducts of the carbenes **A-G**. ^{31}P NMR spectra were recorded in C_6D_6 and the ^{77}Se NMR spectra were recorded in $CDCl_3$ (or THF-d_8 (blue) / acetone-d_6 (red)).[37, 48-49]

Beside his description of the TEP, Tolman also developed a systematic classification of the steric impact of tertiary phosphine ligands by determining the so called Tolman cone angle θ in complexes of the type $[(R_3P)Ni(CO)_3]$.[36] However, the cone angle is not a suitable model for the description of the steric influence of an NHC ligand, due to the different, unsymmetrical umbrella-shaped geometry of NHCs. In 2003, Cavallo and Nolan *et al.*[38a] first reported their studies on the "percent buried volume" (%V_{bur}), which can be calculated from crystallographic or computational data, as a metric for quantifying the steric impact of NHC ligands. The buried volume serves as a measure of the space occupied by a ligand in the first coordination sphere of the metal center.

The calculation requires a definition of the metal center, to which the ligand is coordinated at a certain distance *d*. Then, a sphere of radius *r*, which is centered at the metal atom, is created and the volume the ligand captures is assigned to the buried volume V_{bur} of this sphere. The buried volume V_{bur} indicates the volume of the coordination sphere which is occupied by the ligand, but additionally the percentage of the volume buried by the ligand with respect to the volume of the total sphere (%V_{bur}) leads to a meaningful result, which can be compared. Thus, for the calculation of %V_{bur} a complex is defined as a sphere with the metal atom at the center having a fixed radius (*r*) of 3.5 Å and a metal-carbene distance (*d*) set to 2.00 Å or 2.28 Å (compare Figure I.8).[38] The percentage of the total sphere-volume which is buried by the ligand gives then the %V_{bur}. This approach can also be used for other ligands like phosphines, which allows a better comparison of the different ligand-classes. Cavallo and co-workers additionally developed a very useful open-access online software Samb*V*ca (**Sa**lerno **m**olecular **b**uried **v**olume **ca**lculation),[51] which calculates the %V_{bur} of any ligand after uploading crystallographic data or DFT-derived atomic coordinates. Often the %V_{bur} is calculated from crystal structures of linear gold(I) complexes [(L)AuCl] since the potential steric influence of a co-ligand (here the chloride) is minimized. However, the results obtained strongly depend on the type of the complex, the M–L distance *d* and the sphere radius size *r*. So, these parameters should be chosen wisely and have to be equal if any values are compared. Thus, a proper comparison of %V_{bur} values is in principle only valid if the data were obtained from the same type of complex, using the same metal ligand distance *d* and sphere radius *r*. Concerning coordination numbers of the complexes, the geometry can be decisively affected by the number of co-ligands or by repulsive or attractive interactions between them. A very good example to illustrate this dependence on the ligand environment is the $^{i}Pr_2Im^{Me}$ ligand **G**. For the complex [($^{i}Pr_2Im^{Me}$)AuCl] the %V_{bur} was calculated to be 38.4 %,[35b] while the %V_{bur} of the same ligand in [($^{i}Pr_2Im^{Me}$)Ni(CO)$_3$] was calculated to be only 27.7 %, by our group (compare Figure I.8 and Chapter III).[52] As the steric impact of NHCs is very anisotropic, the Samb*V*ca software was expanded by a tool for calculating topographic steric maps of the ligands, which now allow better information about the spatial distribution of the steric bulk around the metal to be obtained (see Figure I.8).[53]

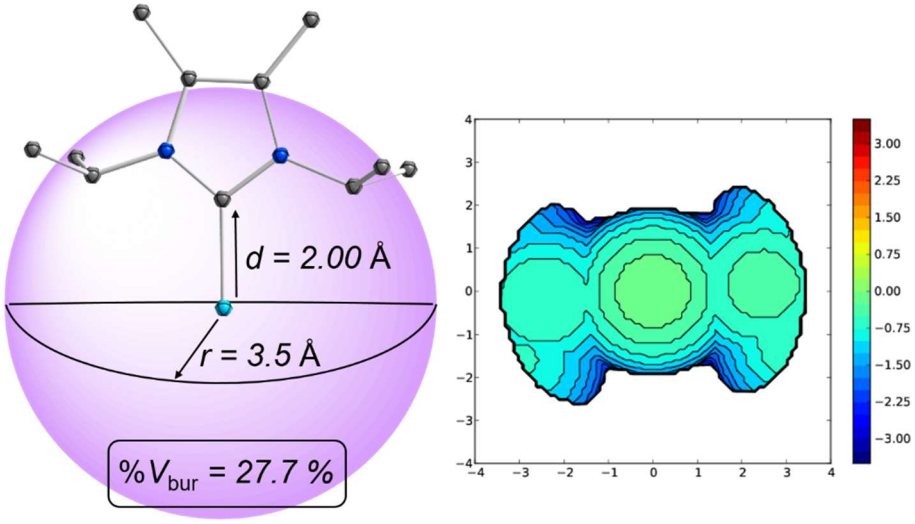

Figure I.8 Percent buried volume %V_{bur} and steric map of $^{i}Pr_2Im^{Me}$ **G** calculated from DFT-derived atomic coordinates of [($^{i}Pr_2Im^{Me}$)Ni(CO)$_3$].[52]

1.4 Synthesis of [Ni(NHC)$_2$] Complexes

First-row, earth-abundant transition metal complexes have attracted a lot of attention in recent years, due to their interesting chemical and physical properties, their relatively low toxicity, and their inexpensive price.[54] In a review of catalysis in organic chemistry from 1922, the Nobel laureate Paul Sabatier compared the metal nickel with “a spirited horse, delicate, difficult to control, and incapable of sustainable work”.[55] Nowadays, contrary to this, nickel complexes have evolved to become very good alternatives to expensive precious-metal catalysts and many powerful nickel-based catalytic systems have been explored.[56] The discovery of NHCs and their easily adjustable stereo-electronic properties, has led to a tremendous amount of new organometallic compounds,[5f, 5g] and unveiled new opportunities in nickel-catalysis.[57] Low-coordinate complexes of nickel especially have shown their outstanding catalytic competence and revealed interesting magnetic behavior.[58] NHC-nickel complexes have been used successfully in a variety of catalytic transformations, such as different C–E (carbon-element) couplings, e.g. alkylations, aminations, hydrosilylations, cycloadditions and oligomerization or polymerization reactions.[57, 59] The section below provides an insight into the reactivity of NHC-stabilized nickel(0)-complexes of the type [Ni(NHC)$_2$]. Since there are too many examples of catalytic reactions using *in situ* generated catalysts by applying [Ni(η^4-COD)$_2$] (COD = 1,5-cyclooctadiene) and different NHC ligands, this overview is limited to the synthesis, properties, and secured reactivities of the readily prepared complexes [Ni(Mes$_2$Im)$_2$] **1**, [Ni(Mes$_2$Im^{H2})$_2$] **2**, [Ni(Dipp$_2$Im)$_2$] **3**, [Ni(Dipp$_2$Im^{H2})$_2$] **4**, [Ni(cAAC^{Me})$_2$] **5**, [Ni(*i*Pr$_2$Im)$_2$] **6** and [Ni(*i*Pr$_2$Im^{Me})$_2$] **7** (see Figure I.9), which are stabilized by the previously described NHCs **A-G** and set the basis for the following chapters of this thesis. It is important to note, that only the complexes **1-5** can be isolated as truly two-coordinate, linear complexes. The complexes [Ni(*i*Pr$_2$Im)$_2$] **6** and [Ni(*i*Pr$_2$Im^{Me})$_2$] **7** are not stable without further stabilizing ligands (*vide infra*), due to the modest steric protection delivered by the *N-iso*-propyl substituents. However, their precursors employed especially in our group typically react as synthons of **6** and **7**, and these synthons will therefore be considered as the two-coordinated linear equivalents [Ni(*i*Pr$_2$Im)$_2$] **6** and [Ni(*i*Pr$_2$Im^{Me})$_2$] **7**.

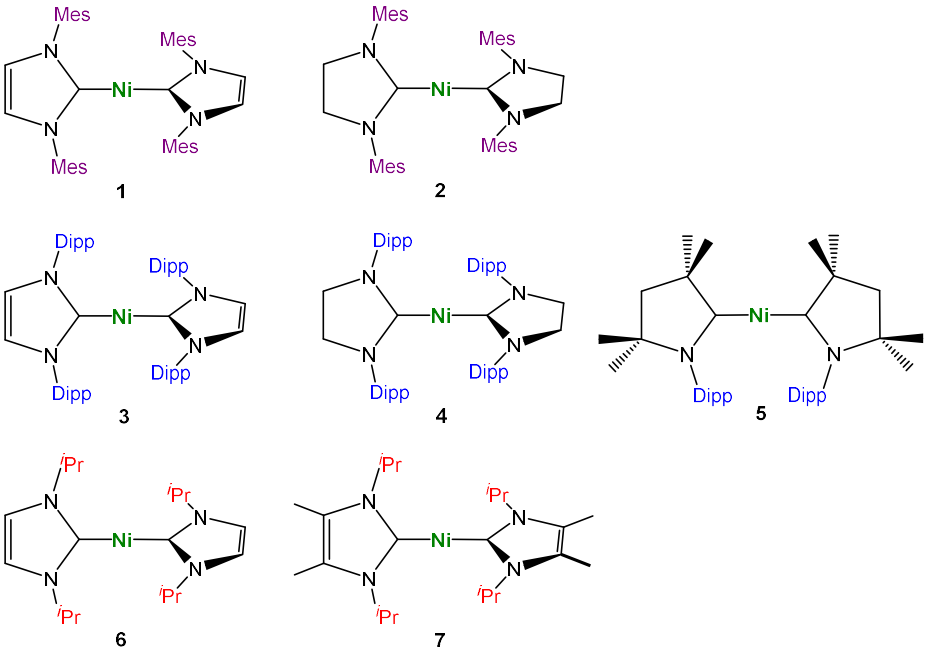

Figure I.9 Bis-NHC-stabilized nickel(0)-complexes **1-7**.

As mentioned at the beginning, the synthesis of [Ni(Mes$_2$Im)$_2$] **1** by Arduengo *et al.* in 1994 was the first isolation of a two-coordinate NHC-stabilized nickel(0)-complex.[15] These authors described the isolated complex **1** as dark violet crystals, which were obtained from the reaction of [Ni(η^4-COD)$_2$] with two equivalents of Mes$_2$Im **A**. Over 20 years, later in 2016, Hillhouse *et al.* used the same direct method for the synthesis of [Ni(Mes$_2$Im^{H2})$_2$] **2**.[60] The *N*-Dipp substituted complex [Ni(Dipp$_2$Im)$_2$] **3** was first reported by Herrmann *et al.* in 2001,[61] but his "Arduengo-like" approach turned out to be pretty inefficient (see below). Alternative synthetic pathways for the synthesis of **3** were independently reported by the groups of Matsubara[62] and Danopoulos[63] starting either from [Ni(acac)$_2$] (acac = acetylacetonate) or from [Ni(CH$_3$)$_2$(tmed)] (tmed = *N,N'*-tetramethylethylenediamine), *via* a direct reduction or ligand substitution with consequent reductive elimination of ethane, respectively. Danopoulos *et al.* also isolated [Ni(Dipp$_2$Im^{H2})$_2$] **4** and [Ni(^{t}Bu$_2$Im)$_2$] from the reaction of [Ni(CH$_3$)$_2$(tmed)] with two equivalents of Dipp$_2$Im^{H2} **D** or ^{t}Bu$_2$Im (1,3-di-*tert*-butylimidazolin-2-ylidene), respectively. Furthermore they postulated the formation of free [Ni(^{i}Pr$_2$Im^{Me})$_2$] **7** by NMR-spectroscopy after heating the bis-alkyl complex *cis*-[Ni(^{i}Pr$_2$Im^{Me})$_2$(CH$_3$)$_2$], but were never able to isolate compound **7**.[63] The direct method using [Ni(η^4-COD)$_2$] and two equivalents of NHC is not a suitable synthetic strategy for the synthesis of the complexes [Ni(Dipp$_2$Im)$_2$] **3** and [Ni(Dipp$_2$Im^{H2})$_2$] **4** or [Ni(^{t}Bu$_2$Im)$_2$]. While the reaction

of [Ni(η^4-COD)$_2$] with ^{t}Bu$_2$Im affords a dimeric complex *via* C–N cleavage of the *tert*-butyl group as the main product,[64] the reaction of Dipp$_2$Im **C** or Dipp$_2$Im^{H2} **D** with [Ni(η^4-COD)$_2$] in THF leads to an equilibrium between the starting materials and the product, which lies on the side of the starting materials.[60, 65] If the reaction is carried out in aromatic solvents, such as benzene or toluene an equilibrium mixture between the [Ni(NHC)$_2$] complexes **3**/**4**, the corresponding mono-NHC complexes [(NHC)Ni(η^6-arene)] (NHC = Dipp$_2$Im **C** or Dipp$_2$Im^{H2} **D**) and the starting material was verified (compare Scheme I.3).[66] However, Ogoshi *et al.* showed that this approach is a useful way to synthesize the mono-NHC complexes [(NHC)Ni(η^6-arene)], if one equivalent of the carbene is used and the reaction is performed under an H_2-atmosphere (8 bar) to reduce the resulting free 1,5-cyclooctadiene to cyclooctane.[66]

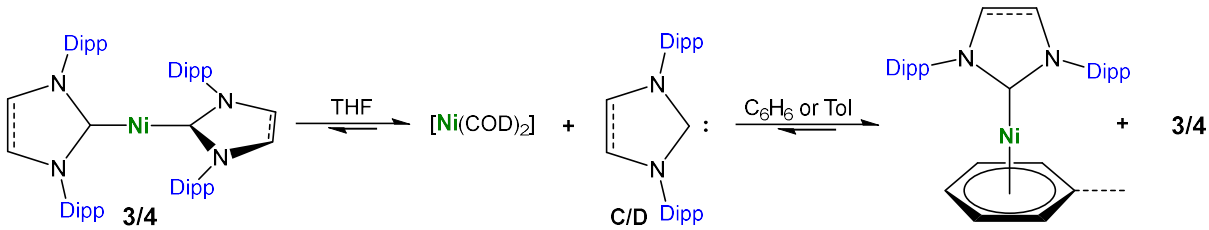

Scheme I.3 Equilibrium reaction between [Ni(η^4-COD)$_2$] and the *N*-Dipp substituted NHCs **C** or **D** in different solvents.[60,65,66]

Complex [Ni(cAAC^{Me})$_2$] **5** was first reported by the groups of Roesky and Ackermann and synthesized by treating anhydrous $NiCl_2$ with two equivalents of cAAC^{Me} **E** and subsequently reducing the obtained nickel(II)-complex [Ni(cAAC^{Me})$_2$Cl$_2$] with lithium di-*iso*-propylamide (LDA) or potassium graphite (KC_8).[67] More recently, Hillhouse *et al.* adopted a comparable reductive route to optimize the synthesis of complex **3**, by a ligand exchange starting from *trans*-[Ni(PPh$_3$)$_2$Cl$_2$].[60] Our group recently reported a general reductive method for the complexes **3-5**, using [NiBr$_2$•DME] and the carbenes **C-E** as starting materials and KC_8 for the reduction of the intermediate complexes *trans*-[Ni(NHC)$_2$Br$_2$] (compare Chapter IV).

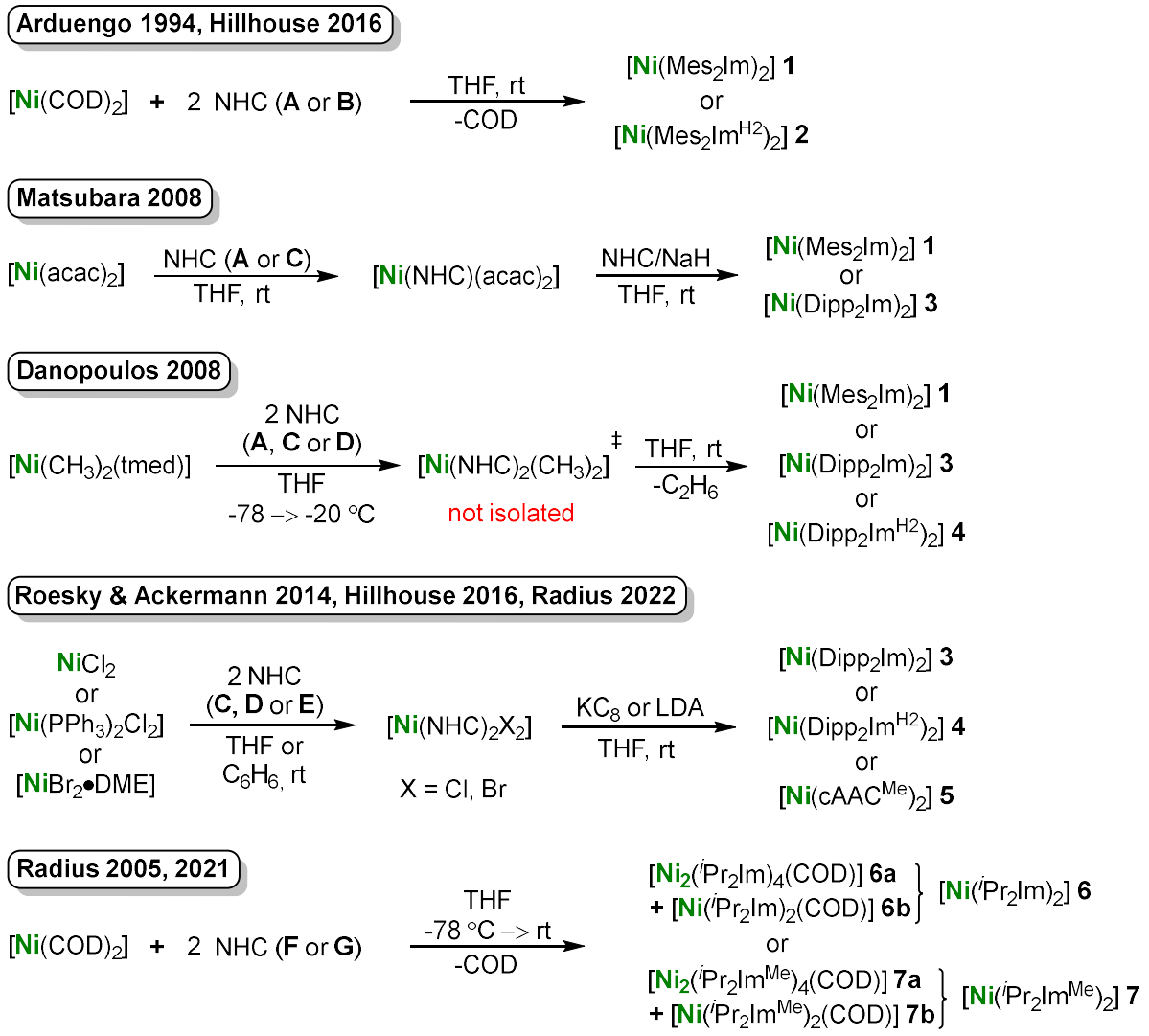

Scheme I.4 Different synthetic procedures for the complexes **1-7**.[15, 52, 60-68]

In 2005, our group first reported the synthesis of the dinuclear complex [Ni$_2$(^{i}Pr$_2$Im)$_4$(μ-(η^2:η^2)-COD)] **6a**, which is a synthon of [Ni(^{i}Pr$_2$Im)$_2$] **6**, *via* the reaction of [Ni(η^4-COD)$_2$] with two equivalents of the NHC ^{i}Pr$_2$Im **F**.[68] Later on it became clear that the reaction always affords small amounts of the mononuclear chelating complex [Ni(^{i}Pr$_2$Im)$_2$(η^4-COD)] **6b** as a by-product (up to 40 %) and that the reaction of [Ni(η^4-COD)$_2$] with the small alkyl substituted NHCs, ^{n}Pr$_2$Im (1,3-di-*n*-propylimidazolin-2-ylidene) or Me^{i}PrIm (1-methyl-3-*iso*-propylimidazolin-2-ylidene), affords similar complexes.[69] Lately, we also synthesized the complexes of the backbone-methylated NHC [Ni$_2$(^{i}Pr$_2$Im^{Me})$_4$(μ-(η^2:η^2)-COD)] **7a** in a mixture with [Ni(^{i}Pr$_2$Im^{Me})$_2$(η^4-COD)] **7b**,[52] which also act as synthons of [Ni(^{i}Pr$_2$Im^{Me})$_2$] **7** (see Scheme I.4 and the following chapters). The complexes **6a** and **7a** can be separated from **6b** and **7b** by crystallization. However, since the complexes **6/7a** and **6/7b** both typically react as

synthons of [Ni(^{i}Pr$_2$Im)$_2$] **6** and [Ni(^{i}Pr$_2$Im^{Me})$_2$] **7**, they were usually not separated for further transformations. The reaction of [Ni(η^4-COD)$_2$] with the smallest NHC Me$_2$Im (1,3-dimethylimidazolin-2-ylidene) interestingly leads to formation of the three-coordinated, trigonal-planar complex [Ni(Me$_2$Im)$_3$], instead of forming a COD-bridged dimer.[69]

The different NHC ligands **A-G** of the complexes **1-7**, of course, lead to different bonding situations between the nickel atom and the carbene, which then influence the electronic properties of the [Ni(NHC)$_2$]-moiety and its reactivity towards other substrates. While the *N*-aryl substituted NHCs **A-D** provide very good steric protection of the nickel atom, the *N*-alkyl substituted complexes **6** and **7** are sterically unsaturated and react readily with all kinds of substrates. Additionally the *N*-*iso*-propyl substituents of **6** and **7** lead to a more electron releasing [Ni(NHC)$_2$]-moiety compared to the *N*-Mes or *N*-Dipp substituted complexes **1-4**, due to better electron transfer from the NHC to the nickel. This effect is further strengthened by the smaller NHC-Ni-NHC bite-angle these smaller carbenes can adopt in the final products if [Ni(NHC)$_2$] is reacted, for example, with π-accepting substrates (see Chapters II and III).[52, 70]

1.5 Reactivity and Application of [Ni(NHC)$_2$] Complexes

Besides the widespread application of *in situ* generated NHC-nickel complexes in catalysis, the reactivity of the well-defined complexes **1-7** towards different substrates, such as olefins, alkynes, silanes, nitriles, phosphorus or sulfur compounds and alkyl- or aryl-halides have been studied by several groups during the last few years. Most of this fundamental work has been done on the complexes [Ni(Mes$_2$Im)$_2$] **1**, [Ni(Dipp$_2$Im)$_2$] **3** and [Ni(^{i}Pr$_2$Im)$_2$] **6** and the results of these studies are summarized and compared below.

The first important substrate class which must be mentioned here are simple olefins. Cavell *et al.* reported the reaction of [Ni(Mes$_2$Im)$_2$] **1** with dimethylfumarate (DMFU) in 2006, which leads to different bis- and mono-NHC complexes [Ni(Mes$_2$Im)$_2$(η^2-MeOOCC=CCOOMe)], [Ni(Mes$_2$Im)(η^2-MeOOCC=CCOOMe)$_2$], [{Ni(Mes$_2$Im)(η^2-MeOOCC=CCOOMe)}$_2$] and a NHC-olefin coupling product, depending on the amount of DMFU used.[71] Around the same time Walther and co-workers isolated the dimeric complex **8** from the reaction of **1** with four equivalents of 2,3-dimethylbutadiene under an atmosphere of pressurized CO_2 (see Scheme I.5).[72] This product resulted from the oxidative coupling of two dienes and subsequent insertion of CO_2. Again, one NHC dissociates from **1** forming the carboxylation product Mes$_2$Im-CO_2 as a side-product.[73] If **1** was reacted with CO_2 only, the dimeric complex [{Ni(Mes$_2$Im)}$_2$(μ-CO)(μ-η^2,η^2-CO_2)] was formed, as reported by Sadighi *et al.*[74]

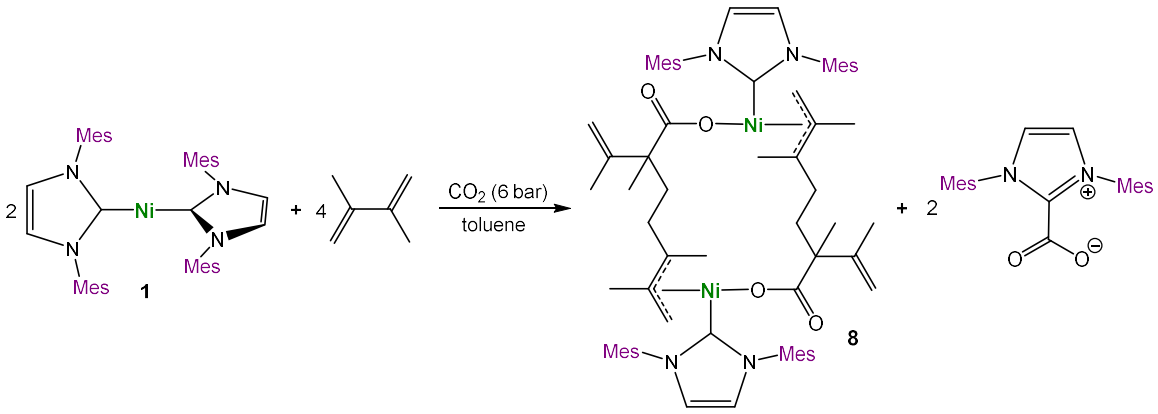

Scheme I.5 Reaction of [Ni(Mes$_2$Im)$_2$] **1** with 2,3-dimethylbutadiene and CO_2.[72]

The reaction of **1** with the unactivated alkene 1-hexene leads to an equilibrium between the starting materials and the *side-on* coordinated complex, [Ni(Mes$_2$Im)$_2$(η^2-H$_2$C=CH(C$_4$H$_9$))], as reported by Hillhouse *et al*.[60] This group further demonstrated that [Ni(Mes$_2$Im)$_2$] **1** catalyzes the cyclopropanation of olefins with diphenyldiazomethane with loss of N$_2$. In the last few years, [Ni(Dipp$_2$Im)$_2$] **3** has also been used as an effective catalyst for different catalytic transformations of alkenes, such as the reductive cyclo-isomerization of enynes with CO$_2$[75] or the diarylation of alkenes,[76] for example. In 2014, Hartwig *et al.* reported on the highly selective hydroarylation of unactivated terminal and internal olefins with trifluoromethyl-arenes, yielding linear products without the need of directing groups on the arene (see Scheme I.6).[77]

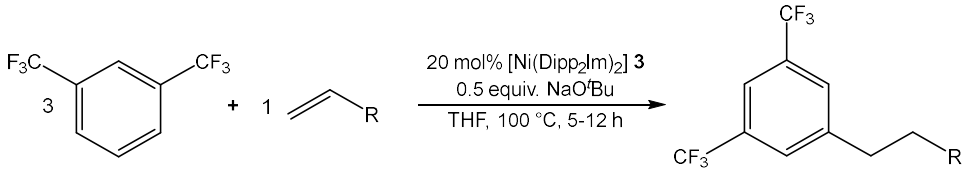

Scheme I.6 Catalytic hydroarylation of terminal alkenes using [Ni(Dipp$_2$Im)$_2$] **3**.[77]

All of these stoichiometric and catalytic reactions share a common characteristic that the olefin complexes bearing two of the bulky NHC ligands Mes$_2$Im **A** or Dipp$_2$Im **C** are labile and tend to extrude one of the NHC ligands to form mono-NHC nickel olefin complexes, however complexes bearing small or activated acceptor olefins behave differently (see Chapter II).[70] This is in contrast to the reactivity of complex **6**, studied by our group, which forms very stable bis-NHC olefin complexes such as [Ni(*i*Pr$_2$Im)$_2$(η^2-H$_2$C=CH$_2$)],[68] [Ni(*i*Pr$_2$Im)$_2$(η^2-Me$_2$C=CHCOMe)] and [Ni(*i*Pr$_2$Im)$_2$(η^2-H$_2$C=CH(4-C$_5$H$_4$N))].[78] Furthermore, complexes **1** and **6** also form *side-on* coordinated complexes of different stabilities with aldehydes and ketones, as discussed in detail in Chapter II.[70] Another good example to illustrate the difference in the reactivity between the complexes stabilized by the bulky NHCs (**1**, **2**, and **3**) and complex **6** stabilized by the smaller NHC *i*Pr$_2$Im **F**, is the reactivity towards diazoalkanes and azides. The complexes **1**, **2** and **3** react with diphenyldiazoalkane leading to *end-on* coordinated complexes of the type [Ni(NHC)$_2$(κ^1-N$_2$CPh$_2$)] (NHC = **A**, **B** and **C**),[60] while the same reaction of complex **6** yields the *side-on* complex [Ni(*i*Pr$_2$Im)$_2$(η^2-*N,N'*-N$_2$CPh$_2$)].[78] On the other hand, the reaction of **1** with 1-azidoadamantane led to the isolation of [Ni(Mes$_2$Im)$_2$(η^2-N$_3$Ad)].[60]

The groups of Louie[59e, 65, 79] and Montgomery[80] have published several catalytic transformations of alkynes, using [Ni(η^4-COD)$_2$] and the *N*-aryl substituted NHC ligands **A-D** over the past few years. Additionally, Louie *et al.* showed in a detailed study about the [Ni(Dipp$_2$Im)$_2$] **3** catalyzed cycloaddition of alkynes and nitriles to form pyridines, that the result of this particular reaction is highly dependent on the competitive binding of nitriles and alkynes to the nickel atom.[81] Influenced by the sterics of the NHC, the initial binding of the nitrile is superior to the coordination of alkynes to the [Ni(NHC)$_2$]-moiety in this special case, thus leading to the desired hetero-coupling pyridine products. The reactivity of [Ni(^{i}Pr$_2$Im)$_2$] **6** towards alkynes and nitriles was investigated by our group in recent years. We have previously shown that the reaction of **6** with a plethora of alkynes leads to stable *side-on* coordinated complexes of the type [Ni(^{i}Pr$_2$Im)$_2$(η^2-RC≡CR')], and that **6** effectively catalyzes the insertion of diphenylacetylene into the 2,2'-bond of biphenylene yielding diphenylphenantrene.[69] Furthermore, Chapter III of this thesis evaluates the reactivity of **1** and the backbone-methylated complex [Ni(^{i}Pr$_2$Im^{Me})$_2$] **7** with alkynes and provides a detailed comparison of the complexes **1**, **6** and **7**.[52] In 2007, our group reported the irreversible C$_\alpha$–CN activation of different organonitriles under thermal or photochemical conditions using complex **6** to afford the cyanide complexes *trans*-[Ni(^{i}Pr$_2$Im)$_2$(CN)(R)] *via* the η^2-coordinated intermediates [Ni(^{i}Pr$_2$Im)$_2$(η^2-N≡CR)] (see Scheme I.7).[82] For the reaction with adiponitrile, the C–C activation step was found to be very slow at room temperature and irradiation of the *side-on* coordinated intermediate led to decomposition to the bis-cyanido complex [Ni(^{i}Pr$_2$Im)$_2$(CN)$_2$]. In contrast to the reactivity towards nitriles, the reaction of [Ni(^{i}Pr$_2$Im)$_2$] **6** with *tert*-butyl-phosphaalkyne afforded the stable η^2-coordinated complex [Ni(^{i}Pr$_2$Im)$_2$(η^2-P≡C^{t}Bu)], which dimerizes upon heating to 100 °C to give the dinuclear compound [{Ni(^{i}Pr$_2$Im)$_2$}$_2$(η^2-η^2-2,4-^{t}Bu$_2$-1,3-diphosphacyclobutadiene)] (see Scheme I.7).[83]

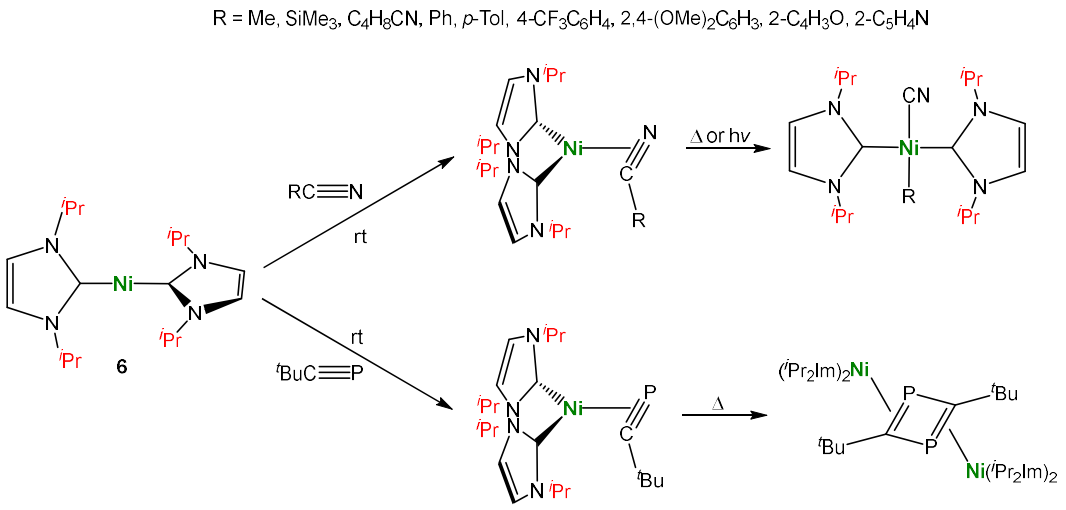

Scheme I.7 Reaction of [Ni(*i*Pr2Im)2] **6** with different organonitriles and *tert*-butyl-phosphaalkyne.[82-83]

In terms of the reactivity towards unsaturated substrates the reaction with carbon monoxide is of particular interest since the mono-NHC carbonyl-complexes [(NHC)Ni(CO)3] may be used to determine the TEP or %V_{bur} of NHC ligands, as mentioned above. While [(NHC)Ni(CO)3] complexes are typically synthesized from [Ni(CO)4] and one equivalent of the corresponding NHC,[35c, 63, 84] the reaction of [Ni(NHC)2] with CO leads to complexes with different numbers of NHC and CO ligands bound to the nickel, depending on the sterics of the carbene. Our group has demonstrated previously that the treatment of **6** with CO leads to formation of [Ni(*i*Pr2Im)2(CO)2] **9**.[68] If [Ni(CO)4] is reacted with the free carbene *i*Pr2Im **F**, complex **9** and the Chini-type cluster [Ni3(*i*Pr2Im)3(μ^2-CO)3(μ^3-CO)] **10** can be isolated, depending on the amount of NHC used (see Figure I.10). For the backbone-methylated carbene *i*Pr2Im^{Me} **G**, the complexes [Ni(*i*Pr2Im^{Me})2(CO)2] or [(*i*Pr2Im^{Me})Ni(CO)3] are derived from [Ni(CO)4].[84] The CO-reaction is also one of the rare well-understood reactions of the complex [Ni(cAAC^{Me})2] **5**, and leads to the tricarbonyl-complex [(cAAC^{Me})Ni(CO)3] **11**, as does the reaction between [Ni(CO)4] and free cAAC^{Me} **E**. Treatment of [(cAAC^{Me})Ni(CO)3] **11** with additional cAAC^{Me} **E** resulted in the formation of [Ni(cAAC^{Me})2(CO)] **12** (see Figure I.10).[48, 85] For the *N*-aryl substituted carbenes **A-D** the mono-NHC carbonyl complexes [(NHC)Ni(CO)3] are known from the [Ni(CO)4]-route,[35c] while the reactivity of **1-4** towards CO is not reported in the literature.

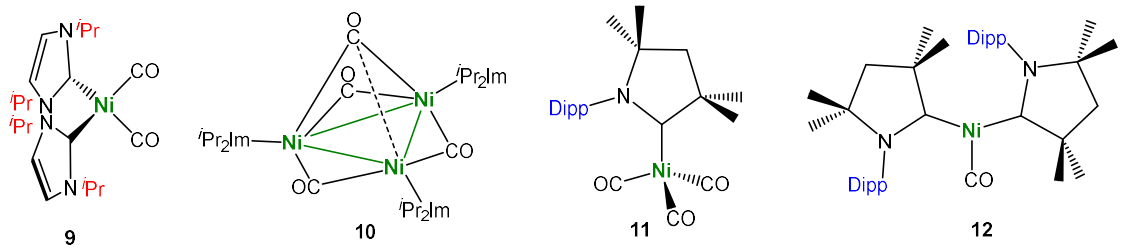

Figure I.10 Selected examples of NHC-stabilized nickel-carbonyl compounds.[48, 68, 85]

The [Ni(NHC)$_2$] complexes have proved to be promising reactants for the activation of different E–E bonds in recent years. Our group reported the Si–H activation of hydrosilanes mediated by [Ni(^{i}Pr$_2$Im)$_2$] **6**, leading to hydrido-silyl and bis-silyl nickel complexes of the general type *cis*-[Ni(^{i}Pr$_2$Im)$_2$(H)(SiH$_{n-1}$R$_{4-n}$)$_2$] (*n* = 1, 2) and *cis*-[Ni(^{i}Pr$_2$Im)$_2$(SiH$_{n-1}$R$_{4-n}$)$_2$].[86] These complexes exhibit remarkably short Si–H and Si–Si distances, caused by remaining Si–H and Si–Si interactions, which stabilize the rare *cis*-configuration. The only exceptions are the reactions with HSi(OEt)$_3$ and with Ph$_2$SiH$_2$ (at elevated temperatures) which yielded the *trans*-configurated complex *trans*-[Ni(^{i}Pr$_2$Im)$_2$(Si(OEt)$_3$)$_2$] or the dinuclear complex [{(^{i}Pr$_2$Im)Ni-μ-(HSiPh$_2$)}$_2$], respectively (see Scheme I.8).[86b] Furthermore, complex **6** is able to catalyze different Si–H functionalization reactions such as Si–H/D exchange, the dehydrogenative coupling of hydrosilanes or the hydrogenation of disilanes to hydrosilanes. In collaboration with Wittlesey *et al.* we recently published comparable P–H and P–P activation products, *trans*-[Ni(NHC)$_2$(H)(PR$_2$)] and *trans*-[Ni(NHC)$_2$(PR$_2$)$_2$], stabilized by different small *N*-alkyl substituted NHCs (^{i}Pr$_2$Im **F**, Me$_2$Im^{Me} and Et$_2$Im^{Me}).[87] In contrast to the activation of silanes, the oxidative addition products formed with phosphines or diphosphines exclusively adopt the *trans*-configuration. Interestingly, we found that complex [Ni(^{i}Pr$_2$Im)$_2$] **6** reacts with an excess of PPhH$_2$ or P(*p*-Tol)H$_2$ at elevated temperatures *via* an unusual dehydrocoupling of the primary phosphines to afford the *side-on* coordinated diphosphene complexes [Ni(^{i}Pr$_2$Im)$_2$(η^2-ArP=PAr)] (Ar = Ph, *p*-Tol). This reaction pathway is suppressed when more sterically demanding phosphines like PMesH$_2$ are applied. Furthermore, the *trans*-[Ni(NHC)$_2$(H)(PR$_2$)] and *trans*-[Ni(NHC)$_2$(PR$_2$)$_2$] complexes are remarkably stable towards NHC dissociation and dimerization reactions.

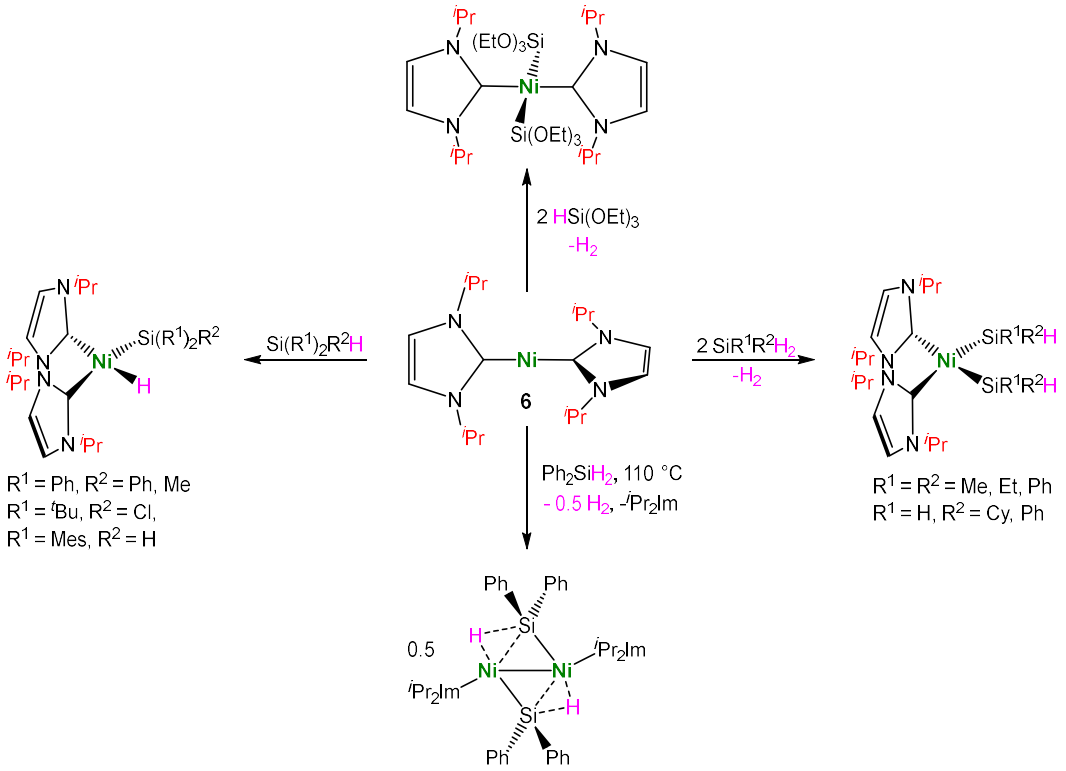

Scheme I.8 Si–H activation of different hydrosilanes using [Ni(*i*Pr2Im)2] **6**.[86]

Other phosphorus containing compounds were also successfully activated by [Ni(NHC)2] complexes. Wolf and co-workers reported different nickel-phosphorus cluster compounds obtained from the activation of white phosphorus (P_4) mediated by [Ni(Mes2Im)2] **1** or [Ni(Dipp2Im)2] **3** (see Figure I.11).[88] The reaction of **1** with P_4 in toluene led to the formation of the trinuclear cluster [(Mes2Im)3Ni3P4] **13**. Changing the solvent to THF decreases the selectivity and affords two additional clusters [(Mes2Im)3Ni3P6] **14** and [(Mes2Im)2Ni2P5] **15**. The same reaction with [Ni(Dipp2Im)2] **3** afforded the octahedral cluster [(Dipp2Im)3Ni3P8] **16**. In contrast to the *N*-aryl substituted complexes, [Ni(*i*Pr2Im)2] **6** reacts without extrusion of a NHC ligand, but instead by degradation of P_4 to yield the butterfly-shaped compound [{Ni(*i*Pr2Im)2}2($\mu,\eta^{2:2}$-P2)] **17**.[89]

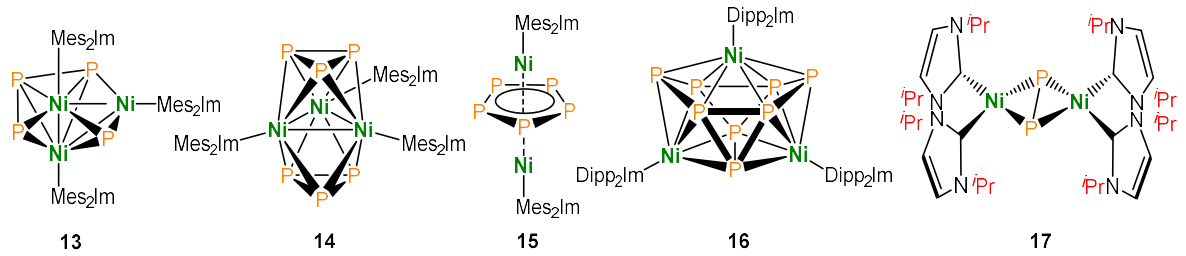

Figure I.11 Mixed Ni-P cluster compounds from the activation of P_4 with **1**, **3** or **6**.[88-89]

Recently, Wolf *et al.* also published the activation of di-*tert*-butyldiphosphatetrahedrane with [Ni(Mes2Im)2] **1** leading to the dinuclear cluster [{(Mes2Im)Ni}2(tBu4C4P4)] which then reacts under elimination of di-*tert*-butylacetylene to form the compound [(Mes2ImNi)2(P2)-(tBu2C2P2)].[90]

In 2011 Hartwig *et al.* reported the difficult to achieve catalytic hydrogenolysis of diaryl ethers, mediated by an *in situ* generated nickel complex stabilized by Dipp2ImH2 **D**.[91] Later, the well-defined complex [Ni(Dipp2ImH2)2] **4** was found to exhibit excellent catalytic activity in this reaction,[92] although the catalytically active species is a mono-NHC nickel complex formed after ligand dissociation in an aromatic solvent (compare Scheme I.3), as already reported by the groups of Surawatanawong[93] and Chung[94] by means of theoretical DFT-calculations.

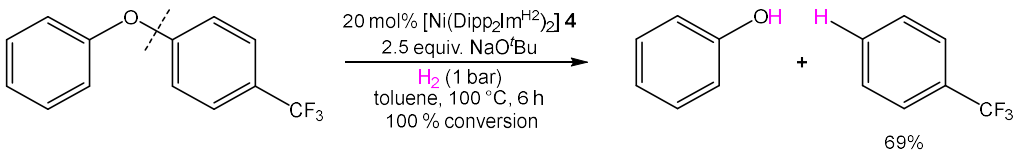

Scheme I.9 Catalytic hydrogenolysis of diaryl ethers using [Ni(Dipp2ImH2)2] **4** as catalyst.[92]

Our group has previously shown that the sterically less bulky complex [Ni(iPr2Im)2] **6** is able to cleave the C–S, S–S and S–H bonds of thioethers, sulfoxides, disulfides and thiols effectively, leading to complexes of the general type *trans*-[Ni(iPr2Im)2(R)(SR')], *trans*-[Ni(iPr2Im)2(R)(SOR')], *trans*-[Ni(iPr2Im)2(SR)2] and *trans*-[Ni(iPr2Im)2(H)(SR)].[95] If the cyclic thioethers benzothiophene or dibenzothiophene were applied, insertion of [Ni(iPr2Im)2] **6** into the C–S bond occurred to yield the *cis*-configurated compounds *cis*-[Ni(iPr2Im)2(1,8-benzothiophenylato)] and *cis*-[Ni(iPr2Im)2(*C,S*-dibenzothiophenylato)]. The C–S bonds of sulfoxides are readily activated to give complexes of the type

trans-[Ni(*i*Pr$_2$Im)$_2$(R)(*S*OR')] or *trans*-[Ni(*i*Pr$_2$Im)$_2$(R)(*O*SR)], in the case of diphenylsulfoxide. This C–S activation reaction has been exploited recently for the nickel-catalyzed borylation of aryl sulfoxides.[96] The reaction with the sulfur(VI) containing sulfones, benzothiophene-1,1-dioxide and methylphenylsulfone, did not afford C–S activation, but instead led to *side-on* coordinated complexes [Ni(*i*Pr$_2$Im)$_2$(η^2-2,3-benzothiophene-1,1-dioxide)] and [Ni(*i*Pr$_2$Im)$_2$(η^2-MeSO$_2$C$_6$H$_5$)]. In contrast to **6**, Jones *et al.* reported that [Ni(Mes$_2$Im)$_2$] **1** reacts with dimethyldisulfide to yield the trinuclear methylthiolate-bridged complex [{(Mes$_2$Im)(MeS)Ni(μ-SMe)$_2$}$_2$Ni] and the NHC-sulfur adduct Mes$_2$Im=S (see Scheme I.10).[97]

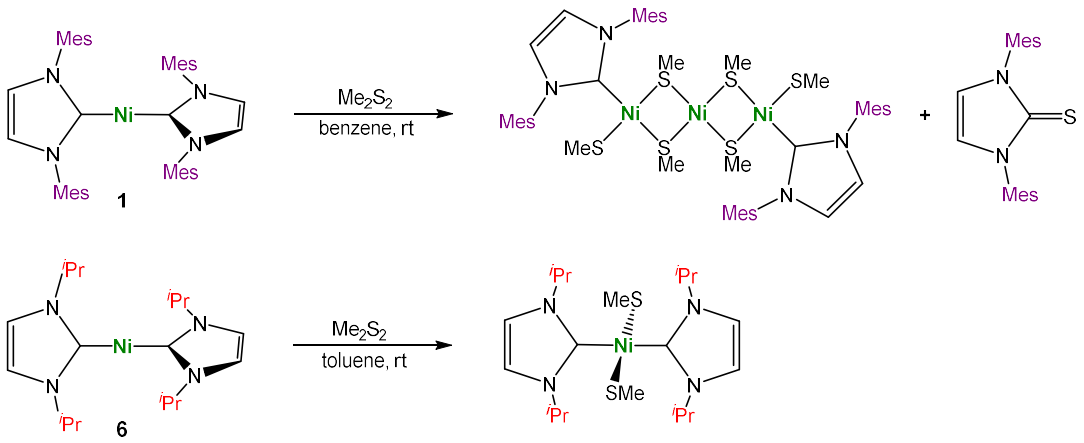

Scheme I.10 Different reactivities of [Ni(Mes$_2$Im)$_2$] **1** and [Ni(*i*Pr$_2$Im)$_2$] **6** towards dimethyl disulfide.[95, 97]

The use of [Ni(NHC)$_2$] complexes in stoichiometric and catalytic C–H and C–X (X = F, Cl, Br, I) bond activation reactions has been studied extensively. Such reactions are of high importance for a variety of catalytic transformations, as they enable the formation of complex molecules from simple, commercially available precursors. The cleavage of C–F bonds of fluoroorganics is an especially challenging task, due to the high stability of such bonds.[98] In 2005, our group first reported the stoichiometric C–F activation of hexafluorobenzene mediated by [Ni(*i*Pr$_2$Im)$_2$] **6** leading to the nickel(II) complex *trans*-[Ni(*i*Pr$_2$Im)$_2$(F)(C$_6$F$_5$)] **18**.[68] In the following years, different square-planar pentafluorophenyl-nickel(II) complexes were synthesized *via* derivatization of the fluorido ligand of complex **18** (see Scheme I.11).[99] Mechanistic studies on the C–F activation of hexafluorobenzene and octafluoronaphthalene revealed that the oxidative addition of the C–F bond proceeds *via* a concerted mechanism including a

η^2-coordinated intermediate. The corresponding octafluoronaphthalene intermediate-complex *trans*-[Ni(^{i}Pr$_2$Im)$_2$(η^2-C$_{10}$F$_8$)] has been isolated and structurally characterized.[100]

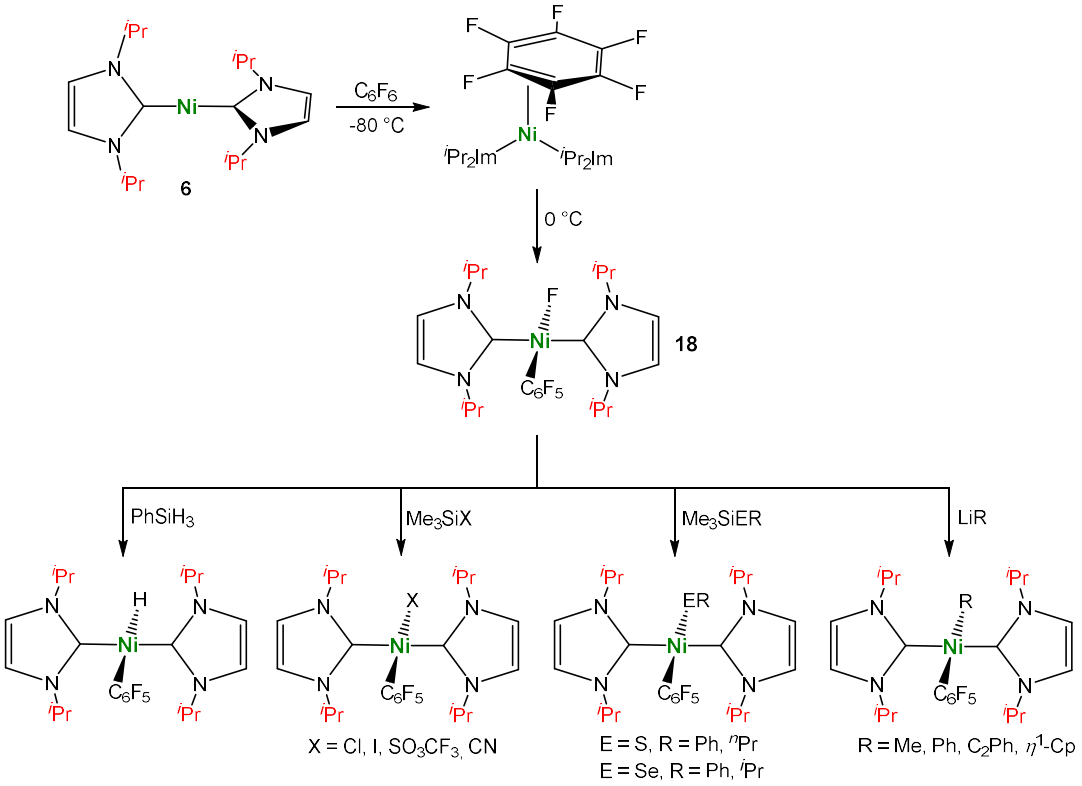

Scheme I.11 Synthesis of *trans*-[Ni(^{i}Pr$_2$Im)$_2$(F)(C$_6$F$_5$)] **18** and consecutive exchange reactions of the fluorido ligand.[68, 99]

Furthermore, we found that complex **6** readily activates the C–F bonds of many different polyfluoroarenes to form *trans*-configurated nickel-fluorido complexes of the general type *trans*-[Ni(^{i}Pr$_2$Im)$_2$(F)(Ar^F)].[100-101] It is also able to catalyze the Suzuki-Miyaura cross-coupling reaction between polyfluoroarenes and aryl boronic acids,[102] as well as the hydrodefluorination of polyfluoroarenes using hydrosilanes as hydride source (see Scheme I.12).[103] The groups of Ohashi and Ogoshi [104] and our group[105] independently reported the Suzuki-Miyaura cross-coupling of fluoroarenes with different aryl boronate esters using complex **6** as catalyst.

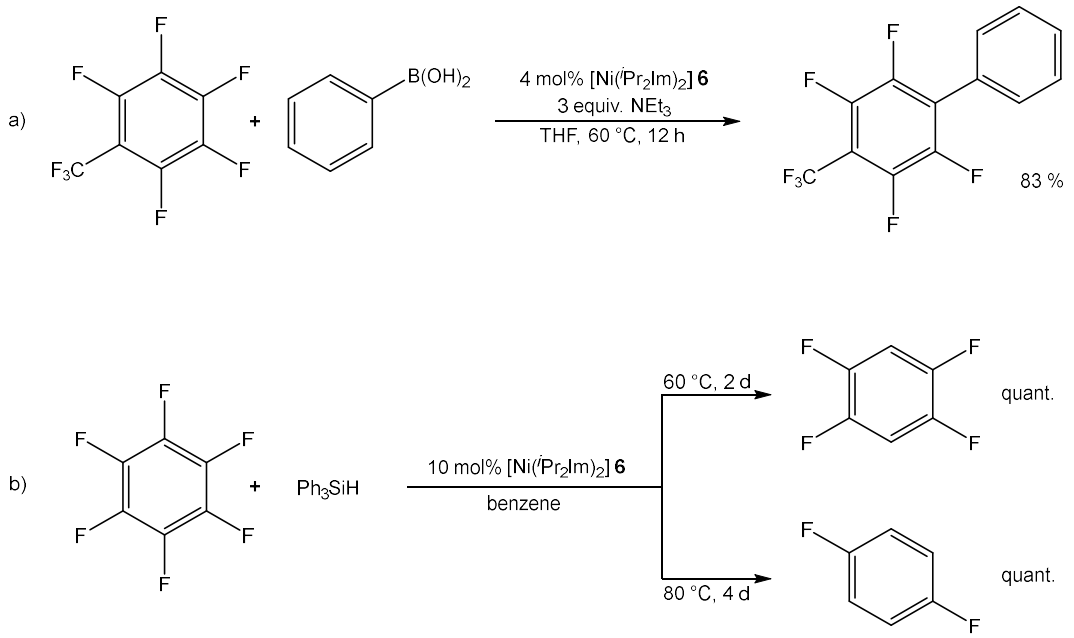

Scheme I.12 Suzuki-Miyaura cross-coupling (a) and hydrodefluorination (b) of polyfluoroarenes catalyzed by [Ni(^{i}Pr$_2$Im)$_2$] **6**.[102-103]

In addition, Ohashi and Ogoshi demonstrated that [Ni(^{i}Pr$_2$Im)$_2$] **6** can be used for the base-free Hiyama cross-coupling between perfluoroarenes and organosilicates of the type ArSi(OMe)$_3$.[106] This finding was later confirmed by our group, however it was also found that the reaction leads to an alkoxy transfer to the fluoroarene in the presence of a base, instead of forming the desired C–C coupling product.[107] We also tried to use complex **6** as catalyst for Negishi cross-couplings between perfluoroarenes and diorganozinc reagents, which was unsuccessful due to the thermal stability of the resulting nickel alkyl complexes *trans*-[Ni(^{i}Pr$_2$Im)$_2$(R)(Ar^F)] (R = Me, Et). These complexes do not undergo reductive elimination at temperatures below 100 °C and on a timescale suitable for catalysis.[107] Just recently, Ogoshi *et al.* reported that complex **6** is also able to activate C(sp^3)–F bonds of neat trifluoromethylarenes at elevated temperatures.[108] In this case, the oxidative addition also proceeds *via* an η^2-coordinated intermediate,[109] which can be isolated at room temperature. Furthermore, the complete hydrodefluorination of the trifluoromethylarenes was achieved using Me$_2$PhSiH, CsF as an additive and catalytic amounts of [Ni(^{i}Pr$_2$Im)$_2$] **6** (see Scheme I.13).

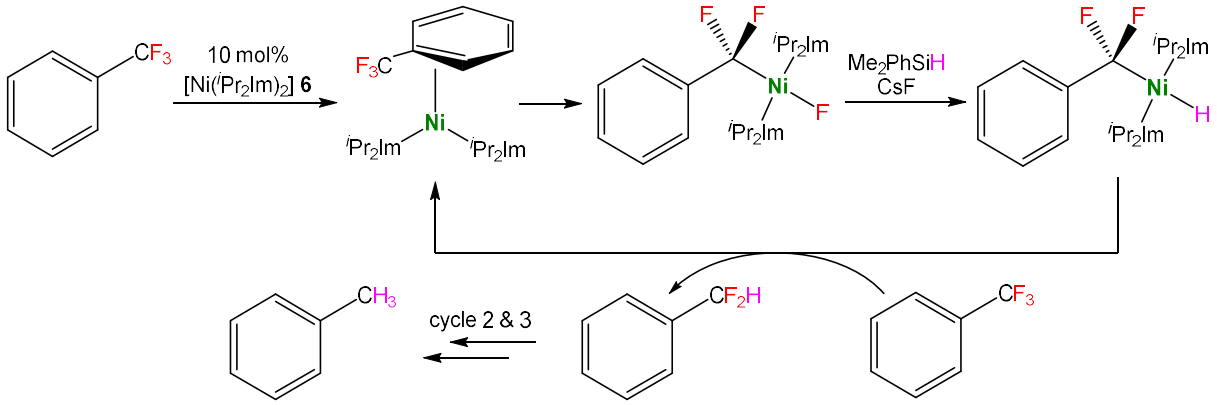

Scheme I.13 C–F activation and hydrodefluorination of trifluoromethylarenes catalyzed by [Ni(^{i}Pr$_2$Im)$_2$] **6**.[108]

Whilst the studies on the Suzuki-Miyaura cross-coupling of polyfluoroarenes with [Ni(^{i}Pr$_2$Im)$_2$] **6** were ongoing, we demonstrated that the sterically more encumbered complex [Ni(Mes$_2$Im)$_2$] **1** effectively catalyzes the thermally induced borylation of polyfluoroarenes *via* C–F bond activation, using B$_2$pin$_2$ (= bis(pinacolato)diboron) as a boron source and NMe$_4$F or CsF as an additive.[110] Later on, it was also possible to accomplish this C–F borylation under photocatalytic conditions at room temperature, by applying a tandem catalyst system containing [Ni(Mes$_2$Im)$_2$] **1** and a rhodium biphenyl complex, which acts as a triplet sensitizer (compare Scheme I.14).[111]

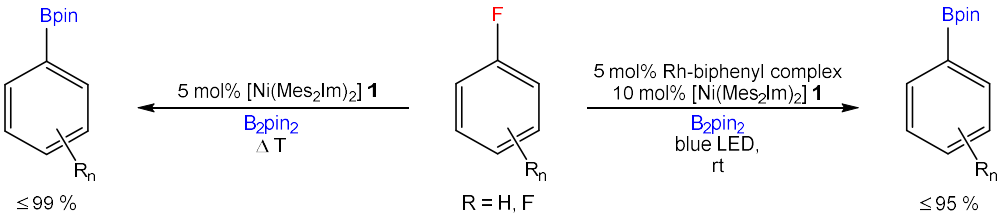

Scheme I.14 Borylation of polyfluoroarenes catalyzed by [Ni(Mes$_2$Im)$_2$] **1**.[110-111]

In 2020, our group presented a detailed study on the role of the different NHCs Mes$_2$Im **A** and ^{i}Pr$_2$Im **F** in the [Ni(NHC)$_2$] catalyzed C–F bond activation of hexafluorobenzene.[112] Both, [Ni(Mes$_2$Im)$_2$] **1** and [Ni(^{i}Pr$_2$Im)$_2$] **6**, cleave the C–F bonds of polyfluoroarenes to yield complexes of the type *trans*-[Ni(Mes$_2$Im)$_2$(F)(Ar^F)] and *trans*-[Ni(^{i}Pr$_2$Im)$_2$(F)(Ar^F)], respectively. For the reaction of **1** with C$_6$F$_6$ different reaction products were obtained. Beside *trans*-[Ni(Mes$_2$Im)$_2$(F)(C$_6$F$_5$)] **19**, also

trans-[Ni(Mes$_2$Im)$_2$F$_2$] **20**, *trans*-[Ni(Mes$_2$Im)$_2$(C$_6$F$_5$)$_2$] **21**, [Ni^{I}(Mes$_2$Im)$_2$(F)] **22** and [Ni^{I}(Mes$_2$Im)$_2$(C$_6$F$_5$)] **23** were detected (see Scheme I.15).

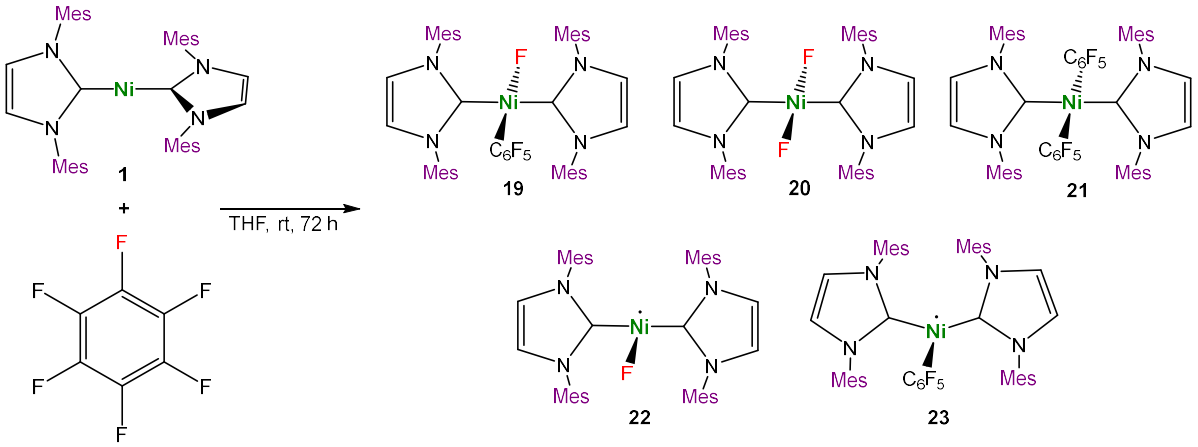

Scheme I.15 Stoichometric reaction of [Ni(Mes$_2$Im)$_2$] **1** with hexafluorobenzene.[112]

The experimental and theoretical investigations revealed that the mechanisms of the C–F activation steps are very different, depending on the NHC co-ligand used. While for the complex **6** of the small NHC a concerted reaction mechanism is favored (*vide supra*), the sterically more demanding complex **1** prefers a radical pathway with fluorine abstraction as the key reaction step. However, an additional NHC-assisted mechanism was found as a competitive pathway for both complexes. These findings are consistent with the calculations reported by Nelson and Maseras, who showed previously in a theoretical study that the reactions of [Ni(NHC)$_2$] with arylhalides Ph–X (X = Cl, Br, I) either lead to oxidative addition products *trans*-[Ni(NHC)$_2$(X)(Ph)] if small NHCs are used or to halide abstraction to form nickel(I) complexes [Ni^{I}(NHC)$_2$(X)] if larger NHCs are used.[113] The barely investigated complex [Ni(cAAC^{Me})$_2$] **5** has been successfully used for the homocoupling of mono-fluoro arenes and mono-chloro arenes in the past. Theoretical investigations concerning the mechanism indicated the involvement of different nickel species with oxidation states of 0, I, II and III.[67] Matsubara *et al.* already demonstrated in 2010 experimentally that the reaction of [Ni(Dipp$_2$Im)$_2$] **3** with aryl chlorides leads to the formation of the three-coordinate nickel(I) complex [Ni^{I}(Dipp$_2$Im)$_2$Cl] and the homocoupling product of the corresponding arene.[114] The resulting nickel(I) complex [Ni^{I}(Dipp$_2$Im)$_2$Cl] was further used as catalyst for Kumada cross-coupling reactions between aryl bromides and phenylmagnesium chloride. One year later, Louie and co-workers showed that the Mes$_2$Im **A** substituted complexes

[Ni^{I}(Mes$_2$Im)$_2$X] (X = Cl, Br, I) are also accessible *via* similar reactions of [Ni(Mes$_2$Im)$_2$] **1** with the corresponding phenyl halide (see Scheme I.16) and that these complexes are also highly active catalysts for Kumada- and Suzuki-Miyaura cross-couplings.[115] Stoichometric control reactions indicated a decisive role of the nickel(I) radical in the catalytic cycle. Simultaneously, Nocera *et al.* reported that [Ni(Mes$_2$Im)$_2$] **1** reacts with 2,6-lutidine•HX (X = Cl, Br) *via* oxidative addition to yield the nickel(II) complexes *trans*-[Ni(Mes$_2$Im)$_2$(H)(X)]. Upon irradiation, these complexes react with H_2 elimination leading to the same nickel(I) complexes [Ni^{I}(Mes$_2$Im)$_2$X] (X = Cl, Br) (see Scheme I.16).

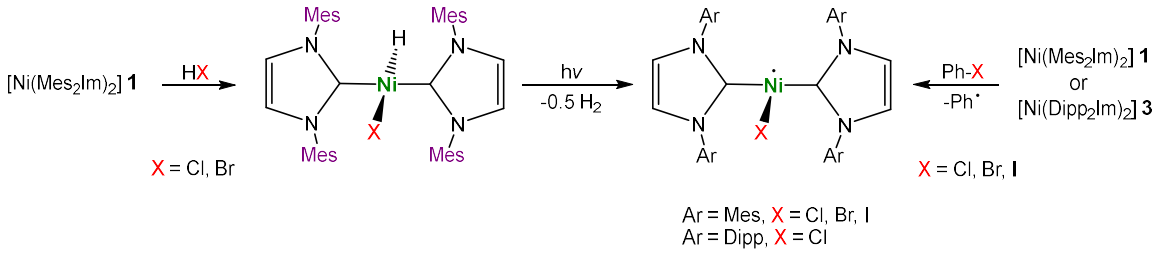

Scheme I.16 Synthesis of three-coordinate nickel(I) halide complexes [Ni^{I}(NHC)$_2$X].[113-115]

In cooperation with the Marder group we recently demonstrated that [Ni(Mes$_2$Im)$_2$] **1** effectively catalyzes the visible-light-induced (400 nm) borylation of aryl chlorides at room temperature, whereby [Ni^{I}(Mes$_2$Im)$_2$Cl] and [Ni(Mes$_2$Im)$_2$Cl$_2$] are important intermediates of the catalytic cycle (see Scheme I.17).[116] As reported previously, the same catalytic reaction can also be performed under thermal conditions in a classical two-electron Ni(0)/Ni(II)-process if synthons of the Cy$_2$Im (1,3-dicyclohexylimidazolin-2-ylidene) substituted nickel(0) complex [Ni(Cy$_2$Im)$_2$] are used as catalyst.[117]

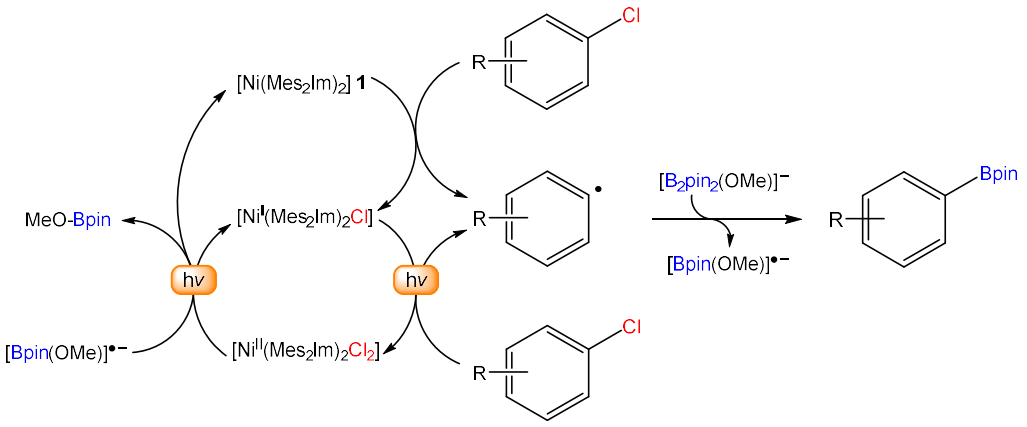

Scheme I.17 Proposed mechanism of the visible-light induced borylation of chloroarenes using [Ni(Mes$_2$Im)$_2$] **1** as catalyst.[116]

In contrast to the complexes [Ni(Mes$_2$Im)$_2$] **1**, [Ni(Dipp$_2$Im)$_2$] **3** and [Ni(cAAC^{Me})$_2$] **5**, which clearly prefer to undergo one-electron processes with aryl chlorides and aryl bromides to yield three-coordinate nickel(I) radicals, the sterically less demanding complex [Ni(^{i}Pr$_2$Im)$_2$] **6** favors classical two-electron oxidative addition reactions with those substrates, akin to what was observed for the fluoroarenes (*vide supra*). We have shown previously that [Ni(^{i}Pr$_2$Im)$_2$] **6** cleanly reacts with aryl chlorides,[118] aryl bromides,[119] benzyl chloride and benzyl bromide[120] to form square-planar C–X (X = Cl, Br) activation products of the type *trans*-[Ni(^{i}Pr$_2$Im)$_2$(X)(Ar)] or *trans*-[Ni(^{i}Pr$_2$Im)$_2$(X)(CH$_2$Ph)], respectively. However, the reaction with aryl bromides only leads to the aryl bromide complexes selectively if the reaction is performed at -78 °C in high dilution. At room temperature, a mixture of *trans*-[Ni(^{i}Pr$_2$Im)$_2$(Br)(Ar)], *trans*-[Ni(^{i}Pr$_2$Im)$_2$Br$_2$] and *trans*-[Ni(^{i}Pr$_2$Im)$_2$(Ar)$_2$] was observed. With a large excess of aryl bromide and using elevated temperatures, i.e. catalytic conditions, the complex *trans*-[Ni(^{i}Pr$_2$Im)$_2$(Br)(Ar)] decomposes, resulting in the final formation of 2[^{i}Pr$_2$Im-Ar]$^+$[NiBr$_4$]$^{2-}$ (see Scheme I.18).[119]

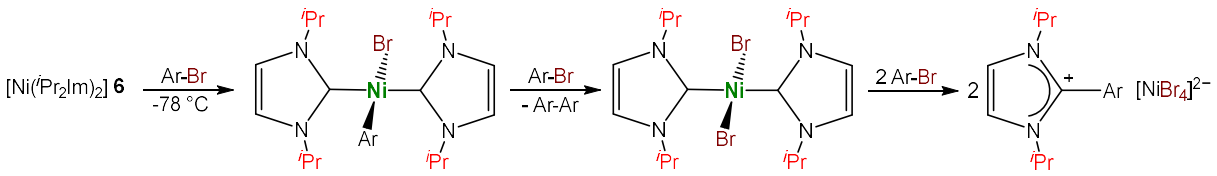

Scheme I.18 Reaction of [Ni(^{i}Pr$_2$Im)$_2$] **6** with aryl bromides.[119]

Nevertheless, [Ni(^{i}Pr$_2$Im)$_2$] **6** turned out to be an excellent catalyst for the Suzuki-Miyaura cross-coupling of aryl chlorides, aryl bromides and benzyl chlorides, provided enough boronic acid is present to avoid catalyst deactivation.[118-120] Furthermore, complex **6** is also able to activate the C–X bond of aroyl halides yielding complexes of the type *trans*-[Ni(^{i}Pr$_2$Im)$_2$(X)(*C*(O)-Ar)].[121] Upon irradiation, these complexes react *via* a decarbonylation to a mixture of the corresponding di-halide, aryl halide and bis-aryl complexes.

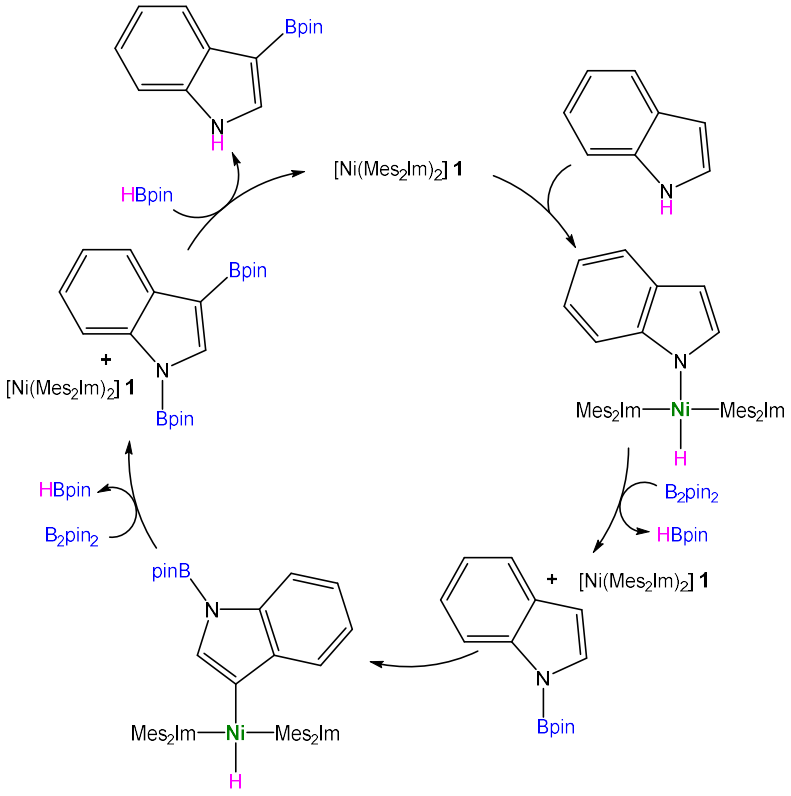

Scheme I.19 Proposed mechanism of the traceless, C3-selective C–H borylation of indoles using [Ni(Mes$_2$Im)$_2$] **1** as catalyst.[122]

Just recently the Radius and the Marder group published a C3-selective C–H borylation of indoles, again using the sterically bulky complex [Ni(Mes$_2$Im)$_2$] **1** as catalyst.[122] Interestingly, in contrast to the C–X borylations described above, no radical species were observed in this case. Instead, complex **1** reacts with indoles *via* an oxidative addition of the N–H bond in the first step leading to nickel(II) complexes of the type *trans*-[Ni(Mes$_2$Im)$_2$(H)(*N*-indolyl)]. Reaction with B$_2$pin$_2$ and reductive elimination of the resulting *N*-borylated indole regenerates complex **1**. In the second step, the *N*-

borylated indole reacts with **1** *via* a selective C–H activation at the 3-position. A second borylation with B_2pin_2 gives the bis-borylated 1,3-(Bpin)$_2$-indole, which finally undergoes auto removal of the C3-directing N–Bpin group with *in situ* generated HBpin to yield the desired 3-Bpin-indole (compare Scheme I.19).

As these studies demonstrate, the [Ni(NHC)$_2$] scaffold shows a versatile range of reactivity towards different substrates, depending on the electronic and steric nature of the NHC ligands used. The chemical behavior of the complexes can be easily tuned by adjusting the properties of the NHCs, allowing numerous applications of these complexes in different catalytic transformations. The following chapters of this thesis provide a deeper insight into the reactivity of the complexes **1-7** and some of the differences encountered are explored in some detail. In the first two chapters, the reactivity of [Ni(Mes$_2$Im)$_2$] **1**, [Ni(^{i}Pr$_2$Im)$_2$] **6** and [Ni(^{i}Pr$_2$Im^{Me})$_2$] **7** towards unsaturated substrates like olefins, alkynes, aldehydes and ketones is reported. Then the one-electron redox behavior of the complexes [Ni(Mes$_2$Im)$_2$] **1**, [Ni(Mes$_2$Im^{H2})$_2$] **2**, [Ni(Dipp$_2$Im)$_2$] **3**, [Ni(Dipp$_2$Im^{H2})$_2$] **4** and [Ni(cAAC^{Me})$_2$] **5** as well as the synthesis of rare linear nickel(I) metalloradicals is examined in detail, including their magnetic properties. In the last part, the synthesis and characterization of the first NHC-stabilized nickel-boryl complexes is presented as well as first investigations concerning the catalytic borylation of alkynes mediated by NHC-nickel complexes.

1.6 References

[1] A. J. Arduengo, R. L. Harlow, M. Kline, *J. Am. Chem. Soc.* **1991**, *113*, 361-363.

[2] a) W. A. Herrmann, C. Köcher, *Angew. Chem.* **1997**, *109*, 2256-2282; *Angew. Chem. Int. Ed.* **1997**, *36*, 2162-2187; b) D. Bourissou, O. Guerret, F. P. Gabbaï, G. Bertrand, *Chem. Rev.* **2000**, *100*, 39-92; c) S. Nolan, *N-Heterocyclic Carbenes in Synthesis*, Wiley-VCH, Weinheim, Germany, **2006**; d) F. E. Hahn, M. C. Jahnke, *Angew. Chem.* **2008**, *120*, 3166-3216; *Angew. Chem. Int. Ed.* **2008**, *47*, 3122-3172; e) T. Dröge, F. Glorius, *Angew. Chem.* **2010**, *122*, 7049-7107; *Angew. Chem. Int. Ed.* **2010**, *49*, 6940-6952; f) W. Kirmse, *Angew. Chem.* **2010**, *122*, 8980-8983; *Angew. Chem. Int. Ed.* **2010**, *49*, 8798-8801; g) L. Benhamou, E. Chardon, G. Lavigne, S. Bellemin-Laponnaz, V. César, *Chem. Rev.* **2011**, *111*, 2705-2733; h) M. N. Hopkinson, C. Richter, M. Schedler, F. Glorius, *Nature* **2014**, *510*, 485-496; i) E. Peris, *Chem. Rev.* **2018**, *118*, 9988-10031; j) F. Nahra, D. J. Nelson, S. P. Nolan, *Trends Chem.* **2020**, *2*, 1096-1113.

[3] a) O. Schuster, L. Yang, H. G. Raubenheimer, M. Albrecht, *Chem. Rev.* **2009**, *109*, 3445-3478; b) M. Melaimi, M. Soleilhavoup, G. Bertrand, *Angew. Chem.* **2010**, *122*, 8992-9032; *Angew. Chem. Int. Ed.* **2010**, *49*, 8810-8849; c) M. Asay, C. Jones, M. Driess, *Chem. Rev.* **2011**, *111*, 354-396; d) J. P. Moerdyk, D. Schilter, C. W. Bielawski, *Acc. Chem. Res.* **2016**, *49*, 1458-1468; e) M. Melaimi, R. Jazzar, M. Soleilhavoup, G. Bertrand, *Angew. Chem.* **2017**, *129*, 10180-10203; *Angew. Chem. Int. Ed.* **2017**, *56*, 10046-10068; f) U. S. D. Paul, U. Radius, *Eur. J. Inorg. Chem.* **2017**, 3362-3375; g) Á. Vivancos, C. Segarra, M. Albrecht, *Chem. Rev.* **2018**, *118*, 9493-9586; h) S. C. Sau, P. K. Hota, S. K. Mandal, M. Soleilhavoup, G. Bertrand, *Chem. Soc. Rev.* **2020**, *49*, 1233-1252.

[4] a) P. P. Power, *Nature* **2010**, *463*, 171-177; b) D. Martin, M. Soleilhavoup, G. Bertrand, *Chem. Sci.* **2011**, *2*, 389-399; c) Y. Wang, G. H. Robinson, *Dalton Trans.* **2012**, *41*, 337-345; d) C. D. Martin, M. Soleilhavoup, G. Bertrand, *Chem. Sci.* **2013**, *4*, 3020-3030; e) Y. Wang, G. H. Robinson, *Inorg. Chem.* **2014**, *53*, 11815-11832; f) V. Nesterov, D. Reiter, P. Bag, P. Frisch, R. Holzner, A. Porzelt, S. Inoue, *Chem. Rev.* **2018**, *118*, 9678-9842; g) Y. Kim, E. Lee, *Chem. Eur. J.* **2018**, *24*, 19110-19121; h) A. Doddi, M. Peters, M. Tamm, *Chem. Rev.* **2019**, *119*, 6994-7112; i) S. Kundu, S. Sinhababu, V. Chandrasekhar, H. W. Roesky, *Chem. Sci.* **2019**, *10*, 4727-4741.

[5] a) P. de Frémont, N. Marion, S. P. Nolan, *Coord. Chem. Rev.* **2009**, *253*, 862-892; b) S. P. Nolan, *N-Heterocyclic Carbenes: Effective Tools for Organometallic Synthesis*, Wiley-VCH, Weinheim, Germany, **2014**; c) K. Riener, S. Haslinger, A. Raba, M. P. Högerl, M. Cokoja, W. A. Herrmann, F. E. Kühn, *Chem. Rev.* **2014**, *114*, 5215-5272; d) D. Zhang, G. Zi, *Chem. Soc. Rev.* **2015**, *44*, 1898-1921; e) J. Cheng, L. Wang, P. Wang, L. Deng, *Chem. Rev.* **2018**, *118*, 9930-9987; f) A. A. Danopoulos, T. Simler, P. Braunstein, *Chem. Rev.* **2019**, *119*, 3730-3961; g) C. Romain, S. Bellemin-Laponnaz, S. Dagorne, *Coord. Chem. Rev.* **2020**, *422*, 213411; h) N. M. Scott, S. P. Nolan, *Eur. J. Inorg. Chem.* **2005**, 1815-1828.

[6] a) F. Glorius, *N-Heterocyclic Carbenes in Transition Metal Catalysis, Vol. 21*, Springer Berlin, Heidelberg, **2007**; b) W. A. Herrmann, *Angew. Chem.* **2002**, *114*, 1342-1363; *Angew. Chem. Int. Ed.* **2002**, *41*, 1290-1309; c) S. Díez-González, *N-Heterocyclic Carbenes: From Laboratory Curiosities to Efficient Synthetic Tools*, Royal Society of Chemistry, Cambridge, **2010**; d) S. Diez-Gonzalez, N. Marion, S. P. Nolan, *Chem. Rev.* **2009**, *109*, 3612-3676; e) D. Janssen-Müller, C. Schlepphorst, F. Glorius, *Chem. Soc. Rev.* **2017**, *46*, 4845-4854.

[7] a) D. Enders, O. Niemeier, A. Henseler, *Chem. Rev.* **2007**, *107*, 5606-5655; b) N. Marion, S. Díez-González, S. P. Nolan, *Angew. Chem.* **2007**, *119*, 3046-3058; *Angew. Chem. Int. Ed.* **2007**, *46*, 2988-3000; c) A. T. Biju, N. Kuhl, F. Glorius, *Acc. Chem. Res.* **2011**, *44*, 1182-1195; d) X. Bugaut, F. Glorius, *Chem. Soc. Rev.* **2012**, *41*, 3511-3522; e) M. Fèvre, J. Pinaud, Y. Gnanou, J. Vignolle, D. Taton, *Chem. Soc. Rev.* **2013**, *42*, 2142-2172; f) D. M. Flanigan, F. Romanov-Michailidis, N. A. White, T. Rovis, *Chem. Rev.* **2015**, *115*, 9307-9387; g) M. H. Wang, K. A. Scheidt, *Angew. Chem.* **2016**, *128*, 15134-15145; *Angew. Chem. Int. Ed.* **2016**, *55*, 14912-14922.

[8] a) K. M. Hindi, M. J. Panzner, C. A. Tessier, C. L. Cannon, W. J. Youngs, *Chem. Rev.* **2009**, *109*, 3859-3884; b) L. Oehninger, R. Rubbiani, I. Ott, *Dalton Trans.* **2013**, *42*, 3269-3284; c) F. Cisnetti, A. Gautier, *Angew. Chem.* **2013**, *125*, 12194-12196; *Angew. Chem. Int. Ed.* **2013**, *52*, 11976-11978; d) W. Liu, R. Gust, *Chem. Soc. Rev.* **2013**, *42*, 755-773; e) C. Hemmert, H. Gornitzka, *Dalton Trans.* **2016**, *45*, 440-447; f) W. Liu, R. Gust, *Coord. Chem. Rev.* **2016**, *329*, 191-213; g) Ö. Karaca, S. M. Meier-Menches, A. Casini, F. E. Kühn, *Chem. Commun.* **2017**, *53*, 8249-8260; h) I. Ott, *Inorganic and Organometallic Transition Metal Complexes*

with Biological Molecules and Living Cells (Ed.: K. K.-W. Lo), Academic Press, **2017**, pp. 147-179; i) S. Bellemin-Laponnaz, *Eur. J. Inorg. Chem.* **2020**, 10-20.

[9] a) H.-W. Wanzlick, F. Esser, H.-J. Kleiner, *Chem. Ber.* **1963**, *96*, 1208-1212; b) H.-W. Wanzlick, E. Schikora, *Chem. Ber.* **1961**, *94*, 2389-2393; c) M. K. Denk, K. Hatano, M. Ma, *Tetrahedron Lett.* **1999**, *40*, 2057-2060; d) Y. Liu, D. M. Lemal, *Tetrahedron Lett.* **2000**, *41*, 599-602; e) V. P. W. Böhm, W. A. Herrmann, *Angew. Chem.* **2000**, *112*, 4200-4202; *Angew. Chem. Int. Ed.* **2000**, *39*, 4036-4038.

[10] H. W. Wanzlick, H. J. Schönherr, *Angew. Chem.* **1968**, *80*, 154-154; *Angew. Chem. Int. Ed.* **1968**, *7*, 141-142.

[11] K. Öfele, *J. Organomet. Chem.* **1968**, *12*, P42-P43.

[12] a) M. F. Lappert, P. L. Pye, G. M. McLaughlin, *ChemInform* **1977**, *8*; b) D. J. Cardin, B. Çetinkaya, M. J. Doyle, M. F. Lappert, *Chem. Soc. Rev.* **1973**, *2*, 99-144; c) D. J. Cardin, B. Cetinkaya, M. F. Lappert, L. Manojlović-Muir, K. W. Muir, *J. Chem. Soc. D* **1971**, 400-401.

[13] A. J. Arduengo, H. V. R. Dias, R. L. Harlow, M. Kline, *J. Am. Chem. Soc.* **1992**, *114*, 5530-5534.

[14] A. J. Arduengo, H. V. R. Dias, J. C. Calabrese, F. Davidson, *Organometallics* **1993**, *12*, 3405-3409.

[15] A. J. Arduengo, S. F. Gamper, J. C. Calabrese, F. Davidson, *J. Am. Chem. Soc.* **1994**, *116*, 4391-4394.

[16] V. Lavallo, Y. Canac, C. Präsang, B. Donnadieu, G. Bertrand, *Angew. Chem.* **2005**, *117*, 5851-5855; *Angew. Chem. Int. Ed.* **2005**, *44*, 5705-5709.

[17] a) K. Chandra Mondal, S. Roy, H. W. Roesky, *Chem. Soc. Rev.* **2016**, *45*, 1080-1111; b) W. Li, S. Kundu, C. Köhler, J. Li, S. Dutta, Z. Yang, D. Stalke, R. Herbst-Irmer, A. C. Stückl, B. Schwederski, D. Koley, W. Kaim, H. W. Roesky, *Organometallics* **2019**, *38*, 1939-1945; c) M. Soleilhavoup, G. Bertrand, *Acc. Chem. Res.* **2015**, *48*, 256-266.

[18] a) Z. Kelemen, O. Hollóczki, J. Oláh, L. Nyulászi, *RSC Adv.* **2013**, *3*, 7970-7978; b) L. Kong, Y. Li, R. Ganguly, D. Vidovic, R. Kinjo, *Angew. Chem.* **2014**, *126*, 9434-9437; *Angew. Chem. Int. Ed.* **2014**, *53*, 9280-9283.

[19] A. J. Arduengo, J. R. Goerlich, W. J. Marshall, *Liebigs Ann.* **1997**, *1997*, 365-374.

[20] D. Enders, K. Breuer, G. Raabe, J. Runsink, J. H. Teles, J.-P. Melder, K. Ebel, S. Brode, *Angew. Chem.* **1995**, *107*, 1119-1122; *Angew. Chem. Int. Ed.* **1995**, *34*, 1021-1023.

[21] R. H. Crabtree, *Coord. Chem. Rev.* **2013**, *257*, 755-766.

[22] a) N. Kuhn, T. J. S. Kratz, *Synthesis* **1993**, *6*, 561-562; b) F. E. Hahn, L. Wittenbecher, R. Boese, D. Bläser, *Chem. Eur. J.* **1999**, *5*, 1931-1935.

[23] B. Bantu, G. M. Pawar, U. Decker, K. Wurst, A. M. Schmidt, M. R. Buchmeiser, *Chem. Eur. J.* **2009**, *15*, 3103-3109.

[24] M. Otto, S. Conejero, Y. Canac, V. D. Romanenko, V. Rudzevitch, G. Bertrand, *J. Am. Chem. Soc.* **2004**, *126*, 1016-1017.

[25] G. W. Nyce, S. Csihony, R. M. Waymouth, J. L. Hedrick, *Chem Eur. J.* **2004**, *10*, 4073-4079.

[26] X. Bantreil, S. P. Nolan, *Nat. Protoc.* **2011**, *6*, 69-77.

[27] T. Schaub, U. Radius, A. Brucks, M. P. Choules, M. T. Olsen, T. B. Rauchfuss, *Inorg. Synth.* **2010**, *35*, 78-91.

[28] a) D. A. Dixon, A. J. Arduengo, *J. Phys. Chem.* **1991**, *95*, 4180-4182; b) J. Cioslowski, *Int. J. Quantum Chem.* **1993**, *48*, 309-319; c) C. Heinemann, W. Thiel, *Chem. Phys. Lett.* **1994**, *217*, 11-16; d) C. Heinemann, T. Müller, Y. Apeloig, H. Schwarz, *J. Am. Chem. Soc.* **1996**, *118*, 2023-2038; e) C. Boehme, G. Frenking, *J. Am. Chem. Soc.* **1996**, *118*, 2039-2046; f) D. Munz, *Organometallics* **2018**, *37*, 275-289; g) K. Breitwieser, D. Munz, *Advances in Organometallic Chemistry, Vol. 78* (Ed.: P. J. Pérez), Academic Press, **2022**, pp. 79-132.

[29] a) M. J. Krahfuss, J. Nitsch, F. M. Bickelhaupt, T. B. Marder, U. Radius, *Chem. Eur. J.* **2020**, *26*, 11276-11292; b) U. Radius, F. M. Bickelhaupt, *Coord. Chem. Rev.* **2009**, *253,* 678-686; c) U. Radius, F. M. Bickelhaupt, *Organometallics* **2008**, *27*, 3410-3414.

[30] E. A. Carter, W. A. Goddard, *J. Phys. Chem.* **1986**, *90*, 998-1001.

[31] a) H. Clavier, A. Correa, L. Cavallo, E. C. Escudero-Adán, J. Benet-Buchholz, A. M. Z. Slawin, S. P. Nolan, *Eur. J. Inorg. Chem.* **2009**, 1767-1773; b) S. Gaillard, X. Bantreil, A. M. Z. Slawin, S. P. Nolan, *Dalton Trans.* **2009**, 6967-6971.

[32] J. J. Dunsford, K. Cavell, *Dalton Trans.* **2011**, *40*, 9131-9135.

[33] O. Kühl, *Chem. Soc. Rev.* **2007**, *36*, 592-607.

[34] K. M. Kuhn, J.-B. Bourg, C. K. Chung, S. C. Virgil, R. H. Grubbs, *J. Am. Chem. Soc.* **2009**, *131*, 5313-5320.

[35] a) D. J. Nelson, S. P. Nolan, *Chem. Soc. Rev.* **2013**, *42*, 6723-6753; b) H. Clavier, S. P. Nolan, *Chem. Commun.* **2010**, *46*, 841-861; c) R. Dorta, E. D. Stevens, N.

M. Scott, C. Costabile, L. Cavallo, C. D. Hoff, S. P. Nolan, *J. Am. Chem. Soc.* **2005**, *127*, 2485-2495; d) H. V. Huynh, *Chem. Rev.* **2018**, *118*, 9457-9492.

[36] C. A. Tolman, *Chem. Rev.* **1977**, *77*, 313-348.

[37] a) S. V. C. Vummaleti, D. J. Nelson, A. Poater, A. Gómez-Suárez, D. B. Cordes, A. M. Z. Slawin, S. P. Nolan, L. Cavallo, *Chem. Sci.* **2015**, *6*, 1895-1904; b) O. Back, M. Henry-Ellinger, C. D. Martin, D. Martin, G. Bertrand, *Angew. Chem.* **2013**, *125*, 3011-3015; *Angew. Chem. Int. Ed.* **2013**, *52*, 2939-2943; c) A. Liske, K. Verlinden, H. Buhl, K. Schaper, C. Ganter, *Organometallics* **2013**, *32*, 5269-5272; d) K. Verlinden, H. Buhl, W. Frank, C. Ganter, *Eur. J. Inorg. Chem.* **2015**, 2416-2425.

[38] a) A. C. Hillier, W. J. Sommer, B. S. Yong, J. L. Petersen, L. Cavallo, S. P. Nolan, *Organometallics* **2003**, *22*, 4322-4326; b) A. Poater, F. Ragone, R. Mariz, R. Dorta, L. Cavallo, *Chem. Eur. J.* **2010**, *16*, 14348-14353.

[39] M. H. Dunn, N. Konstandaras, M. L. Cole, J. B. Harper, *J. Org. Chem.* **2017**, *82*, 7324-7331.

[40] A. B. P. Lever, *Inorg. Chem.* **1990**, *29*, 1271-1285.

[41] N. Wang, J. Xu, J. K. Lee, *Org. Biomol. Chem.* **2018**, *16*, 8230-8244.

[42] L. Perrin, E. Clot, O. Eisenstein, J. Loch, R. H. Crabtree, *Inorg. Chem.* **2001**, *40*, 5806-5811.

[43] D. Setiawan, R. Kalescky, E. Kraka, D. Cremer, *Inorg. Chem.* **2016**, *55*, 2332-2344.

[44] J. Mathew, C. H. Suresh, *Inorg. Chem.* **2010**, *49*, 4665-4669.

[45] C. A. Ramsden, W. P. Oziminski, *J. Org. Chem.* **2016**, *81*, 10295-10301.

[46] Z. Shi, *Sci. Total. Environ.* **1994**, *148*, 293-298.

[47] R. Dorta, E. D. Stevens, C. D. Hoff, S. P. Nolan, *J. Am. Chem. Soc.* **2003**, *125*, 10490-10491.

[48] U. S. D. Paul, C. Sieck, M. Haehnel, K. Hammond, T. B. Marder, U. Radius, *Chem. Eur. J.* **2016**, *22*, 11005-11014.

[49] M. Tretiakov, Y. G. Shermolovich, A. P. Singh, P. P. Samuel, H. W. Roesky, B. Niepötter, A. Visscher, D. Stalke, *Dalton Trans.* **2013**, *42*, 12940-12946.

[50] G. P. Junor, J. Lorkowski, C. M. Weinstein, R. Jazzar, C. Pietraszuk, G. Bertrand, *Angew. Chem.* **2020**, *132*, 22212-22217; *Angew. Chem. Int. Ed.* **2020**, *59*, 22028-22033.

[51] A. Poater, B. Cosenza, A. Correa, S. Giudice, F. Ragone, V. Scarano, L. Cavallo, *Eur. J. Inorg. Chem.* **2009**, 1759-1766.

[52] L. Tendera, M. Helm, M. J. Krahfuss, M. W. Kuntze-Fechner, U. Radius, *Chem. Eur. J.* **2021**, *27*, 17849-17861.

[53] L. Falivene, R. Credendino, A. Poater, A. Petta, L. Serra, R. Oliva, V. Scarano, L. Cavallo, *Organometallics* **2016**, *35*, 2286-2293.

[54] a) C. Xu, A. Vasileff, Y. Zheng, S.-Z. Qiao, *Adv. Mater. Interfaces* **2021**, *8*, 2001904; b) L. Rocard, D. Chen, A. Stadler, H. Zhang, R. Gil, S. Bezzenine, J. Hannedouche, *Catalysts* **2021**, *11*, 674; c) J. Loup, U. Dhawa, F. Pesciaioli, J. Wencel-Delord, L. Ackermann, *Angew. Chem.* **2019**, *131*, 12934-12949; *Angew. Chem. Int. Ed.* **2019**, *58*, 12803-12818; d) Ł. Woźniak, N. Cramer, *Trends Chem.* **2019**, *1*, 471-484; e) S. Bansal, A. B. Shabade, B. Punji, *Adv. Synth. Catal.* **2021**, *363*, 1998-2022; f) P. Gandeepan, T. Müller, D. Zell, G. Cera, S. Warratz, L. Ackermann, *Chem. Rev.* **2019**, *119*, 2192-2452; g) K. D. Vogiatzis, M. V. Polynski, J. K. Kirkland, J. Townsend, A. Hashemi, C. Liu, E. A. Pidko, *Chem. Rev.* **2019**, *119*, 2453-2523; h) S. K. Bose, L. Mao, L. Kuehn, U. Radius, J. Nekvinda, W. L. Santos, S. A. Westcott, P. G. Steel, T. B. Marder, *Chem. Rev.* **2021**, *121*, 13238-13341.

[55] P. Sabatier, *Catalysis in Organic Chemistry*, D. Van Nostrand Company, New York, **1922**.

[56] a) V. P. Ananikov, *ACS Catal.* **2015**, *5*, 1964-1971; b) S. Z. Tasker, E. A. Standley, T. F. Jamison, *Nature* **2014**, *509*, 299-309.

[57] A. P. Prakasham, P. Ghosh, *Inorg. Chim. Acta.* **2015**, *431*, 61-100.

[58] a) L. J. Taylor, D. L. Kays, *Dalton Trans.* **2019**, *48*, 12365-12381; b) P. P. Power, *Chem. Rev.* **2012**, *112*, 3482-3507; c) J. M. Frost, K. L. M. Harriman, M. Murugesu, *Chem. Sci.* **2016**, *7*, 2470-2491.

[59] a) J. Montgomery, *Angew. Chem.* **2004**, *116*, 3980-3998; *Angew. Chem. Int. Ed.* **2004**, *43*, 3890-3908; b) E. P. Jackson, J. Montgomery, *J. Am. Chem. Soc.* **2015**, *137*, 958-963; c) A. J. Nett, J. Montgomery, P. M. Zimmerman, *ACS Catal.* **2017**, *7*, 7352-7362; d) A. W. Rand, J. Montgomery, *Chem. Sci.* **2019**, *10*, 5338-5344; e) A. Thakur, J. Louie, *Acc. Chem. Res.* **2015**, *48*, 2354-2365; f) P. M. Zimmerman, A. Paul, C. B. Musgrave, *Inorg. Chem.* **2009**, *48*, 5418-5433; g) T. Inatomi, Y. Fukahori, Y. Yamada, R. Ishikawa, S. Kanegawa, Y. Koga, K. Matsubara, *Catal. Sci. Technol.* **2019**, *9*, 1784-1793; h) K. Matsubara, Y.

Fukahori, T. Inatomi, S. Tazaki, Y. Yamada, Y. Koga, S. Kanegawa, T. Nakamura, *Organometallics* **2016**, *35*, 3281-3287; i) V. Ritleng, M. Henrion, M. J. Chetcuti, *ACS Catal.* **2016**, *6*, 890-906.

[60] N. D. Harrold, A. R. Corcos, G. L. Hillhouse, *J. Organomet. Chem.* **2016**, *813*, 46-54.

[61] V. P. W. Böhm, C. W. K. Gstöttmayr, T. Weskamp, W. A. Herrmann, *Angew. Chem.* **2001**, *113*, 3500-3503; *Angew. Chem. Int. Ed.* **2001**, *40*, 3387-3389.

[62] K. Matsubara, S. Miyazaki, Y. Koga, Y. Nibu, T. Hashimura, T. Matsumoto, *Organometallics* **2008**, *27*, 6020-6024.

[63] A. A. Danopoulos, D. Pugh, *Dalton Trans.* **2008**, 30-31.

[64] S. Caddick, F. G. N. Cloke, P. B. Hitchcock, A. K. de K. Lewis, *Angew. Chem.* **2004**, *116*, 5948-5951; *Angew. Chem. Int. Ed.* **2004**, *43*, 5824-5827.

[65] J. Louie, J. E. Gibby, M. V. Farnworth, T. N. Tekavec, *J. Am. Chem. Soc.* **2002**, *124*, 15188-15189.

[66] Y. Hoshimoto, Y. Hayashi, H. Suzuki, M. Ohashi, S. Ogoshi, *Organometallics* **2014**, *33*, 1276-1282.

[67] K. C. Mondal, P. P. Samuel, Y. Li, H. W. Roesky, S. Roy, L. Ackermann, N. S. Sidhu, G. M. Sheldrick, E. Carl, S. Demeshko, S. De, P. Parameswaran, L. Ungur, L. F. Chibotaru, D. M. Andrada, *Eur. J. Inorg. Chem.* **2014**, 818-823.

[68] T. Schaub, U. Radius, *Chem. Eur. J.* **2005**, *11*, 5024-5030.

[69] T. Schaub, M. Backes, U. Radius, *Organometallics* **2006**, *25*, 4196-4206.

[70] L. Tendera, T. Schaub, M. J. Krahfuss, M. W. Kuntze-Fechner, U. Radius, *Eur. J. Inorg. Chem.* **2020**, 3194-3207.

[71] N. D. Clement, K. J. Cavell, L.-I. Ooi, *Organometallics* **2006**, *25*, 4155-4165.

[72] J. Langer, D. Walther, H. Görls, *J. Organomet. Chem.* **2006**, *691*, 4874-4881.

[73] H. A. Duong, T. N. Tekavec, A. M. Arif, J. Louie, *Chem. Commun.* **2004**, 112-113.

[74] C. H. Lee, D. S. Laitar, P. Mueller, J. P. Sadighi, *J. Am. Chem. Soc.* **2007**, *129*, 13802-13803.

[75] J. B. Diccianni, T. Heitmann, T. Diao, *J. Org. Chem.* **2017**, *82*, 6895-6903.

[76] H. Wang, C.-F. Liu, R. T. Martin, O. Gutierrez, M. J. Koh, *Nat. Chem.* **2022**, *14*, 188-195.

[77] J. S. Bair, Y. Schramm, A. G. Sergeev, E. Clot, O. Eisenstein, J. F. Hartwig, *J. Am. Chem. Soc.* **2014**, *136*, 13098-13101.

[78] T. Schaub, U. Radius, *Z. Anorg. Allg. Chem.* **2007**, *633*, 2168-2172.

[79] a) P. Kumar, A. Thakur, X. Hong, K. N. Houk, J. Louie, *J. Am. Chem. Soc.* **2014**, *136*, 17844-17851; b) T. N. Tekavec, J. Louie, *J. Org. Chem.* **2008**, *73*, 2641-2648; c) H. A. Duong, J. Louie, *Tetrahedron* **2006**, *62*, 7552-7559; d) M. M. McCormick, H. A. Duong, G. Zuo, J. Louie, *J. Am. Chem. Soc.* **2005**, *127*, 5030-5031; e) H. A. Duong, M. J. Cross, J. Louie, *J. Am. Chem. Soc.* **2004**, *126*, 11438-11439.

[80] a) A. D. Jenkins, A. Herath, M. Song, J. Montgomery, *J. Am. Chem. Soc.* **2011**, *133*, 14460-14466; b) H. A. Malik, G. J. Sormunen, J. Montgomery, *J. Am. Chem. Soc.* **2010**, *132*, 6304-6305; c) M. R. Chaulagain, G. J. Sormunen, J. Montgomery, *J. Am. Chem. Soc.* **2007**, *129*, 9568-9569.

[81] R. M. Stolley, H. A. Duong, J. Louie, *Organometallics* **2013**, *32*, 4952-4960.

[82] T. Schaub, C. Döring, U. Radius, *Dalton Trans.* **2007**, 1993-2002.

[83] T. Schaub, U. Radius, *Z. Anorg. Allg. Chem.* **2006**, *632*, 981-984.

[84] J. H. J. Berthel, M. W. Kuntze-Fechner, U. Radius, *Eur. J. Inorg. Chem.* **2019**, 2618-2623.

[85] U. S. D. Paul, U. Radius, *Organometallics* **2017**, *36*, 1398-1407.

[86] a) T. Zell, T. Schaub, K. Radacki, U. Radius, *Dalton Trans.* **2011**, *40*, 1852-1854; b) D. Schmidt, T. Zell, T. Schaub, U. Radius, *Dalton Trans.* **2014**, *43*, 10816-10827; c) C. Hauf, J. E. Barquera-Lozada, P. Meixner, G. Eickerling, S. Altmannshofer, D. Stalke, T. Zell, D. Schmidt, U. Radius, W. Scherer, *Z. Anorg. Allg. Chem.* **2013**, *639*, 1996-2004.

[87] S. Sabater, D. Schmidt, H. Schmidt, M. Kuntze-Fechner, T. Zell, C. Isaac, N. Rajabi, H. Grieve, W. Blackaby, J. Lowe, S. Macgregor, M. Mahon, U. Radius, M. Whittlesey, *Chem. Eur. J.* **2021**, *27*, 13221-13234.

[88] G. Hierlmeier, P. Coburger, N. P. van Leest, B. de Bruin, R. Wolf, *Angew. Chem.* **2020**, *132*, 14252-14257; *Angew. Chem. Int. Ed.* **2020**, *59*, 14148-14153.

[89] B. Zarzycki, T. Zell, D. Schmidt, U. Radius, *Eur. J. Inorg. Chem.* **2013**, 2051-2058.

[90] G. Hierlmeier, R. Wolf, *Angew. Chem.* **2021**, *133*, 6507-6512; *Angew. Chem. Int. Ed.* **2021**, *60*, 6435-6440.

[91] A. G. Sergeev, J. F. Hartwig, *Science* **2011**, *332*, 439-443.

[92] N. I. Saper, J. F. Hartwig, *J. Am. Chem. Soc.* **2017**, *139*, 17667-17676.

[93] B. Sawatlon, T. Wititsuwannakul, Y. Tantirungrotechai, P. Surawatanawong, *Dalton Trans.* **2014**, *43*, 18123-18133.

[94] L. Xu, L. W. Chung, Y.-D. Wu, *ACS Catal.* **2016**, *6*, 483-493.

[95] a) T. Schaub, M. Backes, O. Plietzsch, U. Radius, *Dalton Trans.* **2009**, 7071-7079; b) T. Schaub, M. Backes, U. Radius, *Chem. Commun.* **2007**, 2037-2039.

[96] M. Huang, Z. Wu, J. Krebs, A. Friedrich, X. Luo, S. A. Westcott, U. Radius, T. B. Marder, *Chem. Eur. J.* **2021**, *27*, 8149-8158.

[97] J. Li, J. Morris, W. W. Brennessel, W. D. Jones, *J. Chem. Crystallogr.* **2013**, *44*, 15-19.

[98] a) K. Muthuvel, T. Gandhi, *ChemCatChem.* **2022**, *14*, e202101579; b) T. Ahrens, J. Kohlmann, M. Ahrens, T. Braun, *Chem. Rev.* **2015**, *115*, 931-972.

[99] T. Schaub, M. Backes, U. Radius, *Eur. J. Inorg. Chem.* **2008**, 2680-2690.

[100] T. Schaub, P. Fischer, A. Steffen, T. Braun, U. Radius, A. Mix, *J. Am. Chem. Soc.* **2008**, *130*, 9304-9317.

[101] T. Schaub, P. Fischer, T. Meins, U. Radius, *Eur. J. Inorg. Chem.* **2011**, 3122-3126.

[102] T. Schaub, M. Backes, U. Radius, *J. Am. Chem. Soc.* **2006**, *128*, 15964-15965.

[103] P. Fischer, K. Götz, A. Eichhorn, U. Radius, *Organometallics* **2012**, *31*, 1374-1383.

[104] M. Ohashi, H. Saijo, M. Shibata, S. Ogoshi, *Eur. J. Org. Chem.* **2013**, 443-447.

[105] J. Zhou, J. H. Berthel, M. W. Kuntze-Fechner, A. Friedrich, T. B. Marder, U. Radius, *J. Org. Chem.* **2016**, *81*, 5789-5794.

[106] H. Saijo, H. Sakaguchi, M. Ohashi, S. Ogoshi, *Organometallics* **2014**, *33*, 3669-3672.

[107] M. W. Kuntze-Fechner, C. Kerpen, D. Schmidt, M. Häring, U. Radius, *Eur. J. Inorg. Chem.* **2019**, 1767-1775.

[108] H. Iwamoto, H. Imiya, M. Ohashi, S. Ogoshi, *J. Am. Chem. Soc.* **2020**, *142*, 19360-19367.

[109] T. Schaub, *Neuartige Nickel-Carbenkomplexe und deren Anwendung in Element-Element-Aktivierungsreaktionen*, Dissertation, Cuvillier Verlag, Universität Karlsruhe, **2006**.

[110] J. Zhou, M. W. Kuntze-Fechner, R. Bertermann, U. S. Paul, J. H. Berthel, A. Friedrich, Z. Du, T. B. Marder, U. Radius, *J. Am. Chem. Soc.* **2016**, *138*, 5250-5253.

[111] Y. Tian, X. Guo, M. Kuntze-Fechner, I. Krummenacher, H. Braunschweig, U. Radius, A. Steffen, T. B. Marder, *J. Am. Chem. Soc.* **2018**, *140*, 17612-17623.

[112] M. W. Kuntze-Fechner, H. Verplancke, L. Tendera, M. Diefenbach, I. Krummenacher, H. Braunschweig, T. B. Marder, M. C. Holthausen, U. Radius, *Chem. Sci.* **2020**, *11*, 11009-11023.

[113] D. J. Nelson, F. Maseras, *Chem. Commun.* **2018**, *54*, 10646-10649.

[114] S. Miyazaki, Y. Koga, T. Matsumoto, K. Matsubara, *Chem. Commun.* **2010**, *46*, 1932-1934.

[115] K. Zhang, M. Conda-Sheridan, S. R. Cooke, J. Louie, *Organometallics* **2011**, *30*, 2546-2552.

[116] Y. M. Tian, X. N. Guo, I. Krummenacher, Z. Wu, J. Nitsch, H. Braunschweig, U. Radius, T. B. Marder, *J. Am. Chem. Soc.* **2020**, *142*, 18231-18242.

[117] L. Kuehn, D. G. Jammal, K. Lubitz, T. B. Marder, U. Radius, *Chem. Eur. J.* **2019**, *25*, 9514-9521.

[118] T. Zell, M. Feierabend, B. Halfter, U. Radius, *J. Organomet. Chem.* **2011**, *696*, 1380-1387.

[119] T. Zell, P. Fischer, D. Schmidt, U. Radius, *Organometallics* **2012**, *31*, 5065-5073.

[120] T. Zell, U. Radius, *Z. Anorg. Allg. Chem.* **2011**, *637*, 1858-1862.

[121] T. Zell, U. Radius, *Z. Anorg. Allg. Chem.* **2013**, *639*, 334-339.

[122] Y.-M. Tian, X.-N. Guo, Z. Wu, A. Friedrich, S. A. Westcott, H. Braunschweig, U. Radius, T. B. Marder, *J. Am. Chem. Soc.* **2020**, *142*, 13136-13144.

Chapter II

Large versus Small NHC Ligands in Nickel(0) Complexes: The Coordination of Olefins, Ketones and Aldehydes at $[Ni(NHC)_2]$

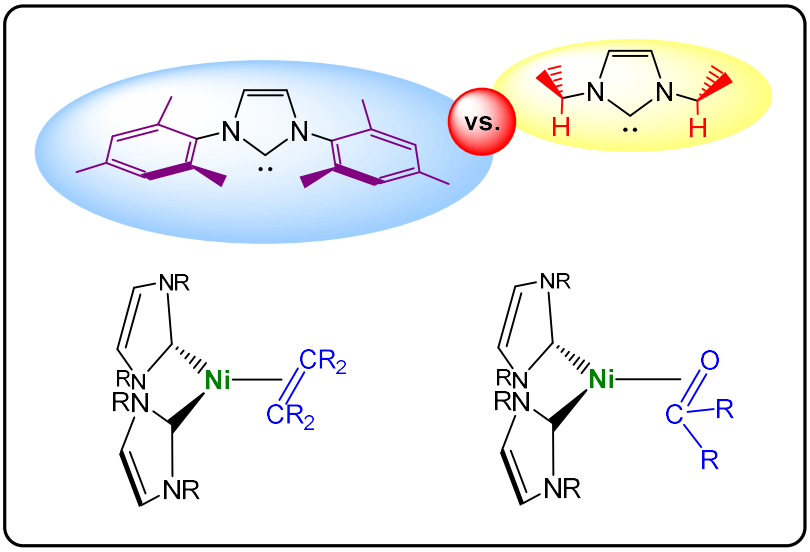

2 Large versus Small NHC Ligands in Nickel(0) Complexes: The Coordination of Olefins, Ketones and Aldehydes at [Ni(NHC)$_2$]

2.1 Introduction

Since the discovery of the first stable crystalline *N*-heterocyclic carbene (NHC) in 1991,[1] NHCs have become considerable alternatives to phosphines as ancillary ligands in transition metal chemistry and in homogeneous catalysis.[2] The 14-electron bis-NHC nickel(0) complex [Ni(Mes$_2$Im)$_2$] **1** (Mes$_2$Im = 1,3-dimesitylimidazolin-2-ylidene), which was reported by Arduengo and co-workers two years after the initial discovery of stable NHCs,[3] provides one of the earliest examples for a low-coordinated, subvalent transition metal complex stabilized by a bulky NHC. The price paid for the stability of the 14 VE (valence electron) complex [Ni(Mes$_2$Im)$_2$] and analogues containing even more bulky *N*-aryl substituents compared to complexes of sterically less demanding NHCs is a limited or altered reactivity. Many transition metal-catalyzed processes consist of steps such as oxidative addition, reductive elimination, migratory insertion, transmetalation, and *β*-hydride elimination, and these elementary steps are significantly influenced by the sterics of the (NHC) co-ligand and by the degree of electron transfer to organic substrates.[4] For example, Nelson and Maseras highlighted recently by means of quantum chemical calculations the dominant mechanistic role of steric effects in the reaction of complexes of the type [Ni(NHC)$_2$] with aryl halides (Ph–X, X = Cl, Br, I) and demonstrated that the outcome of this reaction is controlled by the steric impact of the NHC ligand.[5] Small NHC substituents should favor a concerted oxidative addition of the C–X bond to the Ni(0) complex leading to Ni(II) complexes, while larger NHC ligands should prevent coordination of the aryl halide and favor halide radical abstraction to form Ni(I) complexes.[5] However, even though different nickel complexes bearing the bulky Mes$_2$Im or Dipp$_2$Im ligands are widely used as catalysts in different organic transformations,[6] this difference in the reactivity of mononuclear complexes such as [Ni(Mes$_2$Im)$_2$] **1**, and Ni(0) complexes of sterically less encumbered NHCs is not too well documented.

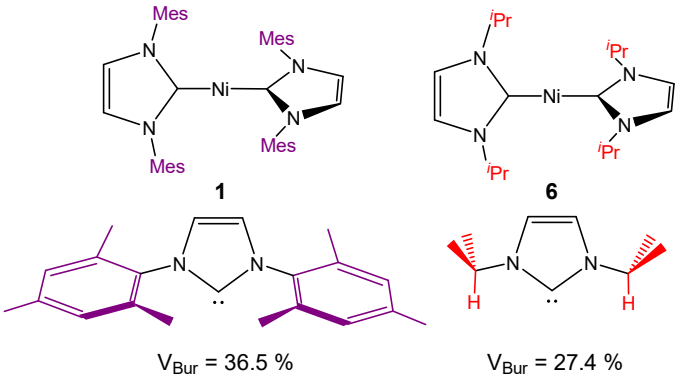

Scheme II.1 The nickel NHC complexes [Ni(Mes$_2$Im)$_2$] **1** and [Ni(^{i}Pr$_2$Im)$_2$] **6** as provided by [Ni$_2$(^{i}Pr$_2$Im)$_4$(*μ-(η^2:η^2)*-COD)] **6a**.

Over the past few years our group investigated the NHC-stabilized nickel(0) complexes [Ni(Mes$_2$Im)$_2$] **1**[7] and [Ni$_2$(^{i}Pr$_2$Im)$_4$(*μ-(η^2:η^2)*-COD)] **6a**[8] (^{i}Pr$_2$Im = 1,3-di-*iso*-propyl-imidazolin-2-ylidene) (Scheme II.1) in stoichiometric and catalytic C–F bond activation reactions as well as the catalytic borylation of polyfluoroarenes. While the general reactivity of the dinuclear complex [Ni$_2$(^{i}Pr$_2$Im)$_4$(*μ-(η^2:η^2)*-COD)] **6a** with different small molecules such as olefins, alkynes, silanes, nitriles, thioethers, sulfoxides, sulfones and carbon monoxide is already well established,[8-10] there is a lack on studies concerning the reactivity of the mononuclear complex [Ni(Mes$_2$Im)$_2$] **1** with these small molecules. We demonstrated earlier that [Ni$_2$(^{i}Pr$_2$Im)$_4$(*μ-(η^2:η^2)*-COD)] **6a** is a source of [Ni(^{i}Pr$_2$Im)$_2$] **6**, which readily coordinates to unsaturated substrates such as alkenes and alkynes to yield complexes [Ni(^{i}Pr$_2$Im)$_2$(η^2-H$_2$C=CH$_2$)], [Ni(^{i}Pr$_2$Im)$_2$(η^2-RC≡CR)] (R = Ph, Et, Me), [Ni(^{i}Pr$_2$Im)$_2$(η^2-P≡C^{t}Bu)],[9] and also inserts readily into different element element bonds.[10] The reaction of **6a** with organonitriles such as benzonitrile and *p*-toluonitrile, for example, leads to the formation of the complexes [Ni(^{i}Pr$_2$Im)$_2$(η^2-N≡CR)] (R = Ph, *p*-tolyl) with η^2-coordinated organonitrile ligand, which leads under thermal or photolytic conditions to insertion of [Ni(^{i}Pr$_2$Im)$_2$] **6** into the nitrile C$_\alpha$-CN bond to yield the aryl cyanide complexes *trans*-[Ni(^{i}Pr$_2$Im)$_2$(CN)(Ph)] and *trans*-[Ni(^{i}Pr$_2$Im)$_2$(CN)(*p*Tol)].[10a] We also demonstrated that alkenes with other potentially coordinating subgroups such as mesityl oxide (4-methyl-3-pentene-2-one) and 4-vinylpyridine selectively coordinate *via* the olefinic moiety to [Ni(^{i}Pr$_2$Im)$_2$].[11] However, there are currently just a few reports in the literature concerning the reactivity of the complex [Ni(Mes$_2$Im)$_2$] **1** towards different “small” molecules in stoichiometric reactions. In 2006, the reaction of [Ni(Mes$_2$Im)$_2$] **1** with dimethylfumarate was

investigated by Cavell *et al.*[12] These authors have shown that, depending on the stoichiometric amount of dimethylfumarate added to **1**, different η^2-complexes [Ni(Mes_2Im)$_2$(η^2-MeOOCC=CCOOMe)], [Ni(Mes_2Im)(η^2-MeOOCC=CCOOMe)$_2$], [{Ni(Mes_2Im)(η^2-MeOOCC=CCOOMe)}$_2$] and an organic NHC-dimethylfumarate coupling product are formed.[12] We presented earlier the synthesis and characterization of a stable, *side-on* η^2-(N,N)-bonded diazoalkane complex [Ni(iPr$_2$Im)$_2$(η^2-*N,N'*-N_2CPh_2)] from the reaction of **6a** with diphenyldiazomethane.[11] Nine years later, Hillhouse *et al.* reported the synthesis of the *end-on* coordinated diazoalkane complexes [Ni(Mes_2Im)$_2$(κ^1-N_2CPh_2)], [Ni($Dipp_2Im$)$_2$(κ^1-N_2CPh_2)] and [Ni(Mes_2Im^{H2})$_2$(κ^1-N_2CPh_2)] (Mes_2Im^{H2} = 1,3-dimesitylimidazolidin-2-ylidene), synthesized from the corresponding bis-carbene nickel(0) complexes and diphenyldiazomethane.[13] They also isolated the *side-on* coordinated azide complex [Ni(Mes_2Im)$_2$(η^2-N_3Ad)] from the reaction of **1** with 1-azidoadamantane. All complexes are stable with respect to N_2 loss and the diazoalkane complex [Ni(Mes_2Im)$_2$(κ^1-N_2CPh_2)] was reacted with olefins to give different cyclopropane products. The cyclization can also be carried out under catalytic conditions using either [Ni(Mes_2Im)$_2$] **1** or [Ni(Mes_2Im)$_2$(κ^1-N_2CPh_2)] as the catalyst.[13]

Herein the reactivity of **1** and **6a** towards simple *π*-acidic substrates such as olefins, ketones and aldehydes is reported, with the aim to establish some of the differences in the reactivity of the 14 VE nickel(0) NHC complexes [Ni(Mes_2Im)$_2$] **1** and [Ni(^{i}Pr$_2$Im)$_2$] **6**.

2.2 Results and Discussion

We reported earlier the reaction of [Ni$_2$(^{i}Pr$_2$Im)$_4$(μ-(η^2:η^2)-COD)] **6a** with different alkenes and alkynes which selectively affords stable complexes of the type [Ni(^{i}Pr$_2$Im)$_2$(η^2-R$_2$C=CR$_2$)] or [Ni(^{i}Pr$_2$Im)$_2$(η^2-RC≡CR)].[8a, 9] The resulting complexes reveal shifted NMR resonances of the olefin and the acetylene hydrogen and carbon atoms typically observed due to the high degree of π-backbonding into the carbon–carbon multiple bond according to the Dewar-Chatt-Duncanson model.[14] Thus, these complexes can be considered in-between metal olefin or alkyne complexes and metallacyclopropanes or metallacyclopropenes, respectively.

Now the reactivity of [Ni(Mes$_2$Im)$_2$] **1** with different olefins is investigated. Most interestingly, in contrast to [Ni$_2$(^{i}Pr$_2$Im)$_4$(μ-(η^2:η^2)-COD)] **6a**, most olefins such as tetramethylethylene, 1,1-diphenylethylene and cyclohexene did not react at all with **1**, even at elevated temperatures. Only the reaction of **1** with the smallest alkene, i.e. ethylene, afforded the complex [Ni(Mes$_2$Im)$_2$(η^2-H$_2$C=CH$_2$)] **II-1** quantitatively if the reaction was performed in the NMR tube. For the synthesis of analytically pure material the isolated yield was only 58 % due to the good solubility of the complex in pentane and hexane (Scheme II.2). Similarly, the reaction of **1** with the more π-acidic olefin methyl acrylate led to the formation of [Ni(Mes$_2$Im)$_2$(η^2-(*C,C*)-H$_2$C=CHCOOMe)] **II-2**, in which nickel binds selectively to the olefinic moiety rather than to the carbonyl function of the Michael system (Scheme II.2). The same selectivity was found for the reaction of methyl acrylate with complex **6**.[11]

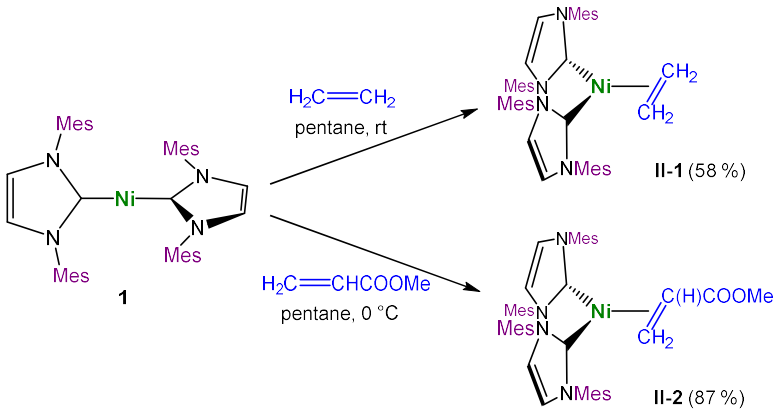

Scheme II.2 Synthesis of [Ni(Mes$_2$Im)$_2$(η^2-C$_2$H$_4$)] **II-1** and [Ni(Mes$_2$Im)$_2$(η^2-(*C,C*)-H$_2$C=CHCOOMe)] **II-2**.

Complex **II-1** was isolated as an orange solid in 58 % yield, while **II-2** was obtained in form of red crystals in 87 % yield. Both complexes were fully characterized by ^{1}H NMR-, ^{13}C NMR-, IR-spectroscopy, X-Ray diffraction, high-resolution mass spectroscopy, and elemental analysis. The ^{1}H NMR spectrum of **II-1** shows one set of signals for the NHC ligands, i.e. resonances of the methyl protons of the mesityl group at 1.99 ppm (*ortho*) and 2.29 ppm (*para*), a signal for the backbone protons at 6.14 ppm and a resonance for the mesityl aryl protons at 6.73 ppm. The ethylene proton resonances show a significant shift towards higher fields compared to uncoordinated ethylene and were detected as a singlet at 1.61 ppm. In the ^{13}C{^{1}H} NMR spectrum the NHC carbene carbon resonance was detected at 206.4 ppm and the ethylene carbon resonance at 35.9 ppm, 86.9 ppm high-field shifted compared to the uncoordinated ethylene (122.8 ppm). The ^{1}H NMR and ^{13}C{^{1}H} NMR spectra of [Ni(Mes$_2$Im)$_2$(η^2-(*C,C*)-H$_2$C=CHCOOMe)] **II-2** reveal both significantly broadened signals due to a hindered rotation of the methacrylate and Mes$_2$Im ligand. However, the characteristic resonances have been assigned (see Experimental Part) and the integration of the resonances in the ^{1}H NMR spectrum leads to the expected number of hydrogen atoms per resonance. The mesityl methyl protons give rise to very broad signals in the region between 1.66 ppm and 2.56 ppm in the ^{1}H NMR spectrum of **II-2**. These signals overlap with the resonances of the diastereotopic protons of the methacrylate olefinic moiety, which appear as three doublets of doublets at 1.26 ppm and 1.81 ppm (CH_2 group) and at 2.47 ppm (CH group). The methyl protons of the acrylate give rise to a singlet at 3.33 ppm. In the ^{13}C{^{1}H} NMR spectrum the NHC carbon atom resonances were detected at 202.2 ppm and 205.3 ppm due to the asymmetric nature of the olefin ligand, the coordinated olefin reveals high-field shifted resonances at 31.3 ppm (CH=*C*H$_2$) and 40.6 ppm (*C*H=CH$_2$). Complex **II-1** slowly decomposes under elevated temperatures in solution (benzene, 80 °C) with formation of [Ni(Mes$_2$Im)$_2$] **1**, free carbene and unidentified decomposition products. Furthermore, [Ni(Mes$_2$Im)$_2$(η^2-H$_2$C=CH$_2$)] **II-1** is labile at reduced pressure and completely dissociates in solution upon evaporation into ethylene and [Ni(Mes$_2$Im)$_2$] **1**.

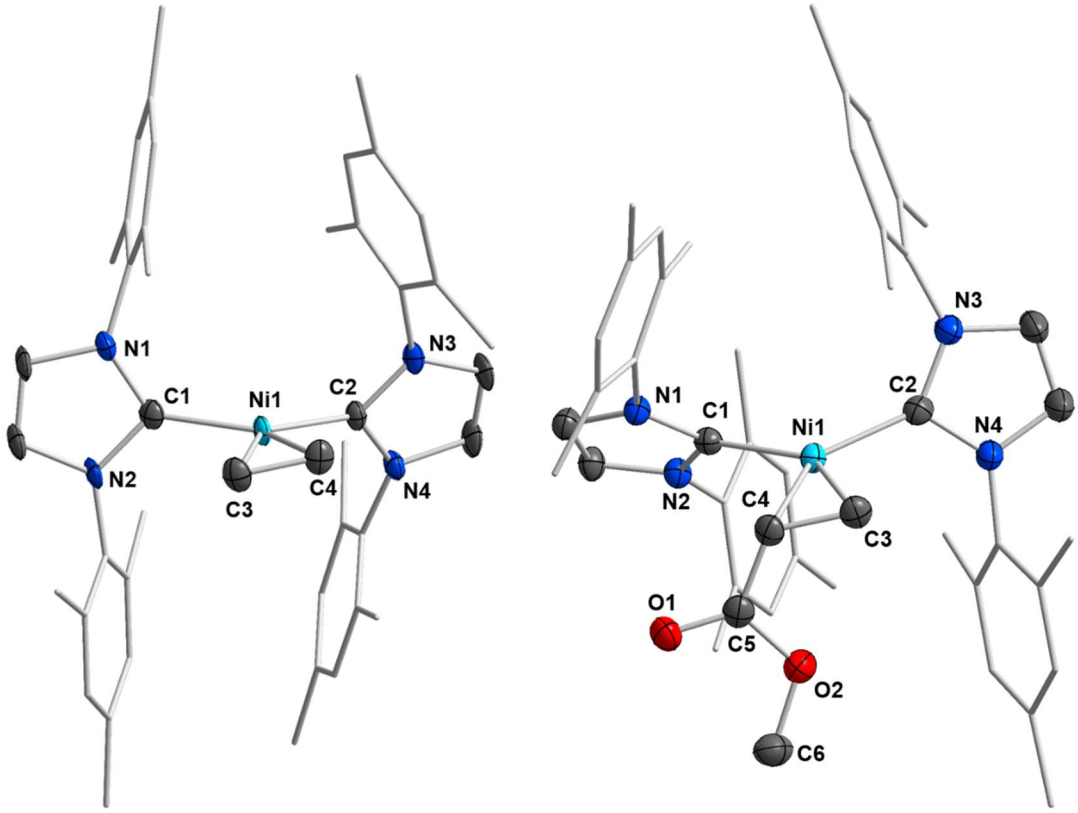

Figure II.1 Molecular structures of [Ni(Mes$_2$Im)$_2$(η^2-H$_2$C=CH$_2$)] **II-1** (left) and [Ni(Mes$_2$Im)$_2$(η^2-(*C,C*)-H$_2$C=CHCOOMe)] **II-2** (right) in the solid state (ellipsoids set at 50 % probability level). Hydrogen atoms have been omitted for clarity. Selected bond lengths [Å] and angles [°] of **II-1**: Ni1–C1 1.900(4), Ni1–C2 1.909(4), Ni1–C3 1.971(4), Ni1–C4 1.973(3), C3–C4 1.405(5), C1–N1 1.382(5), C1–N2 1.383(4), C2–N3 1.376(4), C2–N4 1.377(4), C1–Ni1–C2 131.01(15), C1–Ni1–C3 92.09(16), C2–Ni1–C4 96.22(13), C3–Ni1–C4 41.74(15), N1–C1–N2 101.79(27), N3–C2–N4 101.65(27) plane (C1–Ni1–C2) – plane (C3–Ni1–C4) 13.78(24). Selected bond lengths [Å] and angles [°] of **II-2**: Ni1–C1 1.948(2), Ni1–C2 1.923(2), Ni1–C3 1.961(2), Ni1–C4 2.009(2), C3–C4 1.426(3), C1–N1 1.381(3), C1–N2 1.371(3), C2–N3 1.380(2), C2–N4 1.382(3), C4–C5 1.443(3), C5–O1 1.224(3), C5–O2 1.368(3), O2–C6 1.430(3), C1–Ni1–C2 125.58(9), C1–Ni1–C4 97.62(9), C2–Ni1–C3 94.67(9), C3–Ni1–C4 42.08(9), N1–C1–N2 101.88(17), N3–C2–N4 101.46(17) plane (C1–Ni1–C2) – plane (C3–Ni1–C4) 3.37(12).

Crystals suitable for X-ray diffraction of **II-1** and **II-2** were obtained by storing saturated solutions of the complexes in pentane or hexane at -30 °C for several days. The molecular structures of **II-1** and **II-2** as well as selected bond lengths and bond angles are provided in Figure II.1, important metric parameter of the complexes **II-1**, **II-2** and data obtained for [Ni(*i*Pr$_2$Im)$_2$(η^2-H$_2$C=CH$_2$)] **24**, [Ni(PPh$_3$)$_2$(η^2-H$_2$C=CH$_2$)] **25** and [Ni(Mes$_2$Im)$_2$(η^2-MeOOCC=CCOOMe)] **26** are given in Table II.1. Complex **II-1** crystallizes in the monoclinic space group P2$_1$/n and adopts a distorted pseudo square planar geometry, spanned by the two NHC ligands and the ethylene ligand. The Ni–C distances to the NHC carbene carbon atoms of 1.900(4) Å (Ni1–C1) and 1.909(4) Å (Ni1–C2) are almost identical and in line with other bis-carbene olefin complexes such as [Ni(*i*Pr$_2$Im)$_2$(η^2-H$_2$C=CH$_2$)] **24** (1.905(2) Å and 1.915(2) Å).[8a] The C–C distance of 1.405(5) Å of the ethylene ligand is significantly enlarged compared to that of uncoordinated ethylene (1.33 Å) and lies also in the same range as observed for [Ni(*i*Pr$_2$Im)$_2$(η^2-H$_2$C=CH$_2$)] **24** (1.420(4) Å)[8a] or [Ni(PPh$_3$)$_2$(η^2-H$_2$C=CH$_2$)] **25** (1.391(5) Å).[15] The ethylene ligand (i.e. plane C$_{olefin}$–Ni–C$_{olefin}$) is not perfectly planar aligned to the C$_{carbene}$–Ni–C$_{carbene}$ plane and twisted by 13.78(24)°, which is remarkably larger than the twist observed for [Ni(*i*Pr$_2$Im)$_2$(η^2-H$_2$C=CH$_2$)] **24** (1.85(14)°) and [Ni(PPh$_3$)$_2$(η^2-H$_2$C=CH$_2$)] **25** (6.60(2)°). We attribute this twisting to the increased steric bulk of the Mes$_2$Im ligand, which is in line with the much larger %V_{bur} ("percent buried volume") of Mes$_2$Im (36.5 %) compared to *i*Pr$_2$Im (27.4 %).[16] Complex **II-2** crystallizes with one molecule hexane in the asymmetric unit in the triclinic space group P$\bar{1}$. Complex **II-2** also adopts a distorted pseudo square planar geometry, the Ni–C$_{NHC}$ distances of 1.948(2) Å for Ni1–C1 and 1.923(2) Å for Ni1–C2 are slightly longer than the distances observed for **II-1**. The C–C bond length of the olefin of 1.426(3) Å lies in the same range as observed for the ethylene complexes **II-1**, **24** and **25** and [Ni(Mes$_2$Im)$_2$(η^2-MeOOCC=CCOOMe)] **26**, which was reported earlier by Cavell *et al.*[12] (see also Table II.1). In contrast to complex **I-1,** the olefin is almost perfectly aligned to the C$_{carbene}$–Ni–C$_{carbene}$ plane, the angle between the planes C$_{carbene}$–Ni–C$_{carbene}$ and Ni–C$_{olefin}$–C$_{olefin}$ is 3.37(12)°. Although the methyl acrylate ligand should be larger than the ethylene ligand, increased back-bonding to the electron-poorer alkene seems to override steric effects in this case.

Love and Kennepohl *et al.* published recently a study on the stabilization of square planar d^{10} nickel π-complexes.[17] The geometric and electronic structure of a series of nickel π-complexes [Ni(dtbpe)(X)] (dtbpe = 1,2-bis(di-*tert*-butyl)phosphinoethane; X =

alkene or carbonyl containing π-ligands) was probed using a combination of ^{31}P NMR, Ni K-edge XAS, Ni K_b XES, and DFT calculations. They have demonstrated that these complexes are best described as square planar d^{10} complexes with π-back-bonding acting as the dominant contributor to bonding to the π-ligand. Most interestingly, these authors provide some evidence that backbonding is dominated by charge donation from the co-ligand *via* the metal center, which retains a formal d^{10} electronic configuration, to the π-acidic ligand. This ligand induced backbonding can be described as a 3-centre-4-electron interaction, in which the nickel center mediates charge transfer from the co-ligand σ-donor orbital to the π-ligand π^*-acceptor orbital. Thus, good net donor ligands should allow for strong backdonation, which is in line with our observations for the different C–C distances for the complexes **24** > **II-1** > **25**, which correlate with the net donor properties of the ancillary co-ligands ^{i}Pr$_2$Im > Mes$_2$Im > PPh$_3$. Moreover, it is known for d^{10} ML$_2$ complexes that a larger deviation from linearity (*i.e.* a smaller bite-angle L-M-L) leads to a better backbonding into the π^*-orbital of a π-ligand (and therefore to an elongation of the π-bond of this ligand).[18] For the ethylene complexes [Ni(Mes$_2$Im)$_2$(η^2-H$_2$C=CH$_2$)] **II-1** and [Ni(^{i}Pr$_2$Im)$_2$(η^2-H$_2$C=CH$_2$)] **24** the bite-angles of the ancillary co-ligands are determined by the steric properties of the NHC ligands and much smaller for the ^{i}Pr$_2$Im complex **24** (C_{NHC}-Ni-C_{NHC}: **24**: 102.41(9) Å, **II-1**: 131.01(15) Å), which leads to different electron transfer to the ethylene ligand and thus correlates with different olefin C–C distances observed experimentally (**24**: 1.420(4) Å; **II-1**: 1.405(5) Å; but see also [Ni(^{i}Pr$_2$Im)$_2$(η^2-(*C,C*)-Me$_2$C=CHCOOMe)]: 1.441(3) Å, **II-2**: 1.426(3)). Accordingly, backbonding of the nickel center to the olefin ligand, the "degree of activation" of the π-acidic ligand and thus the reactivity of the resulting coordinated ligand crucially depends on the sterics of the NHC nitrogen substituents also for electronic reasons.

[Ni(^{i}Pr$_2$Im)$_2$] **6** also binds selectively to the olefinic moiety if the substrate contains different other potentially coordinating sites such as keto functionalities.[11] However, in an earlier work of our group Dr. Thomas Schaub has shown, that complex **6** cleanly reacts with the C=O double bond of a carbonyl function of ketones and aldehydes in the absence of an olefinic moiety.[11a] For a better comparison between complex **1** and **6**, his results are represented and discussed in the following section (compounds **II-3 – II-8**).

Table II.1 Important bond lengths, bond angles and chemical shifts of [Ni(Mes_2Im)$_2$(η^2-$H_2C{=}CH_2$)] **II-1**, [Ni(Mes_2Im)$_2$(η^2-(*C,C*)-$H_2C{=}CHCOOMe$)] **II-2**, [Ni($^iPr_2Im$)$_2$(η^2-$H_2C{=}CH_2$)] **24**, [Ni(PPh_3)$_2$(η^2-$H_2C{=}CH_2$)] **25** and [Ni(Mes_2Im)$_2$(η^2-MeOOC-C=C-COOMe) **26** ($d_{C–C}$ = C–C distance of the olefin, L = NHC or phosphine ligands, twist angle: twist between the planes L–Ni–L and C–Ni–C; δ_C = $^{13}C\{^1H\}$ NMR shift of the olefin carbon atoms; δ_H = ^1H NMR shift of the olefin hydrogen atoms; $\delta_{C\ NHC}$ =$^{13}C\{^1H\}$ NMR shift of the NHC carbene carbon atom).

Compound	$d_{Ni–L}$ [Å]	$d_{C–C}$ [Å]	twist angle [°]	δ_C NHC [ppm]	δ_C olefin [ppm]	δ_H olefin [ppm]
II-1	1.900(4)/1.909(4)	1.405(5)	13.78(24)	206.4	35.9	1.61
II-2	1.948(2)/1.923(2)	1.426(3)	3.37(12)	202.2	31.3	1.81
				205.3	40.6	2.47
24[8a]	1.905(2)/1.915(2)	1.420(4)	1.85(14)	203.0	24.9	1.95
25[15, 19]	2.148(4)/2.158(4)	1.391(5)	6.60(24)	-	-	2.55
26[12]	1.947(2)/1.941(2)	1.446(3)	5.58(14)	199.6	37.0	2.78

The reaction of [$Ni_2(^iPr_2Im)_4$(*μ-(η²:η²)*-COD)] **6a** with pivalaldehyde, benzaldehyde, acetophenone, benzophenone, 4,4´-difluorobenzophenone and methyltrifluoroacetate at room temperature leads to the formation of the corresponding ketone or aldehyde complexes with *side-on* η^2-(*C,O*)-coordinating ligands [Ni($^iPr_2Im$)$_2$(η^2-O=CH^{t}Bu)] **II-3**, [Ni($^iPr_2Im$)$_2$(η^2-O=CHPh)] **II-4**, [Ni($^iPr_2Im$)$_2$(η^2-O=CMePh)] **II-5**, [Ni($^iPr_2Im$)$_2$(η^2-$O{=}CPh_2$)] **II-6**, [Ni($^iPr_2Im$)$_2$(η^2-O=C(4-F-C_6H_4)$_2$)] **II-7** and [Ni($^iPr_2Im$)$_2$(η^2-O=C(OMe)(CF_3))] **II-8** in moderate to good yields (Scheme II.3). This is contrary to the behavior of the analogous platinum complex [Pt($^iPr_2Im$)$_2$] which leads upon reaction with acetophenone to an equilibrium with the *α*-C-H bond activation product *trans*-[Pt($^iPr_2Im$)$_2$(H)(–$\underline{C}H_2$-C{O}Ph)].[20] The formation of this complex was quantitative if an excess of acetophenone was used at elevated temperatures (80 °C). Other likely reaction products such as an η^2-ketone complex or a complex resulting from *ortho*-metalation of the phenyl ring of the ketone have not been observed.

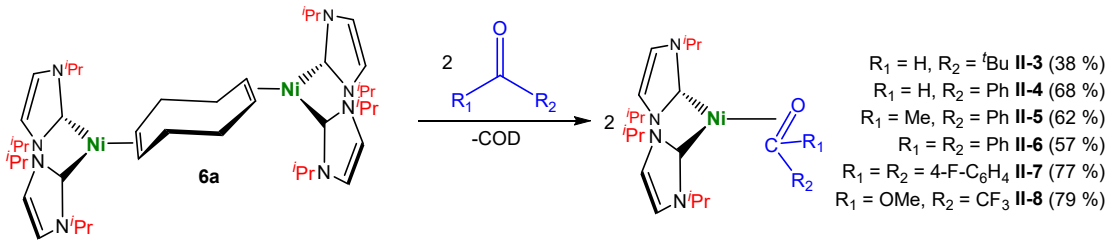

Scheme II.3 Synthesis of [Ni(*i*Pr$_2$Im)$_2$(η^2-O=CH*t*Bu)] **II-3**, [Ni(*i*Pr$_2$Im)$_2$(η^2-O=CHPh)] **II-4**, [Ni(*i*Pr$_2$Im)$_2$(η^2-O=CMePh)] **II-5**, [Ni(*i*Pr$_2$Im)$_2$(η^2-O=CPh$_2$)] **II-6**, [Ni(*i*Pr$_2$Im)$_2$(η^2-O=C(4-F-C$_6$H$_4$)$_2$)] **II-7** and [Ni(*i*Pr$_2$Im)$_2$(η^2-O=C(OMe)(CF$_3$))] **II-8**.

The complexes **II-3 – II-8** were isolated as orange to red colored, air and moisture sensitive solids and have been fully characterized by ^{1}H NMR-, ^{13}C{1H} NMR, IR-spectroscopy and elemental analysis (except complex **II-3**). Under the conditions of mass spectrometry (EI) the complexes tend to decompose and therefore the molecular ion peaks were not detected in the high-resolution mass spectrum. Important ^{1}H and ^{13}C{^{1}H} NMR data of the compounds **II-3 – II-8** are summarized in Table II.2. The ^{1}H NMR spectra reveal the expected signals for the NHC ligands in the typical regions. The low symmetry of the keto and aldehyde ligands are reflected in the inequivalent NHC ligands which give rise to up to four resonances for the *iso*-propyl methyl protons in the range between 0.76 ppm and 1.27 ppm, i.e. typically two septets for the methine protons in the range between 5.24 ppm and 5.79 ppm and two signals for the backbone hydrogen atoms between 6.21 ppm and 6.49 ppm in the ^{1}H NMR spectrum. Two NHC carbene carbon resonances for each complex were found in the range between 192.1 ppm and 199.7 ppm in the ^{13}C{^{1}H} NMR spectra. Similar as observed for the nickel olefin and alkyne complexes, [8a, 9b] the ^{13}C{^{1}H} NMR resonances of the carbonyl carbon atoms show a significant coordination shift due to strong back-bonding from the metal to the ligand. These resonances were observed in the range between 73.9 ppm and 92.2 ppm and are thus shifted by 65.8 ppm up to 122.2 ppm to higher fields compared to the uncoordinated carbonyl compounds. Coordination shifts were also observed in the ^{1}H NMR spectra for the resonances of the aldehyde hydrogen atoms, which were detected at 4.40 ppm (**II-3**) and 5.93 ppm (**II-4**) compared to 9.24 ppm (pivalaldehyde) and 9.64 ppm (benzaldehyde) in the uncoordinated molecule. Coordination has also impact on the C=O stretching mode in the IR spectra as the characteristic stretching vibrations of uncoordinated ketones and aldehydes between 1695 cm^{-1} and 1740 cm^{-1} are shifted into the “fingerprint” region with loss of

intensity. Hence the C=O stretching vibrations of the complexes **II-3 – II-8** were not reliably identified.

Although complex **6a** is known to readily activate C–F bonds of polyfluorinated aromatics, no indication for a side reaction due to C–F bond activation for the reaction of **6a** with 4,4´-difluorobenzophenone or methyltrifluoroacetate was found, i.e. nickel insertion into one of the C–F bonds of the substrates was not observed. Both complexes [Ni(^{i}Pr$_2$Im)$_2$(η^2-O=C(4-F-C$_6$H$_4$)$_2$)] **II-7** and [Ni(^{i}Pr$_2$Im)$_2$(η^2-O=C(OMe)(CF$_3$))] **II-8** are also stable regarding further C–F bond activation pathways under thermal and photolytic conditions. All complexes **II-3 – II-8** are also stable with respect to further C–C and C–H bond cleavage at the carbonyl function, which has some precedence in the literature for other transition metal complexes.[21]

Table II.2 $^{13}C\{^1H\}$ NMR and ^1H NMR shifts [ppm] of the carbonyl carbon atoms and the aldehyde hydrogen atoms of the complexes **II-3 – II-8** (δ_C = $^{13}C\{^1H\}$ NMR shift of the carbonyl carbon atom; $\Delta\delta_C$ = $^{13}C\{^1H\}$ coordination shift of the carbonyl carbon atom; δ_H = ^1H NMR shift of the aldehyde hydrogen atom; $\Delta\delta_H$ = ^1H coordination shift of the aldehyde hydrogen atom; $\delta_{C\ NHC}$ = $^{13}C\{^1H\}$ NMR shift of the NHC carbene carbon atom).

Compound	δ_C	$\Delta\delta_C$	δ_H	$\Delta\delta_H$	$\delta_{C\ NHC}$
II-3	87.6	-105.5	4.40	-4.84	196.9, 199.7
II-4	73.9	-117.6	5.93	-3.71	195.3, 197.1
II-5	74.9	-122.2	-	-	195.3, 196.8
II-6	80.2	-115.8	-	-	194.6, 194.8
II-7	78.1	-115.9	-	-	194.3, 194.4
II-8	92.2	-65.8	-	-	192.1, 192.3

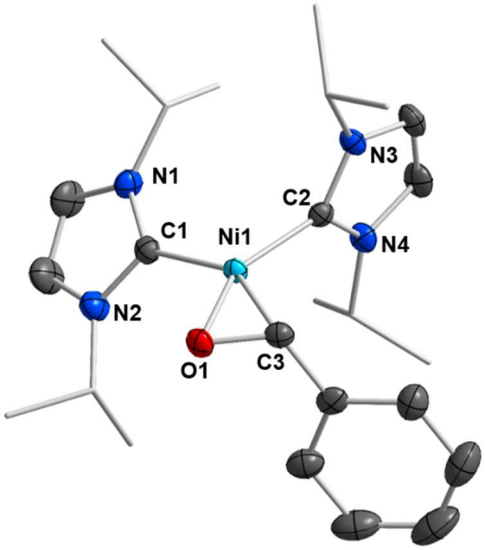

Figure II.2 Molecular structure of [Ni(^{i}Pr$_2$Im)$_2$(η^2-O=CHPh)] **II-4** in the solid state (ellipsoids set at 50 % probability level). Hydrogen atoms have been omitted for clarity. Selected bond lengths [Å] and angles [°] of **II-4**: Ni1–C1 1.949(2), Ni1–C2 1.879(2), Ni1–O1 1.887(2), Ni1–C3 1.924(2), O1–C3 1.343(2), C1–N1 1.367(3), C1–N2 1.371(3), C2–N3 1.366(2), C2–N4 1.364(3), C1–Ni1–C2 103.36(9), C1–Ni1–O1 108.02(8), O1–Ni1–C3 41.24(8), C2–Ni1–C3 107.10(8), N1–C1–N2 102.84(17), N3–C2–N4 103.52(17), plane (C1–Ni1–C2) – plane (Ni1–O1–C3) 9.95(8), plane (N1–C1–N2) – plane (Ni1–O1–C3) 42.55(9), plane (N3–C2–N4) – plane (Ni1–O1–C3) 87.53(10), plane (N1–C1–N2) – plane (N3–C2–N4) 81.08(18).

Crystals suitable for X-ray diffraction of complex **II-4** were obtained from a saturated benzene solution at room temperature (Figure II.2). Complex **II-4** crystallizes in the monoclinic space group P2$_1$/n and adopts a distorted pseudo square planar geometry, spanned by the two NHC ligands and the benzaldehyde ligand. The aldehyde ligand coordinates *via* the carbonyl carbon atom and oxygen atom with a Ni–C distance of 1.924(2) Å and a Ni–O distance of 1.887(2) Å, and lies almost perfectly in the $C_{carbene}$–Ni–$C_{carbene}$ plane, the deviation of the oxygen atom to the plane C_{NHC}-Ni-C_{NHC} is 0.1373(14) Å, the deviation of the carbonyl carbon atom 0.304(2) Å and the twist between the planes C_{NHC}-Ni-C_{NHC} and Ni1–O1–C3 is 9.95(8)°. The asymmetry brought into the complex by the benzaldehyde ligand is reflected in the different Ni–C distances to the NHC carbene carbon atoms of 1.949(2) Å for Ni–C1 *trans* to the benzaldehyde carbonyl carbon atom and 1.879(2) Å for Ni–C2 *trans* to the benzaldehyde carbonyl oxygen atom. Despite of this remarkable difference both Ni–C_{NHC} distances are still in

line with lengths observed previously for related η^2-coordinated nickel-olefin and nickel-alkyne complexes.[8a, 9b, 11] The C3–O1 distance of 1.343(2) Å of the benzaldehyde ligand is slightly larger compared to the bond length of with 1.325(7) Å observed in the analogous phosphine complex [Ni(PCy$_3$)$_2$(η^2-O=CHPh)].[22] The Ni1–C3 distance in **II-4** of 1.924(2) Å is also shorter compared to those of the phosphine complex [Ni(PCy$_3$)$_2$(η^2-O=CHPh)], while the Ni1–O1 bond length of 1.8873(15) Å is almost the same ([Ni(PCy$_3$)$_2$(η^2-O=CHPh)]: Ni–O 1.867(3) Å, Ni–C 1.983(5) Å). These parameter indicate stronger back-donation for **II-4** from nickel to the benzaldehyde ligand in the Ni–C–O three-membered ring.

To get further insight into the general reactivity of [Ni(Mes$_2$Im)$_2$] **1** and to compare the reactivity of **1** with that of the complex with the smaller carbene **6**, complex **1** was also reacted with different ketones and aldehydes (Scheme II.4). As the reactivity of **1** with non-activated olefins is rather limited, highly electron-poor π-systems, in which metal-centered backbonding increases, react readily with **1**. The reactions of **1** with benzaldehyde, *iso*-butyraldehyde, 4-(dimethylamino)benzaldehyde, 4-(methoxy)benzaldehyde, benzophenone and 4,4´-difluorobenzophenone similarly afforded the corresponding η^2-(*C,O*)-complexes [Ni(Mes$_2$Im)$_2$(η^2-O=CHPh)] **II-9**, [Ni(Mes$_2$Im)$_2$(η^2-O=CH(CH(CH$_3$)$_2$))] **II-10**, [Ni(Mes$_2$Im)$_2$(η^2-O=CH(4-NMe$_2$-C$_6$H$_4$))] **II-11**, [Ni(Mes$_2$Im)$_2$(η^2-O=CH(4-OMe-C$_6$H$_4$))] **II-12**, [Ni(Mes$_2$Im)$_2$(η^2-O=CPh$_2$)] **II-13** and [Ni(Mes$_2$Im)$_2$(η^2-O=C(4-F-C$_6$H$_4$)$_2$)] **II-14**.

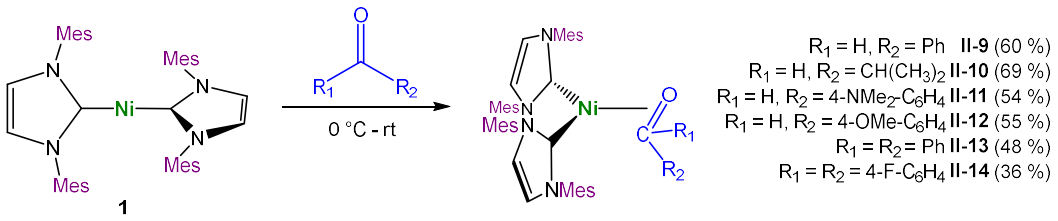

Scheme II.4 Synthesis of [Ni(Mes$_2$Im)$_2$(η^2-O=CHPh)] **II-9**, [Ni(Mes$_2$Im)$_2$(η^2-O=CH(CH(CH$_3$)$_2$))] **II-10**, [Ni(Mes$_2$Im)$_2$(η^2-O=CH(4-NMe$_2$-C$_6$H$_4$))] **II-11**, [Ni(Mes$_2$Im)$_2$(η^2-O=CH(4-OMe-C$_6$H$_4$))] **II-12**, [Ni(Mes$_2$Im)$_2$(η^2-O=CPh$_2$)] **II-13** and [Ni(Mes$_2$Im)$_2$(η^2-O=C(4-F-C$_6$H$_4$)$_2$)] **II-14**.

The complexes were isolated as yellow or red to brown, air and moisture sensitive powders and have been characterized by using ^{1}H NMR-, ^{13}C{^{1}H} NMR-, IR-spectroscopy and elemental analysis (see Experimental). The complexes **II-9 – II-14** also tend to decompose under mass spectrometric conditions (LIFDI). In contrast to the complexes **II-3 – II-8** with the small NHC ligand ^{i}Pr$_2$Im, the complexes **II-9 – II-14** of the bulkier Mes$_2$Im ligand show extremely broadened ^{1}H NMR and ^{13}C{^{1}H} NMR spectra for the NHC ligand due to hindered rotation presumably of both, the NHC and the keto/aldehyde ligand. For example, the mesityl methyl proton resonances in the ^{1}H NMR spectra of **II-9 – II-14** overlap in the region between 1.48 ppm and 2.32 ppm which is caused by signal broadening. Nevertheless, all characteristic resonances have been assigned and the integration of the resonances is consistent with the expectations. Also, the resonances of the backbone hydrogen atoms can be found as broad singlets in the range between 5.94 ppm and 6.15 ppm whereas the mesityl aryl protons were observed as sharp resonances between 6.73 ppm and 6.88 ppm. The ^{1}H NMR resonances of the aldehyde hydrogen atoms and the ^{13}C{^{1}H} NMR signals of the carbonyl carbon atom are shifted into regions between 3.98 ppm and 4.85 ppm and 76.0 ppm and 86.7 ppm, respectively, upon coordination (Table II.3).The ^{13}C{^{1}H} NMR resonances of the NHC carbene carbon atoms for each complex were observed in each case in the region between 199.4 ppm and 202.7 ppm.

EPR measurements were performed on [Ni(Mes$_2$Im)$_2$(η^2-O=CHPh)] **II-9** at room temperature to exclude line broadening of the NMR resonances of isolated **II-9 – II-14** by radical side products or radical impurities, and these EPR experiments confirm the absence of radical species. A variable temperature ^{1}H NMR experiment of **II-9** in THF-d_8 reveals at -90 °C a ^{1}H NMR spectrum with 12 sharp singlets in the region between 1.01 ppm and 2.51 ppm for the 12 methyl groups of the inequivalent mesityl substituents. At the high temperature limit at +90 °C in toluene-d_8 two sharp signals are observed, i.e. one resonance for the *ortho*- and one resonance for the *para*-methyl groups. This observation confirms that the broadening at room temperature is caused by the hindered rotation of the ligand due to the steric demand of the bulky Mes$_2$Im ligands and simultaneously shows the high thermal stability of these compounds.

Table II.3 $^{13}C\{^1H\}$ NMR and ^1H NMR coordination shifts [ppm] of the coordinated carbonyl carbon atoms and the aldehyde hydrogen atoms in the complexes **II-9 – II-14** (δ_C = $^{13}C\{^1H\}$ NMR shift of the carbonyl carbon atom; $\Delta\delta_C$ = $^{13}C\{^1H\}$ coordination shift of the carbonyl carbon atom; δ_H = ^1H NMR shift of the aldehyde hydrogen atom; $\Delta\delta_H$ = ^1H coordination shift of the aldehyde hydrogen atom; $\delta_{C\ NHC}$ = $^{13}C\{^1H\}$ NMR shift of the NHC carbene carbon atom).

Compound	δ_C	$\Delta\delta_C$	δ_H	$\Delta\delta_H$	$\delta_{C\ NHC}$
II-9	76.5	-115.0	4.85	-4.79	199.4, 202.2
II-10	86.7	-118.3	3.98	-5.25	202.3, 202.7
II-11	76.8	-112.2	4.83	-5.02	200.4, 202.7
II-12	76.0	-115.0	4.78	-4.91	199.8, 202.5
II-13	83.5	-112.5	-	-	201.1
II-14	79.7	-113.8	-	-	199.6

Crystals of **II-9** and **II-10** suitable for X-ray diffraction were obtained from storing a saturated solution of the complex in hexane at -30 °C for several weeks (Figure II.3). Complex **II-9** crystallizes in the triclinic space group $P\bar{1}$ and complex **II-10** in the orthorhombic space group $P2_12_12_1$. Important crystallographic data of the complexes **II-4**, **II-9**, **II-10** and the analogous phosphine complex [Ni(PCy_3)$_2$(η^2-O=CHPh)] **27** are summarized in Table II.4. Both complexes adopt a distorted pseudo square planar geometry, but show much larger C_{NHC}-Ni-C_{NHC} angles (i.e. C1–Ni1–C2 angles) of 122.69(6)° (**II-9**) and 130.89(14)° (**II-10**) compared to the aldehyde complex of the small NHC, Ni(^{i}Pr$_2$Im)$_2$(η^2-O=CHPh)] **II-4** (103.36(9)°), which is associated with the increased steric demand of the bulkier NHC Mes$_2$Im compared to ^{i}Pr$_2$Im. The C–O distances of 1.3279(19) Å (**II-9**) and 1.333(4) Å (**II-10**) are in between the distances observed for the phosphine complex [Ni(PCy_3)$_2$(η^2-O=CHPh)] **27** (1.325(7) Å)[22] and for **II-4** (1.343(2) Å), which can be attributed to the net donor properties of the complexes with the co-ligands PCy_3 < Mes$_2$Im < ^{i}Pr$_2$Im. As it was observed for the ethylene complexes before, these values can be correlated to the different donor properties of the NHC ligand and the different C_{NHC}-Ni-C_{NHC} angles of 103.36(9)° (**II-4**), 122.69(6) (**II-9**) and 130.89(14) (**II-10**). Similar as observed for **II-4** and [Ni(PCy_3)$_2$(η^2-

O=CHPh)] **27**, the Ni-C distances from Ni to the NHC carbene carbon atom *trans* to the aldehyde oxygen atom are remarkably longer than those trans to the aldehyde carbonyl carbon atom: Ni1–C1 1.9641(15) Å (**II-9**) and 1.957(4) Å (**II-10**) compared to Ni1–C2 1.8974(15) Å (**II-9**) and 1.902(4) Å (**II-10**). The Ni–C distances to the carbonyl group of 1.9718(15) Å (**II-9**) and 1.923(3) Å (**II-10**) are longer than the Ni–O distances of 1.8752(11) Å (**II-9**) and 1.913(2) Å (**II-10**), as observed for complex **II-4**.

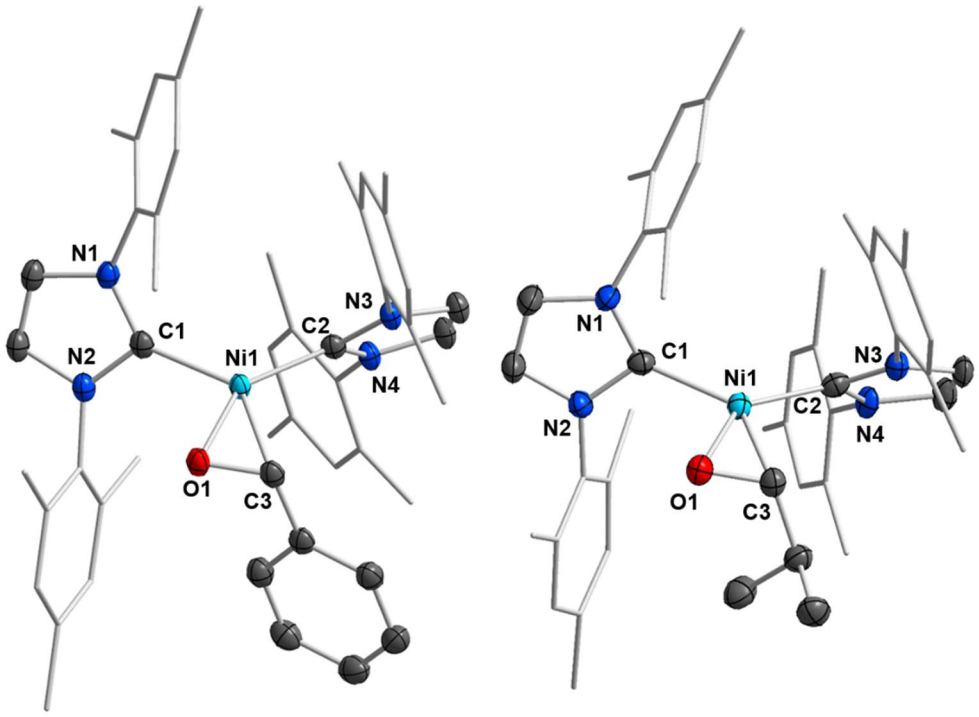

Figure II.3 Molecular structures of [Ni(Mes_2Im)$_2$(η^2-O=CHPh)] **II-9** (left) and [Ni(Mes_2Im)$_2$(η^2-O=CH(CH(CH_3)$_2$))] **II-10** (right) in the solid state (ellipsoids set at 50 % probability level). Hydrogen atoms have been omitted for clarity. Selected bond lengths [Å] and angles [°] of **II-9**: Ni1–C1 1.9641(15), Ni1–C2 1.8974(15), Ni1–O1 1.8752(11), Ni1–C3 1.9718(15), O1–C3 1.3279(19), C1–N1 1.375(2), C1–N2 1.380(2), C2–N3 1.3825(19), C2–N4 1.3789(19), C1–Ni1–C2 122.69(6), C1–Ni1–O1 94.80(5), O1–Ni1–C3 40.29(5), C2–Ni1–C3 102.33(6), N1–C1–N2 102.11(12), N3–C2–N4 101.54(12), plane (C1–Ni1–C2) – plane (Ni1–O1–C3) 5.112(99),plane (N1–C1–N2) – plane (Ni1–O1–C3) 56.22(8), plane (N3–C2–N4) – plane (Ni1–O1–C3) 72.55(10), plane (N1–C1–N2) – plane (N3–C2–N4) 66.18(11). Selected bond lengths [Å] and angles [°] of **II-10**: Ni1–C1 1.957(4), Ni1–C2 1.902(4), Ni1–O1 1.913(2), Ni1–C3 1.923(3), O1–C3 1.333(4), C1–N1 1.376(4), C1–N2 1.377(4), C2–N3 1.382(4), C2–N4 1.375(4), C1–Ni1–C2 130.89(14), C1–Ni1–O1 92.63(12), O1–Ni1–C3 40.67(12), C2–Ni1–C3

95.84(14), N1–C1–N2 101.8(3), N3–C2–N4 101.9(3), plane (C1–Ni1–C2) – plane (Ni1–O1–C3) 3.05(18), plane (N1–C1–N2) – plane (Ni1–O1–C3) 69.90(17), plane (N3–C2–N4) – plane (Ni1–O1–C3) 63.45(20), plane (N1–C1–N2) – plane (N3–C2–N4) 50.77(22).

Table II.4 Selected bond lengths and angles of the complexes [Ni(^{i}Pr$_2$Im)$_2$(η^2-O=CHPh)] **II-4**, [Ni(Mes$_2$Im)$_2$(η^2-O=CHPh)] **II-9**, [Ni(Mes$_2$Im)$_2$(η^2-O=CH(CH(CH$_3$)$_2$))] **II-10**, and [Ni(PCy$_3$)$_2$(η^2-O=CHPh)] **27**[22] (C = carbonyl carbon, L1 = NHC or phosphine on the oxygen side, L2 = NHC or phosphane on the carbon side).

	II-4	**II-9**	**II-10**	**27**[22]
$d_{C–O}$ [Å]	1.343(2)	1.3279(19)	1.333(4)	1.325(7)
$d_{Ni–O}$ [Å]	1.8873(15)	1.8752(11)	1.913(2)	1.867(3)
$d_{Ni–C}$ [Å]	1.924(2)	1.9718(15)	1.923(3)	1.983(5)
$d_{Ni–L1}$ [Å]	1.949(2)	1.9641(15)	1.957(4)	2.244(2)
$d_{Ni–L2}$ [Å]	1.879(2)	1.8974(15)	1.902(4)	2.171(2)
$\sphericalangle_{L1–Ni–L2}$ [°]	103.36(9)	122.69(6)	130.89(14)	118.9(1)

The reaction of different aryl halides with [Ni(Mes$_2$Im)$_2$] **1** or [Ni(Dipp$_2$Im)$_2$] **3**, respectively, lead to the formation of nickel centered radical nickel(I) complexes [Ni^I(NHC)$_2$X] (X = Cl, Br, I), as Louie *et al.* and Matsubara *et al.* demonstrated earlier.[23] Since it is known that ketones and aldehydes tend to form acyl radicals in the presence of transition metal complexes to further react in substitution, cyclization, carbonylation, decarbonylation or coupling reactions,[24] we wondered if the reaction of **1** or **6a** with more than one equivalent aldehyde such as benzaldehyde would lead to [Ni(^{i}Pr$_2$Im)$_2$(η^2-O=CHPh)] **II-4** and [Ni(Mes$_2$Im)$_2$(η^2-O=CHPh)] **II-9** or to a different reaction product. Whereas treatment of [Ni$_2$(^{i}Pr$_2$Im)$_4$(μ-(η^2:η^2)-COD)] **6a** with an excess benzaldehyde still affords the η^2-(*C,*O)-complex [Ni(^{i}Pr$_2$Im)$_2$(η^2-O=CHPh)] **II-4** in good yields, from the reaction of [Ni(Mes$_2$Im)$_2$] **1** with three equivalents benzaldehyde two different reaction products were isolated: the hydride carboxylate complex *trans*-[Ni(Mes$_2$Im)$_2$H(OOCPh)] **II-15** and the dimer [Ni$_2$(Mes$_2$Im)$_2$(μ_2-CO)(μ_2-η^2-*C,O*-PhCOCOPh)] **II-16** (Scheme II.5). These complexes

were crystallized by storing the mother liquor in hexane at -30 °C and were structurally characterized by X-ray diffraction (Figure II.4). Complex **II-15** can also be isolated from the reaction of **1** with benzoic acid as a cream-colored solid in 60 % yield, and was completely characterized by using ^{1}H NMR-, ^{13}C NMR-, IR-spectroscopy and elemental analysis. Complex **II-16** was isolated from the reaction mixture as a red solid but could not be separated from some residual organic impurities. However, the NMR data obtained indicate that **II-15** and **II-16** are formed selectively in a 1:1 ratio by heating the reaction mixture of **1** with three equivalents of benzaldehyde in toluene for one week at 50 °C. The observed structures (Figure II.4) are a hint to the involvement of radical side reactions, since for such electron-poor π-systems metal-centered backbonding increases and it has been shown that nickel(I) character becomes significantly more important.[17]

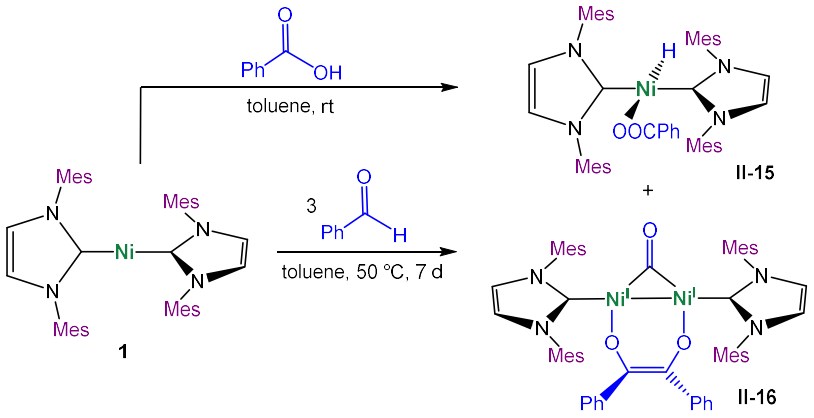

Scheme II.5 Synthesis of *trans*-[Ni(Mes$_2$Im)$_2$H(OOCPh)] **II-15** and [Ni$_2$(Mes$_2$Im)$_2$(μ_2-CO)(μ_2-η^2-C,O-PhCOCOPh)] **II-16**.

The ^{1}H NMR spectrum of **II-15** shows one set of signals for the carbene ligands with four singlet resonances at 2.00, 2.35, 6.02 and 6.84 ppm. The resonances of the aromatic protons of the carboxylate ligand can be found as two multiplets at 7.26 ppm and 7.91 ppm. The resonance for the Ni hydride was detected at -25.12 ppm. In the ^{13}C{^{1}H} NMR spectrum the resonances for the carboxylate carbon atom and the carbene carbon atoms were detected at 169.1 ppm and 187.4 ppm, respectively. In the ^{1}H NMR spectrum of the red solid (**II-16**) the resonances of the mesityl methyl protons can be detected as broad overlapping singlets in the region between 1.97 ppm and 2.27 ppm. The signal for the backbone hydrogen atoms gives rise to a singlet at

6.28 ppm. For the mesityl aryl protons two singlets were detected at 6.53 ppm and 6.75 ppm. The aryl protons of the benzil ligand have been found as multiplets at 6.79, 6.95 and 7.01 ppm. The $^{13}C\{^1H\}$ NMR spectrum reveals three characteristic signals at 111.8 ppm for the carbonyl carbon atoms of the benzil ligand, at 196.5 ppm for the carbene carbon atoms and at 263.8 ppm for the bridging carbon monoxide carbon atom.

Complex **II-15** crystallizes in the monoclinic space group $P2_1/n$ and adopts a slightly distorted square planar geometry. The Ni–NHC distances of 1.891(6) Å and 1.891(5) Å are enlarged compared to the starting complex **1** (1.827(6) Å and 1.830(6) Å).[3] The hydride ligand was refined at a rather short Ni–H distance of 1.18(5) Å [25] Keim *et al.* reported earlier the molecular structure of [{κ^P,κ^O-$Ph_2PCH_2C(CF_3)_2O$}NiH(PCy_3)], which shows a much longer Ni–H bond length of 1.37(3) Å and a shorter Ni–O distance of 1.873(2) Å,[26] compared to 1.949(4) Å (Ni1–O2) in complex **II-15**.
The dinuclear complex **II-16** crystallizes in the monoclinic space group $P2_1/c$ and shows a very short Ni–Ni bond length of 2.4005(7) Å, compared to other CO-bridged nickel complexes (2.5389-2.694(1) Å).[27] The CO-bridge between the nickel centers is asymmetric with Ni–CO distances of 1.852(4) Å (Ni1–C3) and 1.821(4) Å (Ni2–C3). Furthermore, both metal centers are bridged by a benzil ligand. Each carbonyl function of the benzil ligand is η^2 coordinated to a nickel atom with Ni–C distances of 2.044(4) Å (Ni1–C4) and 2.072(4) Å (Ni2–C5) and Ni–O distances of 1.936(3) Å (Ni1–O2) and 1.929(3) Å (Ni2–O3). The C-C axis of the benzil ligand is twisted to the Ni-Ni vector with an angle of 45.56(18)° between the planes Ni1–C3–Ni2 and C3–C4–C5. The bond lengths within the benzil ligand indicate some delocalization of the π-electrons over the four atoms O2, C4, C5 and O3. Different bonding situations can be envisaged for the benzil ligand as 1,2-diketones are known to undergo readily electron transfer with transition metal atoms.[28] 1,2-Diketones in the coordination sphere of a transition metal can be described as neutral 1,2-diketone ligands, as one-electron reduced monoanionic π-radical ligands or as two-electron reduced enediolate(2-) ligands. Referring to the classification of Wieghardt *et al.*[28b, 28c], the benzil ligand in **II-16** may be best considered as an enediolate(2-) ligand. Accordingly, complex **II-16** may be described as a dinuclear Ni(I) complex, in which each nickel center is stabilized by one NHC ligand, the bridging CO ligand and a bridging enediolate(2-) ligand. The unpaired electrons at nickel are localized in a Ni–Ni bond as the Ni1–Ni2 distance of 2.4005(7) Å

is within the region typically observed for Ni-Ni single bonds,[29] which leads to diamagnetic behavior of this complex.

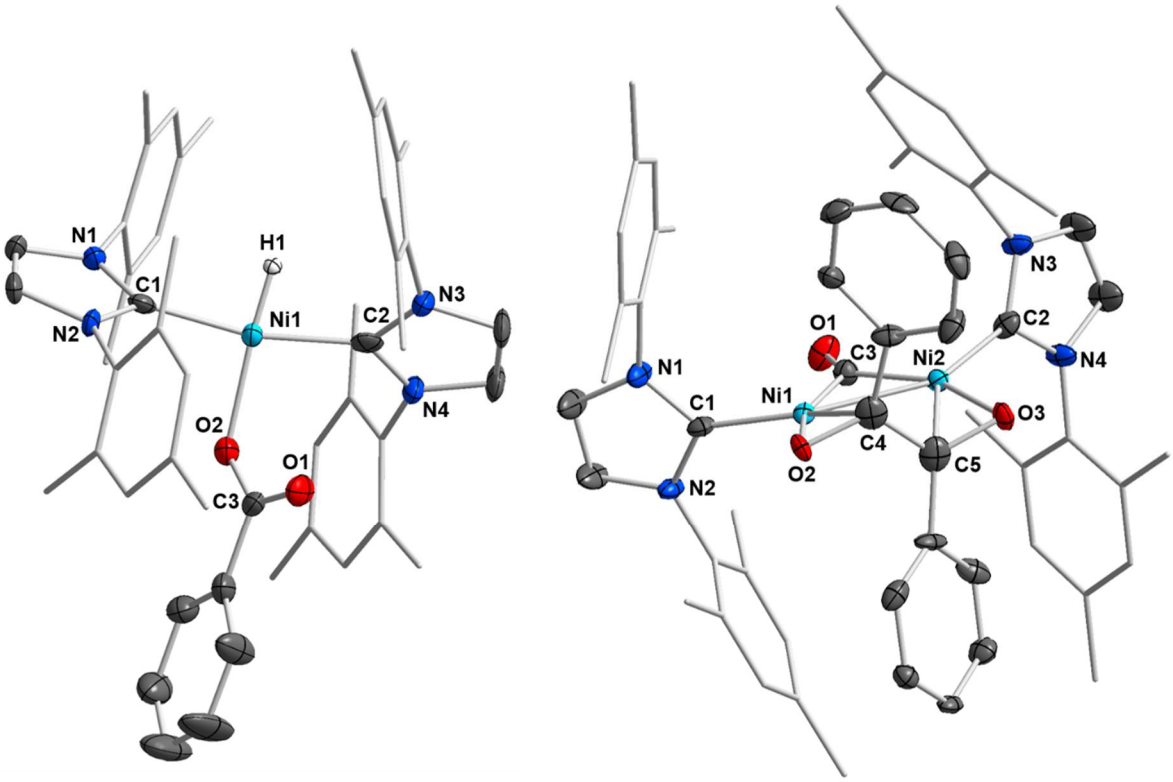

Figure II.4 Molecular structure of *trans*-[Ni(Mes$_2$Im)$_2$H(OOCPh)] **II-15** (left) and [Ni$_2$(Mes$_2$Im)$_2$(μ_2-CO)(μ_2-η^2-*C*,*O*-PhCOCOPh)] **II-16** (right) in the solid state (ellipsoids set at 50 % probability level). Hydrogen atoms have been omitted for clarity. Selected bond lengths [Å] and angles [°] of **II-15**: Ni1–C1 1.891(6), Ni1–C2 1.891(5), Ni1–H1 1.18(5), Ni1–O2 1.949(4), C1–N1 1.366(7), C1–N2 1.366(7), C2–N3 1.371(7), C2–N4 1.362(7), C3–O1 1.248(7), C3–O2 1.276(7), C1–Ni1–H1 90.5(19), C1–Ni1–O2 93.83(19), C2–Ni1–O2 98.37(19), C2–Ni1–H1 77.3(19). Selected bond lengths [Å] and angles [°] of **II-16**: Ni1–Ni2 2.4005(7), Ni1–C1 1.889(4), Ni2–C2 1.890(4), Ni1–C3 1.852(4), Ni2–C3 1.821(4), Ni1–C4 2.044(4), Ni2–C5 2.072(4), Ni1–O2 1.936(3), Ni2–O3 1.929(3), C3–O1 1.196(5), C4–C5 1.430(6), C4–O2 1.336(5), C5–O3 1.337(5), Ni1–C3–Ni2 81.61(16), Ni1–Ni2–C3 49.75(13), Ni2–Ni1–C3 48.64(12), C1–Ni1–O2 106.83(15), C1–Ni1–C3 95.03(17), O2–Ni1–C4 39.09(13), C3–Ni1–C4 119.12(16), C2–Ni2–O3 105.53(14), C2–Ni2–C3 99.37(17), O3–Ni2–C5 38.84(14), C3–Ni2–C5 116.26(17) plane (Ni1–C3–Ni2) – plane (C3–C4–C5) 45.56(18).

Although there is not any information about the mechanism which led to the formation of the complexes **II-15** and **II-16** it seems very likely that the benzil ligand in **II-16** was formed by an oxidative radical coupling of two benzaldehyde molecules with formal hydrogen elimination.[24d, 30] The CO-bridge either could have been formed by a radical decarbonylation reaction[21a, 24a] or *via* C–H activation, CO migration and subsequent elimination of benzene at nickel. Compound **II-15** is formally the O–H activation product of benzoic acid. The latter is often observed as an impurity in commercially available benzaldehyde (or some oxidation of the starting material), [24d] but such impurities were not detected by NMR spectroscopy or GC/MS in our samples. Anyway, these results demonstrate that the reaction of **1** with benzaldehyde (and aldehydes in general) might lead to multiple reaction channels, depending on the reaction conditions applied. Metal radicals generated by **1** seem to play a crucial role in these different reaction channels and investigations to further establish the application of [Ni(Mes_2Im)$_2$] **1** for electron transfer are currently in progress in our group.

2.3 Conclusion

In this chapter the reactivity of two homoleptic NHC nickel(0) complexes of NHCs of different steric demand, i.e. [Ni(Mes$_2$Im)$_2$] **1** and [Ni(iPr$_2$Im)$_2$] **6** (as provided by [Ni$_2$(^{i}Pr$_2$Im)$_4$(μ-(η^2:η^2)-COD)] **6a**) towards simple olefins and organic carbonyl compounds such as ketones and aldehydes is reported. For simple olefins the sterics of the NHC nickel complex seems to be decisive for the reactivity. Whereas it is known for complex **6a** that it readily reacts with olefins of different size, complex **1** reacts only with the smallest olefin ethylene or with activated acceptor olefins such as acrylates. Thus, the NHC nitrogen substituent influences the reactivity substantially for steric reasons. Steric congestion is also reflected in the molecular structure of **II-1**, as ethylene coordination deviates from planarity in **II-1** compared to [Ni(^{i}Pr$_2$Im)$_2$(η^2-H$_2$C=CH$_2$)] **24**, i.e. the plane C$_{olefin}$–Ni–C$_{olefin}$ is twisted by 13.78(24)° with respect to C$_{carbene}$–Ni–C$_{carbene}$ plane in **II-1**, remarkably larger than the twist observed for **24** (1.85(14)°).

Furthermore, the molecular structure of **II-1** unravels a significant enlargement of the angle C$_{NHC}$-Ni-C$_{NHC}$ for the [Ni(NHC)$_2$] moiety as compared to **24** (from 102.41(9)° in **24** to 131.01(15)° in **II-1**). In both cases the good net donor properties of NHC ligands should allow for strong backdonation, which depends on the nature of the NHC, but backdonation is also influenced by the C$_{NHC}$-M-C$_{NHC}$ bite angle. The sterically less demanding, but better electron releasing NHC ^{i}Pr$_2$Im leads to olefin complexes with a smaller C$_{NHC}$-M-C$_{NHC}$ bite-angle and, both, the (i) better donor capabilities and (ii) smaller bite angle allow stronger backbonding into the π^*-orbital of the olefin for [Ni(^{i}Pr$_2$Im)$_2$] **6**. A better charge transfer to the olefin leads to a stronger metal-olefin bond and thus to a more stable olefin complex for [Ni(^{i}Pr$_2$Im)$_2$] **6** as compared to [Ni(Mes$_2$Im)$_2$] **1**. Accordingly, the variation of the sterics at the NHC nitrogen substituents does not only modify reactivity for simple steric reasons (olefins larger than ethylene do not noticeably react to yield stable complexes) but also for electronic reasons (modification of the donor/acceptor properties of the carbene plus modification of the bite angle in [Ni(NHC)$_2$]) which leads to different bonding, different activation of the π-acidic ligand and thus to modification in the reactivity of both complexes [Ni(^{i}Pr$_2$Im)$_2$] **6** and [Ni(Mes$_2$Im)$_2$] **1**.

Whereas the reactivity of **1** with non-activated olefins is rather limited, electron-poor *π*-systems, in which metal-centered backbonding increases, react readily with **1**. The reaction of [Ni(Mes$_2$Im)$_2$] **1** or [Ni$_2$(^{i}Pr$_2$Im)$_4$(*μ*-(*η*^{2}:*η*^{2})-COD)] **6a** with ketones or aldehydes afforded complexes with *side-on* *η*^{2}-(*C,O*)-coordinating ligands: [Ni(^{i}Pr$_2$Im)$_2$(*η*^{2}-O=CH^{t}Bu)] **II-3**, [Ni(^{i}Pr$_2$Im)$_2$(*η*^{2}-O=CHPh)] **II-4**, [Ni(^{i}Pr$_2$Im)$_2$(*η*^{2}-O=CMePh)] **II-5**, [Ni(^{i}Pr$_2$Im)$_2$(*η*^{2}-O=CPh$_2$)] **II-6**, [Ni(^{i}Pr$_2$Im)$_2$(*η*^{2}-O=C(4-F-C$_6$H$_4$)$_2$)] **II-7**, [Ni(^{i}Pr$_2$Im)$_2$(*η*^{2}-O=C(OMe)(CF$_3$))] **II-8** and [Ni(Mes$_2$Im)$_2$(*η*^{2}-O=CHPh)] **II-9**, [Ni(Mes$_2$Im)$_2$(*η*^{2}-O=CH(CH(CH$_3$)$_2$))] **II-10**, [Ni(Mes$_2$Im)$_2$(*η*^{2}-O=CH(4-NMe$_2$-C$_6$H$_4$))] **II-11**, [Ni(Mes$_2$Im)$_2$(*η*^{2}-O=CH(4-OMe-C$_6$H$_4$))] **II-12**, [Ni(Mes$_2$Im)$_2$(*η*^{2}-O=CPh$_2$)] **II-13** and [Ni(Mes$_2$Im)$_2$(*η*^{2}-O=C(4-F-C$_6$H$_4$)$_2$)] **II-14**. All complexes were isolated as yellow, orange or red to brown, air and moisture sensitive solids in moderate to good yields. According to the X-ray structures of **II-4**, **II-9** and **II-10** these complexes adopt a distorted pseudo square planar geometry. Again, the Mes$_2$Im complexes **II-9** and **II-10** have much larger C$_{NHC}$-Ni-C$_{NHC}$ angles (i.e. C1–Ni1–C2 angles) of 122.69(6)° (**II-9**) and 130.89(14)° (**II-10**) compared to the aldehyde complex of the small NHC, Ni(^{i}Pr$_2$Im)$_2$(*η*^{2}-O=CHPh)] **II-4** (103.36(9)°). Accordingly, the C–O distances of 1.3279(19) Å (**II-9**) and 1.333(4) Å (**II-10**) are smaller than the C–O distances observed for **II-4** (1.343(2) Å). Furthermore, two different side products from the reaction of **1** with benzaldehyde were identified, i.e. *trans*-[Ni(Mes$_2$Im)$_2$H(OOCPh)] **II-15** and [Ni$_2$(Mes$_2$Im)$_2$(*μ*$_2$-CO)(*μ*$_2$-*η*^{2}-*C,O*-PhCOCOPh)] **II-16**, which indicate that radical intermediates are important for the reaction of **1** with aldehydes and ketones.

This chapter demonstrates that substrate binding and electron transfer to coordinated substrates in bis-NHC nickel complexes can be very well fine-tuned upon a change of the sterics of the NHC ligand beyond the accessibility of the metal center (steric protection) and the complex stability (co-ligand/NHC dissociation) which lies in the different donor properties of the differently *N*-substituted NHCs, in the C$_{NHC}$-M-C$_{NHC}$ bite-angle NHC ligands of different size adopt in the final product and the propensity of the complexes [Ni(NHC)$_2$] to get involved into radical electron transfer processes. We anticipate that the tuning of both electron-donating properties and the steric size of the NHC (keeping [Ni(NHC)$_2$] intact) will allow for an additional handle in the design of catalysts for a wide range of processes that involve similar starting materials or intermediates.

2.4 References

[1] A. J. Arduengo, R. L. Harlow, M. Kline, *J. Am. Chem. Soc.* **1991**, *113*, 361-363.

[2] a) F. Glorius, *N-Heterocyclic Carbenes in Transition Metal Catalysis,* Springer, Berlin Heidelberg, **2007**, Vol. 21; b) C. S. J. Cazin, *Dalton Trans.* **2013**, *42*; c) P. de Frémont, N. Marion, S. P. Nolan, *Coord. Chem. Rev.* **2009**, *253*, 862-892; d) S. Díez-González, *N-Heterocyclic Carbenes: From Laboratory Curiosities to Efficient Synthetic Tools*, Royal Society of Chemistry, **2010**; e) S. Diez-Gonzalez, N. Marion, S. P. Nolan, *Chem. Rev.* **2009**, *109*, 3612-3676; f) F. E. Hahn, M. C. Jahnke, *Angew. Chem.* **2008**, *120*, 3166-3216; *Angew. Chem. Int. Ed.* **2008**, *47*, 3122-3172. g) W. A. Herrmann, *Angew. Chem.* **2002**, *114*, 1342-1363; *Angew. Chem. Int. Ed.* **2002**, *41*, 1290-1309; h) S. Nolan, *N-Heterocyclic Carbenes in Synthesis*, Wiley-VCH, **2006**; i) S. P. Nolan, *N-Heterocyclic Carbenes: Effective Tools for Organometallic Synthesis*, Wiley-VCH, **2014**; j) M. Poyatos, J. A. Mata, E. Peris, *Chem. Rev.* **2009**, *109*, 3677-3707; k) S. P. Nolan, T. Rovis, *Synlett* **2013**, *24*, 1188-1189.

[3] A. J. Arduengo, S. F. Gamper, J. C. Calabrese, F. Davidson, *J. Am. Chem. Soc.* **1994**, *116*, 4391-4394.

[4] a) R. H. Crabtree, *The organometallic chemistry of the transition metals*, 6th. ed., Wiley-VCH, New York, **2014**; b) J. F. Hartwig, *Organotransition metal chemistry: from bonding to catalysis*, University Science Books, Sausalito, CA., **2010**.

[5] D. J. Nelson, F. Maseras, *Chem. Commun.* **2018**, *54*, 10646-10649.

[6] a) J. Montgomery, *Angew. Chem.* **2004**, *116*, 3980-3998; *Angew. Chem. Int. Ed.* **2004**, *43*, 3890-3908; b) E. P. Jackson, J. Montgomery, *J. Am. Chem. Soc.* **2015**, *137*, 958-963; c) A. J. Nett, J. Montgomery, P. M. Zimmerman, *ACS Catalysis* **2017**, *7*, 7352-7362; d) A. P. Prakasham, P. Ghosh, *Inorg. Chim. Acta.* **2015**, *431*, 61-100; e) A. W. Rand, J. Montgomery, *Chem. Sci.* **2019**, *10*, 5338-5344; f) A. Thakur, J. Louie, *Acc. Chem. Res.* **2015**, *48*, 2354-2365; g) P. M. Zimmerman, A. Paul, C. B. Musgrave, *Inorg. Chem.* **2009**, *48*, 5418-5433; h) A. A. Danopoulos, T. Simler, P. Braunstein, *Chem. Rev.* **2019**, *119*, 3730-3961; i) T. Inatomi, Y. Fukahori, Y. Yamada, R. Ishikawa, S. Kanegawa, Y. Koga, K. Matsubara, *Catal. Sci. Technol.* **2019**, *9*, 1784-1793; j) K. Matsubara, Y. Fukahori, T. Inatomi, S. Tazaki, Y. Yamada, Y. Koga, S. Kanegawa, T. Nakamura, *Organometallics* **2016**, *35*, 3281-3287.

[7] a) J. Zhou, M. W. Kuntze-Fechner, R. Bertermann, U. S. D. Paul, J. H. J. Berthel, A. Friedrich, Z. Du, T. B. Marder, U. Radius, *J. Am. Chem. Soc.* **2016**, *138*, 5250-5253; b) Y. Tian, X. Guo, M. Kuntze-Fechner, I. Krummenacher, H. Braunschweig, U. Radius, A. Steffen, T. B. Marder, *J. Am. Chem. Soc.* **2018**, *140*, 17612-17623.

[8] a) T. Schaub, U. Radius, *Chem. Eur. J.* **2005**, *11*, 5024-5030; b) T. Schaub, M. Backes, U. Radius, *J. Am. Chem. Soc.* **2006**, *128*, 15964-15965; c) T. Schaub, M. Backes, U. Radius, *Eur. J. Inorg. Chem.* **2008**, 2680-2690; d) T. Schaub, P. Fischer, A. Steffen, T. Braun, U. Radius, A. Mix, *J. Am. Chem. Soc.* **2008**, *130*, 9304-9317; e) T. Schaub, P. Fischer, T. Meins, U. Radius, *Eur. J. Inorg. Chem.* **2011**, 3122-3126; f) P. Fischer, K. Götz, A. Eichhorn, U. Radius, *Organometallics* **2012**, *31*, 1374-1383; g) J. Zhou, J. H. Berthel, M. W. Kuntze-Fechner, A. Friedrich, T. B. Marder, U. Radius, *J. Org. Chem.* **2016**, *81*, 5789-5794; h) M. W. Kuntze-Fechner, C. Kerpen, D. Schmidt, M. Häring, U. Radius, *Eur. J. Inorg. Chem.* **2019**, 1767-1775.

[9] a) T. Schaub, U. Radius, *Z. Anorg. Allg. Chem.* **2006**, *632*, 981-984; b) T. Schaub, M. Backes, U. Radius, *Organometallics* **2006**, *25*, 4196-4206; c) P. Fischer, T. Linder, U. Radius, *Z. Anorg. Allg. Chem.* **2012**, *638*, 1491-1496; d) J. H. J. Berthel, L. Tendera, M. W. Kuntze-Fechner, L. Kuehn, U. Radius, *Eur. J. Inorg. Chem.* **2019**, *2019*, 3061-3072.

[10] a) T. Schaub, C. Döring, U. Radius, *Dalton Trans.* **2007**, 1993-2002; b) T. Schaub, M. Backes, U. Radius, *Chem. Commun.* **2007**, 2037-2039; c) T. Schaub, M. Backes, O. Plietzsch, U. Radius, *Dalton Trans.* **2009**, 7071-7079; d) T. Zell, T. Schaub, K. Radacki, U. Radius, *Dalton Trans.* **2011**, *40*, 1852-1854; e) B. Zarzycki, T. Zell, D. Schmidt, U. Radius, *Eur. J. Inorg. Chem.* **2013**, *2013*, 2051-2058; f) C. Hauf, J. E. Barquera-Lozada, P. Meixner, G. Eickerling, S. Altmannshofer, D. Stalke, T. Zell, D. Schmidt, U. Radius, W. Scherer, *Z. Anorg. Allg. Chem.* **2013**, *639*, 1996-2004; g) D. Schmidt, T. Zell, T. Schaub, U. Radius, *Dalton Trans.* **2014**, *43*, 10816-10827.

[11] a) T. Schaub, *Neuartige Nickel-Carbenkomplexe und deren Anwendung in Element-Element-Aktivierungsreaktionen*, Dissertation, Cuvillier Verlag, Universität Karlsruhe, **2006**; b) T. Schaub, U. Radius, *Z. Anorg. Allg. Chem.* **2007**, *633*, 2168-2172.

[12] N. D. Clement, K. J. Cavell, L.-I. Ooi, *Organometallics* **2006**, *25*, 4155-4165.

[13] N. D. Harrold, A. R. Corcos, G. L. Hillhouse, *J. Organomet. Chem.* **2016**, *813*, 46-54.

[14] a) J. Chatt, L. A. Duncanson, *J. Chem. Soc.* **1953**, 2939-2947; b) M. J. S. Dewar, *Bull. Soc. Chim. Fr.* **1951**, C71-79.

[15] W. Dreissig, H. Dietrich, *Acta Crystallogr., Sect. B: Struct.Sci* **1981**, *37*, 931-932.

[16] a) R. Dorta, E. D. Stevens, N. M. Scott, C. Costabile, L. Cavallo, C. D. Hoff, S. P. Nolan, *J. Am. Chem. Soc.* **2005**, *127*, 2485-2495; b) A. Poater, B. Cosenza, A. Correa, S. Giudice, F. Ragone, V. Scarano, L. Cavallo, *Eur. J. Inorg. Chem.* **2009**, 1759-1766; c) H. Clavier, S. P. Nolan, *Chem. Commun.* **2010**, *46*, 841-861.

[17] A. N. Desnoyer, W. He, S. Behyan, W. Chiu, J. A. Love, P. Kennepohl, *Chem. Eur. J.* **2019**, *25*, 5259-5268.

[18] a) P. Hofmann, H. Heiß, G. Müller, *Z. Naturforsch. B* **1987**, *42*, 395-409; b) L. P. Wolters, R. Koekkoek, F. M. Bickelhaupt, *ACS Catalysis* **2015**, *5*, 5766-5775; c) L. P. Wolters, W. J. van Zeist, F. M. Bickelhaupt, *Chem. Eur. J.* **2014**, *20*, 11370-11381.

[19] E. I. Bzowej, F. J. Montgomery, *Ethylenebis(triphenylphosphine)nickel(0). Encyclopedia of Reagents for Organic Synthesis.*, John Wiley & Sons, Chichester, UK, **2001**.

[20] F. Hering, J. Nitsch, U. Paul, A. Steffen, F. M. Bickelhaupt, U. Radius, *Chem. Sci.* **2015**, *6*, 1426-1432.

[21] a) M. A. Garralda, *Dalton Trans.* **2009**, 3635-3645; b) M. Murakami, H. Amii, Y. Ito, *Nature* **1994**, *370*, 540-541; c) J. W. Suggs, *J. Am. Chem. Soc.* **1978**, *100*, 640-641; d) J. W. Suggs, C. H. Jun, *J. Am. Chem. Soc.* **1984**, *106*, 3054-3056; e) T. Morioka, A. Nishizawa, T. Furukawa, M. Tobisu, N. Chatani, *J. Am. Chem. Soc.* **2017**, *139*, 1416-1419.

[22] J. Kaiser, J. Sieler, D. Walther, E. Dinjus, L. Golic, *Acta Crystallogr., Sect. B: Struct.Sci* **1982**, *38*, 1584-1586.

[23] a) S. Miyazaki, Y. Koga, T. Matsumoto, K. Matsubara, *Chem. Commun.* **2010**, *46*, 1932-1934; b) K. Zhang, M. Conda-Sheridan, S. R. Cooke, J. Louie, *Organometallics* **2011**, *30*, 2546-2552.

[24] a) C. Chatgilialoglu, D. Crich, M. Komatsu, I. Ryu, *Chem. Rev.* **1999**, *99*, 1991-2070; b) M. Nakajima, E. Fava, S. Loescher, Z. Jiang, M. Rueping, *Angew. Chem.* **2015**, *127*, 8952-8956; *Angew. Chem. Int. Ed.* **2015**, *54*, 8828-88832; c) S. Winstein, F. H. Seubold, *J. Am. Chem. Soc.* **1947**, *69*, 2916-2917; d) T.

Punniyamurthy, S. J. S. Kalra, J. Iqbal, *Tetrahedron Lett.* **1994**, *35*, 2959-2960; e) Y. Hoshimoto, Y. Hayashi, H. Suzuki, M. Ohashi, S. Ogoshi, *Angew. Chem.* **2012**, *124*, 10970-10973; *Angew. Chem. Int. Ed.* **2012**, *51*, 10812-10815.

[25] N. A. Eberhardt, H. Guan, *Chem. Rev.* **2016**, *116*, 8373-8426.

[26] U. Müller, W. Keim, C. Krüger, P. Betz, *Angew. Chem.* **1989**, *101*, 1066-1067.

[27] I. S. Ignatyev, H. F. Schaefer, R. B. King, S. T. Brown, *J. Am. Chem. Soc.* **2000**, *122*, 1989-1994.

[28] a) G. H. Spikes, E. Bill, T. Weyhermüller, K. Wieghardt, *Chem. Commun.* **2007**, 4339-4341; b) G. H. Spikes, C. Milsmann, E. Bill, T. Weyhermüller, K. Wieghardt, *Inorg. Chem.* **2008**, *47*, 11745-11754; c) G. H. Spikes, S. Sproules, E. Bill, T. Weyhermüller, K. Wieghardt, *Inorg. Chem.* **2008**, *47*, 10935-10944; d) C. G. Pierpont, *Coord. Chem. Rev.* **2001**, *216-217*, 99-125.

[29] a) U. Denninger, J. J. Schneider, G. Wilke, R. Goddard, C. Krüger, *Inorg. Chim. Acta.* **1993**, *213*, 129-140; b) B. R. Dible, M. S. Sigman, A. M. Arif, *Inorg. Chem.* **2005**, *44*, 3774-3776.

[30] C. Liu, D. Liu, A. Lei, *Acc. Chem. Res.* **2014**, *47*, 3459-3470.

Chapter III

A Case Study of *N*-^{i}Pr versus *N*-Mes Substituted NHC Ligands in Nickel Chemistry: The Coordination and Cyclotrimerization of Alkynes at [Ni(NHC)$_2$]

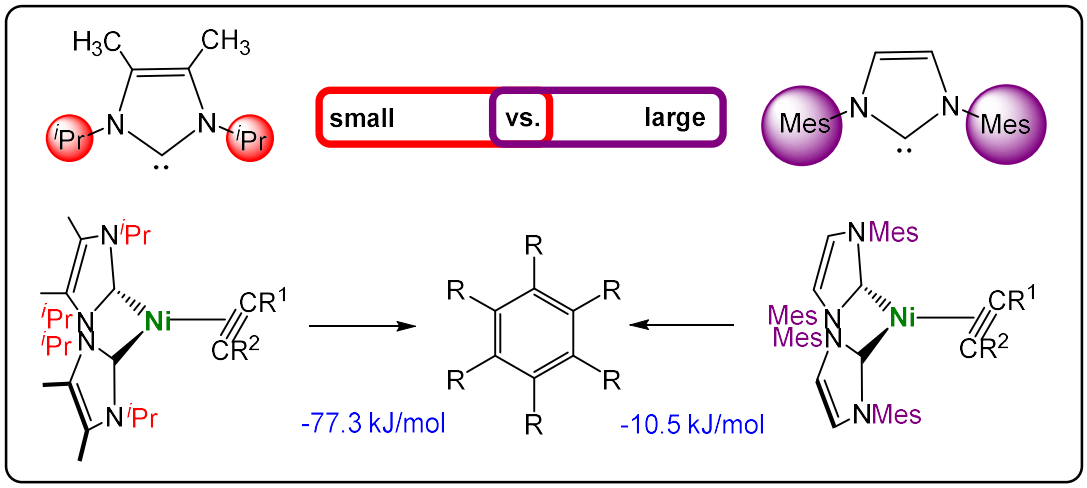

3 A Case Study of *N*-^{i}Pr versus *N*-Mes Substituted NHC Ligands in Nickel Chemistry: The Coordination and Cyclotrimerization of Alkynes at [Ni(NHC)$_2$]

3.1 Introduction

Transition metal catalyzed [2+2+2] cycloaddition reactions are elegant, atom-efficient and group tolerant processes which involve the formation of several C–C bonds in a single step.[1] These reactions offer convenient access to a wide variety of carbocycles and heterocycles, mostly aromatic, starting from simple and inexpensive substrates.[1] After Reppe *et al.* provided their pioneering report on the first cyclopolymerization of acetylene using a mixture of $NiBr_2$ and CaC_2 as the precatalyst,[2] many different unsaturated substrates such as alkynes, diynes, alkenes, imines, *iso*cyanates, *iso*thiocyanates and CO_2 were transformed in cycloaddition reactions to yield highly substituted derivatives of benzenes, pyridines, pyridones, pyrones, thiopyridones and cyclohexanes. Since then, catalytic systems such as $NiBr_2$/dppe in the presence of Zn powder or [Ni(η^4-COD)$_2$]-based systems have been applied to many substrates.[1b-l, 3] Nickel complexes of *N*-heterocyclic carbenes (NHCs) were also explored in cyclo-addition reactions in the last 2 decades, mainly by Louie[3a, 3b] and Montgomery[4] and co-workers. The Louie group commonly employed an *in situ* prepared catalyst system using [Ni(η^4-COD)$_2$] as a nickel source and two equivalents of a sterically bulky and electron rich NHC ligand such as Dipp$_2$Im (= 1,3-(2,6-di-*iso*-propylphenyl)imidazolin-2-ylidene) or Dipp$_2$Im^{H2} (= 1,3-(2,6-di-*iso*-propylphenyl)-imidazolidin-2-ylidene), that supposedly forms complexes of the type [Ni(NHC)$_2$] or [Ni(NHC)] as the pre-catalyst. These catalyst systems are highly efficient in the cyclization of different carbohydrates such as diynes or alkynes with ketones, aldehydes, nitriles, *iso*cyanates and other substrates.[3a,3b,5] For example, the cycloaddition of alkynes or diynes with *iso*cyanates to afford 2-pyridones and pyrimidinediones is highly efficient and occurs with a high degree of chemo-selectivity if a 1:1 mixture of [Ni(η^4-COD)$_2$]/Dipp$_2$Im^{H2} is used as catalyst.[6] For this Ni/NHC-catalyst system, alkyne cyclotrimerization was largely inhibited.[6] However, differences in reactivity, yield, and selectivity have been observed in these Ni/NHC-catalyzed cycloaddition reactions depending on the NHC ligand applied. The influence of the electronic and steric properties of the NHC ligand

employed, e.g. $Dipp_2Im$ vs. $Dipp_2Im^{H2}$ vs. Mes_2Im (= 1,3-dimesitylimidazolin-2-ylidene), to different cyclization reactions seems currently not to be completely understood.[7] However, Montgomery *et al.* demonstrated that stereo-electronic properties of NHC ligands play a crucial role for the regioselectivity observed for related nickel catalyzed allene hydrosilylation and reductive coupling reactions of aldehydes and alkynes.[8, 9] The regioselectivity of the latter is supposedly controlled by steric repulsion between the NHC ligand and the alkyne substituents in the first, rate determining, oxidative addition step.[9e]

We reported earlier that complexes $[Ni_2(NHC)_4(\mu\text{-}(\eta^2\text{:}\eta^2)\text{-COD})]$ of alkyl substituted NHCs such as $^{i}Pr_2Im$ (= 1,3-di-*iso*-propylimidazolin-2-ylidene) or $^{n}Pr_2Im$, which act as a source of $[Ni(NHC)_2]$, are efficient catalysts for the insertion of diphenyl acetylene into the C–C bond of biphenylene leading to 9,10-di(phenyl)phenanthrene.[10] The rate of formation of 9,10-di(phenyl)phenanthrene depends on the steric demand of the NHC employed, with the highest rates observed for the sterically most hindered NHC used. However, alkyne cyclooligomerization was suppressed at the reaction conditions employed (60 – 80 °C) for diphenyl acetylene, but excess of other alkynes (3-hexyne or 2-butyne) afforded traces of the cyclo-oligomerization product. To evaluate the differences in the reactivity of complexes $[Ni(NHC)_2]$ of NHCs of different size,[11] the reactivity of complexes $[Ni(NHC)_2]$ with alkynes is (re-)evaluated in some detail in the following chapter.

As all the work presented so far point to a decisive role of the sterics of the NHC ligand, the steric demand of the *N*-aryl substituted NHC was reduced by going from Dipp to Mes substituted NHC and the steric demand of the *N*-alkyl substituted NHC was increased by backbone methylation. It has been demonstrated previously that backbone substitution at the C4 and C5 position of the imidazole framework, for example by methylation, greatly effects the stereo-electronics of the NHC ligands as repulsion between the C4/C5 methyl group and the *N*-organyl substituent leads to smaller $C_{carbene}\text{-N-}C_{substituent}$ angles.[7, 12] Thus, the NHCs used in this chapter are Mes_2Im and $^{i}Pr_2Im^{Me}$ (= 1,3-di-*iso*-propyl-4,5-dimethylimidazolin-2-ylidene).

3.2 Results and Discussion

The reaction pathways and the results of key-processes in transition metal chemistry and catalysis, such as oxidative addition, reductive elimination, migratory insertion, transmetalation, and *β*-hydride elimination, depend decisively on the sterics of the (NHC) co-ligands used and on the degree of electron transfer from the metal to the substrates and thus to the nature, sterics and number of co-ligands.[13] Our group recently investigated differences in the reactivity of the NHC-stabilized nickel(0) complexes [Ni$_2$(^{i}Pr$_2$Im)$_4$(*μ*-(η^2:η^2)-COD)] **6a**[10] as a source of [Ni(^{i}Pr$_2$Im)$_2$] **6** and [Ni(Mes$_2$Im)$_2$] **1** in some detail.[11] In the course of our work on C–F bond activation and catalytic defluoroborylation of polyfluoroarenes using the complexes **6a**[14] and **1**,[15] we provided evidence from experiment and theory that depending on the NHC ligand used, the insertion of [Ni(NHC)$_2$] into the C–F bond of hexafluorobenzene proceeds *via* a concerted oxidative addition pathway for the small NHC ^{i}Pr$_2$Im and *via* a radical pathway for the more bulky NHC Mes$_2$Im. Additionally, we found for both mechanisms a competitive NHC-assisted reaction pathway which seems to be of general importance in transition metal NHC chemistry.[11a] Furthermore, we provided a detailed study on the steric influence of NHCs of different size on the stabilization of nickel *π*-complexes, since such complexes are very important intermediates in many different catalytic cycles.[16] Therefore the reactions of [Ni$_2$(^{i}Pr$_2$Im)$_4$(*μ*-(η^2:η^2)-COD)] **6a** , i.e. [Ni(^{i}Pr$_2$Im)$_2$] **6**, and [Ni(Mes$_2$Im)$_2$] **1** with different olefins, aldehydes and ketones were investigated (see Chapter II), which led to the formation of complexes of the type [Ni(NHC)$_2$(η^2-R$_2$C=CR$_2$)], [Ni(NHC)$_2$(η^2-O=CHR)] and [Ni(NHC)$_2$(η^2-O=CR$_2$)]. Whereas **6a** readily formed alkene complexes with olefins of different size, complex **1** reacted only with the smallest olefin, ethylene, or with activated acceptor olefins such as acrylates. Thus, the NHC nitrogen substituent influences the reactivity for steric reasons. However, these studies also pointed to the fact that substrate binding and electron transfer in bis-NHC nickel complexes can be very well fine-tuned beyond the accessibility of the metal center by steric protection and complex stability with respect to co-ligand or NHC dissociation. A subtle influence of sterics to the electronic behavior of [Ni(NHC)$_2$] lies in the C_{NHC}-M-C_{NHC} bite-angle the NHC ligands will adopt in the final product and in the propensity of the complexes [Ni(NHC)$_2$] to get involved in radical electron transfer processes.[17] In this chapter the reactivity studies of NHC-stabilized nickel complexes towards simple alkynes are further expanded using [Ni(Mes$_2$Im)$_2$] **1**

and suitable sources of [Ni(*i*Pr$_2$Im^{Me})$_2$] **7**. As mentioned above, our goup reported some alkyne complexes [Ni(*i*Pr$_2$Im)$_2$(η^2-R-C≡C-R‘) starting from [Ni(*i*Pr$_2$Im)$_2$] **6**, earlier,[10, 18] which are also discussed, if appropriate.

The complex [Ni$_2$(*i*Pr$_2$Im^{Me})$_4$(μ-(η^2:η^2)-COD)] **7a**, with the backbone methylated NHC *i*Pr$_2$Im^{Me}, was synthesized – as reported for **6a** – from the reaction of [Ni(η^4-COD)$_2$] with two equivalents of *i*Pr$_2$Im^{Me} (Scheme III.1).

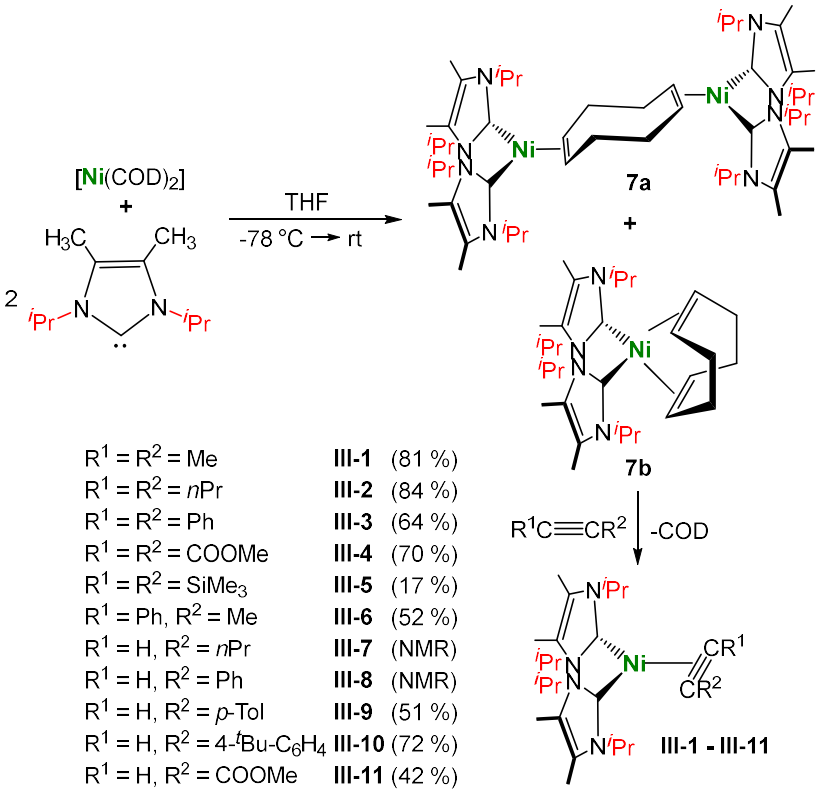

$R^1 = R^2$ = Me	**III-1**	(81 %)
$R^1 = R^2$ = *n*Pr	**III-2**	(84 %)
$R^1 = R^2$ = Ph	**III-3**	(64 %)
$R^1 = R^2$ = COOMe	**III-4**	(70 %)
$R^1 = R^2$ = SiMe$_3$	**III-5**	(17 %)
R^1 = Ph, R^2 = Me	**III-6**	(52 %)
R^1 = H, R^2 = *n*Pr	**III-7**	(NMR)
R^1 = H, R^2 = Ph	**III-8**	(NMR)
R^1 = H, R^2 = *p*-Tol	**III-9**	(51 %)
R^1 = H, R^2 = 4-*t*Bu-C$_6$H$_4$	**III-10**	(72 %)
R^1 = H, R^2 = COOMe	**III-11**	(42 %)

Scheme III.1 Synthesis of [Ni$_2$(*i*Pr$_2$Im^{Me})$_4$(μ-(η^2:η^2)-COD)] **7a** and [Ni(*i*Pr$_2$Im^{Me})$_2$(η^4-COD)] **7b** and the reaction of the mixture with alkynes to yield the complexes [Ni(*i*Pr$_2$Im^{Me})$_2$(η^2-MeC≡CMe)] **III-1**, [Ni(*i*Pr$_2$Im^{Me})$_2$(η^2-H$_7$C$_3$C≡CC$_3$H$_7$)] **III-2**, [Ni(*i*Pr$_2$Im^{Me})$_2$(η^2-PhC≡CPh)] **III-3**, [Ni(*i*Pr$_2$Im^{Me})$_2$(η^2-MeOOCC≡CCOOMe)] **III-4**, [Ni(*i*Pr$_2$Im^{Me})$_2$(η^2-Me$_3$SiC≡CSiMe$_3$)] **III-5**, [Ni(*i*Pr$_2$Im^{Me})$_2$(η^2-PhC≡CMe)] **III-6**, [Ni(*i*Pr$_2$Im^{Me})$_2$(η^2-HC≡CC$_3$H$_7$)] **III-7**, [Ni(*i*Pr$_2$Im^{Me})$_2$(η^2-HC≡CPh)] **III-8**, [Ni(*i*Pr$_2$Im^{Me})$_2$(η^2-HC≡C(*p*-Tol))] **III-9**, [Ni(*i*Pr$_2$Im^{Me})$_2$(η^2-HC≡C(4-*t*Bu-C$_6$H$_4$))] **III-10** and [Ni(*i*Pr$_2$Im^{Me})$_2$(η^2-HC≡CCOOMe)] **III-11**.

As observed for **6a**, the yellow solid obtained consists of two complexes, the dinuclear reaction product **7a** and the mononuclear complex [Ni(^{i}Pr$_2$Im^{Me})$_2$(η^4-COD)] **7b** as a by-product in various amounts (up to approximately 40 %). As **7a** and **7b** typically show identical reactivity with respect to alkynes (the same was observed previously for **6a** and its mononuclear counterpart [Ni(^{i}Pr$_2$Im)$_2$(η^4-COD)]) **6b**, the mixture was not further purified for the following reactions. Dinuclear **7a** and mononuclear **7b** can be distinguished easily in their ^{1}H and ^{13}C{^{1}H} NMR spectra. The resonances of the NHC ligand of **7a** were detected as a broad doublet at 1.42 ppm for the *iso*-propyl methyl protons, a singlet at 1.88 ppm for the backbone methyl protons and a septet at 6.03 ppm for the *iso*-propyl methine protons, whereas sharp resonances were found for the NHC ligand of complex **7b** at 1.33 ppm (d), 1.86 ppm (s) and 5.90 ppm (sept). In the ^{13}C{^{1}H} NMR spectra the resonances for the carbene carbon atoms were detected in close proximity at 206.5 ppm (**7a**) and 205.4 ppm (**7b**). Complex **7a** was structurally characterized (Figure III.1), it adopts in the solid state a distorted pseudo-square planar geometry at both nickel atoms. The complex is isostructural to [Ni$_2$(^{i}Pr$_2$Im)$_4$(μ-(η^2:η^2)-COD)] **6a**, [14a] and both complexes have almost identical Ni–C$_{carbene}$ distances (**7a**: 1.9117(19) Å and 1.9122(19) Å; **6a**: 1.906(3) Å and 1.904(3) Å) and similar C$_{carbene}$–Ni–C$_{carbene}$ angles (**7a**: 138.56(8)°; **6a**: 142.55(14)°).

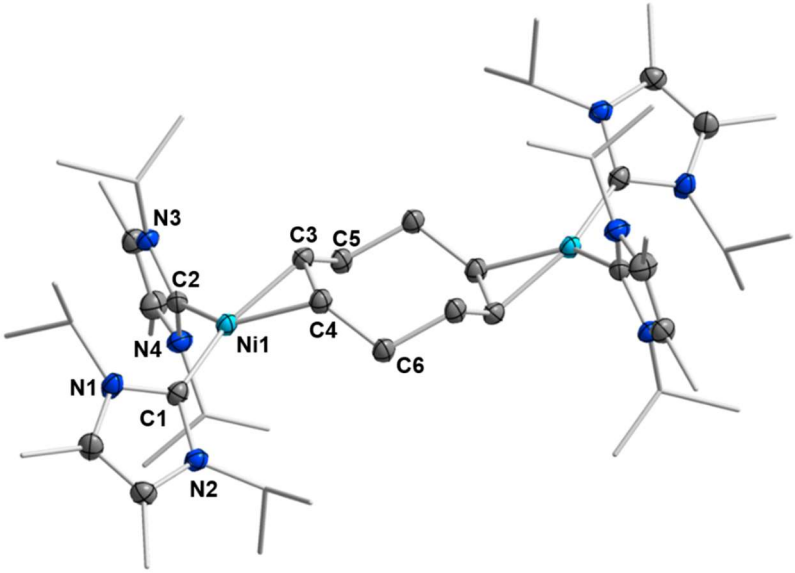

Figure III.1 Molecular structure of [Ni$_2$(^{i}Pr$_2$Im^{Me})$_4$(μ-(η^2:η^2)-COD)] **7a** in the solid state (ellipsoids were set at the 50 % probability level). Hydrogen atoms were omitted for clarity. Selected bond lengths [Å] and angles [°] of **7a**: Ni1–C1 1.9117(19), Ni1–C2

1.9122(19), Ni1–C3 1.9749(19), Ni1–C4 1.9734(19), C3–C4 1.428(2), C3–C5 1.515(3), C4–C6 1.513(3); C1–Ni1–C2 118.65(8), C1–Ni1–C3 138.56(8), C1–Ni1–C4 96.15(8), C2–Ni1–C3 102.72(8), C2–Ni1–C4 145.08(8), C3–Ni1–C4 42.42(7).

The reaction of a mixture of [Ni$_2$(^{i}Pr$_2$Im^{Me})$_4$(μ-(η^2:η^2)-COD)] **7a** and [Ni(^{i}Pr$_2$Im^{Me})$_2$(η^4-COD)] **7b** with equimolar amounts of 2-butyne, 4-octyne, diphenylacetylene, dimethyl acetylendicarboxylate, bis(trimethylsilyl)acetylene, 1-phenyl-1-propyne, 1-pentyne, phenylacetylene, *p*-tolylacetylene, 4-(*tert*-butyl)phenylacetylene and methyl propiolate selectively afforded the corresponding η^2-(*C,C*)-alkyne complexes [Ni(^{i}Pr$_2$Im^{Me})$_2$(η^2-MeC≡CMe)] **III-1**, [Ni(^{i}Pr$_2$Im^{Me})$_2$(η^2-H$_7$C$_3$C≡CC$_3$H$_7$)] **III-2**, [Ni(^{i}Pr$_2$Im^{Me})$_2$(η^2-PhC≡CPh)] **III-3**, [Ni(^{i}Pr$_2$Im^{Me})$_2$(η^2-MeOOCC≡CCOOMe)] **III-4**, [Ni(^{i}Pr$_2$Im^{Me})$_2$(η^2-Me$_3$SiC≡CSiMe$_3$)] **III-5**, [Ni(^{i}Pr$_2$Im^{Me})$_2$(η^2-PhC≡CMe)] **III-6**, [Ni(^{i}Pr$_2$Im^{Me})$_2$(η^2-HC≡CC$_3$H$_7$)] **III-7**, [Ni(^{i}Pr$_2$Im^{Me})$_2$(η^2-HC≡CPh)] **III-8**, [Ni(^{i}Pr$_2$Im^{Me})$_2$(η^2-HC≡C(*p*-Tol))] **III-9**, [Ni(^{i}Pr$_2$Im^{Me})$_2$(η^2-HC≡C(4-^{t}Bu-C$_6$H$_4$))] **III-10** and [Ni(^{i}Pr$_2$Im^{Me})$_2$(η^2-HC≡CCOOMe)] **III-11** (Scheme III.1). The complexes **III-1 – III-11** were isolated as yellow or orange-red, air and moisture sensitive powders and were characterized using ^{1}H NMR, ^{13}C{^{1}H} NMR and IR spectroscopy (see Experimental Details). The complexes were obtained as analytically pure material except for the complexes of the terminal alkynes 1-pentyne and phenylacetylene, [Ni(^{i}Pr$_2$Im^{Me})$_2$(η^2-HC≡CC$_3$H$_7$)] **III-7** and [Ni(^{i}Pr$_2$Im^{Me})$_2$(η^2-HC≡CPh)] **III-8**, which are only stable in solution and decompose upon removal of the solvent. The reactions of **7a/7b** with alkynes proceeded in quantitative yield if performed on NMR scale; the yield of isolated **III-5**, however, is rather low due to losses in the crystallization process to get analytically pure material. Important ^{1}H and ^{13}C{^{1}H} NMR data of the compounds **III-1 – III-11** are summarized in Table III.1. In the ^{1}H NMR and ^{13}C{^{1}H} NMR spectra the signals for the NHC ligands were observed in the typical regions expected, and for the complexes **III-6 – III-11** of unsymmetrical or terminal alkynes the set of NHC resonances is doubled due to a lowering of the complexes symmetry. Each alkyne proton of **III-7 – III-11** is shifted upon coordination to nickel by 4.87 – 5.48 ppm to lower fields compared to the uncoordinated alkyne and was observed as a singlet in the range between 6.71 and 7.64 ppm. Strong backbonding from the metal atom to the ligand is also reflected in the ^{13}C{^{1}H} NMR spectra of these complexes as a significant low-field coordination shift of 41.7 – 61.9 ppm occurs upon complexation.[10, 11b] The observed IR stretching vibrations of the alkyne triple bonds (1659 – 1785 cm^{-1}) in the complexes **III-1 – III-11**

are also significantly shifted to lower wavenumbers compared to the uncoordinated alkynes, which show typical stretching vibrations between 2100 cm^{-1} and 2310 cm^{-1}, and thus reflect a lower bond order upon coordination to nickel.[19] The $\nu_{C\equiv C}$ coordination shift ($\Delta\nu_{C\equiv C}$) of complex **III-3** (1754 cm^{-1}), for example, is -469 cm^{-1} compared to uncoordinated diphenylacetylene (2223 cm^{-1}) and much larger compared to the $\Delta\nu_{C\equiv C}$ reported for the corresponding phosphine complex [$(PPh_3)_2Ni(\eta^2$-PhC≡CPh)] (-419 cm^{-1}).[20] Thus, these complexes may rather be described as metallacyclopropenes, according to the Dewar-Chatt-Duncanson model.[21]

Table III.1 $^{13}C\{^1H\}$ NMR and ^1H NMR shifts [ppm] of the alkyne carbon and terminal alkyne hydrogen atoms as well as IR C≡C stretching vibrations [cm^{-1}] of the complexes **III-1 – III-11** (δ_C = $^{13}C\{^1H\}$ NMR shift of the alkyne carbon atoms; $\Delta\delta_C$ = $^{13}C\{^1H\}$ coordination shift of the alkyne carbon atoms; δ_H = ^1H NMR shift of the terminal alkyne hydrogen atoms; $\Delta\delta_H$ = ^1H coordination shift of the terminal alkyne hydrogen atoms; $\delta_{C\ NHC}$ = $^{13}C\{^1H\}$ NMR shift of the NHC carbene carbon atoms, $\nu_{C\equiv C}$ = IR stretching vibration of the alkyne triple bond).[20b, 22]

Compound	δ_C	$\Delta\delta_C$	δ_H	$\Delta\delta_H$	$\delta_{C\ NHC}$	$\nu_{C\equiv C}$
III-1	121.6	47.2			205.1	1785
III-2	126.4	46.2			205.5	1778
III-3	139.2	49.1	-	-	201.7	1754
III-4	136.8	61.9	-	-	194.3	1749
III-5	159.8	47.3	-	-	205.1	1659
III-6	127.1, 137.2	47.3, 51.4	-	-	203.3	1760
III-7	111.7, 138.1	43.4, 53.6	6.71	4.94	204.2, 204.8	-
III-8	125.3, 127.9	41.7, 50.7	7.64	4.92	202.3, 202.5	-
III-9	123.9, 138.1	46.9, 54.1	7.61	4.87	202.6, 202.9	1687
III-10	123.9, 138.0	46.9, 54.0	7.62	4.87	202.6, 202.9	1683
III-11	129.6, 131.9	53.6, 56.9	7.64	5.48	198.6, 198.8	1702

Crystals of [Ni(^{i}Pr$_2$Im^{Me})$_2$(η^2-MeC≡CMe)] **III-1**, [Ni(^{i}Pr$_2$Im^{Me})$_2$(η^2-PhC≡CPh)] **III-3** and [Ni(^{i}Pr$_2$Im^{Me})$_2$(η^2-Me$_3$SiC≡CSiMe$_3$)] **III-5** suitable for X-ray diffraction were obtained from saturated hexane or pentane solutions at -30 °C (Figure III.2 and Table III.4). Each of the complexes adopt a distorted pseudo-square planar geometry, spanned by the two NHCs and the alkyne ligand. The Ni–C_{NHC} distances lie in the range between 1.9097(14) and 1.9251(13) Å and are thus in line with Ni–C_{NHC} distances reported previously for [Ni(Me^{i}PrIm)$_2$(η^2-PhC≡CPh)] **28** (1.896(6)/1.915(4) Å) and [Ni(^{i}Pr$_2$Im)$_2$(η^2-MeC≡CMe)] **29** (1.917(8)/1.934(7) Å).[10] The distances from nickel to the alkyne carbon atoms (Ni–C_{alkyne}: 1.8804(14) – 1.9047(16) Å) are slightly shorter than the Ni–C_{NHC} distances. The C≡C separation of the alkyne ligands (1.285(2) Å – 1.304(3) Å; **28**: 1.310(6) Å, **29**: 1.286(13) Å) are remarkably enlarged compared to the uncoordinated alkynes.[22] The alkyne ligands are slightly twisted out of the $C_{carbene}$–Ni–$C_{carbene}$ plane with twist angles between 7.90(8)° (**III-3**) and 9.27(12)° (**III-5**). This deviation from planarity is considerably larger compared to the values observed for **28** (1.76(19)°) and **29** (1.96(26)°) and this deviation is attributed to increased steric repulsion of the ligand ^{i}Pr$_2$Im^{Me} with methyl substituents in the backbone compared to ^{i}Pr$_2$Im and/or the Me^{i}PrIm analogues.

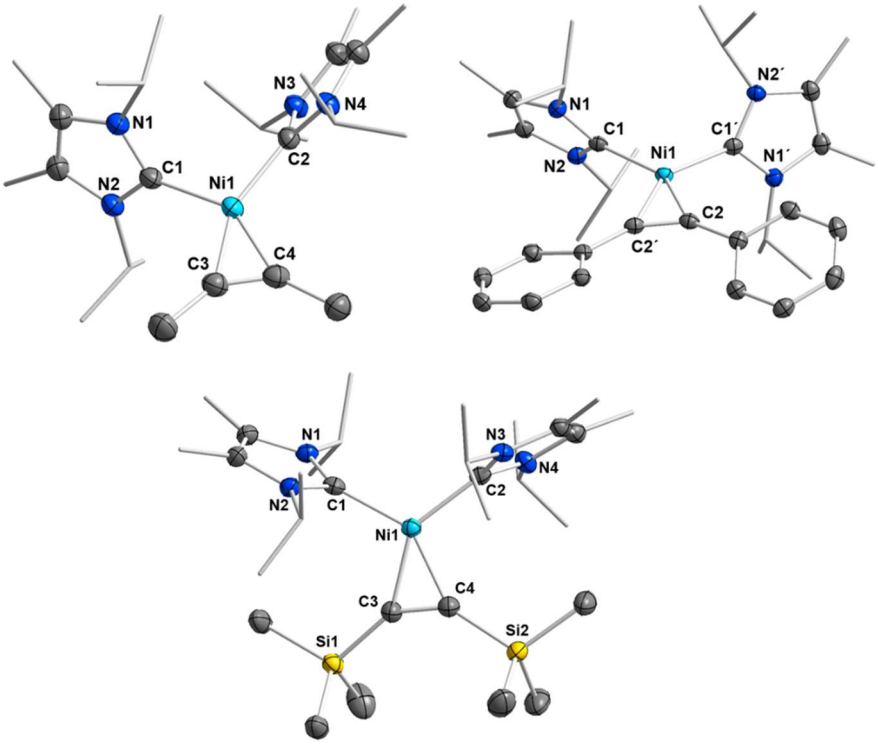

Figure III.2 Molecular structures of [Ni(^{i}Pr$_2$Im^{Me})$_2$(η^2-MeC≡CMe)] **III-1** (top left), [Ni(^{i}Pr$_2$Im^{Me})$_2$(η^2-PhC≡CPh)] **III-3** (top right) and [Ni(^{i}Pr$_2$Im^{Me})$_2$(η^2-Me$_3$SiC≡CSiMe$_3$)]

III-5 (bottom) in the solid state (ellipsoids set at the 50 % probability level). Hydrogen atoms were omitted for clarity. Selected bond lengths [Å] and angles [°] of **III-1**: Ni1–C1 1.9097(14), Ni1–C2 1.9239(14), Ni1–C3 1.8805(15), Ni1–C4 1.9026(14), C3–C4 1.285(2), C1–Ni1–C2 102.42(6), C1–Ni1–C3 105.16(6), C2–Ni1–C4 112.93(6), C3–Ni1–C4 39.70(6), plane (C1–Ni1–C2) – plane (C3–Ni1–C4) 8.32(8). Selected bond lengths [Å] and angles [°] of **III-3**: Ni1–C1/C1´ 1.9251(13), Ni1–C2/C2´ 1.8804(14), C2–C2´ 1.302(3), C1–Ni1–C1´ 110.66(8), C1–Ni1–C2´ 104.57(6), C1´–Ni1–C2 104.57(6), C2–Ni1–C2´ 40.52(8), plane (C1–Ni1–C1´) – plane (C2–Ni1–C2´) 7.90(8). Selected bond lengths [Å] and angles [°] of **III-5**: Ni1–C1 1.9183(15), Ni1–C2 1.9149(15), Ni1–C3 1.9047(16), Ni1–C4 1.9043(16), C3–C4 1.304(2), C3–Si1 1.8310(16), C4–Si2 1.8334(16), C1–Ni1–C2 114.54(6), C1–Ni1–C3 104.69(6), C2–Ni1–C4 101.13(6), C3–Ni1–C4 40.04(7), plane (C1–Ni1–C2) – plane (C3–Ni1–C4) 9.27(12).

Many of the complexes **III-1 – III-11** are unstable upon heating and the result of thermal exposure in solution depends on the alkyne ligand coordinated. While [Ni(^{i}Pr$_2$Im^{Me})$_2$(η^2-PhC≡CPh)] **III-3** and [Ni(^{i}Pr$_2$Im^{Me})$_2$(η^2-MeOOCC≡CCOOMe)] **III-4** are stable in solution at 100 °C for days, complexes [Ni(^{i}Pr$_2$Im^{Me})$_2$(η^2-MeC≡CMe)] **III-1** and [Ni(^{i}Pr$_2$Im^{Me})$_2$(η^2-HC≡CPh)] **III-8** decompose at room temperature, but much more rapidly upon heating with formation of so far unidentified products. Although many of the decomposition products could not be identified, for the thermal decomposition of the terminal alkyne complexes [Ni(^{i}Pr$_2$Im^{Me})$_2$(η^2-HC≡C(*p*-Tol))] **III-9** and [Ni(^{i}Pr$_2$Im^{Me})$_2$(η^2-HC≡C(4-^{t}Bu-C$_6$H$_4$))] **III-10**, the rearrangement products **III-9a** and **III-10a** were characterized (Scheme III.2 and Figure III.3) after heating of benzene or toluene solutions of these complexes to 60 °C for 72 h. In addition to **III-9a** or **III-10a** other, so far unidentified, side-products were formed. However, the complexes **III-9a** and **III-10a** result from an interesting addition of a C–H bond of one of the NHC *N-iso*-propyl substituent methyl groups across the C≡C triple bond of the coordinated alkyne (Scheme III.2).

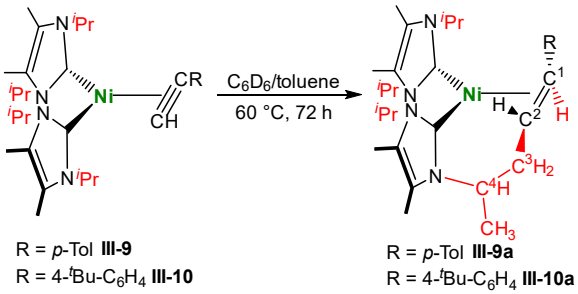

Scheme III.2 Synthesis of the decomposition products **III-9a** and **III-10a**.

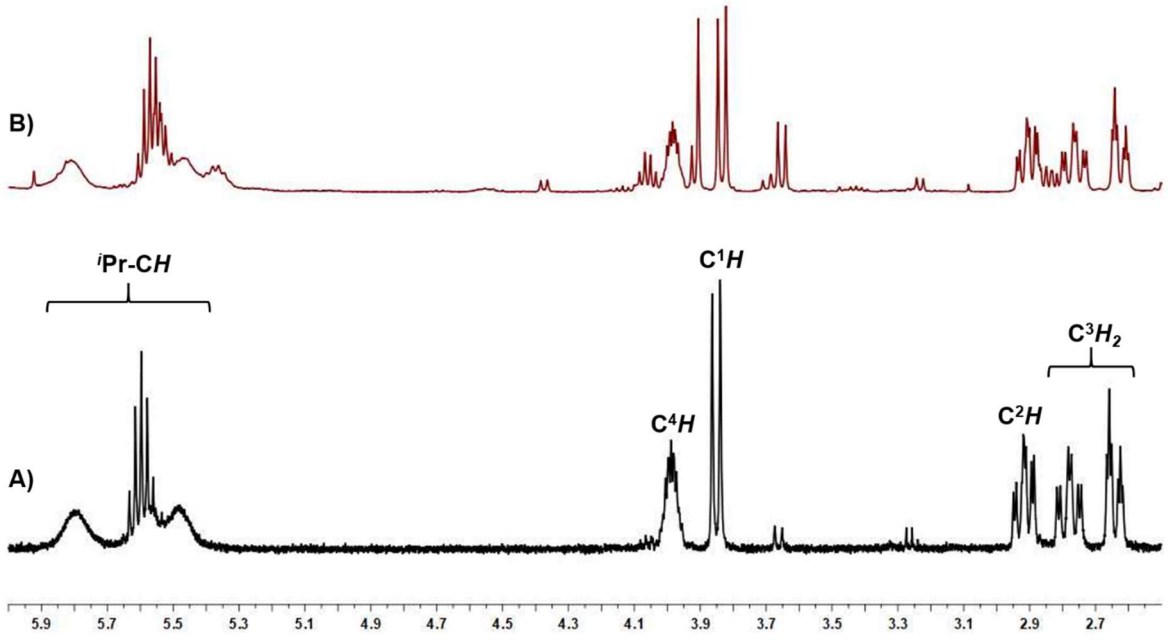

Figure III.3 Part of the ^{1}H NMR spectrum of compound **III-9a** (A, bottom) and the *in situ* ^{1}H NMR spectrum of the synthesis of compound **III-10a** (B, top) in the range between 2.5 ppm and 6.0 ppm, showing the characteristic signals of the 6-membered metallacycles formed.

Our group recently reported that NHC ligands are not good spectator ligands in cobalt NHC half sandwich alkyne chemistry and that they react in the coordination sphere of cobalt with terminal alkynes under coupling of the NHC and the alkyne ligand.[23a] Related decomposition pathways involving coordinated alkynes and NHC ligands are also known.[23] For the alkyne complexes of [Ni(NHC)$_2$] we have not observed this kind of NHC alkyne coupling so far, but the complexes **III-9a** and **III-10a** were formed *via* an intramolecular C–C coupling reaction of the NHC *N*-substituent. Formally, a hydrogen atom is transferred from the nearest *N-iso*-propyl methyl group of the NHC

ligand to the coordinated alkyne carbon atom. The terminal alkyne carbon thus couples with the *iso*-propyl methyl carbon with formation of a 6-membered metallacycle and reduction of the C≡C triple bond to an η^2-(*C,C*)-coordinated alkene.

Red crystals of compound **III-9a** were isolated for a complete characterization of this complex including X-ray analysis, while **III-10a** was only characterized *in situ via* the characteristic ^{1}H NMR resonances in the NMR spectrum (see Figure III.3). In each case, the resonances of the olefinic protons of **III-9a** and **III-10a** were detected as a doublet at 3.85 ppm (C=C*H*R) for the proton at C^1 (see Scheme III.2 and Figure III.3) and a doublet of doublets of doublets at 2.91 ppm for the proton at C^2. The two diastereotopic protons of the CH_2 group at C^3 give rise to two separate resonances at 2.64 ppm (ddd) and 2.78 ppm (ddd), while the former ^{i}Pr methine proton was detected as a broad multiplet at 3.99 ppm. The three remaining *iso*-propyl methine protons of the NHC ligands give rise to three partially overlapping and broadened septets in the range between 5.30 ppm and 5.90 ppm. In the $^{13}C\{^1H\}$ NMR spectrum of complex **III-9a** the resonances of the olefinic carbon atoms are shifted towards higher fields compared to complex **III-9** and were detected at 34.1 ppm (C^2) and 51.9 ppm (C^1). The signals for the C^3 carbon atom and the former *iso*-propyl methine carbon C^4 were observed at 40.2 and 54.1 ppm, respectively. The carbene carbon atom resonance of the NHC ligand involved in the metallacycle is also shifted to higher fields at 191.7 ppm, whereas the resonance of the unaffected NHC carbon atom was found at 204.5 ppm.

Crystals of **III-9a** suitable for X-ray diffraction were obtained from storing a saturated solution of the complex in hexane at -30 °C (Figure III.4). Complex **III-9a** adopts a distorted pseudo-square planar geometry in the solid state. The distance Ni1–C6 of 1.9072(15) Å and Ni1–C7 of 1.9140(15) Å to the NHC ligand carbon atoms are unexceptional and lie in the same range as observed for the alkyne complexes **III-1**, **III-3** and **III-5**. The distances of the nickel center to the olefin carbon atoms of 1.9945(14) Å (Ni1–C1) and 1.9321(14) Å (Ni1–C2) are larger compared to the Ni-C_{alkyne} distances observed for the alkyne complexes, but in line with Ni-C_{olefin} distances observed for **28** and **29** and related compounds. The C1–C2 separation of 1.439(2) Å is consistent with C=C bond lengths observed for other [Ni(NHC)$_2$(η^2-olefin)] complexes.[11b] The nickel atom, the olefin carbon atoms C1, C2 and the NHC carbon atom C7 are perfectly aligned in a plane and the intact NHC ligand is nearly perfectly perpendicular to this plane (88.58(9)°). The NHC ligand of the metallacycle (i.e., plane N3–C6–N4) is twisted towards the plane C1–Ni1–C2 with an angle of 32.51(11)°. The

olefin adopts a *trans*-configuration with angles of 121.19(13)° (C1–C2–C3) and 123.28(13)° (C2–C1–C8) between the C=C-bond vector and the substituents. The C2–C3 distance of the new bond between the olefin and the *iso*-propyl carbon atom is 1.516(2) Å and thus clearly a single bond. The 6-membered metallacycle adopts a distorted chair-conformation.

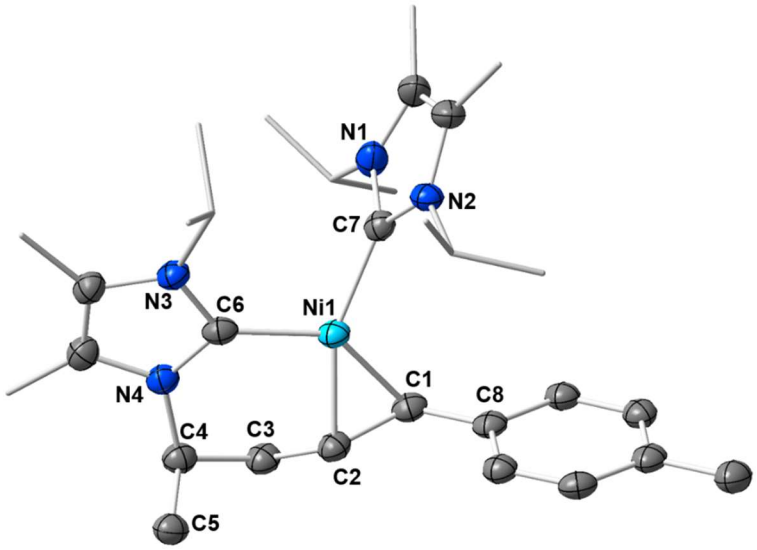

Figure III.4 Molecular structure of **III-9a** in the solid state (ellipsoids set at the 50 % probability level). The hydrogen atoms were omitted for clarity. Selected bond lengths [Å] and angles [°] of **III-9a**: Ni1–C7 1.9140(15), Ni1–C6 1.9072(15), Ni1–C1 1.9945(14), Ni1–C2 1.9321(14), C1–C2 1.439(2), C1–C8 1.474(2), C2–C3 1.516(2), C3–C4 1.532(2), C4–C5 1.533(2); C6–Ni1–C7 109.53(6), C1–Ni1–C7 110.67(6), C1–Ni1–C2 42.96(6), C2–Ni1–C6 95.74(6), C1–C2–C3 121.19(13), C2–C1–C8 123.28(13), plane (C1–Ni1–C2) – plane (N1–C7–N2) 88.58(9), plane (C1–Ni1–C2) – plane (N3–C6–N4) 32.51(11), plane (N3–C6–N4) – plane (N1–C7–N2) 77.05(11).

Scheme III.3 sketches two reasonable reaction pathways for the rearrangement of [Ni(^{i}Pr$_2$Im^{Me})$_2$(η^2-HC≡C(*p*-Tol))] **III-9** to product **III-9a**. The first pathway (i) involves the rearrangement of the terminal alkyne ligand to a nickel vinylidene complex along the typical hydrido alkinyl route, which occurs with insertion of nickel into the C–H bond of the coordinated terminal alkyne ligand and subsequent hydride rearrangement to the *β*-C atom.[24] Insertion of the vinylidene into the NHC methyl C–H bond would lead then to complex **III-9a**. Another likely pathway (ii) involves a concerted or nickel mediated addition of the NHC methyl C–H bond across the C≡C triple bond of the coordinated

alkyne. DFT calculations (BP86//def2-TZVP(Ni)/def2-SVP(C,N,H)) reveal first of all that the rearrangement of **III-9** to yield **III-9a** is a surprisingly strong exothermic process (ΔE=-102.6 kJ/mol), and that the corresponding nickel hydrido alkinyl (+65.5 kJ/mol) and nickel vinylidene (+49.2 kJ/mol) complexes are significantly higher in energy than the alkyne complex, so that the barrier of process (i) is at least +65.5 kJ/mol. For the pathway (ii), either a concerted or a nickel mediated C–H addition to the coordinated alkyne was investigated. However, location of any transition state was not possible here and every attempt to model likely nickel hydrido intermediates resulted in the ground state geometry of **III-9a**. As DFT calculations gave no conclusive answer, complex **III-9** was prepared using deuterated p-tolylacetylene and the rearrangement was repeated with the resulting complex **III-9-D**. As shown in Scheme III.3, the deuterium label of **III-9-D** should appear in the final product at different positions, depending on the pathway involved. The vinylidene pathway should lead to deuterium at the former *β*-position of the coordinated alkyne (H atom marked in red in Scheme III.3), the concerted/nickel-mediated addition should lead to deuterium at the former *α*-position of the coordinated alkyne (H atom marked in blue in Scheme III.3). The result of the deuteration experiment revealed that the deuterium atom stays at the *α*-carbon atom C^2 (see Scheme III.2) and therefore it is likely that the complexes **III-9a** and **III-10a** are formed according to a concerted or nickel-mediated C–H bond activation pathway with addition of the NHC methyl C–H bond to the triple bond, in accordance with pathway (ii) of Scheme III.3.

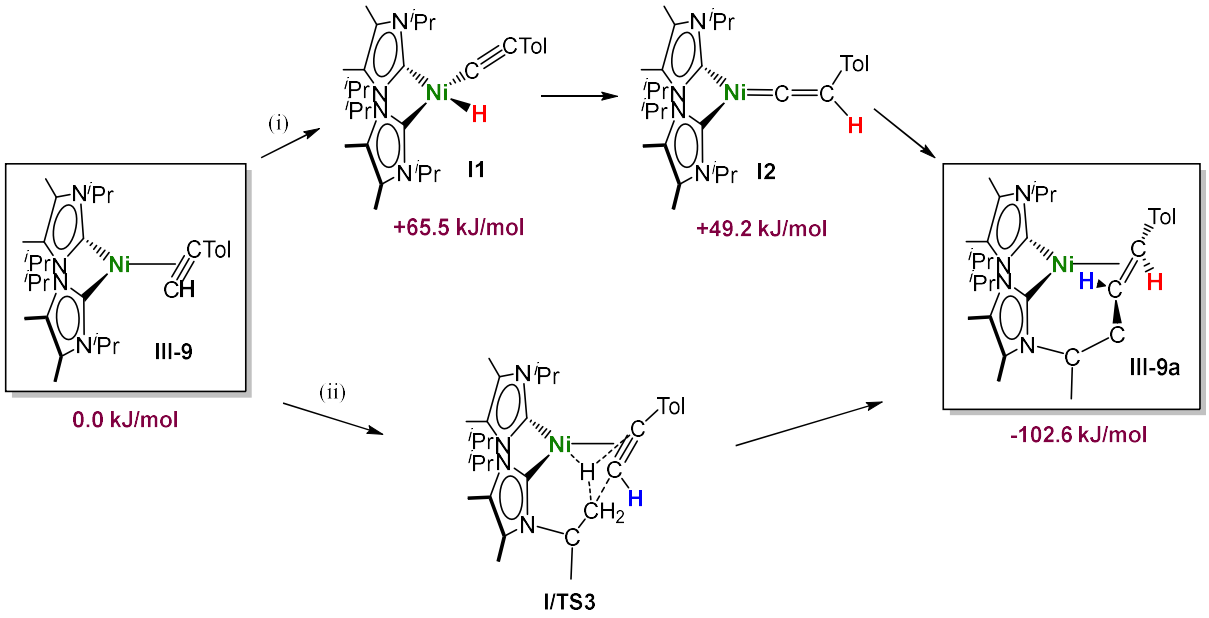

Scheme III.3 Possible pathways for the formation of **III-9a** *via* rearrangement of [Ni(^{i}Pr$_2$Im^{Me})$_2$(η^2-HC≡C(*p*-Tol))] **III-9**. Results obtained from DFT calculations (BP86//def2-TZVP(Ni)/def2-SVP(C,N,H)) are included, given are ZPE corrected energies (maroon).

As it is known that [Ni(NHC)$_2$] catalysts for cyclooligomerization reactions are prepared *in situ* from [Ni(η^4-COD)$_2$] and a bulky and electron rich NHC ligand such as Dipp$_2$Im, Dipp$_2$Im^{H2} or Mes$_2$Im,[3b] isolated [Ni(Mes$_2$Im)$_2$] **1** was reacted with alkynes. Initial NMR experiments revealed that complex **1** cyclotrimerizes 2-butyne quantitatively and therefore the catalytic activity and stereoselectivity of complex **1** in cyclotrimerization reactions was investigated using different internal and terminal alkynes (see Table III.2). NMR spectra of the reactions of 2-butyne, 4-octyne, diphenylacetylene, dimethyl acetylendicarboxylate, 1-pentyne, phenylacetylene and methyl propiolate with 5 mol% of [Ni(Mes$_2$Im)$_2$] **1** in C_6D_6 at 60 °C were recorded and the consumption of the alkynes was monitored. The catalyst was then removed by filtration through a pad of silica gel and the products were analyzed using ^{1}H and ^{13}C{^{1}H} NMR spectroscopy as well as GC/MS. In all cases, the cyclotrimerization of internal alkynes proceeded in quantitative yield on NMR scale (isolated yields were only determined for the preparation of hexaphenylbenzene, in this case the TON is 30) and no formation of side-products was detected, with exception of the cyclotrimerization of 1-pentyne, where traces of tetramerization products were observed.

Table III.2 Scope of the catalytic cyclotrimerization of alkynes with [Ni(Mes$_2$Im)$_2$] **1**.

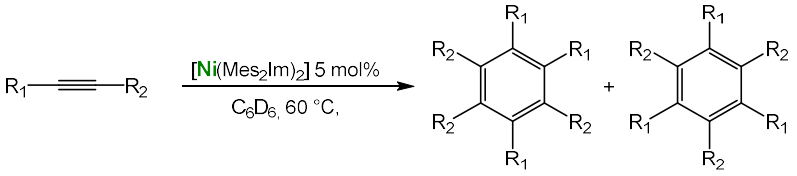

Entry	Substrate	Products[a]	t [h]
1	2-butyne	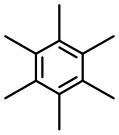	3
2	phenylacetylene	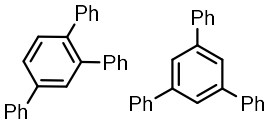	3
3	diphenylacetylene	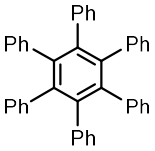 88 %[b,c]	5 min
4	1-pentyne	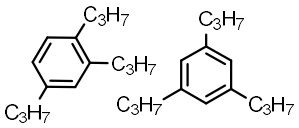 + traces of tetramerization	4
5	4-octyne	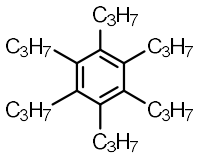	48
6	methylpropiolate	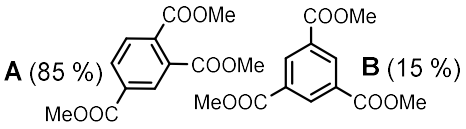 **A** (85 %) **B** (15 %)	4
7	dimethyl acetylenedicarboxylate	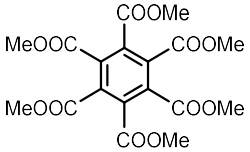	3

[a] Reaction conditions: [Ni(Mes$_2$Im)$_2$] **1** (5 mol%), alkyne (1 equiv.), C_6D_6 (0.6 mL), 60 °C, 20 h. Products after total consumption of the substrates, checked by NMR and GC/MS. Product ratios were determined by ^{1}H NMR integration, if possible. [b] [Ni(Mes$_2$Im)$_2$] **1** (1 mol%), rt, 5 minutes. [c] Yield of isolated material after workup.

The reactions with terminal alkynes did not show any specific stereoselectivity and afforded mixtures of the 1,2,4- and 1,3,5-stereoisomers. The exact determination of the product ratio *via* integration of the ^{1}H NMR spectrum was only possible for the reaction of methyl propiolate due to overlapping NMR resonances for the products of the other alkynes. The use of internal alkynes yielded hexa-substituted benzene derivatives, and the cyclotrimerization of diphenylacetylene to give hexaphenylbenzene proceeded much faster compared to the cyclotrimerization of other alkynes (entry 3, Table III.2). This reaction was finished after five minutes at room temperature using a small catalyst load of just 1 mol%. As the product is almost insoluble in C_6D_6 it was isolated directly from the NMR tube as a colorless solid in 88 % yield.

To gain further insight into the mechanistic details of the catalysis the reaction of **1** with 2-butyne was analyzed. Therefore, initially the reaction of **1** with a slight excess of 2-butyne (4 equiv.) was performed in a Young's tab NMR tube (see Figure III.5a). Addition of the alkyne led to an immediate color change from deep violet, which is the color of **1**, to bright yellow, which rapidly darkened after a few seconds. The analysis of the reaction mixture *via* NMR spectroscopy after five minutes at room temperature revealed the formation of hexamethylbenzene, free NHC Mes_2Im and a new well defined complex **III-A**. After 4 d at room temperature, some re-formation of complex **1** was observed, resonances of free Mes_2Im were still detectable and the signals assigned to complex **III-A** started to decrease. Finally, heating of the sample for 4 h at 60 °C led to a complete disappearance of the resonances for the NHC and for complex **III-A** and a full recovery of complex **1** plus the final cyclotrimerization product hexamethylbenzene was observed. The presence of uncoordinated carbene in the solution indicates that complex **III-A** might be a mono-NHC complex [(Mes_2Im)Ni(η^6-C_6Me_6)] **III-A**, stabilized by hexamethylbenzene. A similar arene-stabilized complex has been reported previously by Ogoshi *et al.*[25] for a larger NHC, i.e., [Ni($Dipp_2Im$)(η^6-C_6H_5Me)]. Despite several attempts, isolation of this complex was not possible. Furthermore, the absence of 2-butyne after five minutes at room temperature indicates that oligomerization proceeds very fast and quantitatively. To learn more details about this process, especially at which temperature the catalysis sets in, a variable temperature NMR experiment of the reaction from -40 °C to +60 °C in steps of 10 °C was performed, additionally (see Figure III.5b).

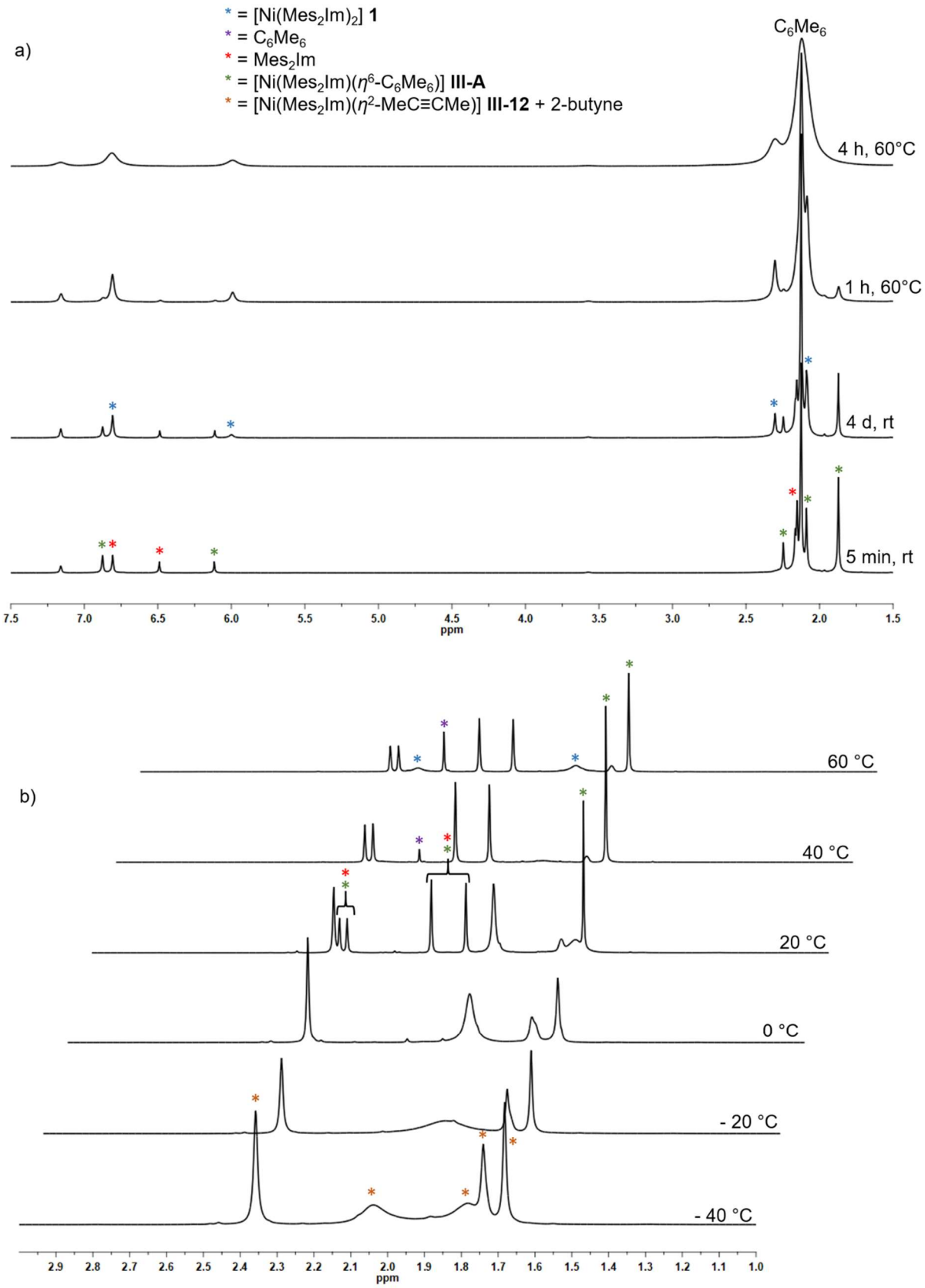

Figure III.5 a) Time resolved ^{1}H NMR spectrum of the reaction of [Ni(Mes$_2$Im)$_2$] **1** with 2-butyne (4 equiv.) (C_6D_6). b) Variable temperature ^{1}H NMR spectrum of the reaction of [Ni(Mes$_2$Im)$_2$] **1** with 2-butyne (4 equiv.) (THF-d$_8$).

At -40 °C, the reaction mixture had a bright yellow color and the NMR spectrum showed the formation of the alkyne complex [Ni(Mes_2Im)$_2$(η^2-MeC≡CMe)] **III-12** (see below), similar as observed for complex **7a/7b** with the smaller NHC ligand. Resonances of the trimerization product, free Mes_2Im as well as the signals of complex **III-A** were already detected at temperatures of 0-10 °C. Integration of the resonances was consistent with the formation of a mono-NHC arene complex [(Mes_2Im)Ni(η^6-C_6Me_6)]. After raising the temperature to 40 °C, the alkyne was completely consumed, the resonance of hexamethylbenzene increased and both, the NHC Mes_2Im as well as the complex [(Mes_2Im)Ni(η^6-C_6Me_6)] **III-A**, were detected. Finally, at 60 °C, the recovery of complex **1** and the decrease of the resonances of the uncoordinated NHC and the mono-NHC complex **III-A** occurred.

To see if **7** is also suitable for catalytic trimerization [Ni(^{i}Pr$_2$Im^{Me})$_2$(η^2-MeC≡CMe)] **III-1** was also reacted with an excess of 2-butyne. In contrast to complex **1**, no cyclization was observed after 20 h at room temperature, but heating the reaction mixture to higher temperatures, of 80 °C and above, led to the slow transformation of 2-butyne to hexamethylbenzene. Isolation of the possible intermediates [Ni(Mes_2Im)$_2$(η^2-R^{1}C≡CR^2)], [Ni(Mes_2Im)(η^2-R^{1}C≡CR^2)$_2$] (for R^1 = R^2 = Me: **III-B**) or [(Mes_2Im)Ni(η^6-C_6R_6)] (for R = Me: **III-A**) of the catalysis was tried by reacting complex **1** with stoichiometric amounts, i.e., 1, 2, or 3 equivalents, of alkyne. However, all attempts to isolate complexes [Ni(Mes_2Im)(η^2-R^{1}C≡CR^2)$_2$] and [(Mes_2Im)Ni(η^6-C_6R_6)] have failed so far, but some complexes of the type [Ni(Mes_2Im)$_2$(η^2-R^{1}C≡CR^2)] were obtained in pure form. The complexes with η^2-(*C,C*)-coordinated alkyne [Ni(Mes_2Im)$_2$(η^2-MeC≡CMe)] **III-12**, [Ni(Mes_2Im)$_2$(η^2-MeOOCC≡CCOOMe)] **III-13**, [Ni(Mes_2Im)$_2$(η^2-PhC≡CMe)] **III-14**, [Ni(Mes_2Im)$_2$(η^2-HC≡C(4-^{t}Bu-C_6H_4))] **III-15** and [Ni(Mes_2Im)$_2$(η^2-HC≡CCOOMe)] **III-16** precipitated as yellow to brown powders if the reactions were carried out at 0 °C in pentane or hexane, which made their isolation possible. These complexes are, once isolated, stable at room temperature in the solid state (see Scheme III.4). The complexes **III-12** to **III-16** were fully characterized including elemental analysis and single crystal X-ray structures for **III-12**, **III-13**, **III-14** and **III-15**. However, due to significant line broadening and signal overlap at room temperature or 0 °C, NMR spectroscopy of **III-12**, **III-14** and **III-15** was performed at -80 °C.

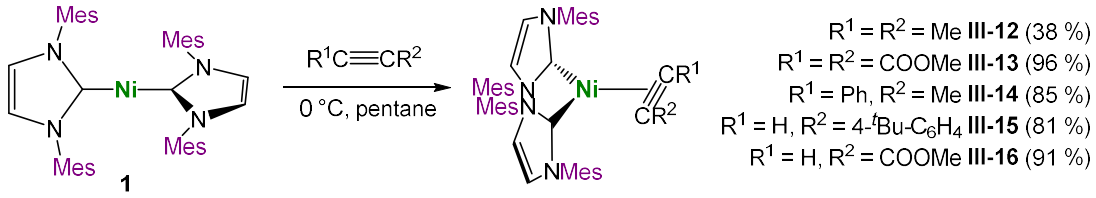

Scheme III.4 Synthesis of [Ni(Mes$_2$Im)$_2$(η^2-MeC≡CMe)] **III-12**, [Ni(Mes$_2$Im)$_2$(η^2-MeOOCC≡CCOOMe)] **III-13**, [Ni(Mes$_2$Im)$_2$(η^2-PhC≡CMe)] **III-14**, [Ni(Mes$_2$Im)$_2$(η^2-HC≡C(4-^{t}Bu-C$_6$H$_4$))] **III-15** and [Ni(Mes$_2$Im)$_2$(η^2-HC≡CCOOMe)] **III-16**.

In general, the stability of complexes [Ni(Mes$_2$Im)$_2$(η^2-R^{1}C≡CR^2)] depend on the steric demand of the alkyne used, but also on the electronic properties of the alkyne ligand. As observed previously for olefin complexes (compare Chapter II), [11b] the steric bulk of the NHC ligand Mes$_2$Im of complex **1** limits the coordination of a third ligand to the nickel atom, which is in stark contrast to the behavior of complexes **6** and **7**. Alkynes with electron withdrawing substituents increase π-backbonding from the nickel atom to the alkyne and increase the stability of the alkyne complex in solution at room temperature. As noted above, alkyl and/or aryl substituted alkynes lead to decomposition of the alkyne complexes with extrusion of one NHC ligand at temperatures slightly above 0 °C. Unlike the complexes **III-1 – III-11**, the NMR spectra of the compounds **III-12 – III-16** reveal remarkably broadened resonances for the bulkier NHC ligand Mes$_2$Im due to hindered rotation, as was previously reported in Chapter II for similar π-complexes with ketone or aldehyde ligands.[11b] Even the low temperature NMR spectra of **III-12**, **III-14** and **III-15** revealed some signal broadening. Nevertheless, all characteristic resonances were assigned and the integration of the resonances is consistent with the presence of one alkyne ligand per two NHC ligands in complexes of the type [Ni(Mes$_2$Im)$_2$(η^2-alkyne)]. Important ^{1}H and ^{13}C{^{1}H} NMR data of **III-12 – III-16** are summarized in Table III.3. In the ^{1}H NMR spectra of **III-12 – III-16** the *ortho* and *para* mesityl methyl protons give rise to up to four broadened resonances in the range between 1.74 and 2.37 ppm. The alkyne protons of the compounds **III-15** and **III-16** each can be observed as a singlet at 6.11 ppm (**III-15**) and 6.94 ppm (**III-16**). In the ^{13}C{^{1}H} NMR spectra the signals of the carbene carbon atoms were detected in the range between 198.2 and 207.0 ppm. The resonances of the alkyne carbon atoms are shifted to lower fields upon coordination and were observed in the range between 118.6 and 136.7 ppm. The $\nu_{C\equiv C}$ stretching vibrations of the complexes **III-12 – III-16** are shifted to lower wavenumbers in the range between 1701 cm^{-1} and 1808 cm^{-1}.

Table III.3 $^{13}C\{^1H\}$ NMR and ^1H NMR shifts [ppm] of the alkyne carbon and terminal alkyne hydrogen atoms as well as IR C≡C stretching vibrations [cm^{-1}] of the complexes **III-12 – III-16** (δ_C = $^{13}C\{^1H\}$ NMR shift of the alkyne carbon atoms; $\Delta\delta_C$ = $^{13}C\{^1H\}$ coordination shift of the alkyne carbon atoms; δ_H = ^1H NMR shift of the terminal alkyne hydrogen atoms; $\Delta\delta_H$ = ^1H coordination shift of the terminal alkyne hydrogen atoms; $\delta_{C\ NHC}$ = $^{13}C\{^1H\}$ NMR shift of the NHC carbene carbon atoms, $\nu_{C\equiv C}$ = IR stretching vibration of the alkyne triple bond).[20b, 22]

Compound	δ_C	$\Delta\delta_C$	δ_H	$\Delta\delta_H$	$\delta_{C\ NHC}$	$\nu_{C\equiv C}$
III-12	118.6[a]	44.2	-	-	207.0[a]	1808
III-13	136.7	61.8	-	-	198.2	1713
III-14	123.9, 135.6[a]	44.1, 49.8	-	-	205.8, 206.0[a]	1756
III-15	122.8, 131.5[a]	45.8, 47.5	6.11[a]	3.36	202.2, 206.5[a]	1701
III-16	134.6, 136.6	58.6, 61.6	6.94	4.78	201.8, 202.4	1711

[a] THF-d_8, -80 °C

Crystals suitable for X-ray diffraction of **III-12**, **III-13**, **III-14** and **III-15** were obtained by either storing a saturated solution of the complex in hexane or pentane at -30 °C or by layering a saturated benzene solution of the complex with hexane at room temperature (**III-13**). The molecular structures of **III-12**, **III-13**, **III-14** and **III-15** are provided in Figure III.6. Important crystallographic data of these complexes and a comparison to the complexes [Ni(Me*i*PrIm)$_2$(η^2-PhC≡CPh)] **28**,[10] [Ni(*i*Pr$_2$Im)$_2$(η^2-MeC≡CMe)] **29**,[10] [Ni(*i*Pr$_2$Im^{Me})$_2$(η^2-MeC≡CMe)] **III-1**, [Ni(*i*Pr$_2$Im^{Me})$_2$(η^2-PhC≡CPh)] **III-3** and [Ni(*i*Pr$_2$Im^{Me})$_2$(η^2-Me$_3$SiC≡CSiMe$_3$)] **III-5** are given in Table III.4. All complexes adopt a distorted pseudo-square planar geometry, spanned by two NHCs and the alkyne ligand. All molecular structures reveal much larger C_{NHC}–N–C_{NHC} bite angles of 122.24(6)° (**III-12**), 118.47(12)° (**III-13**), 118.5(2)° (**III-14**) and 124.59(14)° (**III-15**) compared to the *i*Pr$_2$Im and *i*Pr$_2$Im^{Me} Ni complexes of the *N*-alkyl substituted carbenes (**28**: 109.27(19)°, **29**: 100.4(3)°,[10] **III-1**:102.42(6)°, **III-3**:110.66(8)°, **III-5**: 114.54(6)°), which is associated with the increased steric demand of the bulkier NHC Mes$_2$Im. The C–C distances of the alkyne ligands of the complexes **III-12** (1.280(2) Å) and **III-15** (1.277(5) Å) are slightly shorter compared to the complexes with the small carbenes

(1.285(2) Å (**III-1**) – 1.310(6) Å (**28**)), which is consistent with decreased *π*-backbonding.

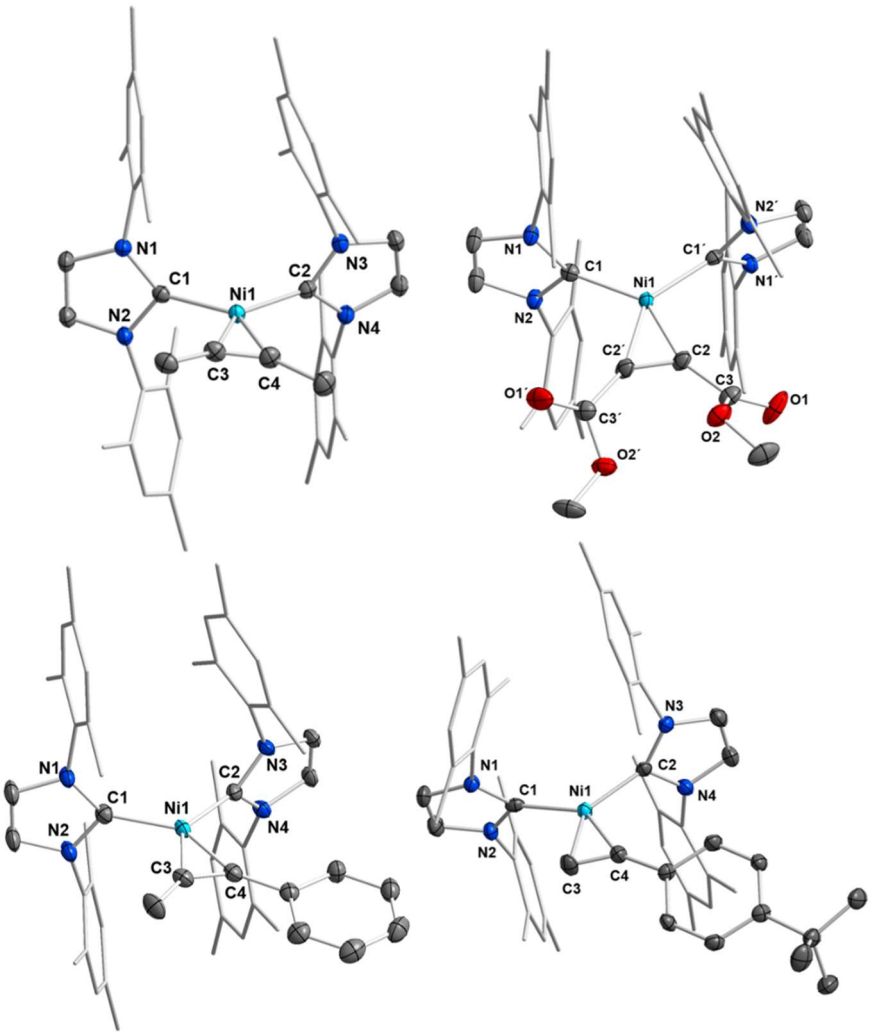

Figure III.6 Molecular structures of [Ni(Mes$_2$Im)$_2$(η^2-MeC≡CMe)] **III-12** (top left), [Ni(Mes$_2$Im)$_2$(η^2-MeOOCC≡CCOOMe)] **III-13** (top right), [Ni(Mes$_2$Im)$_2$(η^2-PhC≡CMe)] **III-14** (bottom left) and [Ni(Mes$_2$Im)$_2$(η^2-HC≡C(4-^{t}Bu-C$_6$H$_4$))] **III-15** (bottom right) in the solid state (ellipsoids set at 50 % probability level). Hydrogen atoms and a hexane molecule (**III-15**) were omitted for clarity. Selected bond lengths [Å] and angles [°] of **III-12**: Ni1–C1 1.9098(14), Ni1–C2 1.9127(14), Ni1–C3 1.9066(14), Ni1–C4 1.9055(15), C3–C4 1.280(2), C1–Ni1–C2 122.24(6), C1–Ni1–C3 99.62(6), C2–Ni1–C4 99.34(6), C3–Ni1–C4 39.24(7), plane (C1–Ni1–C2) – plane (C3–Ni1–C4) 9.60(7). Selected bond lengths [Å] and angles [°] of **III-13**: Ni1–C1/C1´ 1.917(2), Ni1–C2/C2´ 1.873(2), C2–C2´ 1.300(4), C1–Ni1–C1´ 118.47(12), C1–Ni1–C2´ 100.49(9), C1´–Ni1–C2 100.49(9), C2–Ni1–C2´ 40.61(13), plane (C1–Ni1–C1´) – plane (C2–Ni1–C2´) 3.26(13). Selected bond lengths [Å] and angles [°] of **III-14**: : Ni1–C1 1.927(5), Ni1–C2

1.913(5), Ni1–C3 1.902(5), Ni1–C4 1.912(5), C3–C4 1.291(7), C1–Ni1–C2 118.5(2), C1–Ni1–C3 102.6(2), C2–Ni1–C4 99.5(2), C3–Ni1–C4 39.6(2), plane (C1–Ni1–C2) – plane (C3–Ni1–C4) 5.73(22). Selected bond lengths [Å] and angles [°] of **III-15**: : Ni1–C1 1.921(3), Ni1–C2 1.912(3), Ni1–C3 1.876(4), Ni1–C4 1.916(3), C3–C4 1.277(5), C1–Ni1–C2 124.59(14), C1–Ni1–C3 96.26(15), C2–Ni1–C4 99.82(14), C3–Ni1–C4 39.33(15), plane (C1–Ni1–C2) – plane (C3–Ni1–C4) 1.50(17).

Table III.4 Comparison of important bond lengths and bond angles of [Ni(Me^{i}PrIm)$_2$(η^2-PhC≡CPh)] **28**,[10] [Ni(^{i}Pr$_2$Im)$_2$(η^2-MeC≡CMe)] **29**,[10] [Ni(^{i}Pr$_2$Im^{Me})$_2$(η^2-MeC≡CMe)] **III-1**, [Ni(^{i}Pr$_2$Im^{Me})$_2$(η^2-PhC≡CPh)] **III-3**, [Ni(^{i}Pr$_2$Im^{Me})$_2$(η^2-Me$_3$SiC≡CSiMe$_3$)] **III-5**, [Ni(Mes$_2$Im)$_2$(η^2-MeC≡CMe)] **III-12**, [Ni(Mes$_2$Im)$_2$(η^2-MeOOCC≡CCOOMe)] **III-13**, [Ni(Mes$_2$Im)$_2$(η^2-PhC≡CMe)] **III-14** and [Ni(Mes$_2$Im)$_2$(η^2-HC≡C(4-^{t}Bu-C$_6$H$_4$))] **III-15** ($d_{Ni–NHC}$ = Ni–C distance to the carbene carbon atom; $d_{C–C}$ = C–C distance of the alkyne, twist angle: twist between the planes NHC–Ni–NHC and C–Ni–C).

Compound	$d_{Ni–NHC}$ [Å]	$d_{C–C}$ [Å]	∢ NHC-Ni-NHC [°]	twist angle [°]
28	1.896(6)/1.915(4)	1.310(6)	109.27(19)	1.76(19)
29	1.917(8)/1.934(7)	1.286(13)	100.4(3)	1.96(26)
III-1	1.9097(14)/1.9239(14)	1.285(2)	102.42(6)	8.32(8)
III-3	1.9251(13)	1.302(3)	110.66(8)	7.90(8)
III-5	1.9183(15)/1.9149(15)	1.304(2)	114.54(6)	9.27(12)
III-12	1.9098(14)/1.9127(14)	1.280(2)	122.24(6)	9.60(7)
III-13	1.917(2)	1.300(4)	118.47(12)	3.26(13)
III-14	1.927(5)/1.913(5)	1.291(7)	118.5(2)	5.73(22)
III-15	1.921(3)/1.912(3)	1.277(5)	124.59(14)	1.50(17)

NMR experiments as well as the isolation of the NHC nickel alkyne complexes point to a mechanism for the NHC Ni mediated alkyne trimerization as depicted in Scheme III.5 for the trimerization of 2-butyne. The first step of the catalytic cycle is the coordination of the alkyne to deep-purple [Ni(Mes_2Im)$_2$] **1** to yield bright yellow [Ni(Mes_2Im)$_2$(η^2-MeC≡CMe)] **III-12**, a step which occurs at low temperatures. In a second step, another alkyne molecule coordinates to the nickel atom to replace one of the NHC ligands with formation of the bis(alkyne) complex [Ni(Mes_2Im)(η^2-MeC≡Me)$_2$] **III-B**. We have no evidence currently for the formation of **III-B**, but Louie *et al.*[7] and Cavell *et al.*[26] reported previously the synthesis of comparable mono-NHC stabilized nickel olefin complexes of the type [(NHC)Ni(η^2-R_2C=CR_2)$_2$] using bulky NHC ligands such as Mes_2Im or $Dipp_2Im$. As intermediate **III-B** was never detected, it is assumed that the following reaction step, the addition of another equivalent alkyne to **III-B** with cyclization of the alkynes to give [(Mes_2Im)Ni(η^6-C_6R_6)] **III-A**, is very fast. Complex **III-A** was detected by NMR spectroscopy but defied all efforts at isolation. As the complexes **1** or **III-12** were never observed during catalysis, the formation of **1** and **III-12** should be the initial steps to prepare the catalytic active species [Ni(Mes_2Im)(η^2-MeC≡Me)$_2$] **III-B** (“Initiation” in Scheme III.5, highlighted in red) and the effective catalytic process likely occurs as a shuttle between the complexes **III-B** and **III-A** (“Propagation” in Scheme III.5). At the end of the catalysis, the NHC ligand re-coordinates to the nickel atom of **III-A** with elimination of the aromatic trimerization product and recovery of complex **1** (“Termination” in Scheme III.5, highlighted in violet). This last step only occurs if the concentration of alkyne is very low, otherwise [Ni(Mes_2Im)(η^2-MeC≡Me)$_2$] **III-B** will be formed directly to close the catalytic cycle. As the NMR studies on the reaction of **1** with a slight excess of 2-butyne clearly reveal, this last step is associated with the highest barrier.

What is now the difference of [Ni(Mes_2Im)$_2$] **1** and [Ni($^iPr_2Im$)$_2$] **6** or [Ni($^iPr_2Im^{Me}$)$_2$] **7** in the behavior towards alkynes. All three compounds form alkyne complexes, but only the complexes of the sterically more encumbered Mes_2Im ligand enter the catalytic cycle at ambient temperatures. To answer this question DFT calculations (BP86//def2-TZVP(Ni)/def2-SVP(C,N,H)) have been performed on the initiation steps of the cyclotrimerization of 2-butyne with [Ni(NHC)$_2$] (NHC = $^iPr_2Im^{Me}$, Mes_2Im; see Scheme III.5). The results of these computations are given in Figure III.7.

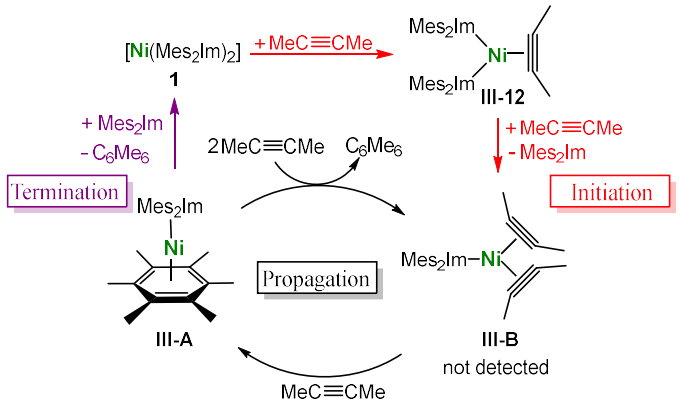

Scheme III.5 Proposed mechanism of the NHC nickel-catalyzed cyclotrimerization of 2-butyne.

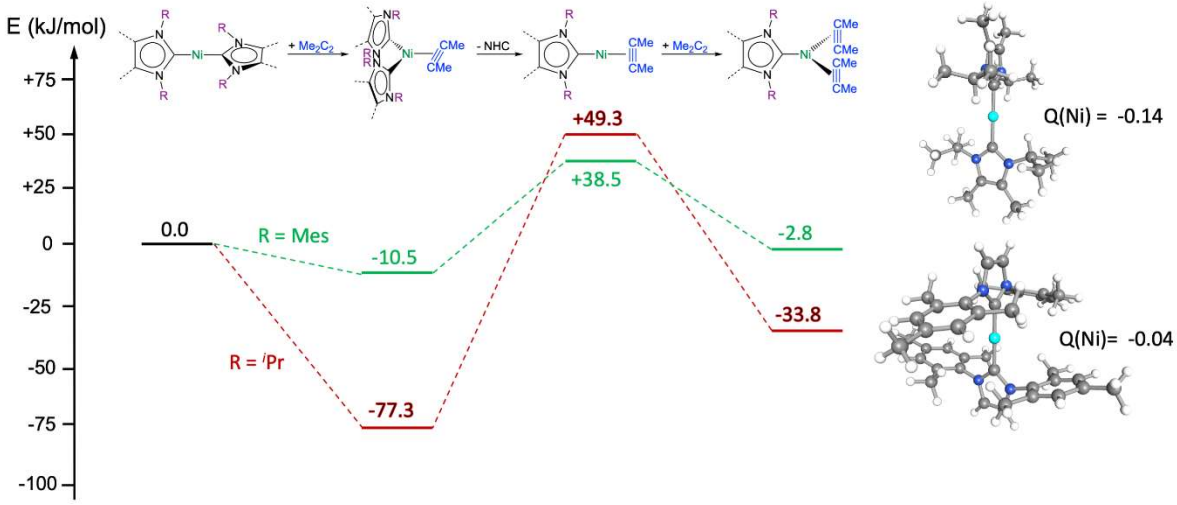

Figure III.7 Energy profile of the initiation steps of the cyclotrimerization of 2-butyne with [Ni(NHC)$_2$] (NHC = ^{i}Pr$_2$Im^{Me} **7**, red; Mes$_2$Im **1**, green) according to DFT calculations (BP86//def2-TZVP(Ni)/def2-SVP(C,N,H)) and calculated NBO charges at the nickel atoms of [Ni(NHC)$_2$]. Given are the ZPE corrected ground state energies in kJ/mol.

A comparison of the energy profile of the cyclotrimerization initiation steps of 2-butyne with [Ni(^{i}Pr$_2$Im^{Me})$_2$] **7** (red) and [Ni(Mes$_2$Im)$_2$] **1** (green) reveals that the profile is very shallow for **1** and each step is associated with a moderate energy change. The formation of the alkyne complexes [Ni(^{i}Pr$_2$Im^{Me})$_2$(η^2-MeC≡CMe)] **III-1** and [Ni(Mes$_2$Im)$_2$(η^2-MeC≡CMe)] **III-12** is connected with a very different energy gain, -77.3 kJ/mol for **III-1** and only -10.5 kJ/mol for **III-12**. Assuming a dissociative process, the dissociation of the NHC ligand from [Ni(NHC)$_2$(η^2-MeC≡CMe)] requires +126.6 kJ/mol

for the $^{i}Pr_2Im^{Me}$ complex, whereas for the Mes_2Im complex only +49 kJ/mol are needed. The attachment of another alkyne to [Ni(NHC)(η^2-MeC≡CMe)] is exothermic in both cases, -41.3 kJ/mol for the formation of [Ni(Mes_2Im)(η^2-MeC≡CMe)$_2$] and -83.1 kJ/mol for [Ni($^{i}Pr_2Im^{Me}$)(η^2-MeC≡CMe)$_2$]. Thus, the potential surface of the nickel complex [Ni(Mes_2Im)$_2$] with both, low energy gain for alkyne addition and low energy loss for NHC dissociation, is nicely suited for catalysis, whereas for [Ni($^{i}Pr_2Im^{Me}$)$_2$] **7** the alkyne complex seems to be too stable for further ligand loss (either alkyne or NHC) to enter a catalytic cycle at ambient temperatures.

As there is a distinct difference in the coordination of alkyne, specifically 2-butyne, to [Ni($^{i}Pr_2Im^{Me}$)$_2$] **7** (red) and [Ni(Mes_2Im)$_2$] **1** (green) it is interesting to track down the differences. Both ligands are different in their stereo-electronic features. For this purpose the steric demand of the NHCs $^{i}Pr_2Im$, $^{i}Pr_2Im^{Me}$ and Mes_2Im expressed by their %V_{bur} ("percent buried volume") [12, 27] was re-evaluated on the basis of DFT geometry optimized structures (BP86//def2-TZVP(all)) of [(NHC)Ni(CO)$_3$]. With the aid of the Web application Samb*V*ca,[28] %V_{bur} values of $^{i}Pr_2Im$ (26.5 %) < $^{i}Pr_2Im^{Me}$ (27.7 %) < Mes_2Im (33.2 %)[29] were obtained, for fixed Ni–$C_{carbene}$ distances of 2.00 Å, which are perfectly in line with our experimental findings. The *σ*-donor and *π*-acceptor properties of the NHC ligands can be described *via* the TEP ("tolman electronic parameter")[27, 30] and ^{31}P or ^{77}Se NMR shifts of NHC phosphinidenes and selenourea compounds,[31] respectively. While our BP86//def2-TZVP(all)-calculated TEP values reveal no significant differences for $^{i}Pr_2Im$ (2054) ~ Mes_2Im (2055) ~ $^{i}Pr_2Im^{Me}$ (2056) in [(NHC)Ni(CO)$_3$], the *π*-acceptor abilities of the NHCs increase in the order $^{i}Pr_2Im$ ($\delta^{31}P$ = -61.2 ppm, $\delta^{77}Se$ = -3 ppm) < $^{i}Pr_2Im^{Me}$ ($\delta^{77}Se$ = -18 ppm) < Mes_2Im ($\delta^{31}P$ = -23 ppm, $\delta^{77}Se$ = +27 ppm).[31]

As a consequence of these different donor and acceptor properties of the NHC ligands used in [Ni(NHC)$_2$], different charges (see Figure III.7; given are NBO charges) were calculated at nickel for the complexes [Ni($^{i}Pr_2Im^{Me}$)$_2$] **7** (-0.14) and [Ni(Mes_2Im)$_2$] **1** (-0.04). Thus, the nickel atom of **7** is more electron-rich compared to the metal atom of **1** and it should be expected that more electron density is transferred to the alkyne ligand of **7**. This is in line with the concept recently provided by Love and Kennepohl *et al.* for the stabilization of square planar d^{10} nickel *π*-complexes bearing phosphine co-ligands.[32] These authors provided evidence that the stability of *π*-complexes depends on the strength of the metal-to-ligand (alkyne or alkene) backbond, which is

critically influenced by charge transfer from the co-ligands (here the NHCs) *via* the metal atom to the *π*-acceptor ligand.

These expectations can be confirmed by the experimental data obtained for the complexes [Ni(*i*Pr$_2$Im)$_2$(η^2-MeC≡CMe)] **29**,[10] [Ni(*i*Pr$_2$Im^{Me})$_2$(η^2-MeC≡CMe)] **III-1** and [Ni(Mes$_2$Im)$_2$(η^2-MeC≡CMe)] **III-12**. As the molecular structure is known for all three complexes it should be noted here that the experimentally determined C≡C bond lengths do not provide in principle a good basis for this discussion, as the differences lie within the experimental error of the structure determination (3σ). However, the trend observed here is as expected, i.e. that the C≡C bond length of the alkyne ligand of the Mes$_2$Im complex [Ni(Mes$_2$Im)$_2$(η^2-MeC≡CMe)] **III-12** is the shortest while those of the complexes **29** and **III-1** are longer due to more electron transfer to the alkyne: 1.280(2) (**III-12**) << 1.285(2) (**III-1**) < 1.286(13) (**29**). This order of the net donor properties is also reflected in the observed coordination shifts of the alkyne carbon atoms ($\Delta\delta_C$ [ppm] = 44.2 (**III-12**) < 47.2 (**III-1**) < 47.5 (**29**))[10, 20b] and even more pronounced in the coordination shifts of the $\nu_{C\equiv C}$ stretching vibrations ($\Delta\nu_{C\equiv C}$ [cm^{-1}] = 425 (**III-12**) < 448 (**III-1**) < 455 (**29**))[10, 20b] (cf. Tables III.1 and III.3).

Different degrees of C≡C bond activation of the alkyne ligands of [Ni(*i*Pr$_2$Im^{Me})$_2$(η^2-MeC≡CMe)] **III-1** and [Ni(Mes$_2$Im)$_2$(η^2-MeC≡CMe)] **III-12** was also confirmed by DFT calculations, either using the C≡C distances (**III-1**: 1.304 Å, **III-12**: 1.297 Å), the calculated charges on the alkyne carbon atoms (e.g., NBO-charges: **III-1**: -0.245, **III-12**: -0.225), calculated (uncorrected) C≡C stretching frequencies (**III-1**: 1852 cm^{-1}; **III-12**: 1876 cm^{-1}) or the C≡C Wiberg bond indices (**III-1**: 1.809, **III-12**: 1.835). A detailed analysis also reveals that alkyne activation (i.e. the strength of the *π*-backbond) is indirectly influenced by the steric demand of the NHC ligand in so far as the complexes [Ni(*i*Pr$_2$Im^{Me})$_2$(η^2-MeC≡CMe)] **III-1** and [Ni(Mes$_2$Im)$_2$(η^2-MeC≡CMe)] **III-12** adopt different angles C_{NHC}–Ni–C_{NHC}. It is well known that a decrease of the bite angle L–M–L (i.e. C_{NHC}–Ni–C_{NHC}) in d^{10}-[ML$_2$] (L = neutral 2VE donor ligand) and related complexes is connected with a more favorable *π*-backbonding in complexes d^{10}-[ML$_2$(alkyne)] and thus an increase of the net charge donation from the metal center to the *π*-ligand.[17a, 17c, 33] The bite angles of the complexes [Ni(NHC)$_2$(η^2-MeC≡CMe)] decrease in the order 122.24(6)° (**III-12**) >> 102.42(6)° (**III-1**) > 100.4(3)° (**29**). To evaluate the contribution of the different bite angles we optimized the geometry of [Ni(*i*Pr$_2$Im^{Me})$_2$(η^2-MeC≡CMe)] **III-1** with the fixed angle of geometry optimized [Ni(Mes$_2$Im)$_2$(η^2-MeC≡CMe)] **III-12** (angle C_{NHC}–Ni–C_{NHC} 123.60°, exp.:122.24(6)°).

The potential for a change of the C_{NHC}–Ni–C_{NHC} angle is very shallow, as the energies of both optimized structures of [Ni(^{i}Pr$_2$Im^{Me})$_2$(η^2-MeC≡CMe)] **III-1** differ by a mere 2.8 kJ/mol. However, the parameters evaluated above for the alkyne ligand of **III-1** and **III-12** adopt for the complex of the constrained geometry complex values within those computed for **III-1** and **III-12**, e.g. 1.301 Å for the C≡C distance (**III-1**: 1.304 Å, **III-12**: 1.297 Å), -0.233 for the NBO-charges on the alkyne carbon atoms (**III-1**: -0.245, **III-12**: -0.225), and 1852 cm^{-1} for the C≡C stretching frequencies (**III-1**: 1852 cm^{-1}; **III-12**: 1876 cm^{-1}).

In total, the much higher stability of [Ni(^{i}Pr$_2$Im^{Me})$_2$(η^2-MeC≡CMe)] **III-1** with respect to [Ni(Mes$_2$Im)$_2$(η^2-MeC≡CMe)] **III-12** can be attributed to three main reasons: (i) electron transfer from the NHC to the metal to the alkyne ligand is higher for the *N*-alkyl compared to the *N*-aryl substituted NHC ligands in [Ni(NHC)$_2$(η^2-MeC≡CMe)] due to different electron donor/acceptor properties of the NHC ligand. (ii) Electron transfer from the metal center to the alkyne ligand is enhanced for the *N*-alkyl compared to the *N*-aryl substituted NHC ligands due to their different steric size, as smaller NHC ligands (such as ^{i}Pr$_2$Im^{Me} or ^{i}Pr$_2$Im) can adopt smaller C_{NHC}–Ni–C_{NHC} bite angles, which leads to increased π-backdonation to the alkyne. (iii) Ligand dissociation is facilitated for the complex of the sterically more encumbered NHC ligand, i.e., [Ni(Mes$_2$Im)$_2$(η^2-MeC≡CMe)] **III-12** loses the NHC ligand more readily than [Ni(^{i}Pr$_2$Im)$_2$(η^2-MeC≡CMe)] **29**[10] and [Ni(^{i}Pr$_2$Im^{Me})$_2$(η^2-MeC≡CMe)] **III-1**. All these factors lead to a significantly enhanced stability of the alkyne complexes of the *N*-alkyl substituted NHCs and are thus the reason why these complexes are not catalytically active for alkyne oligomerization at ambient temperatures.

3.3 Conclusion

This chapter presents a case study on the effect of two different NHC ligands in complexes [Ni(NHC)$_2$] (NHC = ^{i}Pr$_2$Im^{Me} **7**, Mes$_2$Im **1**), including some details to demonstrate how small differences in the stereo-electronic features of closely related ligands can significantly alter the reactivity pattern. The reaction of (suitable precursors of) both complexes with alkynes afforded η^2-(*C,C*)-alkyne complexes [Ni(NHC)$_2$](η^2-alkyne)] (**III-1 – III-16**), although the number of complexes available for [Ni(Mes$_2$Im)$_2$] **1** is limited to small alkynes and good acceptor alkynes. Many of the [Ni(^{i}Pr$_2$Im^{Me})$_2$] complexes **III-1 – III-11** are unstable upon heating, leading to various, in many cases unidentified decomposition products. However, for the thermal reaction of the complexes [Ni(^{i}Pr$_2$Im^{Me})$_2$(η^2-HC≡C(*p*-Tol))] **III-9** and [Ni(^{i}Pr$_2$Im^{Me})$_2$(η^2-HC≡C(4-^{t}Bu-C$_6$H$_4$))] **III-10** the isomers **III-9a** and **III-10a** were identified. DFT calculations as well as deuteration experiments were in accordance with the formation of **III-9a** and **III-10a** *via* a concerted or nickel-mediated C–H addition of a NHC methyl C–H bond across the C≡C triple bond of the coordinated alkyne.

Complex **1** cyclotrimerizes alkynes at ambient conditions, which is in contrast to the behavior found for **6** or **7**. NMR exploration of the reaction of **1** with 2-butyne gave evidence for the formation of the complexes [(Mes$_2$Im)Ni(η^6-C$_6$Me$_6$)] **III-A** and [Ni(Mes$_2$Im)$_2$(η^2-MeC≡CMe)] **III-12** as intermediates of the reaction. A mechanism for the NHC-nickel catalyzed cyclotrimerization of 2-butyne was proposed, which involves coordination of the alkyne to [Ni(Mes$_2$Im)$_2$] **1** to yield [Ni(Mes$_2$Im)$_2$(η^2-MeC≡CMe)] **III-12** and [Ni(Mes$_2$Im)(η^2-MeC≡Me)$_2$] **III-B** with loss of one NHC ligand as the initiation step of the catalysis. The efficient steps of the catalytic cycle involve addition of 2-butyne to [Ni(Mes$_2$Im)(η^2-MeC≡Me)$_2$] **III-B** with cyclization to yield [(Mes$_2$Im)Ni(η^6-C$_6$Me$_6$)] **III-A** and re-formation of **III-B** with arene release. The re-coordination of the NHC ligand to the nickel atom of **III-A** with elimination of the aromatic trimerization product and recovery of complex **1** at the end of the catalysis is the termination of the catalytic cycle.

This chapter demonstrates for the example of bis-NHC nickel alkyne complexes and their reactivity how valuable NHCs are in the fine-tuning of substrate binding, electron transfer and reactivity. Although the differences in the TEP of both NHCs under investigation is small, the differences in the electron transfer of the complexes [Ni(NHC)$_2$] to a coordinated substrate are quite impressive. The increase of the steric

demand of the NHC leads, of course, to a different accessibility of the metal center (steric protection) and to different complex stabilities as co-ligand/NHC dissociation is facilitated for the bulkier ligand. It is also demonstrated here that steric properties of the NHC significantly influence the donor properties of [M(NHC)$_2$]-moieties *via* the C_{NHC}-M-C_{NHC} bite-angle NHC ligands of different size can adopt in the final product.

3.4 References

[1] For a monograph on [2 + 2 + 2] cyclo-addition reactions, see: a) K. Tanaka, *Transition-Metal-Mediated Aromatic Ring Construction*, John Wiley & Sons, Inc., Hoboken, NJ, **2013**; For selected reviews see: b)K. P. C. Vollhardt, *Acc. Chem. Res.* **1977**, *10*, 1-8; c) K. P. C. Vollhardt, *Angew. Chem.* **1984**, *96*, 525-628; *Angew. Chem. Int. Ed.* **1984**, *23*, 539-556; d) N. E. Schore, *Chem. Rev.* **1988**, *88*, 1081-1119; e) S. Saito, Y. Yamamoto, *Chem. Rev.* **2000**, *100*, 2901-2916; f) J. A. Varela, C. Saá, *Chem. Rev.* **2003**, *103*, 3787-3802; g) I. Nakamura, Y. Yamamoto, *Chem. Rev.* **2004**, *104*, 2127-2198; h) B. Heller, M. Hapke, *Chem. Soc. Rev.* **2007**, *36*, 1085-1094; i) G. Domínguez, J. Pérez-Castells, *Chem. Soc. Rev.* **2011**, *40*, 3430-3444; j) E. Ruijter, D. Broere, *Synthesis* **2012**, *44*, 2639-2672; k) A. V. Gulevich, A. S. Dudnik, N. Chernyak, V. Gevorgyan, *Chem. Rev.* **2013**, *113*, 3084-3213; l) A. Roglans, A. Pla-Quintana, M. Solà, *Chem. Rev.* **2021**, *121*, 1894-1979.

[2] W. Reppe, O. Schlichting, K. Klager, T. Toepel, *Liebigs Ann.* **1948**, *560*, 1-92.

[3] a) P. R. Chopade, J. Louie, *Adv. Synth. Catal.* **2006**, *348*, 2307-2327; b) A. Thakur, J. Louie, *Acc. Chem. Res.* **2015**, *48*, 2354-2365; c) J. Montgomery, *Angew. Chem.* **2004** *116*, 3980-3998; *Angew. Chem. Int. Ed*. **2004**, *43*, 3890-3908.

[4] a) A. D. Jenkins, A. Herath, M. Song, J. Montgomery, *J. Am. Chem. Soc.* **2011**, *133*, 14460-14466; b) A. D. Jenkins, M. T. Robo, P. M. Zimmerman, J. Montgomery, *J. Org. Chem.* **2020**, *85*, 2956-2965.

[5] a) P. Kumar, A. Thakur, X. Hong, K. N. Houk, J. Louie, *J. Am. Chem. Soc.* **2014**, *136*, 17844-17851; b) P. Kumar, K. Zhang, J. Louie, *Angew. Chem.* **2012**, *124*, 8730-8734; *Angew. Chem. Int. Ed.* **2012**, *51*, 8602-8606. c) R. M. Stolley, H. A. Duong, J. Louie, *Organometallics* **2013**, *32*, 4952-4960; d) T. N. Tekavec, J. Louie, *J. Org. Chem.* **2008**, *73*, 2641-2648; e) M. M. McCormick, H. A. Duong, G. Zuo, J. Louie, *J. Am. Chem. Soc.* **2005**, *127*, 5030-5031.

[6] a) H. A. Duong, M. J. Cross, J. Louie, *J. Am. Chem. Soc.* **2004**, *126*, 11438-11439; b) H. A. Duong, J. Louie, *Tetrahedron* **2006**, *62*, 7552-7559.

[7] S. Felten, S. F. Marshall, A. J. Groom, R. T. Vanderlinden, R. M. Stolley, J. Louie, *Organometallics* **2018**, *37*, 3687-3697.

[8] Z. D. Miller, W. Li, T. R. Belderrain, J. Montgomery, *J. Am. Chem. Soc.* **2013**, *135*, 15282-15285.

[9] a) G. M. Mahandru, G. Liu, J. Montgomery, *J. Am. Chem. Soc.* **2004**, *126*, 3698-3699; b) B. Knapp-Reed, G. M. Mahandru, J. Montgomery, *J. Am. Chem. Soc.* **2005**, *127*, 13156-13157; c) M. R. Chaulagain, G. J. Sormunen, J. Montgomery, *J. Am. Chem. Soc.* **2007**, *129*, 9568-9569; d) H. A. Malik, G. J. Sormunen, J. Montgomery, *J. Am. Chem. Soc.* **2010**, *132*, 6304-6305; e) P. Liu, J. Montgomery, K. N. Houk, *J. Am. Chem. Soc.* **2011**, *133*, 6956-6959; f) E. P. Jackson, J. Montgomery, *J. Am. Chem. Soc.* **2015**, *137*, 958-963; g) D. P. Todd, B. B. Thompson, A. J. Nett, J. Montgomery, *J. Am. Chem. Soc.* **2015**, *137*, 12788-12791; h) E. P. Jackson, H. A. Malik, G. J. Sormunen, R. D. Baxter, P. Liu, H. Wang, A. R. Shareef, J. Montgomery, *Acc. Chem. Res.* **2015**, *48*, 1736-1745.

[10] T. Schaub, M. Backes, U. Radius, *Organometallics* **2006**, *25*, 4196-4206.

[11] a) M. W. Kuntze-Fechner, H. Verplancke, L. Tendera, M. Diefenbach, I. Krummenacher, H. Braunschweig, T. B. Marder, M. C. Holthausen, U. Radius, *Chem. Sci.* **2020**, *11*, 11009-11023; b) L. Tendera, T. Schaub, M. J. Krahfuss, M. W. Kuntze-Fechner, U. Radius, *Eur. J. Inorg. Chem.* **2020**; c) S. Sabater, D. Schmidt, H. Schmidt, M. Kuntze-Fechner, T. Zell, C. Isaac, N. Rajabi, H. Grieve, W. Blackaby, J. Lowe, S. Macgregor, M. Mahon, U. Radius, M. Whittlesey, *Chem. Eur. J.* **2021**.

[12] H. Clavier, S. P. Nolan, *Chem. Commun.* **2010**, *46*, 841-861.

[13] a) R. H. Crabtree, *The organometallic chemistry of the transition metals*, 6th. ed., Wiley-VCH, New York, **2014**; b) J. F. Hartwig., *Organotransition metal chemistry: from bonding to catalysis*, University Science Books, Sausalito, CA., **2010**.

[14] a) T. Schaub, U. Radius, *Chem. Eur. J.* **2005**, *11*, 5024-5030; b) T. Schaub, M. Backes, U. Radius, *J. Am. Chem. Soc.* **2006**, *128*, 15964-15965; c) T. Schaub, M. Backes, U. Radius, *Eur. J. Inorg. Chem.* **2008**, *2008*, 2680-2690; d) T. Schaub, P. Fischer, A. Steffen, T. Braun, U. Radius, A. Mix, *J. Am. Chem. Soc.* **2008**, *130*, 9304-9317; e) T. Schaub, P. Fischer, T. Meins, U. Radius, *Eur. J. Inorg. Chem.* **2011**, *2011*, 3122-3126; f) P. Fischer, K. Götz, A. Eichhorn, U. Radius, *Organometallics* **2012**, *31*, 1374-1383; g) J. Zhou, J. H. Berthel, M. W. Kuntze-Fechner, A. Friedrich, T. B. Marder, U. Radius, *J. Org. Chem.* **2016**, *81*, 5789-5794; h) M. W. Kuntze-Fechner, C. Kerpen, D. Schmidt, M. Häring, U. Radius, *Eur. J. Inorg. Chem.* **2019**.

[15] a) J. Zhou, M. W. Kuntze-Fechner, R. Bertermann, U. S. Paul, J. H. Berthel, A. Friedrich, Z. Du, T. B. Marder, U. Radius, *J. Am. Chem. Soc.* **2016**, *138*, 5250-5253; b) Y. Tian, X. Guo, M. Kuntze-Fechner, I. Krummenacher, H. Braunschweig, U. Radius, A. Steffen, T. B. Marder, *J. Am. Chem. Soc.* **2018**.

[16] a) K. Muto, J. Yamaguchi, D. G. Musaev, K. Itami, *Nat. Commun.* **2015**, *6*, 7508; b) Y. Bernhard, B. Thomson, V. Ferey, M. Sauthier, *Angew. Chem.* **2017**, *129*, 7568-7572; *Angew. Chem. Int. Ed.* **2017**, *56*, 7460-7464; c) M. L. Lejkowski, R. Lindner, T. Kageyama, G. E. Bodizs, P. N. Plessow, I. B. Muller, A. Schafer, F. Rominger, P. Hofmann, C. Futter, S. A. Schunk, M. Limbach, *Chem.* **2012**, *18*, 14017-14025; d) S. Manzini, N. Huguet, O. Trapp, T. Schaub, *Eur. J. Org. Chem.* **2015**, *2015*, 7122-7130; e) Y. Kita, H. Sakaguchi, Y. Hoshimoto, D. Nakauchi, Y. Nakahara, J. F. Carpentier, S. Ogoshi, K. Mashima, *Chem.* **2015**, *21*, 14571-14578; f) Y. Kita, R. D. Kavthe, H. Oda, K. Mashima, *Angew. Chem.* **2015**, *128*, 1110-1113; *Angew. Chem. Int. Ed.* **2016**, *55*, 1098-1101.

[17] a) P. Hofmann, H. Heiß, G. Müller, **1987**, *42*, 395; b) W. J. van Zeist, F. M. Bickelhaupt, *Dalton Trans.* **2011**, *40*, 3028-3038; c) L. P. Wolters, W. J. van Zeist, F. M. Bickelhaupt, *Chem.* **2014**, *20*, 11370-11381; d) F. Hering, J. Nitsch, U. Paul, A. Steffen, F. M. Bickelhaupt, U. Radius, *Chem. Sci.* **2015**, *6*, 1426-1432; e) J. Nitsch, L. P. Wolters, C. Fonseca Guerra, F. M. Bickelhaupt, A. Steffen, *Chem.* **2017**, *23*, 614-622.

[18] a) T. Schaub, U. Radius, *Z. Anorg. Allg. Chem.* **2006**, *632*, 981-984; b) P. Fischer, T. Linder, U. Radius, *Z. Anorg. Allg. Chem.* **2012**, *638*, 1491-1496; c) J. H. J. Berthel, L. Tendera, M. W. Kuntze-Fechner, L. Kuehn, U. Radius, *Eur. J. Inorg. Chem.* **2019**, *2019*, 3061-3072.

[19] N. Sheppard, D. M. Simpson, *Q. Rev. Chem. Soc.* **1952**, *6*, 1-33.

[20] a) P. W. Jolly, in *Comprehensive Organometallic Chemistry,* Pergamon, Oxford, **1982**, 101-143; b) U. Rosenthal, G. Oehme, V. V. Burlakov, P. V. Petrovskii, V. B. Shur, M. E. Vol'pin, *J. Organomet. Chem.* **1990**, *391*, 119-122.

[21] a) J. Chatt, L. A. Duncanson, *J. Chem. Soc.* **1953**, 2939-2947; b) M. J. S. Dewar, *Bull. Soc. Chim. Fr.* **1951**, C71-79.

[22] a) E. Kleinpeter, A. Frank, *J Phys Chem A* **2009**, *113*, 6774-6778; b) B. Wrackmeyer, K. Horchler, *Progress in Nuclear Magnetic Resonance Spectroscopy* **1990**, *22*, 209-253.

[23] a) K. Lubitz, U. Radius, *Organometallics* **2019**, *38*, 2558-2572; b) E. Becker, V. Stingl, G. Dazinger, M. Puchberger, K. Mereiter, K. Kirchner, *J. Am. Chem. Soc.* **2006**, *128*, 6572-6573, c) Y. Ohki, T. Hatanaka, K. Tatsumi, *J. Am. Chem. Soc.* **2008**, *130*, 17174-17186; d) C. Ma, C. Ai, Z. Li, B. Li, H. Song, S. Xu, B. Wang, *Organometallics* **2014**, 33, 5164-5172; T. Hatanaka, Y. Ohki, K. Tatsumi, *Angew. Chem.* **2014**, *126*, 2765-2767; *Angew. Chem., Int. Ed.* **2014**, *53*, 2727-2729.

[24] a) Y. Wakatsuki, N. Koga, H. Werner, K. Morokuma, *J. Am. Chem. Soc.* **1997**, *119*, 360-366; b) D. B. Grotjahn, X. Zeng, A. L. Cooksy, W. S. Kassel, A. G. DiPasquale, L. N. Zakharov, A. L. Rheingold, *Organometallics* **2007**, *26*, 3385-3402; c) M. I. Bruce, *Chem. Rev.* **1991**, *91*, 197-257; d) H. Werner, *Coord. Chem. Rev.* **2004**, *248*, 1693-1702; e) S. W. Roh, K. Choi, C. Lee, *Chem. Rev.* **2019**, *119*, 4293-4356.

[25] Y. Hoshimoto, Y. Hayashi, H. Suzuki, M. Ohashi, S. Ogoshi, *Organometallics* **2014**, *33*, 1276-1282.

[26] N. D. Clement, K. J. Cavell, L. I. Ooi, *Organometallics* **2006**, *25*, 4155-4165.

[27] R. Dorta, E. D. Stevens, N. M. Scott, C. Costabile, L. Cavallo, C. D. Hoff, S. P. Nolan, *J. Am. Chem. Soc.* **2005**, *127*, 2485-2495.

[28] A. Poater, B. Cosenza, A. Correa, S. Giudice, F. Ragone, V. Scarano, L. Cavallo, *Eur. J. Inorg. Chem.* **2009**, *2009*, 1759-1766.

[29] A. Poater, F. Ragone, S. Giudice, C. Costabile, R. Dorta, S. P. Nolan, L. Cavallo, *Organometallics* **2008**, *27*, 2679-2681.

[30] D. G. Gusev, *Organometallics* **2009**, *28*, 6458-6461.

[31] a) A. Liske, K. Verlinden, H. Buhl, K. Schaper, C. Ganter, *Organometallics* **2013**, *32*, 5269-5272; b) O. Back, M. Henry-Ellinger, C. D. Martin, D. Martin, G. Bertrand, **2013**, *52*, 2939-2943; c) S. V. C. Vummaleti, D. J. Nelson, A. Poater, A. Gómez-Suárez, D. B. Cordes, A. M. Z. Slawin, S. P. Nolan, L. Cavallo, *Chem. Sci.* **2015**, *6*, 1895-1904.

[32] A. N. Desnoyer, W. He, S. Behyan, W. Chiu, J. A. Love, P. Kennepohl, *Chem.* **2019**, *25*, 5259-5268.

[33] L. P. Wolters, R. Koekkoek, F. M. Bickelhaupt, *ACS Catalysis* **2015**, *5*, 5766-5775.

[34] Y. Tian, X. Guo, I. Krummenacher, Z. Wu, J. Nitsch, H. Braunschweig, U. Radius, T. B. Marder, *J. Am. Chem. Soc.* **2020**, *142*, 18231-18242.

Chapter IV

Cationic Nickel d^9-Metalloradicals $[Ni(NHC)_2]^+$

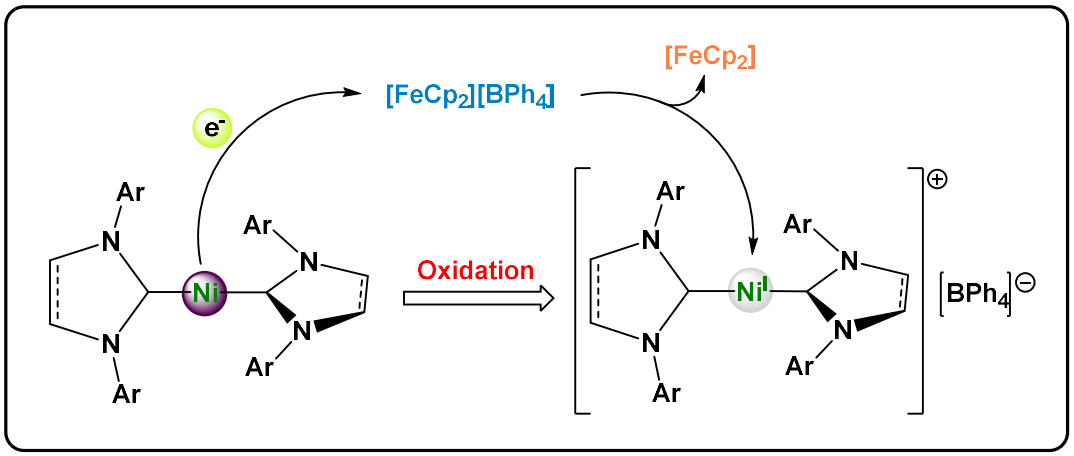

4 Cationic Nickel d^9-Metalloradicals $[Ni(NHC)_2]^+$

4.1 Introduction

Stable two-coordinate, open-shell transition metal complexes have attracted much attention in the last decades[1] due to their high reactivity and to very interesting chemical and physical properties, which allow different applications in small molecule activation, catalysis[2] and magnetism.[3] Bulky ligands are usually necessary to stabilize the monomeric complexes,[4] as they tend to decompose, disproportionate, aggregate to oligomers or form larger ionic lattices. Even with such a steric protection of the metal center, these complexes are often very air and moisture sensitive.

In the past years our group reported on the use of $[Ni^0(NHC)_2]$ synthons in organometallic chemistry and catalysis in stoichiometric[5] and catalytic[6] reactions. We recently highlighted stereo-electronic effects on the reactivity of different *N*-substituted and backbone methylated NHC ligands in the chemistry of $[Ni^0(NHC)_2]$ with small molecules such as alkenes, alkynes, carbonyls and aldehydes (see Chapters II and III).[5j, 5k] This work already revealed that mononuclear, linear nickel complexes $[Ni^0(NHC)_2]$ such as $[Ni(Mes_2Im)_2]$ **1** (Mes_2Im = 1,3-dimesitylimidazolin-2-ylidene) much more readily transfer electrons to substrates compared to synthons with smaller NHC ligands. Our work on C–F bond activation and defluoroborylation of polyfluoroarenes using the NHC stabilized Ni(0) complexes $[Ni_2(^iPr_2Im)_4(\mu\text{-}(\eta^2\text{:}\eta^2)\text{-COD})]$ **6a**[7] and $[Ni(Mes_2Im)_2]$ **1**[8] revealed that $[Ni_2(^iPr_2Im)_4(\mu\text{-}(\eta^2\text{:}\eta^2)\text{-COD})]$ **6a** ($^iPr_2Im$ = 1,3-di-*iso*-propylimidazolin-2-ylidene) favors a concerted (in conjunction with an NHC-assisted) reaction pathway, whereas **1** favors a radical (in conjunction with an NHC-assisted) pathway for the C–F bond activation step.[9] Most interestingly, a detailed exploration of the redox potentials of $[Ni(Mes_2Im)_2]$ **1** and polyfluorinated arenes revealed that in these cases the radical formation is not due to simple electron transfer from **1** to the fluoroarene but due to the approach of the fluoroarene to the nickel center of **1** and the abstraction of a fluoride atom in the first step of the C–F bond activation process. Similarly, for the borylation of aryl chlorides using **1** as a catalyst[6g] we also excluded one electron transfer from **1** to chloroarenes. However, these studies revealed that the reversible redox potential for the process $[Ni(Mes_2Im)_2]$ (**1**) → $[Ni(Mes_2Im)_2]^+$ (**IV-1$^+$**) + e^- lies fairly low, at approximately -1.90 V in THF as a solvent.[8b] Furthermore, we were able to synthesize and characterize

(including X-ray diffraction, XRD) the cationic linear complex $[Ni^{I}(Mes_2Im)_2][BF_4]$ **IV-1^{+BF4}** independently.[9]

As we noticed before that this type of one electron transfer should be very important to many catalytic reactions using nickel complexes $[Ni^{0}(NHC)_2]$ which are stabilized by the "classical" five-membered ring Arduengo-carbenes, we initiated a detailed investigation on the redox potentials of these compounds as well as synthesis and characterization of cationic mononuclear Ni(I) complexes $[Ni^{I}(NHC)_2]^{+}$. In addition to the use in catalysis it has turned out that similar linear coordinated Ni(I) complexes show some interesting properties (see below). Although the examples mentioned below are limited to linear complexes, the nickel(I) oxidation state has been stabilized by many other ligands and in different coordination spheres in the past few years.[1c, 10]

The first neutral NHC-stabilized, two-coordinate Ni(I) complexes were reported in 2008 by Hillhouse and co-workers,[10a] which reacted Sigman's dimer $[(Dipp_2Im)Ni(\mu\text{-}Cl)]_2$[11] ($Dipp_2Im$ = 1,3-(2,6-di-*iso*-propylphenyl)imidazolin-2-ylidene) with $NaN(SiMe_3)_2$ or LiN(H)Dipp to yield the heteroleptic Ni(I) complexes $[(Dipp_2Im)Ni\{N(SiMe_3)_2\}]$ **30** (see Figure IV.1) and [(Dipp$_2$Im)Ni{N(H)Dipp}].[11] A few years later this group also reported alkyl- and aryl-substituted derivatives $[(Dipp_2Im)Ni\{CH(SiMe_3)_2\}]$ and [(Dipp$_2$Im)Ni(dmp)] (dmp = 2,6-dimesitylphenyl).[12] The groups of Tilley *et al.*[13] and Power *et al.*[14] independently demonstrated that one-electron reduction of $[Ni^{II}\{N(SiMe_3)Dipp\}_2]$ is suitable to generate anionic, homoleptic complexes of the type $[Cat][Ni^{I}\{N(SiMe_3)Dipp\}_2]$ **31** (Cat = cation = K, NBu_4), which were subsequently transformed into neutral Ni(I) complexes by protonation with NEt_3HCl in the presence of neutral two-electron donor ligands, yielding complexes $[(L)Ni^{I}\{N(SiMe_3)Dipp\}]$ (L = $Dipp_2Im$, P^tBu_3, P^iPr_3).[15] In a further ligand exchange reaction the second amido ligand was replaced with dtbmp (dtbmp = 2,6-di-*tert*-butyl-4-methylphenol), which either coordinates *via* the oxygen atom or as an η^5-coordinated phenol ligand, respectively. In 2013, Whittlesey *et al.* reported the linear homoleptic $[Ni^{I}(6\text{-}Mes)_2]^{+}$ cation **32a** using the six-membered ring *N*-heterocyclic carbene 6-Mes (= 1,3-dimesityl-3,4,5,6-tetrahydropyrimidin-2-ylidene), which was the first d^9 Ni(I) complex associated with single ion magnet (SIM) behavior. The high magnetic anisotropy of this complex is caused by a very unique orbital splitting resulting in an unquenched angular orbit momentum.[16] Krossing *et al.* reported the related phosphine complex $[Ni^{I}(P^tBu_3)_2]^{+}$ **33**, which was just the second example for a homoleptic, cationic two-coordinate Ni(I) complex.[17] They also described some structural and magnetic similarities to complex

32a, but did not identify SIM behavior for this complex. Just recently, Whittlesey and co-workers expanded their work on linear Ni(I) complexes stabilized by six- or seven-membered NHC ligands and presented three related complexes $[Ni^{I}(7\text{-Mes})_2]^+$ **32b**, $[Ni^{I}(6\text{-Xyl})_2]^+$ **32c**, $[Ni^{I}(7\text{-Xyl})_2]^+$ **32d** including a detailed discussion about their magnetic properties, focusing on the extreme *g*-tensor anisotropy and its dependence on structural distortion.[18] It was demonstrated that these complexes reveal an orbitally degenerate ground state $^2\Delta$, which results from a unique crystal-field splitting (*vide infra*), and therefore leads to very large magnetic anisotropy. The noticeable differences in the low-temperature magnetic relaxation of these compounds were attributed to different vibrational modes and to spin-phonon coupling, while the different torsion angles of the ligands seem to have no influence on the relaxation times, respectively.[18]

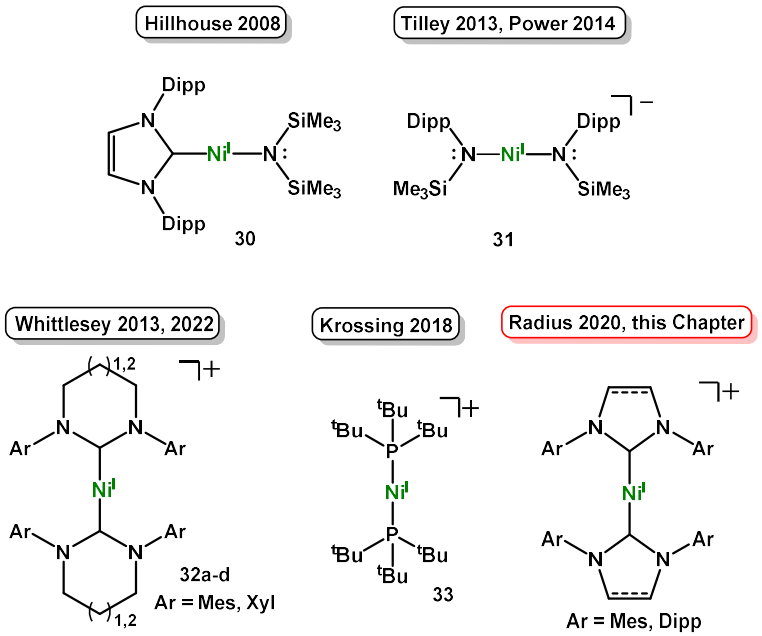

Figure IV.1 Selected examples of two-coordinated, linear Ni(I) complexes.

4.2 Results and Discussion

Our investigations were started with the preparation of a series of five literature known linear Ni(0) complexes stabilized by different saturated and unsaturated five-ring NHC ligands or a cyclic (alkyl)(amino)carbene (cAAC) ligand, respectively. The complexes [Ni(Mes_2Im)$_2$] **1**,[19] [Ni(Mes_2Im^{H2})$_2$] **2**,[20] [Ni($Dipp_2Im$)$_2$] **3**,[21] [Ni($Dipp_2Im^{H2}$)$_2$] **4**[21a] and [Ni($cAAC^{Me}$)$_2$] **5**[22] (Mes_2Im^{H2} = 1,3-dimesitylimidazolidin-2-ylidene, $Dipp_2Im^{H2}$ = 1,3-(2,6-di-*iso*-propylphenyl)imidazolidin-2-ylidene, $cAAC^{Me}$ = 1-(2,6-di-*iso*-propylphenyl)-3,3,5,5-tetramethylpyrrolidin-2-yliden) were synthesized by slightly modified published procedures (see Experimental Details). While **1** and **2** were synthesized by a simple ligand exchange reaction starting from [Ni(η^4-COD)$_2$] and two equivalents of the corresponding NHC, complexes **3**, **4** and **5** were synthesized in two steps *via* a reductive route starting from [$NiBr_2$•DME] and two equivalents of NHC. All compounds **1-5** were isolated as black solids which have a dark purple color in solution, and the NMR spectroscopy of these complexes matched the data reported previously.[19-22] As an X-ray structure of complex **2** has not been reported yet, crystals of this compound suitable for XRD were grown from a saturated hexane solution of the complex at -30 °C (Figure IV.2).

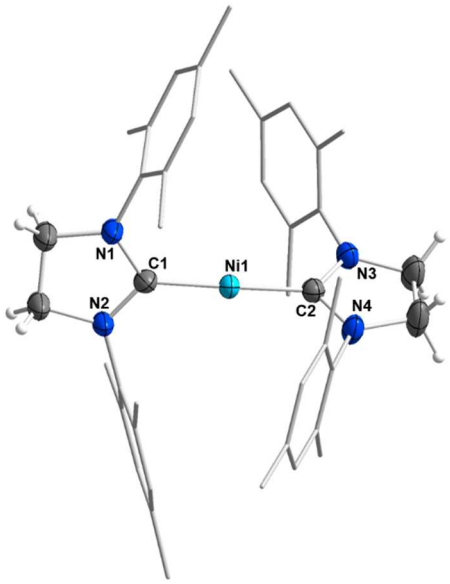

Figure IV.2 Molecular structure of [Ni(Mes_2Im^{H2})$_2$] **2** in the solid state (ellipsoids set at the 50 % probability level). The hydrogen atoms have been omitted for clarity. Selected bond lengths [Å] and angles [°] of **2**: Ni1–C1 1.8187(17), Ni1–C2 1.8332(16), C1–N1 1.363(2), C1–N2 1.361(2), C2–N3 1.351(2), C2–N4 1.353(2); C1–Ni1–C2 176.46(8),

N1–C1–N2 105.99(15), N3–C2–N4 106.64(14), plane (N1–C1–N2) – plane (N3–C2–N4) 66.58(11).

Complex **2** crystallizes in the monoclinic space group $P2_1/c$ and reveals a linear geometry with a $C_{carbene}$–Ni–$C_{carbene}$ angle of 176.46(8)° and Ni–$C_{carbene}$ distances of 1.8187(17) and 1.8332(16) Å, which is perfectly in line with the structural parameters of other complexes [$Ni^0(NHC)_2$] **1** and **3-5** (compare Table IV.1). The torsion angle between the two planes spanned by the NHC rings (plane N1–C1–N2 – plane N3–C2–N4) of 66.6° is slightly larger than those observed for the other complexes (46.1 – 60.7°), presumably due to the increasing steric demand of the NHC imposed by the saturated NHC backbone.[19-22]

The electronic situation for neutral Ni (d^{10}) complexes [$Ni(NHC)_2$][23] and cationic Ni (d^9) complexes can be exemplified for the known complexes [$Ni(Mes_2Im)_2$] **1** and [$Ni(Mes_2Im)_2$]$^+$ **IV-1$^+$**. Density functional theory (DFT) calculations on **1** and **IV-1$^+$** revealed that the energy minimum of both structures optimizes in a D_{2d}-symmetric geometry with distances Ni−C_{calc} of 1.8457 Å in **1** and 1.9283 Å in **IV-1$^+$**, i. e. the Ni–C distances elongate upon oxidation. The electronic structure of the closed-shell species **1** exhibits five occupied metal-based orbitals in an approximate 1:2:2 splitting pattern (Figure IV.3). The HOMO corresponds to the orbital $32a_1$, which is dominated by Ni d_{z^2} and s character (an s-d_{z^2} hybrid orbital, z is the Ni–C axis), and lies at comparable high energies (-3.14 eV). The near-degenerate orbitals $31b_2$ and $15b_2$, which differ by only 0.01 eV in energy, are Ni centered d_{xy} and $d_{x^2-y^2}$ orbitals, and these lie ca. 0.35 eV below the σ-type orbital $32a_1$. These orbitals should be perfectly degenerate e_g orbitals within *pseudo*-$D_{\infty}h$. Below that lie at -3.78 eV the degenerate orbitals 43e (also e_g in *pseudo*-$D_{\infty}h$ symmetry), which are d_{xz} and d_{yz} orbitals in character. While a similar 1:2:2 orbital splitting was reported for $Pd(NHC)_2$,[24] the neutral Ni(0) complex [$Ni(6\text{-}Mes)_2$] was computed to show a different 2:1:2 splitting where the HOMO corresponds to the d_{xz} and d_{yz} orbitals, followed by the d_{z^2} orbital and a low lying set of degenerate d_{xy} and $d_{x^2-y^2}$ orbitals.[16]

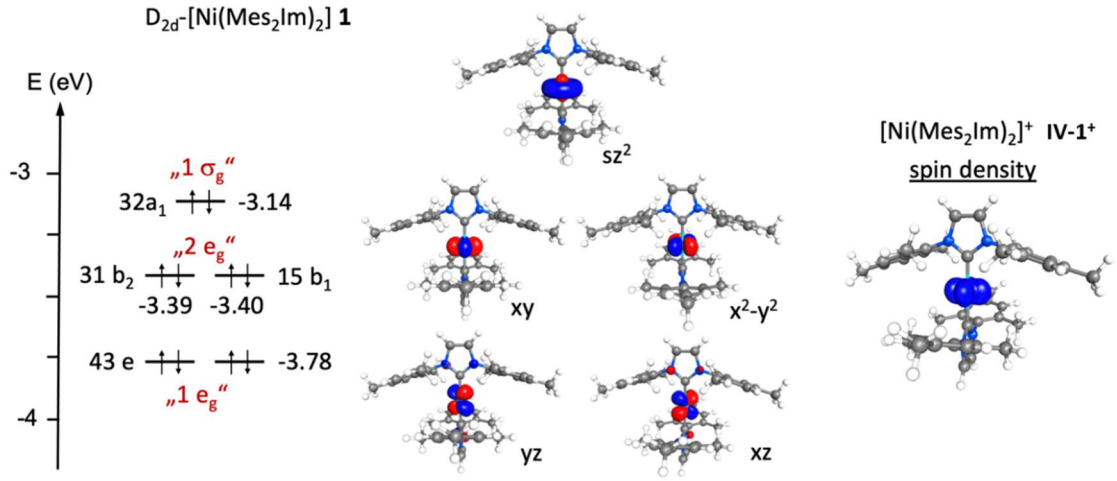

Figure IV.3 Highest-lying occupied molecular orbitals of [Ni(Mes$_2$Im)$_2$] **1**, with associated energies (PBE0//def2-TZVP(Ni)/def2-SVP(C,N,H)). Symmetry labels given in black reflect local D_{2d} geometry, those given in red pseudo-$D_{\infty}h$ symmetry at the metal center. On the right side a plot of the DFT-calculated (PBE0//def2-TZVP(Ni)/def2-SVP(C,N,H)) spin density of [Ni(Mes$_2$Im)$_2$]$^+$ **IV-1$^+$** is shown.

However, for the generation of the complex cation [Ni(Mes$_2$Im)$_2$]$^+$ **IV-1$^+$**, oxidation occurs from the $2e_g$ set of orbitals. The DFT-calculated minimum structure is also of D_{2d} symmetry and oxidation leads to an orbitally degenerated system. The electronic structure of such degenerated systems is not readily described by a single-configuration DFT calculation. However, we also provide in Figure IV.3 the DFT-calculated spin density of this complex which reveals oxidation from the "$2e_g$" set of [Ni(Mes$_2$Im)$_2$]. Whittlesey and co-workers recently described a similar very unique orbital splitting for their six- or seven-membered [Ni^I(NHC)$_2$] complexes **32a-d** by *ab initio* ligand-field analysis (AI-LFT). They reported an orbital order of (d_{xz}, d_{yz}) < d_{z^2} ≈ (d_{xy}, $d_{x^2-y^2}$), where the d_{xz} and d_{yz} orbitals are stabilized by π-backbonding from Ni to the NHCs and d_{z^2} is stabilized by 3d-4s mixing. This leads to an orbitally degenerate ground state $^2\Delta$ and a very large magnetic anisotropy. This orbital degeneracy is also central to understanding of the EPR spectra and the magnetic properties of **IV-1$^+$** and the analogous complexes **IV-2$^+$ – IV-5$^+$** (see below).

To probe if (reversible) one-electron oxidation is possible for all complexes **1-5**, cyclovoltammetry measurements were carried out on these compounds (Figure IV.4). The cyclic voltammograms (CV) show each the presence of a chemically reversible oxidation/reduction associated with a redox potential between -1.89 V (**1**) and -1.37 V

(**5**) for the redox couple Ni^0/Ni^I (in THF vs Fc^+/Fc).[25] All CVs revealed nearly identical oxidation potentials for the NHC complexes in a narrow range between -1.89 V and -1.64 V, whereas $[Ni(cAAC^{Me})_2]$ **5** shows a significantly reduced redox potential in solution (-1.37 V), which is in line with the better accepting capabilities of the $cAAC^{Me}$ ligand and thus reduced electron density at the central nickel atom.[26]

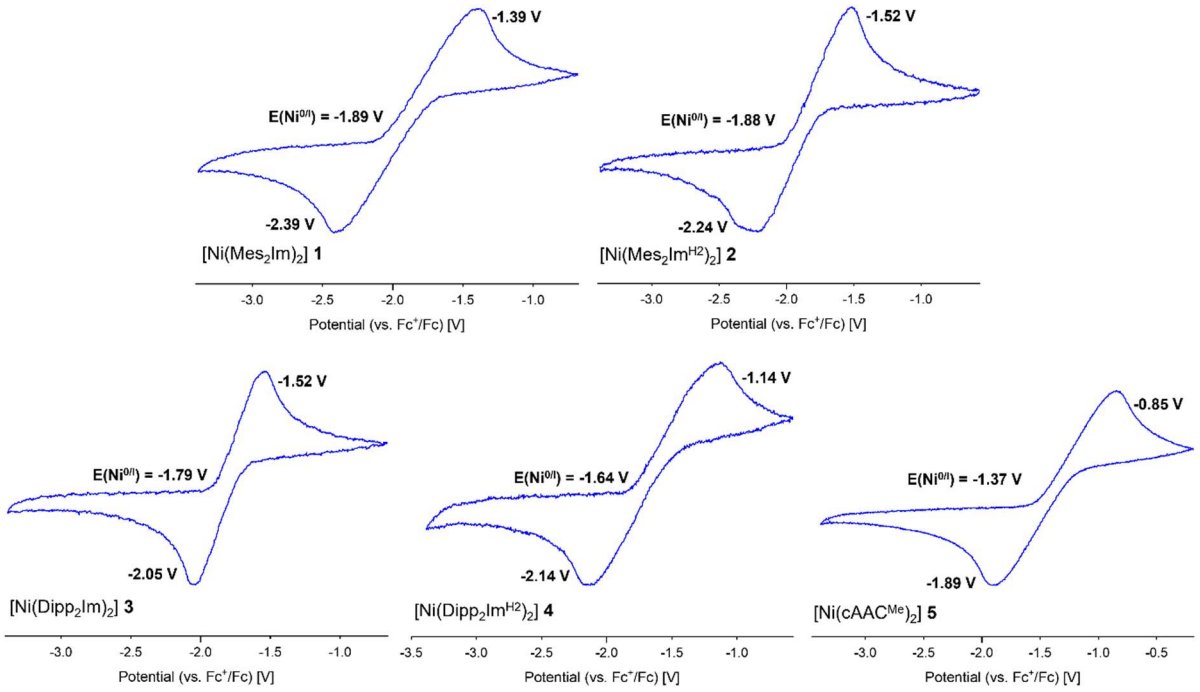

Figure IV.4 Cyclic voltammograms of the Ni^0/Ni^I redox couple of complexes **1-5** (in THF vs Fc^+/Fc).

According to the CV spectra, one-electron oxidation using the $[FeCp_2]^+$ cation, as published previously for the synthesis of $[Ni^I(Mes_2Im)_2][BF_4]$ **IV-1^{+BF4}**, should allow synthesis and preparation of the $[Ni^I(NHC)_2]^+$ cations under consideration. However, since **IV-1^{+BF4}** had only low solubility in common organic solvents and Ni–F contacts to the counter ion (or even a complete fluoride transfer) could not be excluded with certainty, we decided to use the tetraphenyl-borate salt $[FeCp_2][BPh_4]$ as oxidation reagent for this study. This anion should improve solubility of the corresponding nickel complex and prevent anion-cation contact to the cationic metal center. Thus, complexes $[Ni^I(Mes_2Im)_2][BPh_4]$ **IV-1$^+$**, $[Ni^I(Mes_2Im^{H2})_2][BPh_4]$ **IV-2$^+$**, $[Ni^I(Dipp_2Im)_2][BPh_4]$ **IV-3$^+$**, $[Ni^I(Dipp_2Im^{H2})_2][BPh_4]$ **IV-4$^+$** and $[Ni^I(cAAC^{Me})_2][BPh_4]$ **IV-5$^+$** were synthesized upon addition of one equiv. of $[FeCp_2][BPh_4]$ to solutions of the

neutral Ni(0) compounds and isolated as colorless, off-white or yellow (**IV-5$^+$**) solids in good to excellent yields of 66 – 89 % (see Scheme IV.1). The salts are insoluble in non-polar solvents such as hexane, toluene or benzene, **IV-1$^+$ – IV-4$^+$** are soluble in THF, while **IV-5$^+$** is soluble in dichloromethane. The complexes were fully characterized by using elemental analysis, IR and NMR spectroscopy, HRMS and XRD. The paramagnetically shifted ^{1}H NMR spectra of compounds **IV-1$^+$ – IV-5$^+$** all reveal the same number of signals as their neutral Ni(0) analogues plus three broad resonances in the aromatic region which belong to the phenyl rings of the $[BPh_4]^-$ counter ion. For example, the ^{1}H NMR spectra of **IV-1$^+$** and **IV-2$^+$** both reveal seven paramagnetically shifted broad resonances in the range between -3.00 ppm and 21.08 ppm with significant broadening of each signal of ca. 3-4 ppm. For the complexes **IV-3$^+$** and **IV-4$^+$**, nine strongly shifted broad signals were detected in the range between -51.07 and 71.84 ppm, respectively. **IV-5$^+$** reveals 11 signals in a range between -14.36 and 24.66 ppm in the ^{1}H NMR spectrum. The ^{11}B NMR spectra of each salt revealed one sharp singlet for the tetraphenyl-borate salts, with different paramagnetic shifts in the range between -6.50 and -4.15 ppm.

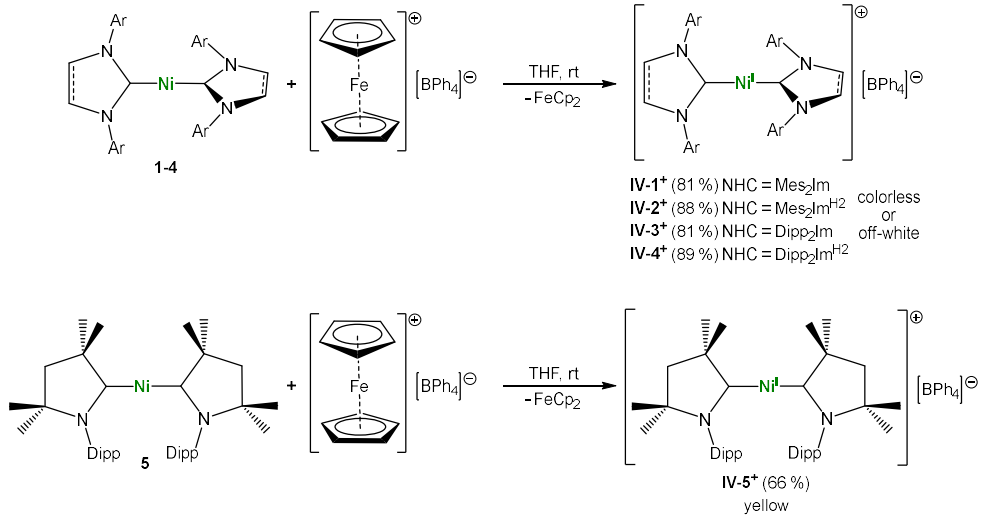

Scheme IV.1 Synthesis of linear Ni(I) complexes $[Ni^I(Mes_2Im)_2][BPh_4]$ **IV-1$^+$**, $[Ni^I(Mes_2Im^{H2})_2][BPh_4]$ **IV-2$^+$**, $[Ni^I(Dipp_2Im)_2][BPh_4]$ **IV-3$^+$**, $[Ni^I(Dipp_2Im^{H2})_2][BPh_4]$ **IV-4$^+$** and $[Ni^I(cAAC^{Me})_2][BPh_4]$ **IV-5$^+$**.

Crystals suitable for X-ray diffraction of compounds **IV-1$^+$ – IV-5$^+$** were obtained either by slow diffusion of hexane into a saturated THF solution (**IV-1$^+$**), slow evaporation of THF (**IV-2$^+$**) or DCM (**IV-5$^+$**) solutions of the corresponding complex, or by storing saturated solutions of the salt in THF at -30 °C (**IV-3$^+$** and **IV-4$^+$**) (see Figure IV.5 and Table IV.1). The complexes crystallize in the monoclinic space groups C2/c (**IV-1$^+$**, **IV-2$^+$** and **IV-5$^+$**) or $P2_1/n$ (**IV-3$^+$**), except for **IV-4$^+$**, which crystallizes in the triclinic space group $P\bar{1}$. All compounds **IV-1$^+$ – IV-5$^+$** reveal linear geometries with $C_{carbene}$–Ni–$C_{carbene}$ angles in the range between 178.27(7)° and 180° and Ni–$C_{carbene}$ distances of 1.8954(12) – 1.9779(16) Å. In each case, the Ni–$C_{carbene}$ bond lengths are slightly longer compared to their neutral analogues **1-5** (see Table IV.1), as predicted by the DFT-calculations (*vide supra*).[19-22] With this elongation of the nickel-carbene bond in the radical cations comes an increase in the N–C–N angle of the coordinated carbene, which corresponds to an increased p-character in the carbene σ-type orbitals due to the polarization of the Ni-C bonds of the cations towards the metal center. The torsion angles between the NHC or cAAC^{Me} ligands (spanned by the two planes N–$C_{carbene}$–N or N–$C_{carbene}$–CMe_2 , respectively, for **IV-5$^+$**), which were observed in the range of 0° - 53° do not follow a simple trend. The cAAC^{Me} complex **IV-5$^+$** reveals no twisting between the cAAC^{Me} ligands (compared to 60.7° in neutral complex **5**) while the torsion angles of **IV-1$^+$** and **IV-2$^+$** strongly decrease and the torsion angles of **IV-3$^+$** and **IV-4$^+$** just slightly increase upon oxidation.

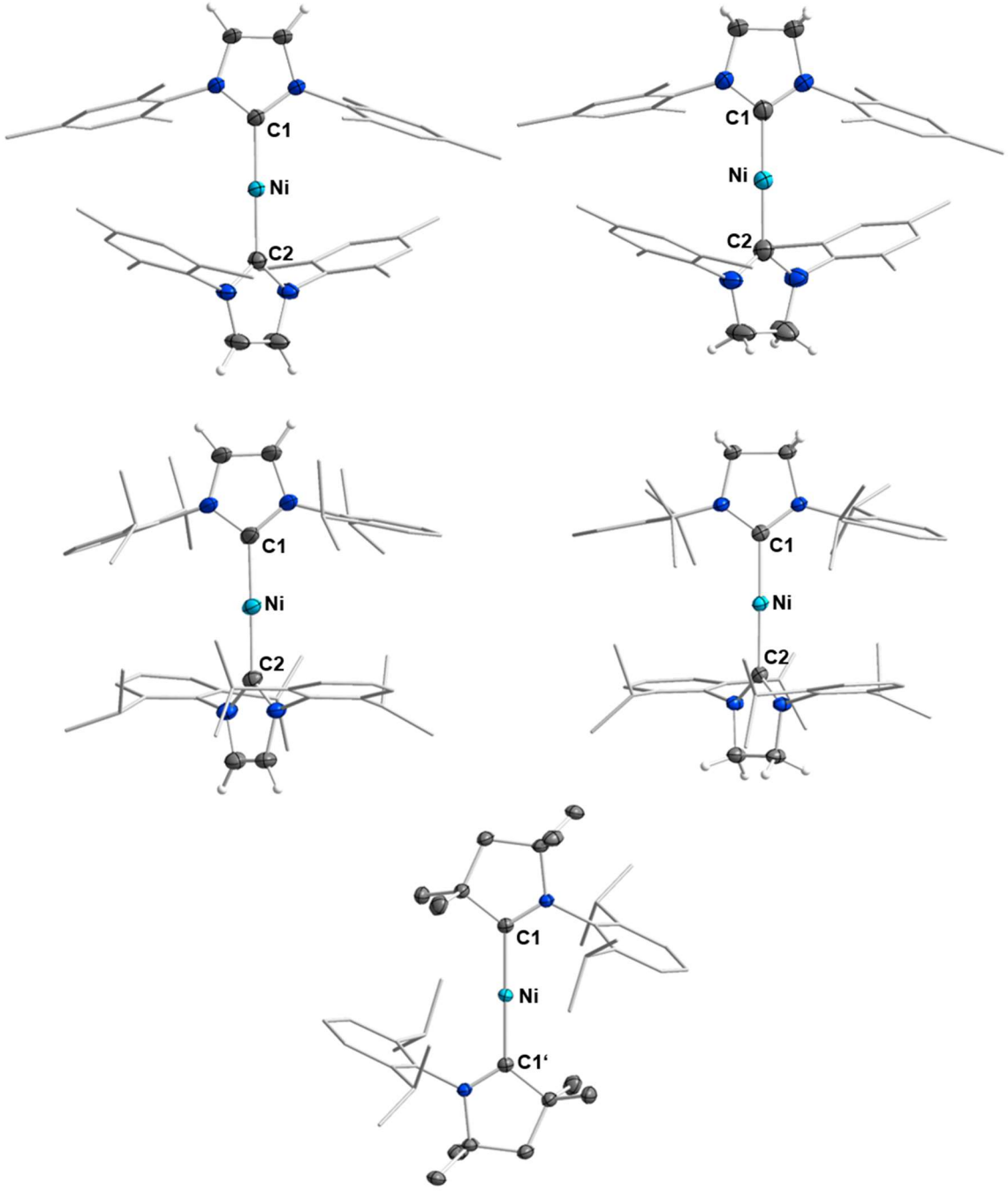

Figure IV.5 Molecular structures of the cations of $[Ni^{I}(NHC)_2][BPh_4]$: $[Ni^{I}(Mes_2Im)_2]^+$ **IV-1⁺** (top left), $[Ni^{I}(Mes_2Im^{H2})_2]^+$ **IV-2⁺** (top right), $[Ni^{I}(Dipp_2Im)_2]^+$ **IV-3⁺** (middle left), $[Ni^{I}(Dipp_2Im^{H2})_2]^+$ **IV-4⁺** (middle right) and $[Ni^{I}(cAAC^{Me})_2]^+$ **IV-5⁺** (bottom center) in the solid state (ellipsoids set at the 50 % probability level). The BPh_4 anions, co-crystallized THF molecules (**IV-3⁺** and **IV-4⁺**) and hydrogen atoms, except of the backbone hydrogen atoms have been omitted for clarity. For selected bond lengths [Å] and angles [°] of **IV-1⁺ – IV-5⁺** see Table IV.1.

Table IV.1 Important structural data and magnetic moments in solution (Evans method) of the literature known Ni(0) complexes [Ni(Mes$_2$Im)$_2$] **1**,[19] [Ni(Mes$_2$Im^{H2})$_2$] **2**,[20] [Ni(Dipp$_2$Im)$_2$] **3**,[21] [Ni(Dipp$_2$Im^{H2})$_2$] **4**[21a] and [Ni(cAAC^{Me})$_2$] **5**[22] and their oxidized Ni(I) analogues [Ni^{I}(Mes$_2$Im)$_2$][BPh$_4$] **IV-1$^+$**, [Ni^{I}(Mes$_2$Im^{H2})$_2$][BPh$_4$] **IV-2$^+$**, [Ni^{I}(Dipp$_2$Im)$_2$][BPh$_4$] **IV-3$^+$**, [Ni^{I}(Dipp$_2$Im^{H2})$_2$][BPh$_4$] **IV-4$^+$** and [Ni^{I}(cAAC^{Me})$_2$][BPh$_4$] **IV-5$^+$**.

Compound	$d_{Ni–NHC}$ [Å]	∢ NHC-Ni-NHC [°]	∢ N-$C_{carbene}$-N/C [°]	torsion angle [°]	μ_{eff} [μ_B]
1	1.827(6)/ 1.830(6)	176.4(3)	101.5(5)/ 102.5(5)	53.0	-
IV-1$^+$	1.8954(12)/ 1.8975(13)	179.31(6)	104.19(11)/ 104.27(11)	39.4	2.42
2	1.8187(17)/ 1.8332(16)	176.46(8)	105.99(15)/ 106.64(14)	66.6	-
IV-2$^+$	1.897(7)/ 1.902(7)	179.8(4)	108.1(6)/ 108.6(6)	32.2	2.49
3	1.856(2)/ 1.872(2)	177.78(10)	101.1(2)/ 101.29(19)	46.1	-
IV-3$^+$	1.9237(18)/ 1.9312(16)	178.27(7)	103.24(14)/ 103.25(15)	47.4	3.15
4	1.865(3)/ 1.886(3)	177.35(15)	104.1(3)/ 104.3(3)	47.9	-
IV-4$^+$	1.9734(17)/ 1.9779(16)	179.13(7)	106.91(14)/ 107.15(14)	53.1	2.26
5	1.8419(13)/ 1.8448(14)	166.42(5)	106.40(10)/ 106.49(10)	60.7	-
IV-5$^+$	1.9311(11)	180	108.29(9)	0	2.82

Measurements of the magnetic moments μ_{eff} in solution of compounds **IV-1$^+$ – IV-5$^+$** (Evans method) in THF-d_8 or CD_2Cl_2 (**IV-5$^+$**) revealed values between 2.26 – 3.15 μ_B. All values are significantly larger than the spin-only value of 1.73 μ_B, but also differ certainly from the values of 3.0 – 3.3 μ_B observed for linear complexes [Ni^{I}(NHC)$_2$]$^+$ **32a-d** stabilized by six- and seven-membered NHC ligands.[18] To get further insight into the magnetic properties of **IV-1$^+$ – IV-5$^+$** EPR experiments were performed on

frozen solutions of each of the complexes (**IV-1$^+$ – IV-4$^+$** in THF and **IV-5$^+$** in DCM) as well as on polycrystalline powder samples (compare Table IV.2 and Figure IV.6). The powder spectra of **IV-1$^+$ – IV-4$^+$** revealed highly anisotropic *g*-tensors, with g_1 values between 5.09 – 5.77, as it was observed previously for comparable compounds (**32a-d**).[18] In contrast to Whittlesey's complexes **32a-d**, the five-ring NHC complex cations produced very different g_2 and g_3 values, depending on the carbene. In general, the complexes bearing NHCs with saturated backbones (**IV-2$^+$:** g_2 = 1.02, g_3 = 0.84 and **IV-4$^+$:** g_2 = 1.37, g_3 = 1.07) revealed higher g_2 and g_3 values than their counterparts with unsaturated NHC-backbones (**IV-1$^+$:** g_2 ~ 0.46, g_3 = outside the range of the magnetic field and **IV-3$^+$:** g_2 = 0.68, g_3 = 0.58) and the *N*-Dipp substituted carbenes led to higher g_2/g_3 values compared to the *N*-Mes substituted NHCs. Thus, we found the most extreme *g*-tensor anisotropy for compound **IV-1$^+$** (g_1 = 5.77, g_2 ~ 0.46, g_3 = outside the range of the magnetic field), which is in the same region as reported for the complexes **32a-d** (g_1 = 5.66 – 5.89, g_2 = 0.56 – 0.62, g_3 = 0.55 – 0.58). [18] For the cAAC^{Me} stabilized complex **IV-5$^+$** *g*-tensors which are much less anisotropic (g_1 = 3.73, g_2 = 2.50, g_3 = 1.67) were observed.

Table IV.2 Experimental *g*-Tensors of the powder samples of **IV-1$^+$ – IV-5$^+$** and in solution (shown in parentheses).

Compound	g_1	g_2	g_3
$[Ni^I(Mes_2Im)_2][BPh_4]$ **IV-1$^+$**	5.77 (2.60)	0.46 (2.39)	- (2.00)
$[Ni^I(Mes_2Im^{H2})_2][BPh_4]$ **IV-2$^+$**	5.32 (2.58)	1.02 (2.36)	0.84 (2.01)
$[Ni^I(Dipp_2Im)_2][BPh_4]$ **IV-3$^+$**	5.58 (5.78)	0.68 (-)	0.58 (-)
$[Ni^I(Dipp_2Im^{H2})_2][BPh_4]$ **IV-4$^+$**	5.09 (5.53)	1.37 (-)	1.07 (-)
$[Ni^I(cAAC^{Me})_2][BPh_4]$ **IV-5$^+$**	3.73	2.50	1.67

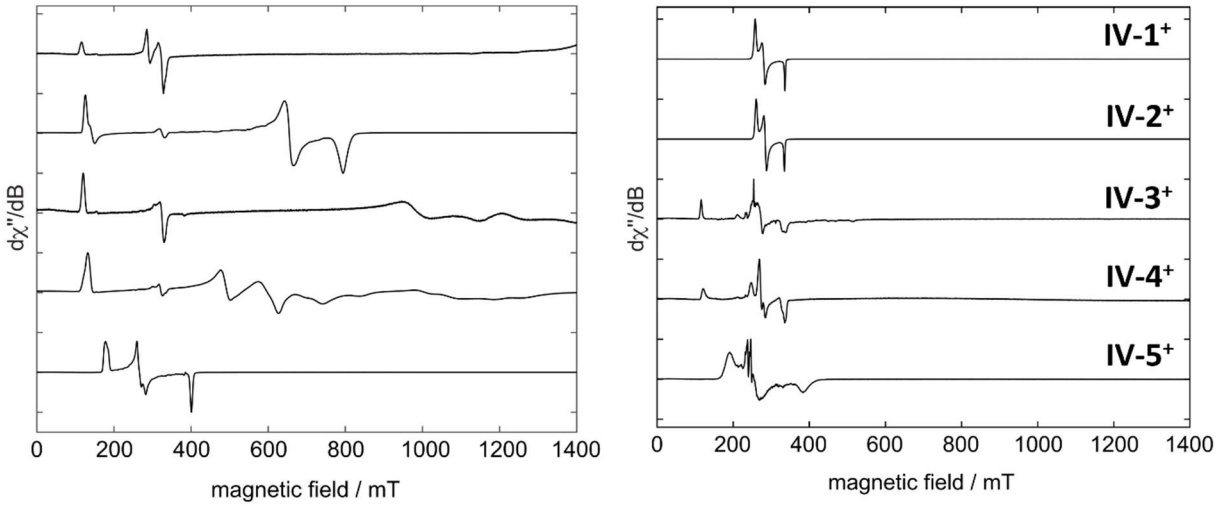

Figure IV.6 Experimental powder X-band CW-EPR spectra of **IV-1$^+$ – IV-5$^+$** (left) and in frozen solution at 10 K (right, **IV-1$^+$ – IV-4$^+$** in THF and **IV-5$^+$** in DCM). For **IV-1$^+$ – IV-4$^+$** the signals in the region of 200 – 400 mT are attributed to paramagnetic impurities or solvent adducts.

Interestingly, the solution EPR spectra of **IV-1$^+$ – IV-4$^+$** differ considerably from the powder spectra. For the *N*-Mes substituted compounds **IV-1$^+$** and **IV-2$^+$**, the EPR spectra measured in THF solutions showed completely new species with *g*-values between 2.60 and 2.00, which are clearly not caused by a linear complex.[9, 17] For *N*-Dipp substituted **IV-3$^+$** and **IV-4$^+$** only the g_1 values could be resolved with a much smaller intensity and some new signals between 200 and 400 mT, arising from impurities or solvent adducts. Interestingly, we obtained a second crystal structure for the complex [Ni^{I}(Mes$_2$Im)$_2$][BF$_4$] **IV-1^{+BF4}** published previously, in which the unit cell contains different cations, of which two-thirds are coordinated by an additional THF molecule (Figure IV.7). This finding is a likely explanation for the EPR resonances found for *N*-Mes substituted complexes **IV-1$^+$**and **IV-2$^+$** in solution, which indicate a non-linear geometry. The resulting signals presumably originate from a T-shaped solvent (THF) adduct formed in solution. For **IV-3$^+$** and **IV-4$^+$** adduct formation is less likely due to the increased steric protection of the nickel atom using the larger *N*-Dipp substituted NHC ligands.

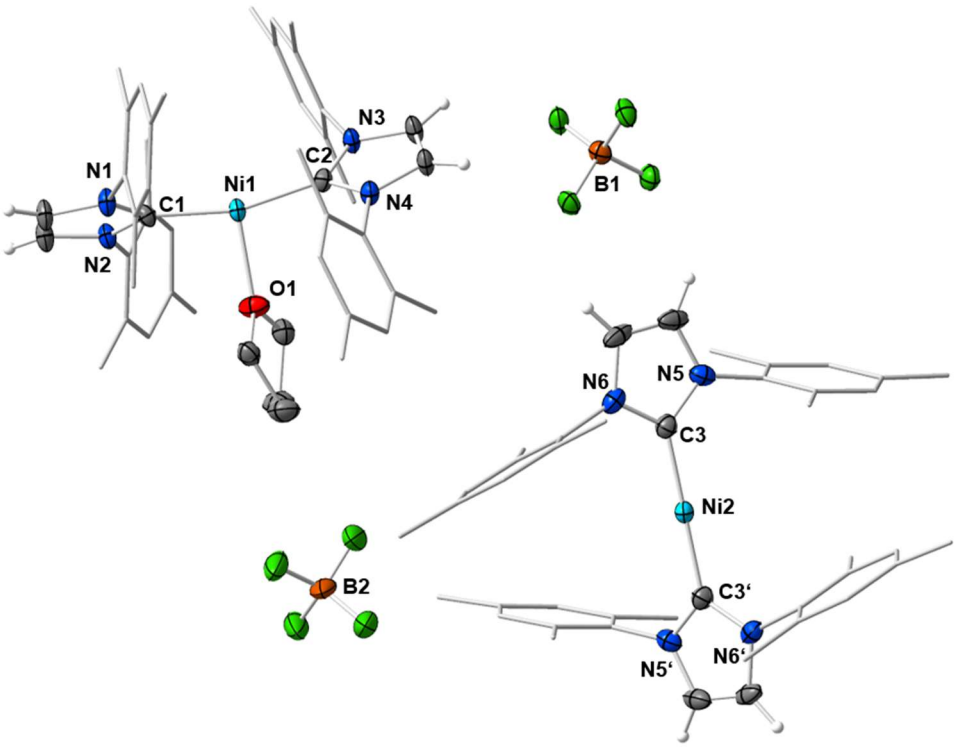

Figure IV.7 Molecular structures of $[Ni^{I}(Mes_2Im)_2(THF)][BF_4]$ **IV-1^{+THF}** and $[Ni^{I}(Mes_2Im)_2][BF_4]$ **IV-1^{+BF4}** in the solid state (ellipsoids set at the 50 % probability level). All hydrogen atoms except of the backbone hydrogen atoms have been omitted for clarity. Selected bond lengths [Å] and angles [°] of **IV-1^{+THF}:** Ni1–C1 1.939(3), Ni1–C2 1.939(3), Ni1–O1 2.094(2), C1–N1 1.362(4), C1–N2 1.365(4), C2–N3 1.365(4), C2–N4 1.358(4); C1–Ni1–C2 164.13(14), C1–Ni1–O1 97.01(12), C2–Ni1–O1 98.86(12), plane (N1–C1–N2) – plane (N3–C2–N4) 54.72(14). Selected bond lengths [Å] and angles [°] of **IV-1^{+BF4}**: Ni2–C3 1.891(3), C3–N5 1.363(4), C3–N6 1.364(4); C3–Ni2–C3’ 179.8(2), N5–C3–N6 103.7(3), plane (N5–C3–N6) – plane (N5’–C3’–N6’) 59.27(13).

4.3 Conclusion

It has been demonstrated previously that homoleptic two-coordinated, linear Ni(I) complexes possess very interesting properties, which allow different applications in small molecule activation, catalysis and magnetism. This chapter demonstrates that redox processes in complexes [Ni(NHC)$_2$], often used in catalysis, easily occur. The redox potentials for a reversible oxidation/reduction process for the redox couple Ni^0/Ni^I lies for the complexes [Ni(Mes$_2$Im)$_2$] **1**, [Ni(Mes$_2$Im^{H2})$_2$] **2**, [Ni(Dipp$_2$Im)$_2$] **3** and [Ni(Dipp$_2$Im^{H2})$_2$] **4** in THF vs Fc^+/Fc in a narrow range between -1.89 V (**1**) and -1.64 V (**4**), depending on the NHC used. [Ni(cAAC^{Me})$_2$] **5** shows a significantly reduced redox potential in solution (-1.37 V), which is in line with the better accepting capabilities of the cAAC^{Me} ligand. Due to the excellent steric protection provided by the NHC ligand and the low lying oxidation potential we believe that electron transfer processes are much more important in catalytic systems using [Ni(NHC)$_2$] as a catalyst as generally accepted. This low lying one-electron oxidation process was used for the synthesis of a variety of stable, two-coordinate nickel-d^9 complexes $[Ni^I(NHC)_2]^+$, stabilized by classical five-ring Arduengo-carbenes and a cyclic (alkyl)(amino)carbene (cAAC). Isolation of the complexes [Ni^I(Mes$_2$Im)$_2$][BPh$_4$] **IV-1$^+$**, [Ni^I(Mes$_2$Im^{H2})$_2$][BPh$_4$] **IV-2$^+$**, [Ni^I(Dipp$_2$Im)$_2$][BPh$_4$] **IV-3$^+$**, [Ni^I(Dipp$_2$Im^{H2})$_2$][BPh$_4$] **IV-4$^+$** and [Ni^I(cAAC^{Me})$_2$][BPh$_4$] **IV-5$^+$** was achieved by one-electron oxidation of the corresponding linear Ni(0) complexes, using ferrocenium tetraphenyl-borate as oxidizing reagent. X-ray diffraction studies of **IV-1$^+$ – IV-5$^+$** revealed linear geometries and the paramagnetic nature of the complexes was verified by NMR measurements, measurement of the magnetic moments in solution (Evans method, range between 2.26 – 3.15 μ_B) and EPR spectroscopy. DFT calculations performed on [Ni(Mes$_2$Im)$_2$] **1** and [Ni(Mes$_2$Im)$_2$]$^+$ **IV-1$^+$** predicted that oxidation occurs from a degenerate e_g set of orbitals, leading to an orbitally degenerate ground state and thus to large magnetic anisotropy in complex **IV-1$^+$**. Theory was confirmed by EPR experiments, showing very high magnetic anisotropies in the solid state for the compounds **IV-1$^+$ – IV-4$^+$**, while the cAAC^{Me}-stabilized complex **IV-5$^+$** revealed significantly reduced anisotropical *g*-tensors. Additional EPR measurements in solution demonstrated extreme variations of the magnetic properties of **IV-1$^+$ – IV-4$^+$**, which culminated in a noticeable decrease of the *g*-tensor anisotropy for the *N*-Mes substituted complexes **IV-1$^+$** and **IV-2$^+$** in solution. This behavior is most likely due to the formation of T-shaped solvent (THF) adducts,

which was exemplified by the observed crystal structure of $[Ni^{I}(Mes_2Im)_2(THF)][BF_4]$ **IV-1^{+THF}**. This study once again illustrates the strong influence of the steric protection by a ligand to the complex metal center with respect to its stability and its magnetic behavior.

4.4 References

[1] a) P. P. Power, *Chem. Rev.* **2012**, *112*, 3482-3507; b) D. L. Kays, *Dalton Trans.* **2011**, *40*, 769-778; c) C. Y. Lin, P. P. Power, *Chem. Soc. Rev.* **2017**, *46*, 5347-5399.

[2] L. J. Taylor, D. L. Kays, *Dalton Trans.* **2019**, *48*, 12365-12381.

[3] a) J. M. Frost, K. L. M. Harriman, M. Murugesu, *Chem. Sci.* **2016**, *7*, 2470-2491; b) A. K. Bar, C. Pichon, J.-P. Sutter, *Coord. Chem. Rev.* **2016**, *308*, 346-380.

[4] P. P. Power, *J. Organomet. Chem.* **2004**, *689*, 3904-3919.

[5] a) T. Schaub, U. Radius, *Z. Anorg. Allg. Chem.* **2006**, *632*, 981-984; b) T. Schaub, M. Backes, U. Radius, *Chem. Commun.* **2007**, 2037-2039; c) T. Schaub, C. Döring, U. Radius, *Dalton Trans.* **2007**, 1993-2002; d) T. Schaub, U. Radius, *Z. Anorg. Allg. Chem.* **2007**, *633*, 2168-2172; e) T. Schaub, M. Backes, O. Plietzsch, U. Radius, *Dalton Trans.* **2009**, 7071-7079; f) T. Zell, T. Schaub, K. Radacki, U. Radius, *Dalton Trans.* **2011**, *40*, 1852-1854; g) B. Zarzycki, T. Zell, D. Schmidt, U. Radius, *Eur. J. Inorg. Chem.* **2013**, 2051-2058; h) J. H. J. Berthel, M. W. Kuntze-Fechner, U. Radius, *Eur. J. Inorg. Chem.* **2019**, 2618-2623; i) J. H. J. Berthel, L. Tendera, M. W. Kuntze-Fechner, L. Kuehn, U. Radius, *Eur. J. Inorg. Chem.* **2019**, 3061-3072; j) L. Tendera, T. Schaub, M. J. Krahfuss, M. W. Kuntze-Fechner, U. Radius, *Eur. J. Inorg. Chem.* **2020**, 3194-3207; k) L. Tendera, M. Helm, M. J. Krahfuss, M. W. Kuntze-Fechner, U. Radius, *Chem. Eur. J.* **2021**, *27*, 17849-17861; l) S. Sabater, D. Schmidt, H. Schmidt, M. Kuntze-Fechner, T. Zell, C. Isaac, N. Rajabi, H. Grieve, W. Blackaby, J. Lowe, S. Macgregor, M. Mahon, U. Radius, M. Whittlesey, *Chem. Eur. J.* **2021**, *27*, 13221-13224.

[6] a) T. Zell, M. Feierabend, B. Halfter, U. Radius, *J. Organomet. Chem.* **2011**, *696*, 1380-1387; b) T. Zell, U. Radius, *Z. Anorg. Allg. Chem.* **2011**, *637*, 1858-1862; c) T. Zell, P. Fischer, D. Schmidt, U. Radius, *Organometallics* **2012**, *31*, 5065-5073; d) D. Schmidt, T. Zell, T. Schaub, U. Radius, *Dalton Trans.* **2014**, *43*, 10816-10827; e) L. Kuehn, D. G. Jammal, K. Lubitz, T. B. Marder, U. Radius, *Chem. Eur. J.* **2019**, *25*, 9514-9521; f) M. W. Kuntze-Fechner, C. Kerpen, D. Schmidt, M. Häring, U. Radius, *Eur. J. Inorg. Chem.* **2019**, 1767-1775; g) Y. M. Tian, X. N. Guo, I. Krummenacher, Z. Wu, J. Nitsch, H. Braunschweig, U. Radius, T. B. Marder, *J. Am. Chem. Soc.* **2020**, *142*, 18231-18242; h) Y.-M. Tian, X.-N. Guo,

Z. Wu, A. Friedrich, S. A. Westcott, H. Braunschweig, U. Radius, T. B. Marder, *J. Am. Chem. Soc.* **2020**, *142*, 13136-13144.

[7] a) T. Schaub, U. Radius, *Chem. Eur. J.* **2005**, *11*, 5024-5030; b) T. Schaub, M. Backes, U. Radius, *J. Am. Chem. Soc.* **2006**, *128*, 15964-15965; c) T. Schaub, P. Fischer, A. Steffen, T. Braun, U. Radius, A. Mix, *J. Am. Chem. Soc.* **2008**, *130*, 9304-9317; d) T. Schaub, P. Fischer, T. Meins, U. Radius, *Eur. J. Inorg. Chem.* **2011**, 3122-3126; e) J. Zhou, J. H. Berthel, M. W. Kuntze-Fechner, A. Friedrich, T. B. Marder, U. Radius, *J. Org. Chem.* **2016**, *81*, 5789-5794.

[8] a) J. Zhou, M. W. Kuntze-Fechner, R. Bertermann, U. S. Paul, J. H. Berthel, A. Friedrich, Z. Du, T. B. Marder, U. Radius, *J. Am. Chem. Soc.* **2016**, *138*, 5250-5253; b) Y. Tian, X. Guo, M. Kuntze-Fechner, I. Krummenacher, H. Braunschweig, U. Radius, A. Steffen, T. B. Marder, *J. Am. Chem. Soc.* **2018**, *140*, 17612-17623.

[9] M. W. Kuntze-Fechner, H. Verplancke, L. Tendera, M. Diefenbach, I. Krummenacher, H. Braunschweig, T. B. Marder, M. C. Holthausen, U. Radius, *Chem. Sci.* **2020**, *11*, 11009-11023.

[10] see for example: a) C. A. Laskowski, G. L. Hillhouse, *J. Am. Chem. Soc.* **2008**, *130*, 13846-13847; b) S. Miyazaki, Y. Koga, T. Matsumoto, K. Matsubara, *Chem. Commun.* **2010**, *46*, 1932-1934; c) K. Zhang, M. Conda-Sheridan, S. R. Cooke, J. Louie, *Organometallics* **2011**, *30*, 2546-2552; d) D. D. Beattie, E. G. Bowes, M. W. Drover, J. A. Love, L. L. Schafer, *Angew. Chem.* **2016**, *128*, 13484–13489; *Angew. Chem. Int. Ed.* **2016**, *55*, 13290-13295; e) S. Pelties, E. Carter, A. Folli, M. F. Mahon, D. M. Murphy, M. K. Whittlesey, R. Wolf, *Inorg. Chem.* **2016**, *55*, 11006-11017; f) K. Matsubara, Y. Fukahori, T. Inatomi, S. Tazaki, Y. Yamada, Y. Koga, S. Kanegawa, T. Nakamura, *Organometallics* **2016**, *35*, 3281-3287. g) P. Zimmermann, C. Limberg, *J. Am. Chem. Soc.* **2017**, *139*, 4233-4242; h) I. Kalvet, Q. Guo, G. J. Tizzard, F. Schoenebeck, *ACS Catal.* **2017**, *7*, 2126-2132; i) R. J. Witzke, T. D. Tilley, *Organometallics* **2022**, *41*, 1565-1571.

[11] B. R. Dible, M. S. Sigman, A. M. Arif, *Inorg. Chem.* **2005**, *44*, 3774-3776.

[12] C. A. Laskowski, D. J. Bungum, S. M. Baldwin, S. A. Del Ciello, V. M. Iluc, G. L. Hillhouse, *J. Am. Chem. Soc.* **2013**, *135*, 18272-18275.

[13] M. I. Lipschutz, X. Yang, R. Chatterjee, T. D. Tilley, *J. Am. Chem. Soc.* **2013**, *135*, 15298-15301.

[14] C.-Y. Lin, J. C. Fettinger, F. Grandjean, G. J. Long, P. P. Power, *Inorg. Chem.* **2014**, *53*, 9400-9406.

[15] M. I. Lipschutz, T. D. Tilley, *Organometallics* **2014**, *33*, 5566-5570.

[16] R. C. Poulten, M. J. Page, A. G. Algarra, J. J. Le Roy, I. Lopez, E. Carter, A. Llobet, S. A. Macgregor, M. F. Mahon, D. M. Murphy, M. Murugesu, M. K. Whittlesey, *J. Am. Chem. Soc.* **2013**, *135*, 13640-13643.

[17] M. M. Schwab, D. Himmel, S. Kacprzak, V. Radtke, D. Kratzert, P. Weis, M. Wernet, A. Peter, Z. Yassine, D. Schmitz, E.-W. Scheidt, W. Scherer, S. Weber, W. Feuerstein, F. Breher, A. Higelin, I. Krossing, *Chem. Eur. J.* **2018**, *24*, 918-927.

[18] W. J. M. Blackaby, K. L. M. Harriman, S. M. Greer, A. Folli, S. Hill, V. Krewald, M. F. Mahon, D. M. Murphy, M. Murugesu, E. Richards, E. Suturina, M. K. Whittlesey, *Inorg. Chem.* **2022**, 61, 1308-1315.

[19] A. J. Arduengo, S. F. Gamper, J. C. Calabrese, F. Davidson, *J. Am. Chem. Soc.* **1994**, *116*, 4391-4394.

[20] N. D. Harrold, A. R. Corcos, G. L. Hillhouse, *J. Organomet. Chem.* **2016**, *813*, 46-54.

[21] a) A. A. Danopoulos, D. Pugh, *Dalton Trans.* **2008**, 30-31; b) K. Matsubara, S. Miyazaki, Y. Koga, Y. Nibu, T. Hashimura, T. Matsumoto, *Organometallics* **2008**, *27*, 6020-6024.

[22] K. C. Mondal, P. P. Samuel, Y. Li, H. W. Roesky, S. Roy, L. Ackermann, N. S. Sidhu, G. M. Sheldrick, E. Carl, S. Demeshko, S. De, P. Parameswaran, L. Ungur, L. F. Chibotaru, D. M. Andrada, *Eur. J. Inorg. Chem.* **2014**, 818-823.

[23] a) U. Radius, F. M. Bickelhaupt, *Organometallics* **2008**, *27*, 3410-3414; b) U. Radius, F. M. Bickelhaupt, *Coord. Chem. Rev.* **2009**, *253*, 678-686.

[24] a) J. C. Green, B. J. Herbert, *Dalton Trans.* **2005**, 1214-1220; b) J. C. Green, R. G. Scurr, P. L. Arnold, F. Geoffrey N. Cloke, *Chem. Commun.* **1997**, 1963-1964; c) M. C. MacInnis, J. C. DeMott, E. M. Zolnhofer, J. Zhou, K. Meyer, R. P. Hughes, O. V. Ozerov, *Chem.* **2016**, *1*, 902-920.

[25] Q. Lin, G. Dawson, T. Diao, *Synlett* **2021**, *32*, 1606-1620.

[26] a) U. S. D. Paul, M. J. Krahfuß, U. Radius, *Chem. unserer Zeit* **2018**, *53*, 212-223; b) U. S. D. Paul, U. Radius, *Eur. J. Inorg. Chem.* **2017**, 3362-3375; c) U. S. D. Paul, U. Radius, *Organometallics* **2017**, *36*, 1398-1407.

Chapter V

Nickel Boryl Complexes and the Nickel-Catalyzed Alkyne-Borylation

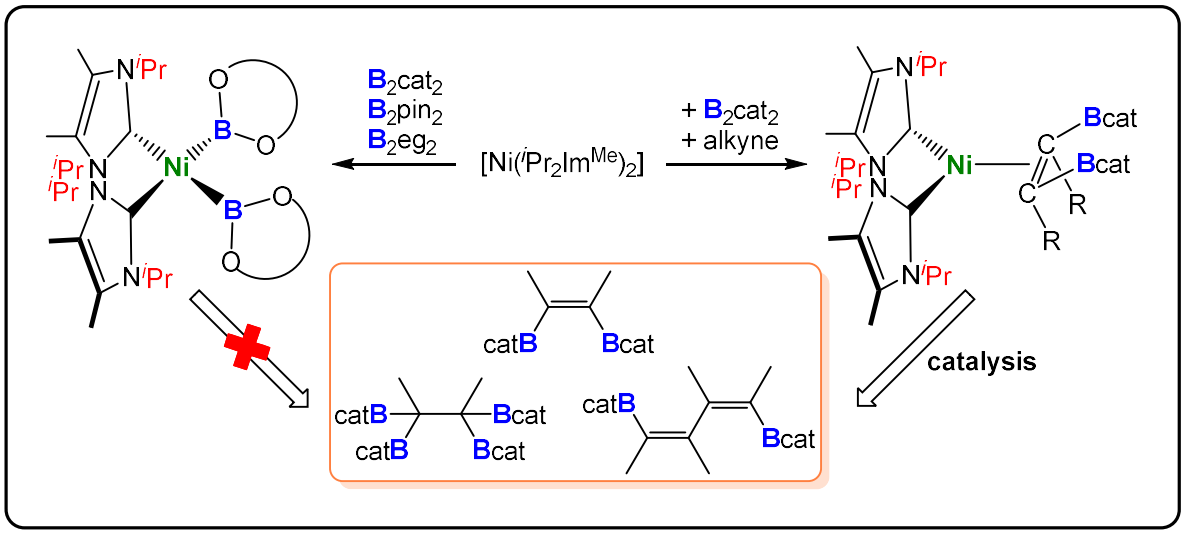

5 Nickel Boryl Complexes and the Nickel-Catalyzed Alkyne-Borylation

5.1 Introduction

Numerous homogeneous catalytic borylation reactions have been developed over the past decades,[1] which include the Suzuki-Miyaura borylation of aryl and alkyl halides,[2] catalytic addition reactions to unsaturated organic molecules such as alkenes, alkynes, allenes, *α,β*–unsaturated compounds, and carbonyl compounds *via* hydroboration, diboration, *β*-borylation or carboboration,[3,4] or the direct functionalization of C–H bonds.[5] In all of these transformations, transition metal boryl complexes[6] play a pivotal role and are key intermediates.[7] Thus, research on transition metal boryl complexes [L_nM-BX_2], in general, is attractive due to their interesting properties and their utility in catalysis, in which poly-boryl complexes often play a dominant role. Among the most important transition metal poly-boryl complexes employed in catalysis are iridium tris-boryl or rhodium bis-boryl complexes, initially synthesized by Baker and Marder *et al.* in 1993 (Figure 1: compounds **34** and **36**),[8] and nowadays frequently employed for C–H borylations of arenes, alkenes and alkanes.[5,9,10] Complexes such as [Ir(dtbpy)(COE)$(Bpin)_3$] **35** (Figure V.1, dtbpy = di-*tert*-butylbipyridine, COE = cyclooctene; pin = pinacolato) are key catalytic intermediates in iridium-catalyzed C–H-borylation reactions. Another well studied class of poly-boryl complexes are platinum bis-boryl complexes such as *cis*-[$Pt(PPh_3)_2(Bcat)_2$] **37** (cat = catecholato),[11] pre-catalysts for the addition of diborane(4) compounds to alkynes, reported independently by the groups of Suzuki and Miyaura[12a-b], M. R. Smith III.[12c] and Marder and Norman.[13] The platinum-catalyzed insertion of alkynes into the B–B bond of a diborane(4) reagent is of interest as it provides the most atom economical route for the stereoselective synthesis of tri- and tetra-substituted alkenes,[4] thus, resulting 1,2-diboryl alkenes are important building blocks in organic synthesis and materials science.[14]

Most of the transition metal-catalyzed borylation reactions developed initially employed precious metals as the catalyst precursors. As first-row d-block metals are less toxic, less expensive, Earth-abundant, and environmentally benign, they are very attractive alternatives to these expensive noble metals. Recently developed borylations employing 3d-metal catalysts show excellent reactivity and selectivity and often

facilitate unique transformations previously unobserved in traditional precious metal-catalyzed processes.[1h] Good examples for outstanding reactivity are copper(I) boryl complexes, using a diverse range of ligands with phosphines and NHCs (*N*-heterocyclic carbenes) being the most commonly employed. These reagents are attractive for different transformations, featuring mild reaction conditions, good functional group tolerance, and low cost of the metal catalyst.[1h,15] For example, *in-situ* generated copper boryl complexes of the type [LCu(Bpin)] (L = phosphine or NHC) have been employed successfully in the borylation of aryl chlorides, bromides and iodides.[15]

We recently investigated the use of NHC nickel complexes for the borylation of aryl chlorides, aryl fluorides and indoles.[16] For each of our nickel-catalyzed borylation reactions, a nickel boryl complex was proposed as a key intermediate, but has never been fully characterized *in situ* or isolated.[17] Nickel boryl complexes are generally considered to be elusive, in contrast to other 3d-metals such as iron,[18] cobalt,[19] or copper.[15,20] Only a few structurally characterized nickel boryl complexes have been isolated thus far, all of them bearing large, rigid pincer ligands (Figure V.1). In 2007, Mindiola *et al.*[21a] reported the synthesis of the first nickel mono-boryl complex [(PNP)Ni(Bcat)] **38** (PNP = N[2-P($CHMe_2$)$_2$-4-methylphenyl]$_2$) and Rodriguez *et al.* introduced the terminal boryl complex [(PBP)Ni(Bcat)] **39** (Figure V.1) among several boryl complexes of PBP pincer ligands [(PBP)NiL] (L = H, Br, Me, Bcat; PBP = C_6H_4{N($CH_2P^tBu_2$)}$_2$B), in which the boryl moiety is embedded in the pincer system.[21c,d] The reactivity of these complexes is unexplored so far.

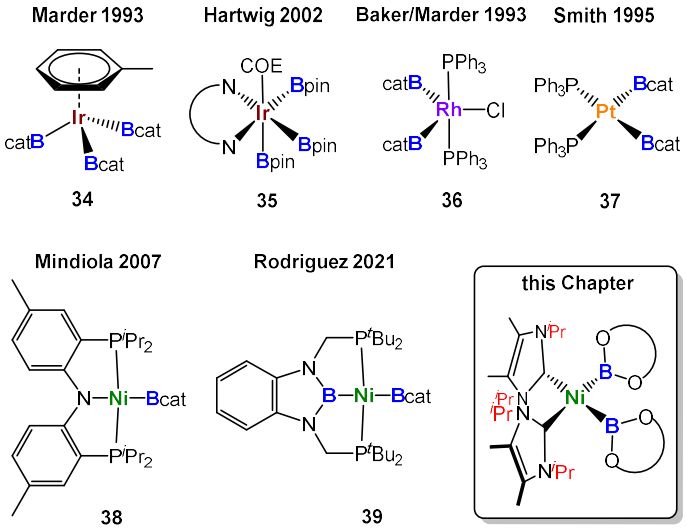

Figure V.1 Selected examples of transition-metal boryl complexes.

Herein we report the synthesis of the first nickel bis-boryl complexes as well as the first investigations concerning the application of the nickel NHC complexes in the diboration of alkynes. We demonstrate that [Ni(NHC)$_2$] catalyst precursors provide excellent catalytic activity for the borylation of alkynes, and that these 3d-metal catalysts provide the potential for new selectivities for this process compared to their well-established platinum-phosphine analogues.

5.2 Results and Discussion

We recently investigated, in detail, the differences in the reactivity of NHC nickel complexes of the type [Ni(NHC)$_2$] dependent upon the stereoelectronic features of NHC ligands,[22] which was the key to the success of the present study. In earlier work, we found that reactions of synthetic equivalents of the complexes [Ni(^{i}Pr$_2$Im)$_2$] **6**, [Ni(Cy$_2$Im)$_2$] and [Ni(Mes$_2$Im)$_2$] **1** (R$_2$Im = 1,3-di-organyl-imidazolin-2-ylidene; Cy = cyclohexyl; Mes = mesityl; ^{i}Pr = *iso*-propyl) with B$_2$cat$_2$, B$_2$pin$_2$, or B$_2$eg$_2$ (= bis(ethylene glycolato)diboron) did not lead to isolable nickel boryl complexes. For the smaller NHCs, decomposition with formation of nickel black and NHC diborane adducts typically occurred. The NHC diborane adducts often underwent subsequent NHC ring expansion reactions, which destroyed the core structure of the NHC and made the process irreversible.[23] Furthermore, in the course of our work on the defluoroborylation of polyfluoroarenes, on the borylation of aryl chlorides, and on the C–H borylation of indoles using [Ni(Mes$_2$Im)$_2$] as a catalyst,[16] we postulated nickel boryl complexes as decisive intermediates, but never detected such compounds. Complexes of the type [Ni(Mes$_2$Im)$_2$(Ar^F)(B{OR}$_2$)] (B{OR}$_2$ = Bcat, Bpin) were not observed in stoichiometric reactions of [Ni(Mes$_2$Im)$_2$(Ar^F)F] with B$_2$pin$_2$ or B$_2$cat$_2$, as reductive elimination leading to the borylation product Ar^F-B(OR)$_2$ was rapid, reforming [Ni(Mes$_2$Im)$_2$].[16a] However, in the course of our work on the borylation of aryl chlorides, a resonance at 44.5 ppm was observed in the ^{11}B{^{1}H} NMR spectrum for the reaction of [Ni(Cy$_2$Im)$_2$(Ar)Cl] with B$_2$pin$_2$, which indicated the formation of a nickel-boryl complex.[16d] Unfortunately, this complex of the *N*-cyclohexyl substituted NHC was not stable in solution and defied isolation despite several attempts. Therefore, we reasoned that using an NHC ligand with similar donor properties and only slightly modified steric demand might lead to the successful synthesis of nickel boryl complexes. As it has been demonstrated previously that backbone substitution at the C4 and C5 position of the imidazole framework by methylation effects the sterics of the NHC ligands as repulsion between the C4/C5 methyl group and the *N*-organyl substituent leads to smaller C$_{carbene}$-N-C$_{substituent}$ angles,[24] we used synthetic equivalents of the backbone-methylated [Ni(^{i}Pr$_2$Im^{Me})$_2$] **7** for this study.

[Ni(^{i}Pr$_2$Im^{Me})$_2$] **7** was provided from a mixture of [Ni$_2$(^{i}Pr$_2$Im^{Me})$_4$(*μ*-(*η*^{2}:*η*^{2})-COD)] **7a** and [Ni(^{i}Pr$_2$Im^{Me})$_2$(*η*^{4}-COD)] **7b**, which can be prepared by the reaction of [Ni(*η*^{4}-COD)$_2$] with two equivalents of ^{i}Pr$_2$Im^{Me}, as reported in Chapter III.[22l] The stoichiometric

reaction of such a mixture of **7a** and **7b** with B_2cat_2 at room temperature cleanly led to the formation of *cis*-[Ni(^{i}Pr$_2$Im^{Me})$_2$(Bcat)$_2$] **V-1a** (Scheme V.1), which is the first nickel bis-boryl complex synthesized and isolated thus far. This complex was isolated as a pale brown solid in 58 % yield and was characterized by IR- and NMR-spectroscopy, X-ray diffraction, and elemental analysis (*vide infra*).

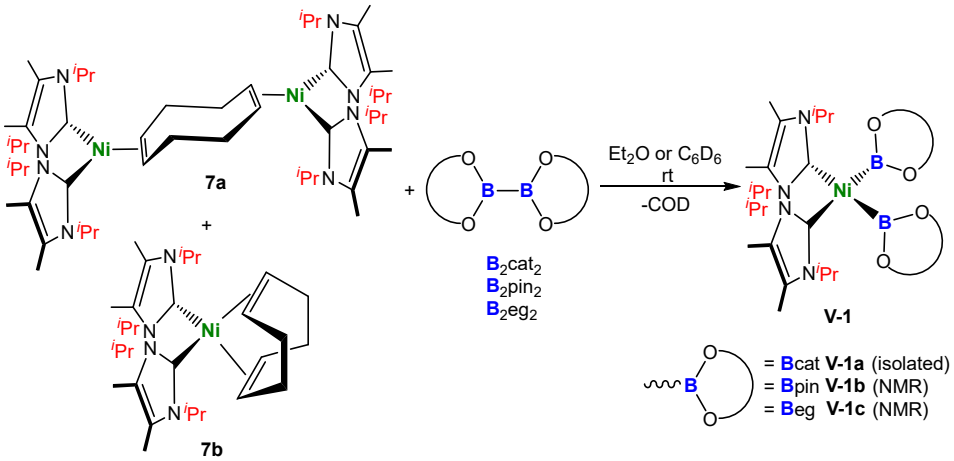

Scheme V.1 Synthesis of *cis*-[Ni(^{i}Pr$_2$Im^{Me})$_2$(Bcat)$_2$] **V-1a**, *cis*-[Ni(^{i}Pr$_2$Im^{Me})$_2$(Bpin)$_2$] **V-1b** and *cis*-[Ni(^{i}Pr$_2$Im^{Me})$_2$(Beg)$_2$] **V-1c**.

If the reaction was carried out with either B_2pin_2 or B_2eg_2 instead of B_2cat_2, it did not proceed quantitatively at room temperature, even if a large excess of the diboron(4) reagent was employed. In all cases, the reaction starts at approximately 0 °C, but does not proceed at lower temperatures. An increase of the temperature above room temperature rapidly leads to a darkening of the reaction mixture with decomposition of the bis-boryl complexes, which is especially rapid for **V-1b** and **V-1c**. This behavior reflects that of copper(I) boryl complexes, which easily decompose upon warming.[20d-g] The use of modified starting materials, such as the ethylene complex [Ni(^{i}Pr$_2$Im^{Me})$_2$(η^2-C_2H_4)] **7c** or the cyclooctene (COE) complex [Ni(^{i}Pr$_2$Im^{Me})$_2$(η^2-COE)] **7d** (see Experimental and Figures XIII.1 and XIII.2), was also unsuccessful for the bulk production of pure **V-1b** and **V-1c**. However, the formation of the bis-boryl complexes *cis*-[Ni(^{i}Pr$_2$Im^{Me})$_2$(Bpin)$_2$] **V-1b** and *cis*-[Ni(^{i}Pr$_2$Im^{Me})$_2$(Beg)$_2$] **V-1c** was clearly detected by NMR spectroscopy, and small amounts of these complexes suitable for X-ray diffraction crystallized from these reaction mixtures (Figure V.2). The bis-boryl complexes reveal different stabilities in solution. Whereas *cis*-[Ni(^{i}Pr$_2$Im^{Me})$_2$(Bpin)$_2$]

V-1b can still be detected in the reaction mixture in a solution kept at room temperature for one month, complexes **V-1a** and **V-1c** completely decompose in C_6D_6 over a period of 6 – 14 days with formation of multiple, as yet unidentified, species.

Characteristic for complexes **V-1a-c** is a broad resonance at 48.7 ppm (**V-1a**), 46.1 ppm (**V-1b**) and 46.5 ppm (**V-1c**) in the $^{11}B\{^1H\}$ NMR spectrum (see Table V.1), which is the region typically observed for transition metal boryl complexes,[6] c.f. 47.0 ppm for *cis*-[Pt(PPh_3)$_2$(Bcat)$_2$].[13] In the $^{13}C\{^1H\}$ NMR spectra, the NHC carbene carbon resonances are also significantly shifted compared to those of the starting materials **7a** (206.5 ppm) and **7b** (205.4 ppm) to 194.3 ppm (**V-1a**), 199.4 ppm (**V-1b**) and 198.5 ppm (**V-1c**). The complexes adopt *cis*-configurations in solution as their ^1H NMR spectra indicate pseudo-C_{2v} species with two resonances for the *N-iso*-propyl methyl protons (**V-1a**: 1.28 ppm and 1.45 ppm, **V-1b**: 1.32 ppm and 1.69 ppm, **V-1c**: 1.28 ppm and 1.58 ppm) and only one signal for the *N-iso*-propyl methine (**V-1a**: 6.05 ppm, **V-1b**: 5.99 ppm, **V-1c**: 6.04 ppm) and for the backbone methyl protons (**V-1a**: 1.63 ppm, **V-1b**: 1.84 ppm, **V-1c**: 1.78 ppm).

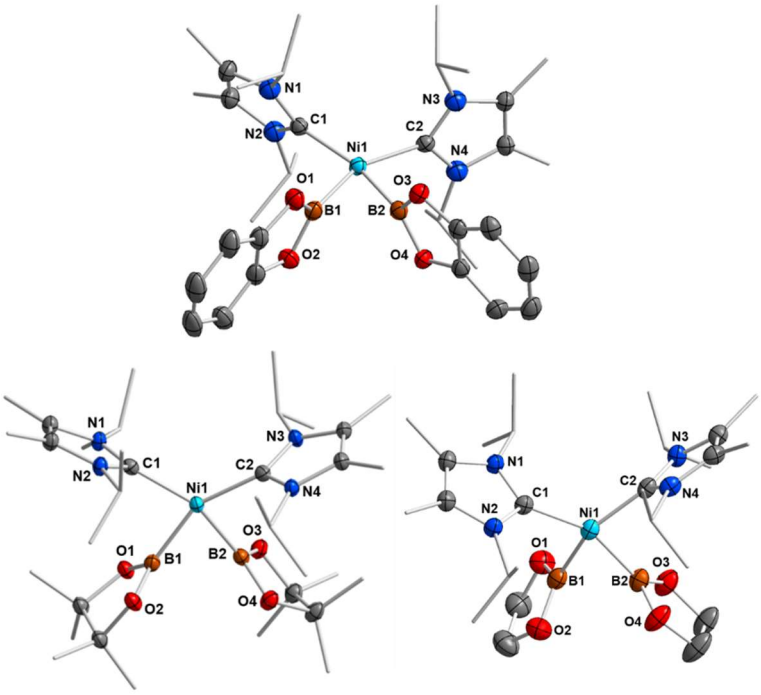

Figure V.2 Molecular structures of *cis*-[Ni(^{i}Pr$_2$Im^{Me})$_2$(Bcat)$_2$] **V-1a** (top), *cis*-[Ni(^{i}Pr$_2$Im^{Me})$_2$(Bpin)$_2$] **V-1b** (bottom left) and *cis*-[Ni(^{i}Pr$_2$Im^{Me})$_2$(Beg)$_2$] **V-1c** (bottom right) in the solid state (ellipsoids shown at 50 % probability level). Hydrogen atoms are omitted for clarity. For selected bond lengths and angles see Table V.1.

Crystals suitable for X-ray diffraction of **V-1a-c** were obtained by storing the reaction mixtures in diethylether at -30 °C. Complexes **V-1a-c** crystallize in the triclinic space group $P\bar{1}$ and adopt a distorted square planar geometry with *cis*-boryl ligands, as observed for platinum bis-boryl complexes *cis*-[Pt(PR_3)$_2$(B{OR}$_2$)$_2$].[6,11] The Ni–C and Ni–B distances lie in a narrow range between 1.9092(18) Å and 1.9448(15) Å (see Table V.1). We attribute the formation of *cis*-configured complexes to the strong *trans* influence of boryl ligands[25] and a remaining B–B interaction between the two boryl boron atoms (*vide infra*). This situation is similar to that observed previously for NHC-stabilized bis-silyl and hydro silyl complexes *cis*-[Ni(NHC)$_2$(SiR_3)$_2$] and *cis*-[Ni(NHC)$_2$(H)(SiR_3)$_2$].[26] The B–B separations of 2.156(3) Å (**V-1a**), 2.247(3) Å (**V-1b**), and 2.189(4) Å (**V-1c**) (see Table V.1) are much smaller than those observed for bis-boryl platinum complexes (2.451 – 2.667 Å),[11-13] consistent with small B1–Ni1–B2 angles of 68.45(7)°(**V-1a**), 70.82(8)° (**V-1b**) and 68.79(8)° (**V-1c**). Thus, the B–B distances are only 0.478 Å (**V-1a**), 0.540 Å (**V-1b**), and 0.485 Å (**V-1c**) longer than those in the solid state molecular structures of B_2cat_2 (1.678(3) Å), B_2pin_2 (1.707(5) Å) and B_2eg_2 (1.704(3) Å).[23d, 27] The BO_2 planes of both boryl ligands are nearly perpendicular to the NiC_2B_2 square plane with angles of 87.85(7)° and 86.21(6)° (**V-1a**), 88.41(9)° and 88.07(9)° (**V-1b**) and 85.85(10)° and 85.30(10)° (**V-1c**). Thus, the structures are best represented by **V-B** in Scheme V.2, which lies in-between the limiting resonance structures of a Ni(II) bis-boryl complex **V-A** and a Ni(0) diborane(4) complex **V-C**, i.e., incomplete oxidative addition with a residual B···B interaction. This is reminiscent to “non-classical” H_2 complexes. As the Ni–B distances of 1.9231(19) Å and 1.9092(18) Å (**V-1a**), 1.936(2) Å and 1.942(2) Å (**V-1b**), and 1.939(2) Å and 1.9353(19) Å (**V-1c**) are of similar magnitude as those observed in [(PNP)Ni(Bcat)] **38** (1.9091(18) Å)[21a] and [(PBP)Ni(Bcat)] **39** (1.942(2) Å; 2.015(2) Å), which feature 2-center-2-electron Ni–B bonds, the oxidative addition is nearly complete.

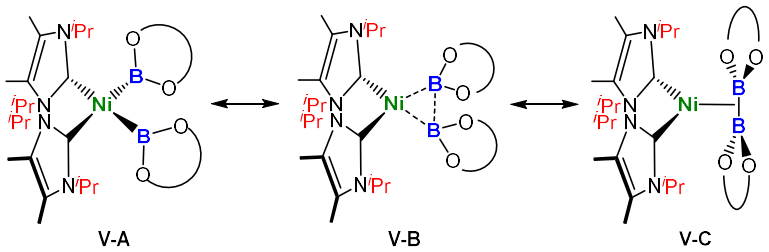

Scheme V.2 Resonance structures of complexes *cis*-[Ni(*i*Pr$_2$Im^{Me})$_2$(B{OR}$_2$)$_2$] **V-1a-c**.

This situation is closely related to that observed for the paramagnetic cobalt complexes [Co(PMe$_3$)$_3$(Bcat)$_2$] (B–B: 2.185 Å, B–Co–B: 67.9(4)°) and *mer*-[Co(PMe$_3$)$_3$(Bcat)$_3$] (B–B: 2.1541(5) Å, B–Co–B: 65.78(1)°), which also feature two Bcat ligands with short B–B distances.[19a,g] DFT calculations on *mer*-[Co(PMe$_3$)$_3$(Bcat)$_3$] revealed bond critical points at the Co–B vector with substantial electron densities and a bond critical point along the B–B vector, which was characterized by a substantial electron density associated with a much smaller yet positive Laplacian compared to the Ni–B bond. It was concluded that *mer*-[Co(PMe$_3$)$_3$(Bcat)$_3$] maintains a degree of B−B interaction, which is essential for the stabilization of this boryl complex.

The preference of the resonance structure **V-B** to characterize the bonding situation of the NiB$_2$ motif in **V-1a-c** is also supported by DFT computations on complex **V-1a**. Inspection of the canonical Kohn-Sham molecular orbitals of **V-1a** reveals that the HOMO (Figure V.3a) is mainly composed of a combination of 3*d* orbitals of nickel that expands across the B–B bonding region. Accordingly, a Mayer bond order (MBO) [28] of 0.451 is found for the B–B bond, whereas the corresponding MBOs of the Ni–B bonds are 0.711 each. These findings strongly suggest that a delocalized, multicenter bonding scheme dictates the bonding situation of the NiB$_2$ moiety. This picture is corroborated by further calculations based on the intrinsic bond orbital (IBO) approach.[29] Analysis of the IBOs of **V-1a** indicates that two doubly occupied IBOs are participating in the NiB$_2$ bonding. The first orbital (Figure V.3b) is mainly localized at the B–B bonding region, with partial delocalization on the Ni center and across the Ni–B bonds. In contrast, the second orbital (Figure V.3c) is mostly localized across the Ni–B bonds, but with a larger contribution coming from the Ni center. From the IBO point of view, the bonding situation of the NiB$_2$ motif is better described as composed of two three-center two-electron (3c,2e) bonds. Taken together, these results are in accordance with the analysis based on the X-ray structures of **V-1a-c** and support the multicenter bonding situation depicted in resonance structure **V-B**.

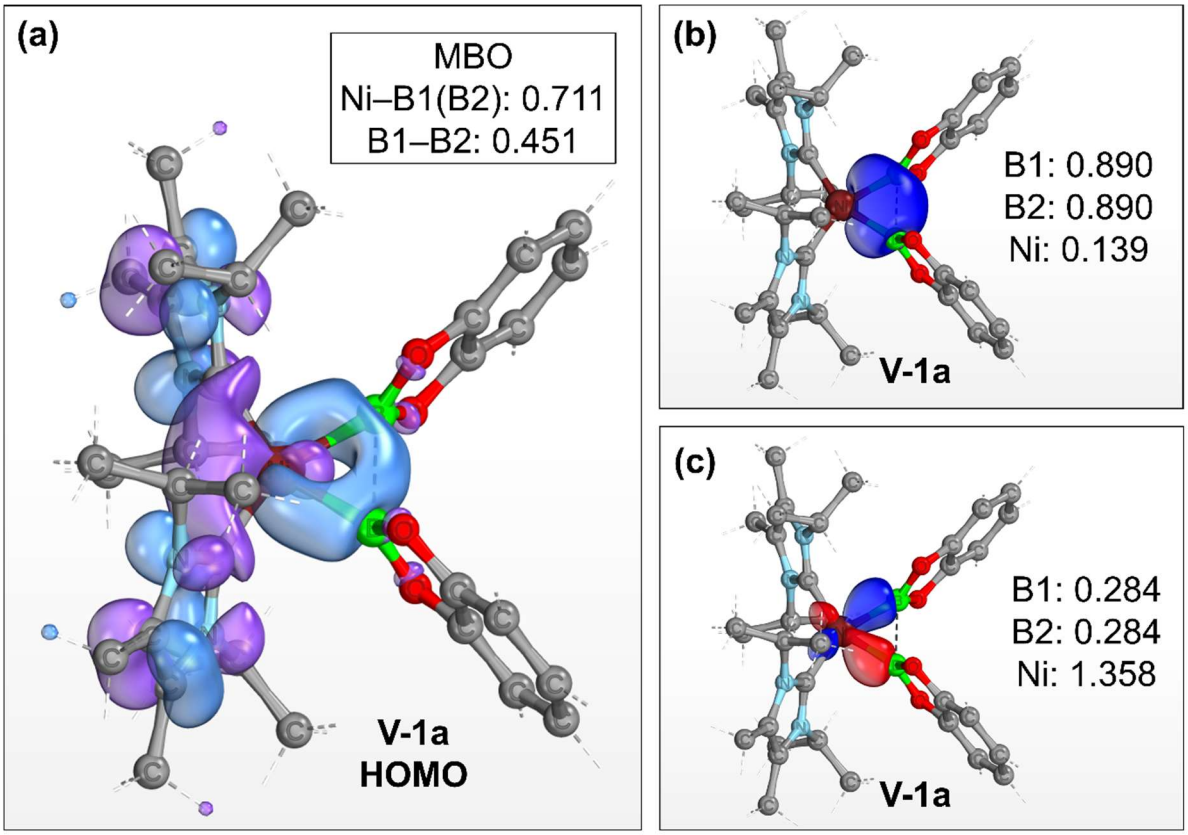

Figure V.3 (a) HOMO of **V-1a** (isovalue: 0.03 au). The Ni–B and B–B Mayer bond orders of **V-1a** are shown in the top right box. (b) and (c) Intrinsic bond orbitals of **V-1a** involved in the bonding of the NiB_2 motif. Numerical values indicate the fraction of electrons of the doubly occupied orbital assigned to the individual atoms. Level of theory: PBE0-D3(BJ)/def2-SVP/def2-TZVP(Ni).[30] Hydrogen atoms are omitted for clarity.

Table V.1 Important bond lengths, bond angles and chemical shifts of *cis*-[Ni(^{i}Pr$_2$Im^{Me})$_2$(Bcat)$_2$] **V-1a**, *cis*-[Ni(^{i}Pr$_2$Im^{Me})$_2$(Bpin)$_2$] **V-1b**, *cis*-[Ni(^{i}Pr$_2$Im^{Me})$_2$(Beg)$_2$] **V-1c** and [(PNP)Ni(Bcat)] **38** (δ_B B(OR)$_2$ = ^{11}B{^{1}H} NMR shift of the boron atoms, δ_c NHC = ^{13}C{^{1}H} NMR shift of the NHC carbene carbon atoms).

Compound	Ni–B [Å]	B–B [Å]	Ni–C [Å]	B–Ni–B [°]	δ_B B(OR)$_2$ [ppm]	δ_c NHC [ppm]
V-1a	1.9231(19)/ 1.9092(18)	2.156(3)	1.9393(16)/ 1.9448(15)	68.45(7)	48.7	194.3
V-1b	1.936(2)/ 1.942(2)	2.247(3)	1.9318(18)/ 1.9185(17)	70.82(8)	46.1	199.4
V-1c	1.939(2)/ 1.9353(19)	2.189(4)	1.9180(15)/ 1.9265(17)	68.79(8)	46.5	198.5
38[21a]	1.9091(18)	-	-	-	47.0	-

Bis-boryl complexes are regarded as the key intermediates for the catalytic diboration of alkynes in platinum chemistry.[11-13] It has been demonstrated that complexes *cis*-[Pt(PR$_3$)$_2$(Bcat)$_2$] or synthetic equivalents for [Pt(PR$_3$)$_2$] are highly active catalyst precursors for the *cis*-stereospecific diboration of alkynes and 1,3-diynes. In the platinum system, phosphine dissociation is a critical step in the catalytic cycle (see Figure XIII.4 in the Appendix), which includes formation of the bis-boryl complex *cis*-[Pt(PR$_3$)$_2$(B{OR}$_2$)$_2$] from the catalyst precursor and subsequent phosphine dissociation to give sterically and electronically unsaturated [Pt(PR$_3$)(B{OR}$_2$)$_2$]. This complex can add the alkyne, and insertion of the alkyne into the Pt-B{OR}$_2$ bond and reductive elimination lead to the corresponding *cis*-alkene-1,2-bis(boronate) ester with regeneration of [Pt(PR$_3$)] or [Pt(PR$_3$)$_2$]. DFT calculations have shown that similar Pd(0) complexes cannot catalyze the alkyne diboration due to differences in the oxidative addition step of the B–B bond of the diborane to [M(PR$_3$)$_2$].[12d] Although the kinetic barrier is lower, the addition is endothermic for the palladium complex and thus the addition product is not stable due to a very small reverse barrier. For the diboration of alkynes using B$_2$pin$_2$ as the boron source, the optimized phosphine:platinum ratio was later shown to be 1:1, with catalyst activity being strongly dependent on the nature of the phosphine.[13b] Sterically bulky, strong electron donors, such as PCy$_3$, allowed diborations to be performed at ambient temperatures. Thus, the isolable and stable compound [Pt(PCy$_3$)(η^2-C$_2$H$_4$)$_2$] was shown to be an excellent catalyst precursor for

alkyne diboration even at room temperature.[13b] We were thus interested to see whether our nickel complexes are also able to catalyze this reaction.

Catalytic reactions were typically carried out in a Young's tab NMR tube using different internal and terminal alkynes (see Table V.2). As standard reaction conditions, 4 mol% of [Ni(^{i}Pr$_2$Im^{Me})$_2$] **7** (the mixture of **7a** and **7b** was used directly) and equimolar amounts of alkyne and B_2cat_2 were reacted using C_6D_6 as solvent at 50 °C. Reaction progress was monitored *via* ^{1}H and ^{11}B{^{1}H} NMR spectroscopy. After completion, the resulting products were identified by NMR spectroscopy and GC/MS analysis of the reaction mixture. Internal alkynes led selectively to the quantitative formation of the *cis*-1,2-diborylalkenes *Z*-(Bcat)(Ph)C=C(Ph)(Bcat) **V-2**, *Z*-(Bcat)(4-Me-C_6H_4)C=C(4-Me-C_6H_4)(Bcat) **V-3**, *Z*-(Bcat)(4-CF_3-C_6H_4)C=C(4-CF_3-C_6H_4)(Bcat) **V-4** *Z*-(Bcat)(C_3H_7)C=C(C_3H_7)(Bcat) **V-5** and *Z*-(Bcat)(Me)C=C(Ph)(Bcat) **V-6**. However, for the synthesis of **V-2**, **V-3** and **V-4** a higher catalyst loading of 10 mol% was necessary to reach full conversion as the catalyst is deactivated by transfer of the NHC ligands to the borylation product to yield the corresponding mono NHC-adducts (*vide infra*). The NHC adduct of compound **V-3**, *Z*-(Bcat)(4-Me-C_6H_4)C=C(4-Me-C_6H_4)(Bcat) • (^{i}Pr$_2$Im^{Me}) **V-3^{NHC}**, was isolated and characterized separately by the reaction of **V-3** with one equivalent of ^{i}Pr$_2$Im^{Me} (see Scheme V.3 and Figure V.4).

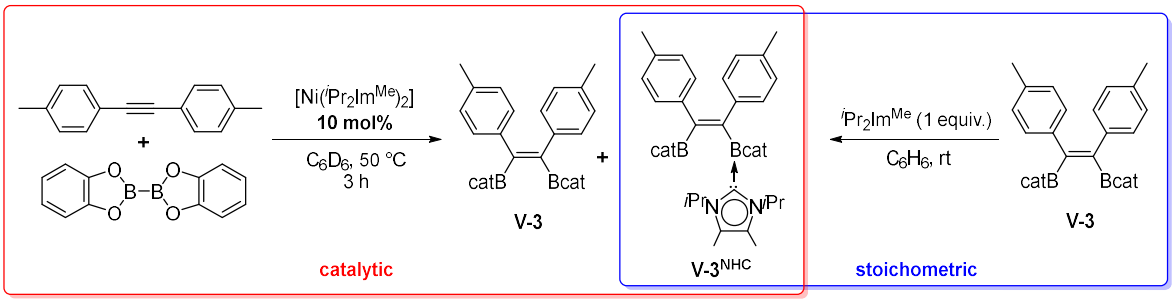

Scheme V.3 Deactivation of the catalyst and independent synthesis to yield *Z*-(Bcat)(4-Me-C_6H_4)C=C(4-Me-C_6H_4)(Bcat) • (^{i}Pr$_2$Im^{Me}) **V-3^{NHC}.**

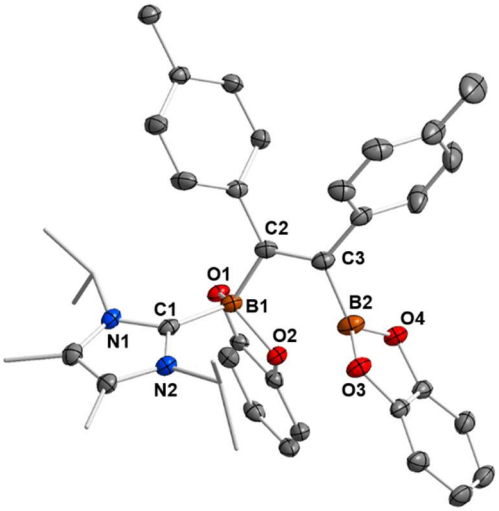

Figure V.4 Molecular structure of *Z*-(Bcat)(4-Me-C_6H_4)C=C(4-Me-C_6H_4)(Bcat) • (^{i}Pr$_2$Im^{Me}) **V-3^{NHC}** in the solid state (ellipsoids set at 50 % probability level). Hydrogen atoms have been omitted for clarity. Selected bond lengths [Å] and angles [°] of **V-3^{NHC}**: C1–B1 1.6604(17), C2–C3 1.3451(17), B1–C2 1.5976(16), B2–C3 1.5816(17), B1–O1 1.4936(14), B1–O2 1.5370(14), B2–O3 1.4257(16), B2–O4 1.4252(17), B2···O2 1.9633(17); C1–B1–C2 116.03(9), C1–B1–O1 108.75(9), C1–B1–O2 108.08(9).

The reaction of aryl substituted terminal alkynes also led to the formation of the *cis*-1,2-diborylalkenes *E*-(Bcat)HC=C(Ph)(Bcat) **V-8**, *E*-(Bcat)HC=C(4-Me-C_6H_4)(Bcat) **V-9** and *E*-(Bcat)HC=C(4-^{t}Bu-C_6H_4)(Bcat) **V-10**, but after consumption of the alkyne approximately 40 % unreacted B_2cat_2 was always detected besides the 1,2-diborylalkene products. Analysis of the reaction mixtures *via* HRMS spectrometry revealed that alkyne cyclotrimerization products and different partially borylated coupling products were formed as side-products, which are hard to identify *via* NMR spectroscopy. Note that the use of more than one equivalent of the alkynes inhibits the borylation, so that no transformation at all was observed when 4 equivalents of the alkynes were applied.

Table V.2 Scope of the borylation of internal and terminal alkynes.

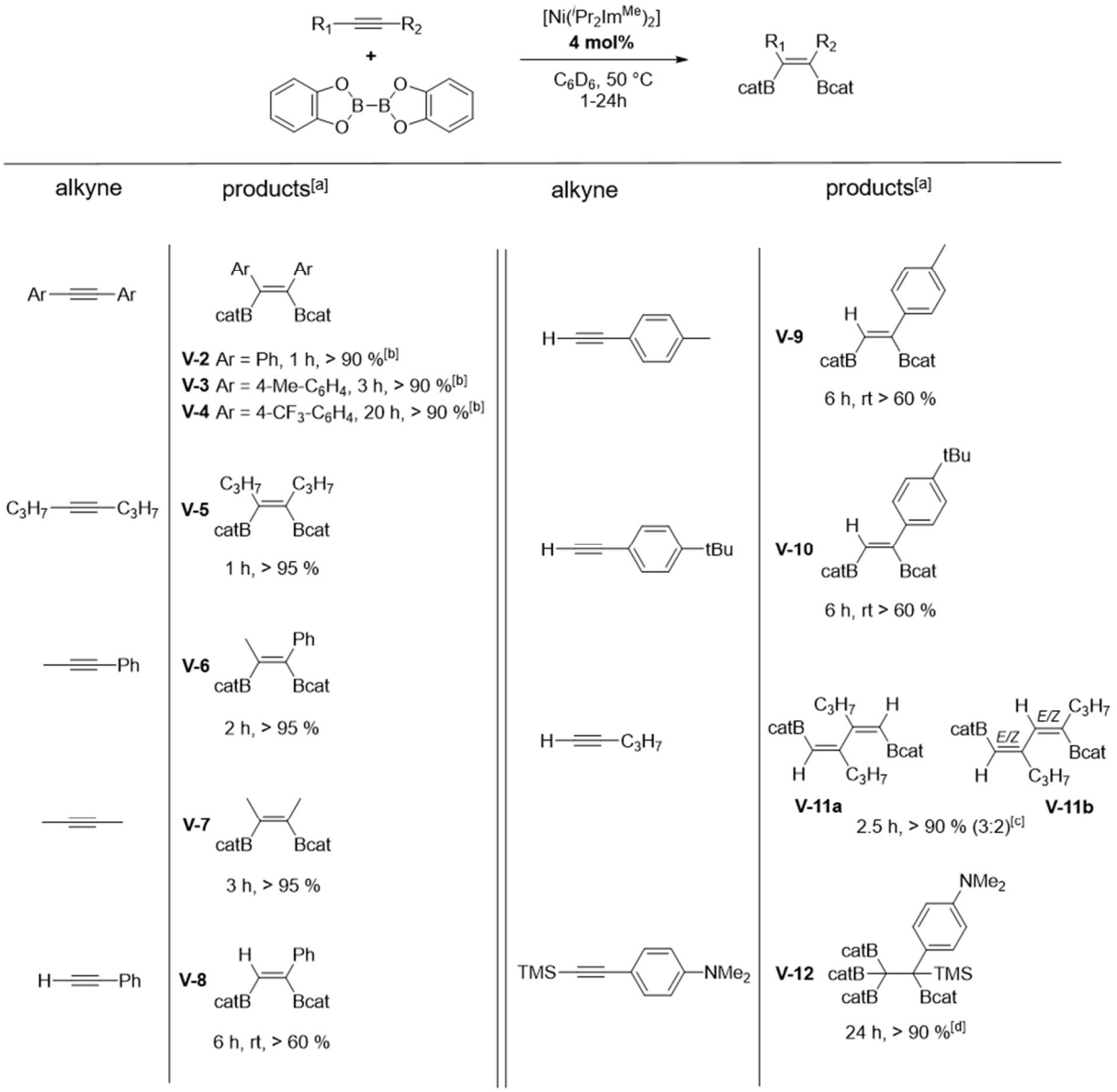

[a] Reaction conditions: [Ni(^{i}Pr$_2$Im^{Me})$_2$] **7a/7b** (4 mol%), alkyne (1 equiv.), B_2cat_2 (1 equiv.), C_6D_6 (0.6 mL), 50 °C (if not otherwise stated). Products after total consumption of the alkynes, monitored by NMR and GC/MS. Yields are combined yields of the products and were estimated by ^{1}H NMR with respect to the consumption of B_2cat_2. [b] [Ni(^{i}Pr$_2$Im^{Me})$_2$] **7a/7b** (10 mol% needed for completion). [c] excess of alkyne (> 4 equiv.). Products after total consumption of B_2cat_2. [d] B_2cat_2 (2 equiv.).

Compared to the well-established platinum catalysts,[12-13] our nickel complex shows very good activity towards internal alkynes under mild conditions. Only the mono-phosphine platinum complexes reported by Marder *et al.*[13b] show a higher efficiency, as they catalyze the diboration at room temperature with a low catalyst loading. For terminal alkynes, the platinum diphosphine complexes and, especially, the

palladium NHC complex [Pd(Me_2Im^{Me})$_2$(η^2-PhC≡CPh)] reported by Navarro *et al.,* deliver higher yields (79 – 95 %).[31] Interestingly, the reactions of alkyl substituted 1-pentyne or TMS-substituted *N*,*N*-dimethyl-4-[(trimethylsilyl)-ethynyl]aniline led to new, previously unknown reaction products. The borylation of 1-pentyne selectively afforded the C–C coupled borylation products *Z,Z*-(Bcat)HC=C(C_3H_7)–(C_3H_7)C=CH(Bcat) **V-11a** (for proof of connectivity see Figure XIII.3 in the Appendix) and *E/Z,E/Z*-(Bcat)HC=C(C_3H_7)–HC=C(Bcat)(C_3H_7) **V-11b** in a 3:2 ratio, according to NMR and GC/MS analysis. An excess of 1-pentyne (4 equiv.) was needed to reach full consumption of B_2cat_2. On the other hand, the borylation of the TMS-substituted alkyne selectively afforded the formation of polyborylated (4-NMe_2-C_6H_4)(Bcat)(TMS)C–C(Bcat)$_3$ **V-12**. In this case, 2 equivalents of B_2cat_2 were needed for a full conversion and the TMS-group undergoes a formal 1,2-shift.

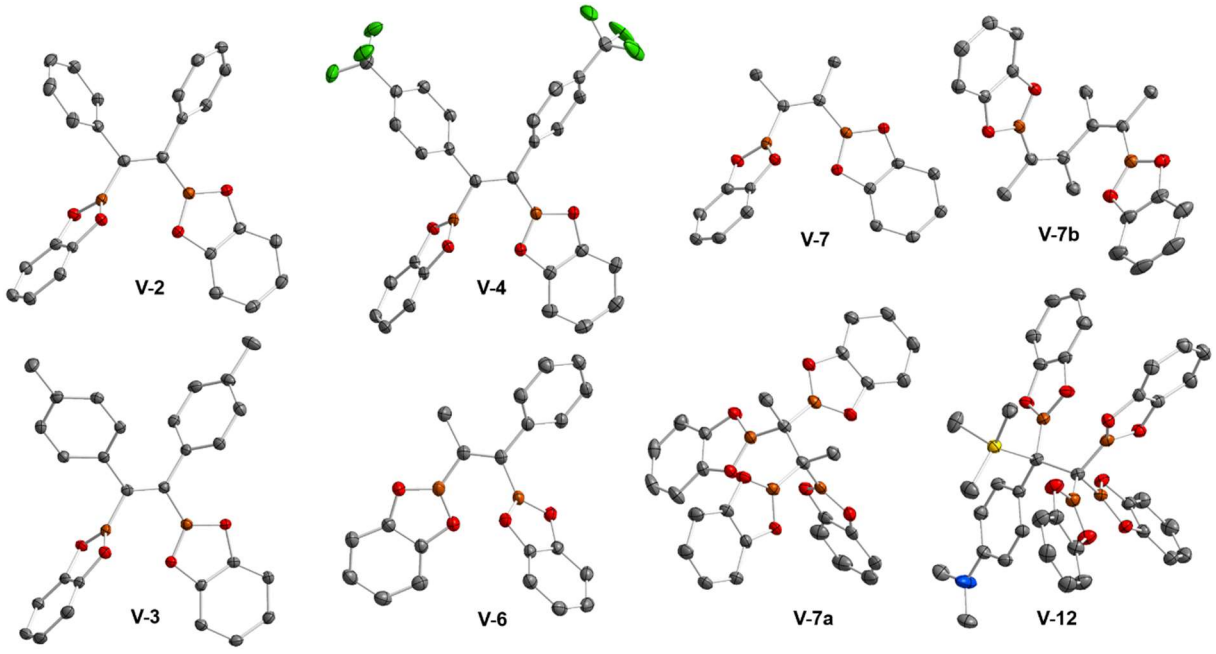

Figure V.5 Molecular structures of *Z*-(Bcat)(Ph)C=C(Ph)(Bcat) **V-2**, *Z*-(Bcat)(4-Me-C_6H_4)C=C(4-Me-C_6H_4)(Bcat) **V-3**, *Z*-(Bcat)(4-CF_3-C_6H_4)C=C(4-CF_3-C_6H_4)(Bcat) **V-4**, *Z*-(Bcat)(Me)C=C(Ph)(Bcat) **V-6**, *Z*-(Bcat)(Me)C=C(Me)(Bcat) **V-7**, (Bcat)$_2$(Me)C–C(Me)(Bcat)$_2$ **V-7a**, *E,E*-(Bcat)(Me)C=C(Me)–(Me)C=C(Me)(Bcat) **V-7b** and (4-NMe_2-C_6H_4)(Bcat)(TMS)C–C(Bcat)$_3$ **V-12** in the solid state (ellipsoids shown at 50 % probability level). Hydrogen atoms are omitted for clarity.

As we observed the formation of coupled and tetra-borylated products **V-11a/b** and **V-12**, we had a closer look at the catalytic borylation reaction of the internal alkyne 2-butyne, which is another special case (Scheme V.4).

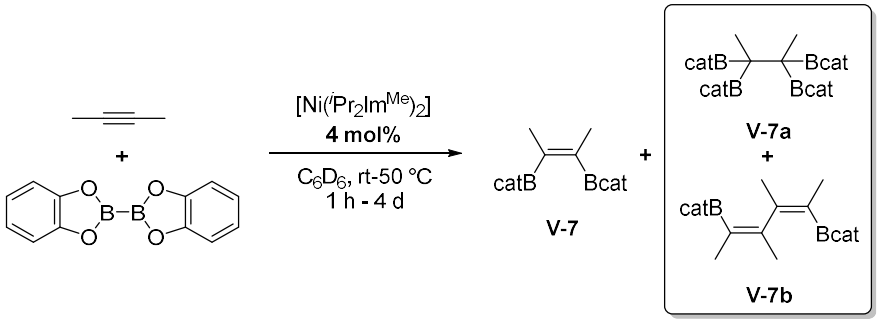

Scheme V.4 Borylation of 2-butyne yielding *Z*-(Bcat)(Me)C=C(Me)(Bcat) **V-7,** $(Bcat)_2(Me)C–C(Me)(Bcat)_2$ **V-7a** or *E,E*-(Bcat)(Me)C=C(Me)–(Me)C=C(Me)(Bcat) **V-7b**, depending on the stoichiometry used.

The reaction of 2-butyne with B_2cat_2 and $[Ni(^iPr_2Im^{Me})_2]$ as a catalyst afforded three different reaction products depending on the reaction conditions, namely *Z*-(Bcat)(Me)C=C(Me)(Bcat) **V-7,** $(Bcat)_2(Me)C–C(Me)(Bcat)_2$ **V-7a** or *E,E*-(Bcat)(Me)C=C(Me)–(Me)C=C(Me)(Bcat) **V-7b** (compare Scheme V.4). The products obtained were often mixtures which cannot be separated by column chromatography, but the product ratios can be controlled to some extent *via* the ratio of alkyne to B_2cat_2 employed. The reaction of one equivalent of 2-butyne with a slight excess of B_2cat_2 and 4 mol% of $[Ni(^iPr_2Im^{Me})_2]$ **7** in C_6D_6 was monitored by ^1H and $^{11}B\{^1H\}$ NMR spectroscopy, which showed complete consumption of the alkyne and B_2cat_2 after 3 h at 50 °C. NMR spectroscopy and GC/MS analysis of the final reaction products revealed the selective formation of the bis-borylated product *Z*-(Bcat)(Me)C=C(Me)(Bcat) **V-7** as the main product and traces of tetra-borylated product $(Bcat)_2(Me)C–C(Me)(Bcat)_2$ **V-7a** in a combined quantitative yield. If 2 equivalents of B_2cat_2 were used, **V-7a** was formed exclusively in quantitative yields. Applying a large excess of 2-butyne (> 4 equiv.) led to a mixture of **V-7**, **V-7a** and **V-7b**, with **V-7b** being the main product, after full consumption of the diboron reagent (4 d, rt). To our knowledge, the formation of compounds **V-7a** and **V-12** are the only examples for tetra-borylation of alkynes, beside the Pt-catalyzed tetra-borylation of (Bcat)C≡C(Bcat) to yield hexa-borylated ethane $(Bcat)_3C–C(Bcat)_3$, which was

reported by Siebert *et al.* in 1999.[32] Products **V-7b** and **V-11a/b** are very rare examples for a combined one-step coupling and borylation of alkynes, which was first described by Marder *et al.,* who observed small amounts of coupling products (*via* GC/MS) during the borylation of phenylacetylene with their platinum-catalyst.[13a]
The use of alternative diboron sources B_2pin_2, B_2eg_2 and B_2neop_2 did not achieve borylation at all or showed large quantities of byproducts from oligomerization reactions. Employing only the free carbene $^{i}Pr_2Im^{Me}$ as a catalyst also failed completely. No major differences in catalytic activity were observed using **7(a-d)**, [Ni($^{i}Pr_2Im^{Me}$)$_2$(η^2-MeC≡CMe)] **III-1**, [Ni($^{i}Pr_2Im^{Me}$)$_2$(η^2-*cis*-(Bcat)(Me)C=C(Me)(Bcat))] **V-13** (*vide infra*) or even the bis-boryl complex **V-1a** as the catalyst precursor, as all of them appear to serve as a source of [Ni($^{i}Pr_2Im^{Me}$)$_2$]. We were also able to isolate analytically pure compounds **V-3** (60 % yield), **V-6** (65 % yield), **V-7a** (38 % yield) and **V-12** (46 % yield) from scaled-up reactions, allowing full characterization, including X-ray diffraction. Additionally, crystals of the compounds **V-2** (structures of **V-2** and **V-3** were reported earlier by Marder et al.),[13a, 33] **V-4**, **V-7** and **V-7b** were obtained by slow evaporation of the reaction mixtures.

To study the catalytic reaction of 2-butyne, B_2cat_2, and [Ni($^{i}Pr_2Im^{Me}$)$_2$] **7** in more detail, we investigated several stoichiometric reactions. Interestingly, the reaction of *cis*-[Ni($^{i}Pr_2Im^{Me}$)$_2$(Bcat)$_2$] **V-1a** with stoichiometric amounts of 2-butyne did not lead to the cis-alkene-1,2-bis(boronate) ester or to exchange of the boryl ligands with the alkyne to form [Ni($^{i}Pr_2Im^{Me}$)$_2$(η^2-MeC≡CMe)] **III-1**.[22l] Instead, the formation of small amounts of the $[Bcat_2]^-$ anion, traces of a species which was later identified as [Ni($^{i}Pr_2Im^{Me}$)$_2$(η^2-*cis*-(Bcat)(Me)C=C(Me)(Bcat))] **V-13**, and the slow formation of hexamethylbenzene was detected *via* NMR spectroscopy. After the complete consumption of 2-butyne in ca. 20 h, complex **V-1a** began to decompose. Although we did not observe the formation of alkyne complex **III-1**, the formation of hexamethylbenzene, especially at higher temperatures, suggests that the boryl ligands of **V-1a** are labile *via* B–B reductive elimination and exchange with the alkyne. However, the reaction of the alkyne complex [Ni($^{i}Pr_2Im^{Me}$)$_2$(η^2-MeC≡CMe)] **III-1**[22l] with B_2cat_2 led to the isolation of the complex of the *cis*-alkene-1,2-bis(boronate) ester [Ni($^{i}Pr_2Im^{Me}$)$_2$(η^2-*cis*-(Bcat)(Me)C=C(Me)(Bcat))] **V-13**. This contrasts with the platinum phosphine system, for which Iverson and Smith demonstrated previously that the stoichiometric reaction of [Pt(PPh_3)$_2$(η^2-$H_7C_3C{\equiv}CC_3H_7$)] with B_2cat_2 yields the bis-boryl

complex [Pt(PPh$_3$)$_2$(Bcat)$_2$] with extrusion of free alkyne. [11a] We verified this reactivity by using the octyne complex [Ni(^{i}Pr$_2$Im^{Me})$_2$(η^2-H$_7$C$_3$C≡CC$_3$H$_7$)] **III-2**, which led to the isolation of [Ni(^{i}Pr$_2$Im^{Me})$_2$(η^2-*cis*-(Bcat)(H$_7$C$_3$)C=C(C$_3$H$_7$)(Bcat))] **V-14** (Scheme V.5). These reactions are quantitative if performed in an NMR tube.

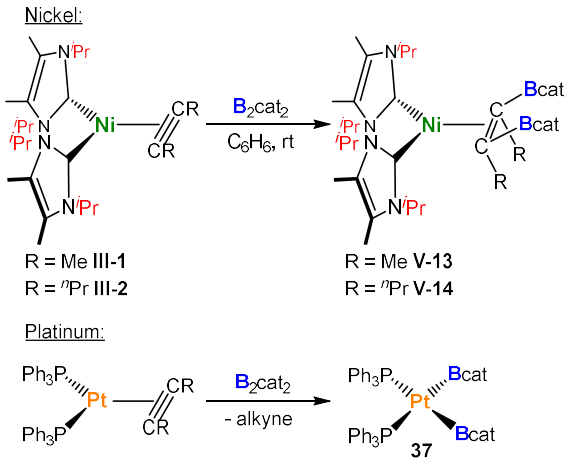

Scheme V.5 Reactivity of NHC nickel alkyne complexes and platinum phosphine alkyne complexes with B$_2$cat$_2$.

Complexes **V-13** and **V-14** were isolated as orange to brown solids and were completely characterized using IR- and NMR-spectroscopy, elemental analysis, and X-ray diffraction. The reduction of symmetry on going from **V-1a** (*pseudo*-C$_{2v}$) to **V-13** and **V-14** (*pseudo*-C$_s$) is reflected in the resonances in the ^{1}H and ^{13}C{^{1}H} NMR spectra of these complexes, which are doubled. The olefinic carbon atoms of the alkene ligand were not detected in the ^{13}C{^{1}H} NMR spectra due to the quadrupolar coupling to boron, but were assigned from an HMBC spectrum to be at 40.0 ppm (**V-13**) and at 47.3 ppm (**V-14**). One broad resonance was observed at 33.3 ppm (**V-13**) and 31.9 ppm (**V-14**) for the boryl substituents in the ^{11}B{^{1}H} NMR spectrum, which are clearly distinct from the resonance of **V-1a** at 48.7 ppm.

Crystals of **V-13** and **V-14** suitable for X-ray diffraction were obtained from saturated hexane solutions of the compounds at -30 °C (Figure V.6). The complexes crystallize in the monoclinic space groups P2$_1$c (**V-13**) and P2$_1$n (**V-14**). Both complexes adopt a pseudo-trigonal planar structure with Ni–C$_{NHC}$ distances of 1.9454(14) – 1.9560(13) Å in a typical range.[22] The C3–C4 distances of the coordinated alkene of 1.453(2) Å (**V-13**) and 1.4550(17) Å (**V-14**) are in line with those of coordinated olefins reported

previously [22a, 22j] and are much larger compared to those of alkyne complexes (c.f. **III-1**: 1.285(2) Å).[22l] Both olefin ligands are distorted such, that one of the electron-deficient boryl substituents can interact with the electron-rich nickel center, which results in very different Ni···B distances of 2.3694(16) Å (Ni1–B2) and 3.0525(19) Å (Ni1–B1) for complex **V-13** and 2.3376(14) Å (Ni1–B2) and 3.0262(14) Å (Ni1–B1) for complex **V-14**, respectively.

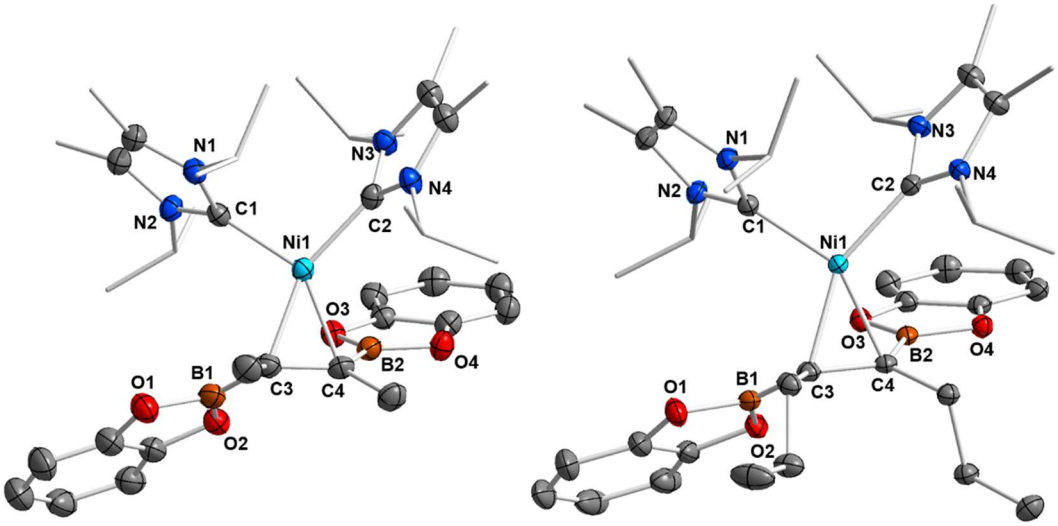

Figure V.6 Molecular structures of [Ni(^{i}Pr$_2$Im^{Me})$_2$(η^2-*cis*-(Bcat)(Me)C=C(Me)(Bcat))] **V-13** (left) and [Ni(^{i}Pr$_2$Im^{Me})$_2$(η^2-*cis*-(Bcat)(H$_7$C$_3$)C=C(C$_3$H$_7$)(Bcat))] **V-14** (right) in the solid state (ellipsoids shown at 50 % probability level). Hydrogen atoms have been omitted for clarity. Selected bond lengths [Å] and angles [°] of **V-13**: Ni1–C1 1.9454(14), Ni1–C2 1.9470(14), Ni1–C3 2.0161(14), Ni1–C4 2.0288(14), Ni1···B1 3.0525(19), Ni1···B2 2.3694(16) C3–C4 1.453(2), C3–B1 1.514(2), C4–B2 1.508(2); C1–Ni1–C2 100.55(6), C1–Ni1–C3 103.18(6), C3–Ni1–C4 42.09(6), C2–Ni1–C4 115.01(6), Ni1–C3–B1 119.02(11), Ni1–C4–B2 82.71(9), B1–C3–C4 124.06(14), B2–C4–C3 123.01(13). Selected bond lengths [Å] and angles [°] of **V-14**: Ni1–C1 1.9517(13), Ni1–C2 1.9560(13), Ni1–C3 2.0373(12), Ni1–C4 2.0070(12), Ni1···B1 3.0262(14), Ni1···B2 2.3376(14), C3–C4 1.4550(17), C3–B1 1.5188(19), C4–B2 1.5122(18); C1–Ni1–C2 99.47(5), C1–Ni1–C3 107.70(5), C3–Ni1–C4 42.16(5), C2–Ni1–C4 111.80(5), Ni1–C3–B1 115.88(9), Ni1–C4–B2 81.94(7), B1–C3–C4 123.63(11), B2–C4–C3 121.28(11).

The formation of **V-13** and **V-14** indicates that the catalytic bis-borylation of alkynes at d^{10}-[Ni(^{i}Pr$_2$Im^{Me})$_2$] most likely proceeds *via* a different mechanistic pathway than reported previously for the d^{10}-[PtL$_n$] platinum system. However, the addition of 2-butyne to **V-13** did not lead to the extrusion of the borylation product and regeneration of the alkyne complex **V-14** even at higher temperatures, but to formation of hexamethylbenzene.

By combining the results obtained from the stoichiometric reactions with additional DFT computations, we were able to rationalize the formation of the borylated products **V-7**, **V-7a** and **V-7b** from 2-butyne, B_2cat_2, and [Ni(^{i}Pr$_2$Im^{Me})$_2$]. Our proposed catalytic cycles are shown in Schemes V.6 and V.7. Initially, [Ni(^{i}Pr$_2$Im^{Me})$_2$] **7** reacts with 2-butyne to form **III-1** (ΔG_1 = –13.7 kcal mol^{-1}), which is competitive to the reaction with B_2cat_2 ($\Delta G_{1'}$ = –17.5 kcal mol^{-1}). The next step is the subsequent borylation at the activated alkyne leading to **V-13**, which is very exergonic (ΔG_2 = –41.3 kcal mol^{-1}). Our DFT calculations show that the barrier for the direct addition of B_2cat_2 to the alkyne is too high ($\Delta G^{‡}$ = +32.0 kcal mol^{-1}, see Figure XIII.5 in the Appendix). Alternatively, **V-13** could be formed by a B_2 insertion across the Ni–C bond ($\Delta G^{‡}$ = +13.7 kcal mol^{-1}), which leads to a five-membered NiC_2B_2 intermediate that exergonically isomerizes to a nickel monoboryl species (ΔG = –16.6 kcal mol^{-1}) and then to **V-13**. The direct release of **V-7** from **V-13** is rather endergonic (ΔG = +19.6 kcal mol^{-1}), and therefore we propose that in the next step an NHC is transferred from **V-13** to another B_2cat_2 molecule (ΔG_3 = +3.4 kcal mol^{-1}). This leads to the mono-NHC intermediate **I1**. Addition of an alkyne to **I1** leads to **I2** and is slightly exergonic (ΔG_4 = –4.7 kcal mol^{-1}). The release of **V-7** from **I2** is then mediated by the transfer of the NHC ligand from the ligand-activated B_2cat_2 species, whose step is endergonic by ΔG_5 = +7.2 kcal mol^{-1} and regenerates **III-1** and B_2cat_2.

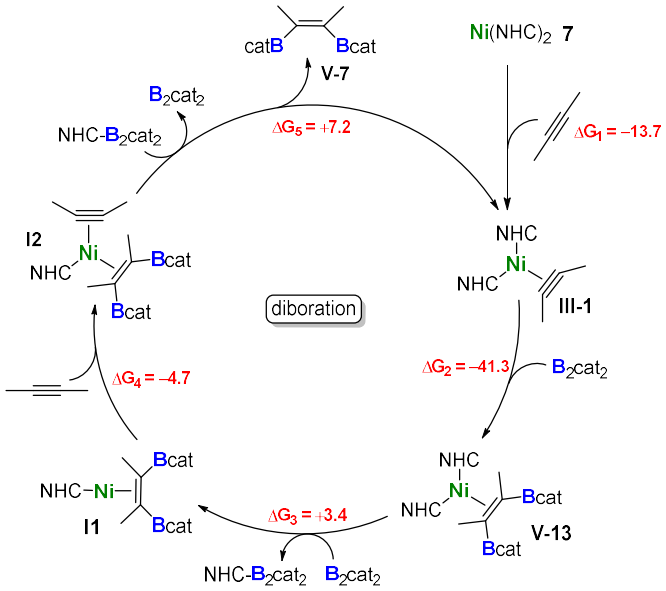

Scheme V.6 Proposed catalytic cycle for the formation of **V-7**. Reaction free energies (kcal mol^{-1}) calculated at the DFT level are shown in red.

The catalytic cycles leading to the tetra-borylated product **V-7a** and the alkyne coupling species **V-7b** are shown in Scheme 7. The mono-NHC intermediate **I1** can react with B_2cat_2 leading exergonically to **I3** (ΔG_6 = –5.4 kcal mol^{-1}). This species can undergo facile B–B bond dissociation and formation of the nickel monoboryl species **I4** (ΔG_7 = +5.6 kcal mol^{-1}), where the other boryl group is transferred to the alkene moiety. The release of the tetra-borylated product **V-7a** (ΔG_8 = –1.8 kcal mol^{-1}) is then mediated by the NHC-activated B_2cat_2 species, with further regeneration of B_2cat_2 and **7**. In turn, **V-13** can transfer an NHC to the product **V-7** (NHC-prod, ΔG_9 = +3.7 kcal mol^{-1}), which would lead to **I1**. As already discussed, this intermediate can be converted to **I2** after addition of an alkyne. We propose that the alkyne coupling can start from **I2**, which would lead to **I5**, a bis-borylated butadiene stabilized by a mono-NHC nickel moiety (ΔG_{10} = –4.1 kcal mol^{-1}). The release of **V-7b** would then be mediated by the transfer of the NHC ligand from the ligand-activated NHC-prod (ΔG_{11} = +2.1 kcal mol^{-1}), regenerating **V-7** and [Ni(^{i}Pr$_2$Im^{Me})$_2$] **7**.

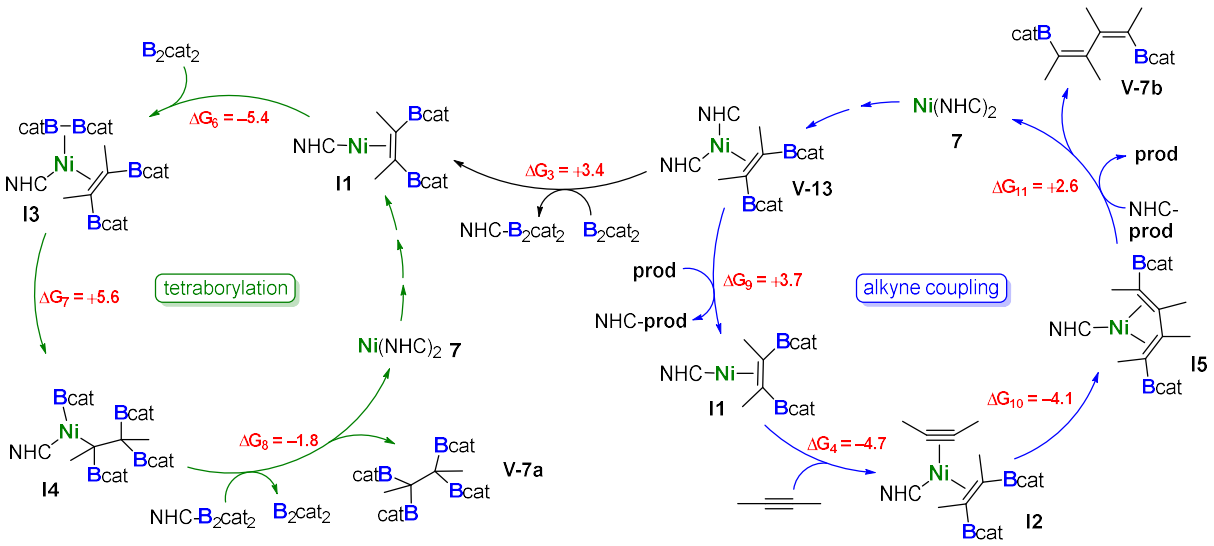

Scheme V.7 Proposed catalytic cycles for the formation of **V-7a** (left) and **V-7b** (right). Reaction free energies (kcal mol^{-1}) calculated at the DFT level are shown in red.

5.3 Conclusion

It has been shown over the last decades that transition metal poly-boryl complexes play pivotal roles and are key intermediates in many borylation processes. Such complexes were typically associated with noble metals, but as first-row d-block metals are less toxic, less expensive, Earth-abundant, and environmentally benign, they are very attractive alternatives to these expensive noble metals. Nickel boryl complexes are generally considered to be elusive, in contrast to other 3d-metals such as iron, cobalt, or copper. We report herein the first nickel bis-boryl complexes *cis*-[Ni(^{i}Pr$_2$Im^{Me})$_2$(Bcat)$_2$] **V-1a**, *cis*-[Ni(^{i}Pr$_2$Im^{Me})$_2$(Bpin)$_2$] **V-1b** and *cis*-[Ni(^{i}Pr$_2$Im^{Me})$_2$(Beg)$_2$] **V-1c**, which can be synthesized from the reaction of a source of [Ni(^{i}Pr$_2$Im^{Me})$_2$] **7** with the diboron(4) compounds B$_2$cat$_2$, B$_2$pin$_2$ and B$_2$eg$_2$. Key to the successful synthesis was the choice of the NHC used, showing the right stereoelectronic properties. Whereas *cis*-[Ni(^{i}Pr$_2$Im^{Me})$_2$(Bcat)$_2$] **V-1a** was isolated as a pale brown solid in 58 % yield, the reaction with either B$_2$pin$_2$ or B$_2$eg$_2$ instead of B$_2$cat$_2$ did not proceed quantitatively at room temperature, as observed by NMR spectroscopy. X-ray diffraction studies on **V-1a-c** and DFT calculations on **V-1a** suggest that a delocalized, multicenter bonding scheme best describes the bonding situation of the NiB$_2$ moiety in these complexes, which is reminiscent of the bonding situation in “non-classical” H$_2$ complexes.

We also demonstrate that [Ni(^{i}Pr$_2$Im^{Me})$_2$] **7** catalyst precursors provide excellent catalytic activity for the diboration of alkynes under mild conditions, using B$_2$cat$_2$ as boron source. Beside the well-known *cis*-alkene-1,2-bis(boronate) esters, the formation of C–C coupled borylation products such as **V-7b**, **V-11a** and **V-11b** as well as tetra-borylated products such as **V-7a** and **V-12** were observed or produced as main products of the reaction, which significantly expands the (poly)borylation of alkynes and the scope of accessible boron compounds for further transformations. Therefore, we demonstrated that these 3d-metal catalysts provide the potential for new selectivities for the borylation of alkynes compared to the well-established catalysts.

Mechanistic investigations supported by DFT calculations revealed significant differences between our NHC nickel system and the well-established platinum-phosphine chemistry. The formation of borylated alkyne complexes **V-13** and **V-14** as catalytic intermediates is crucial to understand the new catalytic pathway and the

formation of new borylation products. Further studies concerning the reactivity of nickel bis-boryl complexes are currently under investigation.

5.4 References

[1] General reviews borylation: a) H. C. Brown, From Little Acorns to Tall Oaks: From Boranes through Organoboranes (Nobel Lecture), **1979**, http://www.nobelprize.org; b) N. Miyarura, *Top. Curr. Chem.* **2002**, *219*, 11-59; c) D. E. Kaufmann, D. S. Matteson (eds), Boron compounds, Science of Syntheses, Vol 6, Georg Thieme Verlag, Stuttgart **2005**; d) D. G. Hall (ed.), *Boronic Acids-Preparation and Applications in Organic Synthesis, Medicine and Materials*, 2nd Edition; Wiley−VCH, Weinheim, Germany, **2011**; e) E. C. Neeve, S. J. Geier, I. A. I. Mkhalid, S. A. Westcott, T. B. Marder, *Chem. Rev.* **2016**, *116*, 9091-9161; f) M. Wang, Z. Shi, *Chem. Rev.* **2020**, *120*, 7348-7398; g) Y. Tian, X. Guo, H. Braunschweig, U. Radius, T. B. Marder, *Chem. Rev.* **2021**, *121*, 3561-3597; h) S. K. Bose, L. Mao, L. Kuehn, U. Radius, J. Nekvinda, W. L. Santos, S. A. Westcott, P. G. Steel, T. B. Marder, *Chem. Rev.* **2021**, *121*, 13238-13341; i) J. Hu, M. Ferger, Z. Shi, T. B. Marder, *Chem. Soc. Rev.* **2021**, *50*, 13129-13188; j) S. Manna, K. K. Das, S. Nandy, D. Aich, S. Paul, S. Panda, *Coord. Chem. Rev.* **2021**, *448*, 214165.

[2] a) T. Ishiyama, M. Murata, N. Miyaura, *J. Org. Chem.* **1995**, *60*, 7508-7510; b) L. T. Pilarski, K. J. Szabó, *Angew. Chem.* **2011**, *123*, 8380-8382; *Angew. Chem. Int. Ed.* **2011**, *50*, 8230-8232; c) M. Murata, *Heterocycles* **2012**, *85*, 1795-1819; d) C. M. Vogels, S. A. Westcott, *ChemCatChem.* **2012**, *4*, 47-49; e) W. K. Chow, O. Y. Yuen, P. Y. Choy, C. M. So, C. P. Lau, W. T. Wong, F. Y. Kwong, *RSC Adv.* **2013**, *3*, 12518-12539; f) K. Kubota, H. Iwamoto, H. Ito, *Org. Biomol. Chem.* **2017**, *15*, 285-300; g) Y. P. Budiman, S. A. Westcott, U. Radius, T. B. Marder, *Adv. Synth. Catal.* **2021**, *363*, 2224-2255.

[3] a) I. Beletskaya, A. Pelter, *Tetrahedron* **1997**, *53*, 4957-5026; b) V. Lillo, A. Bonet, E. Fernández, *Dalton Trans.* **2009**, 2899-2908; c) J. Takaya, N. Iwasawa, *ACS Catal.* **2012**, *2*, 1993-2006; d) H. Wen, G. Liu, Z. Huang, *Coord. Chem. Rev.* **2019**, *386*, 138-153; e) W. Fan, L. Li, G. Zhang, *J. Org. Chem.* **2019**, *84*, 5987-5996; f) O. Salvadó, E. Fernández, *Molecules* **2020**, *25*, 1758; g) X. Wang, Y. Wang, W. Huang, C. Xia, L. Wu, *ACS Catal.* **2021**, *11*, 1-18.

[4] a) T. B. Marder, N. C. Norman, *Top. Catal.* **1998**, 63-73; b) R. Barbeyron, E. Benedetti, J. Cossy, J.-J. Vasseur,S. Arseniyadis, M. Smietana, *Tetrahedron* **2014**, *70*, 8431-8452; c) H. Yoshida, *ACS Catal.* **2016**, *6*, 1799-1811; d) M. B.

Ansell, O. Navarro, J. Spencer, *Coord. Chem. Rev.* **2017**, *336*, 54-77; e) F. Zhao, X. Jia, P. Li, J. Zhao, Y. Zhou, J. Wang, H. Liu, *Org. Chem. Front.* **2017**, 4, 2235-2255; f) J. Carreras, A. Caballero, P. J. Perez, *Chem. Asian J.* **2019**, *14*, 329-343.

[5] a) T. Ishiyama, N. Miyaura, *J. Organomet. Chem.* **2003**, *680*, 3-11; b) I. A. I. Mkhalid, J. H. Barnard, T. B. Marder, J. M. Murphy, J. F. Hartwig, *Chem. Rev.* **2010**, *110*, 890-931; c) J. F. Hartwig, *Chem. Soc. Rev.* **2011**, *40*, 1992-2002; d) J. F. Hartwig, *Acc. Chem. Res.* **2012**, *45*, 864-873; e) A. Ros, R. Fernández, J. M. Lassaletta, *Chem. Soc. Rev.* **2014**, *43*, 3229-3243; f) J. F. Hartwig, *J. Am. Chem. Soc.* **2016**, *138*, 2-24; g) Y. Ping, L. Wang, Q. Ding, Y. Peng, *Adv. Synth. Catal.* **2017**, *359*, 3274-3291; h) T. Gensch, M. J. James, T. Dalton, F. Glorius, *Angew. Chem.* **2018**, *130*, 2318-2328; *Angew. Chem. Int. Ed.* **2018**, *57*, 2296-2306; i) Y. Shi, Q. Gao, S. Xu, *Synlett* **2019**, *30*, 2107-2112; j) E. Fernandez, *Top. Organomet. Chem.* **2021**, *69*, 207-225.

[6] a) G. J. Irvine, M. J. Lesley, T. B. Marder, N. C. Norman, C. R. Rice, E. G. Robins, W. R. Roper, G. R. Whittell, L. J. Wright, *Chem. Rev.* **1998**, *98*, 2685-2722; b) H. Braunschweig, *Angew. Chem.* **1998**, *110*, 1882-1898; *Angew. Chem. Int. Ed.* **1998**, *37*, 1786-1801; c) H. Braunschweig, M. Colling, *Coord. Chem. Rev.* **2001**, *223*, 1-51; d) S. Aldridge, D. L. Coombs, *Coord. Chem. Rev.* **2004**, *248*, 535-559; e) H. Braunschweig, C. Kollann, D. Rais, *Angew. Chem.* **2006**, *118*, 5380-5400; *Angew. Chem. Int. Ed.* **2006**, *45*, 5254-5274; f) D. L. Kays, S. Aldridge, *Struct. Bond.* **2008**, *130*, 29-122; g) U. Kaur, K. Saha, S. Gayen, S. Ghosh, *Coord. Chem. Rev.* **2021**, *446,* 214106.

[7] a) T. Ishiyama, N. Miyaura, *J. Organomet. Chem.* **2000**, *611*, 392-402; b) N. Miyaura, *Bull. Chem. Soc. Jpn.* **2008**, *81*, 1535-1553; c) L. Dang, Z. Lin, T. B. Marder, *Chem. Commun.* **2009**, 3987-3995; d) X. Guo, T. Yang, F. K. Sheong, Z. Lin, *ACS Catal.* **2021**, *11*, 5061-5068.

[8] a) P. Nguyen, H. P. Blom, S. A. Westcott, N. J. Taylor, T. B. Marder, *J. Am. Chem. Soc.* **1993**, *115*, 9329-9330; b) R. T. Baker, J. C. Calabrese, S. A. Westcott, P. Nguyen, T. B. Marder, *J. Am. Chem. Soc.* **1993**, *115*, 4367-4368; c) K. Burgess, W. A. Van der Donk, S. A. Westcott, T. B. Marder, R. T. Baker, J. C. Calabrese, *J. Am. Chem. Soc.* **1992**, *114*, 9350-9359.

[9] a) T. Ishiyama, J. Takagi, K. Ishida, N. Miyaura, N. R. Anastasi, J. F. Hartwig, *J. Am. Chem. Soc.* **2002**, *124*, 390-391; b) J.-Y. Cho, M. K. Tse, D. Holmes, R. E.

Maleczka, M. R. Smith, *Science* **2002**, *295*, 305-308; c) M. A. Larsen, J. F. Hartwig, *J. Am. Chem. Soc.* **2014**, *136*, 4287-4299.

[10] a) A. K. Cook, S. D. Schimler, A. J. Matzger, M. S. Sanford, *Science* **2016**, *351*, 1421-1424; b) K. T. Smith, S. Berritt, M. González-Moreiras, S. Ahn, M. R. Smith, M.-H. Baik, D. J. Mindiola, *Science* **2016**, *351*, 1424-142; c) S. Ahn, D. Sorsche, S. Berritt, M. R. Gau, D. J. Mindiola, M.-H. Baik, *ACS Catal.* **2018**, *8*, 10021-10031.

[11] a) C. N. Iverson, M. R. Smith, *J. Am. Chem. Soc.* **1995**, *117*, 4403-4404; b) C. Borner, C. Kleeberg, *Eur. J. Inorg. Chem.* **2014**, 2486-2489.

[12] a) T. Ishiyama, N. Matsuda, N. Miyaura, A. Suzuki, *J. Am. Chem. Soc.* **1993**, *115*, 11018-11019; b) T. Ishiyama, N. Matsuda, M. Murata, F. Ozawa, A. Suzuki, N. Miyaura, *Organometallics* **1996**, *15*, 713-720; c) C. N. Iverson, M. R. Smith, *Organometallics* **1996**, *15*, 5155-5165; d) Q. Cui, D, G. Musaev, K. Morokuma, *Organometallics* **1998**, *17*, 742-751.

[13] a) G. Lesley, P. Nguyen, N. J. Taylor, T. B. Marder, A. J. Scott, W. Clegg, N. C. Norman, *Organometallics* **1996**, *15*, 5137-5154; b) R. L. Thomas, F. E. S. Souza, T. B. Marder, *Dalton Trans.* **2001**, 1650-1656.

[14] a) T. Ishiyama, N. Miyaura, *Chem. Rec.* **2004**, *4*, 271-280; b) M. W. Carson, M. W. Giese, M. J. Coghlan, *Org. Lett.* **2008**, *10*, 2701-2704; c) K. Yavari, S. Moussa, B. Ben Hassine, P. Retailleau, A.Voituriez, A. Marinetti, *Angew. Chem.* **2012**, *124*, 6852-6856; *Angew. Chem., Int. Ed.* **2012**, *51*, 6748-6752; d) Q.-X. Lin, T.-L. Ho, *Tetrahedron* **2013**, *69*, 2996-3001; e) M. W. Carson, J. G. Luz, C. Suen, C. Montrose, R. Zink, X. Ruan, C. Cheng, H. Cole, M. D. Adrian, D. T. Kohlman, T. Mabry, N. Snyder, B. Condon, M. Maletic, D. Clawson, A. Pustilnik and M. J. Coghlan, *J. Med. Chem.* **2014**, *57*, 849-860; f) J. Yang, M. Chem, J. Ma, W. Huang, H. Zhu, Y. Huang, W. Wang, *J. Mater. Chem. C* **2015**, *3*, 10074-10078.

[15] a) C. Kleeberg, L. Dang, Z. Lin, T. B. Marder, *Angew. Chem.* **2009**, *121*, 5454-5458; *Angew. Chem. Int. Ed.* **2009**, *48*, 5350-5354; b) C.-T. Yang, Z.-Q. Zhang, H. Tajuddin, C.-C. Wu, J. Liang, J.-H. Liu, Y. Fu, M. Czyzewska, P. G. Steel, T. B. Marder, L. Liu, *Angew. Chem.* **2012**, *124*, 543-547; *Angew. Chem. Int. Ed.* **2012**, *51*, 528-532; c) S. K. Bose, S. Brand, H. O. Omoregie, M. Haehnel, J. Maier, G. Bringmann, T. B. Marder, *ACS Catal.* **2016**, *6*, 8332-8335; d) D. Hemming, R. Fritzemeier, S. A. Westcott, W. L. Santos, P. G. Steel, *Chem. Soc. Rev.* **2018**, *47*, 7477-7494; e) L. Kuehn, M. Huang, U. Radius, T. B. Marder, *Org.*

Biomol. Chem. **2019**, *17*, 6601-6606; f) B. S. Takale, R. R. Thakore, E. Etemadi-Davan, B. H. Lipshutz, *Beilstein J. Org. Chem.* **2020**, *16*, 691-737; g) A. Whyte, A. Torelli, B. Mirabi, A. Zhang, M. Lautens, *ACS Catal.* **2020**, *10*, 11578-11622.

[16] a) J. Zhou, M. W. Kuntze-Fechner, R. Bertermann, U. S. Paul, J. H. Berthel, A. Friedrich, Z. Du, T. B. Marder, U. Radius, *J. Am. Chem. Soc.* **2016**, *138*, 5250-5253; b) Y.-M Tian, X.-N. Guo, M. Kuntze-Fechner, I. Krummenacher, H. Braunschweig, U. Radius, A. Steffen, T. B. Marder, *J. Am. Chem. Soc.* **2018**, *140*, 17612-17623; c) M. W. Kuntze-Fechner, H. Verplancke, L. Tendera, M. Diefenbach, I. Krummenacher, H. Braunschweig, T. B. Marder, M. C. Holthausen, U. Radius, *Chem. Sci.* **2020**, *11*, 11009-11023; d) L. Kuehn, D. G. Jammal, K. Lubitz, T. B. Marder, U. Radius, *Chem. Eur. J.* **2019**, *25*, 9514-9521; e) Y.-M. Tian, X.-N. Guo, I. Krummenacher, Z. Wu, J. Nitsch, H. Braunschweig, U. Radius, T. B. Marder, *J. Am. Chem. Soc.* **2020**, *142*, 18231-18242; f) Y.-M. Tian, X.-N. Guo, Z. Wu, A. Friedrich, S. A. Westcott, H. Braunschweig, U. Radius, T. B. Marder, *J. Am. Chem. Soc.* **2020**, *142*, 13136-13144.

[17] The reaction of [Ni(Cy_2Im)$_2$(Ar)Cl] with stoichiometric amounts of B_2pin_2 at room temperature led to a resonance 44.5 ppm in the $^{11}B\{^1H\}$ NMR spectrum of the reaction mixture which indicated the formation of a nickel-boryl complex, see the Supporting Information of ref 16 d.

[18] a) J. F. Hartwig, S. Huber, *J. Am. Chem. Soc.* **1993**, *115*, 4908-4909; b) X. He, J. F. Hartwig, *Organometallics* **1996**, *15*, 400-407; c) K. M. Waltz, C. N. Muhoro, J. F. Hartwig, *Organometallics* **1999**, *18*, 3383-3393; d) S. Aldridge, R. J. Calder, R. E. Baghurst, M. E. Light, M. B. Hursthouse, *J. Organomet. Chem.* **2002**, *649*, 9-14; e) A. Rossin, S. Aldridge, L.-l. Ooi, *Appl. Organomet. Chem*. **2005**, *19*, 181-182; f) T. J. Mazzacano, N. P. Mankad, *Chem. Commun.* **2015**, *51*, 5379-5382; g) R. B. Bedford, P. B. Brenner, E. Carter, T. Gallagher, D. M. Murphy, D. R. Pye, *Organometallics* **2014**, *33*, 5940-5943; h) T. Dombray, C. G. Werncke, S. Jiang, M. Grellier, L. Vendier, S. Bontemps, J.-B. Sortais, S. Sabo-Etienne, C. Darcel, *J. Am. Chem. Soc.* **2015**, *137*, 4062-4065; i) L. Vondung, N. Frank, M. Fritz, L. Alig, R. Langer, *Angew. Chem.* **2016**, *128*, 14665-14670; *Angew. Chem. Int. Ed.* **2016**, *55*, 14450-14454; j) K. Nakajima, T. Kato, Y. Nishibayashi, *Org. Lett.* **2017**, *19*, 4323-4326; k) T. Kato, S. Kuriyama, K. Nakajima, Y. Nishibayashi, *Chem. As. J.* **2019**, *14*, 2097-2101.

[19] a) C. Dai, G. Stringer, J. F. Corrigan, N. J. Taylor, T. B. Marder, N. C. Norman, *J. Organomet. Chem.* **1996**, *513*, 273-275; b) C. J. Adams, R. A. Baber, A. S. Batsanov, G. Bramham, J. P. Charmant, M. F. Haddow, J. A. Howard, W. H. Lam, Z. Lin, T. B. Marder, N. C. Norman, A. G. Orpen, *Dalton Trans.* **2006**, 1370-1373; c) J. V. Obligacion, S. P. Semproni, P. J. Chirik, *J. Am. Chem. Soc.* **2014**, *136*, 4133-4136; d) J. V. Obligacion, S. P. Semproni, I. Pappas, P. J. Chirik, *J. Am. Chem. Soc.* **2016**, *138*, 10645-10653; e) S. M. Rummelt, H. Zhong, N. G. Léonard, S. P. Semproni, P. J. Chirik, *Organometallics* **2019**, *38*, 1081-1090; f) R. Arevalo, T. P. Pabst, P. J. Chirik, *Organometallics* **2020**, *39*, 2763-2773; g) W. Drescher, D. Schmitt-Monreal, C. R. Jacob, C. Kleeberg, *Organometallics* **2020**, *39*, 538-543.

[20] a) D. S. Laitar, P. Müller, J. P. Sadighi, *J. Am. Chem. Soc.* **2005**, *127*, 17196-17197; b) K. Semba, M. Shinomiya, T. Fujihara, J. Terao, Y. Tsuji, *Chem. Eur. J.* **2013**, *19*, 7125-7132; c) C. M. Wyss, J. Bitting, J. Bacsa, T. G. Gray, J. P. Sadighi, *Organometallics* **2016**, *35*, 71-74; d) C. Borner, L. Anders, K. Brandhorst, C. Kleeberg, *Organometallics* **2017**, *36*, 4687-4690; e) C. Kleeberg, C. Borner, *Organometallics* **2018**, *37*, 4136-4146; f) W. Drescher, C. Kleeberg, *Inorg. Chem.* **2019**, *58*, 8215-8229; g) W. Drescher, C. Borner, C. Kleeberg, *New J. Chem.* **2021**, *45*, 14957-14964; h) P. Ríos, M. S. See, R. C. Handford, S. J. Teat, T. D. Tilley, *Chem. Sci.* **2022**, *13*, 6619-6625.

[21] a) D. Adhikari, J. C. Huffman, D. J. Mindiola, *Chem. Commun.* **2007**, 4489-4491; b) B. L. Tran, D. Adhikari, H. Fan, M. Pink, D. J. Mindiola, *Dalton Trans.* **2010**, *39*, 358-360; c) N. Curado, C. Maya, J. López-Serrano, A. Rodríguez, *Chem. Commun.* **2014**, *50*, 15718-15721; d) P. Ríos, J. Borge, F. Fernández de Córdova, G. Sciortino, A. Lledós, A. Rodríguez, *Chem. Sci.* **2021**, *12*, 2540-2548;

[22] a) T. Schaub, U. Radius, *Chem. Eur. J.* **2005**, *11*, 5024-5030; b) T. Schaub, M. Backes, U. Radius, *Organometallics* **2006**, *25*, 4196-4206; c) U. S. D. Paul, C. Sieck, M. Hähnel, K. Hammond, T. B. Marder, U. Radius, *Chem. Eur. J.* **2016**, *21*, 11005-11014; d) U. S. D. Paul, U. Radius, *Chem. Eur. J.* **2017**, *23*, 3993-4009; e) U. S. D. Paul, U. Radius, *Organometallics* **2017**, *36*, 1398-1407; f) J. H. J. Berthel, M. W. Kuntze-Fechner, U. Radius, *Eur. J. Inorg. Chem.* **2019**, 2618-2623; g) J. H. J. Berthel, L. Tendera, M. W. Kuntze-Fechner, L. Kuehn, U. Radius, *Eur. J. Inorg. Chem.* **2019**, 3061-3072; h) J. H. J. Berthel, M. J. Krahfuss, U. Radius, *Z. Anorg. Allg. Chem.* **2020**, *646*, 692-704; i) M. J. Krahfuss, J. Nitsch, F.

M. Bickelhaupt, T. B. Marder, U. Radius, *Chem. Eur. J.* **2020**, *26*, 11276-11292; j) L. Tendera, T. Schaub, M. J. Krahfuss, M. W. Kuntze-Fechner, U. Radius, *Eur. J. Inorg. Chem.* **2020**, 3194-3207; k) S. Sabater, D. Schmidt, H. Schmidt nee Schneider, M. Kuntze-Fechner, T. Zell, C. J. Isaac, H. Grieve, W. J. M. Blackaby, J. P. Lowe, S. A. Macgregor, M. F. Mahon, F. M. Miloserdov, N. Rajabi, U. Radius, M. K. Whittlesey, *Chem. Eur. J.* **2021**, *27*, 13221-13234; l) L. Tendera, M. Helm, M. J. Krahfuss, M. W. Kuntze-Fechner, U. Radius, *Chem. Eur. J.* **2021**, *27*, 17849-17861.

[23] a) S. Würtemberger-Pietsch, U. Radius, T. B. Marder, *Dalton Trans.* **2016**, *45*, 5880-5895; b) S. Pietsch, U. Paul, I. A. Cade, M. J. Ingleson, U. Radius, T. B. Marder, *Chem. Eur. J.* **2015**, *21*, 9018-9021; c) S. Würtemberger-Pietsch, H. Schneider, T. B. Marder, U. Radius, *Chem. Eur. J.* **2016**, *22*, 13032-13036; d) M. Eck, S. Würtemberger-Pietsch, A. Eichhorn, J. H. J. Berthel, R. Bertermann, U. S. D. Paul, H. Schneider, A. Friedrich, C. Kleeberg, U. Radius, T. B. Marder, *Dalton Trans.* **2017**, *46*, 3661-3680.

[24] a) H. Clavier, S. P. Nolan, *Chem. Commun.* **2010**, *46*, 841-861; b) S. Felten, S. F. Marshall, A. J. Groom, R. T. Vanderlinden, R. M. Stolley, J. Louie, *Organometallics* **2018**, *37*, 3687-3697.

[25] a) W. Clegg, F. J. Lawlor, G. Lesley, T. B. Marder, N. C. Norman, A. G. Orpen, M. J. Quayle, C. R. Rice, A. J. Scott, F. E. S. Souza, *J. Organomet. Chem.* **1998**, *550*, 183-192; b) J. Zhu, Z. Lin, T. B. Marder, *Inorg. Chem.* **2005**, *44*, 9384-9390; c) H. Braunschweig, P. Brenner, A. Müller, K. Radacki, D. Rais, K. Uttinger, *Chem. Eur. J.* **2007**, *13*, 7171-7176.

[26] a) T. Zell, T. Schaub, K. Radacki, U. Radius, *Dalton Trans.* **2011**, *40*, 1852-1854; b) C. Hauf, J. E. Barquera-Lozada, P. Meixner, G. Eickerling, S. Altmannshofer, D. Stalke, T. Zell, D. Schmidt, U. Radius, W. Scherer, *Z. Anorg. Allg. Chem.* **2013**, *639*, 1996-2004; c) D. Schmidt, T. Zell, T. Schaub, U. Radius, *Dalton Trans.* **2014**, *43*, 10816-10827.

[27] W. Clegg, M. R. J. Elsegood, F. J. Lawlor, N. C. Norman, N. L. Pickett, E. G. Robins, A. J. Scott, P. Nguyen, N. J. Taylor, T. B. Marder, *Inorg. Chem.* **1998**, *37*, 5289-5293.

[28] a) I. Mayer, *Chem. Phys. Lett.* **1983**, *97*, 270-274; b) I. Mayer, *Int. J. Quantum Chem.* **1984**, *26*, 151-154.

[29] G. Knizia, *J. Chem. Theory Comput.* **2013**, *9*, 4834-4843.

[30] a) M. Ernzerhof, G. E. Scuseria, *J. Chem. Phys.* **1999**, *110*, 5029-5036; b) C. Adamo, V. Barone, *J. Chem. Phys.* **1999**, *110*, 6158-6170; c) S. Grimme, J. Antony, S. Ehrlich, H. Krieg, *J. Chem. Phys.* **2010**, *132*, 154104; d) S. Grimme, S. Ehrlich, L. Goerigk, *J. Comput. Chem.* **2011**, *32*, 1456-1465; e) F. Weigend, R. Ahlrichs, *Phys. Chem. Chem. Phys.* **2005**, *7*, 3297-3305.

[31] M. B. Ansell, V. H. Menezes da Silva, G. Heerdt, A. A. C. Braga, J. Spencer, O. Navarro, *Catal. Sci. Technol.* **2016**, *6*, 7461-7467.

[32] M. Bluhm, A. Maderna, H. Pritzkow, S. Bethke, R. Gleiter, W. Siebert, *Eur. J. Inorg. Chem.* **1999**, 1693-1700.

[33] W. Clegg, A. J. Scott, G. Lesley, T. B. Marder, N. C. Norman, *Acta Crystallogr. C* **1996**, *52*, 1991-1995.

Chapter VI

The Reactivity of Nickel NHC Bis-Boryl Complexes: Reductive Elimination and Formation of Mono-Boryl Complexes

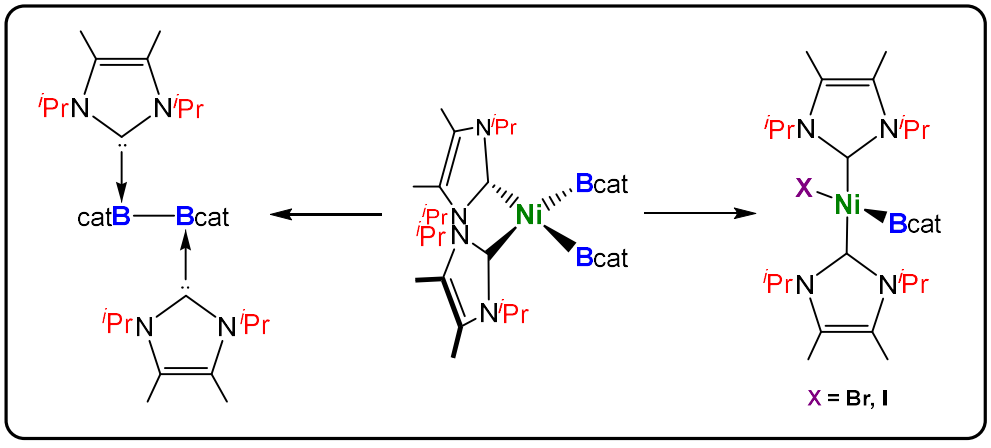

6 The Reactivity of Nickel NHC Bis-Boryl Complexes: Reductive Elimination and Formation of Mono-Boryl Complexes

6.1 Introduction

Since the beginning of the 1990s, when Merola and the groups of Baker and Marder first characterized the molecular structures of the iridium-boryl complexes *mer*-[Ir(H)(Bcat)(Cl)(PMe_3)$_3$][1] and *fac*-[Ir(H)$_2$(PMe_3)$_3$(BC_8H_{14})][2] by single crystal X-ray diffraction, research on transition metal boryl complexes [L_nM-BX_2][3] has evolved enormously. Due to their interesting properties and their decisive role as key-intermediates in different catalytic transformations,[4] such as the Miyaura-borylation of aryl and alkyl halides,[5] catalytic addition reactions to unsaturated organic molecules *via* hydroboration, diboration, *β*-borylation or carboboration,[6,7] or the direct functionalization of C–H bonds,[8] these compounds have been studied intensively. The most commonly used ligands of metal boryls are Bcat or Bpin, mainly due to their application as boron sources in catalytic processes.[9] Those ligands are often introduced *via* oxidative addition of the corresponding diboron(4), hydroborane or haloborane compounds to a low valent transition metal, and can either be coordinated terminally or as bridging ligands between two metals.[3] For group 10 metals, a large number of platinum mono- and bis-boryl complexes of haloboryls, aminoboryls, aryl(halo)boryls or aryloxyboryls are known.[10,11] Well known examples are platinum bis-boryl complexes, such as *cis*-[Pt(PPh_3)$_2$(Bcat)$_2$] **37**,[10a] a pre-catalysts for the addition of diborane(4) compounds to alkynes.[12] The groups of Marder[11b] and Braunschweig[11c] independently provided theoretical and experimental evidence for the strong *trans*-influence of different boryl ligands based on platinum mono-boryl complexes of the type *trans*-[Pt(PR_3)$_2$(B{OR'}$_2$)X] **40**. For the lighter homologues, palladium and nickel, isolated boryl complexes are scarce. The first structurally characterized palladium boryl complex was reported in 1996 by Tanaka *et al.*, who prepared [(dmpe)Pd($SnMe_3$)(B{NMe(C_2H_4)NMe})] **41** by oxidative addition of the corresponding borylstannane to [(dmpe)$PdMe_2$].[13] In 2005, Braunschweig *et al.* presented the complexes *trans*-[M(PCy_3)$_2$(B≡N{$SiMe_3$})Br] **42** (M = Pt and Pd), which are the first examples of complexes containing iminoboryl ligands with B≡N triple bonds.[14] Only a few structurally characterized nickel boryl complexes have been

isolated thus far. In 2007, Mindiola *et al.*[15a] reported the first nickel mono-boryl complex [(PNP)Ni(Bcat)] **38** (PNP = N[2-P(CHMe$_2$)$_2$-4-methylphenyl]$_2$) and Rodriguez *et al.* introduced the *trans*-halo-boryl complex [(PBP)Ni(Br)] **43,** among several boryl complexes [(PBP)NiL] (L = H, Br, Me, Bcat; PBP = C_6H_4{N(CH$_2$P^{t}Bu$_2$)}$_2$B), in which the boryl moiety is embedded in the PBP pincer system.[15c,d]

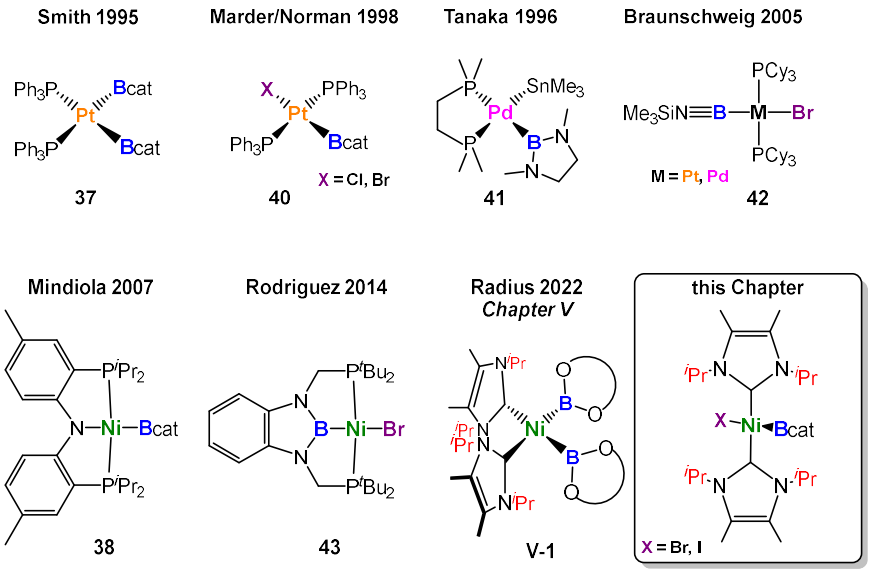

Figure VI.1 Selected examples of group 10 boryl complexes.

During the last years we investigated the stereoelectronic features of different NHC ligands and their influence on the reactivity of nickel complexes of the type [Ni(NHC)$_2$] in some detail.[16] In course of our work on the borylation of polyfluorarenes, aryl chlorides, and indoles using synthetic equivalents of the complexes [Ni(Mes$_2$Im)$_2$] or [Ni(Cy$_2$Im)$_2$] as catalysts (R$_2$Im = 1,3-di-organyl-imidazolin-2-ylidene; Cy = cyclohexyl; Mes = mesityl) we postulated the formation of nickel-boryl species, which defied isolation.[17] In Chapter V the synthesis of novel nickel bis-boryl complexes *cis*-[Ni(*i*Pr$_2$Im^{Me})$_2$(B{OR}$_2$)$_2$] (**V-1**) ({OR}$_2$ = catecholato (**V-1a**), pinakolato (**V-1b**), ethylene glycolato (**V-1c**)) stabilized by monodentate NHC ligands *i*Pr$_2$Im^{Me} (*i*Pr$_2$Im^{Me} = 1,3-di-*iso*-propyl-4,5-dimethylimidazolin-2-ylidene) was reported.[18] Furthermore, the application of [Ni(*i*Pr$_2$Im^{Me})$_2$] as effective catalyst in the borylation of alkynes was reported, providing interesting new selectivities compared to the well established platinum-phosphine systems. In this chapter some detailed reactivity studies of the nickel bis-boryl complex *cis*-[Ni(*i*Pr$_2$Im^{Me})$_2$(Bcat)$_2$] **V-1a** are reported, including the

formation of NHC stabilized mono-boryl complexes and the reductive elimination of B_2cat_2.

6.2 Results and Discussion

In Chapter V the synthesis of *cis*-[Ni(^{i}Pr$_2$Im^{Me})$_2$(Bcat)$_2$] **V-1a** was reported[18] *via* oxidative addition of B_2cat_2 (bis-catecholatodiboron) to synthetic equivalents of [Ni(^{i}Pr$_2$Im^{Me})$_2$] **7**, which were typically provided from a mixture of the complexes [Ni$_2$(^{i}Pr$_2$Im^{Me})$_4$(μ-(η^2:η^2)-COD)] **7a** and [Ni(^{i}Pr$_2$Im^{Me})$_2$(η^4-COD)] **7b**.[16l] In course of our work on the [Ni(^{i}Pr$_2$Im^{Me})$_2$]-catalyzed borylation of alkynes with B_2cat_2, we further investigated some basic reactivity of **V-1a** (Scheme VI.1).

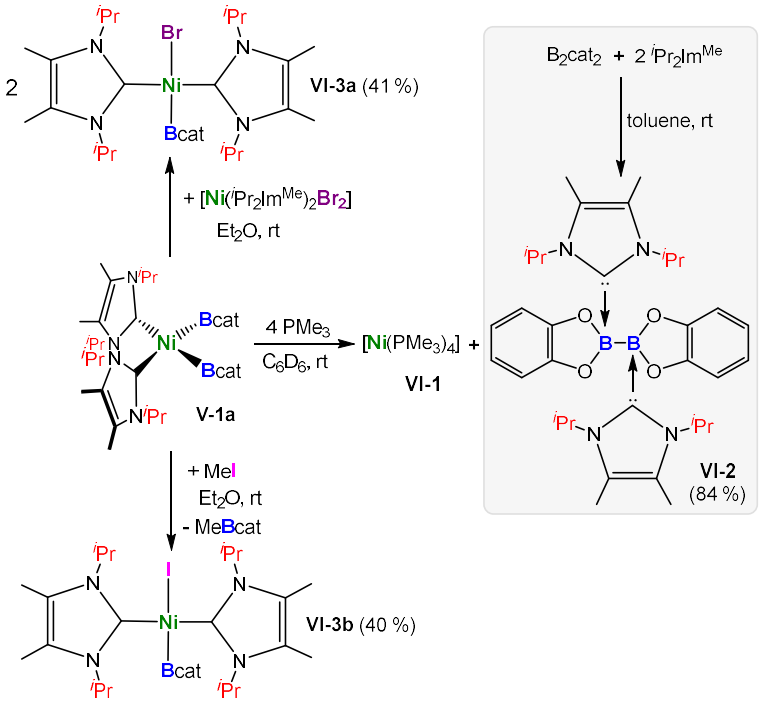

Scheme VI.1 Reactions of *cis*-[Ni(^{i}Pr$_2$Im^{Me})$_2$(Bcat)$_2$] **V-1a** with PMe_3, MeI and *trans*-[Ni(^{i}Pr$_2$Im^{Me})$_2$(Br)$_2$].

First of all, we were interested if ligand exchange of the boryls of *cis*-[Ni(^{i}Pr$_2$Im^{Me})$_2$(Bcat)$_2$] **V-1a** with 2VE donor ligands, electrophilic attack and ligand dismutation with other complexes would be possible (Scheme VI.1). Interestingly, the reaction of **V-1a** with PMe_3 did not lead to the formation of a nickel phosphine bis-boryl complex with NHC ligand exchange but to a complete disrupture of both NHC and boryl ligands to yield the literature known nickel phosphine complex [Ni(PMe_3)$_4$] **VI-1**[19] and the bis-NHC adduct [B_2cat_2 · (^{i}Pr$_2$Im^{Me})$_2$] **VI-2**, which were both identified by NMR spectroscopy. The result of this reaction is independent on the amount of phosphine

used, but four equivalents of phosphine are necessary for a full conversion of the starting material **V-1a**. In an earlier work of our group from Dr. Laura Kuehn, compound **VI-2** was prepared independently in 84 % yield from the reaction of two equivalents $^{i}Pr_2Im^{Me}$ with B_2cat_2,[20] as similarly reported previously for other NHC adducts of diboron(4) compounds.[21] The ^{1}H NMR spectrum of **VI-2** reveals one set of signals for the two NHCs with a doublet at 1.35 ppm for the *iso*-propyl methyl protons, a singlet at 1.48 ppm for the backbone methyl protons and a septet at 6.27 ppm for the *iso*-propyl methine protons. The catechol hydrogen atoms were detected as two signals at 6.77 ppm and 6.90 ppm. The equivalent sp^3-hybridized boron atoms give rise to one broad resonance at 11.5 ppm in the $^{11}B\{^{1}H\}$ NMR spectrum. The NHC carbene carbon atom resonance was observed extremely broadened due to a strong quadrupolar coupling to boron at 166.5 ppm in the $^{13}C\{^{1}H\}$ NMR spectrum of the compound.

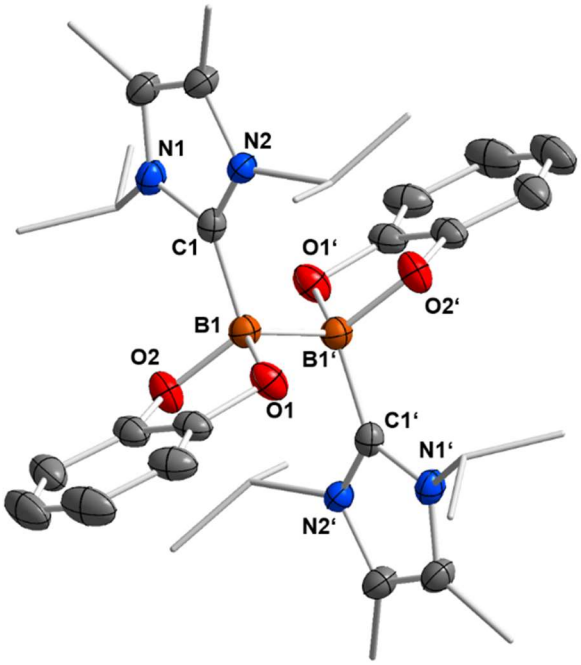

Figure VI.2 Molecular structure of [$B_2cat_2 \cdot (^{i}Pr_2Im^{Me})_2$] **VI-2** in the solid state (ellipsoids set at the 50 % probability level). Hydrogen atoms and co-crystallized benzene molecules have been omitted for clarity. Selected bond lengths [Å] and angles [°] of **VI-2**: B1–C1 1.656(4), B1−B1’ 1.732(6), B1−O1 1.541(3), B1−O2 1.564(3), C1-B1-O1 112.1(2), C1-B1-O2 112.4(3).[20]

Colorless crystals suitable for X-ray diffraction of compound **VI-2** were obtained by slow evaporation of a saturated benzene solution at room temperature (Figure VI.2).[20] The molecular structure of **VI-2** matches that previously reported for [$B_2cat_2 \cdot (Me_2Im^{Me})_2$],[21a] with both boron atoms being sp^3-hybridized and tetrahedrally coordinated. The B1–B1' bond distance of 1.732(6) Å is slightly longer compared to that observed for the bis-NHC adduct [$B_2cat_2 \cdot (Me_2Im^{Me})_2$] (1.710(8) Å).[21a] The B–B distances of both bis-NHC adducts are elongated compared to that observed in uncoordinated B_2cat_2 (1.678(3) Å).[22] The B1–C1 bond length of 1.656(4) Å is similar to that found in [$B_2cat_2 \cdot (Me_2Im^{Me})_2$] (1.658(9) Å).[21a]

Complex **V-1a** reacts readily at room temperature with stoichometric amounts of *trans*-[Ni(^{i}Pr$_2$Im^{Me})$_2$Br$_2$], resulting in ligand dismutation of one boryl and one bromide ligand to yield *trans*-[Ni(^{i}Pr$_2$Im^{Me})$_2$(Bcat)Br] **VI-3a** (Scheme VI.1). As several transition metal complexes are known to give mono-boryl complexes *via* oxidative addition of haloboranes,[3,11] we also reacted synthetic equivalents of [Ni(^{i}Pr$_2$Im^{Me})$_2$] **7** with BrBcat, which led to a complex mixture of thus far unidentified products. However, the reaction of **V-1a** with alkyl halides also seems to be a viable route for the synthesis of nickel boryl complexes of the type *trans*-[Ni(^{i}Pr$_2$Im^{Me})$_2$(Bcat)X], as the reaction of **V-1a** with methyl iodide leads selectively to formation of *trans*-[Ni(^{i}Pr$_2$Im^{Me})$_2$(Bcat)I] **VI-3b** with elimination of MeBcat (which was characterized by NMR spectroscopy). Complexes **VI-3a** and **VI-3b** were isolated as pale brown solids in moderate yields of approximately 40 %. As these complexes always contain small amounts of the corresponding di-halo complexes *trans*-[Ni(^{i}Pr$_2$Im^{Me})$_2$X$_2$] and the spiro-borate anion [$Bcat_2$]$^-$ which were difficult to separate, yields of analytically pure material are generally low. The boryl ligands of **VI-3a** and **VI-3b** give rise to resonances at 43.4 ppm (**VI-3a**) and 45.0 ppm (**VI-3b**), respectively, in the $^{11}B\{^1H\}$ NMR spectrum, slightly shifted compared to the resonance at 48.7 ppm observed for **V-1a** (see Table VI.1). More pronounced are the differences of the $^{13}C\{^1H\}$ NMR NHC carbene carbon atom resonances at 184.1 ppm (**VI-3a**) and 183.7 ppm (**VI-3b**) compared to that at 194.3 ppm (**V-1a**) (see Table V.1).

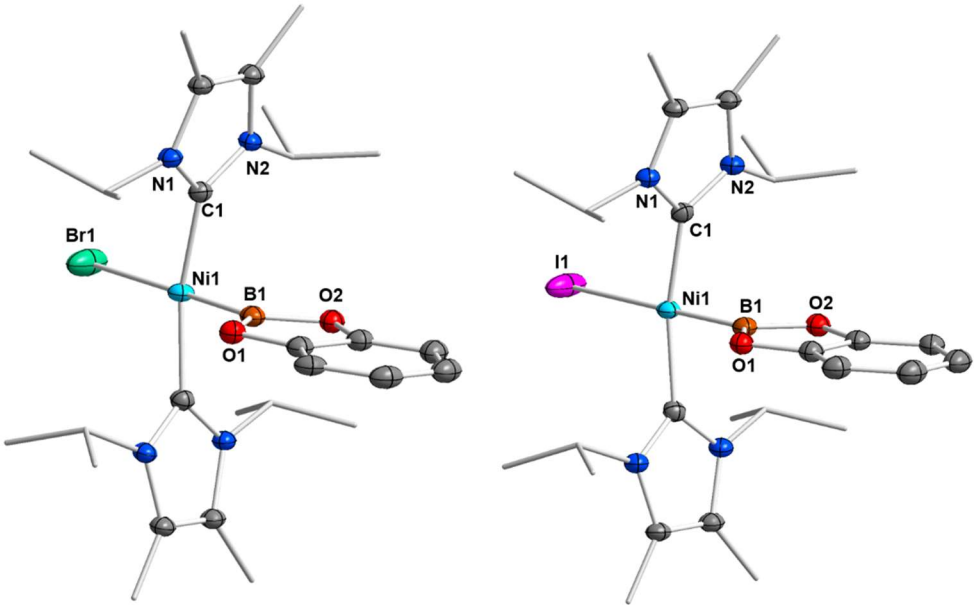

Figure VI.3 Molecular structures of *trans*-[Ni(^{i}Pr$_2$Im^{Me})$_2$(Bcat)Br] **VI-3a** (left) and *trans*-[Ni(^{i}Pr$_2$Im^{Me})$_2$(Bcat)I] **VI-3b** (right) in the solid state (ellipsoids shown at 50 % probability level). Hydrogen atoms have been omitted for clarity. Selected bond lengths [Å] and angles [°] of **VI-3a**: Ni1–C1 1.905(2), Ni1–B1 1.872(4), Ni1–Br1 2.4002(6), B1–O1 1.415(4), B1–O2 1.405(4); C1–Ni1–B1 81.75(6), C1–Ni1–Br1 98.25(6), plane (C1–Ni1–B1) – plane (O1–B1–O2) 89.95(6). Selected bond lengths [Å] and angles [°] of **VI-3b**: Ni1–C1 1.903(2), Ni1–B1 1.864(4), Ni1–I1 2.5706(7), B1–O1 1.404(4), B1–O2 1.415(4); C1–Ni1–B1 82.57(6), C1–Ni1–Br1 97.43(6), plane (C1–Ni1–B1) – plane (O1–B1–O2) 89.93(6).

Crystals suitable for X-ray diffraction of the mono-boryl complexes **VI-3a** and **VI-3b** were obtained by slow evaporation of saturated C_6D_6 solutions of these complexes at room temperature. Both complexes crystallize in the orthorhombic space group Pnma and adopt square planar structures with *trans*-arrangement of the boryl and the halide ligands. Both crystals contain small amounts (approximately 3 %) of the di-halide complex as impurities, which were included as partial disorder in the refinement of the structure. The *trans*-configuration can be rationalized by the strengths of the *trans*-influence of the ligands in the decreasing order $[Bcat]^-$ > NHC > $[X]^-$.[11] A similar geometry was observed in the solid state structures of the platinum complexes *trans*-[Pt(PR$_3$)$_2$(B{OR'}$_2$)X] (**40**) reported previously.[11] The Ni–C distances of 1.905(2) Å (**VI-3a**) and 1.903(2) Å (**VI-3b**) are unexceptional, and the Ni–B distances of 1.872(4) Å (**VI-3a**) and 1.864(4) Å (**VI-3b**) (see Table VI.1) are slightly shorter as those of *cis*-

configured **V-1a** (1.9231(19) Å and 1.9092(18) Å) and the *trans*-halo-boryl complex **43** (see Figure VI.1, 1.900(3) Å).[15c] The Ni–Br bond length of **VI-3a** (2.4002(6) Å) is also slightly longer than the Ni–Br distance of **43** (2.370(3) Å),[15c] which indicates a stronger *trans*-influence of the Bcat ligand compared to the boryl-pincer ligand of **43**.[11] The Bcat ligand is aligned perpendicular to the square plane of the complex (**VI-3a**: 89.95(6)°, **VI-3b**: 89.93(6)°) to minimize intramolecular steric repulsion, like it was observed previously for other group 10 mono-boryl complexes, bearing monodentate ligands.[11]

Table VI.1 Important bond lengths, bond angles and chemical shifts of *cis*-[Ni(^{i}Pr$_2$Im^{Me})$_2$(Bcat)$_2$] **V-1a**, *trans*-[Ni(^{i}Pr$_2$Im^{Me})$_2$(Bcat)Br] **VI-3a**, *trans*-[Ni(^{i}Pr$_2$Im^{Me})$_2$(Bcat)I] **VI-3b** and [(PNP)Ni(Br)] **43** (δ_B B(OR)$_2$ = ^{11}B{^{1}H} NMR shift of the boron atoms, δ_c NHC = ^{13}C{^{1}H} NMR shift of the NHC carbene carbon atoms).

Compound	Ni–B [Å]	Ni–X [Å]	Ni–C [Å]	δ_B B(OR)$_2$ [ppm]	δ_c NHC [ppm]
V-1a[18]	1.9231(19)/ 1.9092(18)	-	1.9393(16)/ 1.9448(15)	48.7	194.3
VI-3a	1.872(4)	2.4002(6)	1.905(2)	43.4	184.1
VI-3b	1.864(4)	2.5706(7)	1.903(2)	45.0	183.7
43[15c]	1.900(3)	2.370(3)	-	39.0	-

6.3 Conclusion

In this chapter some basic reactivity of the nickel bis-boryl complex *cis*-[Ni(^{i}Pr$_2$Im^{Me})$_2$(Bcat)$_2$] **V-1a** is reported. The reaction with the small donor ligand PMe_3 led to a complete ligand exchange at nickel with reductive elimination of B_2cat_2, and formation of the bis-NHC adduct [B_2cat_2 · (^{i}Pr$_2$Im^{Me})$_2$] **VI-2** and [Ni(PMe_3)$_4$] **VI-1** as the metal-containing species. This experiment demonstrates that the boryl ligands in complex **V-1a** are very labile, as has also been observed previously.[18] Furthermore, we demonstrated that oxidative addition of haloboranes to [Ni(^{i}Pr$_2$Im^{Me})$_2$] **7** is no viable route for the synthesis of nickel mono-boryl complexes, but either electrophilic attack of MeI to complex **V-1a** or ligand dismutation of **V-1a** with *trans*-[Ni(^{i}Pr$_2$Im^{Me})$_2$Br$_2$] led to loss of only one boryl ligand and formation of the first NHC stabilized mono-boryl complexes *trans*-[Ni(^{i}Pr$_2$Im^{Me})$_2$(Bcat)Br] **VI-3a** and *trans*-[Ni(^{i}Pr$_2$Im^{Me})$_2$(Bcat)I] **VI-3b**.

6.4 References

[1] J. R. Knorr, J. S. Merola, *Organometallics* **1990**, *9*, 3008-3010.

[2] R. T. Baker, D. W. Ovenall, J. C. Calabrese, S. A. Westcott, N. J. Taylor, I. D. Williams, T. B. Marder, *J. Am. Chem. Soc.* **1990**, *112*, 9399-9400.

[3] a) G. J. Irvine, M. J. Lesley, T. B. Marder, N. C. Norman, C. R. Rice, E. G. Robins, W. R. Roper, G. R. Whittell, L. J. Wright, *Chem. Rev.* **1998**, *98*, 2685-2722; b) H. Braunschweig, *Angew. Chem.* **1998**, *110*, 1882-1898; *Angew. Chem. Int. Ed.* **1998**, *37*, 1786-1801; c) H. Braunschweig, M. Colling, *Coord. Chem. Rev.* **2001**, *223*, 1-51; d) S. Aldridge, D. L. Coombs, *Coord. Chem. Rev.* **2004**, *248*, 535-559; e) H. Braunschweig, C. Kollann, D. Rais, *Angew. Chem.* **2006**, *118*, 5380-5400; *Angew. Chem. Int. Ed.* **2006**, *45*, 5254-5274; f) D. L. Kays, S. Aldridge, *Struct. Bond.* **2008**, *130*, 29-122; g) U. Kaur, K. Saha, S. Gayen, S. Ghosh, *Coord. Chem. Rev.* **2021**, *446,* 214106.

[4] a) H. C. Brown, H. C. From Little Acorns to Tall Oaks: From Boranes through Organoboranes (Nobel Lecture), 1979, http://www.nobelprize.org; b) N. Miyarura, *Top. Curr. Chem.* **2002**, *219*, 11-59; c) D. E. Kaufmann, D. S. Matteson (eds), Boron compounds, Science of Syntheses, Vol 6, Georg Thieme Verlag, Stuttgart **2005**; d) D. G. Hall (ed.), *Boronic Acids-Preparation and Applications in Organic Synthesis, Medicine and Materials*, 2nd Edition; Wiley−VCH, Weinheim, Germany, **2011**; e) E. C. Neeve, S. J. Geier, I. A. I. Mkhalid, S. A. Westcott, T. B. Marder, *Chem. Rev.* **2016**, *116*, 9091-9161; f) M. Wang, Z. Shi, *Chem. Rev.* **2020**, *120*, 7348-7398; g) Y. Tian, X. Guo, H. Braunschweig, U. Radius, T. B. Marder, *Chem. Rev.* **2021**, *121*, 3561-3597; h) S. K. Bose, L. Mao, L. Kuehn, U. Radius, J. Nekvinda, W. L. Santos, S. A. Westcott, P. G. Steel, T. B. Marder, *Chem. Rev.* **2021**, *121*, 13238-13341; i) J. Hu, M. Ferger, Z. Shi, T. B. Marder, *Chem. Soc. Rev.* **2021**, *50*, 13129-13188; j) S. Manna, K. K. Das, S. Nandy, D. Aich, S. Paul, S. Panda, *Coord. Chem. Rev.* **2021**, *448*, 214165.

[5] a) T. Ishiyama, M. Murata, N. Miyaura, *J. Org. Chem.* **1995**, *60*, 7508-7510; b) L. T. Pilarski, K. J. Szabó, *Angew. Chem.* **2011**, *123*, 8380-8382; *Angew. Chem. Int. Ed.* **2011**, *50*, 8230-8232; c) M. Murata, *Heterocycles* **2012**, *85*, 1795-1819; d) C. M. Vogels, S. A. Westcott, *ChemCatChem.* **2012**, *4*, 47-49; e) W. K. Chow, O. Y. Yuen, P. Y. Choy, C. M. So, C. P. Lau, W. T. Wong, F. Y. Kwong, *RSC Adv.* **2013**, *3*, 12518-12539; f) K. Kubota, H. Iwamoto, H. Ito, *Org. Biomol. Chem.* **2017**,

15, 285-300; g) Y. P. Budiman, S. A. Westcott, U. Radius, T. B. Marder, *Adv. Synth. Catal.* **2021**, *363*, 2224-2255.

[6] a) I. Beletskaya, A. Pelter, *Tetrahedron* **1997**, *53*, 4957-5026; b) V. Lillo, A. Bonet, E. Fernández, *Dalton Trans.* **2009**, 2899-2908; c) J. Takaya, N. Iwasawa, Catalytic, *ACS Catal.* **2012**, *2*, 1993-2006; d) H. Wen, G. Liu, Z. Huang, *Coord. Chem. Rev.* **2019**, *386*, 138-153; e) W. Fan, L. Li, G. Zhang, *J. Org. Chem.* **2019**, *84*, 5987-5996; f) O. Salvadó, E. Fernández, *Molecules* **2020**, *25*, 1758; g) X. Wang, Y. Wang, W. Huang, C. Xia, L. Wu, *ACS Catalysis* **2021**, *11*, 1-18.

[7] a) T. B. Marder, N. C. Norman, Top*. Catal.* **1998**, 63-73; b) R. Barbeyron, E. Benedetti, J. Cossy, J.-J. Vasseur,S. Arseniyadis, M. Smietana, *Tetrahedron* **2014**, *70*, 8431-8452; c) H. Yoshida, *ACS Catal.* **2016**, *6*, 1799-1811; d) M. B. Ansell, O. Navarro, J. Spencer, *Coord. Chem. Rev.* **2017**, *336*, 54-77; e) F. Zhao, X. Jia, P. Li, J. Zhao, Y. Zhou, J. Wang, H. Liu, *Org. Chem. Front.* **2017**, 4, 2235-2255; f) J. Carreras, A. Caballero, P. J. Perez, *Chem. Asian J.* **2019**, *14*, 329-343.

[8] a) T. Ishiyama, N. Miyaura, *J. Organomet. Chem.* **2003**, *680*, 3-11; b) I. A. I. Mkhalid, J. H. Barnard, T. B. Marder, J. M. Murphy, J. F. Hartwig, *Chem. Rev.* **2010**, *110*, 890-931; c) J. F. Hartwig, *Chem. Soc. Rev.* **2011**, *40*, 1992-2002; d) J. F. Hartwig, *Acc. Chem. Res.* **2012**, *45*, 864-873; e) A. Ros, R. Fernández, J. M. Lassaletta, *Chem. Soc. Rev.* **2014**, *43*, 3229-3243; f) J. F. Hartwig, *J. Am. Chem. Soc.* **2016**, *138*, 2-24; g) Y. Ping, L. Wang, Q. Ding, Y. Peng, *Adv. Synth. Catal.* **2017**, *359*, 3274-3291; h) T. Gensch, M. J. James, T. Dalton, F. Glorius, *Angew. Chem.* **2018**, *130*, 2318-2328; *Angew. Chem. Int. Ed.* **2018**, *57*, 2296-2306; i) Y. Shi, Q. Gao, S. Xu, *Synlett* **2019**, *30*, 2107-2112; j) E. Fernandez, *Top. Organomet. Chem.* **2021**, *69*, 207-225.

[9] a) T. Ishiyama, N. Miyaura, *J. Organomet. Chem.* **2000**, *611*, 392-402; b) N. Miyaura, *Bull. Chem. Soc. Jpn.* **2008**, *81*, 1535-1553; c) L. Dang, Z. Lin, T. B. Marder, *Chem. Commun.* **2009**, 3987-3995; d) X. Guo, T. Yang, F. K. Sheong, Z. Lin, *ACS Catal.* **2021**, *11*, 5061-5068.

[10] a) C. N. Iverson, M. R. Smith, *J. Am. Chem. Soc.* **1995**, *117*, 4403-4404; b) T. Ishiyama, N. Matsuda, M. Murata, F. Ozawa, A. Suzuki, N. Miyaura, *Organometallics* **1996**, *15*, 713-720; c) G. Lesley, P. Nguyen, N. J. Taylor, T. B. Marder, A. J. Scott, W. Clegg, N. C. Norman, *Organometallics* **1996**, *15*, 5137-5154; d) C. Borner, C. Kleeberg, *Eur. J. Inorg. Chem.* **2014**, *2014*, 2486-2489.

[11] a) W. Clegg, F. J. Lawlor, G. Lesley, T. B. Marder, N. C. Norman, A. G. Orpen, M. J. Quayle, C. R. Rice, A. J. Scott, F. E. S. Souza, *J. Organomet. Chem.* **1998**, *550*, 183-192; b) J. Zhu, Z. Lin, T. B. Marder, *Inorg. Chem.* **2005**, *44*, 9384-9390; c) H. Braunschweig, P. Brenner, A. Müller, K. Radacki, D. Rais, K. Uttinger, *Chem. Eur. J.* **2007**, *13*, 7171-7176.

[12] a) T. Ishiyama, N. Matsuda, N. Miyaura, A. Suzuki, *J. Am. Chem. Soc.* **1993**, *115*, 11018-11019; b) C. N. Iverson, M. R. Smith, *Organometallics* **1996**, *15*, 5155-5165; c) Q. Cui, D, G. Musaev, K. Morokuma, *Organometallics* **1998**, *17*, 742-751; d) R. L. Thomas, F. E. S. Souza, T. B. Marder, *Dalton Trans.* **2001**, 1650-1656.

[13] S. Onozawa, Y. Hatanaka, T. Sakakura, S. Shimada, M. Tanaka, *Organometallics* **1996**, *15*, 5450-5452.

[14] H. Braunschweig, K. Radacki, D. Rais, K. Uttinger, *Angew. Chem.* **2005***, 118*, 169-172; *Angew. Chem. Int. Ed.* **2006**, *45*, 162-165.

[15] a) D. Adhikari, J. C. Huffman, D. J. Mindiola, *Chem. Commun.* **2007**, 4489-4491; b) B. L. Tran, D. Adhikari, H. Fan, M. Pink, D. J. Mindiola, *Dalton Trans.* **2010**, *39*, 358-360; c) N. Curado, C. Maya, J. López-Serrano, A. Rodríguez, *Chem. Commun.* **2014**, *50*, 15718-15721; d) P. Ríos, J. Borge, F. Fernández de Córdova, G. Sciortino, A. Lledós, A. Rodríguez, *Chem. Sci.* **2021**, *12*, 2540-2548.

[16] a) T. Schaub, U. Radius, *Chem. Eur. J.* **2005**, *11*, 5024-5030; b) T. Schaub, M. Backes, U. Radius, *Organometallics* **2006**, *25*, 4196-4206; c) U. S. D. Paul, C. Sieck, M. Hähnel, K. Hammond, T. B. Marder, U. Radius, *Chem. Eur. J.* **2016**, *21*, 11005-11014; d) U. S. D. Paul, U. Radius, *Chem. Eur. J.* **2017**, *23*, 3993-4009; e) U. S. D. Paul, U. Radius, *Organometallics* **2017**, *36*, 1398-1407; f) J. H. J. Berthel, M. W. Kuntze-Fechner, U. Radius, *Eur. J. Inorg. Chem.* **2019**, 2618-2623; g) J. H. J. Berthel, L. Tendera, M. W. Kuntze-Fechner, L. Kuehn, U. Radius, *Eur. J. Inorg. Chem.* **2019**, 3061-3072; h) J. H. J. Berthel, M. J. Krahfuss, U. Radius, *Z. Anorg. Allg. Chem.* **2020**, *646*, 692-704; i) M. J. Krahfuss, J. Nitsch, F. M. Bickelhaupt, T. B. Marder, U. Radius, *Chem. Eur. J.* **2020**, *26*, 11276-11292; j) L. Tendera, T. Schaub, M. J. Krahfuss, M. W. Kuntze-Fechner, U. Radius, *Eur. J. Inorg. Chem.* **2020**, 3194-3207; k) S. Sabater, D. Schmidt, H. Schmidt nee Schneider, M. Kuntze-Fechner, T. Zell, C. J. Isaac, H. Grieve, W. J. M. Blackaby, J. P. Lowe, S. A. Macgregor, M. F. Mahon, F. M. Miloserdov, N. Rajabi, U. Radius, M. K. Whittlesey, *Chem. Eur. J.* **2021**, *27*, 13221-13234; l) L. Tendera, M. Helm,

M. J. Krahfuss, M. W. Kuntze-Fechner, U. Radius, *Chem. Eur. J.* **2021**, *27*, 17849-17861.

[17] a) J. Zhou, M. W. Kuntze-Fechner, R. Bertermann, U. S. Paul, J. H. Berthel, A. Friedrich, Z. Du, T. B. Marder, U. Radius, *J. Am. Chem. Soc.* **2016**, *138*, 5250-5253; b) Y.-M Tian, X.-N. Guo, M. Kuntze-Fechner, I. Krummenacher, H. Braunschweig, U. Radius, A. Steffen, T. B. Marder, *J. Am. Chem. Soc.* **2018**, *140*, 17612-17623; c) M. W. Kuntze-Fechner, H. Verplancke, L. Tendera, M. Diefenbach, I. Krummenacher, H. Braunschweig, T. B. Marder, M. C. Holthausen, U. Radius, *Chem. Sci.* **2020**, *11*, 11009-11023; d) L. Kuehn, D. G. Jammal, K. Lubitz, T. B. Marder, U. Radius, *Chem. Eur. J.* **2019**, *25*, 9514-9521; e) Y.-M. Tian, X.-N. Guo, I. Krummenacher, Z. Wu, J. Nitsch, H. Braunschweig, U. Radius, T. B. Marder, *J. Am. Chem. Soc.* **2020**, *142*, 18231-18242; f) Y.-M. Tian, X.-N. Guo, Z. Wu, A. Friedrich, S. A. Westcott, H. Braunschweig, U. Radius, T. B. Marder, *J. Am. Chem. Soc.* **2020**, *142*, 13136-13144.

[18] Chapter V: *"Nickel Boryl Complexes and the Nickel-Catalyzed Alkyne-Borylation"*, L. Tendera, F. Fantuzzi, T. B. Marder, U. Radius, *submitted* (22.08.**2022**).

[19] A. G. Avent, F. G. N. Cloke, J. P. Day, E. A. Seddon, K. R. Seddon, S. M. Smedley, *J. Organomet. Chem.* **1988**, *341*, 535-541.

[20] L. Kuehn, *Earth-Abundant Metal-Catalyzed and Transition Metal-Free Borylation of Aryl Halides*, Dissertation, Universität Würzburg, **2020**.

[21] a) S. Pietsch, U. Paul, I. A. Cade, M. J. Ingleson, U. Radius, T. B. Marder, *Chem. Eur. J.* **2015**, *21*, 9018-9021; b) S. Würtemberger-Pietsch, H. Schneider, T. B. Marder, U. Radius, *Chem. Eur. J.* **2016**, *22*, 13032-13036; c) M. Eck, S. Würtemberger-Pietsch, A. Eichhorn, J. H. J. Berthel, R. Bertermann, U. S. D. Paul, H. Schneider, A. Friedrich, C. Kleeberg, U. Radius, T. B. Marder, *Dalton Trans.* **2017**, *46*, 3661-3680; d) L. Kuehn, L. Zapf, L. Werner, M. Stang, S. Würtemberger-Pietsch, I. Krummenacher, H. Braunschweig, E. Lacôte, T. B. Marder, U. Radius, *Chem. Sci.* **2022**, *13*, 8321-8333.

[22] W. Clegg, M. R. J. Elsegood, F. J. Lawlor, N. C. Norman, N. L. Pickett, E. G. Robins, A. J. Scott, P. Nguyen, N. J. Taylor, T. B. Marder, *Inorg. Chem.* **1998**, *37*, 5289-5293.

7 Experimental Details

7.1 General Procedures

All reactions and subsequent manipulations were performed under an argon atmosphere using standard Schlenk techniques or in a glovebox (Innovative Technology Inc. or Braun Uni Lab). All reactions were carried out in oven-dried glassware. Solvents were purified by distillation from an appropriate drying agent (toluene, benzene, and ethers from sodium/potassium alloy with benzophenone as indicator). Halocarbons, hexane and acetonitrile were dried and deoxygenated using an Innovative Technology Inc. Pure-Solv 400 Solvent Purification System, and further deoxygenated by using the freeze-pump-thaw method.
Deuterated solvents (C_6D_6, THF-d_8, toluene-d_8, CD_2Cl_2, $CDCl_3$, CD_3CN and D_2O) were purchased from Sigma-Aldrich or ABCR and stored over molecular sieves.

7.1.1 Analytical Methods

Elemental analysis

Elemental analyses were performed in the microanalytical laboratory of the Institute of Inorganic Chemistry at the University of Würzburg, using an Elementar vario MICRO cube.

High-Resolution Mass Spectrometry (HRMS)

High-resolution mass spectra were obtained using a Thermo Scientific Exactive Plus spectrometer equipped with an Orbitrap Mass Analyzer. Measurements were accomplished using an ASAP/APCI source with a corona needle, and carrier-gas (N_2) temperature of 400 °C, 350 °C or 250 °C, respectively. Ionizations were accomplished in Liquid Injection Field Desorption Ionization mode using a LIFDI 700 from Linden CMS with 10 kV at the emitter and an accelerating voltage of 5 V. ESI mass spectrometry was performed using a HESI source with an auxiliary gas temperature of 50 °C.

Gas Chromatography (GC)

GC-MS analyses were performed using a Thermo Fisher Scientific Trace 1310 gas chromatograph (column: TG-SQC 5 % phenyl methyl siloxane, 15 m, Ø 0.25 mm, film 0.25 *µ*m; injector: 250 °C; oven: 40 °C (2 min), 40 °C to 280 °C; carrier gas: He (1.2 mL min^{-1})).

Cyclic Voltammetry (CV)

Cyclic voltammetry experiments were performed using a PINE Instruments AFCBP1 bipotentiostat with a commercially available cell (ALS Co. Ltd., VC-4) in an argon filled glovebox. Commercial glassy carbon disk electrodes (2 mm diameter, BaSi) and platinum wire (0.4 mm x 5.7 mm, ALS Co. Ltd.) counter electrodes, as well as commercial silver wire reference electrodes (RE-7, ALS Co. Ltd.), separated from the main compartment by ion permeable porous glass and filled with a 0.01 M $AgNO_3$ stock solution in acetonitrile, were used. Measurements were performed in argon purged THF using 0.1 M [TBA][PF_6] (bought from Fluka, 98+ %) as supporting electrolyte. Potentials are referenced to the ferrocene/ferrocenium couple.[1]

7.1.2 Spectroscopic Methods

IR Spectroscopy

All infrared spectra were recorded on solid samples at room temperature on a Bruker Alpha FT-IR spectrometer using an ATR unit. Dependent on the intensity of the vibration bands, the intensity was assigned to the following abbreviations: very strong (vs), strong (s), middle (m), weak (w) and very weak (vw).

NMR Spectroscopy

All NMR spectra were recorded on Bruker Avance 400 (^{1}H, 400.1 MHz; ^{13}C, 100.6 MHz; ^{11}B, 128.5 MHz; ^{19}F, 376.8 MHz; ^{31}P, 162.0 MHz; ^{29}Si, 79.5 MHz), Bruker Avance NEO 400 (^{1}H, 400.1 MHz; ^{13}C, 100.6 MHz; ^{11}B, 128.5 MHz; ^{19}F, 376.8 MHz; ^{31}P, 162.0 MHz; ^{29}Si, 79.5 MHz), DRX-300 (^{1}H, 300.1 MHz; ^{13}C, 75.5 MHz, ^{11}B, 96.3 MHz) or Avance 500 (^{1}H, 500.1 MHz; ^{13}C, 125.8 MHz; ^{11}B, 160.5 MHz; ^{19}F, 470.6 MHz) spectrometers and were measured at 298 K. ^{1}H NMR chemical shifts are expressed in parts per million (ppm) and are referenced *via* residual proton resonances

of the corresponding deuterated solvent C_6D_5H (^1H: δ = 7.16 ppm, C_6D_6), C_4D_7HO (^1H: δ = 1.72, 3.58 ppm, THF-d_8), C_7D_7H (^1H: δ = 2.08, 6.97, 7.01, 7.09 ppm, toluene-d_8), $CDHCl_2$ (^1H: δ = 5.32 ppm, CD_2Cl_2), $CHCl_3$ (^1H: δ = 7.26 ppm, $CDCl_3$), CD_2HCN (^1H: δ = 1.94 ppm, CD_3CN), HDO (^1H: δ = 4.79 ppm, D_2O). ^{13}C NMR spectra are reported relative to TMS using the carbon resonances of the deuterated solvent C_6D_6 (^{13}C: δ = 128.06 ppm), THF-d_8 (^{13}C: δ = 25.31, 67.21 ppm), toluene-d_8 (^{13}C: δ = 20.43, 125.13, 127.96, 128.87, 137.48 ppm), CD_2Cl_2 (^{13}C: δ = 53.84 ppm), $CDCl_3$ (^{13}C: δ = 77.16 ppm), CD_3CN (^{13}C: δ = 1.32, 118.26 ppm). All ^{13}C NMR spectra are ^1H broadband decoupled. ^{11}B NMR chemical shifts are reported relative to $BF_3{\cdot}Et_2O$ and ^{19}F NMR chemical shifts relative to $CFCl_3$ as external standard. The coupling constants (*J*) are given in Hertz (Hz) without consideration of the sign. For multiplicities, the following abbreviations are used: s = singlet, d = doublet, t = triplet, q = quartet, sept = septet, m = multiplet, br = broad, vbr = very broad.

Magnetic moments in solution were determined by the Evans method at 298 K with a capillary, filled with pure deuterated solvent, as reference.[2]

EPR Spectroscopy

EPR measurements at X-band (9.38 GHz) were carried out using a Bruker ELEXSYS E580 CW EPR spectrometer equipped with an Oxford Instruments helium cryostat (ESR900) and a MercuryiTC temperature controller. The spectral simulations were performed using MATLAB 9.11.0 (R2021b) and the EasySpin 5.2.33 toolbox.[3]

7.2 Starting Materials

Mes_2Im, Mes_2Im^{H2}, $Dipp_2Im$, $Dipp_2Im^{H2}$,[4] $cAAC^{Me}$,[5] $^{i}Pr_2Im$, $^{i}Pr_2Im^{Me}$,[4a, 6] B_2eg_2,[7] and *trans*-$[Ni(^{i}Pr_2Im^{Me})_2(Br)_2]$[8] were prepared according to published procedures. $[NiBr_2•DME]$ was prepared from the bromination of nickel in DME. The diboron reagents B_2pin_2 and B_2cat_2 were a generous gift from AllyChem Co. Ltd. All other reagents were purchased from Aldrich or ABCR and used without further purification.

$[Ni(\eta^4\text{-}COD)_2]$ [9]

1,5-cyclooctadiene (14 mL, 12.4 g, 114 mmol, 3.3 equiv.) was added to a suspension of (15.3 g, 34.4 mmol, 1 equiv.) $[Ni(Py)_4(Cl)_2]$ in 60 mL of THF. The reaction mixture was cooled to -25 °C and small portions of metallic sodium (2.55 g, 110 mmol) and a spatula tip of naphthalene were added, successively. After stirring at -25 °C over night, the reaction mixture was allowed to warm to room temperature and was then transferred *via* cannula into a schlenk flask filled with 300 mL of methanol, whereby $[Ni(\eta^4\text{-}COD)_2]$ precipitates as bright yellow solid. The supernatant NaCl-suspension was removed *via* cannula and the precipitate was washed four times with 100 mL of methanol (by adding methanol to the precipitate, and removal of the supernatant solution *via* cannula). Finally the product was again suspended in 200 mL of methanol, collected by filtration and dried in vacuo to yield a crystalline yellow solid (8.32 g, 30.4 mmol, 88 %).

^{1}H NMR (400.1 MHz, C_6D_6, 298 K): δ = 2.08 (s, 16H, CH_2), 4.30 (s, 8H, C*H*).

^{13}C{^{1}H} NMR (100.6 MHz, C_6D_6, 298 K): δ = 30.9 (*C*H_2) 89.7 (*C*H).

$[Ni(Mes_2Im)_2]$ (1) [10]

A solution of Mes_2Im (2.29 g, 7.47 mmol) in 20 mL of THF was added at room temperature to a solution of $[Ni(\eta^4\text{-}COD)_2]$ (1.03 g, 3.74 mmol) in 10 mL of THF. The dark purple reaction mixture was stirred for 24 h at room temperature and was then filtered through a pad of celite. All volatiles were removed in vacuo and the remaining residue was suspended in 15 mL of hexane. The product was collected by filtration,

washed with 5 mL of hexane and dried in vacuo to give a dark black crystalline solid (2.00 g, 3.00 mmol, 80 %).

^{1}H NMR (400.1 MHz, C_6D_6, 298 K): δ = 2.10 (s, 24H, aryl$_{NHC}$-CH_{3ortho}), 2.30 (s, 12H, aryl$_{NHC}$-CH_{3para}), 5.99 (s, 4H, NC*H*C*H*N), 6.82 (s, 8H, aryl$_{NHC}$-CH_{meta}).

^{13}C{^{1}H} NMR (100.6 MHz, C_6D_6, 298 K): δ = 18.5 (aryl$_{NHC}$-*C*H$_{3ortho}$), 21.4 (aryl$_{NHC}$-*C*H$_{3para}$), 117.8 (N*C*H*C*HN), 128.6 (aryl$_{NHC}$-*C*H$_{meta}$), 135.4 (aryl$_{NHC}$-*C*CH$_{3ortho}$), 136.2 (aryl$_{NHC}$-*C*CH$_{3para}$), 138.7 (aryl$_{NHC}$-*C$_{ipso}$*), 192.4 (N*C*N).

[Ni(Mes$_2$Im^{H2})$_2$] (2) [11]

A solution of Mes$_2$Im^{H2} (1.50 g, 4.89 mmol) in 5 mL of THF was added at room temperature to a solution of [Ni(η^4-COD)$_2$] (673 mg, 2.45 mmol) in 15 mL of THF. The dark purple reaction mixture was stirred for 24 h at room temperature and was then filtered through a pad of celite. All volatiles were removed in vacuo and the remaining residue was suspended in 10 mL of hexane. The product was collected by filtration, washed with 5 mL of hexane and dried in vacuo to give a dark black crystalline solid (1.04 g, 1.55 mmol, 63 %).

Black crystals of [Ni(Mes$_2$Im^{H2})$_2$] **2** suitable for single-crystal X-ray diffraction were obtained by storing a saturated solution of the complex in hexane at -30 °C.

^{1}H NMR (400.1 MHz, C_6D_6, 298 K): δ = 2.18 (s, 24H, aryl$_{NHC}$-CH_{3ortho}), 2.32 (s, 12H, aryl$_{NHC}$-CH_{3para}), 2.80 (s, 8H, NCH_2CH_2N), 6.88 (s, 8H, aryl$_{NHC}$-CH_{meta}).

^{13}C{^{1}H} NMR (100.6 MHz, C_6D_6, 298 K): δ = 18.4 (aryl$_{NHC}$-*C*H$_{3ortho}$), 21.4 (aryl$_{NHC}$-*C*H$_{3para}$), 50.0 (N*C*H$_2$*C*H$_2$N), 128.9 (aryl$_{NHC}$-*C*H$_{meta}$), 135.3 (aryl$_{NHC}$-*C*CH$_{3ortho}$), 136.5 (aryl$_{NHC}$-*C*CH$_{3para}$), 139.1 (aryl$_{NHC}$-C$_{ipso}$), 210.4 (N*C*N).

[Ni(Dipp$_2$Im)$_2$] (3) [11, 12]

A solution of Dipp$_2$Im (1.32 g, 3.40 mmol) in 6 mL of benzene was added at room temperature to a suspension of [NiBr$_2$•DME] (500 mg, 1.62 mmol) in 15 mL of benzene. The reaction mixture was stirred for 24 h at room temperature and was then filtered through a pad of celite. All volatiles were removed in vacuo and the remaining residue was suspended in 20 mL of hexane. The precipitate was collected by filtration

and dried in vacuo to give the intermediate complex *trans*-[Ni(Dipp$_2$Im)$_2$(Br)$_2$] as pink powder (1.30 g, 1.31 mmol, 81 %).

^{1}H NMR (400.1 MHz, $CDCl_3$, 298 K): δ = 0.84 (d, 24H, $^3J_{HH}$ = 6.7 Hz, ^{i}Pr-C*H$_3$*), 0.99 (d, 24H, $^3J_{HH}$ = 6.7 Hz, ^{i}Pr-C*H$_3$*), 2.93 (sept, 8H, $^3J_{HH}$ = 6.7 Hz, ^{i}Pr-C*H*), 6.60 (s, 4H, NC*H*C*H*N), 7.15 (d, 8H, $^3J_{HH}$ = 7.8 Hz, aryl$_{NHC}$-C*H$_{meta}$*), 7.43 (t, 4H, $^3J_{HH}$ = 7.8 Hz, aryl$_{NHC}$-C*H$_{para}$*).

trans-[Ni(Dipp$_2$Im)$_2$(Br)$_2$] (1.04 g, 1.04 mmol) and KC_8 (445 mg, 3.29 mmol) were suspended in 20 mL of THF. The dark purple reaction mixture was stirred for 24 h at room temperature and was then filtered through a pad of celite. All volatiles were removed in vacuo and the remaining residue was redissolved in 20 mL of toluene and then again filtered through a pad of celite. The solvent was removed in vacuo and the product was suspended in 20 mL of hexane, collected by filtration and dried in vacuo to give a dark black crystalline solid (539 mg, 645 μmol, 62 %).

^{1}H NMR (400.1 MHz, C_6D_6, 298 K): δ = 1.10 (d, 24H, $^3J_{HH}$ = 6.9 Hz, ^{i}Pr-C*H$_3$*), 1.24 (d, 24H, $^3J_{HH}$ = 6.9 Hz, ^{i}Pr-C*H$_3$*), 3.06 (sept, 8H, $^3J_{HH}$ = 6.9 Hz, ^{i}Pr-C*H*), 6.11 (s, 4H, NC*H*C*H*N), 7.08 (d, 8H, $^3J_{HH}$ = 7.7 Hz, aryl$_{NHC}$-C*H$_{meta}$*), 7.28 (t, 4H, $^3J_{HH}$ = 7.7 Hz, aryl$_{NHC}$-C*H$_{para}$*).

^{13}C{^{1}H} NMR (100.6 MHz, C_6D_6, 298 K): δ = 24.3 (^{i}Pr-*C*H$_3$), 24.9 (^{i}Pr-*C*H$_3$), 28.7 (^{i}Pr-*C*H), 121.1 (N*C*H*C*HN), 123.7 (aryl$_{NHC}$-*C*H$_{meta}$), 128.4 (aryl$_{NHC}$-*C*H$_{para}$), 139.7 (aryl$_{NHC}$-*C$_{ipso}$*), 145.8 (aryl$_{NHC}$-*C$_{ortho}$*), 193.9 (N*C*N).

[Ni(Dipp$_2$Im^{H2})$_2$] (4) [11, 12]

A solution of Dipp$_2$Im^{H2} (764 mg, 1.96 mmol) in 15 mL of benzene was added at room temperature to a suspension of [$NiBr_2$•DME] (287 mg, 931 μmol) in 5 mL of benzene. The reaction mixture was stirred for 24 h at room temperature and was then filtered through a pad of celite. All volatiles were removed in vacuo and the remaining residue was suspended in 10 mL of hexane. The precipitate was collected by filtration and dried in vacuo to give the intermediate complex *trans*-[Ni(Dipp$_2$Im^{H2})$_2$(Br)$_2$] as pink powder (910 mg, 910 μmol, 98 %).

^{1}H NMR (400.1 MHz, $CDCl_3$, 298 K): δ = 0.97 (d, 24H, $^3J_{HH}$ = 6.7 Hz, ^{i}Pr-C*H$_3$*), 1.00 (d, 24H, $^3J_{HH}$ = 6.7 Hz, ^{i}Pr-C*H$_3$*), 3.26 (sept, 8H, $^3J_{HH}$ = 6.7 Hz, ^{i}Pr-C*H*), 3.50 (s, 8H,

NC*H*$_2$C*H*$_2$N), 7.06 (d, 8H, $^3J_{HH}$ = 7.7 Hz, aryl$_{NHC}$-C*H*$_{meta}$), 7.30 (t, 4H, $^3J_{HH}$ = 7.7 Hz, aryl$_{NHC}$-C*H*$_{para}$).

trans-[Ni(Dipp$_2$Im^{H2})$_2$(Br)$_2$] (800 mg, 800 *µ*mol) and KC_8 (335 mg, 2.48 mmol) were suspended in 15 mL of THF. The dark purple reaction mixture was stirred for 24 h at room temperature and was then filtered through a pad of celite. All volatiles were removed in vacuo and the remaining residue was redissolved in 20 mL of toluene and then again filtered through a pad of celite. The solvent was removed in vacuo and the product was suspended in 10 mL of hexane, collected by filtration and dried in vacuo to give a dark black crystalline solid (460 mg, 548 *µ*mol, 68 %).

^{1}H NMR (400.1 MHz, C_6D_6, 298 K): *δ* = 1.18 (d, 24H, $^3J_{HH}$ = 6.9 Hz, ^{i}Pr-C*H*$_3$), 1.25 (d, 24H, $^3J_{HH}$ = 6.9 Hz, ^{i}Pr-C*H*$_3$), 2.95 (s, 8H, NC*H*$_2$C*H*$_2$N), 3.25 (sept, 8H, $^3J_{HH}$ = 6.9 Hz, ^{i}Pr-C*H*), 7.08 (d, 8H, $^3J_{HH}$ = 7.6 Hz, aryl$_{NHC}$-C*H*$_{meta}$), 7.23 (t, 4H, $^3J_{HH}$ = 7.6 Hz, aryl$_{NHC}$-C*H*$_{para}$).

^{13}C{^{1}H} NMR (100.6 MHz, C_6D_6, 298 K): *δ* = 24.6 (^{i}Pr-*C*H$_3$), 25.4 (^{i}Pr-*C*H$_3$), 28.6 (^{i}Pr-*C*H), 54.1 (N*C*H$_2$*C*H$_2$N), 124.3 (aryl$_{NHC}$-*C*H$_{meta}$), 127.7 (aryl$_{NHC}$-*C*H$_{para}$), 140.5 (aryl$_{NHC}$-*C*$_{ipso}$), 146.7 (aryl$_{NHC}$-*C*$_{ortho}$), 211.2 (N*C*N).

[Ni(cAAC^{Me})$_2$] (5) [13]

A solution of cAAC^{Me} (777 mg, 2.72 mmol) in 10 mL of benzene was added at room temperature to a suspension of [NiBr$_2$•DME] (400 mg, 1.30 mmol) in 5 mL of benzene. The reaction mixture was stirred for 24 h at room temperature and was then filtered through a pad of celite. All volatiles were removed in vacuo and the remaining residue was suspended in 5 mL of hexane. The precipitate was collected by filtration and dried in vacuo to give the intermediate complex *trans*-[Ni(cAAC^{Me})$_2$(Br)$_2$] as pink powder (710 mg, 899 *µ*mol, 69 %).

^{1}H NMR (400.1 MHz, C_6D_6, 298 K): *δ* = 0.92 (s, 12H, C(C*H*$_3$)$_2$), 1.14 (d, 12H, $^3J_{HH}$ = 5.8 Hz, ^{i}Pr-C*H*$_3$), 1.32 (d, 12H, $^3J_{HH}$ = 5.8 Hz, ^{i}Pr-C*H*$_3$), 1.43 (s, 4H, C*H*$_2$), 2.35 (s, 12H, NC(C*H*$_3$)$_2$), 3.23 (sept, $^3J_{HH}$ = 5.8 Hz, 4H, ^{i}Pr-C*H*), 7.13-7.24 (m, 6H, aryl-C*H*$_{meta/para}$).

The isolated compound contains 20 % of the *cis*-isomer:

^{1}H NMR (400.1 MHz, C_6D_6, 298 K): δ = 0.90 (s, 12H, C(C*H*$_3$)$_2$), 1.20 (d, 12H, ^{i}Pr-C*H*$_3$), 1.30 (s, 4H, C*H*$_2$), 1.83 (d, 12H, ^{i}Pr-C*H*$_3$), 1.94 (s, 12H, NC(C*H*$_3$)$_2$), 3.44 (sept, 4H, ^{i}Pr-C*H*), 7.29-7.36 (m, 6H, aryl-C*H*$_{meta/para}$).

[Ni(cAAC^{Me})$_2$(Br)$_2$] (600 mg, 760 μmol) and KC_8 (318 mg, 2.36 mmol) were suspended in 15 mL of THF. The dark purple reaction mixture was stirred for 24 h at room temperature and was then filtered through a pad of celite. All volatiles were removed in vacuo and the remaining residue was redissolved in 15 mL of toluene and then again filtered through a pad of celite. The solvent was removed in vacuo and the product was suspended in 3 mL of hexane. The suspension was stored for 30 min at -30 °C, collected by filtration and dried in vacuo to give a dark black crystalline solid (208 mg, 330 μmol, 43 %).

^{1}H NMR (400.1 MHz, C_6D_6, 298 K): δ = 0.92 (s, 12H, C(C*H*$_3$)$_2$), 1.24 (d, 12H, ^{i}Pr-C*H*$_3$), 1.25-1.62 (br, 12H, ^{i}Pr-C*H*$_3$), 1.65 (m, 16H, NC(C*H*$_3$)$_2$ and C*H*$_2$), 2.96 (sept, br, 4H, ^{i}Pr-C*H*), 7.03-7.13 (m, 6H, aryl-C*H*$_{meta/para}$).

^{13}C{^{1}H} NMR (100.6 MHz, C_6D_6, 298 K): δ = 22.7 (^{i}Pr-*C*H$_3$), 27.7 (C(*C*H$_3$)$_2$), 28.1 (^{i}Pr-*C*H), 29.0 (NC(*C*H$_3$)$_2$), 52.4 (*C*H$_2$), 55.5 (N*C*Me$_2$), 75.5 (*C*Me$_2$), 123.9 (aryl-*C*H), 127.5 (aryl-*C*H), 138.2 (aryl-*C*$_{ipso}$), 145.1 (aryl-*C*$_{ortho}$), 242.5 (N*C*CMe$_2$).

Synthons of [Ni(^{i}Pr$_2$Im)$_2$] (6)

[Ni$_2$(^{i}Pr$_2$Im)$_4$(μ-(η^2:η^2)-COD)] ***6a*** *and [Ni(^{i}Pr$_2$Im)$_2$(COD)]* ***6b*** [14]

A solution of ^{i}Pr$_2$Im (2.26 g, 14.9 mmol) in 20 mL of THF was cooled to -78 °C and added at this temperature to a solution of [Ni(η^4-COD)$_2$] (2.04 mg, 7.42 mmol) in 60 mL of THF. The reaction mixture was allowed to slowly warm to room temperature overnight and was then filtered through a pad of celite. All volatiles were removed in vacuo and the remaining residue was suspended in 20 mL of hexane. The product was collected by filtration and dried in vacuo to give a yellow powder (2.44 g). The isolated product contains a mixture of [Ni$_2$(^{i}Pr$_2$Im)$_4$(μ-(η^2:η^2)-COD)] **6a** and [Ni(^{i}Pr$_2$Im)$_2$(η^4-COD)] **6b** (60:40).

[Ni$_2$(^{i}Pr$_2$Im)$_4$(μ-(η^2:η^2)-COD)] ***6a***

^{1}H NMR (500.1 MHz, C_6D_6, 298 K): *δ* = 1.19 (d, 48H, $^3J_{HH}$ = 6.8 Hz, ^{i}Pr-C*H*$_3$), 2.21 (m, 4H, COD-C*H*$_2$), 2.42 (d, 4H, $^3J_{HH}$ = 10.5 Hz, COD-C*H*$_2$), 2.89 (d, 4H, $^3J_{HH}$= 7.2 Hz, COD-C*H*), 5.51 (sept, 8H, $^3J_{HH}$ = 6.8 Hz, ^{i}Pr-C*H*), 6.50 (s, 8H, NC*H*C*H*N).

^{13}C{^{1}H} NMR (125.8 MHz, C_6D_6, 298 K): *δ* = 23.8 (^{i}Pr-*C*H$_3$), 32.0 (COD-*C*H$_2$), 38.6 (COD-*C*H), 50.6 (^{i}Pr-*C*H), 54.6 (COD-*C*H), 113.9 (N*C*H*C*HN), 204.2 (N*C*N).

[Ni(^{i}Pr$_2$Im)$_2$(η^4-COD)] ***6b***

^{1}H NMR (500.1 MHz, C_6D_6, 298 K): *δ* = 1.18 (d, 24H, $^3J_{HH}$ = 6.8 Hz, ^{i}Pr-C*H*$_3$), 2.42 (s, 8H, COD-C*H*$_2$), 4.41 (s, 4H, COD-C*H*), 5.40 (sept, 4H, $^3J_{HH}$ = 6.8 Hz, ^{i}Pr-C*H*), 6.48 (s, 4H, NC*H*C*H*N).

Synthons of [Ni(^{i}Pr$_2$Im^{Me})$_2$] (7)

[Ni$_2$(^{i}Pr$_2$Im^{Me})$_4$(μ-(η^2:η^2)-COD)] ***7a*** *and [Ni(^{i}Pr$_2$Im^{Me})$_2$(COD)]* ***7b*** [15]

A solution of ^{i}Pr$_2$Im^{Me} (680 mg, 3.77 mmol) in 15 mL of THF was cooled to -78 °C and added at this temperature to a solution of [Ni(*η*^{4}-COD)$_2$] (520 mg,1.89 mmol) in 15 mL of THF. The reaction mixture was allowed to slowly warm to room temperature overnight and was then filtered through a pad of celite. All volatiles were removed in vacuo and the remaining residue was suspended in 15 mL of hexane. The product was collected by filtration and dried in vacuo to give a yellow powder (653 mg). The isolated product contains a mixture of [Ni$_2$(^{i}Pr$_2$Im^{Me})$_4$(*μ-(η^2:η^2)*-COD)] **7a** and [Ni(^{i}Pr$_2$Im^{Me})$_2$(*η*^{4}-COD)] **7b** (60:40).

Yellow crystals of [Ni$_2$(^{i}Pr$_2$Im^{Me})$_4$(*μ-(η^2:η^2)*-COD)] **7a** suitable for single-crystal X-ray diffraction were obtained by slow evaporation of a saturated benzene solution at room temperature.

[Ni$_2$(^{i}Pr$_2$Im^{Me})$_4$(μ-(η^2:η^2)-COD)] ***7a***

^{1}H NMR (400.1 MHz, C_6D_6, 298 K): *δ* = 1.42 (d, br, 48H, ^{i}Pr-C*H*$_3$), 1.88 (s, 24H, NCC*H*$_3$CC*H*$_3$N), 2.22 (m, 4H, COD-C*H*$_2$), 2.59 (d, br, 4H, COD-C*H*$_2$), 2.84 (m, 4H, COD-C*H*), 6.03 (sept, 8H, $^3J_{HH}$ = 7.1 Hz, ^{i}Pr-C*H*).

$^{13}C\{^1H\}$ NMR (100.6 MHz, C_6D_6, 298 K): δ = 10.6 (NC*C*H$_3$C*C*H$_3$N), 23.0 (^{i}Pr-*C*H$_3$), 38.7 (COD-*C*H$_2$), 51.8 (^{i}Pr-*C*H), 54.5 (COD-*C*H), 122.2 (N*C*CH$_3$*C*CH$_3$N), 206.5 (N*C*N).

[Ni(^{i}Pr$_2$Im^{Me})$_2$(η^4-COD)] ***7b***

^1H NMR (400.1 MHz, C_6D_6, 298 K): δ = 1.33 (d, 24H, $^3J_{HH}$ = 7.2 Hz, ^{i}Pr-C*H*$_3$), 1.86 (s, 12H, NCC*H*$_3$CC*H*$_3$N), 2.47 (s, 8H, COD-C*H*$_2$), 4.38 (s, 4H, COD-C*H*), 5.90 (sept, 4H, $^3J_{HH}$ = 7.2 Hz, ^{i}Pr-C*H*).

$^{13}C\{^1H\}$ NMR (100.6 MHz, C_6D_6, 298 K): δ = 10.6 (NC*C*H$_3$C*C*H$_3$N), 22.8 (^{i}Pr-*C*H$_3$), 33.6 (COD-*C*H$_2$), 51.9 (^{i}Pr-*C*H), 122.6 (N*C*CH$_3$*C*CH$_3$N), 205.4 (N*C*N).

[Ni(^{i}Pr$_2$Im^{Me})$_2$(η^2-C$_2$H$_4$)] (7c)

A 60:40 mixture of [Ni$_2$(^{i}Pr$_2$Im^{Me})$_4$(μ-(η^2:η^2)-COD)] **7a** and [Ni(^{i}Pr$_2$Im^{Me})$_2$(η^4-COD)] **7b** (770 mg, 1.58 mmol) was dissolved in 20 mL of toluene. The flask was evacuated and charged with 1 bar of ethylene. After stirring the reaction mixture for 2 h at room temperature all volatiles were removed in vacuo to give a pale-yellow powder (680 mg, 1.52 mmol, 96 %).

Yellow crystals of [Ni(^{i}Pr$_2$Im^{Me})$_2$(η^2-C$_2$H$_4$)] **7c** suitable for single-crystal X-ray diffraction were obtained by storing a saturated solution of the compound in hexane at -30 °C.

Elemental analysis $C_{24}H_{44}N_4Ni$ [447.33 g/mol] calculated (found): C 64.44 (64.49), H 9.91 (10.12), N 12.52 (12.54).

^1H NMR (400.1 MHz, C_6D_6, 298 K): δ = 1.32 (d, 24H, $^3J_{HH}$ = 7.0 Hz, ^{i}Pr-C*H*$_3$), 1.86 (s, 12H, NCC*H*$_3$CC*H*$_3$N), 1.87 (s, 4H, *H*$_2$C=C*H*$_2$), 5.89 (sept, 4H, $^3J_{HH}$ = 7.0 Hz, ^{i}Pr-C*H*).

$^{13}C\{^1H\}$ NMR (100.6 MHz, C_6D_6, 298 K): δ = 10.4 (NC*C*H$_3$C*C*H$_3$N), 22.4 (^{i}Pr-*C*H$_3$), 26.0 (H$_2$*C*=*C*H$_2$), 51.9 (^{i}Pr-*C*H), 122.8 (N*C*CH$_3$*C*CH$_3$N), 205.0 (N*C*N).

IR (ATR [cm^{-1}]): 2968 (m), 2922 (m), 2870 (m), 1686 (vw), 1641 (vw), 1463 (w), 1405 (m), 1364 (m), 1364 (s), 1305 (m), 1281 (m), 1257 (vs), 1208 (m), 1142 (s), 1098 (m), 1061 (m), 1018 (m), 960 (w), 924 (w), 903 (w), 881 (w), 854 (w), 796 (m), 754 (w), 673 (m), 614 (w), 549 (w), 460 (m).

[Ni(^{i}Pr$_2$Im^{Me})$_2$(η^2-COE)] (7d)

Cyclooctene (411 μL, 349 mg, 3.17 mmol) and KC_8 (1.46 g, 10.8 mmol) were added successively at -78 °C to a suspension of [Ni(^{i}Pr$_2$Im^{Me})$_2$(Br)$_2$] (1.53 g, 2.64 mmol) in 60 mL of THF. The reaction mixture was allowed to warm to room temperature overnight and was then filtered through a pad of celite. All volatiles were removed in vacuo and the remaining residue was suspended in 20 mL of toluene and again filtered through a pad of celite. The solvent was removed in vacuo and the product was suspended in 6 mL of hexane, filtered, and dried in vacuo to give a pale-yellow powder (850 mg, 1.61 mmol, 61 %).

Yellow crystals of [Ni(^{i}Pr$_2$Im^{Me})$_2$(η^2-COE)] **7d** suitable for single-crystal X-ray diffraction were obtained by storing a saturated solution of the compound in hexane at -30 °C.

Elemental analysis $C_{30}H_{54}N_4Ni$ [529.48 g/mol] calculated (found): C 68.05 (67.62), H 10.28 (10.34), N 10.58 (10.39).

^{1}H NMR (400.1 MHz, C_6D_6, 298 K): δ = 1.34 (d, 12H, $^3J_{HH}$ = 7.1 Hz, ^{i}Pr-CH_3), 1.36 (d, 12H, $^3J_{HH}$ = 7.1 Hz, ^{i}Pr-CH_3), 1.69-2.37 (m, 14H, COE-CH_2 and COE-CH), 1.88 (s, 12H, NCCH_3CCH_3N), 5.92 (sept, 4H, $^3J_{HH}$ = 7.1 Hz, ^{i}Pr-CH).

^{13}C{^{1}H} NMR (100.6 MHz, C_6D_6, 298 K): δ = 10.6 (NCCH$_3$CCH$_3$N), 22.9 (^{i}Pr-CH$_3$), 27.7 (COE-CH$_2$), 30.8 (COE-CH$_2$), 33.7 (COE-CH$_2$), 47.9 (COE-CH), 51.9 (^{i}Pr-CH), 122.5 (NCCH$_3$$CCH_3$N), 205.9 (N$C$N).

IR (ATR [cm^{-1}]): 2972 (w), 2918 (m), 2899 (m), 2870 (m), 2820 (w), 1461 (w), 1433 (vw), 1419 (vw), 1399 (m), 1381 (m), 1361 (m), 1335 (vs), 1306 (w), 1281 (s), 1253 (vs), 1205 (s), 1195 (m), 1161 (w), 1141 (w), 1127 (m), 1097 (m), 1055 (m), 1017 (w), 962 (vw), 917 (vw), 903 (vw), 890 (vw), 865 (vw), 837 (vw), 806 (vw), 789 (w), 750 (w), 731 (vw), 684 (m), 671 (w), 652 (vw), 594 (vw), 541 (s), 459 (w), 445 (w).

7.3 Synthetic Procedures for Chapter II

The compounds **II-3 – II-8** have been synthesized and characterized previously in our group by Dr. Thomas Schaub. Detailed synthetic procedures and analytical data can be found in ref [16].

[Ni(Mes$_2$Im)$_2$(η^2-H$_2$C=CH$_2$)] (II-1)

[Ni(Mes$_2$Im)$_2$] **1** (240 mg, 356 μmol) was suspended in 8 mL of pentane. The flask was degassed and charged with 1 bar of ethylene. An orange precipitate was formed immediately, and the mixture was then stirred for 3 h at room temperature. The product was collected by filtration, washed with 5 mL of pentane and dried in vacuo to give an orange powder (145 mg, 208 μmol, 58 %).

Orange crystals of [Ni(Mes$_2$Im)$_2$(η^2-H$_2$C=CH$_2$)] **II-1** suitable for single-crystal X-ray diffraction were obtained by storing a saturated solution of the complex in pentane at -30 °C.

Elemental analysis $C_{44}H_{52}N_4Ni$ [695.62 g/mol] calculated (found): C 75.97 (76.37), H 7.54 (7.68), N 8.05 (8.28).

HRMS-LIFDI m/z (%) calculated for [$C_{44}H_{52}N_4Ni$]: 694.3545(100) $[M]^+$; found: 694.3534(5) $[M]^+$, 666.3229(100) $[Ni(Mes_2Im)_2]^+$, 305.2013(30) $[Mes_2Im+H]^+$.

^{1}H NMR (400.1 MHz, C_6D_6, 298 K): δ = 1.61 (s, 4H, CH_2CH_2), 1.99 (s, 24H, aryl$_{NHC}$-CH_{3ortho}), 2.29 (s, 12H, aryl$_{NHC}$-CH_{3para}), 6.14 (s, 4H, NC*H*C*H*N), 6.73 (s, 8H, aryl$_{NHC}$-CH_{meta}).

^{13}C{^{1}H} NMR (100.6 MHz, C_6D_6, 298 K): δ = 18.7 (aryl$_{NHC}$-*C*H$_{3ortho}$), 21.3 (aryl$_{NHC}$-*C*H$_{3para}$), 35.9 (*C*H2*C*H2), 121.1 (N*C*H*C*HN), 129.2 (aryl$_{NHC}$-*C*H$_{meta}$), 136.1 (aryl$_{NHC}$-*C*CH$_{3ortho}$), 136.2 (aryl$_{NHC}$-*C*CH$_{3para}$), 139.5 (aryl$_{NHC}$-*C$_{ipso}$*) 206.4 (N*C*N).

IR (ATR [cm^{-1}]): 3020(w), 3002 (w), 2961 (w), 2944 (w), 2910 (w), 2851 (w), 2728 (vw), 1507 (vw), 1484 (m), 1374 (m), 1350 (w), 1254 (vs), 1182 (m), 1168 (w), 1089 (w), 1056 (s), 1034 (m), 1013 (m), 964 (w), 915 (m), 889 (w), 848 (s), 807 (w), 703 (m), 640 (w), 575 (m), 426 (m).

[Ni(Mes$_2$Im)$_2$(η^2-(*C,C*)-H$_2$C=CHCOOMe)] (II-2)

Methyl acrylate (26.3 μL, 25.0 mg, 291 μmol) was added at 0 °C to a suspension of [Ni(Mes$_2$Im)$_2$] **1** (97.0 mg, 145 μmol) in 8 mL of hexane. The reaction mixture was stirred at 0 °C for 30 min and was then stored at -30 °C for 3 d. The supernatant solution was removed with a syringe and the red crystals obtained were dried in vacuo (95.0 mg, 126 μmol, 87 %).

Red crystals of [Ni(Mes$_2$Im)$_2$(η^2-(*C,C*)-H$_2$C=CHCOOMe)] **II-2** suitable for single-crystal X-ray diffraction were obtained by storing a saturated solution of the complex in hexane at -30 °C.

Elemental analysis $C_{46}H_{54}N_4NiO_2$ [753.66 g/mol] calculated (found): C 73.31 (73.21), H 7.22 (7.63), N 7.43 (7.10).

HRMS-LIFDI m/z (%) calculated for [$C_{46}H_{54}N_4NiO_2$]: 752.36004(100) $[M]^+$; found: 752.3583(5) $[M]^+$, 666.3217(60) $[Ni(Mes_2Im)_2]^+$, 305.2005(100) $[Mes_2Im+H]^+$.

^{1}H NMR (400.1 MHz, C_6D_6, 298 K): δ = 1.26 (dd, 1H, $^2J_{HH}$ = 2.6 Hz, $^3J_{HH}$ = 9.3 Hz, CH=C*H*$_2$), 1.66 (br, 7H, aryl$_{NHC}$-C*H*$_3$), 1.81 (dd, 1H, $^2J_{HH}$ = 2.6 Hz, $^3J_{HH}$ = 10.7 Hz, CH=C*H*$_2$), 1.96-2.26 (br, 26H, aryl$_{NHC}$-C*H*$_3$), 2.47 (dd, 1H, $^3J_{HH}$ = 9.3 Hz, $^3J_{HH}$ = 10.7 Hz, C*H*=CH$_2$), 2.56 (br, 3H, aryl$_{NHC}$-C*H*$_3$), 3.33 (s, 3H, COOC*H*$_3$), 6.09 (s, 4H, NC*H*C*H*N), 6.79 (s, 8H, aryl$_{NHC}$-C*H*$_{meta}$).

^{13}C{^{1}H} NMR (100.6 MHz, C_6D_6, 298 K): δ = 18.6 (aryl$_{NHC}$-*C*H$_3$), 19.2 (aryl$_{NHC}$-*C*H$_3$), 21.2 (aryl$_{NHC}$-*C*H$_3$), 31.3 (CH=*C*H$_2$), 40.6 (*C*H=CH$_2$), 49.0 (COO*C*H$_3$), 122.3 (N*C*H*C*HN), 129.3 (aryl$_{NHC}$-*C*H$_{meta}$), 135.8 (aryl$_{NHC}$-*C*CH$_{3ortho}$), 136.8 (aryl$_{NHC}$-*C*CH$_{3para}$), 139.2 (aryl$_{NHC}$-*C*$_{ipso}$), 175.4 (*C*OOCH$_3$), 202.2 (N*C*N), 205.3 (N*C*N).

IR (ATR [cm^{-1}]): 3135 (vw), 2954 (w), 2914 (w), 2855 (w), 2729 (vw), 1652 (s), 1609 (w), 1485 (s), 1427 (m), 1380 (s), 1346 (w), 1264 (w), 1225 (s), 1201 (vs), 1091 (m), 1034 (s), 1014 (m), 918 (w), 892 (s), 847 (s), 817 (m), 713 (s), 680 (vs), 635 (w), 592 (m), 565 (m), 499 (w), 458 (m), 424 (m).

[Ni(Mes$_2$Im)$_2$(η^2-O=CHPh)] (II-9)

Benzaldehyde (49.5 μL, 51.5 mg, 485 μmol) was added to a suspension of [Ni(Mes$_2$Im)$_2$] **1** (324 mg, 485 μmol) in 5 mL of hexane at 0 °C. The reaction mixture

was then stirred for 2 h at 0 °C and another 24 h at room temperature whereby a redish precipitate was formed. The product was collected by filtration, washed with 5 mL of hexane and dried in vacuo to give a red powder (226 mg, 292 *µ*mol, 60 %).

Red crystals of [Ni(Mes$_2$Im)$_2$(η^2-O=CHPh)] **II-9** suitable for single-crystal X-ray diffraction were obtained by storing a saturated solution of the complex in hexane at -30 °C.

Elemental analysis $C_{49}H_{54}N_4NiO$ [773.69 g/mol] calculated (found): C 76.07 (75.78), H 7.04 (7.04), N 7.24 (7.14).

HRMS-LIFDI m/z (%) calculated for [$C_{49}H_{54}N_4NiO$]: 772.36512(100) $[M]^+$; found: 666.3214(100) $[Ni(Mes_2Im)_2]^+$, 305.2006(10) $[Mes_2Im+H]^+$.

^{1}H NMR (400.1 MHz, C_6D_6, 298 K): δ = 1.48 (s, br, 6H, aryl$_{NHC}$-C*H*$_3$), 2.01 (s, br, 12H, aryl$_{NHC}$-C*H*$_3$), 2.31 (s, br, 18H, aryl$_{NHC}$-C*H*$_3$), 4.85 (s, 1H, C*H*O), 5.95 (s, 2H, NC*H*C*H*N), 6.13 (s, 2H, NC*H*C*H*N), 6.82 (s, 8H, aryl$_{NHC}$-C*H*$_{meta}$), 7.02-7.10 (m, 5H, aryl-C*H*$_{Ph}$).

^{13}C{^{1}H} NMR (125.8 MHz, C_6D_6, 298 K): δ = 17.6 (aryl$_{NHC}$-*C*H$_3$), 18.8 (aryl$_{NHC}$-*C*H$_3$), 19.5 (aryl$_{NHC}$-*C*H$_3$), 21.3 (aryl$_{NHC}$-*C*H$_3$), 76.4 (*C*HO), 122.1 (NC*H*C*H*N), 122.2 (aryl-*C*H$_{Ph}$), 123.0 (NC*H*C*H*N), 125.6 (aryl-*C*H$_{Ph}$), 127.6 (aryl-*C*H$_{Ph}$), 129.0 (aryl$_{NHC}$-*C*H$_{meta}$), 129.3 (aryl$_{NHC}$-*C*H$_{meta}$), 135.0 (aryl$_{NHC}$-*C*$_q$), 137.1 (aryl$_{NHC}$-*C*$_q$), 137.5 (aryl$_{NHC}$-*C*$_q$), 139.1 (aryl$_{NHC}$-*C*$_q$), 154.2 (aryl-*C*$_{qPh}$), 199.4 (N*C*N), 202.2 (N*C*N).

IR (ATR [cm^{-1}]): 2951 (w), 2906 (w), 2851 (w), 1589 (w), 1482 (m), 1461 (m), 1434 (w), 1377 (m), 1268 (m), 1243 (s), 1236 (m), 1162 (w), 1095 (w), 1066 (m), 1029 (m), 996 (w), 965 (w), 917 (m), 877 (w), 849 (s), 747 (w), 721 (m), 686 (s), 648 (w), 615 (w), 592 (w), 570 (m), 535 (m), 524 (w), 422 (m).

[Ni(Mes$_2$Im)$_2$(η^2-O=CH(CH(CH$_3$)$_2$))] (II-10)

Isobutyraldehyde (23.5 *µ*L, 18.6 mg, 258 *µ*mol) was added to a suspension of [Ni(Mes$_2$Im)$_2$] **1** (86.0 mg, 129 *µ*mol) in 5 mL of hexane at 0 °C. The reaction mixture was then stirred for 45 min at 0 °C whereby a yellow precipitate was formed. The product was collected by filtration, washed with 5 mL of hexane and dried in vacuo to give a yellow powder (66.0 mg, 89.2 *µ*mol, 69 %).

Yellow crystals of [Ni(Mes$_2$Im)$_2$(η^2-O=CH(CH(CH$_3$)$_2$))] **II-10** suitable for single-crystal X-ray diffraction were obtained by storing a saturated solution of the complex in hexane at -30 °C.

Elemental analysis $C_{46}H_{56}N_4NiO$ [739.67 g/mol] calculated (found): C 74.70 (74.25), H 7.63 (7.66), N 7.57 (7.30).

HRMS-LIFDI m/z (%) calculated for [$C_{46}H_{56}N_4NiO$]: 738.38077(100) $[M]^+$; found: 305.2008(100) $[Mes_2Im+H]^+$.

^{1}H NMR (400.1 MHz, C_6D_6, 298 K): δ = 0.85 (d, 3H, $^3J_{HH}$ = 6.3 Hz, CH(C*H*$_3$)$_2$), 1.11 (d, 3H, $^3J_{HH}$ = 6.3 Hz, CH(C*H*$_3$)$_2$), 1.53 (sept, 1H, $^3J_{HH}$ = 6.3 Hz, C*H*(CH$_3$)$_2$), 1.88 (s, br, 6H, aryl$_{NHC}$-C*H*$_3$), 2.07 (s, br, 12H, aryl$_{NHC}$-C*H*$_3$), 2.29 (s, br, 18H, aryl$_{NHC}$-C*H*$_3$), 3.98 (s, 1H, C*H*O), 6.04 (s, 2H, NC*H*C*H*N), 6.15 (s, 2H, NC*H*C*H*N), 6.80 (m, 8H, aryl$_{NHC}$-C*H*$_{meta}$).

^{13}C{^{1}H} NMR (100.6 MHz, C_6D_6, 298 K): δ = 18.4 (aryl$_{NHC}$-*C*H$_3$), 18.6 (aryl$_{NHC}$-*C*H$_3$), 19.1 (aryl$_{NHC}$-*C*H$_3$), 20.5 (CH(*C*H$_3$)$_2$), 21.3 (aryl$_{NHC}$-*C*H$_3$), 22.4 (CH(*C*H$_3$)$_2$), 36.5 (*C*H(CH$_3$)$_2$), 86.7 (*C*HO), 121.5 (N*C*H*C*HN), 122.3 (N*C*H*C*HN), 128.9 (aryl$_{NHC}$-*C*H$_{meta}$), 129.1 (aryl$_{NHC}$-*C*H$_{meta}$), 129.4 (aryl$_{NHC}$-*C*H$_{meta}$), 135.1 (aryl$_{NHC}$-*C*$_q$), 136.8 (aryl$_{NHC}$-*C*$_q$), 139.1 (aryl$_{NHC}$-*C*$_q$), 202.3 (N*C*N), 202.7 (N*C*N).

IR (ATR [cm^{-1}]): 3053 (w), 2920 (w), 2853 (w), 1483 (s), 1449 (m), 1382 (s), 1319 (m), 1269 (s), 1255 (s), 1238 (s), 1202 (m), 1063 (s), 1035 (m), 1014 (w), 952 (w), 910 (m), 847 (vs), 795 (w), 738 (m), 711 (s), 683 (vs), 579 (s), 423 (s).

[Ni(Mes$_2$Im)$_2$(η^2-O=CH(4-NMe$_2$-C$_6$H$_4$))] (II-11)

A suspension of 4-(dimethylamino)benzaldehyde (35.8 mg, 240 μmol) and [Ni(Mes$_2$Im)$_2$] **1** (80.0 mg, 120 μmol) in 5 mL of hexane was stirred for 24 h at room temperature whereby an orange precipitate was formed. The product was then collected by filtration, washed with 10 mL of hexane and dried in vacuo to give an orange powder (53.0 mg, 64.9 μmol, 54 %).

Elemental analysis $C_{51}H_{59}N_5NiO$ [816.76 g/mol] calculated (found): C 75.00 (75.04), H 7.28 (7.42), N 8.57 (8.67).

HRMS-LIFDI m/z (%) calculated for [$C_{51}H_{59}N_5NiO$]: 815.40732(100) [M]$^+$; found: 769.3611(15) [M - $HNMe_2$]$^+$, 666.3216(100) [Ni(Mes_2Im)$_2$]$^+$, 305.2005(60) [Mes_2Im+H]$^+$.

^{1}H NMR (400.1 MHz, C_6D_6, 298 K): δ = 1.53 (s, br, 6H, aryl$_{NHC}$-CH_3), 2.05 (s, br, 12H, aryl$_{NHC}$-CH_3), 2.32 (s, br, 18H, aryl$_{NHC}$-CH_3), 2.75 (s, 6H, N(CH_3)$_2$), 4.83 (s, 1H, C*H*O), 5.96 (s, 2H, NC*H*C*H*N), 6.15 (s, 2H, NC*H*C*H*N), 6.54 (d, 2H, $^3J_{HH}$ = 7.0 Hz, C_6H_4-CH_{aryl}), 6.81-6.86 (m, 8H, aryl$_{NHC}$-CH_{meta}), 7.00 (d, 2H, $^3J_{HH}$ = 7.0 Hz, C_6H_4-CH_{aryl}).

^{13}C{^{1}H} NMR (100.6 MHz, C_6D_6, 298 K): δ = 17.8 (aryl$_{NHC}$-*C*H$_3$), 18.7 (aryl$_{NHC}$-*C*H$_3$), 19.5 (aryl$_{NHC}$-*C*H$_3$), 21.3 (aryl$_{NHC}$-*C*H$_3$), 41.6 (N(*C*H$_3$)$_2$), 76.8 (*C*HO), 113.8 (C_6H_4-*C*H$_{aryl}$), 121.9 (N*C*H*C*HN), 122.8 (N*C*H*C*HN), 127.8 (C_6H_4-*C*H$_{aryl}$), 129.3 (aryl$_{NHC}$-*C*H$_{meta}$), 135.0 (aryl$_{NHC}$-*C*$_q$), 136.9 (aryl$_{NHC}$-*C*$_q$), 139.3 (aryl$_{NHC}$-*C*$_q$), 143.7 (*C*CHO), 147.6 (*C*N(CH$_3$)$_2$), 200.4 (N*C*N), 202.7 (N*C*N).

IR (ATR [cm^{-1}]): 3195 (w), 3062 (w), 2911 (w), 1537 (w), 1507 (m), 1483 (m), 1402 (w), 1379 (s), 1268 (m), 1252 (s), 1238 (s), 1181 (w), 1134 (m), 1080 (w), 1068 (m), 1025 (m), 987 (w), 944 (m), 916 (m), 865 (w), 845 (s), 733 (m), 708 (m), 683 (s), 639 (m), 578 (m), 565 (m), 549 (m), 421 (m).

[Ni(Mes_2Im)$_2$(η^2-O=CH(4-OMe-C_6H_4))] (II-12)

4-methoxybenzaldehyde (23.3 μL, 26.1 mg, 192 μmol) was added to a suspension of [Ni(Mes_2Im)$_2$] **1** (128 mg, 192 μmol) in 5 mL of pentane. Immediately a brown precipitate was formed and the reaction mixture was then stirred for 2 h at room temperature. All volatiles were removed in vacuo and the remaining residue was again suspended in 5 mL of pentane. The product was collected by filtration and dried in vacuo to give a brown powder (85.0 mg, 106 μmol, 55 %).

Elemental analysis $C_{50}H_{56}N_4NiO_2$ [803.72 g/mol] calculated (found): C 74.72 (73.94), H 7.02 (7.11), N 6.97 (6.61).

HRMS-LIFDI m/z (%) calculated for [$C_{50}H_{56}N_4NiO_2$]: 802.38334(100) [M]$^+$; found: 666.3225(100) [Ni(Mes_2Im)$_2$]$^+$, 305.2011(100) [Mes_2Im+H]$^+$.

^{1}H NMR (400.1 MHz, C_6D_6, 298 K): δ = 1.52 (s, br, 6H, aryl$_{NHC}$-CH_3), 2.02 (s, br, 12H, aryl$_{NHC}$-CH_3), 2.30 (s, br, 18H, aryl$_{NHC}$-CH_3), 3.54 (s, 3H, OCH_3), 4.78 (s, 1H, C*H*O),

5.94 (s, 2H, NC*H*C*H*N), 6.14 (s, 2H, NC*H*C*H*N), 6.67 (d, 2H, $^3J_{HH}$ = 8.0 Hz, C_6H_4-C*H*$_{aryl}$), 6.78-6.88 (m, 8H, aryl$_{NHC}$-C*H*$_{meta}$), 7.00 (d, 2H, $^3J_{HH}$ = 8.0 Hz, C_6H_4-C*H*$_{aryl}$).

^{13}C{^{1}H} NMR (100.6 MHz, C_6D_6, 298 K): δ = 17.8 (aryl$_{NHC}$-*C*H$_3$), 18.7 (aryl$_{NHC}$-*C*H$_3$), 19.6 (aryl$_{NHC}$-*C*H$_3$), 21.3 (aryl$_{NHC}$-*C*H$_3$), 54.9 (O*C*H$_3$), 76.1 (*C*HO), 113.3 (C_6H_4-*C*H$_{aryl}$), 121.9 (N*C*H*C*HN), 122.9 (N*C*H*C*HN), 126.4 (C_6H_4-*C*H$_{aryl}$), 129.0 (aryl$_{NHC}$-*C*H$_{meta}$), 129.4 (aryl$_{NHC}$-*C*H$_{meta}$), 137.0 (aryl$_{NHC}$-*C*CH$_{3ortho/para}$), 137.5 (aryl$_{NHC}$-*C*CH$_{3ortho/para}$), 139.2 (aryl$_{NHC}$-*C*$_{ipso}$), 146.7 (C_6H_4-*C*$_q$), 156.3 (C_6H_4-*C*$_q$-OMe), 199.8 (N*C*N), 202.5 (N*C*N).

IR (ATR [cm^{-1}]): 2942 (w), 2912 (w), 2855 (w), 1603 (w), 1486 (m), 1439 (m), 1382 (m), 1274 (m), 1254 (m), 1229 (s), 1160 (w), 1070 (m), 1036 (m), 958 (w), 919 (m), 848 (m), 797 (m), 713 (m), 685 (s), 593 (m), 569 (m), 542 (m), 422 (m).

[Ni(Mes$_2$Im)$_2$(η^2-O=CPh$_2$)] (II-13)

A solution of benzophenone (22.9 mg, 126 μmol) in 5 mL of toluene was added to a solution of [Ni(Mes$_2$Im)$_2$] **1** (84.0 mg, 126 μmol) in 5 mL of toluene. The reaction mixture was then stirred for 2 h at room temperature. All volatiles were removed in vacuo and the remaining residue was suspended in 5 mL of hexane. The product was collected by filtration and dried in vacuo to give a brown powder (51.0 mg, 60.0 μmol, 48 %).

Elemental analysis $C_{55}H_{58}N_4NiO$ [849.79 g/mol] calculated (found): C 77.74 (77.38), H 6.08 (7.01), N 6.59 (6.67).

HRMS-LIFDI m/z (%) calculated for [$C_{55}H_{58}N_4NiO$]: 848.39642(100) [M]$^+$; found: 848.3914(5) [M]$^+$, 666.3216(60) [Ni(Mes$_2$Im)$_2$]$^+$, 305.2004(100) [Mes$_2$Im+H]$^+$.

^{1}H NMR (500.1 MHz, C_6D_6, 298 K): δ = 1.97 (s, 24H, aryl$_{NHC}$-C*H*$_{3ortho}$), 2.31 (s, 12H, aryl$_{NHC}$-C*H*$_{3para}$), 5.99 (s, 4H, NC*H*C*H*N), 6.73 (s, 8H, aryl$_{NHC}$-C*H*$_{meta}$), 6.92 (m, 4H, aryl-*H*$_{meta}$), 7.22 (m, 2H, aryl-*H*$_{para}$), 7.85 (m, 4H, aryl-*H*$_{ortho}$).

^{13}C{^{1}H} NMR (100.6 MHz, C_6D_6, 298 K): δ = 19.0 (aryl$_{NHC}$-*C*H$_{3ortho}$), 21.3 (aryl$_{NHC}$-*C*H$_{3para}$), 83.5 (*C*=O), 123.0 (N*C*H*C*HN), 129.2 (aryl$_{NHC}$-*C*H$_{meta}$), 136.1 (aryl$_{NHC}$-*C*CH$_{3ortho}$), 136.8 (aryl$_{NHC}$-*C*CH$_{3para}$), 139.1 (aryl$_{NHC}$-*C*$_{ipso}$), 152.1 (aryl-*C*$_{qPh}$), 201.1 (N*C*N).

IR (ATR [cm^{-1}]): 2911 (w), 1587 (m), 1483 (s), 1445 (m), 1379 (s), 1255 (s), 1067 (m), 1029 (m), 917 (m), 846 (s), 762 (m), 737 (m), 720 (m), 692 (s), 629 (m), 609 (s), 592 (m), 571 (m), 422 (w).

[Ni(Mes$_2$Im)$_2$(η^2-O=C(4-F-C$_6$H$_4$)$_2$)] (II-14)

A solution of 4,4´-difluorobenzophenone (42.2 mg, 193 μmol) in 5 mL of toluene was added to a solution of [Ni(Mes$_2$Im)$_2$] **1** (129 mg, 193 μmol) in 5 mL of toluene. The reaction mixture was then stirred for 5 d at room temperature. All volatiles were removed in vacuo and the remaining residue was suspended in 5 mL of pentane. The product was collected by filtration and dried in vacuo to give a brown powder (69.5 mg, 78.5 μmol, 36 %).

Elemental analysis $C_{55}H_{56}F_2N_4NiO$ [885.77 g/mol] calculated (found): C 74.58 (74.71), H 6.37 (6.54), N 6.33 (6.25).

HRMS-LIFDI m/z (%) calculated for [$C_{55}H_{56}F_2N_4NiO$]: 884.3776(100) $[M]^+$; found: 884.3738(5) $[M]^+$, 666.3236(80) $[Ni(Mes_2Im)_2]^+$, 305.2012(100) $[Mes_2Im+H]^+$.

^{1}H NMR (400.1 MHz, C_6D_6, 298 K): δ = 1.90 (s, 24H, aryl$_{NHC}$-CH_{3ortho}), 2.30 (s, 12H, aryl$_{NHC}$-CH_{3para}), 5.95 (s, 4H, NCHCHN), 6.62 (m, 4H, aryl-H_{ortho}) 6.67 (s, 8H, aryl$_{NHC}$-CH_{meta}), 7.56 (m, 4H, aryl-H_{meta}).

^{13}C{^{1}H} NMR (125.8 MHz, C_6D_6, 298 K): δ = 19.0 (aryl$_{NHC}$-CH$_{3ortho}$), 21.2 (aryl$_{NHC}$-CH$_{3para}$), 79.5 (C=O), 113.9 (C$_6$H$_4$-CH$_{aryl}$), 123.4 (NCHCHN), 128.3 (C$_6$H$_4$-CH$_{aryl}$), 129.3 (aryl$_{NHC}$-CH$_{meta}$), 136.1 (aryl$_{NHC}$-CCH$_{3ortho}$), 137.2 (aryl$_{NHC}$-CCH$_{3para}$), 139.0 (aryl$_{NHC}$-C_{ipso}), 199.5 (NCN).

^{19}F{^{1}H} NMR (376.8 MHz, C_6D_6, 298 K): δ = -121.61 (s, 2F, aryl-F).

IR (ATR [cm^{-1}]): 2953 (w), 2914 (w), 2857 (w), 1595 (w), 1490 (s), 1437 (m), 1388 (m), 1376 (m), 1256 (s), 1207 (s), 1146 (m), 1066 (m), 1034 (m), 966 (w), 913 (m), 848 (m), 842 (m), 832 (m), 793 (m), 724 (m), 685 (m), 603 (m), 557 (m), 507 (w), 487 (w), 414 (w).

trans-[Ni(Mes$_2$Im)$_2$H(OOCPh)] (II-15)

[Ni(Mes$_2$Im)$_2$] **1** (137 mg, 205 μmol) and benzoic acid (25.1 mg, 205 μmol) were dissolved in 5 mL of toluene. Immediately the color of the solution changed from black to yellow. The reaction mixture was stirred for 2 h at room temperature and was then filtered through a pad of celite. All volatiles were removed in vacuo and the remaining residue was suspended in 5 mL of hexane. The product was collected by filtration, washed with 5 mL of hexane and dried in vacuo to give a cream-colored powder (98.0 mg, 124 μmol, 60 %).

Yellow crystals of *trans*-[Ni(Mes$_2$Im)$_2$H(OOCPh)] **II-15** suitable for X-ray diffraction were obtained by storing a saturated solution of the complex in hexane at -30 °C.

Elemental analysis $C_{49}H_{54}N_4NiO_2$ [789.69 g/mol] calculated (found): C 74.53 (74.22), H 6.89 (7.21), N 7.09 (7.16).

^{1}H NMR (500.1 MHz, C_6D_6, 298 K): δ = -25.12 (s, 1H, Ni-*H*), 2.00 (s, 24H, aryl$_{NHC}$-C*H*$_{3ortho}$), 2.35 (s, 12H, aryl$_{NHC}$-C*H*$_{3para}$), 6.02 (s, 4H, NC*H*C*H*N), 6.84 (s, 8H, aryl$_{NHC}$-C*H*$_{meta}$), 7.26 (m, 3H, aryl-*H*$_{para/ortho}$), 7.92 (m, 2H, aryl-*H*$_{meta}$).

^{13}C{^{1}H} NMR (125.8 MHz, C_6D_6, 298 K): δ = 18.4 (aryl$_{NHC}$-*C*H$_{3ortho}$), 21.4 (aryl$_{NHC}$-*C*H$_{3para}$), 120.9 (N*C*H*C*HN), 126.6 (aryl-*C*H$_{Ph}$), 128.4 (aryl-*C*H$_{Ph}$), 129.2 (aryl$_{NHC}$-*C*H$_{meta}$), 130.4 (aryl-*C*H$_{Ph}$), 136.2 (aryl$_{NHC}$-*C*CH$_{3ortho}$), 137.1 (aryl$_{NHC}$-*C*CH$_{3para}$), 137.7 (aryl$_{NHC}$-*C*$_{ipso}$), 140.2 (aryl-*C*$_{ipso/Ph}$), 169.1 (Ph*C*OO), 187.4(N*C*N).

IR (ATR [cm^{-1}]): 3132 (w), 2913 (w), 2855 (w), 1927 (m), 1725 (s), 1613 (m), 1488 (s), 1401 (m), 1355 (vs), 1321 (s), 1266 (m), 1022 (m), 926 (w), 845 (s), 693 (vs), 677 (m), 530 (m), 424 (w).

[Ni$_2$(Mes$_2$Im)$_2$(μ_2-CO)(μ_2-η^2-*C,O*-PhCOCOPh)] (II-16)

[Ni(Mes$_2$Im)$_2$] **1** (250 mg, 375 μmol) and benzaldehyde (115 μL, 119 mg, 1.12 mmol) were dissolved in 15 mL of toluene. The reaction mixture was stirred at 50 °C for 7 d and was then filtered through a pad of celite. All volatiles were removed in vacuo and the remaining residue was suspended in 20 mL of hexane. The product was collected by filtration and washed with hexane until the filtrate was colorless. The filter cake was dried in vacuo to yield a red powder (120 mg). The isolated red solid contains some residual organic impurities.

Red crystals of [$Ni_2(Mes_2Im)_2(\mu_2$-CO)(μ_2-η^2-*C,O*-PhCOCOPh)] **II-16** suitable for X-ray diffraction were obtained by storing a saturated solution of the complex in hexane at -30 °C for several days.

^{1}H NMR (400.1 MHz, C_6D_6, 298 K): δ = 1.97 (s, aryl$_{NHC}$-C*H*$_3$), 1.99 (s, aryl$_{NHC}$-C*H*$_3$), 2.00 (s, aryl$_{NHC}$-C*H*$_3$), 2.25 (s, aryl$_{NHC}$-C*H*$_3$), 2.27 (s, aryl$_{NHC}$-C*H*$_3$), 6.28 (s, 4H, NC*H*C*H*N), 6.53 (s, 4H, aryl$_{NHC}$-C*H*$_{meta}$), 6.75 (s, 4H, aryl$_{NHC}$-C*H*$_{meta}$), 6.80 (m, 4H, aryl-*H*$_{Benzil}$), 6.95 (m, 4H, aryl-*H*$_{Benzil}$), 7.01 (m, 2H, aryl-*H*$_{Benzil}$).

^{13}C{^{1}H} NMR (100.6 MHz, C_6D_6, 298 K): δ = 17.7 (aryl$_{NHC}$-*C*H$_3$), 18.3 (aryl$_{NHC}$-*C*H$_3$), 18.3 (aryl$_{NHC}$-*C*H$_3$), 21.0 (aryl$_{NHC}$-*C*H$_3$), 21.4 (aryl$_{NHC}$-*C*H$_3$), 111.8 (*C*=O$_{Benzil}$), 122.0 (N*C*H*C*HN), 125.8 (aryl-*C*H$_{Benzil}$), 126.8 (aryl-*C*H$_{Benzil}$), 128.9, 129.3, 129.7, 130.2 (aryl-*C*H$_{Benzil}$), 131.9, 134.8, 136.4, 136.8, 137.3, 140.1, 144.2 (aryl-*C*$_{ipso/Benzil}$), 196.5 (N*C*N), 263.8 (*C*=O$_{bridge}$).

7.4 Synthetic Procedures for Chapter III

[Ni(*i*Pr$_2$Im^{Me})$_2$(η^2-MeC≡CMe)] (III-1)

2-butyne (12.6 *µL*, 8.68 mg, 161 *µ*mol) was added at room temperature to a solution of a 60:40 mixture of [Ni$_2$(*i*Pr$_2$Im^{Me})$_4$(*µ-(η^2:η^2)*-COD)] **7a** and [Ni(*i*Pr$_2$Im^{Me})$_2$(*η^4*-COD)] **7b** (76.0 mg, 156 *µ*mol Ni) in 5 mL of benzene. The reaction mixture was stirred for 10 min at room temperature. All volatiles were removed in vacuo and the remaining residue was dried in vacuo to give a yellow powder (60.0 mg, 127 *µ*mol, 81 %).

Yellow crystals of [Ni(*i*Pr$_2$Im^{Me})$_2$(η^2-MeC≡CMe)] **III-1** suitable for single-crystal X-ray diffraction were obtained from a saturated solution in hexane at -30 °C.

Elemental analysis $C_{26}H_{46}N_4Ni$ [473.38 g/mol] calculated (found): C 65.97 (65.33), H 9.80 (9.88), N 11.84 (11.56).

^{1}H NMR (400.1 MHz, C_6D_6, 298 K): *δ* = 1.27 (d, 24H, $^3J_{HH}$ = 7.2 Hz, *i*Pr-C*H$_3$*), 1.87 (s, 12H, NCC*H$_3$*CC*H$_3$*N), 2.75 (s, 6H, *H$_3$*CC≡CC*H$_3$*), 6.22 (sept, 4H, $^3J_{HH}$ = 7.2 Hz, *i*Pr-C*H*).

^{13}C{^{1}H} NMR (100.6 MHz, C_6D_6, 298 K): *δ* = 10.5 (NC*C*H$_3$C*C*H$_3$N), 13.4 (H$_3$*C*C≡C*C*H$_3$), 22.3 (*i*Pr-*C*H$_3$), 52.0 (*i*Pr-*C*H), 121.6 (*C*≡*C*), 122.8 (N*C*CH$_3$*C*CH$_3$N), 205.1 (N*C*N).

IR (ATR [cm^{-1}]): 2969 (w), 2932 (w), 2884 (w), 2829 (w), 1785 (m), 1640 (vw), 1464 (w), 1407 (w), 1377 (vw), 1362 (w), 1338 (s), 1289 (s), 1264 (vs), 1203 (w), 1161 (vw), 1125 (w), 1098 (m), 1060 (w), 1027 (m), 961 (vw), 902 (w), 775 (vw), 753 (w), 693 (w), 678 (m), 574 (w), 551 (w), 469 (vw), 432 (vw).

[Ni(*i*Pr$_2$Im^{Me})$_2$(η^2-H$_7$C$_3$C≡CC$_3$H$_7$)] (III-2)

4-octyne (35.5 *µ*L, 26.6 mg, 242 *µ*mol) was added at room temperature to a solution of a 60:40 mixture of [Ni$_2$(*i*Pr$_2$Im^{Me})$_4$(*µ-(η^2:η^2)*-COD)] **7a** and [Ni(*i*Pr$_2$Im^{Me})$_2$(*η^4*-COD)] **7b** (109 mg, 224 *µ*mol Ni) in 5 mL of toluene. The reaction mixture was stirred for 16 h at room temperature and was then filtered through a pad of celite. All volatiles were removed in vacuo and the remaining residue was dried in vacuo to give a yellow powder (100 mg, 188 *µ*mol, 84 %).

Elemental analysis $C_{30}H_{54}N_4Ni$ [529.48 g/mol] calculated (found): C 68.05 (67.39), H 10.28 (10.53), N 10.58 (10.01).

^{1}H NMR (400.1 MHz, C_6D_6, 298 K): δ = 1.18 (t, 6H, $^3J_{HH}$ = 7.3 Hz, $CH_2CH_2CH_3$), 1.26 (d, 24H, $^3J_{HH}$ = 7.2 Hz, ^{i}Pr-CH_3), 1.85 (m, 4H, $CH_2CH_2CH_3$), 1.86 (s, 12H, $NCCH_3CCH_3N$), 3.07 (t, 4H, $^3J_{HH}$ = 7.3 Hz, $CH_2CH_2CH_3$), 6.15 (sept, 4H, $^3J_{HH}$ = 7.2 Hz, ^{i}Pr-C*H*).

^{13}C{^{1}H} NMR (100.6 MHz, C_6D_6, 298 K): δ = 10.5 ($NCCH_3CCH_3N$), 14.8 ($CH_2CH_2CH_3$), 22.1 (^{i}Pr-CH_3), 25.1 ($CH_2CH_2CH_3$), 31.5 ($CH_2CH_2CH_3$), 51.8 (^{i}Pr-C*H*), 122.8 ($NCCH_3CCH_3N$), 126.4 ($H_7C_3C{\equiv}CC_3H_7$), 205.5 (N*C*N).

IR (ATR [cm^{-1}]): 2968 (m), 2925 (m), 2863 (w), 2805 (w), 2166 (wv), 2055 (vw), 1996 (wv), 1935 (vw), 1778 (w), 1639 (wv), 1462 (w), 1406 (w), 1379 (m), 1363 (s), 1338 (w), 1305 (m), 1286 (m), 1263 (vs), 1205 (w), 1160 (vw), 1124 (w), 1097 (w), 1059 (w), 1018 (w), 959 (w), 924 (vw), 857 (vw), 751 (w), 691 (w), 679 (w), 594 (w), 461 (w).

[Ni(^{i}Pr$_2$Im^{Me})$_2$(η^2-PhC≡CPh)] (III-3)

A solution of diphenylacetylene (44.6 mg, 250 μmol) in 5 mL of toluene was added at room temperature to a solution of a 60:40 mixture of [Ni$_2$(^{i}Pr$_2$Im^{Me})$_4$(μ-(η^2:η^2)-COD)] **7a** and [Ni(^{i}Pr$_2$Im^{Me})$_2$(η^4-COD)] **7b** (118 mg, 243 μmol Ni) in 10 mL of toluene. The mixture was stirred for 3 h at room temperature and was then filtered through a pad of celite. All volatiles were removed in vacuo and the remaining residue was suspended in 10 mL of pentane. The product was collected by filtration, washed with 3 mL of pentane and dried in vacuo to give a purple powder (93.0 mg, 155 μmol, 64 %).

Red crystals of [Ni(^{i}Pr$_2$Im^{Me})$_2$(η^2-PhC≡CPh)] **III-3** suitable for single-crystal X-ray diffraction were obtained from a saturated solution in hexane at -30 °C.

Elemental analysis $C_{36}H_{50}N_4Ni$ [597.52 g/mol] calculated (found): C 72.37 (72.44), H 8.43 (8.55), N 9.38 (9.22).

^{1}H NMR (400.1 MHz, C_6D_6, 298 K): δ = 1.17 (d, 24H, $^3J_{HH}$ = 7.1 Hz, ^{i}Pr-CH_3), 1.81 (s, 12H, $NCCH_3CCH_3N$), 6.09 (sept, 4H, $^3J_{HH}$ = 7.1 Hz, ^{i}Pr-C*H*), 6.99 (m, 2H, aryl-CH_{para}), 7.20 (m, 4H, aryl-CH_{meta}), 7.69 (m, 4H, aryl-CH_{ortho}).

$^{13}C\{^1H\}$ NMR (100.6 MHz, C_6D_6, 298 K): δ = 10.5 (NC*C*H$_3$C*C*H$_3$N), 22.1 (^{i}Pr-*C*H$_3$), 52.5 (^{i}Pr-*C*H), 123.5 (N*C*CH$_3$*C*CH$_3$N), 123.8 (aryl-*C*H$_{para}$), 128.9 (aryl-*C*H$_{ortho}$), 139.0 (aryl-*C*$_{ipso}$), 139.2 (*C*≡*C*), 201.7 (N*C*N).

IR (ATR [cm^{-1}]): 3062 (w), 3035 (w), 2968 (w), 2930 (w), 2872 (w), 1754 (m), 1734 (m), 1635 (vw), 1582 (m), 1514 (vw), 1474 (w), 1434 (w), 1401 (m), 1347 (s), 1274 (s), 1210 (m), 1164 (w), 1129 (m), 1100 (m), 1065 (m), 1019 (m), 994 (w), 961 (w), 904 (w), 882 (w), 797 (w), 756 (vs), 692 (vs), 626 (w), 596 (m), 551 (w), 510 (w), 455 (w).

[Ni(^{i}Pr$_2$Im^{Me})$_2$(η^2-MeOOCC≡CCOOMe)] (III-4)

Dimethyl acetylene dicarboxylate (35.1 μL, 40.5 mg, 285 μmol) was added at room temperature to a solution of a 60:40 mixture of [Ni$_2$(^{i}Pr$_2$Im^{Me})$_4$(μ-(η^2:η^2)-COD)] **7a** and [Ni(^{i}Pr$_2$Im^{Me})$_2$(η^4-COD)] **7b** (135 mg, 277 μmol Ni) in 5 mL of toluene. The mixture was stirred for 1 h at room temperature and was then filtered through a pad of celite. All volatiles were removed in vacuo and the remaining residue was suspended in 6 mL of hexane. The product was collected by filtration, washed with 3 mL of hexane and dried in vacuo to give an orange powder (108 mg, 192 μmol, 70 %).

Elemental analysis $C_{28}H_{46}N_4NiO_4$ [561.39 g/mol] calculated (found): C 59.91 (58.90), H 8.26 (7.98), N 9.98 (8.62).

^1H NMR (400.1 MHz, C_6D_6, 298 K): δ = 1.17 (d, 24H, $^3J_{HH}$ = 7.2 Hz, ^{i}Pr-C*H*$_3$), 1.74 (s, 12H, NCC*H*$_3$CC*H*$_3$N), 3.55 (s, 6H, COOC*H*$_3$), 5.97 (sept, 4H, $^3J_{HH}$ = 7.2 Hz, ^{i}Pr-C*H*).

$^{13}C\{^1H\}$ NMR (100.6 MHz, C_6D_6, 298 K): δ = 10.3 (NC*C*H$_3$C*C*H$_3$N), 21.9 (^{i}Pr-*C*H$_3$), 50.5 (COO*C*H$_3$), 53.1 (^{i}Pr-*C*H), 124.4 (N*C*CH$_3$*C*CH$_3$N), 136.8 (MeOOC*C*≡*C*COOMe), 170.7 (*C*OOCH$_3$), 194.3 (N*C*N).

IR (ATR [cm^{-1}]): 2973 (w), 2875 (w), 1749 (m), 1683 (s), 1659 (m), 1463 (w), 1426 (w), 1408 (w), 1354 (m), 1301 (w), 1290 (w), 1180 (m), 1125 (s).

[Ni(^{i}Pr$_2$Im^{Me})$_2$(η^2-Me$_3$SiC≡CSiMe$_3$] (III-5)

Bis(trimethylsilyl)acetylene (48.1 μL, 37.0 mg, 217 μmol) was added at room temperature to a solution of a 60:40 mixture of [Ni$_2$(^{i}Pr$_2$Im^{Me})$_4$(μ-(η^2:η^2)-COD)] **7a** and [Ni(^{i}Pr$_2$Im^{Me})$_2$(η^4-COD)] **7b** (98.0 mg, 201 μmol Ni) in 5 mL of benzene. The mixture

was stirred for 18 h at room temperature and was then filtered through a pad of celite. All volatiles were removed in vacuo and the remaining residue was dissolved in 3 mL of hexane and stored at -30 °C for one week. The supernatant solution was removed *via* syringe to obtain yellow crystals (20.0 mg, 34.0 μmol, 17 %).
The obtained crystals of [Ni(*i*Pr$_2$Im^{Me})$_2$(η^2-Me$_3$SiC≡CSiMe$_3$] **III-5** were also suitable for single-crystal X-ray diffraction.

Elemental analysis $C_{30}H_{58}N_4NiSi_2$ [589.69 g/mol] calculated (found): C 61.11 (61.21), H 9.91 (10.12), N 9.50 (9.64).

^{1}H NMR (400.1 MHz, C_6D_6, 298 K): δ = 0.41 (s, 18H, Si(C*H*$_3$)$_3$), 1.15 (d, 12H, $^3J_{HH}$ = 7.1 Hz, *i*Pr-C*H*$_3$), 1.41 (d, 12H, $^3J_{HH}$ = 7.1 Hz, *i*Pr-C*H*$_3$), 1.86 (s, 12H, NCC*H*$_3$CC*H*$_3$N), 5.90 (sept, 4H, $^3J_{HH}$ = 7.1 Hz, *i*Pr-C*H*).

^{13}C{^{1}H} NMR (100.6 MHz, C_6D_6, 298 K): δ = 2.3 (Si(*C*H$_3$)$_3$), 10.6 (NC*C*H$_3$C*C*H$_3$N), 22.2 (*i*Pr-*C*H$_3$), 22.4 (*i*Pr-*C*H$_3$), 51.8 (*i*Pr-*C*H), 123.0 (N*C*CH$_3$*C*CH$_3$N), 159.8 (Me$_3$Si*C*≡*C*SiMe$_3$), 205.1 (N*C*N).

IR (ATR [cm^{-1}]): 2969 (m), 1659 (w), 1466 (w), 1438 (w), 1410 (w), 1358 (s), 1293 (m), 1253 (w), 1235 (w), 1216 (w), 1164 (vw), 1132 (w), 1106 (w), 1058 (w), 905 (vw), 849 (vs), 753 (m), 699 (w), 682 (w), 612 (vw), 587 (vw), 550 (w), 531 (w), 455 (vw).

[Ni(*i*Pr$_2$Im^{Me})$_2$(η^2-PhC≡CMe)] (III-6)

1-phenyl-1-propyne (26.0 μL, 24.3 mg, 209 μmol) was added at room temperature to a solution a 60:40 mixture of [Ni$_2$(*i*Pr$_2$Im^{Me})$_4$(*μ*-(η^2:η^2)-COD)] **7a** and [Ni(*i*Pr$_2$Im^{Me})$_2$(η^4-COD)] **7b** (94.0 mg, 193 μmol Ni) in 5 mL of benzene. The mixture was stirred for 2 h at room temperature and was then filtered through a pad of celite. All volatiles were removed in vacuo and the remaining residue was suspended in 4 mL of hexane. The product was collected by filtration, washed with 3 mL of hexane and dried in vacuo to give an orange powder (54.0 mg, 101 μmol, 52 %).

Elemental analysis $C_{31}H_{48}N_4Ni$ [535.45 g/mol] calculated (found): C 69.54 (67.95), H 9.04 (8.89), N 10.46 (10.17).

^{1}H NMR (400.1 MHz, C_6D_6, 298 K): δ = 1.20 (d, 12H, $^3J_{HH}$ = 7.1 Hz, *i*Pr-C*H*$_3$), 1.26 (d, 12H, $^3J_{HH}$ = 7.1 Hz, *i*Pr-C*H*$_3$), 1.82 (s, 6H, NCC*H*$_3$CC*H*$_3$N), 1.87 (s, 6H, NCC*H*$_3$CC*H*$_3$N),

2.90 (s, 3H, C≡CC*H*$_3$), 6.11 (sept, 2H, $^3J_{HH}$ = 7.1 Hz, ^{i}Pr-C*H*), 6.17 (sept, 2H, $^3J_{HH}$ = 7.1 Hz, ^{i}Pr-C*H*), 6.99 (m, 1H, aryl-C*H*$_{para}$), 7.25 (m, 2H, aryl-C*H*$_{meta}$), 7.54 (m, 1H, aryl-C*H*$_{ortho}$), 7.56 (m, 1H, aryl-C*H*$_{ortho}$).

^{13}C{^{1}H} NMR (100.6 MHz, C_6D_6, 298 K): δ = 10.5 (NC*C*H$_3$C*C*H$_3$N), 10.6 (NC*C*H$_3$C*C*H$_3$N), 15.3 (C≡C*C*H$_3$), 22.1 (^{i}Pr-*C*H$_3$), 22.3 (^{i}Pr-*C*H$_3$), 52.2 (^{i}Pr-*C*H), 52.4 (^{i}Pr-*C*H), 122.7 (aryl-*C*H$_{para}$), 123.2 (N*C*CH$_3$*C*CH$_3$N), 123.2 (N*C*CH$_3$*C*CH$_3$N), 127.1 (Ph*C*≡*C*), 127.9 (aryl-*C*H$_{meta}$), 129.5 (aryl-*C*H$_{ortho}$), 137.2 (C≡*C*Me), 138.8 (aryl-*C*$_{ipso}$), 203.32 (N*C*N).

IR (ATR [cm^{-1}]): 2967 (m), 2930 (w), 2872 (w), 2820 (w), 2082 (vw), 1760 (m), 1584 (m), 1478 (w), 1463 (w), 1436 (w), 1404 (w), 1385 (w), 1364 (w), 1344 (m), 1290 (s), 1270 (vs), 1208 (w), 1162 (w), 1099 (w), 1064 (w), 1025 (vw), 962 (w), 904 (w), 779 (w), 756 (s), 697 (s), 680 (m), 657 (w), 613 (vw), 552 (w), 530 (w), 460 (vw).

NMR Experiment for the Synthesis of [Ni(^{i}Pr$_2$Im^{Me})$_2$(η^2-HC≡CC$_3$H$_7$)] (III-7)

A Young's tab NMR tube was charged with a solution of a 60:40 mixture of [Ni$_2$(^{i}Pr$_2$Im^{Me})$_4$(μ-(η^2:η^2)-COD)] **7a** and [Ni(^{i}Pr$_2$Im^{Me})$_2$(η^4-COD)] **7b** (13.0 mg, 26.5 μmol Ni) in 0.6 mL of C_6D_6. 1-pentyne (2.84 μL, 1.96 mg, 28.8 μmol) was added at room temperature and the mixture was shaken to give a yellow solution. After 5 min the solution was analyzed *via* NMR spectroscopy and the formation of [Ni(^{i}Pr$_2$Im^{Me})$_2$(η^2-HC≡CC$_3$H$_7$)] **III-7** was detected.

^{1}H NMR (400.1 MHz, C_6D_6, 298 K): δ = 1.22 (t, 3H, $^3J_{HH}$ = 7.2 Hz, CH$_2$CH$_2$C*H*$_3$), 1.23 (d, 12H, $^3J_{HH}$ = 7.2 Hz, ^{i}Pr-C*H*$_3$), 1.29 (d, 12H, $^3J_{HH}$ = 7.2 Hz, ^{i}Pr-C*H*$_3$), 1.86 (s, 6H, NCC*H*$_3$CC*H*$_3$N), 1.88 (s, 6H, NCC*H*$_3$CC*H*$_3$N), 1.94 (tq, 2H, $^3J_{HH}$ = 7.2 Hz, CH$_2$C*H*$_2$CH$_3$), 3.13 (td, 2H, $^3J_{HH}$ = 7.2 Hz, $^4J_{HH}$ = 1.7 Hz, C*H*$_2$CH$_2$CH$_3$), 6.16 (sept, 2H, $^3J_{HH}$ = 7.2 Hz, ^{i}Pr-C*H*), 6.20 (sept, 2H, $^3J_{HH}$ = 7.2 Hz, ^{i}Pr-C*H*), 6.71 (t, 1H, $^4J_{HH}$ = 1.7 Hz, C≡C*H*).

^{13}C{^{1}H} NMR (100.6 MHz, C_6D_6, 298 K): δ = 10.4 (NC*C*H$_3$C*C*H$_3$N), 10.5 (NC*C*H$_3$C*C*H$_3$N), 14.8 (CH$_2$CH$_2$*C*H$_3$), 22.0 (^{i}Pr-*C*H$_3$), 22.2 (^{i}Pr-*C*H$_3$), 25.4 (CH$_2$*C*H$_2$CH$_3$), 32.8 (*C*H$_2$CH$_2$CH$_3$), 52.0 (^{i}Pr-*C*H), 52.1 (^{i}Pr-*C*H), 111.7 (C≡*C*H), 122.9 (N*C*CH$_3$*C*CH$_3$N), 138.1 (H$_7$C$_3$*C*≡C), 204.2 (N*C*N), 204.8 (N*C*N).

NMR Experiment for the Synthesis of [Ni(^{i}Pr$_2$Im^{Me})$_2$(η^2-HC≡CPh)] (III-8)

A Young's tab NMR tube was charged with a solution of a 60:40 mixture of [Ni$_2$(^{i}Pr$_2$Im^{Me})$_4$(μ-(η^2:η^2)-COD)] **7a** and [Ni(^{i}Pr$_2$Im^{Me})$_2$(η^4-COD)] **7b** (22.2 mg, 45.5 μmol Ni) in 0.6 mL of C_6D_6. Phenylacetylene (5.00 μL, 4.65 mg, 45.5 μmol) was added at room temperature and the mixture was shaken to give an orange solution. After 5 min the solution was analyzed *via* NMR spectroscopy and the formation of [Ni(^{i}Pr$_2$Im^{Me})$_2$(η^2-HC≡CPh)] **III-8** was detected.

^{1}H NMR (400.1 MHz, C_6D_6, 298 K): δ = 1.20 (d, 12H, $^3J_{HH}$ = 7.2 Hz, ^{i}Pr-CH_3), 1.24 (d, 12H, $^3J_{HH}$ = 7.2 Hz, ^{i}Pr-CH_3), 1.82 (s, 6H, NCCH_3CCH_3N), 1.87 (s, 6H, NCCH_3CCH_3N), 6.06 (sept, $^3J_{HH}$ = 7.2 Hz, 2H, ^{i}Pr-CH), 6.18 (sept, $^3J_{HH}$ = 7.2 Hz, 2H, ^{i}Pr-CH), 7.01 (m, 1H, aryl-CH_{para}), 7.22 (m, 2H, aryl-CH_{meta}), 7.63 (m, 2H, aryl-CH_{ortho}), 7.64 (s, 1H, C≡CH).

^{13}C{^{1}H} NMR (100.6 MHz, C_6D_6, 298 K): δ = 10.5 (NCCH$_3$CCH$_3$N), 22.0 (^{i}Pr-CH$_3$), 22.2 (^{i}Pr-CH$_3$), 52.3 (^{i}Pr-CH), 52.5 (^{i}Pr-CH), 123.3 (NCCH$_3$$CCH_3$N), 123.4 (N$CCH_3$$CCH_3$N), 123.7 (aryl-$CH_{para}$), 125.3 (C≡$C$H), 128.0 (aryl-$CH_{meta}$), 129.7 (aryl-$CH_{ortho}$), 138.6 (aryl-$C_{ipso}$), 202.3 (N$C$N), 202.5 (N$C$N).

[Ni(^{i}Pr$_2$Im^{Me})$_2$(η^2-HC≡C(*p*-Tol))] (III-9)

p-Tolylacetylene (27.6 μL, 25.3 mg, 217 μmol) was added at room temperature to a solution of a 60:40 mixture of [Ni$_2$(^{i}Pr$_2$Im^{Me})$_4$(μ-(η^2:η^2)-COD)] **7a** and [Ni(^{i}Pr$_2$Im^{Me})$_2$(η^4-COD)] **7b** (98.0 mg, 201 μmol Ni) in 5 mL of benzene. The mixture was stirred for 1 h at room temperature and was then filtered through a pad of celite. All volatiles were removed in vacuo and the remaining residue was suspended in 6 mL of hexane. The product was collected by filtration, washed with 3 mL of hexane and dried in vacuo to give a light brown powder (55.0 mg, 103 μmol, 51 %)

Elemental analysis $C_{31}H_{48}N_4Ni$ [535.45 g/mol] calculated (found): C 69.54 (68.95), H 9.04 (8.84), N 10.46 (9.99).

^{1}H NMR (400.1 MHz, C_6D_6, 298 K): δ = 1.23 (d, 12H, $^3J_{HH}$ = 6.9 Hz, ^{i}Pr-CH_3), 1.24 (d, 12H, $^3J_{HH}$ = 6.9 Hz, ^{i}Pr-CH_3), 1.84 (s, 6H, NCCH_3CCH_3N), 1.87 (s, 6H, NCCH_3CCH_3N), 2.14 (s, 3H, aryl-CH_3), 6.08 (sept, 2H, $^3J_{HH}$ = 6.9 Hz, ^{i}Pr-CH), 6.19 (sept, 2H, $^3J_{HH}$ =

6.9 Hz, ^{i}Pr-C*H*), 7.04 (d, 2H, $^{3}J_{HH}$ = 7.8 Hz, aryl-CH_{meta}), 7.58 (d, 2H, $^{3}J_{HH}$ = 7.8 Hz, aryl-CH_{ortho}), 7.61 (s, 1H, C≡C*H*).

^{13}C{^{1}H} NMR (100.6 MHz, C_6D_6, 298 K): δ = 10.4 (NC*C*H$_3$C*C*H$_3$N), 10.5 (NC*C*H$_3$C*C*H$_3$N), 21.4 (aryl-*C*H$_3$), 22.0 (^{i}Pr-*C*H$_3$), 22.2 (^{i}Pr-*C*H$_3$), 52.2 (^{i}Pr-*C*H), 52.5 (^{i}Pr-*C*H), 123.2 (N*C*CH$_3$*C*CH$_3$N), 123.3 (N*C*CH$_3$*C*CH$_3$N), 123.9 (C≡*C*H), 128.7 (aryl-*C*H$_{meta}$), 129.9 (aryl-*C*H$_{ortho}$), 132.6 (aryl-*C*(CH$_3$)), 135.4 (aryl-C_{ipso}), 138.1 (*p*-Tol*C*≡C), 202.6 (N*C*N), 202.9 (N*C*N).

IR (ATR [cm^{-1}]): 2964 (m), 2930 (w), 2158 (w), 2031 (w), 1976 (w), 1687 (w), 1668 (m), 1597 (wv), 1492 (w), 1462 (w), 1407 (w), 1383 (w), 1345 (s), 1291 (s), 1274 (vs), 1210 (w), 1162 (vw), 1128 (w), 1099 (vw), 1062 (w), 1018 (w), 961 (vw), 929 (w), 904 (vw), 869 (m), 817 (w), 748 (m), 718 (w), 679 (m), 644 (vw), 570 (m), 555 (w), 527 (w), 462 (vw), 418 (vw).

[Ni(^{i}Pr$_2$Im^{Me})$_2$(η^2-HC≡C(4-^{t}Bu-C$_6$H$_4$))] (III-10)

4-(*tert*-butyl)phenylacetylene (36.2 µL, 32.5 mg, 203 µmol) was added at room temperature to a solution of a 60:40 mixture of [Ni$_2$(^{i}Pr$_2$Im^{Me})$_4$(*µ*-(η^2:η^2)-COD)] **7a** and [Ni(^{i}Pr$_2$Im^{Me})$_2$(η^4-COD)] **7b** (92.0 mg, 184 µmol Ni) in 5 mL of benzene. The mixture was stirred for 1 h at room temperature and was then filtered through a pad of celite. All volatiles were removed in vacuo and the remaining residue was washed with 1 mL of hexane and dried in vacuo to give an orange powder (77.0 mg, 133 µmol, 72 %).

Elemental analysis $C_{34}H_{54}N_4Ni$ [577.53 g/mol] calculated (found): C 70.71 (71.92), H 9.43 (9.46), N 9.70 (8.63).

^{1}H NMR (400.1 MHz, C_6D_6, 298 K): δ = 1.23 (d, 12H, $^{3}J_{HH}$ = 7.0 Hz, ^{i}Pr-C*H*$_3$), 1,25 (s, 9H, C(C*H*$_3$)$_3$), 1.25 (d, 12H, $^{3}J_{HH}$ = 7.0 Hz, ^{i}Pr-C*H*$_3$), 1.84 (s, 6H, NCC*H*$_3$CC*H*$_3$N), 1.88 (s, 6H, NCC*H*$_3$CC*H*$_3$N), 6.09 (sept, 2H, $^{3}J_{HH}$ = 7.0 Hz, ^{i}Pr-C*H*), 6.21 (sept, 2H, $^{3}J_{HH}$ = 7.0 Hz, ^{i}Pr-C*H*), 7.27 (d, 2H, $^{3}J_{HH}$ = 8.5 Hz, aryl-CH_{meta}), 7.61 (d, 2H, $^{3}J_{HH}$ = 8.5 Hz, aryl-CH_{ortho}), 7.62 (s, 1H, C≡C*H*).

^{13}C{^{1}H} NMR (100.6 MHz, C_6D_6, 298 K): δ = 10.4 (NC*C*H$_3$C*C*H$_3$N), 10.5 (NC*C*H$_3$C*C*H$_3$N), 22.0 (^{i}Pr-*C*H$_3$), 22.1 (^{i}Pr-*C*H$_3$), 31.7 (C(*C*H$_3$)$_3$), 34.5 (*C*(CH$_3$)$_3$), 52.2 (^{i}Pr-*C*H), 52.5 (^{i}Pr-*C*H), 123.2 (N*C*CH$_3$*C*CH$_3$N), 123.3 (N*C*CH$_3$*C*CH$_3$N), 123.9 (C≡*C*H),

124.8 (aryl-*C*H$_{meta}$), 129.5 (aryl-*C*H$_{ortho}$), 135.6 (aryl-*C*$_{ipso}$), 138.0 (H$_4$C$_6$*C*≡C), 146.0 (aryl-*C*H$_{para}$), 202.6 (N*C*N), 202.9 (N*C*N).

IR (ATR [cm^{-1}]): 2964 (m), 2869 (w), 1683 (m), 1596 (vw), 1492 (w), 1460 (w), 1406 (w), 1382 (w), 1346 (vs), 1292 (m), 1275 (s), 1209 (w), 1163 (w), 1132 (w), 1101 (w), 1063 (vw), 1019 (m), 961 (vw), 905 (vw), 870 (w), 839 (w), 826 (w), 804 (w), 753 (vw), 688 (m), 677 (m), 649 (vw), 563 (w), 549 (w), 468 (vw).

[Ni(*i*Pr$_2$Im^{Me})$_2$(*η*^{2}-HC≡CCOOMe)] (III-11)

Methyl propiolate (27.2 *µ*L, 27.4 mg, 325 *µ*mol) was added at room temperature to a solution of a 60:40 mixture of [Ni$_2$(*i*Pr$_2$Im^{Me})$_4$(*µ*-(*η*^{2}:*η*^{2})-COD)] **7a** and [Ni(*i*Pr$_2$Im^{Me})$_2$(*η*^{4}-COD)] **7b** (154 mg, 316 *µ*mol Ni) in 5 mL of toluene. The mixture was stirred for 2 h at room temperature and was then filtered through a pad of celite. All volatiles were removed in vacuo and the remaining residue was suspended in 6 mL of hexane. The product was collected by filtration, washed with 3 mL of hexane and dried in vacuo to give an orange powder (66.0 mg, 131 *µ*mol, 42 %).

Elemental analysis C$_{26}$H$_{44}$N$_4$NiO$_2$ [503.36 g/mol] calculated (found): C 62.04 (61.94), H 8.81 (8.91), N 11.13 (10.90).

^{1}H NMR (400.1 MHz, C$_6$D$_6$, 298 K): *δ* = 1.13 (d, 12H, $^3J_{HH}$ = 7.1 Hz, *i*Pr-C*H*$_3$), 1.26 (d, 12H, $^3J_{HH}$ = 7.1 Hz, *i*Pr-C*H*$_3$), 1.79 (s, 6H, NCC*H*$_3$CC*H*$_3$N), 1.80 (s, 6H, NCC*H*$_3$CC*H*$_3$N), 3.66 (s, 3H, COOC*H*$_3$), 6.01 (sept, 2H, $^3J_{HH}$ = 7.1 Hz, *i*Pr-C*H*), 6.07 (sept, 2H, $^3J_{HH}$ = 7.1 Hz, *i*Pr-C*H*), 7.64 (s, 1H, C≡C*H*).

^{13}C{^{1}H} NMR (100.6 MHz, C$_6$D$_6$, 298 K): *δ* = 10.3 (NC*C*H$_3$C*C*H$_3$N), 10.4 (NC*C*H$_3$C*C*H$_3$N), 21.8 (*i*Pr-*C*H$_3$), 22.1 (*i*Pr-*C*H$_3$), 50.2 (COO*C*H$_3$), 52.5 (*i*Pr-*C*H), 52.8 (*i*Pr-*C*H), 123.7 (N*C*CH$_3$*C*CH$_3$N), 123.8 (N*C*CH$_3$*C*CH$_3$N), 129.6 (C≡*C*H), 131.9 (MeOOC*C*≡*C*), 173.1 (*C*OOCH$_3$), 198.6 (N*C*N), 198.8 (N*C*N).

IR (ATR [cm^{-1}]): 3018 (wv), 2968 (w), 2934 (w), 2162 (wv), 2056 (wv), 1702 (m), 1634 (m), 1464 (w), 1407 (m), 1381 (w), 1384 (w), 1300 (w), 1281 (w), 1213 (vw), 1157 (s), 1130 (w), 1102 (w), 1019 (w), 963 (vw), 896 (w), 849 (w), 777 (w), 754 (w), 735 (w), 688 (w), 665 (vw), 555 (w), 464 (vw), 430 (vw), 410 (wv).

Synthesis of III-9a (^{i}Pr C–H activation of **III-9**)

p-Tolylacetylene (43.6 *µ*L, 39.9 mg, 343 *µ*mol) was added at room temperature to a solution of a 60:40 mixture of [Ni$_2$(^{i}Pr$_2$Im^{Me})$_4$(*µ*-(*η*^{2}:*η*^{2})-COD)] **7a** and [Ni(^{i}Pr$_2$Im^{Me})$_2$(*η*^{4}-COD)] **7b** (148 mg, 304 *µ*mol Ni) in 6 mL of toluene. After 1 h at room temperature all volatiles were removed in vacuo to remove 1,5-cyclooctadiene and residual alkyne. The remaining residue was dissolved again in 6 mL of toluene and the solution was stirred for 72 h at 60 °C. The mixture was then filtered through a pad of celite, all volatiles were removed in vacuo and the remaining residue was suspended in 3 mL of hexane. The resulting precipitate was filtered off and the remaining solution was stored at -30 °C for 6 days. The supernatant solution was removed *via* syringe and the residue was dried in vacuo to give a red crystalline powder (30.0 mg, 56.0 *µ*mol, 18 %).

The obtained crystals of **III-9a** were also suitable for single-crystal X-ray diffraction.

^{1}H NMR (400.1 MHz, C_6D_6, 298 K): *δ* = 0.94 (d, 3H, $^{3}J_{HH}$ = 7.2 Hz, ^{i}Pr-C*H*$_3$), 1.21 (d, 6H, $^{3}J_{HH}$ = 7.2 Hz, ^{i}Pr-C*H*$_3$), 1.36 (d, 3H, $^{3}J_{HH}$ = 6.5 Hz, NCHCH$_2$C*H*$_3$), 1.48 (br, 3H, ^{i}Pr-C*H*$_3$), 1.62 (s, 3H, NCC*H*$_3$CC*H*$_3$N), 1.73 (s, 6H, NCC*H*$_3$CC*H*$_3$N), 1.83 (s, 3H, NCC*H*$_3$CC*H*$_3$N), 2.19 (s, 3H, aryl-C*H*$_3$), 2.64 (ddd, 1H, $^{2}J_{HH}$ = 3.5 Hz, $^{3}J_{HH}$ = 3.5 Hz, $^{3}J_{HH}$ = 13.5 Hz, C=CHC*H*$_2$) 2.78 (ddd, 1H, $^{2}J_{HH}$ = 3.5 Hz, $^{3}J_{HH}$ = 12.0 Hz, $^{3}J_{HH}$ = 13.5 Hz, C=CHC*H*$_2$), 2.91 (ddd, 1H, $^{3}J_{HH}$ = 3.5 Hz, $^{3}J_{HH}$ = 9.8 Hz, $^{3}J_{HH}$ = 12.0 Hz, C=C*H*CH$_2$), 3.85 (d, 1H, $^{3}J_{HH}$ = 9.8 Hz, *p*-Tol*H*C=C), 3.99 (m, 1H, NC*H*CH$_2$CH$_3$), 5.48 (br, 1H, *i*Pr-C*H*), 5.60 (sept, 1H, $^{3}J_{HH}$ = 7.2 Hz, ^{i}Pr-C*H*), 5.80 (br, 1H, ^{i}Pr-C*H*), 7.00 (d, 2H, $^{3}J_{HH}$ = 7.8 Hz, aryl-C*H*$_{meta}$), 7.32 (d, 2H, $^{3}J_{HH}$ = 7.8 Hz, aryl-C*H*$_{ortho}$).

^{13}C{^{1}H} NMR (100.6 MHz, C_6D_6, 298 K): *δ* = 8.7 (NC*C*H$_3$C*C*H$_3$N), 10.3 (NC*C*H$_3$C*C*H$_3$N), 10.8 (NC*C*H$_3$C*C*H$_3$N), 21.3 (aryl-*C*H$_3$), 21.5 (NCHCH$_2$*C*H$_3$), 22.1 (^{i}Pr-*C*H$_3$), 22.1 ^{i}Pr-*C*H$_3$), 22.2 (^{i}Pr-*C*H$_3$), 22.5 (^{i}Pr-*C*H$_3$), 22.7 (^{i}Pr-*C*H$_3$), 34.1 (C=*C*HCH$_2$), 40.2 (C=CH*C*H$_2$), 51.3 (^{i}Pr-*C*H), 51.9 (PhH*C*=C), 52.7 (^{i}Pr-*C*H), 54.1 (N*C*HCH$_2$CH$_3$), 120.9 (N*C*CH$_3$*C*CH$_3$N), 122.8 (N*C*CH$_3$*C*CH$_3$N), 123.9 (aryl-*C*H$_{meta}$), 124.4 (N*C*CH$_3$*C*CH$_3$N), 126.2 (aryl-*C*(CH$_3$)), 129.2 (aryl-*C*H$_{ortho}$) 150.5 (aryl-*C*$_{ipso}$), 191.7 (N*C*N), 204.5 (N*C*N).

NMR Experiment for the Synthesis of III-10a (^{i}Pr C–H activation of **III-10**)

A Young's tab NMR tube was charged with a solution of a 60:40 mixture of [Ni$_2$(^{i}Pr$_2$Im^{Me})$_4$(μ-(η^2:η^2)-COD)] **7a** and [Ni(^{i}Pr$_2$Im^{Me})$_2$(η^4-COD)] **7b** (15.0 mg, 30.5 μmol Ni) in 0.6 mL of C_6D_6. 4-(*tert*-butyl)phenylacetylene (4.02 μL, 3.68 mg, 31.7 μmol) was added at room temperature and the mixture was shaken to give a red solution. After 72 h at 60 °C the solution was analyzed *via* NMR spectroscopy and the formation of **III-10a** was detected.

[Ni(Mes$_2$Im)$_2$(η^2-MeC≡CMe)] (III-12)

2-butyne (100 μL, 69.0 mg, 1.28 mmol) was added at 0 °C to a suspension of [Ni(Mes$_2$Im)$_2$] **1** (110 mg, 165 μmol) in 8 mL of hexane. A yellow precipitate was formed which was collected by filtration immediately and dried in vacuo to give a yellow powder (45.0 mg, 62.5 μmol, 38 %).

Yellow crystals of [Ni(Mes$_2$Im)$_2$(η^2-MeC≡CMe)] **III-12** suitable for single-crystal X-ray diffraction were obtained from a saturated solution in hexane at -30 °C.

Elemental analysis $C_{46}H_{54}N_4Ni$ [721.66 g/mol] calculated (found): C 76.56 (74.25), H 7.54 (7.50), N 7.76 (7.51).

^{1}H NMR (400.1 MHz, THF-d$_8$, 193 K): δ = 1.74 (s, 6H, H_3CC≡CCH_3), 1.78 (s, 12H, aryl$_{NHC}$-CH_{3ortho}), 2.04 (s, 12H, aryl$_{NHC}$-CH_{3ortho}), 2.36 (s, 12H, aryl$_{NHC}$-CH_{3para}), 6.52 (s, 4H, NC*H*C*H*N), 6.67 (s, 8H, aryl$_{NHC}$-CH_{meta}).

^{13}C{^{1}H} NMR (100.6 MHz, THF-d$_8$, 193 K): δ = 13.7 (H$_3$*C*C≡C*C*H$_3$), 19.5 (aryl$_{NHC}$-*C*H$_{3ortho}$), 19.6 (aryl$_{NHC}$-*C*H$_{3ortho}$), 21.4 (aryl$_{NHC}$-*C*H$_{3para}$), 118.6 (*C*≡*C*), 122.3 (N*C*H*C*HN), 129.0 (aryl$_{NHC}$-*C*H$_{meta}$), 135.9 (aryl$_{NHC}$-*C*CH$_{3ortho/para}$), 136.0 (aryl$_{NHC}$-*C*CH$_{3ortho/para}$), 136.1 (aryl$_{NHC}$-*C*CH$_{3ortho/para}$), 139.3 (aryl$_{NHC}$-*C*$_{ipso}$), 207.0 (N*C*N).

IR (ATR [cm^{-1}]): 2911 (vw), 2837 (vw), 1808 (vw), 1483 (m), 1434 (w), 1375 (m), 1245 (vs), 1158 (vw), 1092 (vw), 1060 (m), 1031 (m), 966 (w), 914 (m), 847 (s), 713 (w), 679 (vs), 630 (vw), 591 (w), 572 (m), 446 (vw), 425 (m).

[Ni(Mes$_2$Im)$_2$(η^2-MeOOCC≡CCOOMe)] (III-13)

Dimethyl acetylene dicarboxylate (28.9 *µ*L, 33.5 mg, 236 *µ*mol) was added at 0 °C to a suspension of [Ni(Mes$_2$Im)$_2$] **1** (121 mg, 181 *µ*mol) in 5 mL of pentane. Immediately a brown precipitate was formed, and the mixture was then stirred for 1 h at 0 °C. The supernatant solution was removed *via* syringe and the residue was dried in vacuo to give a light brown powder (140 mg, 173 *µ*mol, 96 %).

Brown crystals of [Ni(Mes$_2$Im)$_2$(η^2-MeOOCC≡CCOOMe)] **III-13** suitable for single-crystal X-ray diffraction were obtained by layering a saturated benzene solution with hexane at room temperature.

Elemental analysis $C_{48}H_{54}N_4NiO_4$ [809.68 g/mol] calculated (found): C 71.20 (70.80), H 6.72 (6.90), N 6.92 (6.75).

^{1}H NMR (400.1 MHz, C_6D_6, 298 K): δ = 2.06 (s, 24H, aryl$_{NHC}$-CH_{3ortho}), 2.23 (s, 12H, aryl$_{NHC}$-CH_{3para}), 3.47 (s, 6H, COOCH_3), 6.11 (s, 4H, NC*H*C*H*N), 6.61 (s, 8H, aryl$_{NHC}$-CH_{meta}).

^{13}C{^{1}H} NMR (100.6 MHz, C_6D_6, 298 K): δ = 19.2 (aryl$_{NHC}$-*C*H$_{3ortho}$), 21.3 (aryl$_{NHC}$-*C*H$_{3para}$), 50.4 (COO*C*H$_3$), 123.4 (N*C*H*C*HN), 129.3 (aryl$_{NHC}$-*C*H$_{meta}$), 136.0 (aryl$_{NHC}$-*C*CH$_{3ortho}$), 136.6 (aryl$_{NHC}$-*C*CH$_{3para}$), 136.7 (*C*≡*C*), 138.4 (aryl$_{NHC}$-*C*$_{ipso}$), 165.9 (*C*OOMe), 198.2 (N*C*N).

IR (ATR [cm^{-1}]): 3161 (vw), 3116 (w), 2981 (w), 2914 (w), 2853 (w), 1713 (m), 1680 (s), 1590 (w), 1484 (m), 1441 (m), 1386 (m), 1290 (m), 1258 (m), 1193 (s), 1180 (s), 1107 (m), 1036 (m), 1015 (m), 919 (m), 844 (s), 740 (m), 693 (m), 569 (m), 424 (m).

[Ni(Mes$_2$Im)$_2$(η^2-PhC≡CMe)] (III-14)

1-phenyl-1-propyne (29.3 *µL*, 27.0 mg, 232 *µ*mol) was added at 0 °C to a suspension of [Ni(Mes$_2$Im)$_2$] **1** (155 mg, 232 *µ*mol) in 6 mL of pentane. Immediately an orange precipitate was formed, and the mixture was then stirred for 1 h at 0 °C. The supernatant solution was removed *via* syringe and the residue was dried in vacuo to give an orange powder (155 mg, 198 *µ*mol, 85 %).

Orange crystals of [Ni(Mes$_2$Im)$_2$(η^2-PhC≡CMe) **III-14** suitable for single-crystal X-ray diffraction were obtained from a saturated solution in pentane at -30 °C.

Elemental analysis $C_{51}H_{56}N_4Ni$ [783.73 g/mol] calculated (found): C 78.16 (77.89), H 7.20 (7.53), N 7.15 (7.05).

^{1}H NMR (500.1 MHz, THF-d_8, 193 K): δ = 1.77 (s, 12H, aryl$_{NHC}$-CH_{3ortho}), 1.82 (s, 6H, aryl$_{NHC}$-CH_{3ortho}), 2.10 (s, 6H, aryl$_{NHC}$-CH_{3ortho}), 2.14 (s, 3H, C≡CCH_3), 2.34 (s, 6H, aryl$_{NHC}$-CH_{3para}), 2.37 (s, 6H, aryl$_{NHC}$-CH_{3para}), 6.50 (s, br, 2H, aryl$_{NHC}$-CH_{meta}), 6.53 (s, br, 4H, aryl$_{NHC}$-CH_{meta}), 6.65 (d, 2H, $^3J_{HH}$ = 7.8 Hz, aryl-CH_{ortho}), 6.70 (s, br, 2H, aryl$_{NHC}$-CH_{meta}), 6.73 (m, 1H, aryl-CH_{para}), 6.77 (s, 2H, NCHCHN), 6.82 (s, 2H, NCHCHN), 6.91 (m, 2H, aryl-CH_{meta}).

^{13}C{^{1}H} NMR (125.8 MHz, THF-d_8, 193 K): δ = 16.9 (C≡CCH$_3$), 19.5 (aryl$_{NHC}$-CH$_{3ortho}$), 19.6 (aryl$_{NHC}$-CH$_{3ortho}$), 19.9 (aryl$_{NHC}$-CH$_{3ortho}$), 20.5 (aryl$_{NHC}$-CH$_{3ortho}$), 21.3 (aryl$_{NHC}$-CH$_{3para}$), 21.4 (aryl$_{NHC}$-CH$_{3para}$), 122.6 (aryl-CH$_{para}$), 123.0 (NCHCHN), 123.9 (PhC≡C), 127.0 (aryl-CH$_{meta}$), 129.0 (aryl$_{NHC}$-CH$_{meta}$), 129.1 (aryl$_{NHC}$-CH$_{meta}$), 129.3 (aryl$_{NHC}$-CH$_{meta}$), 129.6 (aryl$_{NHC}$-CH$_{meta}$), 131.0 (aryl-CH$_{ortho}$), 134.2 (aryl-C_{ipso}), 135.6 (C≡CMe), 135.8 (aryl$_{NHC}$-CCH$_{3ortho}$), 136.0(aryl$_{NHC}$-CCH$_{3ortho}$), 136.1 (aryl$_{NHC}$-CCH$_{3ortho}$), 136.2 (aryl$_{NHC}$-CCH$_{3ortho}$), 136.3 (aryl$_{NHC}$-CCH$_{3para}$), 136.4 (aryl$_{NHC}$-CCH$_{3para}$), 139.0 (aryl$_{NHC}$-C_{ipso}), 139.1 (aryl$_{NHC}$-C_{ipso}), 205.8 (NCN), 206.0 (NCN).

IR (ATR [cm^{-1}]): 2949 (w), 2912 (w), 2837 (w), 1756 (m), 1585 (m), 1480 (s), 1434 (m), 1375 (s), 1262 (vs), 1245 (vs), 1158 (w), 1093 (w), 1063 (m), 1033 (m), 967 (w), 916 (m), 846 (vs), 757 (m), 716 (m), 700 (m), 682 (vs), 653 (m), 571 (m), 521 (w), 423 (m).

[Ni(Mes$_2$Im)$_2$(η^2-HC≡C(4-^{t}Bu-C$_6$H$_4$))] (III-15)

4-(*tert*-butyl)phenylacetylene (44.5 μL, 39.1 mg, 247 μmol) was added at 0 °C to a suspension of [Ni(Mes$_2$Im)$_2$] **1** (165 mg, 247 μmol) in 6 mL of pentane. Immediately an orange precipitate was formed, and the mixture was then stirred for 1 h at 0 °C. The supernatant solution was removed *via* syringe and the residue was dried in vacuo to give an orange powder (166 mg, 201 μmol, 81 %).

Red crystals of [Ni(Mes$_2$Im)$_2$(η^2-HC≡C(4-^{t}Bu-C$_6$H$_4$))] **III-15** suitable for single-crystal X-ray diffraction were obtained from a saturated solution in hexane at -30 °C.

Elemental analysis $C_{54}H_{62}N_4Ni$ [825.81 g/mol] calculated (found): C 78.54 (78.13), H 7.57 (8.16), N 6.78 (5.75).

^{1}H NMR (400.1 MHz, THF-d_8, 193 K): δ = 1.22 (s, 9H, ^{t}Bu-CH_3), 1.76 (s, br, 6H, aryl$_{NHC}$-CH_{3ortho}), 1.82 (s, br, 6H, aryl$_{NHC}$-CH_{3ortho}), 1.85 (s, br, 12H, aryl$_{NHC}$-CH_{3ortho}), 2.34 (s, 12H, aryl$_{NHC}$-CH_{3para}), 6.11 (s, 1H, *H*C≡C), 6.59 (s, br, 2H, aryl$_{NHC}$-CH_{meta}), 6.61 (s, br, 2H, aryl-C$_6H_4$), 6.63 (s, br, 6H, aryl$_{NHC}$-CH_{meta}), 6.78 (s, 2H, NC*H*C*H*N), 6.84 (s, 2H, NC*H*C*H*N), 6.94 (d, 2H, $^3J_{HH}$ = 8.5 Hz, aryl-C$_6H_4$).

^{13}C{^{1}H} NMR (100.6 MHz, THF-d_8, 193 K): δ = 19.2 (aryl$_{NHC}$-*C*H$_{3ortho}$), 19.7 (aryl$_{NHC}$-*C*H$_{3ortho}$), 20.8 (aryl$_{NHC}$-*C*H$_{3ortho}$), 21.1 (aryl$_{NHC}$-*C*H$_{3para}$), 21.3 (aryl$_{NHC}$-*C*H$_{3para}$), 31.6 (C(*C*H$_3$)$_3$), 34.7 (*C*(CH$_3$)$_3$), 122.6 (N*C*H*C*HN), 122.8 (H*C*≡C), 123.0 (N*C*H*C*HN), 123.8 (*C*$_6$H$_4$), 129.1 (aryl$_{NHC}$-*C*H$_{meta}$), 129.2 (aryl$_{NHC}$-*C*H$_{meta}$), 129.6 (aryl$_{NHC}$-*C*H$_{meta}$), 130.7 (aryl-*C*$_{ipso}$), 130.9 (*C*$_6$H$_4$), 131.5 (C≡*C*(C$_6$H$_4$)), 135.5 (aryl$_{NHC}$-*C*CH$_{3para}$), 136.4 (aryl$_{NHC}$-*C*CH$_{3ortho}$), 136.5 (aryl$_{NHC}$-*C*CH$_{3ortho}$), 136.8 (aryl$_{NHC}$-*C*CH$_{3ortho}$), 139.0 (aryl$_{NHC}$-*C*$_{ipso}$), 139.4 (aryl$_{NHC}$-*C*$_{ipso}$), 145.6 (aryl-*C*(^{t}Bu)), 202.2 (N*C*N), 206.5 (N*C*N).

IR (ATR [cm^{-1}]): 2953 (m), 2917 (m), 2856 (m), 1701 (w), 1596 (w), 1548 (s), 1485 (m), 1373 (m), 1291 (m), 1258 (vs), 1242 (vs), 1158 (w), 1086 (s), 1063 (m), 915 (m), 848 (s), 837 (s), 725 (m), 680 (vs), 571 (s), 546 (m), 422 (m).

[Ni(Mes$_2$Im)$_2$(η^2-HC≡CCOOMe)] (III-16)

Methyl propiolate (20.7 μL, 20.8 mg, 247 μmol) was added at 0 °C to a suspension of [Ni(Mes$_2$Im)$_2$] **1** (127 mg, 190 μmol) in 5 mL of pentane. Immediately a brown precipitate was formed, and the mixture was then stirred for 1 h at 0 °C. The supernatant solution was removed *via* syringe and the residue was dried in vacuo to give a light brown powder (130 mg, 173 μmol, 91 %).

Elemental analysis $C_{46}H_{52}N_4NiO_2$ [751.64 g/mol] calculated (found): C 73.51 (73.53), H 6.97 (7.11), N 7.45 (7.27).

^{1}H NMR (400.1 MHz, C_6D_6, 298 K): δ = 1.92 (s, 12H, aryl$_{NHC}$-CH_{3ortho}), 2.12 (s, 12H, aryl$_{NHC}$-CH_{3ortho}), 2.23 (s, 6H, aryl$_{NHC}$-CH_{3para}), 2.26 (s, 6H, aryl$_{NHC}$-CH_{3para}), 3.50 (s, 3H, COOCH_3), 6.06 (s, 2H, NC*H*C*H*N), 6.18 (s, 2H, NC*H*C*H*N), 6.60 (s, 4H, aryl$_{NHC}$-CH_{meta}), 6.66 (s, 4H, aryl$_{NHC}$-CH_{meta}), 6.94 (s, 1H, *H*C≡C).

^{13}C{^{1}H} NMR (100.6 MHz, C_6D_6, 298 K): δ = 19.0 (aryl$_{NHC}$-*C*H$_{3ortho}$), 19.1 (aryl$_{NHC}$-*C*H$_{3ortho}$), 21.3 (aryl$_{NHC}$-*C*H$_{3para}$), 50.2 (COO*C*H$_3$), 122.3 (N*C*H*C*HN), 122.6 (N*C*H*C*HN), 129.2 (aryl$_{NHC}$-*C*H$_{meta}$), 134.6 (H*C*≡C), 135.5 (aryl$_{NHC}$-*C*CH$_{3ortho}$), 136.3 (aryl$_{NHC}$-

*C*CH$_{3\,para}$), 136.6 (C≡*C*COOMe), 138.5 (aryl$_{NHC}$-*C*$_{ipso}$), 138.8 (aryl$_{NHC}$-*C*$_{ipso}$), 165.8 (*C*OOMe), 201.8 (N*C*N), 202.4 (N*C*N).

IR (ATR [cm^{-1}]): 2947 (w), 2912 (w), 2851 (w), 1711 (m), 1656 (m), 1484 (m), 1380 (m), 1284 (m), 1274 (m), 1256 (m), 1160 (vs), 1070 (m), 1034 (m), 968 (w), 917 (m), 846 (s), 724 (m), 689 (s), 577 (m), 424 (m).

General Procedure for the Synthesis of substituted benzene derivatives

In a Young's tab NMR tube [Ni(Mes$_2$Im)$_2$] **1** (10.0 mg, 15.0 *µ*mol, 5 mol%) was dissolved in 0.7 mL of C_6D_6. The alkyne (1 equiv.) was then added to the solution. The reaction mixture was heated to 60 °C and the reaction progress was monitored hourly by ^{1}H NMR spectroscopy. After the alkyne consumption was complete the reaction mixture was poured in air into 5 mL of benzene and was then filtered through a pad of silica gel. The filtrate was evaporated in vacuo and the products were determined by NMR spectroscopy and GC/MS.

Hexamethylbenzene

^{1}H NMR (400.1 MHz, C_6D_6, 298 K): *δ* = 2.13 (s, 18H, $C_6(CH_3)_6$).

^{13}C{^{1}H} NMR (100.6 MHz, C_6D_6, 298 K): *δ* = 16.9 ($C_6(CH_3)_6$), 131.8 ($C_6(CH_3)_6$).

GC/MS Ret.: 7.72 min; (m/z): 162 [M]$^+$.

Hexapropylbenzene

^{1}H NMR (400.1 MHz, C_6D_6, 298 K): *δ* = 1.02 (t, 18H, $^3J_{HH}$ = 7.4 Hz, $CH_2CH_2CH_3$), 1.62 (m, 12H, $CH_2CH_2CH_3$), 2.65 (m, 12H, $CH_2CH_2CH_3$).

^{13}C{^{1}H} NMR (100.6 MHz, C_6D_6, 298 K): *δ* = 15.4 ($CH_2CH_2CH_3$), 25.7 ($CH_2CH_2CH_3$), 32.7 ($CH_2CH_2CH_3$), 137.0 (aryl-C_q).

GC/MS Ret.: 10.70 min; (m/z): 330 [M]$^+$.

Hexamethyl-benzenehexacarboxylate

^{1}H NMR (400.1 MHz, C_6D_6, 298 K): δ = 3.43 (s, 18H, OC*H*$_3$).

^{13}C{^{1}H} NMR (100.6 MHz, C_6D_6, 298 K): δ = 52.9 (O*C*H$_3$), 134.5 (aryl-*C*$_q$), 165.5 (*C*OOMe).

GC/MS Ret.: 13.39 min; (m/z): 395 $[M\text{-}OMe]^+$.

Trimethyl-1,2,4-benzenetricarboxylate and

Trimethyl-1,3,5-benzenetricarboxylate

Trimethyl-1,2,4-benzenetricarboxylate (85 %)

^{1}H NMR (400.1 MHz, C_6D_6, 298 K): δ = 3.38 (s, 3H, OC*H*$_3$), 3.44 (s, 3H, OC*H*$_3$), 3.53 (s, 3H, OC*H*$_3$), 7.37 (d, 1H, $^{3}J_{HH}$ = 8.0 Hz, aryl-6-C*H*), 7.90 (dd, 1H, $^{3}J_{HH}$ = 8.0 Hz, $^{4}J_{HH}$ = 1.6 Hz aryl-5-C*H*), 8.52 (d, 1H, $^{4}J_{HH}$ = 1.6 Hz, aryl-3-C*H*).

^{13}C{^{1}H} NMR (100.6 MHz, C_6D_6, 298 K): δ = 51.9 (O*C*H$_3$), 52.3 (O*C*H$_3$), 52.4 (O*C*H$_3$), 129.1 (aryl-6-*C*H), 130.5 (aryl-3-*C*H), 132.3 (aryl-5-*C*H), 132.3 (aryl-2-*C*$_q$), 132.7 (aryl-1-*C*$_q$), 137.0 (aryl-4-*C*$_q$), 165.0 (4-*C*OOMe), 166.6 (2-*C*OOMe), 167.4 (1-*C*OOMe).

GC/MS Ret.: 9.92 min; (m/z): 252 $[M]^+$.

Trimethyl-1,3,5-benzenetricarboxylate (15 %)

^{1}H NMR (400.1 MHz, C_6D_6, 298 K): δ = 3.41 (s, 9H, OC*H*$_3$), 9.02 (s, 3H, aryl-2,4,6-C*H*).

^{13}C{^{1}H} NMR (100.6 MHz, C_6D_6, 298 K): δ = 52.0 (O*C*H$_3$), 131.7 (aryl-1,3,5-*C*$_q$), 134.6 (aryl-2,4,6-*C*H), 165.1 (1,3,5-*C*OOMe).

GC/MS Ret.: 10.26 min; (m/z): 252 $[M]^+$.

1,2,4-Triphenylbenzene and 1,3,5-Triphenylbenzene

GC/MS Ret.: 13.64, 14.52 min; (m/z): 306 $[M]^+$.

1,2,4-Tripropylbenzene and 1,3,5-Tripropylbenzene

GC/MS Ret.: 7.77, 7.87 min; (m/z): 204 $[M]^+$.

Hexaphenylbenzene

In a Young's tab NMR tube $[Ni(Mes_2Im)_2]$ **1** (3.00 mg, 1 mol%) and diphenylacetylene (80.1 mg, 449 *µ*mol) were dissolved in 0.7 mL C_6D_6. The reaction mixture was sonicated for five minutes whereby a colorless solid precipitated. The supernatant solution was removed *via* syringe and the residue was washed with hexane and dried in vacuo to give an off-white powder (71.0 mg, 133 *µ*mol, 88 %).

Elemental analysis $C_{42}H_{30}$ [534.70 g/mol] calculated (found): C 94.34 (94.28), H 5.66 (5.81).

^{1}H NMR (400.1 MHz, C_6D_6, 298 K): δ = 6.73 (m, 6H, aryl-C_6H_{5para}), 6.83 (m, 12H, aryl-C_6H_{5meta}), 7.12 (m, 12H, aryl-C_6H_{5ortho}).

^{13}C{^{1}H} NMR (100.6 MHz, C_6D_6, 298 K): δ = 125.9 (aryl-C_6H_{5para}), 127.3 (aryl-C_6H_{5meta}), 132.0 (aryl-C_6H_{5ortho}), 141.2 (aryl-C_q), 141.3 (aryl-C_q).

GC/MS Ret.: 14.33 min; (m/z): 534 $[M]^+$.

7.5 Synthetic Procedures for Chapter IV

$[FeCp_2][BPh_4]$

Ferrocene (1.50 g, 8.06 mmol) was dissolved in 30 mL of concentrated sulfuric acid and stirred for 30 min at room temperature. The blue solution was then poured into 300 mL of water and a solution of sodium tetraphenylborate (3.28 g, 9.59 mmol) in 150 mL of water was added. The mixture was then stirred for 2 h at room temperature whereby a light blue preticipate was formed. The product was collected by filtration and washed with 300 mL of water, 100 mL of ethanol and 150 mL of diethylether, successively. The product was dried in vacuo to give a light blue powder (3.30 g, 6.53 mmol, 81 %).

$[Ni^{I}(Mes_2Im)_2][BPh_4]$ (**IV-1$^+$**)

$[Ni(Mes_2Im)_2]$ **1** (200 mg, 300 μmol) and ferrocenium tetraphenylborate (151 mg, 300 μmol) were dissolved in 10 mL of THF. The reaction mixture was stirred for 2 h at room temperature and was then filtered through a pad of celite. All volatiles were removed in vacuo and the remaining residue was suspended in 5 mL of hexane. The product was collected by filtration, washed with 5 mL of benzene and again with 15 mL of hexane. The product was dried in vacuo to give an off-white powder (240 mg, 243 μmol, 81 %).

Colorless crystals of $[Ni^{I}(Mes_2Im)_2][BPh_4]$ **IV-1$^+$** suitable for single-crystal X-ray diffraction were obtained by slow diffusion of hexane into a saturated THF solution of **IV-1$^+$**.

Elemental analysis $C_{66}H_{68}BN_4Ni$ [986.80 g/mol] calculated (found): C 80.33 (79.58), H 6.95 (7.04), N 5.68 (5.79).

HRMS-LIFDI m/z (%) calculated for $[C_{42}H_{48}N_4Ni]^+$: 666.3233(100) $[M]^+$; found: 666.3213(100) $[M]^+$, 305.2006(10) $[Mes_2Im+H]^+$.

^{1}H NMR (400.1 MHz, THF-d_8, 298 K): δ = 0-2.5 (vbr, s), 1.31 (br, s), 4.81 (br, s), 6.76 (br, s, 4H, $B(C_6H_5)_4$), 6.93 (br, s, 8H, $B(C_6H_5)_4$), 7.47 (br, s, 8H, $B(C_6H_5)_4$), 17.87 (vbr, s).

^{11}B NMR (128.5 MHz, THF-d_8, 298 K): δ = -6.32 (s, 1B, BPh_4).

IR (ATR [cm^{-1}]): 3122 (vw), 3054 (vw), 2913 (vw), 1579 (vw), 1484 (w), 1406 (vw), 1377 (vw), 1334 (vw), 1241 (w), 1031 (w), 925 (vw), 850 (m), 741 (m), 729 (m), 705 (vs), 612 (m), 573 (w), 475 (vw), 435 (vw).

Magnetic moment (Evans): μ_{eff} (THF-d_8, 298 K) = 2.42 μ_B.

$[Ni^{I}(Mes_2Im^{H2})_2][BPh_4]$ (IV-2$^+$)

$[Ni(Mes_2Im^{H2})_2]$ **2** (200 mg, 298 μmol) and ferrocenium tetraphenylborate (150 mg, 298 μmol) were dissolved in 10 mL of THF. The reaction mixture was stirred for 2 h at room temperature and was then filtered through a pad of celite. All volatiles were removed in vacuo and the remaining residue was suspended in 5 mL of benzene. The product was collected by filtration, washed with 5 mL of benzene and with 15 mL of hexane. The product was dried in vacuo to give a colorless powder (260 mg, 262 μmol, 88 %).

Colorless crystals of $[Ni^{I}(Mes_2Im^{H2})_2][BPh_4]$ **IV-2$^+$** suitable for single-crystal X-ray diffraction were obtained by slow evaporation of a saturated THF solution.

Elemental analysis $C_{66}H_{72}BN_4Ni$ [990.83 g/mol] calculated (found): C 80.01 (79.99), H 7.32 (7.46), N 5.65 (5.53).

HRMS-LIFDI m/z (%) calculated for $[C_{42}H_{52}N_4Ni]^+$: 670.3546(100) $[M]^+$; found: 670.3529(60) $[M]^+$, 307.2162(10) $[Mes_2Im^{H2}+H]^+$.

^{1}H NMR (400.1 MHz, THF-d_8, 298 K): δ = -3.0-0.5 (vbr, s), -0.62 (br, s), 0.76 (br, s), 7.15 (br, s, 4H, $B(C_6\mathit{H}_5)_4$), 7.43 (br, s, 8H, $B(C_6\mathit{H}_5)_4$), 8.25 (br, s, 8H, $B(C_6\mathit{H}_5)_4$), 21.08 (vbr, s).

^{11}B NMR (128.5 MHz, THF-d_8, 298 K): δ = -5.47 (s, 1B, $\mathit{B}Ph_4$).

IR (ATR [cm^{-1}]): 3055 (w), 3033 (w), 2998 (vw), 2981 (w), 2911 (w), 2852 (vw), 1609 (vw), 1579 (vw), 1487 (s), 1453 (m), 1425 (m), 1374 (w), 1319(w), 1299 (w), 1266 (s), 1178 (w), 1133 (w), 1067 (vw), 1030 (m), 1011 (w), 916 (vw), 848 (m), 811 (w), 743 (m), 739 (s), 705 (vs), 682 (w), 612 (s), 571 (m), 529 (vw), 500 (vw), 464 (w), 425 (w).

Magnetic moment (Evans): μ_{eff} (THF-d_8, 298 K) = 2.49 μ_B.

[Ni^{I}(Dipp$_2$Im)$_2$][BPh$_4$] (IV-3$^+$)

[Ni(Dipp$_2$Im)$_2$] **3** (190 mg, 227 μmol) and ferrocenium tetraphenylborate (115 mg, 227 μmol) were dissolved in 10 mL of THF. The reaction mixture was stirred for 2 h at room temperature and was then filtered through a pad of celite. All volatiles were removed in vacuo and the remaining residue was suspended in 5 mL of benzene. The product was collected by filtration, washed with 5 mL of benzene and with 15 mL of hexane. The product was dried in vacuo to give a colorless powder (211 mg, 183 μmol, 81 %).

Colorless crystals of [Ni^{I}(Dipp$_2$Im)$_2$][BPh$_4$] **IV-3$^+$** suitable for single-crystal X-ray diffraction were obtained by storing a saturated solution in THF at -30 °C.

Elemental analysis $C_{78}H_{92}BN_4Ni$ [1155.13 g/mol] calculated (found): C 81.10 (80.51), H 8.03 (8.02), N 4.85 (4.74).

HRMS-LIFDI m/z (%) calculated for $[C_{54}H_{72}N_4Ni]^+$: 834.5111(100) $[M]^+$; found: 834.5095(40) $[M]^+$, 389.2948(100) [Dipp$_2$Im+H]$^+$.

^{1}H NMR (400.1 MHz, THF-d$_8$, 298 K): δ = -51.07 (vbr, s), -11.57 (br, s), -8.71 (br, s), 7.10 (br, s, 4H, B(C$_6$*H*$_5$)$_4$), 7.50 (br, s, 8H, B(C$_6$*H*$_5$)$_4$), 8.18 (br, s), 8.52 (br, s, 8H, B(C$_6$*H*$_5$)$_4$), 37.24 (vbr, s), 71.84 (vbr, s).

^{11}B NMR (128.5 MHz, THF-d$_8$, 298 K): δ = -5.15 (s, 1B, *B*Ph$_4$).

IR (ATR [cm^{-1}]): 3150 (vw), 3054 (vw), 2962 (w), 2926 (vw), 2868 (vw), 1580 (vw), 1561 (vw), 1460 (m), 1425 (vw), 1399 (w), 1385 (vw), 1364 (w), 1327 (w), 1270 (vw), 1211 (vw), 1181 (vw), 1107 (vw), 1061 (w), 1032 (vw), 940 (w), 842 (vw), 802 (m), 758 (s), 746 (m), 731 (s), 703 (vs), 612 (s), 551 (vw), 469 (w), 454 (w).

Magnetic moment (Evans): μ_{eff} (THF-d$_8$, 298 K) = 3.15 μ_B.

[Ni^{I}(Dipp$_2$Im^{H2})$_2$][BPh$_4$] (IV-4$^+$)

[Ni(Dipp$_2$Im^{H2})$_2$] **4** (200 mg, 238 μmol) and ferrocenium tetraphenylborate (120 mg, 238 μmol) were dissolved in 10 mL of THF. The reaction mixture was stirred for 2 h at room temperature and was then filtered through a pad of celite. All volatiles were removed in vacuo and the remaining residue was suspended in 5 mL of benzene. The product was collected by filtration, washed with 5 mL of benzene and with 15 mL of

hexane. The product was dried in vacuo to give a colorless powder (245 mg, 211 μmol, 89 %).

Colorless crystals of $[Ni^{I}(Dipp_2Im^{H2})_2][BPh_4]$ **IV-4$^+$** suitable for single-crystal X-ray diffraction were obtained by storing a saturated solution in THF at -30 °C.

Elemental analysis $C_{78}H_{96}BN_4Ni$ [1159.16 g/mol] calculated (found): C 80.82 (80.62), H 8.35 (8.65), N 4.83 (4.62).

HRMS-LIFDI m/z (%) calculated for $[C_{54}H_{76}N_4Ni]^+$: 838.5424(100) $[M]^+$; found: 838.5399(10) $[M]^+$, 391.3097(100) $[Dipp_2Im^{H2}+H]^+$.

^{1}H NMR (400.1 MHz, THF-d_8, 298 K): δ = -48.19 (vbr, s), -9.21 (br, s), -7.23 (br, s), 6.01 (br, s), 7.74 (br, s, 4H, $B(C_6\mathit{H}_5)_4$), 8.26 (br, s, 8H, $B(C_6\mathit{H}_5)_4$), 9.49 (br, s, 8H, $B(C_6\mathit{H}_5)_4$), 36.71 (vbr, s), 59.96 (vbr, s).

^{11}B NMR (128.5 MHz, THF-d_8, 298 K): δ = -4.15 (s, 1B, $\mathit{B}Ph_4$).

IR (ATR [cm^{-1}]): 3053 (w), 2962 (m), 2926 (w), 2869 (w), 1580 (vw), 1472 (m), 1455 (s), 1425 (m), 1384 (w), 1363 (w), 1324 (w), 1270 (s), 1242 (w), 1180 (w), 1133 (vw), 1103 (vw), 1058 (w), 1032 (w), 995 (vw), 936 (vw), 907 (vw), 842 (w), 804 (m), 759 (m), 746 (w), 731 (s), 703 (vs), 680 (m), 611 (s), 574 (vw), 549 (w), 506 (vw), 467 (w), 450 (m), 424 (w).

Magnetic moment (Evans): μ_{eff} (THF-d_8, 298 K) = 2.26 μ_B.

$[Ni^{I}(cAAC^{Me})_2][BPh_4]$ (IV-5$^+$)

$[Ni(cAAC^{Me})_2]$ **5** (60.0 mg, 95.3 μmol) and ferrocenium tetraphenylborate (48.2 mg, 95.3 μmol) were dissolved in 6 mL of THF. The reaction mixture was stirred for 2 h at room temperature whereby a yellow preticipate was formed. The product was collected by filtration, washed with 3 mL of THF and with 15 mL of hexane. The product was dried in vacuo to give a yellow powder (60.0 mg, 63.2 μmol, 66 %).

Yellow crystals of $[Ni^{I}(cAAC^{Me})_2][BPh_4]$ **IV-5$^+$** suitable for single-crystal X-ray diffraction were obtained by slow evaporation of a saturated DCM solution.

Elemental analysis $C_{64}H_{82}BN_2Ni$ [948.88 g/mol] calculated (found): C 81.01 (80.90), H 8.71 (8.77), N 2.95 (2.88).

HRMS-LIFDI m/z (%) calculated for $[C_{40}H_{62}N_2Ni]^+$: 628.4266(100) $[M]^+$; found: 628.4254(10) $[M]^+$; 320.2134 $[cAAC^{Me}\text{-}Cl]^+$.

^{1}H NMR (400.1 MHz, CD_2Cl_2, 298 K): δ = -14.36 (vbr, s), -8.11 (br, s), -6.97 (vbr, s), 0.09 (br, s), 1.27 (vbr, s), 6.89 (br, s, 4H, $B(C_6\textit{H}_5)_4$), 7.06 (br, s, 8H, $B(C_6\textit{H}_5)_4$), 7.39 (br, s, 8H, $B(C_6\textit{H}_5)_4$), 14.56 (vbr, s), 20.13 (vbr, s), 24.66 (vbr, s).

^{11}B NMR (128.5 MHz, CD_2Cl_2, 298 K): δ = -6.50 (s, 1B, $\textit{B}Ph_4$).

IR (ATR [cm^{-1}]): 3053 (vw), 3032 (vw), 2967 (w), 2946 (w), 2857 (vw), 1579 (w), 1498 (m), 1456 (m), 1424 (w), 1386 (w), 1370 (w), 1362 (w), 1344 (w), 1328 (w), 1265 (w), 1208 (w), 1179 (w), 1129 (m), 1112 (w), 1064 (w), 1053 (w), 1032 (w), 1001 (w), 968 (vw), 934 (vw), 846 (w), 809 (m), 780 (w), 748 (m), 737 (s), 729 (s), 703 (vs), 612 (s), 570 (w), 559 (vw), 489 (w), 475 (w), 465 (vw), 449 (w), 420 (w).

Magnetic moment (Evans): μ_{eff} (CD_2Cl_2, 298 K) = 2.82 μ_B.

7.6 Synthetic Procedures for Chapter V

cis-[Ni(*i*Pr$_2$Im^{Me})$_2$(Bcat)$_2$] (V-1a)

A 60:40 mixture of [Ni$_2$(*i*Pr$_2$Im^{Me})$_4$(*μ*-(*η*^{2}:*η*^{2})-COD)] **7a** and [Ni(*i*Pr$_2$Im^{Me})$_2$(*η*^{4}-COD)] **7b** (461 mg, 946 *μ*mol Ni) and B$_2$cat$_2$ (225 mg, 946 *μ*mol) were suspended in 5 mL of diethylether. The mixture was stirred for 2 h at room temperature with a color change of the suspension from bright to pale yellow. The product was collected by filtration, washed with 1 mL of cold diethyl ether and dried in vacuo to give a pale-yellow powder (360 mg, 548 *μ*mol, 58 %).

Yellow crystals of *cis*-[Ni(*i*Pr$_2$Im^{Me})$_2$(Bcat)$_2$] **V-1a** suitable for single-crystal X-ray diffraction were obtained by storing the mother liquor at -30 °C.

Elemental analysis $C_{34}H_{48}B_2N_4NiO_4$ [657.10 g/mol] calculated (found): C 62.15 (62.09), H 7.36 (7.49), N 8.53 (8.61).

^{1}H NMR (500.1 MHz, C_6D_6, 298 K): *δ* = 1.28 (s, br, 12H, *i*Pr-C*H*$_3$), 1.45 (s, br, 12H, *i*Pr-C*H*$_3$), 1.63 (s, 12H, NCC*H*$_3$CC*H*$_3$N), 6.05 (sept, 4H, $^3J_{HH}$ = 7.0 Hz, *i*Pr-C*H*), 6.65 (dd, 4H, $^3J_{HH}$ = 5.5 Hz, $^4J_{HH}$ = 3.4 Hz, BO$_2$C$_6$-4,5-*H*$_4$), 7.01 (dd, 4H, $^3J_{HH}$ = 5.5 Hz, $^4J_{HH}$ = 3.4 Hz, BO$_2$C$_6$-3,6-*H*$_4$).

^{13}C{^{1}H} NMR (125.8 MHz, C_6D_6, 298 K): *δ* = 10.2 (NC*C*H$_3$C*C*H$_3$N), 22.2 (*i*Pr-*C*H$_3$), 22.5 (*i*Pr-*C*H$_3$), 52.9 (*i*Pr-*C*H), 110.7 (BO$_2$-3,6-*C*$_6$H$_4$), 120.3 (BO$_2$-4,5-*C*$_6$H$_4$), 123.7 (N*C*CH$_3$*C*CH$_3$N), 151.4 (BO$_2$-1,2-*C*$_6$H$_4$), 194.3 (N*C*N).

^{11}B{^{1}H} NMR (160.5 MHz, C_6D_6, 298 K): *δ* = 48.69 (s, 2B, *B*cat).

IR (ATR [cm^{-1}]): 2972 (w), 2932 (vw), 2875 (vw), 1471 (m), 1403 (w), 1352 (m), 1282 (m), 1228 (s), 1147 (vw), 1117 (m), 1097 (s),1060 (m), 1014 (vs), 972 (m), 906 (m), 863 (vw), 806 (w), 754 (w), 736 (vs), 696 (vw), 681 (w), 618 (vw), 594 (m), 551 (w), 425 (m).

cis-[Ni(*i*Pr$_2$Im^{Me})$_2$(Bpin)$_2$] (V-1b)

In a Young's tab NMR tube, a 60:40 mixture of [Ni$_2$(*i*Pr$_2$Im^{Me})$_4$(*μ*-(*η*^{2}:*η*^{2})-COD)] **7a** and [Ni(*i*Pr$_2$Im^{Me})$_2$(*η*^{4}-COD)] **7b** (20.0 mg, 41.1 *μ*mol Ni) and B$_2$pin$_2$ (4 equiv.) were dissolved in 0.6 mL of C_6D_6. The mixture was shaken until all components were

completely dissolved. After 16 h at room temperature, the mixture was analyzed by NMR spectroscopy and the partial formation of *cis*-[Ni(*i*Pr$_2$Im^{Me})$_2$(Bpin)$_2$] **V-1b** (ca. 30-40 %) was detected. The reaction never proceeded quantitatively and is very sensitive to temperature. Hence, isolation of bulk pure material of the complex *cis*-[Ni(*i*Pr$_2$Im^{Me})$_2$(Bpin)$_2$] **V-1b** for further characterization was not possible. However, yellow crystals of *cis*-[Ni(*i*Pr$_2$Im^{Me})$_2$(Bpin)$_2$] **V-1b** suitable for single-crystal X-ray diffraction were obtained from an equilibrium mixture of the reaction components in diethyl ether at -30 °C.

^{1}H NMR (400.1 MHz, C_6D_6, 298 K): δ = 1.21 (s, 24H, C*H*$_{3Bpin}$), 1.32 (d, 12H, $^3J_{HH}$ = 7.1 Hz, *i*Pr-C*H*$_3$), 1.69 (d, 12H, $^3J_{HH}$ = 7.1 Hz, *i*Pr-C*H*$_3$), 1.84 (s, 12H, NCC*H*$_3$CC*H*$_3$N), 5.99 (sept, 4H, $^3J_{HH}$ = 7.1 Hz, *i*Pr-C*H*).

^{13}C{^{1}H} NMR (100.6 MHz, C_6D_6, 298 K): δ = 10.5 (NC*C*H$_3$C*C*H$_3$N), 22.3 (*i*Pr-*C*H$_3$), 25.7 (Bpin-*C*H$_3$), 52.3 (*i*Pr-*C*H), 79.6 (Bpin-*C*$_q$), 122.5 (N*C*CH$_3$*C*CH$_3$N), 199.4 (N*C*N).

^{11}B{^{1}H} NMR (128.5 MHz, C_6D_6, 298 K): δ = 46.08 (s, 2B, *B*pin).

cis-[Ni(*i*Pr$_2$Im^{Me})$_2$(Beg)$_2$] (V-1c)

In a Young's tab NMR tube, a 60:40 mixture of [Ni$_2$(*i*Pr$_2$Im^{Me})$_4$(*μ*-(*η*^{2}:*η*^{2})-COD)] **7a** and [Ni(*i*Pr$_2$Im^{Me})$_2$(*η*^{4}-COD)] **7b** (15.0 mg, 31.0 *μ*mol Ni) and B$_2$eg$_2$ (4.72 mg, 33.3 *μ*mol) were dissolved in 0.6 mL of C_6D_6. The mixture was shaken and, after 15 min at room temperature, analyzed by NMR spectroscopy. The partial formation of *cis*-[Ni(*i*Pr$_2$Im^{Me})$_2$(Beg)$_2$] **V-1c** (ca. 50-60 %) was detected. The reaction never proceeded quantitatively and is very sensitive to temperature. Hence, the isolation of bulk pure material of the complex *cis*-[Ni(*i*Pr$_2$Im^{Me})$_2$(Beg)$_2$] **V-1c** for further characterization was not possible. However, yellow crystals of *cis*-[Ni(*i*Pr$_2$Im^{Me})$_2$(Beg)$_2$] **V-1c** suitable for single-crystal X-ray diffraction were obtained from an equilibrium mixture of the reaction components in hexane at -30 °C.

^{1}H NMR (500.1 MHz, C_6D_6, 298 K): δ = 1.28 (d, br, 12H, *i*Pr-C*H*$_3$), 1.58 (d, br, 12H *i*Pr-C*H*$_3$), 1.78 (s, 12H, NCC*H*$_3$CC*H*$_3$N), 3.83 (s, 8H, C*H*$_{2Beg}$), 6.04 (sept, 4H, $^3J_{HH}$ = 7.0 Hz, *i*Pr-C*H*).

^{13}C{^{1}H} NMR (160.5 MHz, C_6D_6, 298 K): δ = 10.4 (NC*C*H$_3$C*C*H$_3$N), 22.3 (*i*Pr-*C*H$_3$), 22.5 (*i*Pr-*C*H$_3$), 52.6 (*i*Pr-*C*H), 64.0 (Beg-*C*H$_2$), 123.0 (N*C*CH$_3$*C*CH$_3$N), 198.5 (N*C*N).

$^{11}B\{^1H\}$ NMR (128.5 MHz, C_6D_6, 298 K): δ = 46.46 (s, 2B, *B*eg).

Z-(Bcat)(4-Me-C_6H_4)C=C(4-Me-C_6H_4)(Bcat) • (^{i}Pr$_2$Im^{Me}) (V-3^{NHC})

Z-(Bcat)(4-Me-C_6H_4)C=C(4-Me-C_6H_4)(Bcat) **V-3** (62.0 mg, 140 μmol) and ^{i}Pr$_2$Im^{Me} (25.2 mg, 140 μmol) were dissolved in 5 mL of benzene. The mixture was stirred for 48 h at room temperature and was then filtered through a pad of celite. All volatiles were removed in vacuo and the remaining residue was suspended in 5 mL of hexane. The product was collected by filtration and dried in vacuo to give an off-white powder (45.0 mg, 72.1 μmol, 52 %).

Colorless crystals of *Z*-(Bcat)(4-Me-C_6H_4)C=C(4-Me-C_6H_4)(Bcat) • (^{i}Pr$_2$Im^{Me}) **V-3^{NHC}** suitable for single-crystal X-ray diffraction were obtained by slow evaporation of a saturated solution of the compound in C_6D_6.

Elemental analysis $C_{39}H_{42}B_2N_2O_4$ [624.40 g/mol] calculated (found): C 75.02 (73.84), H 6.78 (6.80), N 4.49 (3.88).

HRMS-LIFDI m/z (%) calculated for [$C_{39}H_{42}B_2N_2O_4$]: 624.3331(100) $[M]^+$; found 625.3398(100) $[M+H]^+$, 299.1921 [^{i}Pr$_2$Im^{Me}Bcat]$^+$, 181.1698 [^{i}Pr$_2$Im^{Me}+H]$^+$.

^1H NMR (400.1 MHz, C_6D_6, 298 K): δ = 1.12 (d, 12H, $^3J_{HH}$ = 7.0 Hz, ^{i}Pr-C*H*$_3$), 1.36 (s, 6H, NCC*H*$_3$CC*H*$_3$N), 1.94 (s, 3H, C_6H_4-C*H*$_3$), 2.04 (s, 3H, C_6H_4-C*H*$_3$), 6.03 (sept, 2H, $^3J_{HH}$ = 7.0 Hz, ^{i}Pr-C*H*), 6.60 (dd, 2H, $^3J_{HH}$ = 5.7 Hz, $^4J_{HH}$ = 3.4 Hz, $BO_2C_6H_4$), 6.70 (dd, 2H, $^3J_{HH}$ = 5.7 Hz, $^4J_{HH}$ = 3.4 Hz, $BO_2C_6H_4$), 6.81 (d, 2H, $^3J_{HH}$ = 8.0 Hz, aryl-C*H*$_{meta}$), 6.89 (d, 2H, $^3J_{HH}$ = 8.0 Hz, aryl-C*H*$_{meta}$), 6.91 (dd, 2H, $^3J_{HH}$ = 5.7 Hz, $^4J_{HH}$ = 3.4 Hz, $BO_2C_6H_4$), 7.14 (dd, 2H, $^3J_{HH}$ = 5.7 Hz, $^4J_{HH}$ = 3.4 Hz, $BO_2C_6H_4$), 7.26 (d, 2H, $^3J_{HH}$ = 8.0 Hz, aryl-C*H*$_{ortho}$), 7.50 (d, 2H, $^3J_{HH}$ = 8.0 Hz, aryl-C*H*$_{ortho}$).

$^{13}C\{^1H\}$ NMR (100.6 MHz, C_6D_6, 298 K): δ = 10.0 (NC*C*H$_3$C*C*H$_3$N), 21.0 (C_6H_4-*C*H$_3$), 21.1 (C_6H_4-*C*H$_3$), 21.5 (^{i}Pr-*C*H$_3$), 50.3 (^{i}Pr-*C*H), 111.6 ($BO_2C_6H_4$), 111.9 ($BO_2C_6H_4$), 120.4 ($BO_2C_6H_4$), 121.0 ($BO_2C_6H_4$), 125.7 (N*C*CH$_3$*C*CH$_3$N), 128.8 (aryl-*C*H$_{meta}$), 128.9 (aryl-*C*H$_{ortho}$), 129.0 (aryl-*C*H$_{meta}$), 129.7 (aryl-*C*H$_{ortho}$), 134.2 (aryl-*C*$_{para}$), 134.7 (aryl-*C*$_{para}$), 139.5 (aryl-*C*$_{ipso}$), 140.7 (*C*=*C*, assigned *via* HMBC), 142.1 (aryl-C$_{ipso}$), 151.2 ($BO_2C_6H_4$), 151.3 ($BO_2C_6H_4$), 157.5 (*C*=*C*, assigned *via* HMBC), 157.9 (N*C*N, assigned *via* HMBC).

$^{11}B\{^1H\}$ NMR (128.5 MHz, C_6D_6, 298 K): δ = 9.71 (s, br, 1B, sp^3-*B*cat), 28.02 (s, br, 1B, sp^2-*B*cat).

IR (ATR [cm^{-1}]): 3019 (vw), 2981 (vw), 2935 (vw), 1632 (vw), 1605 (vw), 1553 (vw), 1506 (w), 1485 (s), 1403 (w), 1362 (w), 1314 (w), 1300 (w), 1243 (s), 1233 (s), 1186 (w), 1170 (w), 1139 (w), 1097 (m), 1086 (m), 1060 (w), 1022 (w), 1007 (w), 951 (m), 934 (w), 896 (m), 880 (w), 848 (w), 817 (m), 800 (m), 778 (m), 747 (w), 729 (vs), 703 (vw), 654 (vw), 630 (vw), 607 (w), 572 (vw), 544 (vw), 528 (w), 512 (m), 496 (w), 422 (w).

[Ni(^{i}Pr$_2$Im^{Me})$_2$(η^2-*cis*-(Bcat)(Me)C=C(Me)(Bcat))] (V-13)

[Ni(^{i}Pr$_2$Im^{Me})$_2$(η^2-MeC≡CMe)] **III-1** (286 mg, 604 μmol) and B_2cat_2 (144 mg, 604 μmol) were dissolved in 8 mL of benzene. The orange-colored mixture was stirred for 20 min at room temperature and was then filtered through a pad of celite. All volatiles were removed in vacuo and the remaining residue was suspended in 15 mL of hexane. The product was collected by filtration and dried in vacuo to give an orange-colored powder (340 mg, 478 μmol, 79 %).

Orange-colored crystals of [Ni(^{i}Pr$_2$Im^{Me})$_2$(η^2-*cis*-(Bcat)(Me)C=C(Me)(Bcat))] **V-13** suitable for single-crystal X-ray diffraction were obtained by storing a saturated solution in hexane at -30 °C.

Elemental analysis $C_{38}H_{54}B_2N_4NiO_4$ [657.10 g/mol] calculated (found): C 64.18 (65.00), H 7.65 (7.97), N 7.88 (7.68).

^{1}H NMR (400.1 MHz, C_6D_6, 298 K): δ = 0.78 (d, 6H, $^3J_{HH}$ = 7.2 Hz, ^{i}Pr-C*H*$_3$), 0.91 (d, 6H, $^3J_{HH}$ = 7.2 Hz, ^{i}Pr-C*H*$_3$), 0.93 (d, 6H, $^3J_{HH}$ = 7.2 Hz, ^{i}Pr-C*H*$_3$), 1.34 (d, 6H, $^3J_{HH}$ = 7.2 Hz, ^{i}Pr-C*H*$_3$), 1.60 (s, 6H, NCC*H*$_3$CC*H*$_3$N), 1.63 (s, 6H, NCC*H*$_3$CC*H*$_3$N), 2.11 (s, 6H, *H*$_3$CC=CC*H*$_3$), 5.78 (sept, 2H, $^3J_{HH}$ = 7.2 Hz, ^{i}Pr-C*H*), 5.98 (sept, 2H, $^3J_{HH}$ = 7.2 Hz, ^{i}Pr-C*H*), 6.81 (dd, 4H, $^3J_{HH}$ = 5.5 Hz, $^4J_{HH}$ = 3.3 Hz, BO_2C_6-4,5-*H*$_4$), 7.07 (dd, 4H, $^3J_{HH}$ = 5.5 Hz, $^4J_{HH}$ = 3.3 Hz, BO_2C_6-3,6-*H*$_4$).

$^{13}C\{^1H\}$ NMR (100.6 MHz, C_6D_6, 298 K): δ = 10.2 (NC*C*H$_3$C*C*H$_3$N), 10.4 (NC*C*H$_3$C*C*H$_3$N), 19.4 (H$_3$*C*C=C*C*H$_3$), 20.7 (^{i}Pr-*C*H$_3$), 21.3 (^{i}Pr-*C*H$_3$), 22.3 (^{i}Pr-*C*H$_3$), 23.6 (^{i}Pr-*C*H$_3$), 40.0 (*C*=*C*, assigned *via* HMBC), 52.5 (^{i}Pr-*C*H), 52.7 (^{i}Pr-*C*H), 111.4

(BO_2-3,6-C_6H_4), 120.7 (BO_2-4,5-C_6H_4), 124.5 (N*C*CH_3*C*CH_3N), 124.7 (N*C*CH_3*C*CH_3N), 151.5 (BO_2-1,2-C_6H_4), 196.0 (N*C*N).

$^{11}B\{^1H\}$ NMR (128.5 MHz, C_6D_6, 298 K): δ = 33.25 (s, 2B, *B*cat).

IR (ATR [cm^{-1}]): 2978 (vw), 2933 (vw), 2871 (vw), 2840 (vw), 1479 (m), 1444 (w), 1401 (m), 1377 (m), 1340 (s), 1288 (w), 1261 (m), 1233 (vs), 1215 (s), 1165 (vw), 1147 (vw), 1127 (w), 1113 (w), 1103 (w), 1072 (vs), 1034 (m), 1005 (m), 962 (vw), 923 (w), 905 (w), 868 (vw), 823 (w), 810 (w), 762 (w), 740 (vs), 696 (vw), 670 (w), 613 (w), 596 (m), 550 (vw), 515 (vw), 484 (vw), 451 (vw), 423 (w).

[Ni(^{i}Pr$_2$Im^{Me})$_2$(η^2-*cis*-(Bcat)(H_7C_3)C=C(C_3H_7)(Bcat))] (V-14)

[Ni(^{i}Pr$_2$Im^{Me})$_2$(η^2-H_7C_3C≡CCC_3H_7)] **III-2** (50.0 mg, 94.4 μmol) and B_2cat_2 (22.5 mg, 94.4 μmol) were dissolved in 3 mL of benzene. The yellow mixture was stirred for 48 h at room temperature and was then filtered through a pad of celite. All volatiles were removed in vacuo and the remaining residue was suspended in 3 mL of hexane. The product was collected by filtration and dried in vacuo to give an orange powder (25.0 mg, 32.6 μmol, 35 %).

Orange-colored crystals of [Ni(^{i}Pr$_2$Im^{Me})$_2$(η^2-*cis*-(Bcat)(H_7C_3)C=C(C_3H_7)(Bcat))] **V-14** suitable for single-crystal X-ray diffraction were obtained by storing a saturated solution in hexane at -30 °C.

Elemental analysis $C_{42}H_{62}B_2N_4NiO_4$ [767.30 g/mol] calculated (found): C 65.75 (64.97), H 8.14 (8.01), N 7.30 (6.79).

^{1}H NMR (400.1 MHz, C_6D_6, 298 K): δ = 0.76 (d, 6H, $^3J_{HH}$ = 7.1 Hz, ^{i}Pr-C*H*$_3$), 0.92 (d, 12H, $^3J_{HH}$ = 7.1 Hz, ^{i}Pr-C*H*$_3$), 1.28 (t, 6H, $^3J_{HH}$ = 7.1 Hz, $CH_2CH_2CH_3$), 1.39 (d, 6H, $^3J_{HH}$ = 7.1 Hz, ^{i}Pr-C*H*$_3$), 1.62 (s, 6H, NCC*H*$_3$CC*H*$_3$N), 1.64 (s, 6H, NCC*H*$_3$CC*H*$_3$N), 1.97 (m, 2H, $CH_2CH_2CH_3$), 2.13 (m, 2H, $CH_2CH_2CH_3$), 2.40 (m, 2H, $CH_2CH_2CH_3$), 2.81 (m, 2H $CH_2CH_2CH_3$), 5.81 (sept, 2H, $^3J_{HH}$ = 7.1 Hz, ^{i}Pr-C*H*), 5.96 (sept, 2H, $^3J_{HH}$ = 7.1 Hz, ^{i}Pr-C*H*), 6.81 (dd, 4H, $^3J_{HH}$ = 5.6 Hz, $^4J_{HH}$ = 3.3 Hz, BO_2C_6-4,5-*H*$_4$), 7.05 (dd, 4H, $^3J_{HH}$ = 5.6 Hz, $^4J_{HH}$ = 3.3 Hz, BO_2C_6-3,6-*H*$_4$).

$^{13}C\{^1H\}$ NMR (100.6 MHz, C_6D_6, 298 K): δ = 10.2 (NC*C*H_3C*C*H_3N), 10.4 (NC*C*H_3C*C*H_3N), 15.7 ($CH_2CH_2CH_3$), 20.7 (^{i}Pr-*C*H_3), 21.4 (^{i}Pr-*C*H_3), 22.2 (^{i}Pr-*C*H_3), 23.8 (^{i}Pr-*C*H_3), 26.7 ($CH_2CH_2CH_3$), 38.3 ($CH_2CH_2CH_3$), 47.3 (*C*=*C*, assigned *via*

HMBC), 52.4 (^{i}Pr-*C*H), 52.8 (^{i}Pr-*C*H), 111.4 (BO_2-3,6-*C*$_6H_4$), 120.7 (BO_2-4,5-*C*$_6H_4$), 124.6 (N*C*CH$_3$*C*CH$_3$N), 124.7 (N*C*CH$_3$*C*CH$_3$N), 151.5 (BO_2-1,2-*C*$_6H_4$), 196.2 (N*C*N).

^{11}B{^{1}H} NMR (128.5 MHz, C_6D_6, 298 K): δ = 31.91 (s, 2B, *B*cat).

IR (ATR [cm^{-1}]): 2952 (w), 2867 (w), 1635 (vw), 1596 (vw), 1484 (vs), 1415 (w), 1372 (m), 1302 (w), 1238 (vs), 1131 (w), 1096 (w), 1055 (s), 1007 (m), 906 (m), 813 (w), 729 (s), 702 (w), 550 (vw), 466 (vw), 432 (vw).

General procedures for the synthesis of organoboronic esters

Method A:

A Young's tap NMR tube was charged with a 60:40 mixture of [Ni$_2$(^{i}Pr$_2$Im^{Me})$_4$(μ-(η^2:η^2)-COD)] **7a** and [Ni(^{i}Pr$_2$Im^{Me})$_2$(η^4-COD)] **7b** (4-10 mol% [Ni(^{i}Pr$_2$Im^{Me})$_2$]) and B_2cat_2 (23.8 mg, 100 μmol). In close succession, 1 equiv. of alkyne (0.5 equiv. for tetra-borylation; 4 equiv. for alkyne coupling + borylation) and 0.6 mL C_6D_6 were added. The mixture was shaken, and the reaction progress was monitored by ^{1}H and ^{11}B{^{1}H} NMR spectroscopy. If necessary, the reaction mixture was heated to 50 °C until the alkyne (or B_2cat_2 if an excess alkyne was used) was completely consumed. Upon completion, an aliquot was removed and analyzed by GC/MS. From the remaining mixture all volatiles were removed in vacuo and the crude product was analyzed by ^{1}H, ^{11}B{^{1}H} and ^{13}C{^{1}H} NMR spectroscopy (C_6D_6).

Method B:

The synthesis of **V-3**, **V-6**, **V-7a** and **V-12** were scaled-up to a preparative scale. As column chromatography is not suitable for the purification of the compounds, work-up cannot be described in a general method. Scaled-up procedures and purification are therefore reported separately for each case.

***Z*-(Bcat)(Ph)C=C(Ph)(Bcat) (V-2)**

Method A was employed for the preparation of **V-2**, using diphenylacetylene (17.8 mg, 100 μmol, 1 equiv.) as the alkyne and 10 mol% [Ni(^{i}Pr$_2$Im^{Me})$_2$].

^{1}H NMR (400.1 MHz, C_6D_6, 298 K): δ = 6.74 (dd, 4H, $^{3}J_{HH}$ = 5.8 Hz, $^{4}J_{HH}$ = 3.4 Hz, $BO_2C_6H_4$), 6.89 (dd, 4H, $^{3}J_{HH}$ = 5.8 Hz, $^{4}J_{HH}$ = 3.4 Hz, $BO_2C_6H_4$), 6.91 (m, 2H, aryl-CH_{para}), 6.99 (m, 4H, aryl-CH_{meta}), 7.24 (m, 4H, aryl-CH_{ortho}).

^{13}C{^{1}H} NMR (100.6 MHz, C_6D_6, 298 K): δ = 112.8 ($BO_2C_6H_4$), 123.1 ($BO_2C_6H_4$), 127.4 (aryl-CH_{para}), 128.6 (aryl-CH_{meta}), 129.8 (aryl-CH_{ortho}), 139.9 (aryl-C_{ipso}), 146.4 (*C*=*C*, assigned *via* HMBC), 148.8 ($BO_2C_6H_4$).

^{11}B{^{1}H} NMR (128.5 MHz, C_6D_6, 298 K): δ = 32.22 (s, br, 2B, *B*cat).

GC/MS Ret.: 15.42 min, (m/z): 416.0 $[M]^+$.

The spectroscopic data for **V-2** match those reported in the literature.[17]

Z-(Bcat)(4-Me-C_6H_4)C=C(4-Me-C_6H_4)(Bcat) (V-3)

Method A was employed for the preparation of **V-3**, using bis-(*p*-tolyl)acetylene (20.7 mg, 100 μmol, 1 equiv.) as the alkyne and 10 mol% [Ni(^{i}Pr$_2$Im^{Me})$_2$].

The reaction was also performed on a preparative scale:

A Schlenk-tube was charged with a 60:40 mixture of [Ni$_2$(^{i}Pr$_2$Im^{Me})$_4$(μ-(η^2:η^2)-COD)] **7a** and [Ni(^{i}Pr$_2$Im^{Me})$_2$(η^4-COD)] **7b** (20.0 mg, 40.4 μmol, 9.6 mol% [Ni(^{i}Pr$_2$Im^{Me})$_2$]), B_2cat_2 (100 mg, 421 μmol, 1 equiv.) and bis-(*p*-tolyl)acetylene (86.8 mg, 421 μmol, 1 equiv.). The mixture was dissolved in 4 mL of benzene, stirred for 20 h at 50 °C and was then filtered through a pad of celite. All volatiles were removed in vacuo and the remaining residue was suspended in 30 mL of hexane. The product was collected by filtration and dried in vacuo to give an off-white powder of **V-3** (112 mg, 252 μmol, 60 %). The crude product was re-crystallized by storing a saturated hexane solution at -30 °C.

Elemental analysis $C_{28}H_{22}B_2O_4$ [444.10 g/mol] calculated (found): C 75.73 (75.64), H 4.99 (4.96).

^{1}H NMR (400.1 MHz, C_6D_6, 298 K): δ = 1.98 (s, 6H, CH_3), 6.74 (dd, 4H, $^{3}J_{HH}$ = 5.8 Hz, $^{4}J_{HH}$ = 3.4 Hz, $BO_2C_6H_4$), 6.84 (d, 4H, $^{3}J_{HH}$ = 8.0 Hz, aryl-CH_{meta}), 6.90 (dd, 4H, $^{3}J_{HH}$ = 5.8 Hz, $^{4}J_{HH}$ = 3.4 Hz, $BO_2C_6H_4$), 7.23 (d, 4H, $^{3}J_{HH}$ = 8.0 Hz, aryl-CH_{ortho}).

$^{13}C\{^1H\}$ NMR (100.6 MHz, C_6D_6, 298 K): δ = 21.1 (*C*H_3), 112.8 (BO_2*C*$_6H_4$), 123.0 (BO_2*C*$_6H_4$), 129.4 (aryl-*C*H$_{meta}$), 129.9 (aryl-*C*H$_{ortho}$), 136.9 (aryl-*C*$_{ipso}$), 137.2 (aryl-C$_{para}$), 146.2 (*C*=*C*, assigned *via* HMBC), 148.9 (BO_2*C*$_6H_4$).

$^{11}B\{^1H\}$ NMR (128.5 MHz, C_6D_6, 298 K): δ = 32.54 (s, br, 2B, *B*cat).

GC/MS Ret.: 16.53 min, (m/z): 444.1 $[M]^+$.

IR (ATR [cm^{-1}]): 2920 (vw), 1603 (vw), 1575 (vw), 1507 (w), 1470 (s), 1412 (w), 1397 (w), 1372 (m), 1350 (w), 1322 (s), 1308 (s), 1281 (w), 1253 (w), 1228 (vs), 1187 (w), 1167 (m), 1131 (m), 1119 (w), 1083 (w), 1036 (w), 1022 (w), 1004 (w), 993 (w), 970 (w), 944 (vw), 923 (w), 891 (w), 865 (w), 841 (vw), 807 (s), 746 (vs), 738 (vs), 703 (m), 654 (m), 578 (w), 550 (m), 522 (w), 505 (w), 490 (m), 473 (m), 426 (m).

The spectroscopic data for **V-3** match those reported in the literature.[17]

Z-(Bcat)(4-CF_3-C_6H_4)C=C(4-CF_3-C_6H_4)(Bcat) (V-4)

Method A was employed for the preparation of **V-4**, using 1,2-bis[*p*-(trifluoromethyl)phenyl]acetylene (31.5 mg, 100 μmol, 1 equiv.) as the alkyne and 10 mol% [Ni(^{i}Pr$_2$Im^{Me})$_2$].

^1H NMR (400.1 MHz, C_6D_6, 298 K): δ = 6.78 (dd, 4H, $^3J_{HH}$ = 5.9 Hz, $^4J_{HH}$ = 3.4 Hz, BO_2C_6*H*$_4$), 6.92 (dd, 4H, $^3J_{HH}$ = 5.9 Hz, $^4J_{HH}$ = 3.4 Hz, BO_2C_6*H*$_4$), 6.96 (d, 4H, $^3J_{HH}$ = 8.1 Hz, aryl-C*H*$_{meta}$), 7.13 (d, 4H, $^3J_{HH}$ = 8.1 Hz, aryl-C*H*$_{ortho}$).

$^{13}C\{^1H\}$ NMR (100.6 MHz, C_6D_6, 298 K): δ = 113.0 (BO_2*C*$_6H_4$), 123.6 (BO_2*C*$_6H_4$), 125.6 (aryl-*C*H$_{meta}$), 129.9 (aryl-*C*H$_{ortho}$), 142.7 (aryl-*C*$_{ipso}$), 148.5 (BO_2*C*$_6H_4$).

$^{11}B\{^1H\}$ NMR (128.5 MHz, C_6D_6, 298 K): δ = 31.3(s, br, 2B, *B*cat).

$^{19}F\{^1H\}$ NMR (376.8 MHz, C_6D_6, 298 K): δ = -62.40 (s, 6F, C*F*$_3$).

GC/MS Ret.: 14.34 min, (m/z): 552.0 $[M]^+$.

The spectroscopic data for **V-4** match those reported in the literature.[18]

***Z*-(Bcat)(C_3H_7)C=C(C_3H_7)(Bcat) (V-5)**

Method A was employed for the preparation of **V-5**, using 4-octyne (14.7 µL, 11.0 mg, 100 µmol, 1 equiv.) as the alkyne and 4 mol% [Ni(^{i}Pr$_2$Im^{Me})$_2$].

^{1}H NMR (400.1 MHz, C_6D_6, 298 K): δ = 0.91 (t, 6H, $^3J_{HH}$ = 7.5 Hz, $CH_2CH_2CH_3$), 1.54 (m, 4H, $CH_2CH_2CH_3$), 2.50 (t, 4H, $^3J_{HH}$ = 7.5 Hz, $CH_2CH_2CH_3$), 6.74 (dd, 4H, $^3J_{HH}$ = 5.8 Hz, $^4J_{HH}$ = 3.4 Hz, $BO_2C_6H_4$), 6.91 (dd, 4H, $^3J_{HH}$ = 5.8 Hz, $^4J_{HH}$ = 3.4 Hz, $BO_2C_6H_4$).

^{13}C{^{1}H} NMR (100.6 MHz, C_6D_6, 298 K): δ = 14.4 ($CH_2CH_2CH_3$), 23.2 ($CH_2CH_2CH_3$), 33.3 ($CH_2CH_2CH_3$), 112.7 ($BO_2C_6H_4$), 122.9 ($BO_2C_6H_4$), 148.8 ($BO_2C_6H_4$).

^{11}B{^{1}H} NMR (128.5 MHz, C_6D_6, 298 K): δ = 32.38 (s, br, 2B, *B*cat).

GC/MS Ret.: 12.29 min, (m/z): 348.0 $[M]^+$.

***Z*-(Bcat)(Me)C=C(Ph)(Bcat) (V-6)**

Method A was employed for the preparation of **V-6**, using 1-phenyl-1-propyne (12.5 µL, 11.6 mg, 100 µmol, 1 equiv.) as the alkyne and 4 mol% [Ni(^{i}Pr$_2$Im^{Me})$_2$].

The reaction was also performed on a preparative scale:

A Schlenk-tube was charged with a 60:40 mixture of [Ni$_2$(^{i}Pr$_2$Im^{Me})$_4$(*µ*-(η^2:η^2)-COD)] **7a** and [Ni(^{i}Pr$_2$Im^{Me})$_2$(η^4-COD)] **7b** (26.0 mg, 53.5 µmol, 3.6 mol% [Ni(^{i}Pr$_2$Im^{Me})$_2$]) and B_2cat_2 (352 mg, 1.48 mmol, 1 equiv.). In close succession, 1-phenyl-1-propyne (184 µL, 172 mg, 1.48 mmol, 1 equiv.) and 10 mL benzene were added. The reaction mixture was stirred for 3 h at 50 °C and was then filtered through a pad of celite. All volatiles were removed in vacuo, the remaining residue was suspended in 30 mL of hexane and filtered again through a pad of celite. The filtrate was then stored for 24 h at -30 °C. The supernatant solution was removed from the precipitated product *via* a syringe and the product was dried in vacuo to yield light brown crystals of **V-6** (341 mg, 963 µmol, 65 %).

Elemental analysis $C_{21}H_{16}B_2O_4$ [353.98 g/mol] calculated (found): C 71.26 (71.54), H 4.56 (4.87).

^{1}H NMR (400.1 MHz, C_6D_6, 298 K): δ = 2.00 (s, 3H, C*H*$_3$), 6.74 (m, 4H, BO_2C_6*H*$_4$), 6.86 (m, 2H, BO_2C_6*H*$_4$), 6.94 (m, 2H, BO_2C_6*H*$_4$), 7.07 (m, 1H, aryl-C*H*$_{para}$), 7.18 (m, ,2H, aryl-C*H*$_{meta}$), 7.29 (m, 2H, aryl-C*H*$_{ortho}$).

^{13}C{^{1}H} NMR (100.6 MHz, C_6D_6, 298 K): δ = 18.2 (*C*H$_3$), 112.7 (BO_2*C*$_6$H$_4$), 112.8 (BO_2*C*$_6$H$_4$), 122.9 (BO_2*C*$_6$H$_4$), 123.0 (BO_2*C*$_6$H$_4$), 127.4 (aryl-*C*H$_{para}$), 128.7 (aryl-*C*H$_{meta}$), 128.8 (aryl-*C*H$_{ortho}$), 140.1 (aryl-*C*$_{ipso}$), 148.7 (BO_2*C*$_6$H$_4$), 148.9 (BO_2*C*$_6$H$_4$).

^{11}B{^{1}H} NMR (128.5 MHz, C_6D_6, 298 K): δ = 31.97 (s, br, 2B, *B*cat).

GC/MS Ret.: 13.43 min, (m/z): 354.0 $[M]^+$.

IR (ATR [cm^{-1}]): 3063 (vw), 1590 (vw), 1470 (s), 1441 (w), 1390 (w), 1371 (m), 1350 (w), 1323 (s), 1312 (s), 1274 (w), 1230 (vs), 1198 (m), 1124 (m), 1108 (s), 1006 (w), 914 (w), 866 (w), 812 (m), 779 (w), 762 (w), 737 (vs), 706 (s), 688 (m), 672 (s), 611 (w), 583 (w), 539 (w), 499 (w), 488 (w), 428 (m).

Z-(Bcat)(Me)C=C(Me)(Bcat) (V-7)

Method A was employed for the preparation of **V-7**, using 2-butyne (7.85 μL, 5.41 mg, 100 μmol, 1 equiv.) as the alkyne and 4 mol% [Ni(^{i}Pr$_2$Im^{Me})$_2$].

^{1}H NMR (400.1 MHz, C_6D_6, 298 K): δ = 1.88 (s, 6H, C*H*$_3$), 6.75 (dd, 4H, $^{3}J_{HH}$ = 5.8 Hz, $^{4}J_{HH}$ = 3.3 Hz, BO_2C_6*H*$_4$), 6.92 (dd, 4H, $^{3}J_{HH}$ = 5.8 Hz, $^{4}J_{HH}$ = 3.3 Hz, BO_2C_6*H*$_4$).

^{13}C{^{1}H} NMR (100.6 MHz, C_6D_6, 298 K): δ = 16.7 (*C*H$_3$), 112.7 (BO_2*C*$_6$H$_4$), 122.9 (BO_2*C*$_6$H$_4$), 148.9 (BO_2*C*$_6$H$_4$).

^{11}B{^{1}H} NMR (128.5 MHz, C_6D_6, 298 K): δ = 31.90 (s, br, 2B, *B*cat).

GC/MS Ret.: 11.28 min, (m/z): 292.0 $[M]^+$.

(Bcat)$_2$(Me)C–C(Me)(Bcat)$_2$ (V-7a)

Method A was employed for the preparation of **V-7a**, using 2-butyne (3.92 μL, 2.71 mg, 50.0 μmol, 0.5 equiv.) as the alkyne and 4 mol% [Ni(^{i}Pr$_2$Im^{Me})$_2$].

The reaction was also performed on a preparative scale:

A Schlenk-tube was charged with a 60:40 mixture of [Ni$_2$(^{i}Pr$_2$Im^{Me})$_4$(μ-(η^2:η^2)-COD)] **7a** and [Ni(^{i}Pr$_2$Im^{Me})$_2$(η^4-COD)] **7b** (14.0 mg, 28.7 μmol, 3.9 mol% [Ni(^{i}Pr$_2$Im^{Me})$_2$]) and B_2cat_2 (352 mg, 1.48 mmol, 2 equiv.). In close succession, 2-butyne (58.0 μL, 40.0 mg, 740 μmol, 1 equiv.) and 10 mL benzene were added. The reaction mixture was stirred for 20 h at 50 °C and was then filtered through a pad of celite. All volatiles were removed in vacuo and the remaining residue was suspended in 25 mL of hexane. The product was collected by filtration and dried in vacuo to give an off-white powder of **V-7a** (150 mg, 283 μmol, 38 %).

Elemental analysis $C_{28}H_{22}B_4O_8$ [529.72 g/mol] calculated (found): C 63.49 (63.82), H 4.19 (4.60).

^{1}H NMR (400.1 MHz, C_6D_6, 298 K): δ = 2.01 (s, 6H, CH_3), 6.67 (dd, 8H, $^3J_{HH}$ = 5.8 Hz, $^4J_{HH}$ = 3.3 Hz, $BO_2C_6H_4$), 6.86 (dd, 8H, $^3J_{HH}$ = 5.8 Hz, $^4J_{HH}$ = 3.3 Hz, $BO_2C_6H_4$).

^{13}C{^{1}H} NMR (100.6 MHz, C_6D_6, 298 K): δ = 16.5 (CH_3), 112.8 ($BO_2C_6H_4$), 122.8 ($BO_2C_6H_4$), 148.8 ($BO_2C_6H_4$).

^{11}B{^{1}H} NMR (128.5 MHz, C_6D_6, 298 K): δ = 35.90 (s, br, 4B, *B*cat).

GC/MS Ret.: 13.54 min, (m/z): 530.1 $[M]^+$.

IR (ATR [cm^{-1}]): 1470 (s), 1423 (vw), 1390 (vw), 1362 (vw), 1273 (s), 1149 (vw), 1132 (m), 1084 (w), 1053 (m), 1006 (w), 960 (vw), 919 (vw), 865 (w), 853 (vw), 809 (m), 740 (vs), 695 (w), 631 (vw), 613 (w), 557 (vw), 452 (vw), 424 (m).

E,E-(Bcat)(Me)C=C(Me)–(Me)C=C(Me)(Bcat) (V-7b)

Method A was employed for the preparation of **V-7b**, using 2-butyne (31.2 μL, 21.7 mg, 400 μmol, 4 equiv.) as the alkyne and 4 mol% [Ni(^{i}Pr$_2$Im^{Me})$_2$].

^{1}H NMR (400.1 MHz, C_6D_6, 298 K): δ = 1.97 (q, br, 6H, $^5J_{HH}$ = 1 Hz, CH_3), 2.01(q, br, 6H, $^5J_{HH}$ = 1 Hz, CH_3), 6.73 (dd, 4H, $^3J_{HH}$ = 5.9 Hz, $^4J_{HH}$ = 3.3 Hz, $BO_2C_6H_4$), 6.95 (dd, 4H, $^3J_{HH}$ = 5.9 Hz, $^4J_{HH}$ = 3.3 Hz, $BO_2C_6H_4$).

$^{13}C\{^1H\}$ NMR (100.6 MHz, C_6D_6, 298 K): δ = 16.4 (*C*H_3), 19.3 (*C*H_3), 112.4 (BO_2*C*$_6H_4$), 119.8 (C=*C*(Me)(Bcat), assigned *via* HMBC), 122.6 (BO_2*C*$_6H_4$), 148.9 (BO_2*C*$_6H_4$), 159.5 ((Me)*C*=C).

$^{11}B\{^1H\}$ NMR (128.5 MHz, C_6D_6, 298 K): δ = 31.88 (s, br, 4B, *B*cat).

GC/MS Ret.: 12.05 min, (m/z): 346.1 $[M]^+$.

E-(Bcat)HC=C(Ph)(Bcat) (V-8)

Method A was employed for the preparation of **V-8**, using phenylacetylene (11.0 μL, 10.2 mg, 100 μmol, 1 equiv.) as the alkyne and 4 mol% [Ni(^{i}Pr$_2$Im^{Me})$_2$].

^1H NMR (400.1 MHz, C_6D_6, 298 K): δ = 6.68 (dd, 2H, $^3J_{HH}$ = 5.8 Hz, $^4J_{HH}$ = 3.4 Hz, BO_2C_6*H*$_4$), 6.78 (dd, 2H, $^3J_{HH}$ = 5.8 Hz, $^4J_{HH}$ = 3.4 Hz, BO_2C_6*H*$_4$), 6.85 (dd, 2H, $^3J_{HH}$ = 5.8 Hz, $^4J_{HH}$ = 3.4 Hz, BO_2C_6*H*$_4$), 6.89 (s, 1H, C=*C*H), 7.05-7.10 (m, 2H, BO_2C_6*H*$_4$, 3H aryl-C*H*$_{para/meta}$), 7.45 (m, 2H, aryl-C*H*$_{ortho}$).

$^{13}C\{^1H\}$ NMR (100.6 MHz, C_6D_6, 298 K): δ = 112.7 (BO_2*C*$_6H_4$), 112.9 (BO_2*C*$_6H_4$), 123.0 (BO_2*C*$_6H_4$), 123.2 (BO_2*C*$_6H_4$), 127.4 (aryl-*C*H$_{ortho}$), 129.0 (aryl-*C*H$_{meta}$), 129.1 (aryl-*C*H$_{para}$), 141.1 (aryl-*C*$_{ipso}$), 148.6 (BO_2*C*$_6H_4$), 149.0 (BO_2*C*$_6H_4$), 154.7 (*C*=CH, assigned *via* HMBC).

$^{11}B\{^1H\}$ NMR (128.5 MHz, C_6D_6, 298 K): δ = 30.87 (s, br, 2B, *B*cat).

GC/MS Ret.: 13.58 min, (m/z): 340.0 $[M]^+$.

The spectroscopic data for **V-8** match those reported in the literature.[17]

E-(Bcat)HC=C(4-Me-C$_6$H$_4$)(Bcat) (V-9)

Method A was employed for the preparation of **V-9**, using *p*-tolylacetylene (12.7 μL, 11.6 mg, 100 μmol, 1 equiv.) as the alkyne and 4 mol% [Ni(^{i}Pr$_2$Im^{Me})$_2$].

^1H NMR (400.1 MHz, C_6D_6, 298 K): δ = 2.05 (s, 3H, C*H*$_3$), 6.67 (dd, 2H, $^3J_{HH}$ = 5.8 Hz, $^4J_{HH}$ = 3.4 Hz, BO_2C_6*H*$_4$), 6.78 (dd, 2H, $^3J_{HH}$ = 5.8 Hz, $^4J_{HH}$ = 3.4 Hz, BO_2C_6*H*$_4$), 6.86 (dd, 2H, $^3J_{HH}$ = 5.8 Hz, $^4J_{HH}$ = 3.4 Hz, BO_2C_6*H*$_4$), 6.92 (d, 2H, $^3J_{HH}$ = 7.8 Hz, aryl-C*H*$_{meta}$), 6.93 (s, 1H, C=C*H*), 7.10 (dd, 2H, $^3J_{HH}$ = 5.8 Hz, $^4J_{HH}$ = 3.4 Hz, BO_2C_6*H*$_4$), 7.42 (d, 2H, $^3J_{HH}$ = 7.8 Hz, aryl-C*H*$_{ortho}$).

$^{13}C\{^1H\}$ NMR (100.6 MHz, C_6D_6, 298 K): δ = 21.2 (CH_3), 112.7 ($BO_2C_6H_4$), 113.0 ($BO_2C_6H_4$), 122.9 ($BO_2C_6H_4$), 123.2 ($BO_2C_6H_4$), 127.4 (aryl-CH_{ortho}), 129.8 (aryl-CH_{meta}), 138.3 (aryl-C_{ipso}), 139.2 (aryl-CCH_3), 148.6 ($BO_2C_6H_4$), 149.0 ($BO_2C_6H_4$), 154.8 (*C*=CH, assigned *via* HMBC).

$^{11}B\{^1H\}$ NMR (128.5 MHz, C_6D_6, 298 K): δ = 30.84 (s, br, 2B, *B*cat).

GC/MS Ret.: 14.05 min, (m/z): 354.0 $[M]^+$.

E-(Bcat)HC=C(4-^{t}Bu-C_6H_4)(Bcat) (V-10)

Method A was employed for the preparation of **V-10**, using 4-(*tert*-butyl)phenylacetylene (17.8 µL, 15.8 mg, 100 µmol, 1 equiv.) as the alkyne and 4 mol% [Ni(^{i}Pr$_2$Im^{Me})$_2$].

^1H NMR (400.1 MHz, C_6D_6, 298 K): δ = 1.20 (s, 9H, $C(CH_3)_3$), 6.67 (dd, 2H, $^3J_{HH}$ = 5.8 Hz, $^4J_{HH}$ = 3.4 Hz, $BO_2C_6H_4$), 6.78 (dd, 2H, $^3J_{HH}$ = 5.8 Hz, $^4J_{HH}$ = 3.4 Hz, $BO_2C_6H_4$), 6.87 (dd, 2H, $^3J_{HH}$ = 5.8 Hz, $^4J_{HH}$ = 3.4 Hz, $BO_2C_6H_4$), 6.97 (s, 1H, C=C*H*), 7.13 (dd, 2H, $^3J_{HH}$ = 5.8 Hz, $^4J_{HH}$ = 3.4 Hz, $BO_2C_6H_4$), 7.18 (d, 2H, $^3J_{HH}$ = 8.6 Hz, aryl-CH_{meta}), 7.46 (d, 2H, $^3J_{HH}$ = 8.6 Hz, aryl-CH_{ortho}).

$^{13}C\{^1H\}$ NMR (100.6 MHz, C_6D_6, 298 K): δ = 31.3 ($C(CH_3)_3$), 34.7 ($C(CH_3)_3$), 112.7 ($BO_2C_6H_4$), 113.0 ($BO_2C_6H_4$), 122.9 ($BO_2C_6H_4$), 123.2 ($BO_2C_6H_4$), 126.1 (aryl-CH_{meta}), 127.3 (aryl-CH_{ortho}), 138.2 (aryl-C_{ipso}), 148.6 ($BO_2C_6H_4$), 149.1 ($BO_2C_6H_4$), 152.3 (aryl-*C*-^{t}Bu), 154.9 (*C*=CH, assigned *via* HMBC).

$^{11}B\{^1H\}$ NMR (128.5 MHz, C_6D_6, 298 K): δ = 30.81 (s, br, 2B, *B*cat).

GC/MS Ret.: 15.06 min, (m/z): 396.1 $[M]^+$.

Z,Z-(Bcat)HC=C(C_3H_7)–(C_3H_7)C=CH(Bcat) (V-11a)

Method A was employed for the preparation of **V-11a** and **V-11b**, using 1-pentyne (39.4 µL, 27.3 mg, 100 µmol, 4 equiv.) as the alkyne and 4 mol% [Ni(^{i}Pr$_2$Im^{Me})$_2$].

^1H NMR (400.1 MHz, C_6D_6, 298 K): δ = 0.90 (t, 6H, $^3J_{HH}$ = 7.3 Hz, $CH_2CH_2CH_3$), 1.57 (m, 4H, $CH_2CH_2CH_3$), 2.31 (m, 4H, $CH_2CH_2CH_3$), 5.89 (t, 2H, $^4J_{HH}$ = 1.3 Hz,

*H*C=C(C_3H_7)–(C_3H_7)C=C*H*), 6.69 (dd, 4H, $^3J_{HH}$ = 5.8 Hz, $^4J_{HH}$ = 3.4 Hz, $BO_2C_6H_4$), 6.96 (dd, 4H, $^3J_{HH}$ = 5.8 Hz, $^4J_{HH}$ = 3.4 Hz, $BO_2C_6H_4$).

$^{13}C\{^1H\}$ NMR (100.6 MHz, C_6D_6, 298 K): δ = 14.1 ($CH_2CH_2CH_3$), 21.0 ($CH_2CH_2CH_3$), 41.9 ($CH_2CH_2CH_3$), 112.5 ($BO_2C_6H_4$), 122.7 ($BO_2C_6H_4$), 148.7 ($BO_2C_6H_4$), 169.0 (HC=*C*(C_3H_7)–(C_3H_7)*C*=CH).

$^{11}B\{^1H\}$ NMR (128.5 MHz, C_6D_6, 298 K): δ = 31.33 (s, br, 2B, *B*cat).

GC/MS Ret.: 12.93 min, (m/z): 374.1 $[M]^+$.

E/Z,E/Z-(Bcat)HC=C(C_3H_7)–HC=C(Bcat)(C_3H_7) (V-11b)

^1H NMR (400.1 MHz, C_6D_6, 298 K): δ = 0.82 (t, 3H, $^3J_{HH}$ = 7.3 Hz, $CH_2CH_2CH_3$), 1.00 (t, 3H, $^3J_{HH}$ = 7.3 Hz, $CH_2CH_2CH_3$), 1.51 (m, 2H, $CH_2CH_2CH_3$), 1.67 (m, 2H, $CH_2CH_2CH_3$), 2.28 (m, 2H, $CH_2CH_2CH_3$), 2.52 (m, 2H, $CH_2CH_2CH_3$), 5.81 (dt, 1H, $^4J_{HH}$ = 1.2 Hz, $^4J_{HH}$ = 1.0 Hz, (Bcat)*H*C=C(C_3H_7)), 6.71 (dd, 2H, $^3J_{HH}$ = 5.8 Hz, $^4J_{HH}$ = 3.4 Hz, $BO_2C_6H_4$), 6.75 (dd, 2H, $^3J_{HH}$ = 5.8 Hz, $^4J_{HH}$ = 3.4 Hz, $BO_2C_6H_4$), 6.98 (dd, 2H, $^3J_{HH}$ = 5.8 Hz, $^4J_{HH}$ = 3.4 Hz, $BO_2C_6H_4$), 7.01 (dd, 2H, $^3J_{HH}$ = 5.8 Hz, $^4J_{HH}$ = 3.4 Hz, $BO_2C_6H_4$), 7.17 (br, 1H, *H*C=C(Bcat)(C_3H_7)).

$^{13}C\{^1H\}$ NMR (100.6 MHz, C_6D_6, 298 K): δ = 13.9 ($CH_2CH_2CH_3$), 14.1 ($CH_2CH_2CH_3$), 21.9 ($CH_2CH_2CH_3$), 23.5 ($CH_2CH_2CH_3$), 40.1 ($CH_2CH_2CH_3$), 42.6 ($CH_2CH_2CH_3$), 112.5 ($BO_2C_6H_4$), 112.7 ($BO_2C_6H_4$), 114.0 (Bcat)H*C*=C(C_3H_7), assigned *via* HMBC), 122.7 ($BO_2C_6H_4$), 123.0 ($BO_2C_6H_4$), 133.3 (HC=*C*(Bcat)(C_3H_7), assigned *via* HMBC), 145.9 (H*C*=C(Bcat)(C_3H_7)), 148.5 ($BO_2C_6H_4$), 148.7 ($BO_2C_6H_4$), 164.6 (Bcat)HC=*C*(C_3H_7)).

$^{11}B\{^1H\}$ NMR (128.5 MHz, C_6D_6, 298 K): δ = 31.33 (s, br, 2B, *B*cat).

GC/MS Ret.: 13.04 min, (m/z): 374.1 $[M]^+$.

(4-NMe_2-C_6H_4)(Bcat)(TMS)C–C(Bcat)$_3$ (V-12)

Method A was employed for the preparation of **V-12**, using *N*,*N*-dimethyl-4-[(trimethylsilyl)-ethinyl]-aniline (10.9 mg, 50 μmol, 0.5 equiv.) as the alkyne and 4 mol% [Ni(^{i}Pr$_2$Im^{Me})$_2$].

The reaction was also performed on a preparative scale:

A Schlenk-tube was charged with a 60:40 mixture of [Ni$_2$(^{i}Pr$_2$Im^{Me})$_4$(μ-(η^2:η^2)-COD)] **7a** and [Ni(^{i}Pr$_2$Im^{Me})$_2$(η^4-COD)] **7b** (6.00 mg, 12.3 μmol, 3.9 mol% [Ni(^{i}Pr$_2$Im^{Me})$_2$]), *N*,*N*-dimethyl-4-[(trimethylsilyl)-ethinyl]-aniline (69.0 mg, 317 μmol, 1 equiv.) and B_2cat_2 (151 mg, 635 μmol, 2 equiv.). The mixture was dissolved in 10 mL of benzene and stirred for 48 h at 50 °C. All volatiles were removed in vacuo and the remaining residue was suspended in 5 mL of hexane. The product was collected by filtration and dried in vacuo to give an off-white powder (101 mg, 146 μmol, 46 %).

Colorless crystals of (4-NMe$_2$-C$_6$H$_4$)(Bcat)(TMS)C–C(Bcat)$_3$ **V-12** suitable for single-crystal X-ray diffraction were obtained by slow evaporation of a saturated solution of the compound in C_6D_6.

Elemental analysis $C_{37}H_{35}B_4NO_8Si$ [693.01 g/mol] calculated (found): C 64.13 (64.27), H 5.09 (5.30), N 2.02 (2.13).

HRMS-LIFDI m/z (%) calculated for [$C_{37}H_{35}B_4NO_8Si$]: 693.2505(100) $[M]^+$; found 693.2489(100) $[M]^+$, 575.2237 $[M\text{-Bcat+H}]^+$, 502.1797 $[M\text{-Bcat-TMS+H}]^{+\cdot}$.

^{1}H NMR (400.1 MHz, C_6D_6, 298 K): δ = 0.49 (s, 9H, Si(CH_3)$_3$), 2.38 (s, 6H, N(CH_3)$_2$), 6.52 (d, 2H, $^3J_{HH}$ = 8.8 Hz, aryl-CH_{meta}), 6.65 (dd, 6H, $^3J_{HH}$ = 5.9 Hz, $^4J_{HH}$ = 3.4 Hz, BO$_2$C$_6$$H_4$), 6.67 (dd, 2H, $^3J_{HH}$ = 5.9 Hz, $^4J_{HH}$ = 3.4 Hz, BO$_2$C$_6$$H_4$), 6.84 (dd, 2H, $^3J_{HH}$ = 5.9 Hz, $^4J_{HH}$ = 3.4 Hz, BO$_2$C$_6$$H_4$), 6.85 (dd, 6H, $^3J_{HH}$ = 5.9 Hz, $^4J_{HH}$ = 3.4 Hz, BO$_2$C$_6$$H_4$), 7.85 (d, 2H, $^3J_{HH}$ = 8.8 Hz, aryl-CH_{ortho}).

^{13}C{^{1}H} NMR (100.6 MHz, C_6D_6, 298 K): δ = 1.43 (Si(*C*H$_3$)$_3$), 32.2 (*C*–C(Bcat)$_3$, assigned *via* HMBC), 40.3 (N(*C*H$_3$)$_2$), 112.6 (BO$_2$*C*$_6$H$_4$), 112.8 (BO$_2$*C*$_6$H$_4$), 112.9 (aryl-*C*H$_{meta}$), 122.8 (BO$_2$*C*$_6$H$_4$), 122.9 (BO$_2$*C*$_6$H$_4$), 131.4 (aryl-*C*H$_{ortho}$), 131.7 (aryl-*C*$_{ipso}$), 148.3 (aryl-*C*NMe$_2$), 148.6 (BO$_2$*C*$_6$H$_4$), 148.7 (BO$_2$*C*$_6$H$_4$).

^{11}B{^{1}H} NMR (128.5 MHz, C_6D_6, 298 K): δ = 35.94 (s, br, 4B, *B*cat).

^{29}Si NMR (79.5 MHz, C_6D_6, 298 K): 8.82 (s, 1Si, *Si*(CH$_3$)$_3$).

IR (ATR [cm^{-1}]): 2896 (vw), 1609 (vw), 1519 (w), 1470 (s), 1367 (vw), 1291 (s), 1251 (m), 1226 (vs), 1212 (vs), 1153 (vw), 1127 (w), 1058 (vw), 1004 (vw), 939 (w), 918 (vw), 862 (m), 840 (m), 810 (m), 791 (w), 748 (s), 740 (s), 731 (s), 706 (vw), 679 (vw) 630 (vw), 602 (w), 567 (vw), 531 (vw), 520 (vw), 421 (m).

7.7 Synthetic Procedures for Chapter VI

[Ni(PMe$_3$)$_4$] (VI-1) and [B$_2$cat$_2$ • (^{i}Pr$_2$Im^{Me})$_2$] (VI-2)

In a Young's tap NMR tube, trimethylphosphine (8.00 μL, 5 equiv) was added to a solution of *cis*-[Ni(^{i}Pr$_2$Im^{Me})$_2$(Bcat)$_2$] **V-1a** (10.0 mg, 15.2 μmol) in 0.6 mL of C_6D_6. The mixture was shaken and directly analyzed *via* NMR spectroscopy. After a few minutes the formation of [Ni(PMe$_3$)$_4$] **VI-1** and [B$_2$cat$_2$ • (^{i}Pr$_2$Im^{Me})$_2$] **VI-2** was detected.

[Ni(PMe$_3$)$_4$] ***VI-1***

^{1}H NMR (400.1 MHz, C_6D_6, 298 K): δ = 1.15 (s, 36H, P(C*H*$_3$)$_3$).

^{13}C{^{1}H} NMR (100.6 MHz, C_6D_6, 298 K): δ = 25.1 (quint., J_{CP} = 10 Hz, P(*C*H$_3$)$_3$).

^{31}P{^{1}H} NMR (162.1 MHz, C_6D_6, 298 K): δ = -21.85 (s, 4P, *P*(CH$_3$)$_3$).

The NMR data of compound **VI-1** are consistent with those reported in the literature.[19]

[B$_2$cat$_2$ • (^{i}Pr$_2$Im^{Me})$_2$] ***VI-2***

^{1}H NMR (400.1 MHz, C_6D_6, 298 K): δ = 1.33 (d, 24H, $^3J_{HH}$ = 7 Hz, ^{i}Pr-C*H*$_3$), 1.51 (s, 12H, NCC*H*$_3$CC*H*$_3$N), 6.23 (sept, 4H, $^3J_{HH}$ = 7 Hz, ^{i}Pr-C*H*), 6.71 (m, 4H, BO$_2$C$_6$-4,5-*H*$_4$), 6.83 (m, 4H, BO$_2$C$_6$-3,6-*H*$_4$).

^{13}C{^{1}H} NMR (100.6 MHz, C_6D_6, 298 K): δ = 10.3 (NC*C*H$_3$C*C*H$_3$N), 22.1 (^{i}Pr-*C*H$_3$), 49.9 (^{i}Pr-*C*H), 108.5 (BO$_2$-3,6-*C*$_6$H$_4$), 117.8 (BO$_2$-4,5-*C*$_6$H$_4$), 124.2 (N*C*CH$_3$*C*CH$_3$N), 156.2 (BO$_2$-1,2-*C*$_6$H$_4$), 166.5 (N*C*N).

^{11}B{^{1}H} NMR (128.5 MHz, C_6D_6, 298 K): δ = 11.63 (s, 2B, *B*$_2$cat$_2$).

Compound **VI-2** was synthesized and characterized previously in our group by Dr. Laura Kuehn:[20]

Direct synthesis of [B$_2$cat$_2$ • (^{i}Pr$_2$Im^{Me})$_2$] (VI-2)

B$_2$cat$_2$ (150 mg, 631 μmol) and ^{i}Pr$_2$Im^{Me} (227 mg, 1.26 mmol) were dissolved in 15 mL of toluene and stirred overnight at room temperature. The white precipitate was filtered and washed with 3 mL of toluene and 6 mL of hexane and dried in vacuo to give an off-white solid (317 mg, 530 μmol, 84 %).

Colorless crystals suitable for X-ray diffraction of [B_2cat_2 • (^{i}Pr$_2$Im^{Me})$_2$] **VI-2** were obtained by slow evaporation of the solvent of a saturated solution of the compound in benzene.

Elemental analysis $C_{34}H_{48}B_2N_4O_4$ [598.40 g/mol]: calculated (found) C 68.24 (70.98), H 8.09 (8.23), N 9.36 (7.99). Although this elemental analysis results are outside the range viewed as established for analyzed purity, they are provided to illustrate the best values obtained to date. Notably, a significant amount of toluene still remains in the final product (not removable under reduced pressure or by washing with hexane). Taking the amount of one solvent molecule of toluene into account (determined by the integration of the ^{1}H NMR spectrum), the elemental analysis results match the calculation; for $C_{34}H_{48}B_2N_4O_4$ + (toluene) C_7H_8: calculated (found) C 71.31 (70.98), H 8.17 (8.23), N 8.11 (7.99).

HRMS-ASAP (m/z): calculated (found) for $C_{34}H_{49}B_2N_4O_4$ $[M+H]^+$ 599.3934 (599.3922).

^{1}H NMR (300.2 MHz, C_6D_6, 298 K): δ = 1.35 (d, $^3J_{HH}$ = 7.0 Hz, 24H, ^{i}Pr-CH_3), 1.48 (s, 12H, NCCH_3CCH_3N), 6.27 (sept, $^3J_{HH}$ = 7.0 Hz, 4H, ^{i}Pr-CH), 6.77 (m, 4H, BO_2C_6-4,5-H_4), 6.90 (m, 4H, BO_2C_6-3,6-H_4).

^{13}C{^{1}H} NMR (75.5 MHz, C_6D_6, 298 K): δ = 10.2 (NCCH$_3$CCH$_3$N), 22.1 (^{i}Pr-CH$_3$), 49.9 (^{i}Pr-CH), 108.6 (BO_2-3,6-C_6H_4), 117.8 (BO_2-4,5-C_6H_4), 124.2 (NCCH$_3$$CCH_3$N), 156.2 ($BO_2$-1,2-$C_6H_4$), 166.5 (N$C$N).

^{11}B{^{1}H} NMR (96.3 MHz, CD_2Cl_2, 298 K): δ = 11.49 (s, 2B, B_2cat$_2$).

HRMS-ASAP (m/z): calculated (found) for $C_{34}H_{49}B_2N_4O_4$ $[M+H]^+$ 599.3934 (599.3922).

trans-[Ni(^{i}Pr$_2$Im^{Me})$_2$(Bcat)Br] (VI-3a)

The complexes *cis*-[Ni(^{i}Pr$_2$Im^{Me})$_2$(Bcat)$_2$] **V-1a** (65.5 mg, 99.6 μmol) and [Ni(^{i}Pr$_2$Im^{Me})$_2$Br$_2$] (57.7 mg, 99.6 μmol) were suspended in 3 mL of diethyl ether. The mixture was stirred for 2 h at room temperature with a color change of the suspension from yellow to pale brown. The product was collected by filtration, washed with 2 mL of cold diethyl ether, and dried in vacuo to give a pale brown powder (50.0 mg, 80.9 μmol, 41 %).

Brown crystals of *trans*-[Ni(*i*Pr$_2$Im^{Me})$_2$(Bcat)Br] **VI-3a** suitable for single-crystal X-ray diffraction were obtained by slow evaporation of a saturated solution of the compound in C_6D_6.

Elemental analysis $C_{28}H_{44}BBrN_4NiO_2$ [618.09 g/mol] calculated (found): C 54.41 (53.75), H 7.18 (7.32), N 9.06 (8.61).

^{1}H NMR (400.1 MHz, C_6D_6, 298 K): δ = 1.59 (d, 12H, $^3J_{HH}$ = 7.0 Hz, ^{i}Pr-C*H$_3$*), 1.63 (s, 12H, NCC*H$_3$*CC*H$_3$*N), 1.75 (d, 12H, $^3J_{HH}$ = 7.0 Hz, ^{i}Pr-C*H$_3$*), 6.63 (sept, 4H, $^3J_{HH}$ = 7.0 Hz, ^{i}Pr-C*H*), 6.66 (m, 2H, BO_2C_6-4,5-*H$_4$*), 6.95 (m, 2H, BO_2C_6-3,6-*H$_4$*).

^{13}C{^{1}H} NMR (100.6 MHz, C_6D_6, 298 K): δ = 10.0 (NC*C*H$_3$C*C*H$_3$N), 22.0 (^{i}Pr-*C*H$_3$), 22.1 (^{i}Pr-*C*H$_3$), 53.3 (^{i}Pr-*C*H), 110.7 (BO_2-3,6-*C*$_6$H$_4$), 120.9 (BO_2-4,5-*C*$_6$H$_4$), 124.6 (N*C*CH$_3$*C*CH$_3$N), 150.3 (BO_2-1,2-*C*$_6$H$_4$), 184.1 (N*C*N).

^{11}B{^{1}H} NMR (128.5 MHz, C_6D_6, 298 K): δ = 43.41 (s, 1B, *B*cat).

IR (ATR [cm^{-1}]): 2976 (w), 2938 (vw), 2876 (vw), 1633 (vw), 1555 (vw), 1476 (m), 1368 (m), 1297 (m), 1232 (s), 1170 (vw), 1138 (m), 1100 (vs), 1067 (s), 1011 (m), 908 (w), 862 (vw), 807 (m), 768 (s), 703 (w), 639 (w), 618 (m), 551 (w), 441 (w).

trans-[Ni(*i*Pr$_2$Im^{Me})$_2$(Bcat)I] (VI-3b)

Methyl iodide (6.30 µL, 14.4 mg, 101 µmol) was added to a suspension of *cis*-[Ni(*i*Pr$_2$Im^{Me})$_2$(Bcat)$_2$] **V-1a** (66.5 mg, 101 µmol) in 3 mL of diethyl ether. The mixture was stirred for 1 h at room temperature with a color change of the suspension from yellow to pale brown. The product was collected by filtration, washed with 2 mL of cold diethyl ether, and dried in vacuo to give a pale brown powder (26.8 mg, 40.3 µmol, 40 %).

Brown crystals of *trans*-[Ni(*i*Pr$_2$Im^{Me})$_2$(Bcat)I] **VI-3b** suitable for single-crystal X-ray diffraction were obtained by slow evaporation of a saturated solution of the compound in C_6D_6.

Elemental analysis $C_{28}H_{44}BIN_4NiO_2$ [665.09 g/mol] calculated (found): C 50.57 (52.32), H 6.67 (6.75), N 8.42 (8.23).

^{1}H NMR (400.1 MHz, C_6D_6, 298 K): δ = 1.57 (d, 12H, $^{3}J_{HH}$ = 7.0 Hz, ^{i}Pr-C*H*$_3$), 1.61 (s, 12H, NCC*H*$_3$CC*H*$_3$N), 1.74 (d, 12H, $^{3}J_{HH}$ = 7.0 Hz, ^{i}Pr-C*H*$_3$), 6.56 (sept, 4H, $^{3}J_{HH}$ = 7.0 Hz, ^{i}Pr-C*H*), 6.66 (m, 2H, BO_2C_6-4,5-*H*$_4$), 6.94 (m, 2H, BO_2C_6-3,6-*H*$_4$).

^{13}C{^{1}H} NMR (100.6 MHz, C_6D_6, 298 K): δ = 10.0 (NC*C*H$_3$C*C*H$_3$N), 21.4 (^{i}Pr-*C*H$_3$), 22.0 (^{i}Pr-*C*H$_3$), 53.2 (^{i}Pr-*C*H), 110.7 (BO_2-3,6-*C*$_6$H$_4$), 121.1 (BO_2-4,5-*C*$_6$H$_4$), 124.9 (N*C*CH$_3$*C*CH$_3$N), 150.3 (BO_2-1,2-*C*$_6$H$_4$), 183.7 (N*C*N).

^{11}B{^{1}H} NMR (128.5 MHz, C_6D_6, 298 K): δ = 45.01 (s, 1B, *B*cat).

IR (ATR [cm^{-1}]): 3054 (vw), 3020 (vw), 2976 (w), 2938 (vw), 2875 (vw), 1635 (vw), 1601 (vw), 1555 (vw), 1475 (m), 1449 (w), 1410 (w), 1368 (s), 1296 (m), 1230 (vs), 1169 (vw), 1138 (s), 1100 (vs), 1067 (vs), 1016 (m), 961 (w), 934 (w), 908 (m), 861 (w), 807 (m), 765 (s), 735 (w), 702 (w), 657 (vw), 636 (w), 615 (m), 588 (vw), 551 (w), 439 (w).

8 Crystallographic Details

8.1 Collection Parameters

Crystal data were collected with a Bruker D8 Apex-2 diffractometer equipped with an Oxford Cryosystems low-temperature device using a CCD area detector and graphite monochromated Mo-K_α radiation or a Rigaku XtaLAB Synergy-DW diffractometer equipped with an Oxford Cryo 800 using a HyPix-6000HE detector and copper monochromated Cu-K_α radiation. Crystals were immersed in a film of perfluoropolyether oil on a MicroMount™ and data were collected at 100 K. The images were processed with the Bruker or Crysalis software packages and equivalent reflections were merged. Corrections for Lorentz-polarization effects and absorption were performed if necessary and the structures were solved by direct methods. Subsequent difference Fourier syntheses revealed the positions of all other non-hydrogen atoms. The structures were solved by using the ShelXTL software package.[21] All non-hydrogen atoms were refined anisotropically. Hydrogen atoms were included in structure factor calculations and assigned to idealized positions. Diamond software was used for graphical representation.

8.2 CCDC numbers of published compounds

Crystallographic data for the compounds presented in this thesis have been deposited with the Cambridge Crystallographic Data Centre as supplementary publication nos.

CCDC-2004880 (**II-1**), CCDC-2004882 (**II-2**), CCDC-2004877 (**II-4**), CCDC-2004878 (**II-9**), CCDC-2004879 (**II-10**), CCDC-2004881 (**II-15**), CCDC-2004883 (**II-16**).

CCDC-2100093 (**III-13**), CCDC-2100094 (**III-3**), CCDC-2100095 (**III-12**), CCDC-2100096 (**III-1**), CCDC-2100097 (**7a**), CCDC-2100098 (**III-15**), CCDC-2100099 (**III-9a**), CCDC-2100100 (**III-14**), CCDC-2100101 (**III-5**).

CCDC-2182812 (**2**), CCDC-2182813 (**IV-2$^+$**), CCDC-2182814 (**IV-1^{+THF}**), CCDC-2182815 (**IV-5$^+$**), CCDC-2182816 (**IV-1$^+$**), CCDC-2182817 (**IV-4$^+$**), CCDC-2182818 (**IV-3$^+$**).

These data can be obtained free of charge from The Cambridge Crystallographic Data Centre *via* www.ccdc.cam.ac.uk/data_request/cif.

8.3 Crystallographic Data for Chapter V

Crystal data for 7c: $C_{24}H_{44}N_4Ni$, M_r = 447.34, yellow block, 0.118 x 0.080 x 0.059 mm, monoclinic space group $P2_1/c$, a = 15.5164(2) Å, b = 9.42990(10) Å, c = 17.7244(3) Å, α = 90°, β = 108.412(2)°, γ = 90°, V = 2460.64(6) Å^3, T = 99.9(3) K, Z = 4, $\rho_{calcd.}$ = 1.208 g cm^{-3}, μ = 1.242 mm^{-1}, F(000) = 976, 26885 reflections in h(–19/19), k(–11/10), l(–22/21) measured in the range 3.002° < θ < 74.500°, 5027 independent reflections, 5027 observed reflections [$I > 2\sigma(I)$], 274 parameters, 0 restraints; all data: R_1 = 0.0369 and wR_2 = 0.0824, $I > 2\sigma(I)$: R_1 = 0.0318 and wR_2 = 0.0794, *Goof* 1.039, largest difference peak/hole 0.301/–0.365 e Å^{-3}.

Crystal data for 7d: $C_{30}H_{54}N_4Ni$, M_r = 529.48, yellow block, 0.378 x 0.334 x 0.284 mm, monoclinic space group C2/c, a = 15.7119(3) Å, b = 9.6716(2) Å, c = 19.5224(3) Å, α = 90°, β = 94.027(2)°, γ = 90°, V = 2959.28(10) Å^3, T = 100.00(10) K, Z = 4, $\rho_{calcd.}$ = 1.188 g cm^{-3}, μ = 1.106 mm^{-1}, F(000) = 1160, 15596 reflections in h(–19/18), k(–11/12), l(–23/24) measured in the range 4.541° < θ < 74.498°, 3034 independent reflections, 3034 observed reflections [$I > 2\sigma(I)$], 202 parameters, 96 restraints; all data: R_1 = 0.0453 and wR_2 = 0.1132, $I > 2\sigma(I)$: R_1 = 0.0433 and wR_2 = 0.1115, *Goof* 1.044, largest difference peak/hole 0.469/–0.983 e Å^{-3}.

Crystal data for V-1a: $C_{34}H_{48}B_2N_4NiO_4$, M_r = 657.07, yellow block, 0.151 x 0.131 x 0.052 mm, triclinic space group P-1, a = 10.8305(2) Å, b = 18.8820(3) Å, c = 19.1567(3) Å, α = 62.566(2)°, β = 83.687(2)°, γ = 81.6060(10)°, V = 3435.70(11) Å^3, T = 100.0(3) K, Z = 4, $\rho_{calcd.}$ = 1.270 g cm^{-3}, μ = 1.146 mm^{-1}, F(000) = 1400, 59441 reflections in h(–12/13), k(–23/23), l(–23/23) measured in the range 2.602° < θ < 74.498°, 14025 independent reflections, 14025 observed reflections [$I > 2\sigma(I)$], 835 parameters, 0 restraints; all data: R_1 = 0.0451 and wR_2 = 0.1076, $I > 2\sigma(I)$: R_1 = 0.0396 and wR_2 = 0.1039, *Goof* 1.074, largest difference peak/hole 0.508/–0.472 e Å^{-3}.

Crystal data for V-1b: $C_{34}H_{64}B_2N_4NiO_4$, M_r = 673.20, yellow block, 0.230 x 0.103 x 0.087 mm, monoclinic space group $P2_1/c$, a = 12.04960(10) Å, b = 19.77260(10) Å, c = 16.77860(10) Å, α = 90°, β = 110.8770(10)°, γ = 90°, V = 3735.09(5) Å^3,

T = 100.00(10) K, Z = 4, $\rho_{calcd.}$ = 1.197 g cm^{-3}, μ = 1.055 mm^{-1}, F(000) = 1464, 76585 reflections in h(–15/15), k(–20/24), l(–20/20) measured in the range 3.598° < θ < 74.501°, 7608 independent reflections, 7608 observed reflections [I > 2σ(I)], 426 parameters, 0 restraints; all data: R_1 = 0.0408 and wR_2 = 0.0949, I > 2σ(I): R_1 = 0.0397 and wR_2 = 0.0945, *Goof* 1.201, largest difference peak/hole 0.315/–0.236 e Å^{-3}.

Crystal data for V-1c: $C_{26}H_{48}B_2N_4NiO_4$, M_r = 561.01, yellow plate, 0.333 x 0.083 x 0.050 mm, triclinic space group P-1, a = 10.2981(2) Å, b = 17.9201(2) Å, c = 18.0389(3) Å, α = 116.089(2)°, β = 93.6880(10)°, γ = 93.5090(10)°, V = 2968.67(9) Å^3, T = 99.9(7) K, Z = 4, $\rho_{calcd.}$ = 1.255 g cm^{-3}, μ = 1.229 mm^{-1}, F(000) = 1208, 61400 reflections in h(–12/12), k(–22/19), l(–22/22) measured in the range 2.742° < θ < 74.503°, 12093 independent reflections, 12093 observed reflections [I > 2σ(I)], 750 parameters, 240 restraints; all data: R_1 = 0.0485 and wR_2 = 0.1246, I > 2σ(I): R_1 = 0.0445 and wR_2 = 0.1212, *Goof* 1.017, largest difference peak/hole 0.812/–0.854 e Å^{-3}.

Crystal data for V-2: $C_{26}H_{18}B_2O_4$, M_r = 416.02, colorless block, 0.337 x 0.216 x 0.108 mm, triclinic space group P-1, a = 9.80080(10) Å, b = 11.16390(10) Å, c = 20.6104(3) Å, α = 81.5130(10)°, β = 82.3600(10)°, γ = 66.2130(10)°, V = 2034.20(4) Å^3, T = 100.00(10) K, Z = 4, $\rho_{calcd.}$ = 1.358 g cm^{-3}, μ = 0.717 mm^{-1}, F(000) = 864, 42444 reflections in h(–12/11), k(–13/13), l(–25/25) measured in the range 2.175° < θ < 74.502°, 8287 independent reflections, 8287 observed reflections [I > 2σ(I)], 577 parameters, 0 restraints; all data: R_1 = 0.0397 and wR_2 = 0.0973, I > 2σ(I): R_1 = 0.0368 and wR_2 = 0.0941, *Goof* 0.647, largest difference peak/hole 0.291/–0.241 e Å^{-3}.

Crystal data for V-3: $C_{28}H_{22}B_2O_4$, M_r = 444.07, colorless block, 0.190 x 0.150 x 0.070 mm, triclinic space group P-1, a = 10.3698(2) Å, b = 10.8321(2) Å, c = 11.1405(3) Å, α = 94.791(2)°, β = 108.533(2)°, γ = 103.715(2)°, V = 1135.37(5) Å^3, T = 100.00(10) K, Z = 2, $\rho_{calcd.}$ = 1.299 g cm^{-3}, μ = 0.675 mm^{-1}, F(000) = 464, 23004 reflections in h(–12/12), k(–13/12), l(–13/13) measured in the range 4.249° < θ < 72.114°, 4475 independent reflections, 4475 observed reflections [I > 2σ(I)], 309 parameters, 0 restraints; all data: R_1 = 0.0399 and wR_2 = 0.0985, I > 2σ(I): R_1 = 0.0370 and wR_2 = 0.0959, *Goof* 1.050, largest difference peak/hole 0.240/–0.221 e Å^{-3}.

Crystal data for V-3^{NHC}: $C_{39}H_{42}B_2N_2O_4$, M_r = 624.36, colorless block, 0.260 x 0.180 x 0.080 mm, monoclinic space group $P2_1/c$, a = 10.35860(10) Å, b = 16.2208(2) Å, c = 20.3367(2) Å, α = 90°, β = 94.8820(10)°, γ = 90°, V = 3404.67(6) Å^3, T = 100(2) K, Z = 4, $\rho_{calcd.}$ = 1.218 g cm^{-3}, μ = 0.608 mm^{-1}, F(000) = 1328, 34811 reflections in h(–12/12), k(–19/20), l(–25/25) measured in the range 3.490° < θ < 72.124°, 6704 independent reflections, 6704 observed reflections [I > 2σ(I)], 432 parameters, 0 restraints; all data: R_1 = 0.0422 and wR_2 = 0.0987, I > 2σ(I): R_1 = 0.0372 and wR_2 = 0.0953, *Goof* 1.055, largest difference peak/hole 0.292/–0.221 e Å^{-3}.

Crystal data for V-4: $C_{28}H_{16}B_2F_6O_4$ + C_6H_6, M_r = 630.13, colorless block, 0.320 x 0.120 x 0.030 mm, triclinic space group P-1, a = 10.2370(2) Å, b = 11.4631(2) Å, c = 13.6600(3) Å, α = 113.599(2)°, β = 91.470(2)°, γ = 93.724(2)°, V = 1463.47(5) Å^3, T = 100.00(10) K, Z = 2, $\rho_{calcd.}$ = 1.430 g cm^{-3}, μ = 1.006 mm^{-1}, F(000) = 644, 29131 reflections in h(–12/12), k(–12/14), l(–16/16) measured in the range 3.537° < θ < 72.106°, 5750 independent reflections, 5750 observed reflections [I > 2σ(I)], 445 parameters, 36 restraints; all data: R_1 = 0.0461 and wR_2 = 0.1114, I > 2σ(I): R_1 = 0.0405 and wR_2 = 0.1069, *Goof* 1.071, largest difference peak/hole 0.386/–0.284 e Å^{-3}.

Crystal data for V-6: $C_{21}H_{16}B_2O_4$, M_r = 353.96, colorless block, 0.193 x 0.137 x 0.096 mm, triclinic space group P-1, a = 6.35850(10) Å, b = 8.8436(2) Å, c = 16.0653(4) Å, α = 100.552(2)°, β = 97.420(2)°, γ = 93.988(2)°, V = 876.64(3) Å^3, T = 99.9(6) K, Z = 2, $\rho_{calcd.}$ = 1.341 g cm^{-3}, μ = 0.729 mm^{-1}, F(000) = 368, 18064 reflections in h(–7/7), k(–9/11), l(–19/20) measured in the range 2.828° < θ < 74.490°, 3562 independent reflections, 3562 observed reflections [I > 2σ(I)], 245 parameters, 0 restraints; all data: R_1 = 0.0464 and wR_2 = 0.1173, I > 2σ(I): R_1 = 0.0419 and wR_2 = 0.1127, *Goof* 1.047, largest difference peak/hole 0.293/–0.290 e Å^{-3}.

Crystal data for V-7: $C_{16}H_{14}B_2O_4$, M_r = 291.89, colorless block, 0.365 x 0.162 x 0.060 mm, triclinic space group P-1, a = 5.7823(2) Å, b = 8.4295(4) Å, c = 14.2439(5) Å, α = 87.274(3)°, β = 84.401(3)°, γ = 89.585(3)°, V = 690.18(5) Å^3, T = 100.00(10) K, Z = 2, $\rho_{calcd.}$ = 1.405 g cm^{-3}, μ = 0.796 mm^{-1}, F(000) = 304, 2746 reflections in h(–7/7), k(–10/10), l(–3/17) measured in the range 5.253° < θ < 74.502°, 2746 independent reflections, 2746 observed reflections [I > 2σ(I)], 202 parameters, 0 restraints; all data: R_1 = 0.0687 and wR_2 = 0.2231, I > 2σ(I): R_1 = 0.0668 and wR_2 = 0.2217, *Goof* 1.187, largest difference peak/hole 0.383/–0.329 e Å^{-3}.

Crystal data for V-7a: $C_{28}H_{22}B_4O_8$ + 0.5(C_6H_6), M_r = 568.75, colorless block, 0.313 x 0.213 x 0.127 mm, triclinic space group P-1, a = 10.03360(10) Å, b = 12.4047(2) Å, c = 12.9515(3) Å, α = 62.329(2)°, β = 78.2950(10)°, γ = 83.9380(10)°, V = 1397.82(5) Å^3, T = 100.00(10) K, Z = 2, $\rho_{calcd.}$ = 1.351 g cm^{-3}, μ = 0.773 mm^{-1}, F(000) = 590, 29158 reflections in h(–12/12), k(–15/15), l(–16/16) measured in the range 3.914° < θ < 74.497°, 5723 independent reflections, 5723 observed reflections [I > 2σ(I)], 416 parameters, 237 restraints; all data: R_1 = 0.0470 and wR_2 = 0.1144, I > 2σ(I): R_1 = 0.0440 and wR_2 = 0.1120, *Goof* 1.020, largest difference peak/hole 0.451/–0.353 e Å^{-3}.

Crystal data for V-7b: $C_{20}H_{20}B_2O_4$, M_r = 345.98, colorless plate, 0.386 x 0.190 x 0.071 mm, monoclinic space group P2$_1$/c, a = 12.9444(2) Å, b = 15.05970(10) Å, c = 9.51950(10) Å, α = 90°, β = 98.5030(10)°, γ = 90°, V = 1835.32(4) Å^3, T = 100.00(10) K, Z = 4, $\rho_{calcd.}$ = 1.252 g cm^{-3}, μ = 0.678 mm^{-1}, F(000) = 728, 36922 reflections in h(–16/16), k(–18/12), l(–11/11) measured in the range 3.452° < θ < 74.479°, 3750 independent reflections, 3750 observed reflections [I > 2σ(I)], 239 parameters, 0 restraints; all data: R_1 = 0.0469 and wR_2 = 0.1185, I > 2σ(I): R_1 = 0.0436 and wR_2 = 0.1156, *Goof* 1.046, largest difference peak/hole 0.326/–0.311 e Å^{-3}.

Crystal data for V-12: $C_{37}H_{35}B_4NO_8Si$, M_r = 692.99, colorless block, 0.410 x 0.240 x 0.050 mm, triclinic space group P-1, a = 9.7326(2) Å, b = 10.1947(2) Å, c = 19.1912(5) Å, α = 76.146(2)°, β = 86.927(2)°, γ = 64.991(2)°, V = 1672.98(7) Å^3, T = 100(2) K, Z = 2, $\rho_{calcd.}$ = 1.376 g cm^{-3}, μ = 1.087 mm^{-1}, F(000) = 724, 33072 reflections in h(–12/12), k(–11/12), l(–23/23) measured in the range 2.375° < θ < 72.100°, 6524 independent reflections, 6524 observed reflections [I > 2σ(I)], 465 parameters, 0 restraints; all data: R_1 = 0.0495 and wR_2 = 0.1210, I > 2σ(I): R_1 = 0.0429 and wR_2 = 0.1164, *Goof* 1.040, largest difference peak/hole 0.416/–0.352 e Å^{-3}.

Crystal data for V-13: $C_{38}H_{54}B_2N_4NiO_4$, M_r = 711.18, orange block, 0.211 x 0.099 x 0.086 mm, monoclinic space group P2$_1$/c, a = 12.33620(10) Å, b = 17.5427(2) Å, c = 17.1923(2) Å, α = 90°, β = 97.9660(10)°, γ = 90°, V = 3684.69(7) Å^3, T = 99.9(4) K, Z = 4, $\rho_{calcd.}$ = 1.282 g cm^{-3}, μ = 1.108 mm^{-1}, F(000) = 1520, 39700 reflections in h(–15/15), k(–21/13), l(–21/21) measured in the range 3.618° < θ < 74.488°, 7534 independent reflections, 7534 observed reflections [I > 2σ(I)], 456 parameters,

0 restraints; all data: R_1 = 0.0399 and wR_2 = 0.1003, $I > 2\sigma(I)$: R_1 = 0.0362 and wR_2 = 0.0977, *Goof* 1.046, largest difference peak/hole 0.301/–0.256 e Å^{-3}.

Crystal data for V-14: $C_{42}H_{62}B_2N_4NiO_4$, M_r = 767.28, orange plate, 0.321 x 0.155 x 0.043 mm, monoclinic space group $P2_1/n$, a = 11.23960(10) Å, b = 19.39160(10) Å, c = 19.42560(10) Å, α = 90°, β = 97.7140(10)°, γ = 90°, V = 4195.57(5) Å^3, T = 99.99(10) K, Z = 4, $\rho_{calcd.}$ = 1.215 g cm^{-3}, μ = 1.007 mm^{-1}, F(000) = 1648, 45015 reflections in h(–14/14), k(–19/24), l(–24/23) measured in the range 3.235° < θ < 74.502°, 8567 independent reflections, 8567observed reflections [$I > 2\sigma(I)$], 492 parameters, 0 restraints; all data: R_1 = 0.0379 and wR_2 = 0.0910, $I > 2\sigma(I)$: R_1 = 0.0342 and wR_2 = 0.0884, *Goof* 1.063, largest difference peak/hole 0.309/–0.312 e Å^{-3}.

8.4 Crystallographic Data for Chapter VI

Crystal data for VI-2: $C_{34}H_{48}B_2N_4O_4 \cdot 2(C_6H_6)$, M_r = 754.60, colorless block, 0.274 x *0.236 x 0.173 mm, triclinic space group P-1, a = 11.5699(2) Å, b = 11.5794(3) Å, c = 16.3012(3) Å, α = 90.095(2)°, β = 90.074(2)°, γ = 101.071(2)°, V = 2143.26(8) Å^3, T = 100(2) K, Z = 2, $\rho_{calcd.}$ = 1.169 g cm^{-3}, μ = 0.575 mm^{-1}, F(000) = 812, 42040 reflections in h(–14/10), k(–14/14), l(–20/20) measured in the range 2.711° < θ < 72.263°, 8434 independent reflections, 8434 observed reflections [I > 2σ(I)], 717 parameters, 648 restraints; all data: R_1 = 0.0532 and wR_2 = 0.1276, I > 2σ(I): R_1 = 0.0500 and wR_2 = 0.1249, Goof 1.052, largest difference peak/hole 0.390/–0.280 e Å^{-3}.*[20]

Crystal data for VI-3a: $C_{27.94}H_{43.96}B_{0.99}Br_{1.03}N_4NiO_{1.98}$, M_r = 619.31, brown block, 0.158 x 0.063 x 0.035 mm, orthorombic space group Pnma, a = 19.2627(4) Å, b = 17.3065(2) Å, c = 8.9510(2) Å, α = 90°, β = 90°, γ = 90°, V = 2983.99(10) Å^3, T = 100.00(10) K, Z = 4, $\rho_{calcd.}$ = 1.379 g cm^{-3}, μ = 2.788 mm^{-1}, F(000) = 1298, 16962 reflections in h(–23/24), k(–18/21), l(–11/10) measured in the range 4.591° < θ < 74.475°, 3155 independent reflections, 3155 observed reflections [$I > 2\sigma(I)$], 195 parameters, 159 restraints; all data: R_1 = 0.0419 and wR_2 = 0.0930, $I > 2\sigma(I)$: R_1 = 0.0375 and wR_2 = 0.0907, *Goof* 1.089, largest difference peak/hole 0.724/–0.605 e Å^{-3}.

Crystal data for VI-3b: $C_{27.91}H_{43.94}B_{0.98}I_{1.03}N_4NiO_{1.97}$, M_r = 667.42, colorless block, 0.227 x 0.140 x 0.082 mm, orthorombic space group Pnma, a = 19.53370(10) Å, b = 17.36040(10) Å, c = 8.93500(10) Å, α = 90°, β = 90°, γ = 90°, V = 3029.97(4) Å^3, T = 99.9(5) K, Z = 4, $\rho_{calcd.}$ = 1.463 g cm^{-3}, μ = 9.415 mm^{-1}, F(000) = 1371, 60076 reflections in h(–21/24), k(–21/21), l(–11/11) measured in the range 4.527° < θ < 74.500°, 3205 independent reflections, 3205 observed reflections [I > 2σ(I)], 199 parameters, 159 restraints; all data: R_1 = 0.0299 and wR_2 = 0.0723, I > 2σ(I): R_1 = 0.0297 and wR_2 = 0.0722, *Goof* 1.127, largest difference peak/hole 0.928/–1.388 e Å^{-3}.

9 Computational Details

9.1 Computational Details for Chapter III and IV

Calculations were carried out using the TURBOMOLE V7.2 2017 program suite, a development of the University of Karlsruhe and the Forschungszentrum Karlsruhe GmbH, 1989-2007, TURBOMOLE GmbH, since 2007; available from http://www.turbomole.com.[22] Geometry optimizations were performed using (RI-)DFT calculations[23] on a m4 grid employing the PBE0[24] functional and a def2-SV(P)[25] basis set for all atoms with the exception of Ni, for which a def2-TZVP basis set was used.

Vibrational frequencies were calculated at the same level of theory with the AOFORCE[26] module and all structures represented true minima without imaginary frequencies.

Natural population analysis,[27] NBO[28] and Wiberg bond indices[29] have been evaluated from the DFT ground state electron density.

For **IV-1$^+$**, the unrestricted formulism was employed and a final $<S^2>$ value of 0.756 indicated an absence of any significant spin-contamination for a doublet spin state.

Cartesian coordinates of the geometry-optimized complexes are provided in the Supporting Informations of the publications [15, 30].

9.2 Computational Details for Chapter V

Geometry optimizations were performed using the PBE0[24] functional. Nickel was described with the def2-TZVP[25] basis set while on all other atoms the def2-SVP[25] basis set was used. Dispersion corrections were considered in the geometry optimizations by using Grimme's D3[31] correction together with the Becke-Johnson (BJ) damping function.[32] All stationary points were fully characterized by analytical frequency calculations as either minima (only positive eigenvalues) or transition states (one negative eigenvalue). The connectivity of the transition states was analyzed by geometry optimizations following the imaginary frequency mode and additional intrinsic

reaction coordinate (IRC)[33] calculations. Solvation corrections were included from using the solvent model based on density (SMD[34]; solvent = benzene; ε = 2.2706) from single-point energy calculations at the PBE0-D3(BJ)/def2-TZVPP level. A concentration correction of $\Delta G^{0\rightarrow *}$ = 1.89 kcal mol^{-1} was included in the free energies of all species to account for the change in standard states in going from the gas phase (1 atm) to the condensed phase (1 M), and to properly describe associative/dissociative steps.[35] Mayer bond orders (MBI)[36] were obtained for selected bonds. The bonding situation of **V-1a** was investigated by inspection of the canonical Kohn-Sham molecular orbitals and by further calculations based on the intrinsic bond orbital (IBO)[37] approach. WBI calculations were done in Multiwfn 3.8.[38] All geometry optimizations and vibrational frequencies were performed in Gaussian 16, revision C.01.[39] The IBO calculations were done in IboView.

10 References for Experimental, Crystallographic and Computational Section

[1] Q. Lin, G. Dawson, T. Diao, *Synlett* **2021**, *32*, 1606-1620.

[2] a) D. F. Evans, *J. Chem. Soc.* **1959**, 2003-2005; b) D. H. Grant, *J. Chem. Educ*. **1995**, *72*, 39-40; c) S. K. Sur, *J. Magn. Reson.* **1989**, *82*, 169-173.

[3] S. Stoll, A. Schweiger, *J. Magn. Reson.* **2006**, *178*, 42-55.

[4] a) A. J. Arduengo, H. V. R. Dias, R. L. Harlow, M. Kline, *J. Am. Chem. Soc.* **1992**, *114*, 5530-5534; b) A. J. Arduengo, R. Krafczyk, R. Schmutzler, H. A. Craig, J. R. Goerlich, W. J. Marshall, M. Unverzagt, *Tetrahedron* **1999**, *55*, 14523-14534; c) X. Bantreil, S. P. Nolan, *Nat. Protoc.* **2011**, *6*, 69-77.

[5] a) V. Lavallo, Y. Canac, C. Präsang, B. Donnadieu, G. Bertrand, *Angew. Chem.* **2005**, *117*, 5851-5855; *Angew. Chem. Int. Ed.* **2005**, *44*, 5705-5709; b) R. Jazzar, R. D. Dewhurst, J.-B. Bourg, B. Donnadieu, Y. Canac, G. Bertrand, *Angew. Chem.* **2007**, *119*, 2957-2960; *Angew. Chem. Int. Ed.* **2007**, *46*, 2899-2902; c) P. Bissinger, H. Braunschweig, A. Damme, I. Krummenacher, A. K. Phukan, K. Radacki, S. Sugawara, *Angew. Chem.* **2014**, *126*, 7488-7491; *Angew. Chem. Int. Ed.* **2014**, *53*, 7360-7363.

[6] a) F. Graf, L. Hupfer, **1981***, DE2940709A1*; b) A. J. Arduengo III, **1991***, US5077414*; c) T. Schaub, U. Radius, A. Brucks, M. P. Choules, M. T. Olsen, T. B. Rauchfuss, *Inorg. Synth.* **2010**, *35*, 78-91.

[7] M. Eck, S. Würtemberger-Pietsch, A. Eichhorn, J. H. J. Berthel, R. Bertermann, U. S. D. Paul, H. Schneider, A. Friedrich, C. Kleeberg, U. Radius, T. B. Marder, *Dalton Trans.* **2017**, *46*, 3661-3680.

[8] J. H. J. Berthel, L. Tendera, M. W. Kuntze-Fechner, L. Kuehn, U. Radius, *Eur. J. Inorg. Chem.* **2019**, 3061-3072.

[9] a) R. A. Schunn, S. D. Ittel, M. A. Cushing, R. Baker, R. J. Gilbert, D. P. Madden, *Inorg. Synth.* **1990**, *28*, 94-98; b) J. W. Wielandt, D. Ruckerbauer, T. Zell, U. Radius, *Inorg. Synth.* **2010**, *35*, 120-125.

[10] A. J. Arduengo, S. F. Gamper, J. C. Calabrese, F. Davidson, *J. Am. Chem. Soc.* **1994**, *116*, 4391-4394.

[11] N. D. Harrold, A. R. Corcos, G. L. Hillhouse, *J. Organomet. Chem.* **2016**, *813*, 46-54.

[12] a) A. A. Danopoulos, D. Pugh, *Dalton Trans.* **2008**, 30-31; b) K. Matsubara, S. Miyazaki, Y. Koga, Y. Nibu, T. Hashimura, T. Matsumoto, *Organometallics* **2008**, *27*, 6020-6024.

[13] K. C. Mondal, P. P. Samuel, Y. Li, H. W. Roesky, S. Roy, L. Ackermann, N. S. Sidhu, G. M. Sheldrick, E. Carl, S. Demeshko, S. De, P. Parameswaran, L. Ungur, L. F. Chibotaru, D. M. Andrada, *Eur. J. Inorg. Chem.* **2014**, 818-823.

[14] T. Schaub, M. Backes, U. Radius, *Organometallics* **2006**, *25*, 4196-4206.

[15] L. Tendera, M. Helm, M. J. Krahfuss, M. W. Kuntze-Fechner, U. Radius, *Chem. Eur. J.* **2021**, *27*, 17849-17861.

[16] a) T. Schaub, *Neuartige Nickel-Carbenkomplexe und deren Anwendung in Element-Element-Aktivierungsreaktionen*, Dissertation, Cuvillier Verlag, Universität Karlsruhe, **2006**; b) L. Tendera, T. Schaub, M. J. Krahfuss, M. W. Kuntze-Fechner, U. Radius, *Eur. J. Inorg. Chem.* **2020**, 3194-3207.

[17] G. Lesley, P. Nguyen, N. J. Taylor, T. B. Marder, A. J. Scott, W. Clegg, N. C. Norman, *Organometallics* **1996**, *15*, 5137-5154.

[18] C. N. Iverson, M. R. Smith, *Organometallics* **1996**, *15*, 5155-5165.

[19] A. G. Avent, F. G. N. Cloke, J. P. Day, E. A. Seddon, K. R. Seddon, S. M. Smedley, *J. Organomet. Chem.* **1988**, *341*, 535-541.

[20] L. Kuehn, *Earth-Abundant Metal-Catalyzed and Transition Metal-Free Borylation of Aryl Halides*, Dissertation, Universität Würzburg, **2020**.

[21] G. M. Sheldrick, *Acta Crystallogr. A* **2015**, *71*, 3-8.

[22] a) F. Furche, R. Ahlrichs, C. Hättig, W. Klopper, M. Sierka, F. Weigend, *WIREs Comput. Mol. Sci.* **2014**, *4*, 91-100; b) R. Ahlrichs, M. Bär, M. Häser, H. Horn, C. Kölmel, *Chem. Phys. Lett.* **1989**, *162*, 165-169.

[23] a) M. Sierka, A. Hogekamp, R. Ahlrichs, *J. Chem. Phys.* **2003**, *118*, 9136-9148; b) O. Treutler, R. Ahlrichs, *J. Chem. Phys.* **1995**, *102*, 346-354; c) M. Häser, R. Ahlrichs, *J. Comput. Chem.* **1989**, *10*, 104-111.

[24] a) A. D. Becke, *Phys. Rev. A* **1988**, *38*, 3098-3100; b) J. P. Perdew, *Phys. Rev. B* **1986**, *33*, 8822-8824; c) M. Ernzerhof, G. E. Scuseria, *J. Chem. Phys.* **1999**, *110*, 5029–5036; d) C. Adamo, V. Barone, *J. Chem. Phys.* **1999**, *110*, 6158–6170.

[25] a) F. Weigend, R. Ahlrichs, *Phys. Chem. Chem. Phys.* **2005**, *7*, 3297-3305; b) K. Eichkorn, F. Weigend, O. Treutler, R. Ahlrichs, *Theor. Chem. Acc.* **1997**, *97*, 119-124; c) K. Eichkorn, O. Treutler, H. Öhm, M. Häser, R. Ahlrichs, *Chem. Phys.*

Lett. **1995**, *242*, 652-660; d) A. Schäfer, C. Huber, R. Ahlrichs, *J. Chem. Phys.* **1994**, *100*, 5829-5835.

[26] P. Deglmann, K. May, F. Furche, R. Ahlrichs, *Chem. Phys. Lett.* **2004**, *384*, 103-107.

[27] Reed, A. E.; Weinstock, R. B.; Weinhold, F., Natural population analysis, *J. Chem. Phys.* **1985**, *83*, 735-746.

[28] NBO 6.0. E. D. Glendening, J. K. Badenhoop, A. E. Reed, J. E. Carpenter, J. A. Bohmann, C. M. Morales, C. R. Landis, and F. Weinhold (Theoretical Chemistry Institute, University of Wisconsin, Madison, WI, 2013); http://nbo6.chem.wisc.edu/.

[29] Wiberg, K. A., Application of the Pople-Santry-Segal CNDO Method to the Cyclopropylcarbinyl and Cyclobutyl Cation and to Bicyclobutane, *Tetrahedron* **1968**, *24*, 1083-1096.

[30] L. Tendera, M. S. Luff, I. Krummenacher, U. Radius, *Eur. J. Inorg. Chem.* **2022**, Accepted Article, DOI: 10.1002/ejic.202200416

[31] S. Grimme, J. Antony, S. Ehrlich, H. Krieg, *J. Chem. Phys.* **2010**, *132*, 154104.

[32] S. Grimme, S. Ehrlich, L. Goerigk, *J. Comput. Chem.* **2011**, *32*, 1456–1465.

[33] K. Ishida, K. Morokuma, A. Komornicki, *J. Chem. Phys.* **1977**, *66*, 2153–2156.

[34] A. V. Marenich, C. J. Cramer, D. G. Truhlar, *J. Phys. Chem. B* **2009**, *113*, 6378–6396.

[35] a) C. P. Kelly, C. J. Cramer, D. G. Truhlar, *J. Chem. Theory Comput.* **2005**, *1*, 1133–1152; b) M. Sparta, C. Riplinger, F. Neese, *J. Chem. Theory Comput.* **2014**, *10*, 1099–1108.

[36] a) I. Mayer, *Chem. Phys. Lett.* **1983**, *97*, 270–274; b) I. Mayer, *Int. J. Quantum Chem.* **1984**, *26*, 151–154.

[37] G. Knizia, *J. Chem. Theory Comput.* **2013**, *9*, 4834–4843.

[38] T. Lu, F. Chen, *J. Comput. Chem.* **2012**, *33*, 580–592.

[39] M. J. Frisch, G. W. Trucks, H. B. Schlegel, G. E. Scuseria, M. A. Robb, J. R. Cheeseman, G. Scalmani, V. Barone, B. Mennucci, G. A. Petersson, H. Nakatsuji, M. Caricato, X. Li, H. P. Hratchian, A. F. Izmaylov, J. Bloino, G. Zheng, J. L. Sonnenberg, M. Hada, M. Ehara, K. Toyota, R. Fukuda, J. Hasegawa, M. Ishida, T. Nakajima, Y. Honda, O. Kitao, H. Nakai, T. Vreven, J. A. Montgomery Jr., J. E. Peralta, F. Ogliaro, M. Bearpark, J. J. Heyd, E. Brothers, K. N. Kudin, V. N. Staroverov, R. Kobayashi, J. Normand, K. Raghavachari, A. Rendell, J. C.

Burant, S. S. Iyengar, J. Tomasi, M. Cossi, N. Rega, J. M. Millam, M. Klene, J. E. Knox, J. B. Cross, V. Bakken, C. Adamo, J. Jaramillo, R. Gomperts, R. E. Stratmann, O. Yazyev, A. J. Austin, R. Cammi, C. Pomelli, J. W. Ochterski, R. L. Martin, K. Morokuma, V. G. Zakrzewski, G. A. Voth, P. Salvador, J. J. Dannenberg, S. Dapprich, A. D. Daniels, Ö. Farkas, J. B. Foresman, J. V Ortiz, J. Cioslowski, D. J. Fox, *Gaussian 16, Revision C.01*, Gaussian, Inc., Wallingford CT, **2016**.

11 Summary

This thesis describes the synthesis and reactivity of bis-NHC ligated nickel(0)-complexes and their application in catalytic cyclization and borylation reactions of alkynes. The focus of the presented work lies on the investigation of the electronic and steric impact of different NHC ligands on the reactivity and catalytic activity of [Ni(NHC)$_2$] complexes. Since d^{10}-ML$_2$ complexes play a decisive role for numerous catalytic reactions, such as the Suzuki-Miyaura cross-coupling, the first chapter provides an overview about the general properties of NHCs and the chemistry of NHC-ligated nickel complexes, their synthesis, characterization, reactivity, and application in catalysis. Due to the large amount of work using systems generated *in situ* from imidazolium salts and nickel precursors the introduction is restricted to the current knowledge for the isolated, well-defined [Ni(NHC)$_2$] complexes **1-7**, as those complexes are employed throughout the thesis.

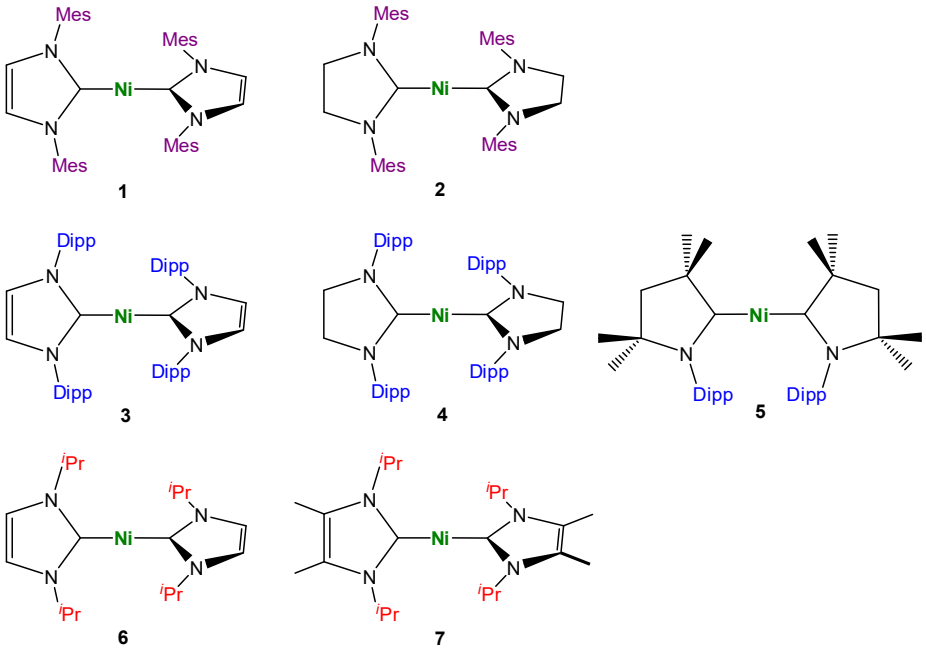

Figure XI.1 Bis-NHC-ligated nickel(0)-complexes **1-7**.

The reactivity of complex [Ni(*i*Pr$_2$Im)$_2$] **6** with different *π*-acidic substrates has already been well investigated in previous studies from our group. Contrary to that, there are just a few studies concerning the reactivity of the long known complex [Ni(Mes$_2$Im)$_2$] **1** with such substrates present in the literature. Therefore, the reactivity of **1** towards

olefins, aldehydes and ketones is examined in Chapter II and compared to the results found for **6**. While [Ni(^{i}Pr$_2$Im)$_2$] **6** readily reacts with olefins of different size, complex [Ni(Mes$_2$Im)$_2$] **1** only reacts with the smallest olefin ethylene or with activated acceptor-olefins, such as acrylates. A comparison of the ethylene-complexes [Ni(^{i}Pr$_2$Im)$_2$(η^2-H$_2$C=CH$_2$)] **24** and [Ni(Mes$_2$Im)$_2$(η^2-H$_2$C=CH$_2$)] **II-1** reveals clearly the different influence of the carbenes ^{i}Pr$_2$Im and Mes$_2$Im. The sterically more encumbered NHC Mes$_2$Im leads to a significant deviation from the square-planar coordination of the central nickel atom in **II-1**. Furthermore, the bigger C_{NHC}-Ni-C_{NHC} bite-angle adopted in the product, together with the poorer net donor properties of the carbene, lead to weaker π-backbonding to the olefin and thus to a more unstable complex. The reactions of **1** and **6** with aldehydes and ketones led in both cases to a *side-on* coordination of the C=O double bond to the nickel atom (compounds **II-3 – II-14**). Since aldehydes and ketones are less electron-rich than olefins, backbonding from the metal to the ligand gets strengthened and the stability of the resulting complexes increases. However, the steric influence of the bigger Mes$_2$Im ligand is also reflected in these compounds. Compared to the ^{i}Pr$_2$Im-stabilized complexes, the complexes stabilized by Mes$_2$Im reveal again significantly larger C_{NHC}-Ni-C_{NHC} bite-angles and, as a result of that, shorter C–O distances of the coordinated aldehyde or ketone ligands. The formation of *trans*-[Ni(Mes$_2$Im)$_2$H(OOCPh)] **II-15** and [Ni$_2$(Mes$_2$Im)$_2$(μ_2-CO)(μ_2-η^2-*C,O*-PhCOCOPh)] **II-16** during the reaction of **1** with three equivalents of benzaldehyde indicated already that radical electron-transfer processes play a pivotal role in the chemistry of complex [Ni(Mes$_2$Im)$_2$] **1**.

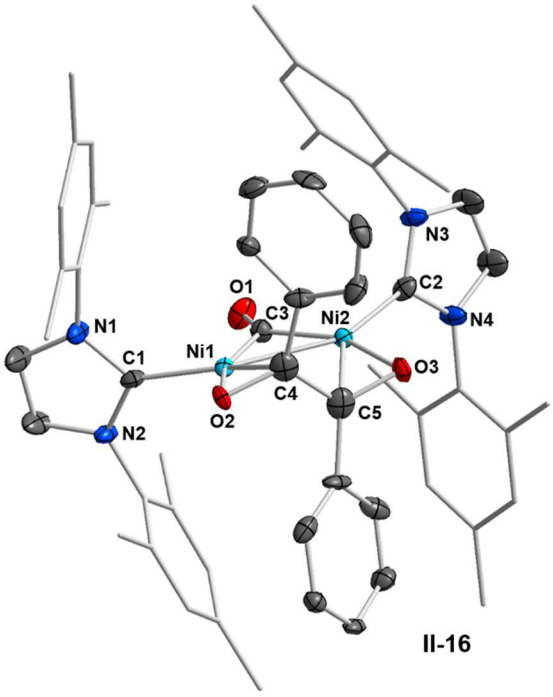

II-16

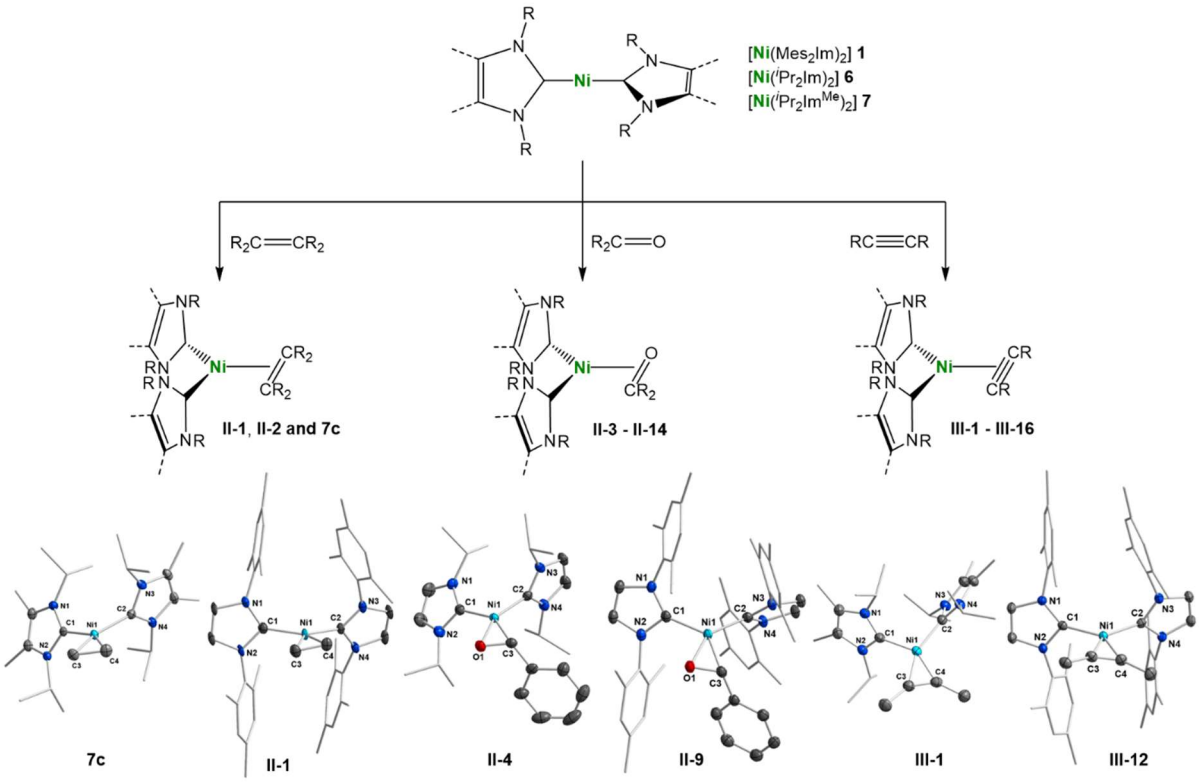

Scheme XI.1 General reactivity of the complexes **1**, **6** and **7** towards olefins, aldehydes, ketones and alkynes.

In Chapter III the studies concerning the reactivity of [Ni(NHC)$_2$] complexes are further expanded towards alkynes. At first, synthons of complex [Ni(^{i}Pr$_2$Im^{Me})$_2$] **7** (i.e. a mixture of [Ni$_2$(^{i}Pr$_2$Im^{Me})$_4$(μ-(η^2:η^2)-COD)] **7a** and [Ni(^{i}Pr$_2$Im^{Me})$_2$(η^4-COD)] **7b**) were synthesized by reacting [Ni(η^4-COD)$_2$] with ^{i}Pr$_2$Im^{Me} to explore the influence of backbone-substituted carbenes. As it was previously observed for complex **6**, the complexes **1** and **7** react with alkynes to form complexes of the type [Ni(NHC)$_2$(η^2-RC≡CR)] (**III-1 – III-16**), whereby the reactivity of **1** is again limited to small and electron-poor alkynes. Otherwise, complex **7** reacts willingly like complex **6** even with electron-rich alkynes. The methylated backbone of ^{i}Pr$_2$Im^{Me} causes only a slight twisting from the square planar geometry compared to the ^{i}Pr$_2$Im-stabilized complexes. Dependent from the alkyne introduced, the [Ni(^{i}Pr$_2$Im^{Me})$_2$] complexes **III-1 – III-11** are partially unstable upon heating. While [Ni(^{i}Pr$_2$Im^{Me})$_2$(η^2-PhC≡CPh)] **III-3** and [Ni(^{i}Pr$_2$Im^{Me})$_2$(η^2-MeOOCC≡CCOOMe)] **III-4** are stable upon heating to 100 °C for several days, the thermal reaction of [Ni(^{i}Pr$_2$Im^{Me})$_2$(η^2-HC≡C(*p*-Tol))] **III-9** and [Ni(^{i}Pr$_2$Im^{Me})$_2$(η^2-HC≡C(4-^{t}Bu-C$_6$H$_4$))] **III-10** leads to activation of one NHC *iso*-propyl methyl group *via* a C–H

addition across the C≡C triple bond of the coordinated alkyne. Thereby, the six-membered metallacycles **III-9a** and **III-10a** are formed. In contrast to [Ni(^{i}Pr$_2$Im)$_2$] **6** and [Ni(^{i}Pr$_2$Im^{Me})$_2$] **7**, complex [Ni(Mes$_2$Im)$_2$] **1** catalyzes the cyclotrimerization of alkynes already at ambient conditions. DFT calculations and experimental investigations reveal that the dissociation of one NHC ligand is the decisive step to enter the catalytic cycle, which is energetically favored for complexes of **1** due to the sterical overload. After the dissociation of a NHC ligand, additional alkyne molecules can coordinate to the resulting mono-NHC nickel moiety and the catalytically active species [Ni(Mes$_2$Im)(η^2-MeC≡CMe)$_2$] **III-B** and [(Mes$_2$Im)Ni(η^6-C$_6$Me$_6$)] **III-A** are formed. The steric impact and the associated donor properties of the NHCs lead here again to considerable differences in the stability and reactivity of the complexes [Ni(Mes$_2$Im)$_2$] **1** and [Ni(^{i}Pr$_2$Im^{Me})$_2$] **7**.

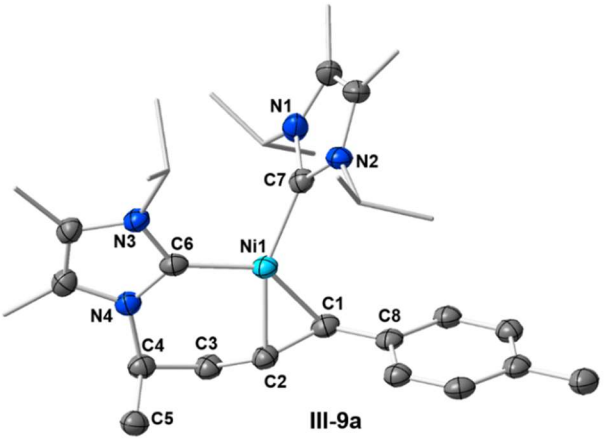

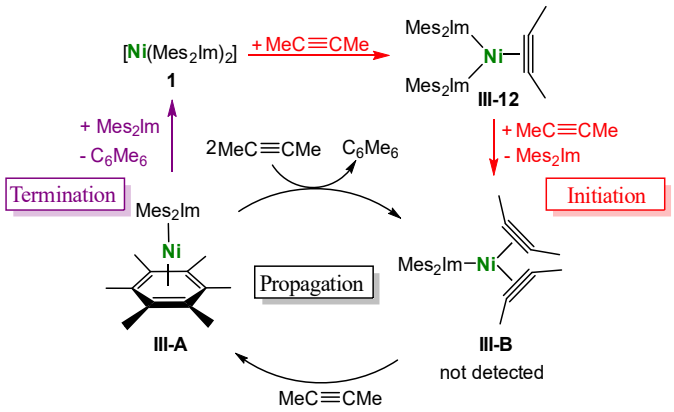

Scheme XI.2 Proposed mechanism of the NHC nickel-catalyzed cyclotrimerization of 2-butyne.

In Chapter II and earlier work of our group on the stoichiometric and catalytic C–F bond activation of fluoroarenes using [Ni(Mes$_2$Im)$_2$] **1**, the participation of metallaradicals has been already demonstrated. Therefore, in Chapter IV the oxidation of literature-known Ni(0)-complexes **1-5** by one-electron transfer to yield the corresponding radical-cations has been investigated. The reaction of **1-5** with ferrocenium tetraphenylborate yielded

the Ni(I) complexes **IV-1$^+$ – IV-5$^+$**, which were isolated as colorless, off-white or yellow (**IV-5$^+$**) solids and have been fully characterized.

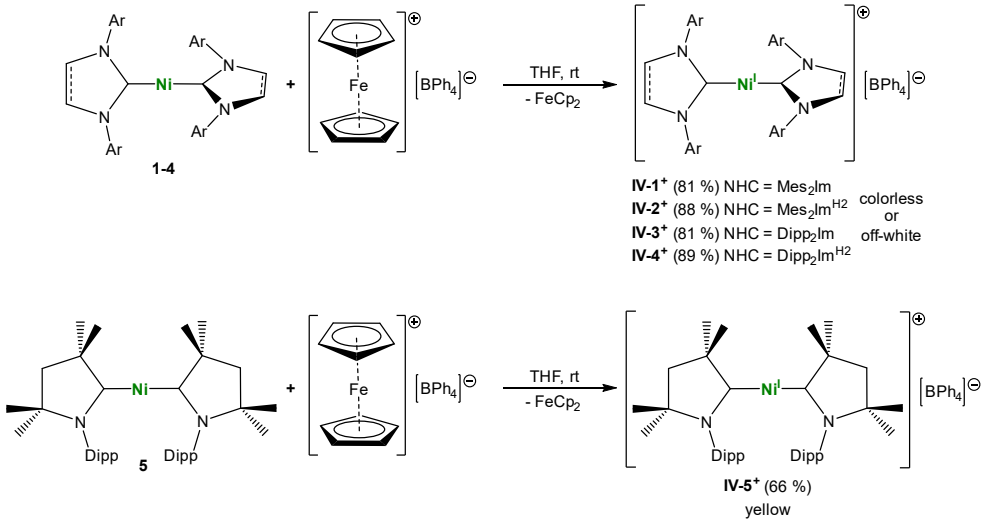

Scheme XI.3 Synthesis of linear Ni(I) complexes [Ni^I(Mes$_2$Im)$_2$][BPh$_4$] **IV-1$^+$**, [Ni^I(Mes$_2$Im^{H2})$_2$][BPh$_4$] **IV-2$^+$**, [Ni^I(Dipp$_2$Im)$_2$][BPh$_4$] **IV-3$^+$**, [Ni^I(Dipp$_2$Im^{H2})$_2$][BPh$_4$] **IV-4$^+$** and [Ni^I(cAAC^{Me})$_2$][BPh$_4$] **IV-5$^+$**.

All complexes adopt linear geometries and their magnetic properties were analyzed by EPR-measurements. Except for the cAAC^{Me}-stabilized complex **IV-5$^+$**, all compounds display strong magnetic anisotropy in the solid state, which is caused by an orbitally degenerate SOMO, according to DFT-calculations. Furthermore, it has been shown that both, the electronic properties of the NHCs as well as the steric protection of the nickel atom, are of central importance for the magnetic behavior of the complexes. An unsaturated NHC-backbone leads to a stronger anisotropy, compared to complexes with saturated NHC-backbones, respectively. The complexes **IV-1$^+$** and **IV-2$^+$**, which are stabilized

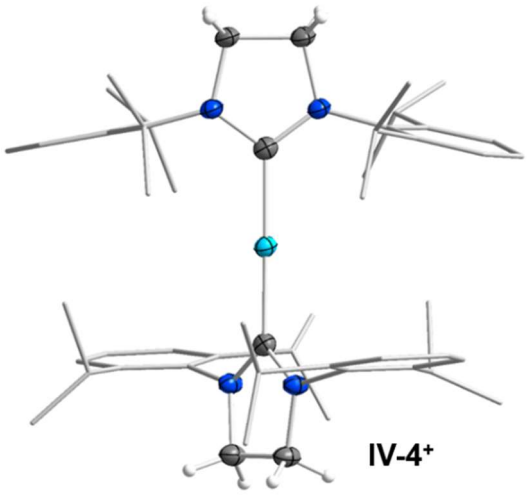

by *N*-Mes substituted carbenes, are sterically less protected than the complexes stabilized by *N*-Dipp substituted carbenes **IV-3**$^{+}$ and **IV-4**$^{+}$, and thus T-shaped THF-adducts are formed in solution to reach steric saturation of the metal. This results in a distinct decrease of the magnetic anisotropy in solution, which was verified by EPR-measurements and by the X-ray crystal structure of **IV-1**$^{+THF}$. For the complexes **IV-3**$^{+}$ and **IV-4**$^{+}$ adduct formation seems less likely due to the increased steric protection of the nickel atom caused by the larger *N*-Dipp substituted NHC ligands.

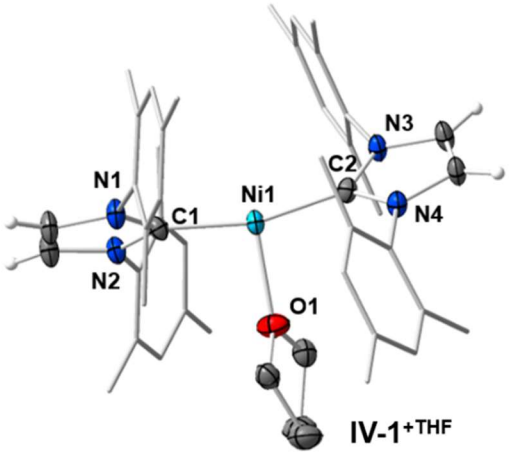

Chapter V reports the first synthesis and characterization of NHC-stabilized nickel bis-boryl complexes, as well as application of the complex [Ni(*i*Pr$_2$Im^{Me})$_2$] **7** as an efficient catalyst for the diboration of alkynes. The bis-boryl complexes **V-1a**, **V-1b** and **V-1c** were synthesized by oxidative addition of the corresponding diboron(4) compound to the [Ni(*i*Pr$_2$Im^{Me})$_2$] moiety.

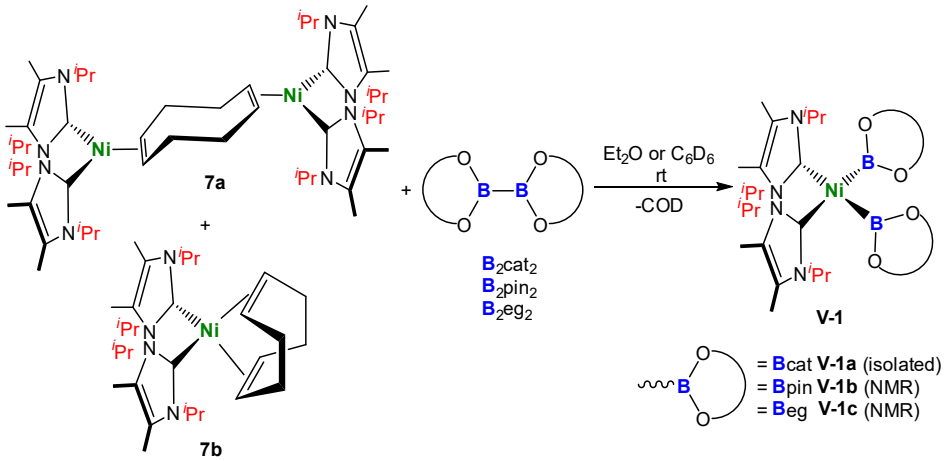

Scheme XI.4 Synthesis of *cis*-[Ni(*i*Pr$_2$Im^{Me})$_2$(Bcat)$_2$] **V-1a**, *cis*-[Ni(*i*Pr$_2$Im^{Me})$_2$(Bpin)$_2$] **V-1b** and *cis*-[Ni(*i*Pr$_2$Im^{Me})$_2$(Beg)$_2$] **V-1c**.

While **V-1a** was isolated as a pale brown solid and has been fully characterized, the reaction with B_2pin_2 or B_2eg_2 did not proceed quantitatively and led to an equilibrium with the [Ni(*i*Pr$_2$Im^{Me})$_2$]-precursors **7a** and **7b**. Thus, the complexes **V-1b** and **V-1c**

were only characterized by NMR-spectroscopy in solution. Identical experiments with other NHC ligands never afforded further nickel-boryl complexes. For all complexes **V-1a-c** single crystal X-ray structures were obtained, which feature extremely short B–B distances and small B–Ni–B angles, indicating a multicenter bonding situation of the NiB_2-moiety, which is in agreement with DFT-calculations.

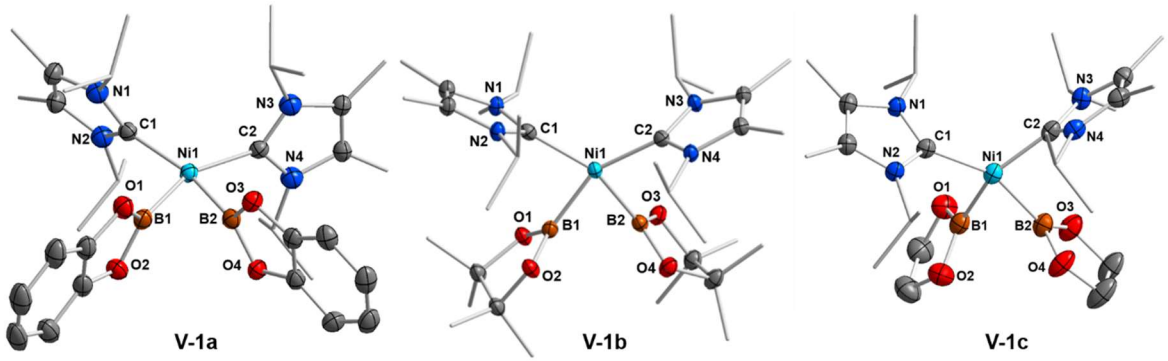

Since analogous phospine-stabilized bis-boryl complexes of the higher homologue platinum evidentially represent key-intermediates in the platinum-catalyzed diboration of alkynes, the catalytic activity of complex [Ni(^{i}Pr$_2$Im^{Me})$_2$] **7** for the borylation of alkynes was additionally studied. In NMR experiments differently substituted internal and terminal alkynes were reacted with equimolar amounts of B_2cat_2 and 4 mol% of [Ni(^{i}Pr$_2$Im^{Me})$_2$] **7**, giving the corresponding 1,2-diborylalkenes **V-2 – V-10** in good to excellent yields. In contrast to the established platinum-catalyzed borylation, new C–C coupled borylation products and tetra-borylation products were also obtained, depending on the alkyne used. The reaction of 1-pentyne selectively afforded the C–C coupled borylation products *Z,Z*-(Bcat)HC=C(C_3H_7)–(C_3H_7)C=CH(Bcat) **V-11a** and *E/Z,E/Z*-(Bcat)HC=C(C_3H_7)–HC=C(Bcat)(C_3H_7) **V-11b** whilst the reaction of the TMS-substituted alkyne *N,N*-Dimethyl-4-[(trimethylsilyl)-ethynyl]aniline afforded the tetra-borylated product (4-NMe_2-C_6H_4)(Bcat)(TMS)C–C(Bcat)$_3$ **V-12**, for instance. Another special case is the borylation of 2-butyne, in such a way as the product formation can be partially controlled by the reaction conditions applied. In dependence of the substrate ratio, the reaction temperature, and the reaction time, three different borylation products were detected. The bis-borylated product **V-7**, the

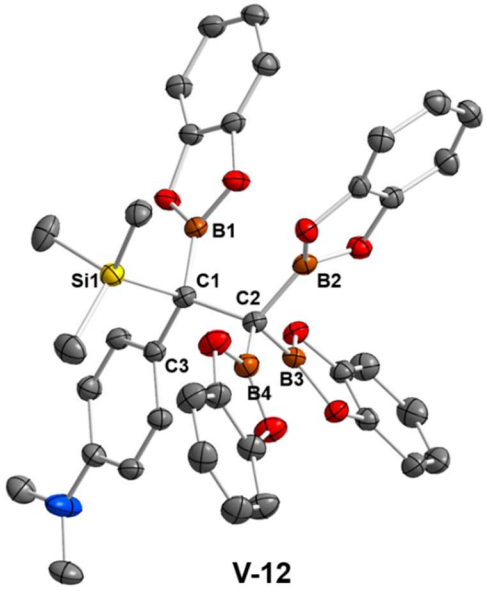

tetra-borylated product **V-7a** and the C–C coupled product **V-7b** were characterized by NMR-spectroscopy and X-ray diffraction analysis. The so far unknown products significantly expand the scope of alkyne borylations and provide an access to new boron-compounds for further transformations.

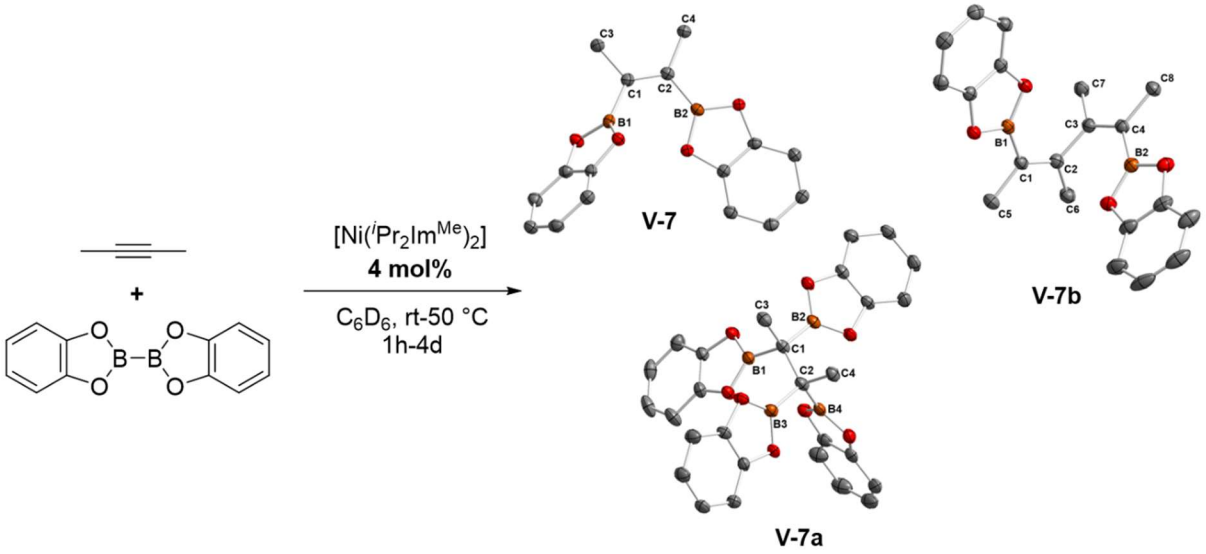

Scheme XI.5 Borylation of 2-butyne yielding *Z*-(Bcat)(Me)C=C(Me)(Bcat) **V-7,** $(Bcat)_2(Me)C–C(Me)(Bcat)_2$ **V-7a** or *E,E*-(Bcat)(Me)C=C(Me)–(Me)C=C(Me)(Bcat) **V-7b**.

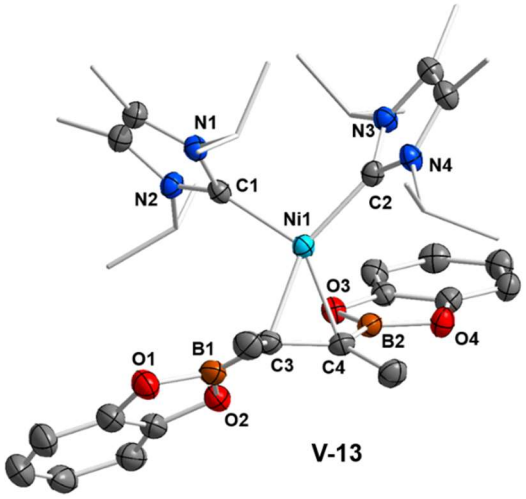

Moreover, mechanistic investigations were performed experimentally and by means of DFT-calculations, which revealed significant differences compared to the well-known catalytic cycle of the platinum-catalyzed bis-borylation. For the $[Ni(NHC)_2]$ system the bis-boryl complexes do not act as key-intermediates in the catalytic cycle. Instead, the alkyne-complexes described in chapter III are formed during the first step of the reaction pathway, which react with B_2cat_2 to the borylated olefin-complexes $[Ni(^iPr_2Im^{Me})_2(\eta^2$-*cis*-(Bcat)(Me)C=C(Me)(Bcat))] **V-13** and $[Ni(^iPr_2Im^{Me})_2(\eta^2$-*cis*-(Bcat)$(H_7C_3)$C=C$(C_3H_7)$(Bcat))] **V-14**. These complexes act as crucial catalytic intermediates and facilitate new catalytic pathways leading to new borylation products.

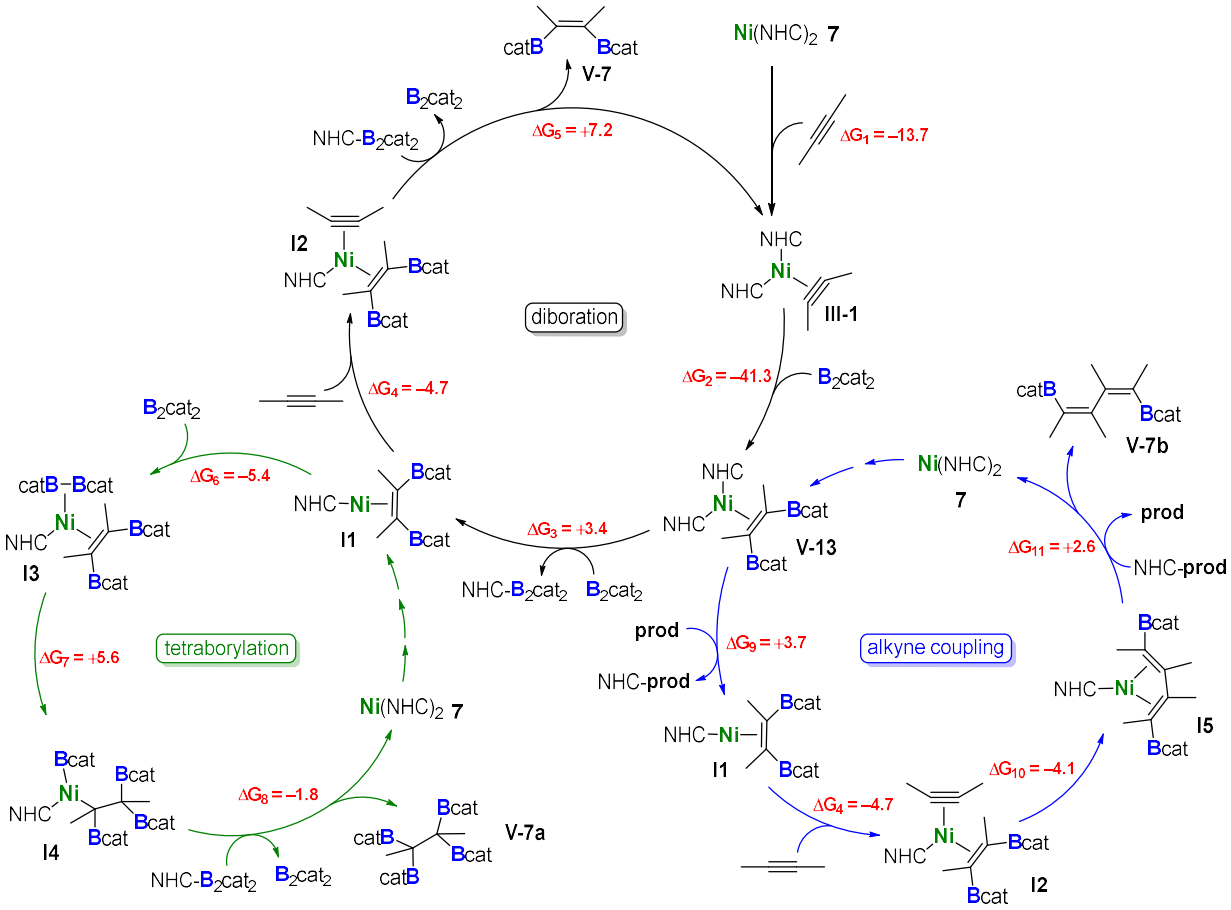

Scheme XI.6 Proposed catalytic cycles for the formation of **V-7** (black), **V-7a** (green) and **V-7b** (blue).

To get a deeper insight into the reactivity of the new bis-boryl complexes, *cis*-[Ni(*i*Pr$_2$Im^{Me})$_2$(Bcat)$_2$] **V-1a** was further investigated in Chapter VI. The reaction of complex **V-1a** with PMe$_3$ leads to a complete ligand exchange at the central nickel atom yielding the homoleptic phosphine-complex [Ni(PMe$_3$)$_4$] **VI-1** and the bis-NHC-adduct [B$_2$cat$_2$ • (*i*Pr$_2$Im^{Me})$_2$] **VI-2** *via* a reductive elimination and re-formation of the previously added B–B bond of B$_2$cat$_2$. This observation again reflects the multicenter bonding interaction described before for complex **V-1a** and shows that the boryl ligands are labile.

Furthermore the synthesis of the first NHC-stabilized mono-boryl complexes *trans*-[Ni(*i*Pr$_2$Im^{Me})$_2$(Bcat)Br] **VI-3a** and *trans*-[Ni(*i*Pr$_2$Im^{Me})$_2$(Bcat)I] **VI-3b** was achieved by an electrophilic attack of methyliodide to **V-1a** or by a ligand dismutation with *trans*-[Ni(*i*Pr$_2$Im^{Me})$_2$Br$_2$].

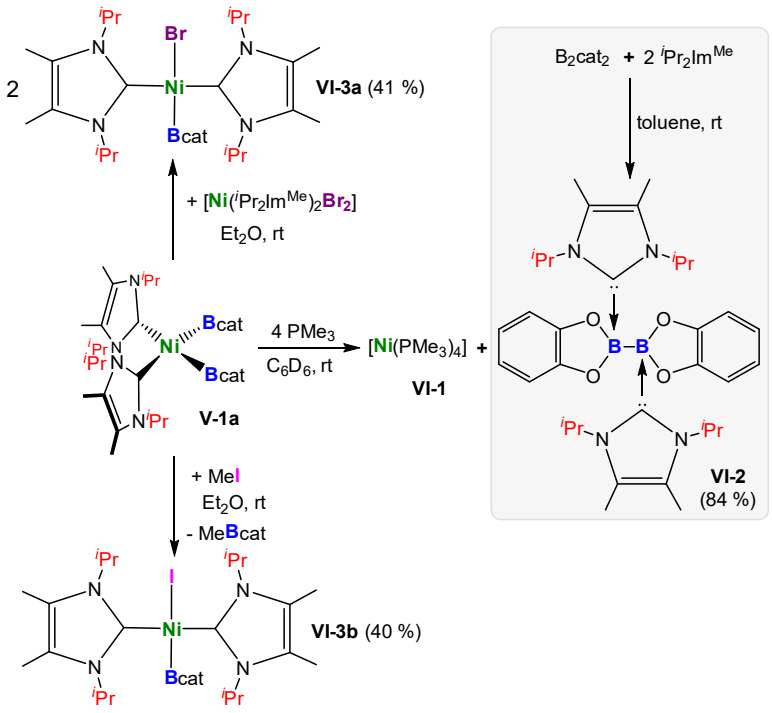

Scheme XI.7 Reactions of *cis*-[Ni(*i*Pr2Im^{Me})2(Bcat)2] **V-1a** with PMe_3, MeI and *trans*-[Ni(*i*Pr2Im^{Me})2(Br)2].

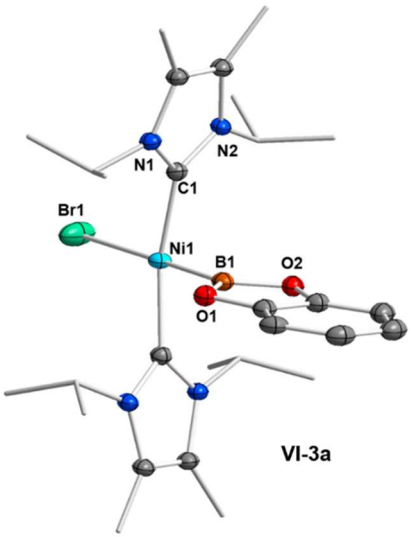

Contrary to the platinum-chemistry, it was found that the simple oxidative addition of haloboranes to [Ni(*i*Pr2Im^{Me})2] is not a suitable synthetic route to afford such mono-boryl complexes. The *trans*-configuration adopted by **VI-3a** and **VI-3b** is the result of the different *trans*-influences of the ligands ([Bcat]$^-$ > NHC > [X]$^-$), similarly as previously observed for the comparable platinum compounds. Due to the electronic overload of the nickel atom, caused by the four strong *σ*-donor ligands, complex **V-1a** is generally very reactive towards many different substrates, but often leads to unidentified decomposition products.

In course of the presented work the influence of different NHC ligands on the properties of [Ni(NHC)2] complexes was explored in detail. It has been proofed that the different steric demand of the NHCs, of course, leads to different steric protection and accessability of the metal center, but also has a significant impact on the donor-properties of the [Ni(NHC)2]-moiety *via* the NHC–Ni–NHC bite-angle the NHCs can

adopt. Furthermore, the stability of complexes coordinated by π-ligands, the tendency for ligand-dissociation and the redox behavior are decisively influenced by the sterics of the carbenes. The choice of suitable NHC ligands therefore is crucial for the potential stabilization of highly reactive nickel complexes, as well as for the design of new catalysts, which enter new reaction pathways, in the future.

12 Zusammenfassung

Die vorliegende Arbeit befasst sich mit der Synthese und Reaktivität von zweifach NHC-stabilisierten Nickel(0)-Komplexen sowie deren Anwendung als Katalysatoren in Zyklisierungs- und Borylierungsreaktionen von Alkinen. Der Fokus liegt auf der Untersuchung von elektronischen und sterischen Einflüssen verschiedener NHC-Liganden auf die Reaktivität und katalytische Aktivität von [Ni(NHC)$_2$]-Komplexen. Da solche d^{10}-ML$_2$ Komplexe heute für eine Vielzahl von katalytischen Reaktionen von immenser Bedeutung sind, wie z. B. der Suzuki-Miyaura-Kreuzkupplung, wird im ersten Kapitel ein Überblick über die grundlegenden Eigenschaften von NHCs und die Chemie NHC-substituierter Nickel-Komplexe, deren Synthese, Charakterisierung, Reaktivität und Anwendung in der Katalyse, gegeben. Aufgrund der großen Anzahl an Studien zu Nickel-NHC-Komplexen, welche *in situ* aus Imidazolium-Salzen und geeigneten Nickel-Vorläuferkomplexen erzeugt werden, wird in der Einleitung vorwiegend auf den aktuellen Kenntnisstand über die isolierten, klar definierten [Ni(NHC)$_2$]-Komplexe **1-7** Bezug genommen, welche im Zuge dieser Arbeit verwendet wurden.

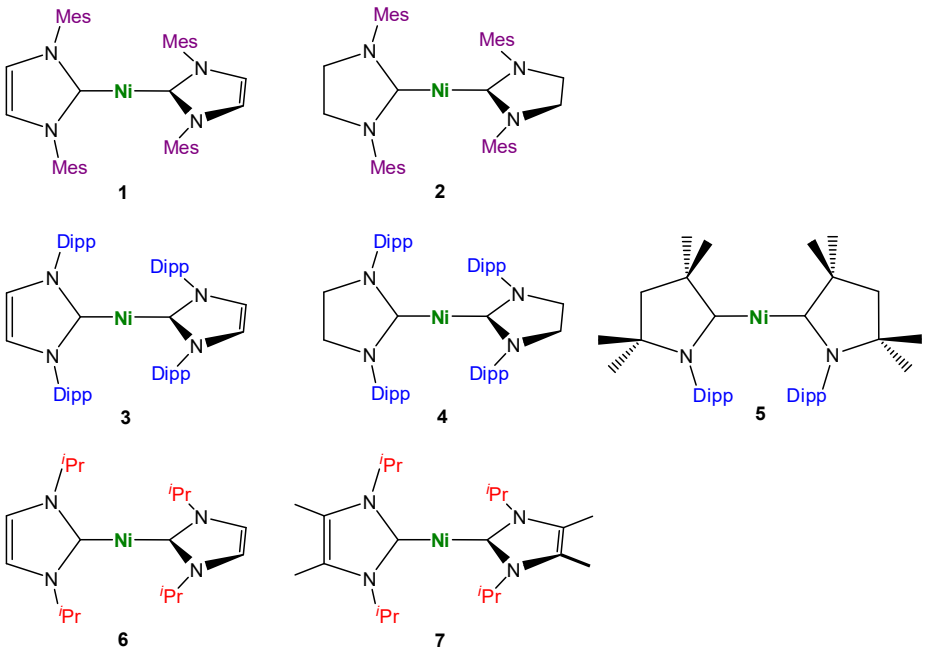

Abbildung XII.1 Zweifach NHC-stabilisierte Nickel(0)-Komplexe **1-7**.

In der eigenen Arbeitsgruppe wurde die Reaktivität des Komplexes [Ni(^{i}Pr$_2$Im)$_2$] **6** gegenüber verschiedenen *π*-aciden Liganden in vorangegangenen Arbeiten bereits weitgehend untersucht, wohingegen für den lange bekannten Komplex [Ni(Mes$_2$Im)$_2$] **1** nur wenige Reaktivitätsstudien mit diesen Substraten bekannt sind. In Kapitel II wird daher die Reaktivität von **1** gegenüber Olefinen, Aldehyden und Ketonen untersucht und mit den bereits bekannten Ergebnissen von Komplex **6** verglichen. Während [Ni(^{i}Pr$_2$Im)$_2$] **6** bereitwillig mit unterschiedlich großen Olefinen unter Ausbildung von stabilen *side-on* koordinierten Komplexen des Typs [Ni(^{i}Pr$_2$Im)$_2$(η^2-R$_2$C=CR$_2$)] reagiert, reagiert Komplex [Ni(Mes$_2$Im)$_2$] **1** nur mit dem kleinsten Olefin Ethylen und mit aktivierten Akzeptor-Olefinen, wie z. B. Acrylaten. Ein Vergleich der beiden Ethylen-Komplexe [Ni(^{i}Pr$_2$Im)$_2$(η^2-H$_2$C=CH$_2$)] **24** und [Ni(Mes$_2$Im)$_2$(η^2-H$_2$C=CH$_2$)] **II-1** zeigt deutlich den unterschiedlichen Einfluss der Carbene ^{i}Pr$_2$Im und Mes$_2$Im. Das sterisch anspruchsvollere Carben Mes$_2$Im führt zu einer deutlichen Abweichung von der quadratisch-planaren Koordination des zentralen Nickelatoms in **II-1**. Zudem wird ein deutlich größerer C_{NHC}-Ni-C_{NHC} Bisswinkel ausgebildet, was zusätzlich zur schlechteren *σ*-Donorfähigkeit des Carbens, zu einer schlechteren *π*-Rückbindung zum Olefin-Liganden und somit zu einem instabileren Komplex führt. Die Umsetzung von Komplex **1** und Komplex **6** mit Aldehyden und Ketonen führte in beiden Fällen zur *side-on* Koordination der C=O-Doppelbindung an das Nickelatom (Verbindungen **II-3 – II-14**). Da Aldehyde und Ketone deutlich elektronenärmer als Olefine sind, wird die Rückbindung vom Metall auf den *π*-Liganden gestärkt und somit die Stabilität der Komplexe erhöht. Jedoch wird auch hier der Einfluss des sterisch anspruchsvollen Mes$_2$Im-Liganden deutlich. Im Vergleich zu den ^{i}Pr$_2$Im-stabilisierten Komplexen weisen die Mes$_2$Im-stabilisierten Komplexe ebenfalls deutlich größere C_{NHC}-Ni-C_{NHC} Bisswinkel und daraus folgend kürzere C–O Abstände im koordinierten Carbonyl-Liganden auf. Die Bildung von *trans*-[Ni(Mes$_2$Im)$_2$H(OOCPh)] **II-15** und [Ni$_2$(Mes$_2$Im)$_2$(μ_2-CO)(μ_2-η^2-*C,O*-PhCOCOPh)] **II-16**, welche bei der Umsetzung von **1**

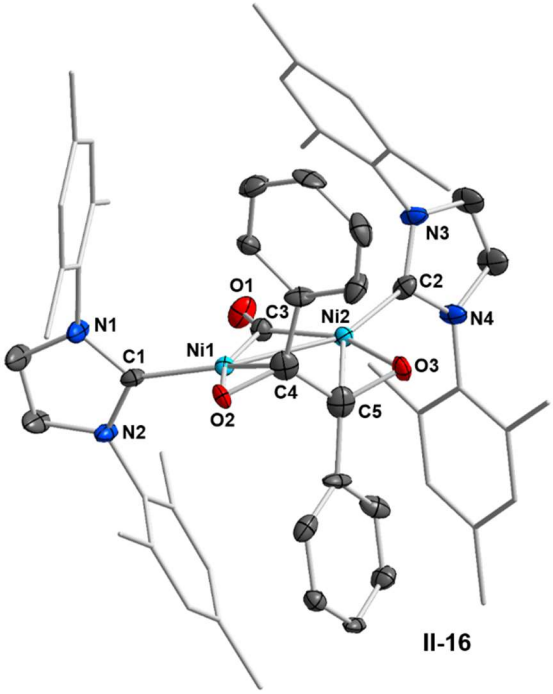

II-16

mit drei Äquivalenten Benzaldehyd gebildet wurden, deutet darauf hin, dass radikalische Elektronentransferprozesse eine entscheidende Rolle für das Reaktionsverhalten von Komplex [Ni(Mes$_2$Im)$_2$] **1** spielen.

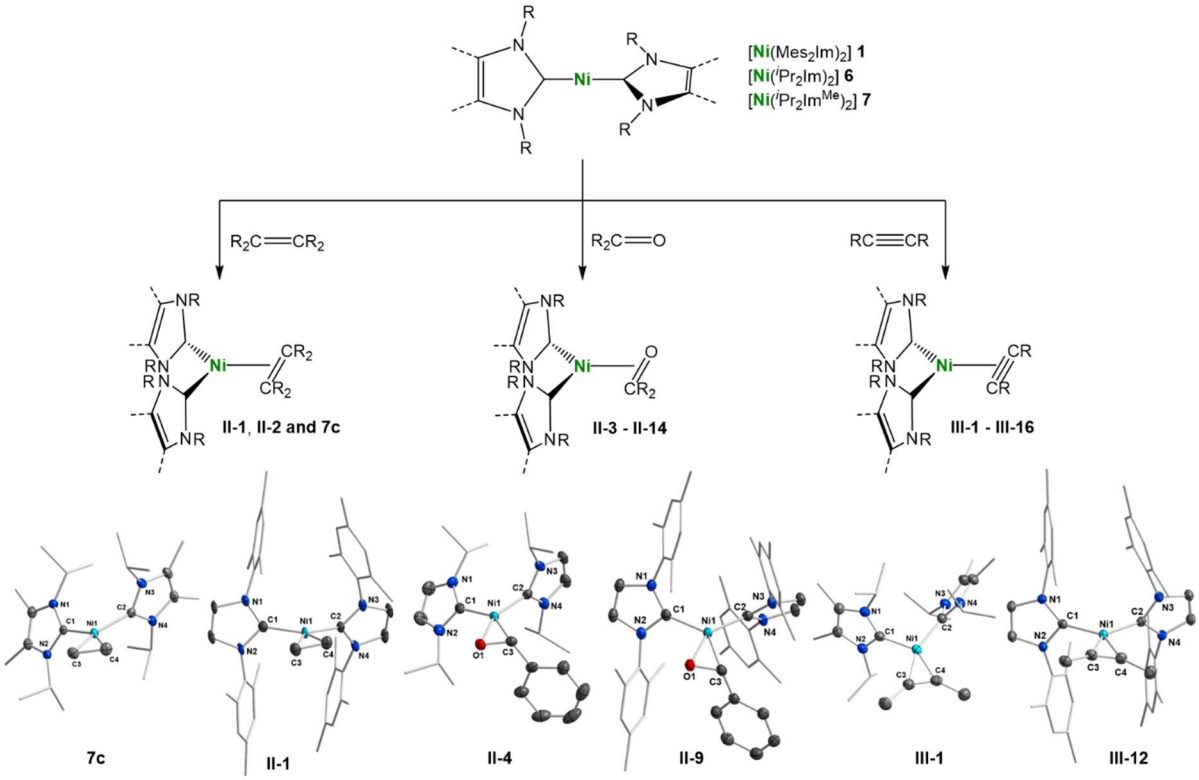

Schema XII.1 Generelle Reaktivität der Komplexe **1**, **6** und **7** gegenüber Olefinen, Aldehyden, Ketonen und Alkinen.

In Kapitel III werden die Reaktivitätsstudien an [Ni(NHC)$_2$] auf Alkine ausgeweitet. Um auch die Auswirkungen von Rückgrat-substituierten Carbenen zu untersuchen, wurden durch Umsetzung von [Ni(η^4-COD)$_2$] mit ^{i}Pr$_2$Im^{Me} zunächst Synthone für [Ni(^{i}Pr$_2$Im^{Me})$_2$] **7** (ein Gemisch aus [Ni$_2$(^{i}Pr$_2$Im^{Me})$_4$(μ-(η^2:η^2)-COD)] **7a** und [Ni(^{i}Pr$_2$Im^{Me})$_2$(η^4-COD)] **7b**) erstmalig dargestellt. Analog zu Komplex **6** reagieren die Komplexe **1** und **7** mit Alkinen unter Ausbildung von Komplexen des Typs [Ni(NHC)$_2$(η^2-RC≡CR)] (**III-1 – III-16**), wobei die Reaktivität von **1** auch hier auf kleine und elektronenarme Alkine beschränkt ist. Komplex **7** hingegen zeigt eine ähnliche Reaktionsfreudigkeit wie der bereits gut untersuchte Komplex **6**, auch mit elektronenreichen Alkinen. Das methylierte Rückgrat von ^{i}Pr$_2$Im^{Me} führt, im Vergleich zu den ^{i}Pr$_2$Im-stabilisierten Komplexen, lediglich zu einer leichten Verdrehung der

Alkin-Liganden aus der quadratisch-planaren Ebene. Die [Ni(^{i}Pr$_2$Im^{Me})$_2$] Komplexe **III-1 – III-11** sind, abhängig vom eingeführten Alkin-Liganden, unter thermischer Belastung in Lösung teilweise instabil und liefern daher verschiedene Zersetzungsprodukte. Während die Komplexe [Ni(^{i}Pr$_2$Im^{Me})$_2$(η^2-PhC≡CPh)] **III-3** und [Ni(^{i}Pr$_2$Im^{Me})$_2$(η^2-MeOOCC≡CCOOMe)] **III-4** selbst bei 100 °C über mehrere Tage stabil sind, führt die thermische Reaktion von [Ni(^{i}Pr$_2$Im^{Me})$_2$(η^2-HC≡C(*p*-Tol))] **III-9** und [Ni(^{i}Pr$_2$Im^{Me})$_2$(η^2-HC≡C(4-^{t}Bu-C$_6$H$_4$))] **III-10** zu einer C–H-Aktivierung einer NHC *iso*-Propyl-Methyl-Gruppe unter C–H-Addition an die C≡C-Dreifachbindung des koordinierten Alkins und zur Ausbildung der sechs-gliedrigen Metallazyklen **III-9a** und **III-10a**. Im Gegensatz zu [Ni(^{i}Pr$_2$Im)$_2$] **6** und [Ni(^{i}Pr$_2$Im^{Me})$_2$] **7**, katalysiert Komplex [Ni(Mes$_2$Im)$_2$] **1** bereits bei Raumtemperatur die Zyklotrimerisierung von Alkinen. DFT-Rechnungen und experimentelle Untersuchungen belegen, dass der entscheidende Schritt die Dissoziation eines NHC Liganden vom Alkinkomplex ist, was für Komplex **1**, aufgrund der sterischen Überfrachtung, energetisch deutlich bevorzugt ist. Nach Dissoziation eines NHC Liganden können weitere Alkine an das Nickel Mono-NHC-Komplexfragment koordinieren, wodurch die Zwischenstufen [Ni(Mes$_2$Im)(η^2-MeC≡Me)$_2$] **III-B** und [(Mes$_2$Im)Ni(η^6-C$_6$Me$_6$)] **III-A** gebildet werden, welche letztendlich die katalytisch aktiven Spezies darstellen. Der sterische Einfluss des NHCs und die damit verbundenen Donorfähigkeiten von [Ni(NHC)$_2$] führen demnach auch hier zu deutlichen Unterschieden in Stabilität und Reaktivität der untersuchten Komplexe [Ni(Mes$_2$Im)$_2$] **1** und [Ni(^{i}Pr$_2$Im^{Me})$_2$] **7**.

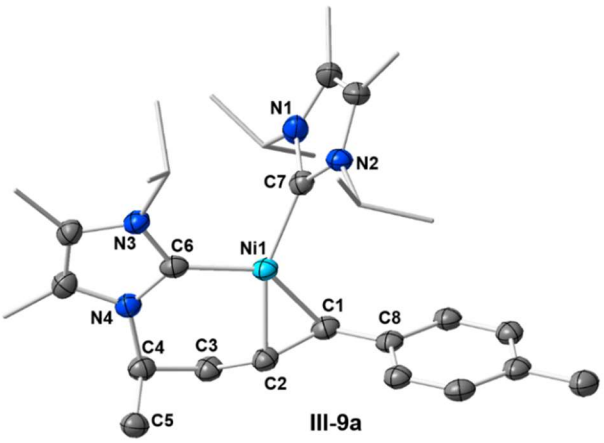

III-9a

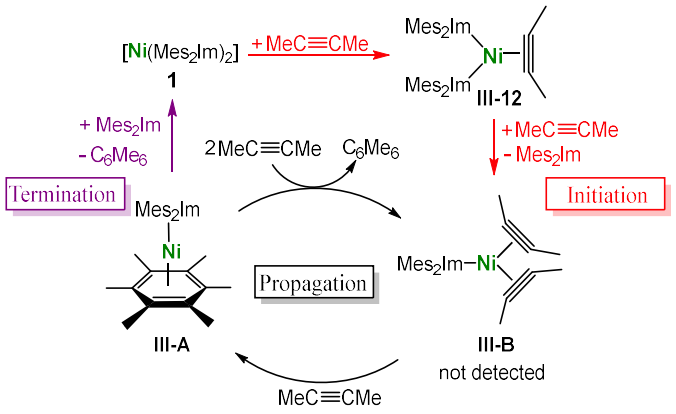

Schema XII.2 Postulierter Mechanismus für die NHC-Nickel-katalysierte Zyklotrimerisierung von 2-Butin.

In Kapitel II und früheren Arbeiten unserer Gruppe zur stöchiometrischen und katalytischen C–F-Bindungsaktivierung von Fluoraromaten mit [Ni(Mes$_2$Im)$_2$] **1** wurde bereits die Beteiligung von Metallradikalen nachgewiesen. Daher beschreibt das vierte Kapitel die Einelektronenoxidation der literaturbekannten, linearen Ni(0)-Komplexe **1-5** hin zu den entsprechenden Radikal-Kationen. Dabei konnten durch die Umsetzung von **1-5** mit Ferroceniumtetraphenylborat die jeweiligen Ni(I)-Komplexe **IV-1$^+$ – IV-5$^+$** isoliert und vollständig charakterisiert werden.

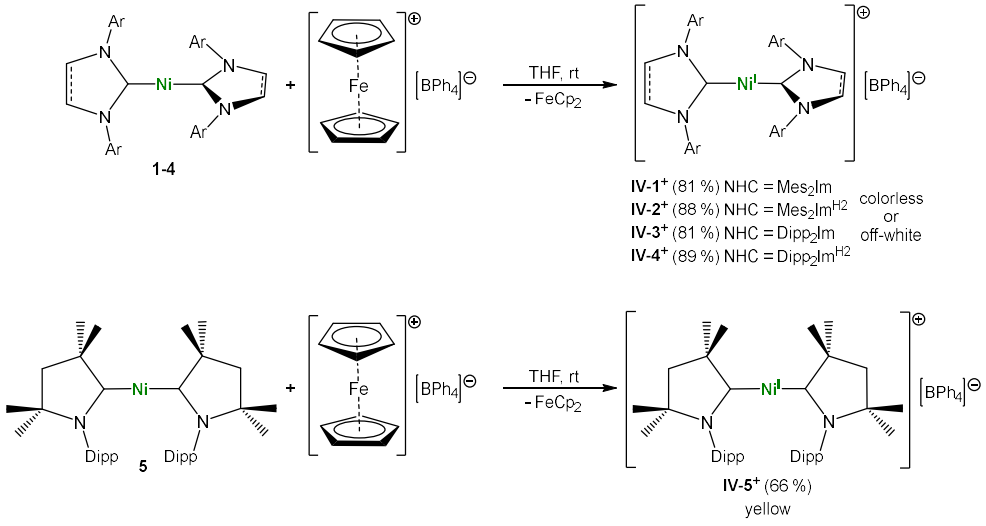

Schema XII.3 Synthese der linearen Ni(I)-Komplexe [Ni^I(Mes$_2$Im)$_2$][BPh$_4$] **IV-1$^+$**, [Ni^I(Mes$_2$Im^{H2})$_2$][BPh$_4$] **IV-2$^+$**, [Ni^I(Dipp$_2$Im)$_2$][BPh$_4$] **IV-3$^+$**, [Ni^I(Dipp$_2$Im^{H2})$_2$][BPh$_4$] **IV-4$^+$** und [Ni^I(cAAC^{Me})$_2$][BPh$_4$] **IV-5$^+$**.

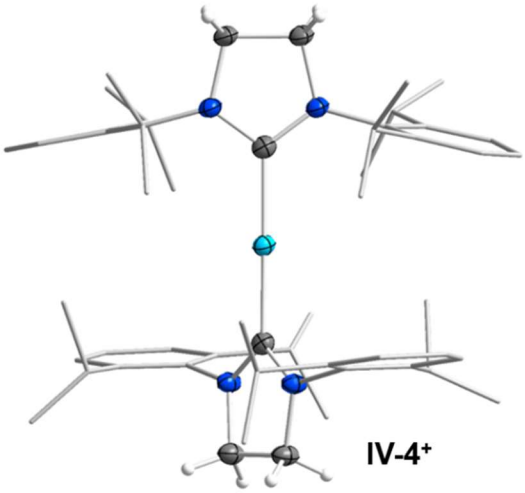

Alle Komplexe weisen eine lineare Geometrie auf und wurden mittels EPR-Messungen auf ihre magnetischen Eigenschaften hin untersucht. Bis auf den cAAC^{Me}-stabilisierten Komplex **IV-5$^+$** wurde für alle Komplexe eine sehr starke magnetische Anisotropie im Festkörper festgestellt, welche laut theoretischen Rechnungen auf die Entartung des SOMOs zurückzuführen ist. Zudem konnte gezeigt werden, dass sowohl die elektronischen Eigenschaften der NHCs als auch die sterische Abschirmung des Nickelatoms von zentraler Bedeutung für die magnetischen Eigenschaften der Komplexe sind. Ein ungesättigtes NHC-Rückgrat führt dementsprechend zu einer stärkeren Anisotropie im Vergleich zu den Komplexen mit gesättigtem Rückgrat. Die Komplexe **IV-1$^+$** und **IV-2$^+$**, welche durch die *N*-Mes-substituierten Carbene stabilisiert werden und somit im Vergleich zu den *N*-Dipp-substituierten Komplexen sterisch etwas weniger abgeschirmt sind, bilden in Lösung T-förmige THF-Addukte, um eine sterische Absättigung des Nickels zu erreichen. Daraus resultiert eine deutliche Verringerung der magnetischen Anisotropie in Lösung, was durch EPR-Messungen und zusätzlich durch die erhaltene Kristallstruktur von **1^{+THF}** belegt werden konnte. Für die Komplexe **IV-3$^+$** und **IV-4$^+$** scheint die Adduktbildung aufgrund des größeren sterischen Anspruchs der *N*-Dipp-substituierten NHCs weniger begünstigt zu sein.

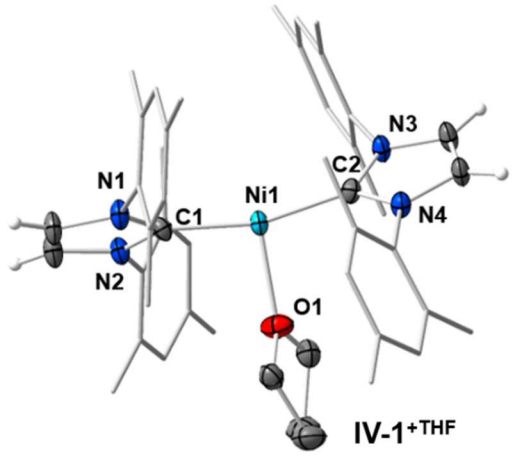

In Kapitel V wird die erstmalige Synthese und Charakterisierung von NHC-stabilisierten Nickel Bis-Boryl Komplexen sowie die Verwendung von **7** als effizienter Katalysator für die Bis-Borylierung von Alkinen beschrieben. Die Bis-Boryl Komplexe **V-1a**, **V-1b** und **V-1c** konnten durch eine oxidative Additionsreaktion der entsprechenden Diboran(4)-Verbindung an das [Ni(^{i}Pr$_2$Im^{Me})$_2$]-Komplexfragment dargestellt werden.

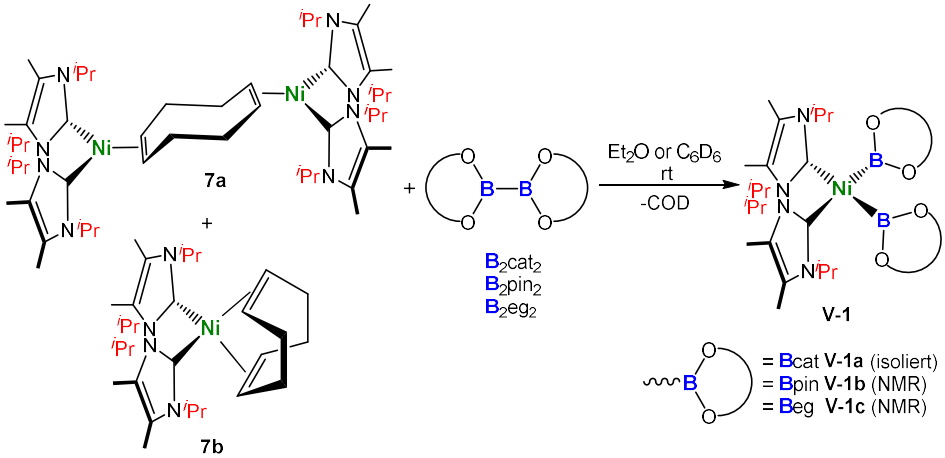

Schema XII.4 Synthese von *cis*-[Ni(*i*Pr$_2$Im^{Me})$_2$(Bcat)$_2$] **V-1a**, *cis*-[Ni(*i*Pr$_2$Im^{Me})$_2$(Bpin)$_2$] **V-1b** und *cis*-[Ni(*i*Pr$_2$Im^{Me})$_2$(Beg)$_2$] **V-1c**.

Während **V-1a** als hellbrauner Feststoff isoliert und vollständig charakterisiert werden konnte, führte die Reaktion mit B_2pin_2 und B_2eg_2 nicht zu einer quantitativen Umsetzung und stattdessen zu einem Gleichgewicht mit den eingesetzten [Ni(*i*Pr$_2$Im^{Me})$_2$]-Precursoren **7a** und **7b**, weshalb die Komplexe **V-1b** und **V-1c** lediglich in Lösung charakterisiert werden konnten. Analoge Versuche mit anderen NHC-Liganden führten in keinem Fall zur erfolgreichen Synthese von Nickel-Boryl Komplexen. Für alle drei Komplexe konnten Molekülstrukturen im Festkörper erhalten werden, welche sich durch extrem kurze B–B-Abstände und kleine B–Ni–B-Winkel auszeichnen. Dies steht in Übereinstimmung mit durchgeführten DFT-Rechnungen, wonach eine delokalisierte Mehrzentrenbindung zwischen dem Nickelatom und den beiden Boryl-Einheiten die entscheidende bindende Wechselwirkung ist.

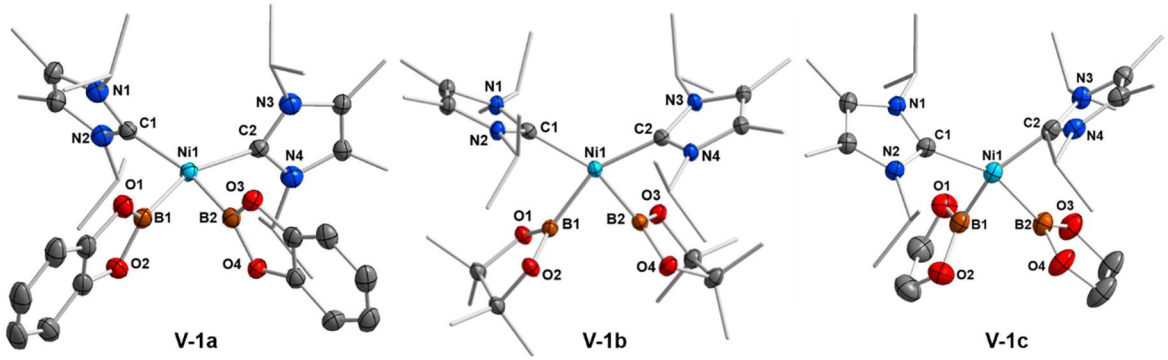

Da analoge Phosphan-stabilisierte Bis-Boryl Komplexe des höheren Homologen Platin erwiesenermaßen entscheidende Schlüsselintermediate in der Platin-katalysierten Bis-Borylierung von Alkinen darstellen, wurde Komplex **7** ebenfalls auf seine katalytische Aktivität für die Borylierung von Alkinen untersucht. Dafür wurden in NMR-Experimenten verschieden substituierte interne und terminale Alkine mit einer äquimolaren Menge an B_2cat_2 und 4 mol% [Ni(^{i}Pr$_2$Im^{Me})$_2$] **7** umgesetzt. Folglich konnten die entsprechenden *cis*-1,2-Diborylalkene **V-2 – V-10** in guten bis sehr guten Ausbeuten erhalten werden. Anders als bei der etablierten Platin-katalysierten Borylierung konnten, je nach eingesetztem Alkin, darüber hinaus neue C–C-gekuppelte und tetra-borylierte Produkte dargestellt werden. Demnach führte die Reaktion mit 1-Pentin selektiv zur Bildung der neuen C–C-gekuppelten Borylierungsprodukte *Z,Z*-(Bcat)HC=C(C_3H_7)–(C_3H_7)C=CH(Bcat) **V-11a** und *E/Z,E/Z*-(Bcat)HC=C(C_3H_7)–HC=C(Bcat)(C_3H_7) **V-11b**. Die Reaktion mit dem TMS-substituierten Alkin *N*,*N*-Dimethyl-4-[(trimethylsilyl)-ethynyl]anilin lieferte hingegen das tetra-borylierte Produkt (4-NMe_2-C_6H_4)(Bcat)(TMS)C–C(Bcat)$_3$ **V-12**. Einen weiteren Sonderfall stellt die Borylierung von 2-Butin dar, da hier die Produktbildung durch Anpassung der Reaktionsbedingungen teilweise gesteuert werden kann. So konnten für diese Reaktion, in Abhängigkeit vom Edukt-Verhältnis, der Reaktionstemperatur und der Reaktionsdauer, drei verschiedene Produkte nachgewiesen werden. Das zweifach borylierte Produkt **V-7**, das vierfach-borylierte Produkt **V-7a** und das C–C-gekuppelte Produkt **V-7b** wurden sowohl mittels NMR-Spektroskopie als auch per Einkristallstrukturanalyse charakterisiert. Die bisher unbekannten Produkte stellen eine deutliche Erweiterung der Produktpalette von Alkin-Borylierungsreaktionen dar und eröffnen einen Zugang zu neuen Bor-Verbindungen, welche weiter funktionalisiert werden können.

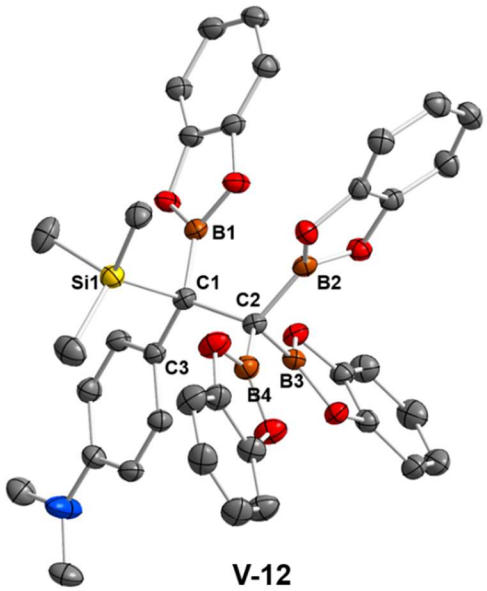

V-12

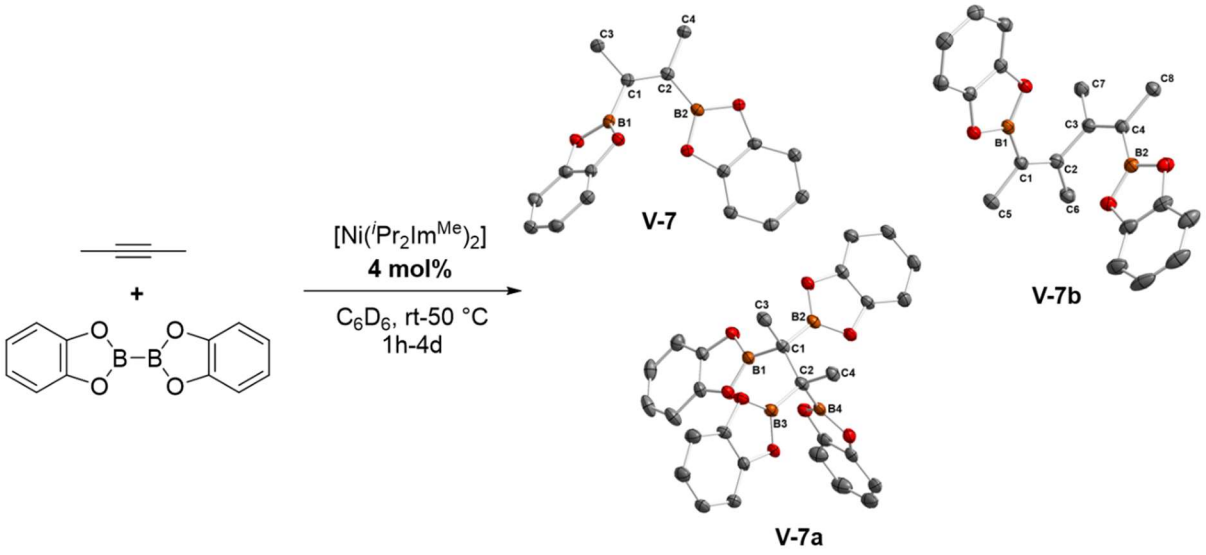

Schema XII.5 Borylierung von 2-Butin unter Ausbildung von *Z*-(Bcat)(Me)C=C(Me)(Bcat) **V-7,** $(Bcat)_2(Me)C–C(Me)(Bcat)_2$ **V-7a** oder *E,E*-(Bcat)(Me)C=C(Me)–(Me)C=C(Me)(Bcat) **V-7b**.

Des Weiteren wurden sowohl experimentelle Untersuchungen als auch DFT-Rechnungen zur Aufklärung des Mechanismus der Katalyse durchgeführt, welche deutliche Unterschiede zur bekannten Platin-Phosphan Chemie aufzeigen. Demnach nehmen die Bis-Boryl Komplexe für das hier beschriebene $[Ni(NHC)_2]$-System keine tragende Rolle im Katalysezyklus ein. Stattdessen konnte gezeigt werden, dass der Reaktionspfad im ersten Schritt zur Bildung der in Kapitel III beschriebenen Alkinkomplexe und anschließend zu den borylierten Olefinkomplexen $[Ni(^iPr_2Im^{Me})_2(\eta^2$-*cis*-(Bcat)(Me)C=C(Me)(Bcat))] **V-13** und $[Ni(^iPr_2Im^{Me})_2(\eta^2$-*cis*-$(Bcat)(H_7C_3)C=C(C_3H_7)(Bcat))]$ **V-14** führt. Diese Komplexe fungieren als entscheidende katalytische Intermediate und eröffnen neue Reaktionspfade, welche die Darstellung neuer Borylierungsprodukte ermöglichen.

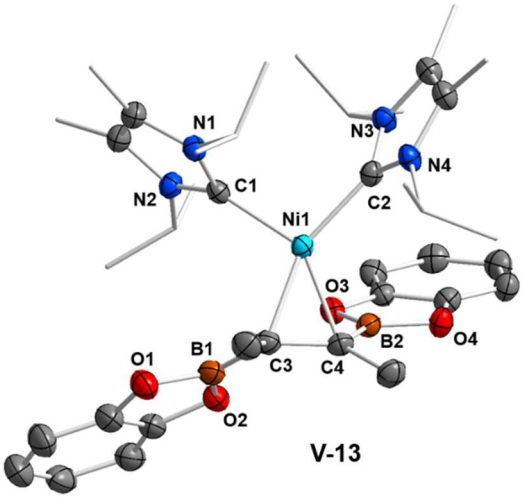

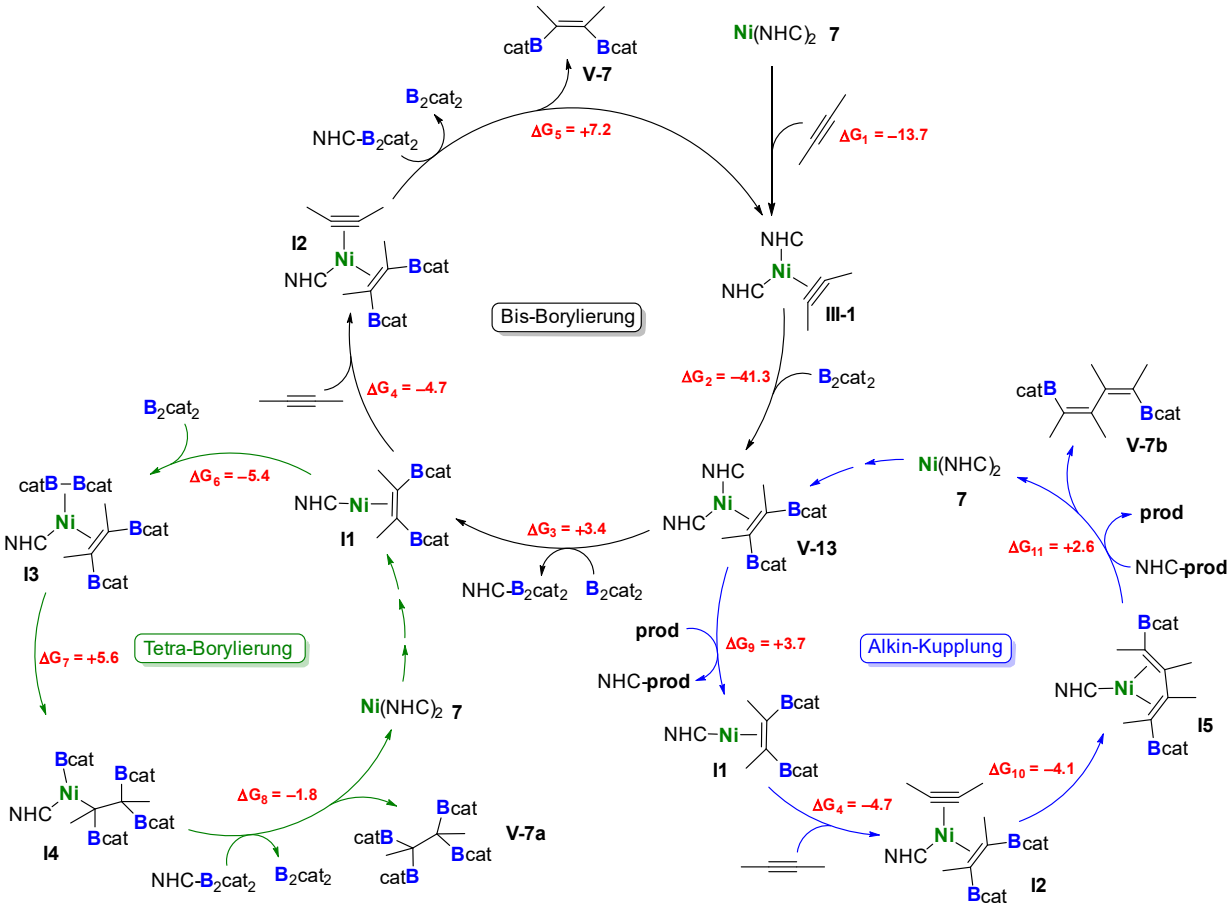

Schema XII.6 Postulierte Katalysezyklen für die Bildung von **V-7** (schwarz), **V-7a** (grün) und **V-7b** (blau).

Um einen besseren Einblick in die Reaktivität der neuen Bis-Boryl Komplexe zu erhalten, wird die Reaktivität von *cis*-[Ni(^{i}Pr$_2$Im^{Me})$_2$(Bcat)$_2$] **V-1a** in Kapitel VI weitergehend untersucht. Die Umsetzung von **V-1a** mit PMe$_3$ führt zu einem vollständigen Ligandenaustausch am zentralen Nickelatom unter Ausbildung des bis-NHC-Addukts [B$_2$cat$_2$ • (^{i}Pr$_2$Im^{Me})$_2$] **VI-2** und des homoleptischen Phosphan-Komplexes [Ni(PMe$_3$)$_4$] **VI-1**. Hierbei wird die zuvor addierte B–B-Bindung von B$_2$cat$_2$ über eine reduktive Eliminierung zurückgebildet, was wiederum ein Indiz für die zuvor beschriebene Mehrzentren-Wechselwirkung in Komplex **V-1a** ist und die Labilität der Boryl-Liganden verdeutlicht. Durch einen elektrophilen Angriff von Methyliodid bzw. eine Liganden-Dismutierung mit *trans*-[Ni(^{i}Pr$_2$Im^{Me})$_2$Br$_2$] können ausgehend von **V-1a** die

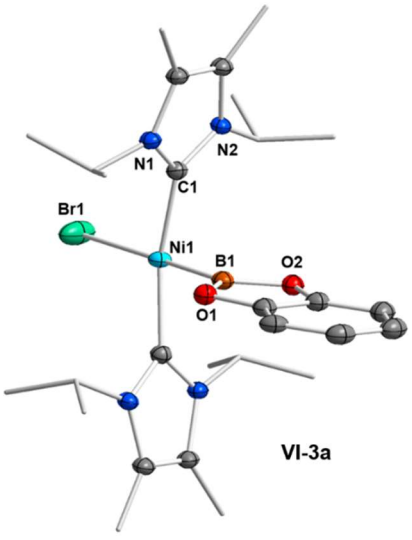

ersten NHC-stabilisierten Mono-Boryl Komplexe *trans*-[Ni(*i*Pr$_2$Im^{Me})$_2$(Bcat)Br] **VI-3a** und *trans*-[Ni(*i*Pr$_2$Im^{Me})$_2$(Bcat)I] **VI-3b** dargestellt werden. Im Gegensatz zur Platin-Chemie stellt eine einfache oxidative Addition von Halogenboranen an [Ni(*i*Pr$_2$Im^{Me})$_2$] keine geeignete Syntheseroute zu derartigen Mono-Boryl Komplexen dar. Die *trans*-Konfiguration der Komplexe **VI-3a** und **VI-3b** wird genau wie bei den vergleichbaren Platin-Komplexen durch den *trans*-Einfluss der Liganden ([Bcat]$^-$ > NHC > [X]$^-$) vorgegeben. Generell sind die Komplexe **V-1** aufgrund der elektronischen Übersättigung des Nickelatoms, durch die vier starken *σ*-Donorliganden, sehr reaktiv gegenüber vielen unterschiedlichen Substraten. Jedoch reagieren diese häufig unter undefinierter Zersetzung.

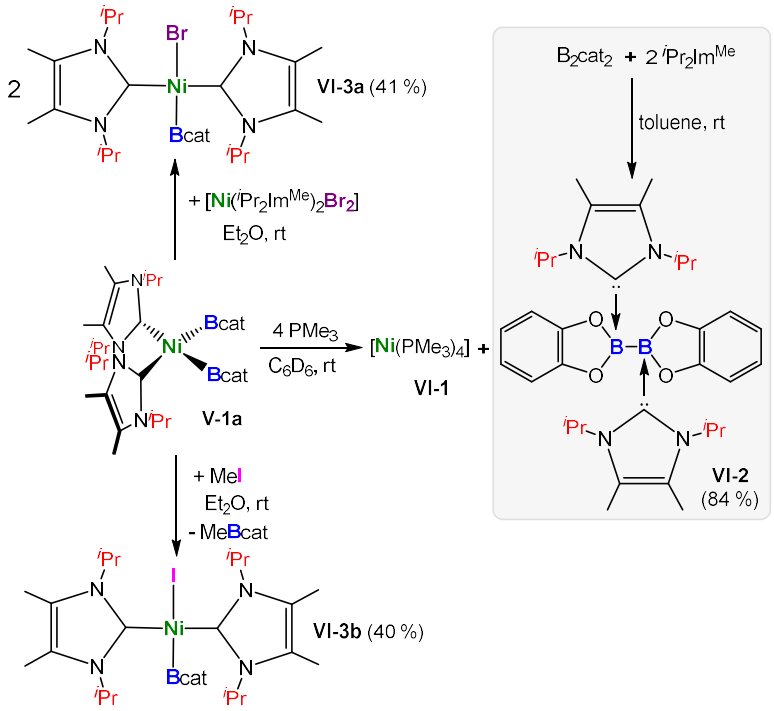

Schema XII.7 Reaktionen von *cis*-[Ni(*i*Pr$_2$Im^{Me})$_2$(Bcat)$_2$] **V-1a** mit PMe$_3$, MeI und *trans*-[Ni(*i*Pr$_2$Im^{Me})$_2$(Br)$_2$].

Im Rahmen dieser Arbeit wurde der Einfluss von unterschiedlichen NHC-Liganden auf die Eigenschaften von [Ni(NHC)$_2$]-Komplexen eingehend untersucht. Es konnte festgestellt werden, dass der unterschiedliche sterische Anspruch der verwendeten Carbene, neben einer unterschiedlichen Abschirmung und Zugänglichkeit des Nickel-Zentrums, einen deutlichen Einfluss auf den NHC–Ni–NHC Bisswinkel und damit auf die Donoreigenschaften des [Ni(NHC)$_2$]-Fragments hat. Zudem wird die Stabilität von

Komplexen mit koordinierten π-Liganden, die Neigung zur Liganden-Dissoziation sowie das Redox-Verhalten entscheidend durch die Sterik des Carbens beeinflusst. Durch die Wahl von geeigneten NHCs als Liganden können so in Zukunft weitere reaktive Nickel-Koordinationsverbindungen stabilisiert und neue Katalysatoren dargestellt werden, welche bisher unbekannte Reaktionswege eröffnen.

13 Appendix

13.1 List of compounds

1 [Ni(Mes_2Im)$_2$]

2 [Ni(Mes_2Im^{H2})$_2$]

3 [Ni($Dipp_2Im$)$_2$]

4 [Ni($Dipp_2Im^{H2}$)$_2$]

5 [Ni($cAAC^{Me}$)$_2$]

6 [Ni($^iPr_2Im$)$_2$]

6a [Ni_2($^iPr_2Im$)$_4$(μ-(η^2:η^2)-COD)]

6b [Ni($^iPr_2Im$)$_2$(η^4-COD)]

7 [Ni($^iPr_2Im^{Me}$)$_2$]

7a [Ni_2($^iPr_2Im^{Me}$)$_4$(μ-(η^2:η^2)-COD)]

7b [Ni($^iPr_2Im^{Me}$)$_2$(η^4-COD)]

7c [Ni($^iPr_2Im^{Me}$)$_2$(η^2-C_2H_4)]

7d [Ni($^iPr_2Im^{Me}$)$_2$(η^2-COE)]

8-43 literature-known compounds

Chapter II

II-1 [Ni(Mes_2Im)$_2$(η^2-H_2C=CH_2)]

II-2 [Ni(Mes_2Im)$_2$(η^2-(*C,C*)-H_2C=CHCOOMe)]

II-3 [Ni($^iPr_2Im$)$_2$(η^2-O=CH^{t}Bu)]

II-4 [Ni($^iPr_2Im$)$_2$(η^2-O=CHPh)]

II-5 [Ni($^iPr_2Im$)$_2$(η^2-O=CMePh)]

II-6 [Ni($^iPr_2Im$)$_2$(η^2-O=CPh_2)]

II-7 [Ni($^iPr_2Im$)$_2$(η^2-O=C(4-F-C_6H_4)$_2$)]

II-8 [Ni($^iPr_2Im$)$_2$(η^2-O=C(OMe)(CF_3))]

II-9 [Ni(Mes_2Im)$_2$(η^2-O=CHPh)]

II-10 [Ni(Mes_2Im)$_2$(η^2-O=CH(C$H(CH_3)_2$))]

II-11 [Ni(Mes_2Im)$_2$(η^2-O=CH(4-NMe_2-C_6H_4))]

II-12 [Ni(Mes$_2$Im)$_2$(η^2-O=CH(4-OMe-C$_6$H$_4$))]

II-13 [Ni(Mes$_2$Im)$_2$(η^2-O=CPh$_2$)]

II-14 [Ni(Mes$_2$Im)$_2$(η^2-O=C(4-F-C$_6$H$_4$)$_2$)]

II-15 *trans*-[Ni(Mes$_2$Im)$_2$H(OOCPh)]

II-16 [Ni$_2$(Mes$_2$Im)$_2$(μ_2-CO)(μ_2-η^2-*C,O*-PhCOCOPh)]

Chapter III

III-1 [Ni(^{i}Pr$_2$Im^{Me})$_2$(η^2-MeC≡CMe)]

III-2 [Ni(^{i}Pr$_2$Im^{Me})$_2$(η^2-H$_7$C$_3$C≡CC$_3$H$_7$)]

III-3 [Ni(^{i}Pr$_2$Im^{Me})$_2$(η^2-PhC≡CPh)]

III-4 [Ni(^{i}Pr$_2$Im^{Me})$_2$(η^2-MeOOCC≡CCOOMe)]

III-5 [Ni(^{i}Pr$_2$Im^{Me})$_2$(η^2-Me$_3$SiC≡CSiMe$_3$]

III-6 [Ni(^{i}Pr$_2$Im^{Me})$_2$(η^2-PhC≡CMe)]

III-7 [Ni(^{i}Pr$_2$Im^{Me})$_2$(η^2-HC≡CC$_3$H$_7$)]

III-8 [Ni(^{i}Pr$_2$Im^{Me})$_2$(η^2-HC≡CPh)]

III-9 [Ni(^{i}Pr$_2$Im^{Me})$_2$(η^2-HC≡C(*p*-Tol))]

III-9a ^{i}Pr C–H activation of **III-9**

III-10 [Ni(^{i}Pr$_2$Im^{Me})$_2$(η^2-HC≡C(4-^{t}Bu-C$_6$H$_4$))]

III-10a ^{i}Pr C–H activation of **III-10**

III-11 [Ni(^{i}Pr$_2$Im^{Me})$_2$(η^2-HC≡CCOOMe)]

III-12 [Ni(Mes$_2$Im)$_2$(η^2-MeC≡CMe)]

III-13 [Ni(Mes$_2$Im)$_2$(η^2-MeOOCC≡CCOOMe)]

III-14 [Ni(Mes$_2$Im)$_2$(η^2-PhC≡CMe)]

III-15 [Ni(Mes$_2$Im)$_2$(η^2-HC≡C(4-^{t}Bu-C$_6$H$_4$))]

III-16 [Ni(Mes$_2$Im)$_2$(η^2-HC≡CCOOMe)]

Chapter IV

IV-1$^+$ [Ni^I(Mes$_2$Im)$_2$][BPh$_4$]

IV-1^{+BF4} [Ni^I(Mes$_2$Im)$_2$][BF$_4$]

IV-1^{+THF} [Ni^I(Mes$_2$Im)$_2$(THF)][BF$_4$]

IV-2$^+$ [Ni^I(Mes$_2$Im^{H2})$_2$][BPh$_4$]

IV-3$^+$ [Ni^I(Dipp$_2$Im)$_2$][BPh$_4$]

IV-4$^+$ [Ni^I(Dipp$_2$Im^{H2})$_2$][BPh$_4$]

IV-5$^+$ [Ni^I(cAAC^{Me})$_2$][BPh$_4$]

Chapter V

V-1a *cis*-[Ni(*i*Pr$_2$Im^{Me})$_2$(Bcat)$_2$]

V-1b *cis*-[Ni(*i*Pr$_2$Im^{Me})$_2$(Bpin)$_2$]

V-1c *cis*-[Ni(*i*Pr$_2$Im^{Me})$_2$(Beg)$_2$]

V-2 *Z*-(Bcat)(Ph)C=C(Ph)(Bcat)

V-3 *Z*-(Bcat)(4-Me-C$_6$H$_4$)C=C(4-Me-C$_6$H$_4$)(Bcat)

V-3^{NHC} *Z*-(Bcat)(4-Me-C$_6$H$_4$)C=C(4-Me-C$_6$H$_4$)(Bcat) • (*i*Pr$_2$Im^{Me})

V-4 *Z*-(Bcat)(4-CF$_3$-C$_6$H$_4$)C=C(4-CF$_3$-C$_6$H$_4$)(Bcat)

V-5 *Z*-(Bcat)(C$_3$H$_7$)C=C(C$_3$H$_7$)(Bcat)

V-6 *Z*-(Bcat)(Me)C=C(Ph)(Bcat)

V-7 *Z*-(Bcat)(Me)C=C(Me)(Bcat)

V-7a (Bcat)$_2$(Me)C–C(Me)(Bcat)$_2$

V-7b *E,E*-(Bcat)(Me)C=C(Me)–(Me)C=C(Me)(Bcat)

V-8 *E*-(Bcat)HC=C(Ph)(Bcat)

V-9 *E*-(Bcat)HC=C(4-Me-C$_6$H$_4$)(Bcat)

V-10 *E*-(Bcat)HC=C(4-*t*Bu-C$_6$H$_4$)(Bcat)

V-11a *Z,Z*-(Bcat)HC=C(C$_3$H$_7$)–(C$_3$H$_7$)C=CH(Bcat)

V-11b *E/Z,E/Z*-(Bcat)HC=C(C$_3$H$_7$)–HC=C(Bcat)(C$_3$H$_7$)

V-12 (4-NMe$_2$-C$_6$H$_4$)(Bcat)(TMS)C–C(Bcat)$_3$

V-13 [Ni(*i*Pr$_2$Im^{Me})$_2$(η^2-*cis*-(Bcat)(Me)C=C(Me)(Bcat))]

V-14 [Ni(*i*Pr$_2$Im^{Me})$_2$(η^2-*cis*-(Bcat)(H$_7$C$_3$)C=C(C$_3$H$_7$)(Bcat))]

Chapter VI

VI-1 [Ni(PMe$_3$)$_4$]

VI-2 [B$_2$cat$_2$ • (*i*Pr$_2$Im^{Me})$_2$]

VI-3a *trans*-[Ni(*i*Pr$_2$Im^{Me})$_2$(Bcat)Br]

VI-3b *trans*-[Ni(*i*Pr$_2$Im^{Me})$_2$(Bcat)I]

13.2 Abbreviations

N-heterocyclic carbenes

Ad_2Im	1,3-diadamantylimidazolin-2-ylidene
$cAAC^{Me}$	1-(2,6-di-*iso*-propylphenyl)-3,3,5,5-tetramethylpyrrolidin-2-yliden
Cy_2Im	1,3-dicyclohexylimidazolin-2-ylidene
$Dipp_2Im$	1,3-(2,6-di-*iso*-propylphenyl)imidazolin-2-ylidene
$Dipp_2Im^{H2}$	1,3-(2,6-di-*iso*-propylphenyl)imidazolidin-2-ylidene
$^{i}Pr_2Im$	1,3-di-*iso*-propylimidazolin-2-ylidene
$^{i}Pr_2Im^{Me}$	1,3-di-*iso*-propyl-4,5-dimethylimidazolin-2-ylidene
Me_2Im^{Me}	1,3,4,5-tetramethylimidazolin-2-ylidene
$Me^{i}PrIm$	1-methyl-3-*iso*-propylimidazolin-2-ylidene
Mes_2Im	1,3-dimesitylimidazolin-2-ylidene
Mes_2Im^{H2}	1,3-dimesitylimidazolidin-2-ylidene
$^{n}Pr_2Im$	1,3-di-*n*-propylimidazolin-2-ylidene
p-Cl-Ph_2Im	1,3-di-(*p*-chlorophenyl)-2-ylidene
$^{t}Bu_2Im$	1,3-di-*tert*-butylimidazolin-2-ylidene
Tol_2Im	1,3-ditolylimidazolin-2-ylidene
6-Mes	1,3-dimesityl-3,4,5,6-tetrahydropyrimidin-2-ylidene
6-Xyl	1,3-dixylyl-3,4,5,6-tetrahydropyrimidin-2-ylidene
7-Mes	1,3-dimesityl-hexahydro-1*H*-1,3-diazepin-2-ylidene
7-Xyl	1,3-dixylyl-hexahydro-1*H*-1,3-diazepin-2-ylidene

General abbreviations

acac	acetylacetonate
Ad	adamantyl
Ar	aryl

BAr^F	tris(pentafluorophenyl)borane
cAAC	cyclic (alkyl)(amino)carbene
cat	catecholato
C_6D_6	deuterated benzene
COD	1,5-cyclooctadiene
COE	cyclooctene
Cp	cyclopentadiene
CSD	Cambridge Structural Database
CV	cyclic voltammetry
Cy	cyclohexyl
DCM	dichloromethane
DFT	density functional theory
Dipp	2,6-di-*iso*-propylphenyl
DME	dimethoxyethane
dmp	2,6-dimesitylphenyl
dmpe	1,2-bis(dimethylphosphino)ethane
DMSO	dimethylsulfoxide
dtbmp	2,6-di-*tert*-butyl-4-methylphenol
dtbpe	1,2-bis(di-*tert*-butyl)phosphinoethane
dtbpy	di-*tert*-butylbipyridine
eg	ethylene glycolato
EPR	electron paramagnetic resonance
Et	ethyl
Et_2O	diethyl ether
Fc^+/Fc	ferrocenium/ferrocene
HMBC	heteronuclear multiple bond correlation

HOMO	highest occupied molecular orbital
HRMS	high resolution mass spectrometry
IBO	intrinsic bond orbital
^{i}Pr	*iso*-propyl
IR	infrared
KO*t*Bu	potassium *tert*-butoxide
LUMO	lowest unoccupied molecular orbital
MBO	molecular bond orbital
Me	methyl
MeCN	acetonitrile
MeOH	methanol
Mes	mesityl
NBO	natural bond orbital
*n*Bu	*n*-butyl
NHC	*N*-heterocyclic carbene
NMR	nuclear magnetic resonance
^{n}Pr	*n*-propyl
neop	neopentyl
OTf	triflate
PBP	$C_6H_4\{N(CH_2P^tBu_2)\}_2B$
Ph	phenyl
pin	pinacolato
PNP	$N[2\text{-}P(CHMe_2)_2\text{-}4\text{-methylphenyl}]_2$
R	organic substituent
SET	single electron transfer
SIM	single ion magnet

SOMO	singly occupied molecular orbital
^{t}Bu	*tert*-butyl
TEP	tolman electronic parameter
THF	tetrahydrofuran
tmed	*N,N'*-tetramethylethylenediamine
TMS	trimethylsilyl
Tol	tolyl, toluene
TON	turnover number
VE	valence electron
XRD	X-ray diffraction
Xyl	2,6-dimethylphenyl
%V_{bur}	percent buried volume

Analytical abbreviations

Å	Ångström, 1 Å = 10^{-10} m
br	broad (in NMR spectroscopy)
d	doublet (in NMR spectroscopy); days
equiv.	equivalent
h	hour
J	coupling constant in NMR spectroscopy, [Hz]
m	multiplet (in NMR spectroscopy)
MHz	megahertz
min	minute
m/z	mass to charge ratio in MS
ppm	parts per million
q	quartet (in NMR spectroscopy)

rt	room temperature
s	singlet (in NMR spectroscopy)
sec	second
sept	septet (in NMR spectroscopy)
t	triplet (in NMR spectroscopy)
Z	number of molecules per unit cell
δ	chemical shift in NMR spectroscopy, [ppm]
λ	wavelength
v	frequency, [s^{-1}]
mol%	percentage per mol
wt%	weight percent

13.3 Additional Figures

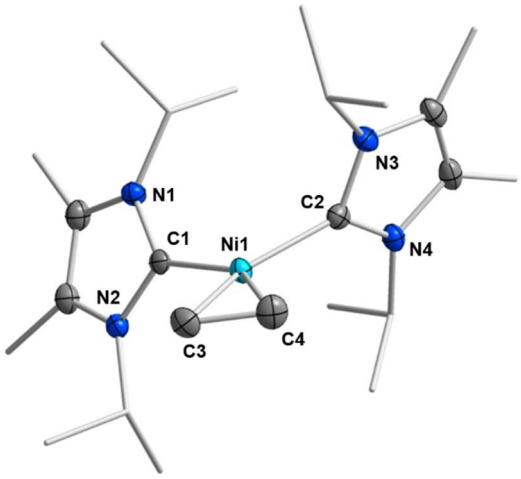

Figure XIII.1 Molecular structure of [Ni(^{i}Pr$_2$Im^{Me})$_2$(η^2-C$_2$H$_4$)] **7c** in the solid state (ellipsoids set at the 50 % probability level). Hydrogen atoms have been omitted for clarity. Selected bond lengths [Å] and angles [°] of **7c**: Ni1–C1 1.9191(16), Ni1–C2 1.9265(13), Ni1–C3 1.9596(16), Ni1–C4 1.9659(18), C3–C4 1.428(2); C1–Ni1–C2 105.25(6), C1–Ni1–C3 105.61(7), C2–Ni1–C4 106.79(6), C3–Ni1–C4 42.67(7).

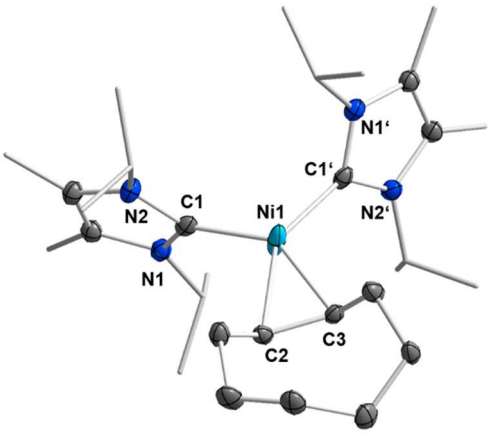

Figure XIII.2 Molecular structure of [Ni(^{i}Pr$_2$Im^{Me})$_2$(η^2-COE)] **7d** in the solid state (ellipsoids set at the 50 % probability level). Hydrogen atoms have been omitted for clarity. Selected bond lengths [Å] and angles [°] of **7d**: Ni1–C1/C1’ 1.9175(16), Ni1–C2 2.047(3), Ni1–C3 1.992(3), C2–C3 1.439(4); C1–Ni1–C1’ 110.88(9), C1–Ni1–C2 100.38(10), C1’–Ni1–C3 104.24(10), C2–Ni1–C3 41.71(12).

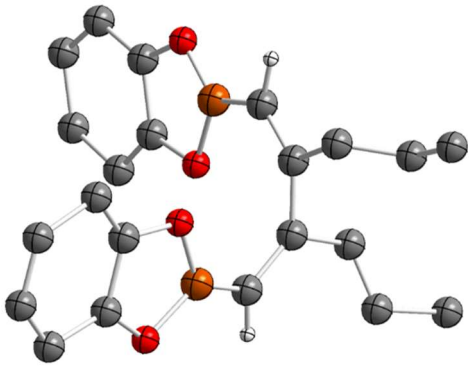

Figure XIII.3 Molecular structure of *Z,Z*-(Bcat)HC=C(C$_3$H$_7$)–(C$_3$H$_7$)C=CH(Bcat) **V-11a** in the solid state. Due to poor crystal quality the structural data is sufficient for proof of connectivity but insufficient for detailed discussion of bond parameters.

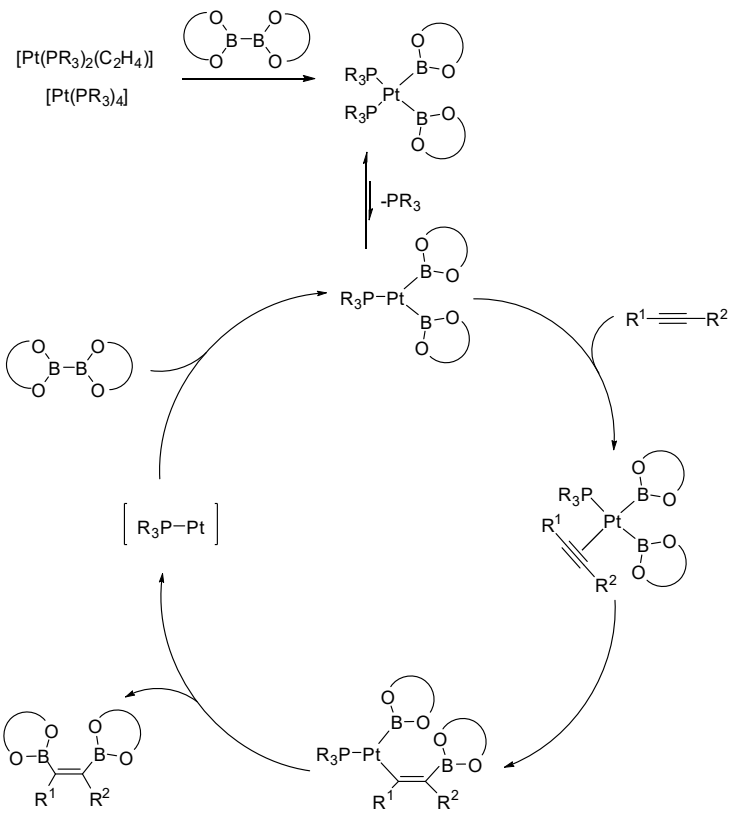

Figure XIII.4 Catalytic cycle for the platinum catalyzed diboration of alkynes.

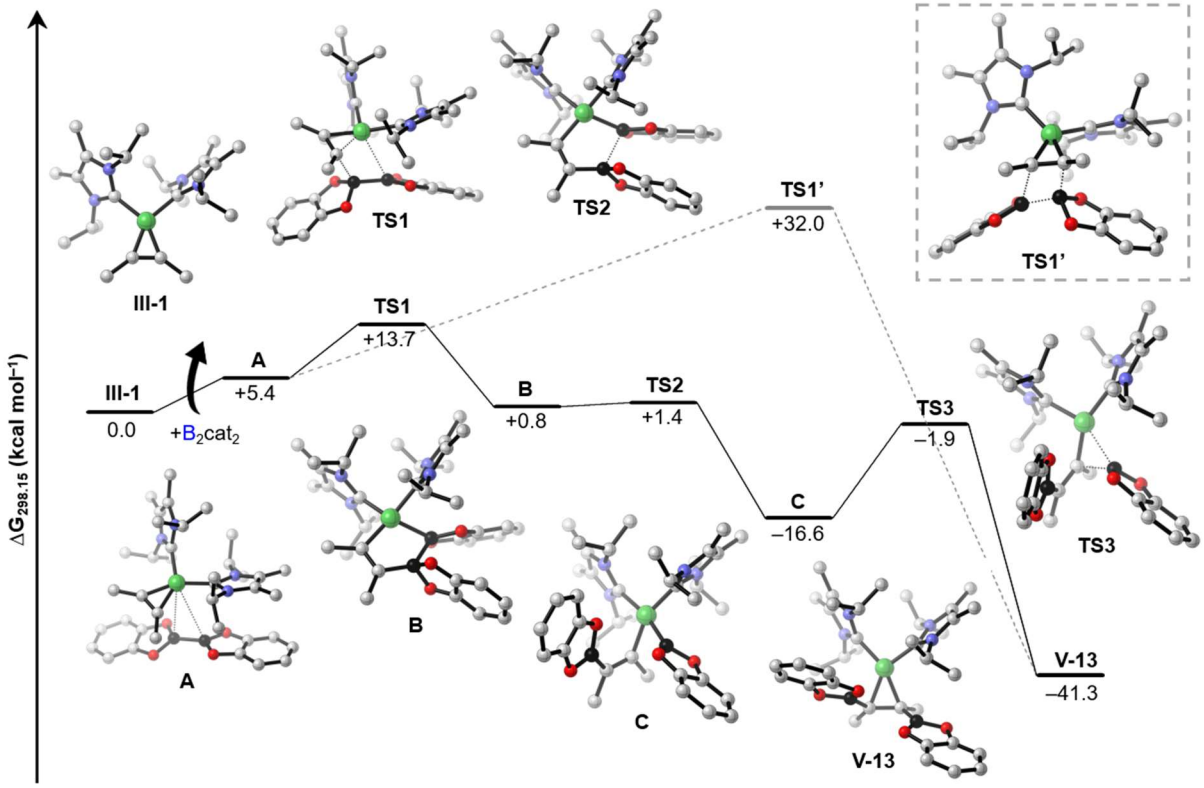

Figure XIII.5 Free energy profile of the formation of **V-13** with important transition states.

13.4 Publications

13.4.1 Reprint Permission

The publications listed below are reproduced and slightly modified in this thesis with permission from Wiley-VCH GmbH, according to the terms and conditions specified within the respective license agreement (Creative Commons Attribution 4.0). The table itemizes at which position in this work, each publication has been reproduced.

Publication	Position
"Large versus Small NHC Ligands in Nickel(0) Complexes: The Coordination of Olefins, Ketones and Aldehydes at [Ni(NHC)$_2$]" Lukas Tendera, Thomas Schaub, Mirjam J. Krahfuss, Maximilian W. Kuntze-Fechner, Udo Radius, *Eur. J. Inorg. Chem.* **2020**, 3194-3207; DOI: 10.1002/ejic.202000493. License: CC-BY 4.0	Chapter II
"A Case Study of N-^{i}Pr versus N-Mes Substituted NHC Ligands in Nickel Chemistry: The Coordination and Cyclotrimerization of Alkynes at [Ni(NHC)$_2$]" Lukas Tendera, Moritz Helm, Mirjam J. Krahfuss, Maximilian W. Kuntze-Fechner, Udo Radius, *Chem. Eur. J.* **2021**, *27*, 17849-17861; DOI: 10.1002/chem.202103093. License: CC-BY 4.0	Chapter III
"Cationic Nickel d9-Metalloradicals [Ni(NHC)$_2$]$^+$" Lukas Tendera, Martin S. Luff, Ivo Krummenacher, Udo Radius, *Eur. J. Inorg. Chem.* **2022**, Accepted Article, DOI: 10.1002/ejic.202200416 License: CC-BY-NC 4.0	Chapter IV
"Nickel Boryl Complexes and the Nickel-Catalyzed Alkyne-Borylation" Lukas Tendera, Felipe Fantuzzi, Todd B. Marder, Udo Radius, *submitted* 22. August **2022**.	Chapter V

13.4.2 Further Publications

Publications in peer-reviewed journals:

„NHC-Stabilized Nickel Olefin, Dialkyl and Dicyanido Complexes“
Johannes H. J. Berthel, Lukas Tendera, Maximilian W. Kuntze-Fechner, Laura Kuehn, Udo Radius, *Eur. J. Inorg. Chem.* **2019**, 3061-3072; DOI: 10.1002/ejic.201900484.

„Coligand Role in the NHC Nickel catalyzed C–F Bond Activation: Investigations on the Insertion of bis(NHC) Nickel into the C–F Bond of Hexafluorobenzene“
Maximilian W. Kuntze-Fechner, Hendrik Verplancke, Lukas Tendera, Martin Diefenbach, Ivo Krummenacher, Holger Braunschweig, Todd B. Marder, Max C. Holthausen, Udo Radius, *Chem. Sci.* **2020**, *11*, 11009-11023; DOI: 10.1039/D0SC04237D.

13.4.3 Erklärung zur Autorenschaft

Chapter II:

Julius-Maximilians-
UNIVERSITÄT
WÜRZBURG

Fakultät für
CHEMIE UND
PHARMAZIE

Erklärung zur Autorenschaft

"Large vs. Small NHC Ligands in Nickel(0) Complexes: The Coordination of Olefins, Ketones and Aldehydes at [Ni(NHC)$_2$]"
L.Tendera, T. Schaub, M.J. Krahfuss, M. W. Kuntze-Fechner, U. Radius, *Eur. J. Inorg. Chem.* **2020**, 3194 – 3207.

Detaillierte Darstellung der Anteile an der Veröffentlichung (in %)

Angabe Autoren/innen (ggf. Haupt- / Ko- / korrespondierende/r Autor/in) mit Vorname Nachname (Initialen)

Hauptautor: Lukas Tendera (LT), Koautoren: Thomas Schaub (TS), Mirjam J. Krahfuss (MK) Maximilian w. Kuntze-Fechner (MKF), korrespondierender Autor: Udo Radius (UR)

Autor	LT	TS	MK	MKF	UR							Σ in Prozent
Konzept	2,5%				5%							7,5%
Synthesen	20%	15%										35%
Analytik	10%	5%	5%	5%								25%
Verfassen der Veröffentlichung	12,5%				5%							17,5%
Korrektur der Veröffentlichung	5%				5%							10%
Koordination der Veröffentlichung					5%							5%
Summe	50%	20%	5%	5%	20%							100%

Julius-Maximilians-
UNIVERSITÄT
WÜRZBURG

Fakultät für
CHEMIE UND
PHARMAZIE

Erklärung zur Autorenschaft

"Case Study of N-^{i}Pr versus N-Mes Substituted NHC Ligands in Nickel Chemistry: The Coordination and Cyclotrimerization of Alkynes at [Ni(NHC)$_2$]"
L.Tendera, M. Helm, M.J. Krahfuss, M. W. Kuntze-Fechner, U. Radius, *Chem. Eur. J.* **2021**, *27*, 17849 – 17861.

Detaillierte Darstellung der Anteile an der Veröffentlichung (in %)
Angabe Autoren/innen (ggf. Haupt- / Ko- / korrespondierende/r Autor/in) mit Vorname Nachname (Initialen)

Hauptautor: Lukas Tendera (LT), Koautoren: Moritz Helm (MH), Mirjam J. Krahfuss (MK) Maximilian w. Kuntze-Fechner (MKF), korrespondierender Autor: Udo Radius (UR)

Autor	LT	MH	MK	MKF	UR							∑ in Prozent
Konzept	2,5%				2,5%							5%
Synthesen	27,5%	2,5%										30%
Analytik	15%	2,5%	5%	5%								27,5%
Rechnungen					2,5%							2,5%
Verfassen der Veröffentlichung	15%				5%							20%
Korrektur der Veröffentlichung	5%				5%							10%
Koordination der Veröffentlichung					5%							5%
Summe	65%	5%	5%	5%	20%							100%

Julius-Maximilians-
UNIVERSITÄT
WÜRZBURG

Fakultät für
CHEMIE UND
PHARMAZIE

Erklärung zur Autorenschaft

"Cationic Nickel d9-Metalloradicals $[Ni(NHC)_2]^+$"

L.Tendera, M. S. Luff, I. Krummenacher, U. Radius, *Eur. J. Inorg. Chem.* **2022**, Accepted Article, DOI: 10.1002/ejic.202200416

Detaillierte Darstellung der Anteile an der Veröffentlichung (in %)

Angabe Autoren/innen (ggf. Haupt- / Ko- / korrespondierende/r Autor/in) mit Vorname Nachname (Initialen)

Hauptautor: Lukas Tendera (LT), Koautoren: Martin S. Luff (ML), Ivo Krummenacher (IK), korrespondierender Autor: Udo Radius (UR)

Autor	LT	ML	IK	UR								Σ in Prozent
Konzept	2,5%			2,5%								5%
Synthesen	30%											30%
Analytik	12,5%	5%	10%									27,5%
Rechnungen				2,5%								2,5%
Verfassen der Veröffentlichung	15%			5%								20%
Korrektur der Veröffentlichung	5%			5%								10%
Koordination der Veröffentlichung				5%								5%
Summe	65%	5%	10%	20%								100%

Julius-Maximilians-
UNIVERSITÄT
WÜRZBURG

Fakultät für
CHEMIE UND
PHARMAZIE

Erklärung zur Autorenschaft

"Nickel Boryl Complexes and the Nickel-Catalyzed Alkyne-Borylation"

L.Tendera, F. Fantuzzi, T. B. Marder, U. Radius, *submitted* 22. August **2022**

Detaillierte Darstellung der Anteile an der Veröffentlichung (in %)

Angabe Autoren/innen (ggf. Haupt- / Ko- / korrespondierende/r Autor/in) mit Vorname Nachname (Initialen)

Hauptautor: Lukas Tendera (LT), Koautoren: Felipe Fantuzzi (FF), Todd B. Marder (TM), korrespondierender Autor: Udo Radius (UR)

Autor	LT	FF	TM	UR								∑ in Prozent
Konzept	2,5%			2,5%								5%
Synthesen	25%											25%
Analytik	20%											20%
Rechnungen		20%										20%
Verfassen der Veröffentlichung	10%	5%		2,5%								17,5%
Korrektur der Veröffentlichung	2,5%		5%	2,5%								10%
Koordination der Veröffentlichung				2,5%								2,5%
Summe	60%	25%	5%	10%								100%

14 Danksagung

An erster Stelle ein riesiges Dankeschön an meinen Doktorvater **Udo Radius**. Danke, dass ich sowohl meine Masterarbeit als auch meine Doktorarbeit in deinem Arbeitskreis machen durfte und dass deine Tür wirklich zu jeder Zeit offen stand. Vielen Dank für dein Vertrauen, deine Hilfestellungen und die super gute Arbeitsatmosphäre, welche man wahrscheinlich nur selten so finden kann. Ich hatte einfach eine unfassbar gute Zeit in deiner Gruppe, egal ob im Laboralltag, auf den Tagungen in Hirschegg und Prag oder einfach nach Feierabend hinter der alten AC oder zwischen den neuen Gebäuden. Neben all dem Wissen, das du mir vermittelt hast, möchte ich dir für den freundschaftlichen Umgang während der kompletten Zeit danken und auch dafür, dass du mir den nächsten Schritt nach der Promotion (nach Karlsruhe) so sehr erleichtert hast. Vielen Dank für alles!

Ein besonderer Dank gilt allen ehemaligen und aktuellen Mitgliedern des AK Radius (und dem erweiterten Kreis). Durch euch bin ich von Anfang an gerne auf die Arbeit gekommen (wenn man das so nennen mag) und hatte immer unglaublich viel Spaß im Labor oder an den Abenden danach. Danke an die „ganz Alten“ – **Schnurres, Heidi, Toni, Ulli, Matti, Shorty** – mit denen ich leider nicht allzu viel Zeit verbringen durfte, aber trotzdem froh bin, dass ihr mich schon während meines Master-Praktikums so nett aufgenommen habt. Das hat auch dafür gesorgt, dass ich mich später für die AC entschieden habe. **Matti** und **Shorty** euch bin ich besonders dankbar für die geile Zeit während meiner Masterarbeit, für die Heimwege (mit Bier) in die Nürnberger, die schier endlosen Gespräche über Basketball (der Killer war der Beste) oder spontane Ausflüge in den Erthalhof. Danke auch an die jetzt schon „alte Generation“ – **Katha, Laura, Steffen, Miri, Kuntze** – für unvergesslich schöne und lustige Momente im Labor, im Kaffeeraum, beim ersten Mal Hirschegg, in der Stadt oder sonst wo. Danke **Miri**, dass du mich damals als Praktikant aufgenommen hast und mir damit den Weg in die Gang eröffnet hast. Vielleicht bezahle ich irgendwann noch die Strafbiere, die ich dir angeblich schulde. Danke **Katja**, dass du mir den Unterschied zwischen Faschings- und Karnevals-Musik erklärt hast (Karneval find ich ok bis ok). Danke **Steffen** für deine fachliche Expertise und für völlig unerwartete Sprüche, welche bis heute regelmäßig zitiert werden. **Laura**, Mama Lauda!!! Udo ist wahrscheinlich froh

nach dem Umzug endlich zwei Türen zwischen sich und dem Labor zu haben, aber ich fand unser altes Labor klasse. Danke dafür **Laura** und für deine endlos gute Laune und viele witzige Erinnerungen. **Kuntze** mein Bester, danke, dass du neben einem premium Laborpartner auch ein richtig guter Kumpel bist. Die Abende, als wir spontan im Tscharlies oder Loma versackt sind oder plötzlich auf irgendeiner Geburtstagsparty Bier-Wiegen gespielt haben, werde ich nie vergessen. Auch unser Trip nach Hamburg war „speziell“, aber trotzdem legendär. Natürlich möchte ich mich auch bei der „aktuellen Gang“ – **Michi, Günther, Luis, Christian, Martin, Melanie und Edu** – für alles bedanken. „Wenn wir kommen, fängt die Stimmung an“ wurde spätestens in Hirschegg auf jeden Fall bestätigt. **Michi**, du hast mir ja jetzt alles knapp vor der Nase weggeschnappt. Also, was soll ich noch sagen… Danke für deine Fröhlichkeit, und dass du für jeden Spaß zu haben bist, für witzige, sehr lange Abende, dass man dich nie lange überreden musste und dass man auch mal ernste Themen mit dir bequatschen konnte. Wir habens geschafft mein Freund! Danke **Günni**, dass du dich als „Mädchen für alles“ immer um den AK kümmerst und so hilfsbereit bist. Du bist auch neben der Arbeit echt ein guter Kumpel, der verlässlich ist und mit dem man sowohl super chillen (meistens am Main oder im Park) als auch ordentlich feiern kann. Vor allem die Tagung in Prag mit **Luis** (trinkt nie Bier im AK, in Prag aber schon) war wirklich nochmal ein richtiges Highlight. Keiner liest so schön vor wie ihr beiden. Dir auch ein großes Dankeschön **Luis**, für deinen Humor, den ich absolut teilen kann und für die vielen guten Ausfahrten auf dem Rad sowie die detaillierten Analysen der Stats, die du zusammen mit diesem **Kimchi Kagawa** durchgeführt hast. Allgemein finde ich, dass die ganze Radgruppe eine echt coole Sache ist, die mir mit Sicherheit sehr fehlen wird. Danke **Christian**, für die tägliche Versorgung mit allen wichtigen Infos aus der digitalen Welt und deine Hilfsbereitschaft für jeden einzelnen. **Martin Alberto Roberto Montenegro (1000 ppm) Luft**, danke auch dir für viele gute Gespräche, deine Hilfe bei den CVs und deine Freundschaft. Deine extreme Risikobereitschaft hat auf jeden Fall immer für Lacher gesorgt. Ich hoffe wirklich, dass du jetzt verletzungsfrei bleibst und die Elektrikerausbildung abschließen kannst. Danke auch an die „Neuen“ **Melaunie** und **Edu**, für die amüsanten Diskussionen, die leckeren Backwaren und die unerwarteten Tischtennis- und Fußballfähigkeiten, welche für großen Spaß gesorgt haben. Wenn die Ehetherapie anschlägt, bin ich mir sicher, dass alles gut wird. Vielen Dank an alle genannten Personen für die unvergesslichen vier Jahre (und ein paar Monate) in diesem Arbeitskreis. Bleibt einfach „immer diese Radien“!

Bei meinen Praktikanten und Praktikantinnen – **Kathrin, Jonas, Anna und Moritz** – möchte ich mich für die gute Arbeit im Labor bedanken, die mir sehr geholfen hat und euch hoffentlich auch ein bisschen.

Bei **Luis**, **Martin**, **Lewis** und **Nicole** möchte ich mich noch einmal für das Korrekturlesen dieser Arbeit bedanken. Vielen Dank auch allen, die bei der Korrektur-Session geholfen haben.

Zudem möchte ich mich bei allen Mitgliedern der anderen Arbeitskreise für jegliche Hilfe und das ein oder andere Feierabendbier bedanken. Ein großes Dankeschön auch an die Angestellten des Hauses, die dafür sorgen, dass der Laden reibungslos läuft. Danke an **Dr. Krzysztof Radacki** und **Dr. Alexandra Friedrich** für die Einführung in die Kristallographie. Bei **Dr. Rüdiger Bertermann, Marie-Luise Schäfer** und **Laura Wolz** möchte ich mich für das Messen von NMR-Proben bedanken. Danke an **Christoph Maler** für die Massenspektren. Danke an **Dr. Ivo Krummenacher** für die ESR-Messungen und danke an **Dr. Felipe Fantuzzi** für die ausführlichen Rechnungen, welche zu gemeinsamen Publikationen geführt haben. Danke an den Glasbläser **Bernhard Werner**, die Werkstätten um **Alois Ruf**, **Manfred Reinhard** und **Wolfgang Obert** und an den technischen Betrieb. Danke auch an die CHN-Abteilung um **Liselotte Michels** und **Sabine Timmroth** sowie an **Cornelia Walter** und **Birgit Zepke** für die Hilfe bei allen organisatorischen Dingen. Danke auch an **Alfred Schertzer**, **Stephan Köper** und **Gertrud Wunderling** für die ständige Hilfsbereitschaft und für das Kümmern ums komplette Haus. Ein großes Dankeschön auch an **Dr. Stephan Wagner** für die komplette Organisation des Instituts.

Ein großer Dank gilt auch meinen Freunden außerhalb der Uni, die mich in den letzten zehn Jahren in Würzburg begleitet und immer unterstützt haben. Besonders möchte ich mich hier bei **Fulli**, **Markus**, **Franzi** und den **Handball-Jungs aus Wabü** bedanken. Es war eine wunderschöne Zeit mit euch allen. Danke auch an **Lars**, **Daniel** und **Fuchsi** für den besten „Gürtel“-Stammtisch der Welt. Leider war diese Zeit viel zu kurz, aber die Freundschaft, die dabei entstanden ist und die Erinnerungen an diese Zeit sind einfach nur Gold wert. Danke auch an meine Freunde aus der Heimat – **Flo, Kröger, Held, Seppo, Fuchsi** – auf euch kann man sich vollständig verlassen und auch wenn wir uns nich mehr so oft sehen, ist alles wie immer, wenn wir uns treffen.

Besonders möchte ich mich noch einmal bei **Seppo** und **Fuchsi** bedanken. Es gibt auf der Welt keine besseren Freunde als euch! Ich bin unglaublich dankbar, dass ihr damals auf mich zugekommen seid und mich verwechselt habt. Das war ein riesiges Glück. Ihr seid die Besten!

Vielen Dank auch an alle, die hier nicht namentlich genannt sind, die mich aber in den letzten zehn Jahren auf irgendeine Weise begleitet haben. Danke!

Das Beste kommt bekanntlich zum Schluss. Ich möchte mich von ganzem Herzen bei meiner gesamten Familie bedanken, die mich nicht nur während dieser Arbeit, sondern während meines gesamten Lebens bei allem bedingungslos unterstützt. Danke vor allem **Mama**, **Papa** und **Christoph**, dass ihr immer für mich da seid und mir immer helft, den richtigen Weg zu finden. Ihr seid unglaublich und ich bin unfassbar froh, euch zu haben.
Zu meiner Familie zähle ich auch dich, liebste **Nicole**. Danke, dass du immer ein offenes Ohr für mich hast und mich ermutigst und beruhigst, wenn es mal stressig wird. Vielen Dank für deine Unterstützung, dein Verständnis, deine Fürsorge und dass du ebenfalls immer für mich da bist. Ich feue mich sehr auf das, was kommt.

Cheers! Auf euch alle!